



**Soil degradation by water erosion in
a sub-humid West-African catchment:
a modelling approach considering
land use and climate change in Benin**

Dissertation
zur
Erlangung des Doktorgrades (Dr. rer. nat.)
der
Mathematisch-Naturwissenschaftlichen Fakultät
der
Rheinischen Friedrich-Wilhelms-Universität Bonn

vorgelegt von

Claudia Hiepe

aus

Jena

Bonn, im Oktober 2008

Angefertigt mit Genehmigung der Mathematisch-Naturwissenschaftlichen Fakultät
der Rheinischen Friedrich-Wilhelms-Universität Bonn

1. Referent: Prof. Dr. B. Diekkrüger

2. Referent: Prof. Dr. B. Reichert

Tag der mündlichen Prüfung: 19.12.2008

Erscheinungsjahr: 2008

Diese Dissertation ist auf dem Hochschulschriftenserver der ULB Bonn

unter http://hss.ulb.uni-bonn.de/diss_online elektronisch publiziert.

For my parents

Acknowledgements

This work was conducted under the IMPETUS project, and was supported by the Federal German Ministry of Education and Research (BMBF) under grant No. 01 LW 0301A and by the Ministry of Science and Research (MWF) of the federal state of Northrhine-Westfalia (grant No. 223-21200200).

This dissertation could only have been possible through the generous contributions of many people. First and foremost, I am grateful to my supervisor Prof. Dr. B. Diekkrüger, who supported me through my doctoral research. In particular, I thank him for his prompt availability whenever needed. I also thank my co-supervisor Prof. Dr. B. Reichert for her interest in my work and her continued cooperation throughout IMPETUS subproject A2.

I am deeply grateful to all my colleagues in the Hydrology Research Group, in particular Dr. Simone Giertz, Gero Steup, Anna Zeyen, Henning Busche, Dr. Anne-Kathrin Jaeger, Herwig Hölzel, Andreas Enders, and Dr. Luc Sintondji for the inspiring working atmosphere that they fostered and the wonderful time we had together in Bonn and Benin. I would also like to extend special thanks to lab workers Elfriede Mainz and Annette Schäfermeier for their commitment to the analysis of my soil samples. Furthermore, I would like to thank all the student assistants who contributed to this work, particularly Beate Ambeck, Eva Lampe, Marianne Wargenau, Ronja Wolter and Dennis Prangenberg.

My gratitude is also extended to all the former and current members of the IMPETUS project. In particular, I would like to thank Dr. Birte Junge, Dr. Luc Sintondji, Dr. Hans-Peter Thamm, Dr. Michael Judex, Prof. Dr. Heiko Paeth, Dr. Andreas Fink, Malte Diederich, and Volker Ermert for providing data for my study. Many thanks also go out to my colleagues Christiane Stadler, Dr. Julia Röhrig, Dr. Ina Gruber, Dr. Valens Mulindabigwi, Moritz Heldmann, and Stefan Klose for their cooperative and pleasant team work throughout the project.

Additionally, I would like to extend a special thank you to all the people of Benin who supported my work; working with them helped to broaden my mind. I want to thank all people who helped me during the field investigations in the Upper Ouémé catchment, particularly Luc Seguis and Christophe Peugeot (IRD France), Claude Kanninkpo; Bouké, Lamidi, Francois and Benoit from Dogué, Drahmane, Adamou and Alaza from Sérrou, Doussi from Parakou, and Dr. Elisabeth van den Akker. Moreover, I would like to thank Dr. Attanda Moinou Igué and Dr. Anastase Azontonde (CENAP), Daniel Loconon (NGO AGEDREN), Dr. Gabi Zink (DED, PAEB-Nord), Werner Dickore (DED, ProCGRN), Marimam Idrissou Yaya and Mr. Albert (NGO Alpha & Omega Environment), Jaques Zanou (NGO Benin 21), and Armande Zanou (MEPN) for many interesting discussions about soil management in Benin.

Special thanks are also extended to Dr. Olaf Post, Prof. Dr. Wolfgang Pekrun, Dr. Ina Mäurer, Henning Busche, and Dr. Simone Giertz for proof-reading this work and providing valuable comments.

Last but not least, I would like to thank Olaf Post, all my friends, and my parents, Renate and Hans-Ulrich Hiepe, for unconditional encouragement.

Abstract

Soil degradation by water erosion in a sub-humid West-African catchment: a modelling approach considering land use and climate change in Benin

Soil degradation threatens agricultural production and food security in Sub-Saharan Africa. In the coming decades, soil degradation, in particular soil erosion, will become worse through the expansion of agriculture into savannah and forest and changes in climate. This study aims to improve the understanding of how land use and climate change affect the hydrological cycle and soil erosion rates at the catchment scale.

We used the semi-distributed, time-continuous erosion model SWAT (Soil Water Assessment Tool) to quantify runoff processes and sheet and rill erosion in the Upper Ouémé River catchment (14500 km², Central Benin) for the period 1998-2005. We could then evaluate a range of land use and climate change scenarios with the SWAT model for the period 2001-2050 using spatial data from the land use model CLUE-S and the regional climate model REMO. Field investigations were performed to parameterise a soil map, to measure suspended sediment concentrations for model calibration and validation and to characterise erosion forms, degraded agricultural fields and soil conservation practices.

Modelling results reveal current “hotspots” of soil erosion in the north-western, eastern and north-eastern parts of the Upper Ouémé catchment. As a consequence of rapid expansion of agricultural areas triggered by high population growth (partially caused by migration) and resulting increases in surface runoff and topsoil erosion, the mean sediment yield in the Upper Ouémé River outlet is expected to increase by 42 to 95% by 2025, depending on the land use scenario. In contrast, changes in climate variables led to decreases in sediment yield of 5 to 14% in 2001-2025 and 17 to 24% in 2026-2050. Combined scenarios showed the dominance of land use change leading to changes in mean sediment yield of -2 to +31% in 2001-2025. Scenario results vary considerably within the catchment. Current “hotspots” of soil erosion will aggravate, and a new “hotspot” will appear in the southern part of the catchment. Although only small parts of the Upper Ouémé catchment belong to the most degraded zones in the country, sustainable soil and plant management

practices should be promoted in the entire catchment. The results of this study can support planning of soil conservation activities in Benin.

Kurzfassung

Bodendegradation durch Wassererosion in einem semi-humiden west-afrikanischen Flusseinzugsgebiet: ein Modellierungsansatz unter Berücksichtigung von Klima- und Landnutzungsänderungen in Benin

Bodendegradation gefährdet die Agrarproduktion und Ernährungssicherheit in Afrika südlich der Sahara. In den nächsten Jahrzehnten wird die Bodendegradation, insbesondere die Bodenerosion, durch die Ausdehnung landwirtschaftlicher Flächen in die Savannen und Wälder und durch Klimaveränderungen zunehmen. Die vorliegende Studie versucht, das Verständnis der Zusammenhänge zwischen Klima- und Landnutzungswandel und dem Wasserkreislauf und Bodenerosionsraten auf der regionalen Skala zu verbessern.

Das semi-distributive, zeit-kontinuierliche Erosionsmodell SWAT (Soil Water Assessment Tool) wurde verwendet, um die Abflussprozesse sowie Flächen- und Rillenerosion im Oberen Ouémé - Flusseinzugsgebiet (14500 km², Zentral-Benin) für den Zeitraum 1998-2005 zu quantifizieren. Anschließend konnten mit dem SWAT-Modell verschiedene Landnutzungs- und Klimaszenarien für den Zeitraum 2001-2050 berechnet werden. Dafür wurden räumliche Daten des Landnutzungsmodells CLUE-S und des regionalen Klima-Modells REMO verwendet. Felduntersuchungen wurden durchgeführt, um die Bodenkarte zu parametrisieren, Schwebstoffkonzentrationen zur Modellkalibrierung und -validierung zu messen sowie Erosionsformen, degradierte Äcker und Bodenschutzmassnahmen zu charakterisieren.

Im Rahmen der Modellierung wurden aktuell besonders erosionsgefährdete Gebiete im Nordwesten, Osten und Nordosten des Oberen Ouémé Einzugsgebietes identifiziert. Infolge der schnellen Expansion von Ackerflächen aufgrund des hohen Bevölkerungswachstums (z.T. bedingt durch Migration) nehmen Oberflächenabfluss und Bodenabtragsmengen zu. Die mittlere Sedimentaustragsrate am Gebietsauslass des Oberen Ouémé - Flusses könnte sich dadurch bis 2025 je nach Landnutzungsszenario um 42 bis 95% erhöhen. Im Gegensatz dazu führten

simuliert Veränderungen der Klimavariablen zu einer Abnahme der mittleren Sedimentaustragsrate um 5 bis 14% in 2001-2025 beziehungsweise 17 bis 24% in 2026-2050. Kombinierte Szenarien ergaben eine Dominanz der Landnutzungsänderungen und daraus resultierende Veränderungen der Sedimentaustragsrate von -2 bis +31% in 2001-2025. Die Ergebnisse der Szenarienanalyse variieren erheblich innerhalb des Einzugsgebietes. Aktuell besonders erosionsgefährdete Gebiete werden in Zukunft noch stärker betroffen sein; hinzu kommt ein zusätzlich erosionsgefährdetes Gebiet im südlichen Teil des Einzugsgebietes. Obwohl nur ein kleiner Teil des Oberen Ouémé - Einzugsgebietes zu den am stärksten degradierten Teilen des Landes gehört, sollten nachhaltige Boden- und Pflanzenmanagement- praktiken im gesamten Gebiet gefördert werden. Die Ergebnisse dieser Studie können die Planung von Bodenschutzmassnahmen in Benin unterstützen.

Résumé

Dégradation des sols soumis à l'érosion par l'eau dans un bassin versant subhumide de l'Afrique de l'Ouest: une modélisation prenant en compte les changements d'utilisation des sols et des changements climatiques au Bénin

La dégradation des sols menace la production agricole et la sécurité alimentaire en Afrique sub-saharienne. Dans les décennies à venir, la dégradation des sols, et plus particulièrement l'érosion des sols, risque de s'aggraver encore du fait de l'extension de l'agriculture vers la savane et la forêt ainsi que des changements climatiques. Cette étude a pour but d'aider à comprendre comment des changements d'utilisation des sols et des changements climatiques affecte le cycle hydrologique et les taux d'érosion des sols à l'échelle du bassin versant.

Nous avons utilisé le modèle d'érosion SWAT (Soil Water Assessment Tool) semi-distribué et continu dans le temps pour quantifier les processus de ruissellement et d'érosion en nappe et linéaire dans le bassin versant de l'Ouémé supérieur (14500 km², au centre du Bénin) entre 1998 et 2005. Nous avons ensuite pu réaliser une gamme de scénarios d'utilisation des sols et de changements climatiques à l'aide du modèle SWAT pour la période 2001-2050 utilisant les données spatiales du modèle CLUE-S d'utilisation des sols et du modèle climatique régional REMO. Des

investigations de terrain ont été réalisées pour paramétrer une carte des sols, pour mesurer les concentrations de sédiments suspendus afin de calibrer et valider le modèle et pour caractériser les formes d'érosion, les sites agricoles dégradés et les pratiques de conservation des sols.

Les résultats de la modélisation révèlent que les « points chauds » actuels de l'érosion des sols se situent dans les parties nord-ouest, est, et nord-est du bassin versant de l'Ouémé supérieur. À la suite d'une rapide expansion des zones d'agriculture liées à la forte croissance démographique (due en partie aux migrations) et de l'augmentation des ruissellements de surface et de l'érosion des sols de surface qui en résultent, la production moyenne de sédiments à la sortie du bassin versant de l'Ouémé supérieur devrait augmenter, selon les scénarios d'utilisation des sols, de 42 à 95% d'ici à 2025. Au contraire, les modifications des variables climatiques ont entraîné une diminution de la production sédimentaire de 5 à 14% pour la période 2001-2025 et de 17 à 24% pour la période 2026-2050. Les scénarios combinés ont montré que les changements d'utilisation des sols dominant, entraînant un changement de la production moyenne de sédiments de -2 à +31% in 2001-2025. Les résultats des scénarios varient considérablement à l'intérieur du bassin versant. La situation des « points chauds » actuels de l'érosion des sols va s'aggraver et un nouveau « point chaud » apparaître dans la partie sud du bassin versant. Même si seules de petites parties du bassin versant de l'Ouémé supérieur font partie des zones les plus dégradées du pays, il faut encourager des pratiques durables de gestion des sols et des plantes dans tous le bassin versant. Les résultats peuvent se révéler utiles pour planifier les activités de conservation des sols au Bénin.

Table of contents

Acknowledgements	<i>i</i>
Abstract	<i>iii</i>
Kurzfassung.....	<i>iv</i>
Résumé	<i>v</i>
Table of contents	<i>vii</i>
List of Figures	<i>xi</i>
List of Tables	<i>xix</i>
Abbreviations.....	<i>xxiii</i>
1. INTRODUCTION.....	1
1.1. Background	1
1.2. Aims of research.....	2
1.3. Structural overview	4
2. RESEARCH AREA.....	5
2.1. Climate	6
2.2. Hydrology	8
2.3. Geology	11
2.4. Geomorphology and soil genesis	12
2.5. Vegetation and land use.....	16
2.6. Population and migration.....	20
3. HYDROLOGICAL PROCESSES AND SOIL DEGRADATION IN THE TROPICS	25
3.1. Hydrological Processes in the tropics.....	25
3.2. Erosion Processes.....	28
3.3. Soil degradation in the tropics	32
4. EROSION MODELS AND THEIR APPLICATION IN THE TROPICS	39

4.1.	Fundamental aspects of hydrological modelling.....	39
4.2.	Soil erosion models	41
4.3.	Application of erosion models in the tropics	42
5.	METHODS	49
5.1.	Soil investigations.....	50
5.2.	Measurements of suspended sediment.....	56
5.3.	Erosion modelling with SWAT and scenario analysis.....	57
5.3.1.	Model description	58
5.3.2.	Modelling procedure.....	70
5.4.	Sensitivity and uncertainty analyses and automatic calibration.....	72
5.4.1.	Sensitivity analysis	72
5.4.2.	Automatic calibration	73
5.4.3.	Uncertainty analysis	74
5.5.	Soil evaluation	75
5.6.	Statistical analysis	77
6.	SOIL DISTRIBUTION AND DEGRADATION IN THE UPPER OUÉMÉ CATCHMENT	79
6.1.	Soil characteristics in the Upper Ouémé catchment.....	79
6.1.1.	Properties of the representative profiles	79
6.1.2.	Evaluation of soil fertility.....	90
6.2.	Soil characteristics in inland valleys	92
6.3.	Soil degradation in the Upper Ouémé catchment.....	97
7.	EROSION MODELLING IN THE UPPER OUÉMÉ CATCHMENT	109
7.1.	Model setup 1998-2005, calibration and validation	109
7.1.1.	Databases and pre-processing	109
7.1.2.	Model calibration/validation - Hydrology.....	118
7.1.3.	Model calibration/validation - Sediment budget	127
7.1.4.	Influence of spatial discretisation on model performance	131
7.1.5.	Discussion of modelling results 1998-2005.....	133
7.1.6.	Conclusions	138
7.2.	Scenario analysis 2001-2050	139
7.2.1.	Databases and pre-processing	139
7.2.2.	Land use change scenarios	150

7.2.3.	Climate change scenarios	158
7.2.4.	Combined scenarios of land use and climate changes.....	166
7.2.5.	Scenario analysis - Conclusions	174
8.	UNCERTAINTIES IN THE MODELLING PROCESS	179
8.1.	Uncertainties in the model input data	179
8.2.	Uncertainties in the model assumptions.....	184
8.3.	Uncertainties in observed data for model calibration and validation.....	194
8.4.	Evaluation of uncertainties in the modelling process.....	198
9.	OPTIONS FOR SUSTAINABLE LAND USE	201
9.1.	Hotspots of soil erosion in the Upper Ouémé catchment	201
9.2.	Soil conservation in Central Benin – Status quo.....	206
9.2.1.	The institutional framework	206
9.2.2.	Promoted soil conservations measures	212
9.2.3.	Challenges in implementing soil conservation measures	217
9.3.	Recommendations.....	224
10.	Literature	229
11.	APPENDIX	253
	Appendix A. Soil investigations	255
	Appendix B. Modelling and suspended sediment measurements.....	292
	Appendix C. Soil conservation	303

List of Figures

Fig. 2.1 Location of the Upper Ouémé catchment in Benin (West Africa)	5
Fig. 2.2 Overview of the Upper Ouémé catchment (HVO), including elevation and commune borders	5
Fig. 2.3 Climate diagram station Parakou, mean rainfall values for 1961–1990	6
Fig. 2.4 Observed rainfall variability for different regions in West-Africa in 1950-2006	7
Fig. 2.5 Structure of the ITCZ over West-Africa, and weather zones in the course of the year in the Upper Ouémé catchment (HVO).....	8
Fig. 2.6 Deviation from the mean yearly discharge of the Ouémé at the Beterou station from 1950-2000	9
Fig. 2.7 Principal gauged subcatchments of the Upper Ouémé catchment.....	10
Fig. 2.8 Rainfall - discharge relationships for the main subcatchments in the Upper Ouémé catchment between 1998 and 2005	11
Fig. 2.9 Main geological units in Benin.....	12
Fig. 2.10 Cross-section of an inland-valley in granite/gneiss in the Sudan-Guinea Zone	13
Fig. 2.11 Morphodynamic activity phases and formation of slope pediments (gravel and Hillwash); polycyclic deposit sequence A–C	14
Fig. 2.12 Simplified soil map of the Upper Ouémé catchment	16
Fig. 2.13 Land use map of the Upper Ouémé catchment derived from Landsat-TM data.....	18
Fig. 2.14 Phase model of ecological degradation developed by Mulindabigwi (2006)	20
Fig. 2.15 Population densities in the communes of Benin for 1992, 2002, and 2025 based on INSAE data and projections	21
Fig. 2.16 Motivations for migration to the southern Upper Ouémé catchment: a) problems in the home village, b) reasons for transmigration.....	22
Fig. 2.17 Demographic projections for the Upper Ouémé catchment	22
Fig. 3.1 Runoff generation mechanisms	26
Fig. 3.2 Prevalent runoff generation processes under natural vegetation and agriculture	27
Fig. 3.3 Main factors affecting soil erosion.....	30
Fig. 3.4 Schematic circle of poverty and soil degradation.....	34
Fig. 3.5 Causes and on-site indicators of soil degradation in Sub-Saharan Africa	35

Fig. 4.1 Classification of hydrological models	40
Fig. 5.1 Flowchart of the components of this study and their interactions	49
Fig. 5.2 Location of investigated transects and representative profiles	51
Fig. 5.3 Percolation tube.....	53
Fig. 5.4 Comparison of Mehlich and AA method for CEC_{pot}	53
Fig. 5.5 Turbidity probe after installation in the river bed	57
Fig. 5.6 Schematic representation of the hydrologic cycle in SWAT	59
Fig. 5.7 Applied procedure for manual calibration of hydrology and sediment budget.....	71
Fig. 5.8 LH-OAT sampling for a two parameter set. Initial parameters of the LH sampling (x) and the two OAT points (·) are shown	72
Fig. 5.9 Example of the Fertility Capability Classification (FCC).....	76
Fig. 6.1 Soil texture of the representative profiles for horizon 1 to 4.....	80
Fig. 6.2 Soil type 56 - representative profile.....	83
Fig. 6.3 Physical and chemical properties of soil type 56 (representative profile)	84
Fig. 6.4 Soil catena in soil unit 56.....	84
Fig. 6.5 Soil type 45 - representative profile.....	85
Fig. 6.6 Physical and chemical properties of soil type 45 (representative profile)	86
Fig. 6.7 Soil type 58 - representative profile.....	86
Fig. 6.8 Physical and chemical properties of soil type 58 (representative profile)	87
Fig. 6.9 Soil catena in soil unit 58.....	87
Fig. 6.10 Soil type 48 - representative profile.....	88
Fig. 6.11 Physical and chemical properties of soil type 48 (representative profile)	89
Fig. 6.12 Soil catena in soil unit 48.....	89
Fig. 6.13 Inland-valley near Parakou	92
Fig. 6.14 Soil catena in inland-valley <i>Boko1</i>	94
Fig. 6.15 Soil texture of inland-valley profiles, horizon 1 to 4	94
Fig. 6.16 Soil catena in inland-valley <i>Dogué2</i>	95
Fig. 6.17 Inventoried inland-valleys from the study of Giertz & Steup (unpublished) in cooperation with the IVC Benin	97
Fig. 6.18 Percentage of farmers facing degraded soils in the HVO based on data from HVO-Survey (2005).....	98

Fig. 6.19 Applied technologies to improve soil quality based on data from HVO-Survey (2005)	98
Fig. 6.20 Applied technologies for improvement of soil quality by commune based on data from HVO-Survey (2005).....	99
Fig. 6.21 Degree of mechanisation in the communes of the Upper Ouémé catchment based on data from HVO-Survey (2005)	99
Fig. 6.22 Sheet and rill erosion on fields	100
Fig. 6.23 Rill erosion (a) and gully erosion (b) along paths and roads.....	100
Fig. 6.24 Surface runoff on crusted surfaces next to road	101
Fig. 6.25 Crusting and soil erosion in former sand excavation sites	101
Fig. 6.26 Gravel accumulation on yam field near Barei	102
Fig. 6.27 Crusting on summits.....	102
Fig. 6.28 Exhausted cassava field and sacred forest in Serou	106
Fig. 6.29 Sorghum field with high variability of plant growth near Copargo	106
Fig. 7.1 Steps for the setting up of a new SWAT project with the ArcView User Interface.....	112
Fig. 7.2 Delineated subcatchments, considered climate stations and locations of calibration and validation outlets	113
Fig. 7.3 Site-specific relationships between turbidity and suspended sediment concentration	114
Fig. 7.4 Sediment and discharge curves in 2005 at the outlets Terou-Igbomakoro and Donga-Pont derived from measurements	115
Fig. 7.5 Baseflow separation based on discharge measurements for an event at Terou-Igbomakoro outlet.....	117
Fig. 7.6 Comparison of baseflow separation according to the baseflow filter program of Arnold & Allen (1999) with separation based on measurements of electrical conductivity and equation 7.1.....	117
Fig. 7.7 Fraction of surface runoff derived from measurements of electrical conductivity	118
Fig. 7.8 Comparison of simulated and measured annual discharge for the calibration period: Terou-Igbomakoro and Donga-Pont outlets	120
Fig. 7.9 Comparison of simulated and measured weekly discharge for the calibration period: Terou-Igbomakoro and Donga-Pont outlets, measures of performance	121
Fig. 7.10 Discharge components: baseflow fraction from measured and simulated discharge data in the Terou-Igbomakoro catchment.....	122
Fig. 7.11 Scatter plot and frequency distribution for measured and simulated weekly discharge values at the Terou-Igbomakoro outlet in the calibration period.....	123

Fig. 7.12 Scatter plot and frequency distribution for measured and simulated weekly discharge values at the Donga-Pont outlet in the calibration period	123
Fig. 7.13 Comparison of measured and simulated annual discharge for the validation period: Terou-Igbomakoro and Donga-Pont outlets	125
Fig. 7.14 Comparison of measured and simulated weekly discharge for the validation period: Terou-Igbomakoro and Donga-Pont outlets, measures of performance	125
Fig. 7.15 Comparison of measured and simulated weekly discharge and sediment yield for 2004 and 2005 at the Terou-Igbomakoro and the Donga-Pont outlets	129
Fig. 7.16 Scatter plots for measured and simulated weekly sediment yields at the Donga-Pont and the Terou-Igbomakoro outlets in the calibration period 2004/2005	129
Fig. 7.17 Measured and simulated daily sediment yield and total discharge at the Terou-Igbomakoro and the Donga-Pont outlets in the calibration period 2004/2005.....	130
Fig. 7.18 Comparison of daily measured and simulated total discharge and sediment yield for 2004 and 2005 at the Ouémé-Beterou outlet	131
Fig. 7.19 Comparison of the land use distribution in the Upper Ouémé catchment for two different discretisations with the original distribution from the Landsat classification	132
Fig. 7.20 Comparison of measured and simulated discharge for the period 2002-2005 at the Donga-Pont outlet for discretisation 1 (left) and 2 (right)	132
Fig. 7.21 Spatial distribution of the mean simulated sediment yield in the Upper Ouémé catchment (1998-2005).....	136
Fig. 7.22 Spatial distribution of the mean simulated surface runoff in the Upper Ouémé catchment (1998-2005).....	136
Fig. 7.23 Annual precipitation, sediment and water yields in the Upper Ouémé catchment (1998-2005)	137
Fig. 7.24 Mean monthly values and standard deviation for sediment and water yields, suspended sediment concentration and precipitation in the Upper Ouémé catchment (1998-2005)	137
Fig. 7.25 Cumulative distribution of sediment yield and rainfall in the Upper Ouémé catchment (1998-2005).....	138
Fig. 7.26 Land use maps 2001 and 2025 for scenario L3 (Business as usual) from CLUE-S model.	141
Fig. 7.27 Disaggregation scheme for the CLUE-S land use maps: Example is for the land use class “Cropland (>20%)”	142
Fig. 7.28 Fractions of cropland in the original model, after aggregation for CLUE-S, and after disaggregation and HRU delineation	143
Fig. 7.29 Fraction of cropland for the land use scenarios before and after HRU delineation in the SWAT model	144

Fig. 7.30 IPCC SRES scenarios: Increase of air temperature until 2100	145
Fig. 7.31 Comparison of measured and simulated climate data for the period 1960 to 2000 at the station Parakou: monthly rainfall (left), calculated ET_{pot} according to Penman-Monteith (right)	146
Fig. 7.32 Comparison of measured and simulated daily rainfall distribution for the period 1960 to 2000 at the station Parakou; the bars reflect the total range of the ensemble runs	147
Fig. 7.33 Simulated annual rainfall in the Upper Ouémé catchment for 1960-2050 from the REMO model. The mean of all three ensemble runs for each scenario (historic, A1B, B1) and the range covered by the ensemble runs are shown	148
Fig. 7.34 Denomination of the SWAT simulation runs based on the land use and climate scenarios from the CLUE-S and REMO models	149
Fig. 7.35 Simulated annual water yield (WY) and sediment yield (SY) for the original model and the Lu00 model	150
Fig. 7.36 Simulated monthly water yield (WY), Q_{surf} , and ET in the Upper Ouémé catchment for the original model and the Lu00 model	151
Fig. 7.37 Simulated monthly sediment yield in the Upper Ouémé catchment for the original model and the Lu00 model	151
Fig. 7.38 Simulated water and sediment yields for the land use scenarios L1, L2, L3 compared to the Lu00 model	152
Fig. 7.39 Regression between the field fraction and the sediment yield for the land use scenarios L1 to L3	153
Fig. 7.40 Comparison of the mean simulated annual sediment yield (1998-2005) for the Lu00 model and the Lu25 model for the land use scenarios L1 to L3.....	153
Fig. 7.41 Comparison of the mean annual simulated surface runoff (1998-2005) for the Lu00 model and the Lu25 model for the land use scenarios L1 to L3.....	154
Fig. 7.42 Relative comparison of the components of the water balance in the Terou-Igbomakoro subcatchment: land use scenarios Lu00 (black), L1_Lu25 (orange), L2_Lu25 (ochre), L3_Lu25 (yellow); mean annual sediment and water yields in the Terou-Igbomakoro subcatchment.....	155
Fig. 7.43 Relative comparison of the components of the water balance in the Donga-Pont subcatchment: land use scenarios Lu00 (black), L1_Lu25 (orange), L2_Lu25 (ochre), L3_Lu25 (yellow); mean annual sediment and water yields in the Donga-Pont subcatchment	156

Fig. 7.44 Relative comparison of the components of the water balance in the Upper Ouémé catchment: land use scenarios Lu00 (black), L1_Lu25 (orange), L2_Lu25 (ochre), L3_Lu25 (yellow).....	156
Fig. 7.45 Comparison of the mean monthly evapotranspiration, water yield and surface runoff in the Upper Ouémé catchment for scenario L3_Lu25.....	157
Fig. 7.46 Comparison of the mean monthly sediment yields in the Upper Ouémé catchment for the Lu25 models and the Lu00 model.....	157
Fig. 7.47 Mean simulated annual values of ET_{pot} and precipitation (PCP) of the three ensemble runs for climate scenarios A1B and B1 for the period 2001-2050 for the Upper Ouémé catchment.....	159
Fig. 7.48 Mean simulated annual values of sediment yield (SY) and water yield (WY) of the three ensemble runs for the climate scenarios A1B and B1 for the period 2001-2050 for the Upper Ouémé catchment.....	160
Fig. 7.49 Mean spatial distribution of sediment yield for the climate scenarios A1B and B1 for the periods 2001-2025 and 2026-2050 compared to the original model (1998-2005) and the model with REMO climate data for 1960-2000	161
Fig. 7.50 Mean spatial distribution of surface runoff for climate scenarios A1B and B1 for the periods 2001-2025 and 2026-2050 compared to the original model (1998-2005) and the model with REMO climate data for 1960-2000	161
Fig. 7.51 Mean simulated annual values of sediment yield (SY) and water yield (WY) of the three ensemble runs for climate scenarios A1B and B1 for the period 2001-2050 in the Terou-Igbomakoro subcatchment.....	162
Fig. 7.52 Mean simulated annual values of sediment yield (SY) and water yield (WY) of the three ensemble runs for climate scenarios A1B and B1 for the period 2001-2050 in the Donga-Pont subcatchment	162
Fig. 7.53 Components of the water balance in the Terou-Igbomakoro and Donga-Pont subcatchments for the climate scenarios relative to the original model (1998-2005)	163
Fig. 7.54 Components of the water balance in the Upper Ouémé catchment for the climate scenarios relative to the original model (1998-2005)	164
Fig. 7.55 Mean monthly water and sediment yields for climate scenarios A1B and B1 for the periods 2001- 2025 and 2026-2050 compared to the period 1960-2000 (REMO climate data) and 1998 (measured climate data).....	165
Fig. 7.56 Mean simulated annual values of sediment yield (SY) and water yield (WY) for the combination of land use scenarios L1, L2, and L3 with climate change scenarios for the period 2001 to 2030. The presented results are an average of three ensemble runs of each climate scenario	167

Fig. 7.57 Mean spatial distribution of sediment yield for the combinations of climate scenarios A1B and B1 with land use scenarios L1-L3 for the period 2001-2030 compared to the original model (1998-2005) and the model with REMO climate data for 1960-2000	168
Fig. 7.58 Mean spatial distribution of surface runoff for the combinations of climate scenarios A1B and B1 with land use scenarios L1-L3 for the period 2001-2030 compared to the original model (1998-2005) and the model with REMO climate data for 1960-2000	170
Fig. 7.59 Mean simulated annual values of sediment yield (SY), and water yield (WY) for the combination of land use scenario L3 with the climate change scenarios for the period 2001 to 2030 for the Terou-Igbomakoro and Donga-Pont subcatchments. The presented results are averages of three ensemble runs for each climate scenario	171
Fig. 7.60 Components of the water balance in the Terou-Igbomakoro and Donga-Pont subcatchments for the combined scenarios relative to the Lu00 model (1998-2005)	172
Fig. 7.61 Components of the water balance in the Upper Ouémé catchment relative to the Lu00 model (1998-2005).....	173
Fig. 7.62 Deviation of mean monthly water and sediment yields for the combined scenarios for the periods 2001-2025 and 1960-2000 (REMO climate data) from the results for 1998-2005 (measured climate data)	173
Fig. 7.63 Mean spatial distribution of sediment yield for the land use, climate, and combined scenarios compared to the Lu00 model (1998-2005) and the model with REMO climate data for 1960-2000.....	177
Fig. 8.1 Sensitivity of mean annual discharge and model efficiency to changes of the parameter ALPHA_BF	189
Fig. 8.2 Sensitivity of mean annual discharge and model efficiency to changes of the parameter RCHRG_DP	190
Fig. 8.3 Sensitivity of mean annual discharge and model efficiency to changes of parameters CN2 and SOL_AWC	191
Fig. 8.4 Sensitivity of mean annual sediment yield to changes of parameters CN2 and SURLAG ..	192
Fig. 8.5 Sensitivity of mean annual sediment yield to changes of parameters ALPHA_BF and CH_K2	193
Fig. 8.6 Confidence interval (90%) for mean weekly discharge and sediment yield at the Terou-Igbomakoro outlet	193
Fig. 8.7 Confidence interval (90%) for mean weekly discharge and sediment yield at the Donga-Pont outlet	194
Fig. 8.8 Stagnant water around the turbidity probe at the Terou-Igbomakoro outlet	195

Fig. 8.9 Temporal resolution of turbidity measurements: comparison of a 3-minute and 30-minute interval at the Donga-Pont outlet	197
Fig. 9.1 Mean sediment yield for 1998-2005 in the Upper Ouémé catchment (left), communes in the Upper Ouémé catchment (right).....	202
Fig. 9.2 Map of soil degradation in Benin	203
Fig. 9.3 Mean sediment yield for the range of climate, land use and combined scenarios in the Upper Ouémé catchment compared to the original model (1998-2005) and the model with REMO data for 1960-2000	204
Fig. 9.4 Actors in the field of sustainable management of soil resources in Benin	207
Fig. 9.5 Promoted tillage directions on fields: (a) yam mounds <i>en quinconce</i> , (b) tillage direction perpendicular to the slope.....	213
Fig. 9.6 Cover crops in association with Maize: <i>Niebe</i> sp. and <i>Mucuna</i> sp.	214
Fig. 9.7 Agro-Forestry: <i>Cajanus cajan</i> and <i>Gliricidia sepium</i>	215
Fig. 9.8 <i>Vetiver</i> hedges near Barei.....	216
Fig. 9.9 Factors influencing the adoption potential for soil conservation measures.....	222

List of Tables

Table 2.1 Mean annual rainfall (1922–2005) for the Beterou, Djougou, and Parakou stations, and classification of rainfall sums for 1998–2005.....	7
Table 2.2 Types of vegetation in the research area.....	17
Table 3.1 Classification of erosion forms	29
Table 4.1 Overview of time-continuous, (semi-)physically-based erosion models	42
Table 4.2 Overview of SWAT applications in tropical developing countries	45
Table 5.1 Determined parameters and applied laboratory methods.....	52
Table 5.2 Definition of the input parameter hydrologic group	56
Table 5.3 Main components of the model SWAT, process description and factors considered in the model.....	61
Table 6.1 Representative profiles – Classification according to the World Reference Base (WRB) and the French soil classification system (CPCS).....	81
Table 6.2 Physical properties of the topsoils.....	82
Table 6.3 Chemical properties of the topsoils	83
Table 6.4 Evaluation of the representative profiles according to the Fertility Capability Classification (FCC).....	91
Table 6.5 Topsoil characteristics of studied inland-valleys	95
Table 6.6 Typical characteristics of observable erosion forms in the Upper Ouémé catchment	102
Table 6.7 Comparison of mean topsoil properties of exhausted fields, fallows and sacred land in the Upper Ouémé catchment	105
Table 7.1 Model input data and corresponding data sources	109
Table 7.2 Attribution of the classes of the land use classification for the Upper Ouémé catchment to the SWAT land use types	110
Table 7.3 Distribution of land use types before and after establishing a threshold of 10% for the definition of hydrological response units (HRUs)	111
Table 7.4 Minimum annual sediment loads derived from turbidity measurements (Donga-Pont, Terou-Igbomakoro, Lower Aguima) and daily water sampling (Ouémé-Beterou).....	115
Table 7.5 Calibrated parameters for hydrological calibration, comparison with default values and assumptions by Sintondji (2005)	119

Table 7.6 Comparison of mean simulated and measured discharge components for the calibration period at the Terou-Igbomakoro and Donga-Pont outlets. Baseflow here includes lateral flow and shallow aquifer recharge. Measured baseflow was derived with a digital baseflow filter.....	121
Table 7.7 Mean simulated annual soil water balance in the Donga-Pont, Terou-Igbomakoro and the Upper Ouémé catchment in the calibration period (1998-2001)	122
Table 7.8 Comparison of mean simulated and measured discharge components for the validation period at the Terou-Igbomakoro and Donga-Pont outlets	124
Table 7.9 Mean simulated annual soil water balance in the Donga-Pont, Terou-Igbomakoro and the Upper Ouémé catchments for the validation period (2002-2005).....	126
Table 7.10 Validation of discharge at several outlets in the Upper Ouémé catchment	126
Table 7.11 Calibrated parameters for sediment calibration, comparison with default values and assumptions used by Sintondji (2005)	127
Table 7.12 Comparison of cumulative sediment and water yields in 2004 and 2005 for days with valid measurements in the Donga-Pont and the Terou-Igbomakoro subcatchments	128
Table 7.13 Comparison of cumulative sediment yields and discharge values in 2004 and 2005 for days with valid measurements the Ouémé-Beterou subcatchment	130
Table 7.14 Comparison of model performance for the period 1998-2001 for two different discretisations.....	132
Table 7.15 Land use and hydrological characteristics of Donga-Pont and Terou-Igbomakoro subcatchments and the whole Upper Ouémé catchment derived from modelling results 1998-2005.....	133
Table 7.16 Mean water balance for the period 1998-2005 in the Donga-Pont and Terou-Igbomakoro subcatchments and the whole Upper Ouémé catchment	134
Table 7.17 USLE factors and mean simulated soil loss rates for the Terou-Igbomakoro, Donga-Pont and Upper Ouémé catchments in the period 1998-2001	134
Table 7.18 Average sediment loadings in % and total sediment loads and sediment yields per land use in the Upper Ouémé catchment	135
Table 7.19 Model input data for scenarios	139
Table 7.20 Definition of land use scenarios L1, L2, and L3 according to Judex (2008)	140
Table 7.21 Percentages for the disaggregation of the CLUE-S land use map	142
Table 7.22 Land use scenarios: change of fractions of cropland according to CLUE-S results before and after implementation in the SWAT model	144
Table 7.23 Changes in simulated rainfall (PCP) for the Upper Ouémé catchment and the two subcatchments compared to the original model for the period 1998-2005.....	147

Table 7.24 Mean simulated annual sediment yield (SY) and water yield (WY) for the period 1998-2005 for the land use scenarios L1, L2, L3 compared to the Lu00 model	152
Table 7.25 Mean simulated annual values of rainfall (PCP), sediment yield (SY), and water yield (WY) of the three ensemble runs for the climate scenarios A1B and B1, change in % from the original model (1998-2005)	158
Table 7.26 Mean simulated annual values of sediment yield (SY), water yield (WY), and surface runoff (Q_{surf}) of the combined land use and climate change scenarios in the Upper Ouémé catchment. The results are averages of three ensemble runs for each climate scenario. Absolute values and change in % from baseline scenario Lu00 (1998-2005) are shown	166
Table 7.27 Mean simulated annual values of sediment yield (SY), water yield (WY), and surface runoff (Q_{surf}) of combined land use and climate change scenarios in the Terou-Igbomakoro and Donga-Pont subcatchments. The results are averages of three ensemble runs for each climate scenario. Absolute values and change in % from baseline scenario Lu00 (1998-2005) are presented	171
Table 7.28 Comparison of effects of land use, climate, and combined scenarios on rainfall (PCP), water yield (WY), sediment yield (SY), and surface runoff (Q_{surf}) in the Upper Ouémé catchment and the Terou-Igbomakoro and Donga-Pont subcatchments for the period 2001-2025 compared to the original model	175
Table 8.1 Most sensitive model parameters for the mean daily discharge for the Upper Ouémé catchment (1998-2001)	186
Table 8.2 Most sensitive model parameters for the mean daily sediment yield for the Upper Ouémé catchment (1998-2001)	187
Table 8.3 Most sensitive model parameters for the daily discharge; relative to measurements at the Terou-Igbomakoro outlet	187
Table 8.4 Parameter ranges for the parameter uncertainty analysis	188
Table 8.5 Evaluation of the different sources of uncertainty in the modelling results	198
Table 9.1 Zones of severity of desertification in Benin according to MEHU (1999).....	202
Table 9.2 Ongoing projects concerning soil conservation acting partially in the Upper Ouémé catchment.....	209
Table 9.3 Institutional obstacles for the sustainability of development projects dealing with soil conservation in Benin.....	220

Abbreviations

ArcView	GIS Software
CV	Coefficient of variation
DEM	Digital elevation model
CEC	Cation Exchange Capacity
ET _{pot}	Potential evapotranspiration
GCM	General Circulation Model
GIS	Geographic Information System
GLOWA	Global change of the water cycle, BMBF programme
GW	Groundwater
HRU	Hydrologic Response Unit
HVO	Upper Ouémé catchment (<i>Haute Vallée de L'Ouémé</i>)
IA	Index of agreement according to Willmott (1981)
LAI	Leaf area index
ME	Model efficiency according to Nash & Sutcliffe (1970)
NTU	Nephelometric unit as a measure of turbidity
Q _{surf}	Surface runoff
Q _{base}	Base flow
Q _{tot}	Total streamflow
PTF	Pedotransfer function
SY	Sediment yield
WY	Water yield

Institutions

ABE	Beninese Agency of the Environment (<i>Agence Béninoise pour l'Environnement</i>)
AFD	French Development Agency (<i>Agence Française de Développement</i>)
AGEDREN	<i>Association pour la GEstion Durable des REssources Naturelles</i> (NGO)
BAD	African Development Bank (<i>Banque Africaine de Développement</i>)
BMBF	Federal Ministry of Education and Research, Germany
BOAD	West-African Development Bank (<i>Banque Ouest Africaine de Développement</i>)
CERABE	<i>CEntre de Recherche et d'Action pour le Bien-être et la sauvegarde de L'Environnement</i> (NGO)
CeRPA	Regional Center of Agricultural Promotion (<i>Centre Régional pour la Promotion Agricole</i>)
DIFOV	Directorate of Extension and Training, Benin (<i>Direction de la Formation Opérationnelle et de la Vulgarisation agricole</i>)
DMN	National Directorate of Meteorology, Benin (<i>Direction Météorologique Nationale du Benin</i>)

FAO	Food and Agriculture Organisation of the United Nations
GEF	Global Environment Facility
GERED	<i>Groupe d'Etude et de Recherche sur l'Environnement et le Développement (NGO)</i>
IFAD	International Fund for Agricultural Development (<i>Fonds International pour le Développement Agricole</i>)
IGN	National Institute of Geography, Benin (<i>Institut Géographique National du Bénin</i>)
INRAB	National Institute of Agricultural Research, Benin (<i>Institut National des Recherches Agricoles du Bénin</i>)
INSAE	National Institute of Statistics and for Economical Analysis, Benin (<i>Institut National de la Statistique et de l'Analyse Economique du Bénin</i>)
IVC	Inland Valley Consortium, Benin

Development and research projects

CATCH	<i>Couplage de l'Atmosphère Tropicale et du Cycle Hydrologique</i>
FALMP	Forests and Adjacent Land Management Programme
IMPETUS	Integrative management project for an efficient and sustainable use of freshwater resources in West Africa
PADSA	<i>Programme d'Appui au Développement du Secteur Agricole</i>
PADSE	<i>Projet d'Amélioration et de Diversification des Systèmes d'Exploitation dans les départements du Zou, des Collines, du Borgou et d'Alibori</i>
PAMF	<i>Projet d'Aménagement des Massifs Forestiers d'Agoua, des Monts Kouffé et de Wari Maro</i>
PAMR-B	<i>Projet Pilote d'Appui au Monde Rural dans le Borgou</i>
PDEBE	<i>Projet de Développement de l'Elevage dans le Borgou Est</i>
PDRT	<i>Projet de Développement des plantes à Racines et des Tubercules</i>
PGRN	<i>Projet de Gestion des Ressources Naturelles</i>
PGTRN	<i>Programme de Gestion des Terroirs et des Ressources Naturelles</i>
PPEA	<i>Projet Promotion de L'Elevage dans L'Atacora</i>
ProCGRN	<i>Programme de Conservation et de Gestion des Ressources Naturelles</i>
PRRF	<i>Projet pour la Restauration de Ressources Forestières dans la région de Bassila</i>

1. INTRODUCTION

1.1. Background

Human-induced soil erosion began when land was first settled and used for intensive agriculture. Today, five to seven million hectares of agricultural land are lost each year, more than any prior time period in human history (Lal 1990). One fourth of the agricultural area worldwide has already been damaged, as overall agricultural productivity has become heavily reduced (Steiner 1994). In Africa, more than 500 million hectares of land are affected by land degradation (Oldeman et al. 1991). The first global assessment of soil degradation (GLASOD) by Oldeman et al. (1991) identified water erosion as the dominant type of soil degradation causing one fourth of the productivity loss in Africa (Oldeman 1998). Nutrient depletion due to extremely low consumption of fertiliser and shortened fallow periods is an additional major cause of soil degradation in Sub-Saharan Africa. The net nutrient removal exceeds the net replenishment by a factor of 3 to 4 in many countries (Stoorvogel & Smaling 1990). As such, soil erosion and nutrient depletion threaten agricultural productivity and food security in Sub-Saharan Africa (Sachs 2005). An agricultural growth of 4% per year would be necessary to ensure food security for the rapidly growing population in Africa (FAO 2001b). Unfortunately, estimations forecast either stagnation or decreases in crop yields resulting from a decline of soil fertility in the region (FAO 2001a).

Soil degradation and climate change display a strong connection, as more frequent and intense extreme weather events, such as floods and droughts, enhance soil erosion and desertification, while reductions in average rainfall diminish soil erosion. Higher surface temperatures lead to an increase in the loss of organic carbon from soil, reducing overall fertility. Soil degradation also aggravates climate change by the decomposition of organic carbon in the soil, resulting in a lower biomass production (Steiner 1994).

Africa is highly vulnerable to climate change. The roots of its vulnerability lie in the harsh climate, its heavy reliance on rain-fed agriculture and its low adaptive capacity due to human poverty, soil degradation, and institutional deficits. Agricultural production in many African nations is projected to be severely compromised due to

climate variability and change (UNEP 2007). Thus, climate change and soil degradation have the potential to undermine recent progress in the fight against hunger in Sub-Saharan Africa where the percentage of population classified as undernourished has declined from 35% in 1990 to 32% in 2003 (FAO 2006).

In West Africa, the mean temperature and climate variability are projected to increase due to climate change. However, for the changes in mean rainfall, climate models do not yet provide consistent results (IPCC 2007). There is evidence from meteorological observations and modelling that the total annual rainfall may decrease in the sub-humid regions in West Africa within the next decades. This applies also to the small West-African country Benin.

Despite the flat relief of the country, soil erosion and nutrient depletion are considerable problems in Benin, because high rainfall intensities and low-input farming systems are prevalent. The dominant erosion forms are sheet and rill erosion. Sheet erosion, i.e. the erosion of a thin layer of soil from the land surface by runoff water, is especially dangerous, because it is difficult to observe and measure at the regional scale (Schmidt 2000). The traditional fallow farming systems in Benin are only sustainable for long fallow periods of at least 5 to 10 years. However, population growth and poverty force people to reduce the fallow periods without compensation by other soil fertilisation strategies. In Benin, the use of mineral fertiliser is limited to cotton and maize. The integration of agriculture and animal husbandry is only practised by semi-sedentary Fulani herders. Additionally, Benin displays a moderate nutrient depletion rate comparable to that of Burkina Faso and Niger, while Nigeria and Ghana are characterized by high rates of nutrient depletion, and Kenya by very high rates of depletion (Stoorvogel & Smaling 1990). The dominant strategy for farmers in Benin is to increase the area of land under crop cultivation, which leads to extreme negative impacts on the environment on the whole (Mama & Oloukoi 2003).

1.2. Aims of research

The effects of global change on the water cycle are not yet well understood. A quantitative understanding of the effects of climate and land use change on water availability and soil degradation in tropical developing countries is scarce, and

management strategies for adaptation are still insufficient. Studies which assess the effects of climate change on hydrology at the catchment scale are hampered by uncertainties in climate projections, insufficient knowledge of land cover change, and the inadequate resolution of general circulation models (GCMs) (Mahé et al. 2005).

In order to address these issues, the German Ministry of Education and Research launched the GLOWA programme (GLOWA = global change of the water cycle) in 2000. The multidisciplinary IMPETUS project (Integrated management project for an efficient and sustainable use of freshwater resources in West Africa) is one of five GLOWA projects. The project aims to investigate the effects of global change on the water cycle and water availability at the regional scale in the Wadi Drâa in Morocco, and the Ouémé catchment in Benin. The first phase of IMPETUS (2000–2003) focused on the identification and analysis of factors influencing the water cycle, while the second phase (2003–2006) was dedicated to the modelling of scenarios of future impacts on the water cycle. In the current and final phase (2006–2009), management options for decision making are being elaborated based on scenario analysis and decision support systems for different problem clusters. More details about the IMPETUS-Project are provided in the project reports (e.g. IMPETUS 1999, 2003, 2006, 2008).

The present study is embedded within the IMPETUS project. The primary objective of this work is the analysis of soil degradation in the Upper Ouémé catchment in Central Benin. A special focus is on the quantification of soil erosion by water under recent conditions and future land use and climate change. Junge (2004) investigated current soil erosion at the local scale in the Aguima subcatchment of the Upper Ouémé. This study focuses on the regional scale, and the time periods 1998–2005, 2001–2025, and 2026–2050.

The present study addresses the following questions:

1. What are the characteristics of soil degradation in the Upper Ouémé catchment? What are the physical and chemical properties of the dominant soil types?
2. What amounts of soil are lost in the Upper Ouémé catchment on a regional scale? How do climate and land use changes affect the rates of soil loss in the time periods 2001-2025 and 2026-2050?

3. Where are the current and future “hotspots” of soil erosion, and which measures are appropriate for soil conservation in the Upper Ouémé catchment?

As part of the IMPETUS project, this study is closely linked to both earlier and current investigations carried out by other project members addressing hydrological, hydrogeological, and pedological processes (e.g. Junge, 2004; Giertz, 2004; Sintondji, 2005; El Fahem, 2008), land use/land cover change (Mulindabigwi, 2006; Judex, 2008), socioeconomic aspects related to land degradation and resource management (Doevenspeck, 2005; Singer, 2005) and climate change (Paeth et al. 2008) in the Upper Ouémé catchment.

1.3. Structural overview

After a brief introduction to the background and the aims of this dissertation, Chapter 2 characterizes the Upper Ouémé catchment. Chapters 3 and 4 summarize the scientific knowledge about hydrological and erosive processes and common hydrological and erosion models. Chapter 5 describes the methods applied in the present study, including a description of the Soil Water Assessment Tool (SWAT model). Based on soil investigations in the field, Chapter 6 discusses the characteristics of the soils in the Upper Ouémé catchment and the current status of soil degradation. These soil investigations serve as a basis for model parameterization, calibration, and validation. Chapter 7 presents the primary results of this study, highlighted by the modelling results for the recent time period and for the period between 2001 and 2050, taking into consideration changes in climate and land use. The uncertainties inherent to the modelling process and the input data are analysed in Chapter 8. Finally, conclusions from the modelling results and management options for soil conservation are discussed in Chapter 9.

2. RESEARCH AREA

The Upper Ouémé catchment (HVO) is located in the central part of the Republic of Benin between 9° – 10.5°N and 1.5° – 3°E Greenwich. Benin borders the Gulf of Guinea in West Africa, and is surrounded by the countries Nigeria, Togo, Niger and Burkina Faso (Fig. 2.1). The Ouémé River is the longest river of the country. The Upper Ouémé catchment covers an area of 14500 km², and is delimited by a small ridge to the East, the Atacora Mountains to the West, and low mountain ranges to the North, which serve as a divide to the Niger catchment. Altitude differences in the Upper Ouémé catchment are small

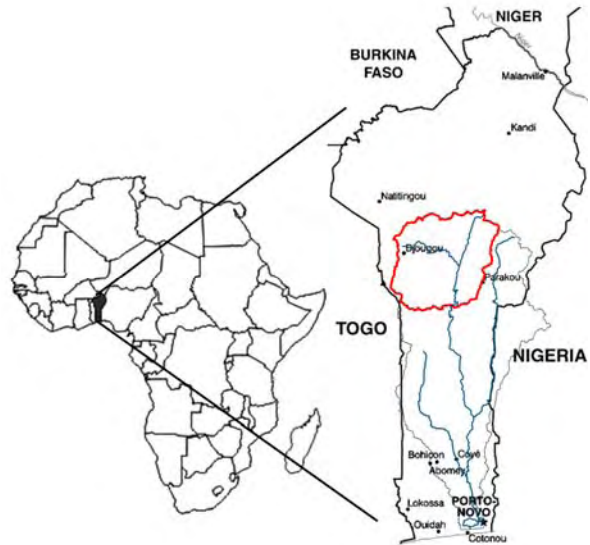


Fig. 2.1 Location of the Upper Ouémé catchment (→) in Benin (West Africa).

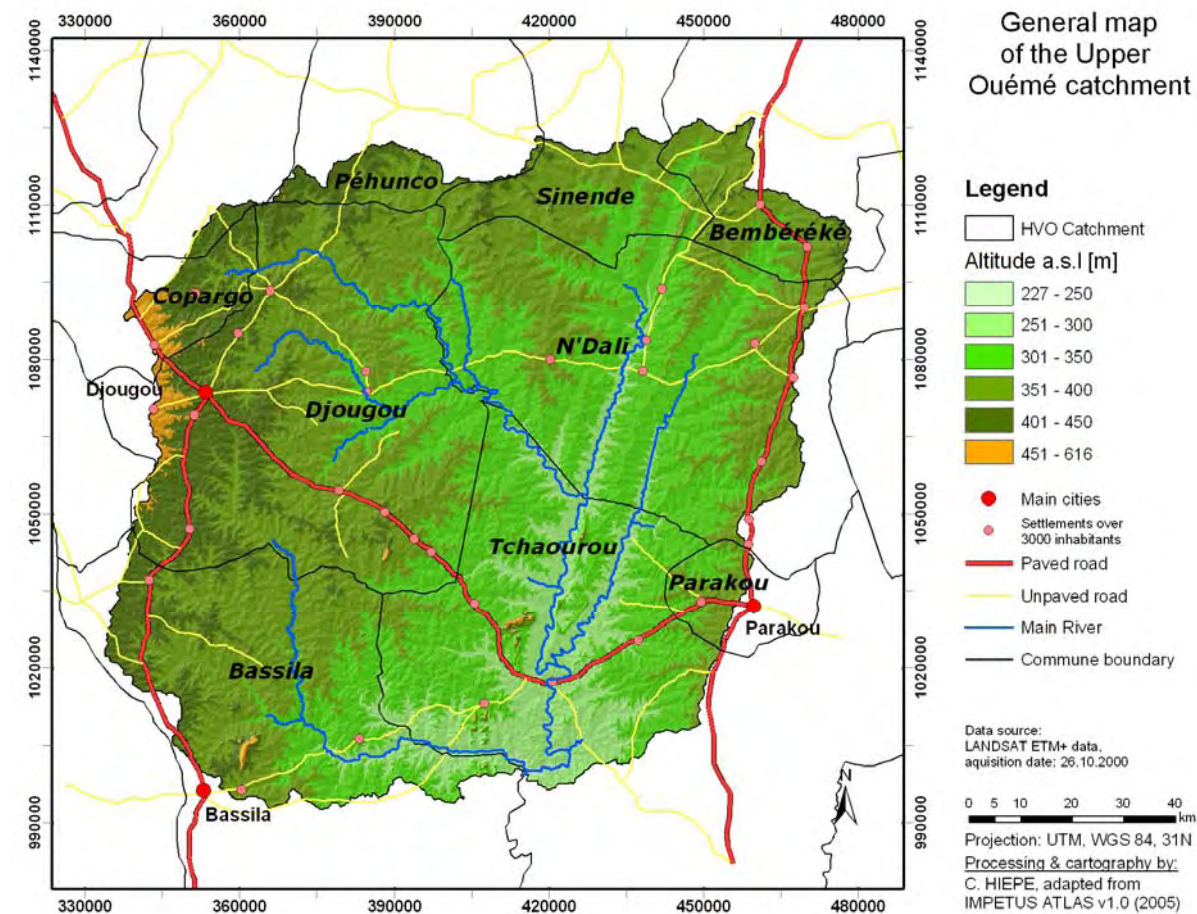


Fig. 2.2 Overview of the Upper Ouémé catchment (HVO), including elevation and commune borders.

(Fig. 2.2). Elevations in the Upper Ouémé catchment range from 225 to 400 meters above sea level, except for some isolated inselbergs in the vicinity of the geological Kandi fault in the southern part of the catchment. This relief rises from the Ouémé flood plain to the Djougou plateau in the West and the Parakou plateau in the East. The Upper Ouémé catchment covers parts of the Atacora department (commune Péhunco), the Donga department (communes Djougou, Copargo, Bassila) and the Borgou department (communes N'Dali, Parakou, Tchaourou, Sinende, Bembéréké).

2.1. Climate

Benin is located in the Dahomey gap, a dryer region of the Guinea coast zone where the Guinean tropical rainforest is interrupted by savannah formations. Benin covers four climatic zones: (1) a littoral humid tropical zone (1200–1400 mm rainfall per year), (2) a littoral and inland sub-humid zone (900–1200 mm rainfall per year), (3) a wetter inland zone (1200–1400 mm rainfall per year) in the West of Djougou and Nikki; and (4) a continental dry northern zone (900–1200 mm rainfall per year) (Faure & Volkoff 1998). In South Benin the rainfall regime is bimodal, with a short dry season during August and a longer dry season from November to March. In central and northern Benin, only one dry season occurs lasting from October to March (Faure & Volkoff 1998).

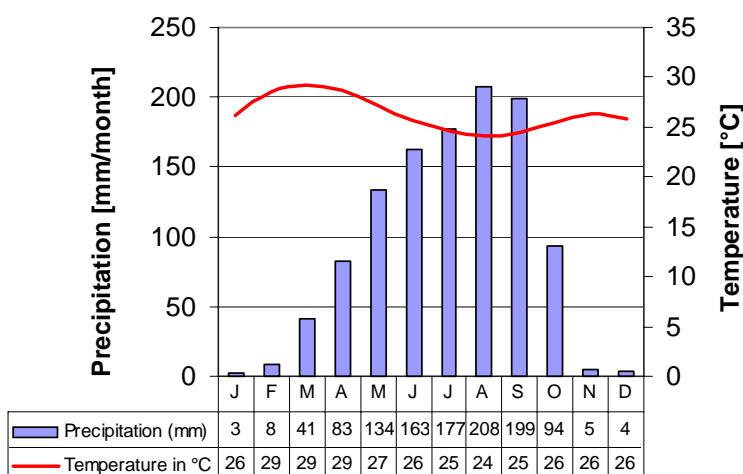


Fig. 2.3 Climate diagram station Parakou, mean rainfall values for 1961–1990 (modified from Giertz (2004)).

The Upper Ouémé catchment belongs partially to the dry northern zone and the wetter inland zone with one dry season and a mean annual rainfall between 1100 and 1400 mm. The climate diagram of the Parakou station (Fig. 2.3) illustrates the monthly distribution of precipitation and temperature

in Central Benin. The highest rainfall totals occur in August and September, whereas the highest temperatures are recorded in March and April, at the beginning of the

rainy season. The average observed annual evapotranspiration in the region is 800 mm (Walling et al. 2001); maximum values are recorded at the end of the dry season.

Interannual rainfall variability in the Upper Ouémé catchment is high. For the Parakou and Beterou stations, the mean rainfall for 1998–2005 was significantly lower than the long-term mean for 1922–2005 (Table 2.1). However, the Djougou station recorded significantly higher values.

Table 2.1 Mean annual rainfall (1922–2005) for the Beterou, Djougou, and Parakou stations, and classification of rainfall sums for 1998–2005 (Data source: DMN Benin, oral comm. Diederich (IMPETUS)), dry/wet year: > 50mm below/above long long-term average.

Station	Long-term mean [mm/yr]	Mean 1998-2005 [mm/yr]	Dry years	Wet years
Beterou	1196 ± 212	1150 ± 142	2000, 2001	2002
Djougou	1301 ± 220	1354 ± 211	2001, 2002	1999, 2003
Parakou	1199 ± 204	1113 ± 173	2000, 2001, 2002, 2005	1998

2000 and 2001 were the driest years on record in the Upper Ouémé catchment, and 1998 and 2003 were the wettest years in the period between 1998 and 2005. Since

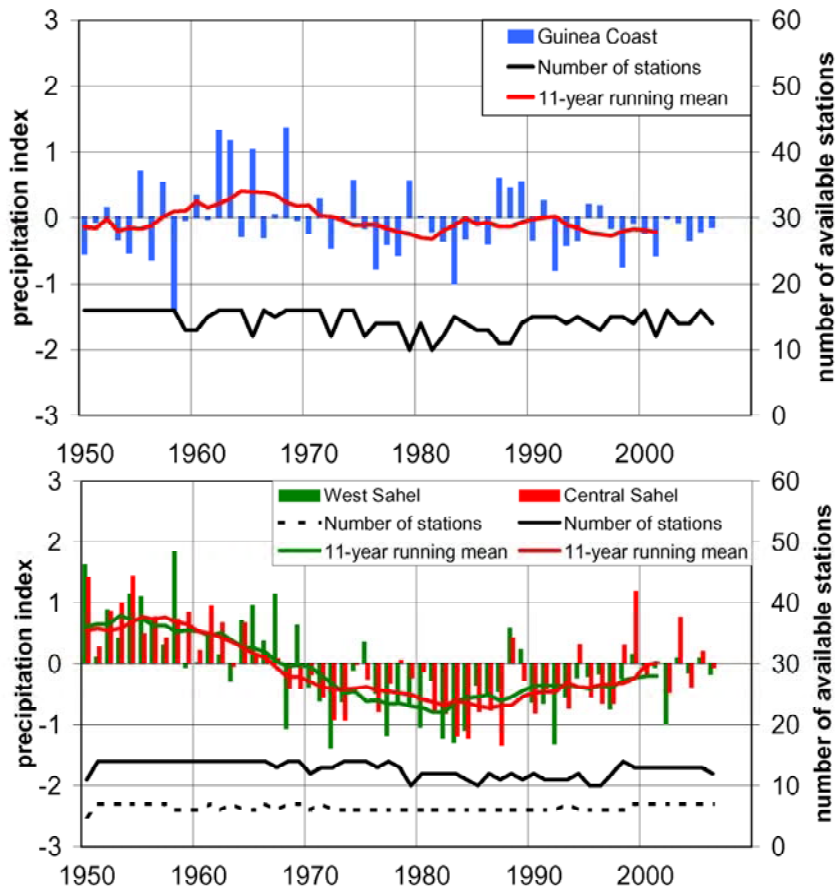


Fig. 2.4 Observed rainfall variability for different regions in West Africa in 1950–2006 (unpublished from Fink & Kotthaus (IMPETUS)). The Upper Ouémé catchment belongs to the climate zone Guinea coast.

the 1970s, a rainfall deficit has been observed in tropical West Africa (Fig. 2.4, Hulme et al. (2001) and Ojo et al. (2004)). Rainfall at Beterou, Djougou and Parakou was almost 10% below the long-term average in the 1970s and 1980s, but has remained near the average since 1990. The rainy seasons in West Africa are primarily triggered by the northward and southward movement

of the Intertropical Convergence Zone (ITCZ). As part of the Hadley circulation, two dominant air masses in the region, the wet South-West monsoon and the dry North-East trade wind (Harmattan) shift in accordance with the ITCZ. As a consequence, four different weather zones determine the seasonal rainfall characteristics in the Upper Ouémé catchment (Fig. 2.5). From November to mid-February, zone A dominates, resulting in dry air masses and low rainfall amounts. In this period, the Harmattan deposits dust from the Sahara desert. Zone B is prevalent between mid-February and mid-April, and between mid-October and the end of November, leading to short localized thunderstorms. Zone C, with its heavy rainfalls due to squall lines, is the main contributor for rainfall in the Upper Ouémé catchment. In 2002, these highly organized convective systems accounted for at least 50% of total annual rainfall in the region (Fink et al. 2006).

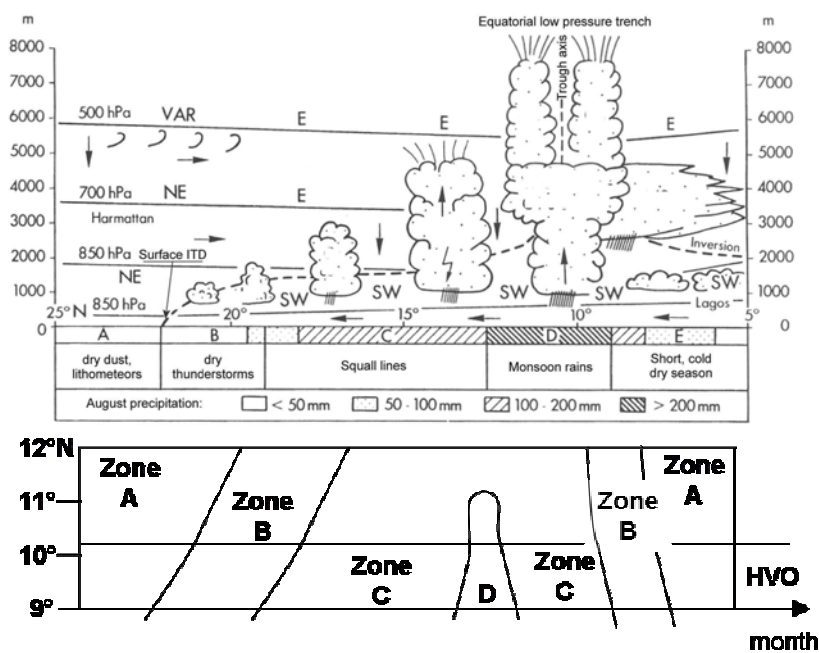


Fig. 2.5 Structure of the ITCZ over West-Africa, and weather zones in the course of the year in the Upper Ouémé catchment (HVO) (modified from Weischet & Endlicher (2000)).

monsoonal rainfalls associated with Zone D occur in the Upper Ouémé catchment only in August.

2.2. Hydrology

The Ouémé River displays significant differences in its water level between the rainy and the dry seasons. All tributaries in the Upper Ouémé catchment are ephemeral

Squall lines develop over the central Nigerian highlands and reach the research area at night between 2:00 am and 3:00 am. The development of squall lines is not yet well understood, but appears to be triggered by the African Easterly Jet stream (IMPETUS, 2003; Leroux, 2001). Low intensity, persistent

ivers that dry up during the dry months. The last limnigraph of the Upper Ouémé at Beterou records continuous water flow from June to mid-December. Large tributaries such as the Terou River in the south-western part of the catchment and the Donga River in the north-western part of the catchment drain eastwards, while the smaller rivers are aligned in NNW-SSE direction like the rift system of the bedrock.

As a consequence of the rainfall deficiencies in the last decades, runoff amounts in West Africa have been significantly lower than the long-term average (Ojo et al. 2004). Figure 2.6 underscores this observation for the Upper Ouémé outlet at Beterou.

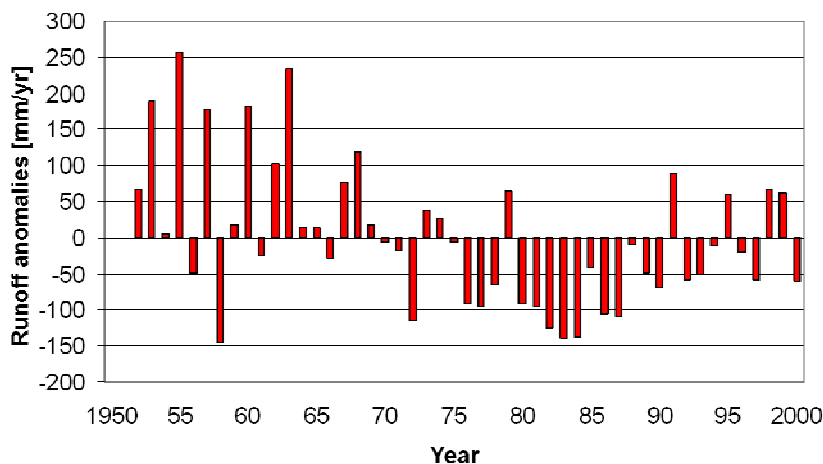


Fig. 2.6 Deviation from the mean annual discharge of the Ouémé at the Beterou station from 1950–2000 (IMPETUS 2002).

still low, and the frequent appearance of macro-pores leads to a fast saturation of the soil. From mid-August through the end of October or November, the hydromorphic soils in the inland valleys are completely saturated. Soil moisture displays a high seasonality and extremely high small-scale variability (Giertz 2004). In general, the water content of savannah soils is lower than that of agricultural soils due to a higher permeability and thus a faster deep infiltration on savannah land (Giertz 2004).

The groundwater table in the Upper Ouémé catchment fluctuates between 12 meters in depth in the dry season and zero to four meters in depth in the rainy season (El Fahem 2008). Two groundwater aquifers can be distinguished: (i) a seasonal aquifer in the saprolite and (ii) a permanent fractured aquifer in the Precambrian basement with a depth of about 40 meters (IMPETUS 2001). The floating ground water table in the saprolite develops during the rainy season as a consequence of accumulating water over impermeable plinthite and clay-rich saprolitic decomposition material (Fass 2004). Groundwater recharge in the Aguima catchment was estimated

The dominant hydrological processes in the catchment vary over the course of the year, and along the hill-slope. At the beginning of the rainy season, surface runoff is the dominant runoff pathway because the vegetation cover is

at 113 mm for 2002 by Fass (2004) from the climatic water balance and the changes in the soil water storage.

The most important discharge gauges in the Upper Ouémé catchment are at the Aguima, Terou (Saramanga, Igbomakoro, Wanou), and Donga Rivers (Pont, Affon) (Fig 2.7).

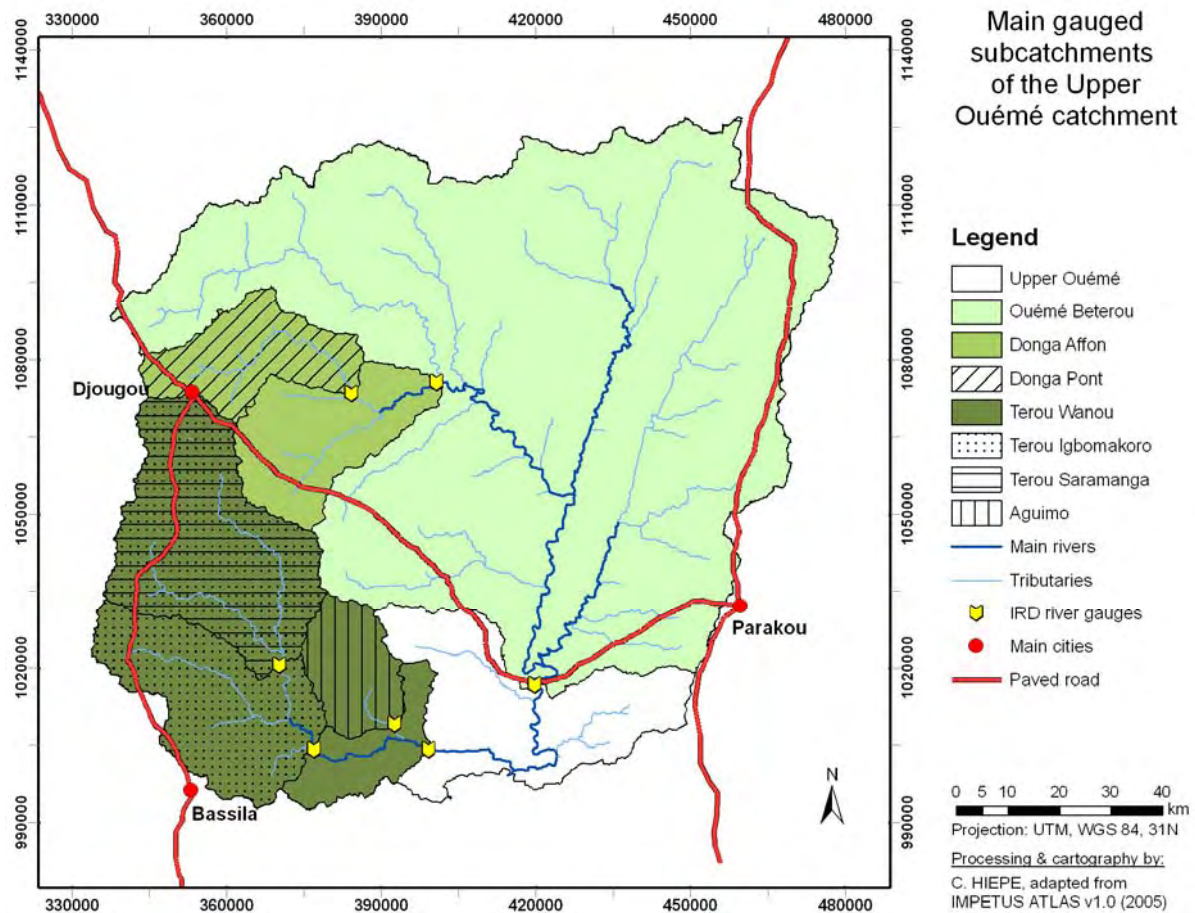


Fig. 2.7 Principal gauged subcatchments of the Upper Ouémé catchment.

In this study, particular attention will be given to the heavily agriculturally used Donga-Pont subcatchment (586 km²) and the less extensively used Terou-Igbomakoro subcatchment (2324 km²).

In the period between 1998 and 2005, the measured runoff amounts in the main subcatchments ranged from 100 to 400 mm per year corresponding to areal annual rainfall sums between 900 and 1650 mm (Fig. 2.8). The highest runoff coefficients were observed at the Donga-Pont outlet, and ranged from 0.11 to 0.26 and from 0.10 to 0.23 for the Donga-Pont and Terou-Igbomakoro subcatchments, respectively. For all studied subcatchments, the highest runoff coefficients were obtained in the years with the highest annual rainfall, specifically 1998, 1999, and 2003. For the Terou-

Wanou subcatchment, discharge data was only available for the comparatively wet period between 1998 and 2000. This might explain the high runoff coefficients at this outlet.

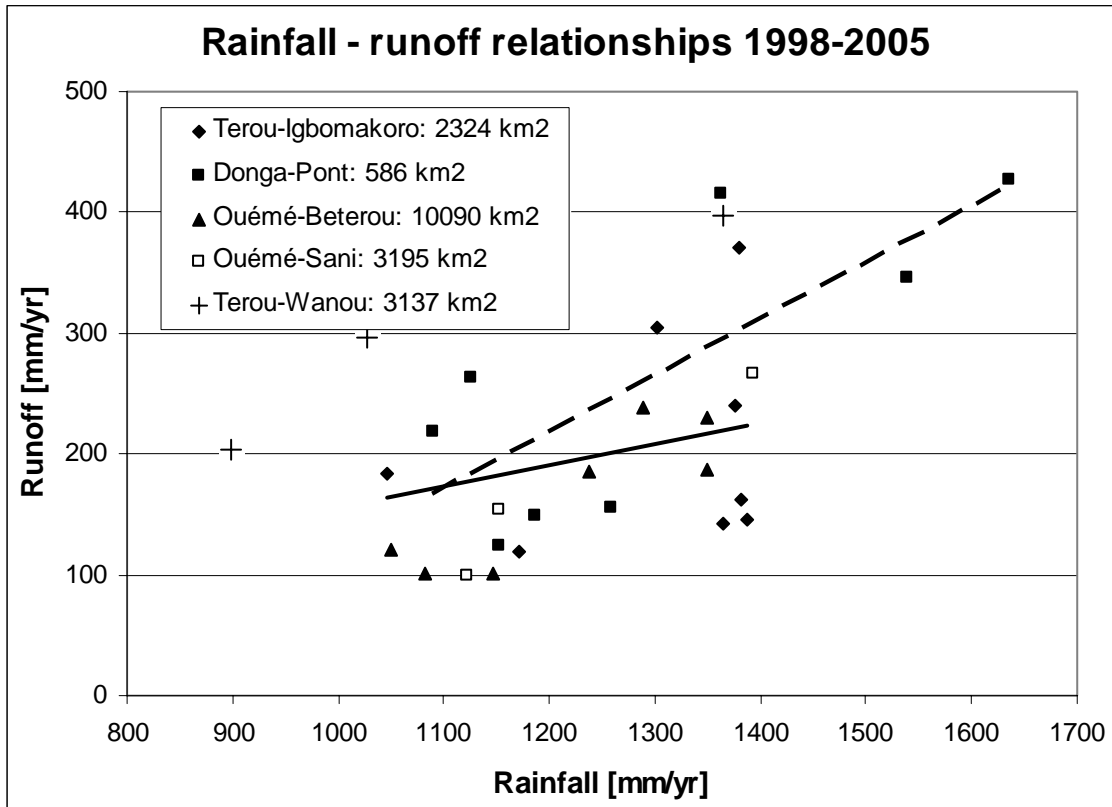


Fig. 2.8 Rainfall - discharge relationships for the main subcatchments in the Upper Ouémé catchment between 1998 and 2005. The regression lines refer to the Terou-Igbomakoro (-) and Donga-Pont (--) subcatchments.

2.3. Geology

The Upper Ouémé catchment is located on metamorphic and crystalline rocks forming the Dahomeyan basement as part of the Precambrian basement (Faure & Volkoff 1998). The Dahomeyan crystalline basement is divided into two main blocs, the western and eastern, separated from each other by a tectonic disruption, the Kandi fault (Fig. 2.9). The eastern bloc is composed of granite gneissic rocks corresponding to a medium metamorphic gradient. In contrast, the western bloc consists of granolithic and aluminous gneissic rocks corresponding to a high metamorphic gradient (Faure & Volkoff 1998). Other major geological units of Benin, outside of the Upper Ouémé catchment, are the Atacora Mountain and three sedimentary basins: the coastal basin, the Kandi basin and the Volta basin.

The geological map of the Upper Ouémé catchment distinguishes four principal litho-stratigraphic units (Faure 1977a). West of Djougou, gneisses with muscovite and two micas and leucocratic rocks, rich in quartz and muscovite, are prevalent. East of Djougou, a large biotitic gneiss panel is located from Gangamou in the northeast to Bassila and Partago in the East (Fig. A.1, Appendix A).

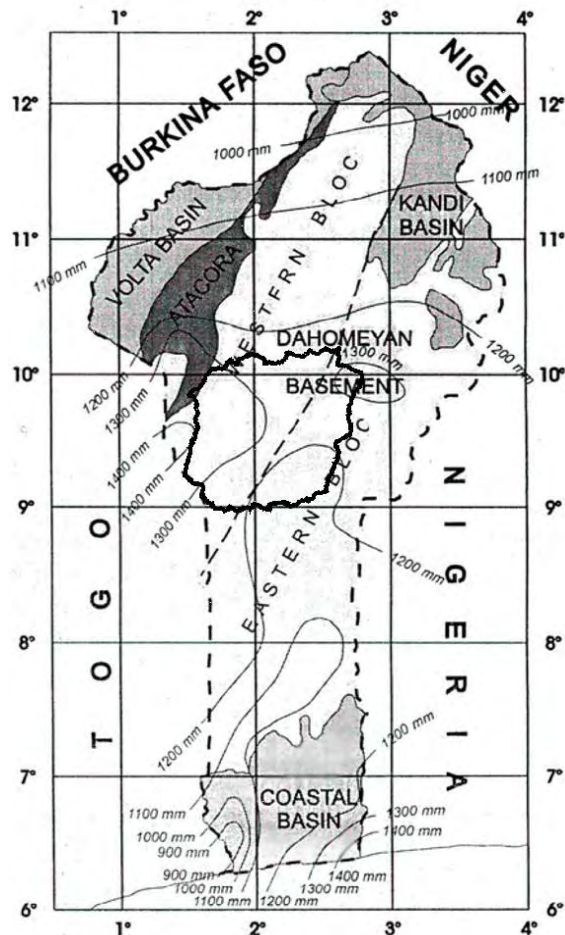


Fig. 2.9 Main geological units in Benin (modified from Faure & Volkoff (1998)).

These gneisses are darker than the ones West of Djougou; the contents of quartz are lower and biotitic micas prevail. Syntectonic granites dominate the north-eastern and the south-western area of the Upper Ouémé catchment. Embrechites, with variable mineralogical compositions, cover the south-eastern part of the catchment and the underground portion of the Ouémé River. A porphyroid formation with large feldspars and melanocratic properties is visible around the Inselbergs of Kpessou and Wari-Marou in the south of the catchment.

The geological map contains two units of particular interest for soil scientists. First, the map classifies alterites, which are strongly weathered rocks corresponding in most cases to ferrallitic soils. The alterites show a thickness up to 10 meters in the western part of the catchment (Office Béninois des Mines 1984). Second, the map classifies lateritic hardened soil horizons on the summits or at the lower slope, at the surface or subsurface.

2.4. Geomorphology and soil genesis

The Upper Ouémé catchment is characterised by a gently undulating relief with slightly inclined slopes. Faure & Volkoff (1998) classified seven geomorphologic units

on the crystalline basement in Benin. Three, in particular, cover the Upper Ouémé catchment: (1) the Djougou plateau, (2) the strongly dissected Pira peneplaine, which is characterized by steep convex slopes and a general lowering of thalwegs; and (3) the Parakou plateau on a granitic substratum. Swoboda (1994) distinguished four geomorphologic units in the savannah zone of northern Benin: peneplains along the main water divide, high and low pediplaines, and inland valleys.

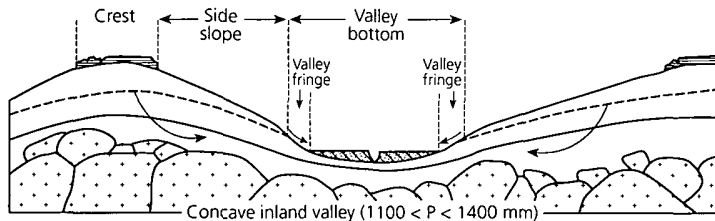


Fig. 2.10 Cross-section of an inland-valley in granite/gneiss in the Sudan-Guinea Zone (from Windmeijer & Andriessse (1993), adapted from Raunet (1985)).

Apart from the prevalent pediments, inland valleys are a characteristic morphological form of the research area. Inland valleys are flat, long valley forms without clear drainage systems, and

covered by grass savannah vegetation (Fig. 2.10). Inland valleys have been formed in the Quaternary, and show recent morpho-dynamics, specifically removal of fine soil fractions and deepening. Morphologically, inland valleys can be flat, concave, or convex. Inland valleys on granite and gneiss are generally U-shaped with concave or flat valley bottoms (Windmeijer & Andriessse 1993). At their borders, inland valleys are connected to the lower slopes of the pediment, which are often characterized by iron crusts and the ex-filtration of interflow.

The pediplaines developed in the Quaternary as a consequence of polycyclic phases of activity and stability. The last phase of activity completed approximately 2000 years ago, and was followed by an on-going period of stability with a predominance of soil formation. The pedimentation process (Fig. 2.11) drastically reduced the influence of the geology on recent geomorphologic forms.

The pedisediments in the Upper Ouémé catchment form a 20–30 cm thick loamy sand layer (Hillwash, A-horizon), which was deposited at the end of the last activity period. The thickness of the Hillwash horizon varies locally and tends to increase downward slope. It compensates for the irregular surface of the underlying gravel and saprolite horizons (Bremer 1995). The gravel-rich B-horizon, bearing rounded crust fragments and concretions, was likely deposited approximately 7000 years ago (Fölster 1983). The pedisediments cover a saprolitic C-horizon.

The autochthonous soils, which developed over the saprolite, were completely removed in the Quaternary (Fölster 1983).

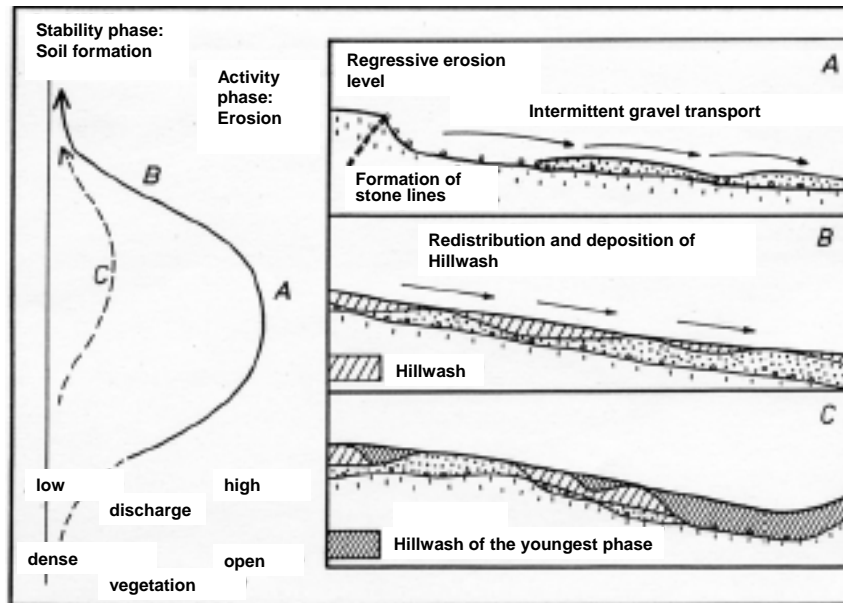


Fig. 2.11 Morpho-dynamic activity phases and formation of slope pediments (gravel and Hillwash); polycyclic deposit sequence A–C (modified from Fölster (1983)).

Saprolite is a highly weathered material. It is characterized by a high percentage of new secondary minerals (kaolinite, sesquioxides) and significant depletions in cations and silica under an extensive maintenance of the rock structure (Fölster 1983). The saprolitic horizon is

often biogeneously aerated, strongly acid, and shows high aluminium saturation, as well as higher nutrient contents than the B-horizon. The material contains 90% kaolinite in the clay fraction and displays a typical pseudo-primary structure and red or heterogeneous mottles, indicating iron oxidation and hydromorphisation. The drainage in saprolite is limited to very coarse pores, but the saturated hydraulic conductivity can be very high in tectonically stressed rocks with many rifts (Wiechmann 1991). In the Aguima subcatchment in the South of the Upper Ouémé catchment, saprolite was found at depths up to 12 meters (IMPETUS 2002).

A number of different processes have formed the soils in the sub-humid tropics. The dominant processes are saprolithisation, humification, clay eluviation, ferralithisation, plinthisation, and hydromorphisation. *Humification* refers to the decomposition of organic material in the topsoil. The mixing of the organic material and mineralized soil is supported by roots and soil fauna, particularly termites and lumbricids. Generally, the wet and warm climate causes a high litter decomposition rate, which results in lower organic carbon contents in the soils of the tropics than in the soils of temperate climates (Lal, 1990; Mulindabigwi, 2006). *Clay eluviation* describes the transport of clay by percolating water in coarse pores, leading to vertical differences in soil texture (Fölster 1983). *Ferralithisation* describes the combined processes of excessive

silica removal and a high accumulation of sesquioxides (Goethite, Hematite, Gibbsite) and kaolinite in clay fractions. Presently, the distribution of ferricretes is irregular due to past polycyclic erosion and accumulation phases. In the Upper Ouémé catchment, large superficial ferricretes can be found on the plateaus around Bassila, Parakou and Djougou (Junge 2004). *Plinthisation* describes the hardening of pediment gravel due to an accumulation of ferri-oxides, primarily Goethite, in the B-horizon. As a consequence of the lateral transport of soluble iron and the accumulation of water in depressions, plinthic horizons generally occur at the lower slopes or, as a result of relief inversion, at the summits (Fölster, 1983; Van Wambeke, 1991). *Hydromorphisation* describes the phenomenon of redox reactions in the subsoil due to a fluctuating water table or impounding water. Hydromorphic horizons frequently occur in inland valley soils or over a plinthic, poorly draining horizon. They are characterized by light grey to blue and red mottles. More details about the soil formation processes in the humid and sub-humid tropics can be found in Junge (2004), Fölster (1983) and Schachtschabel et al. (1998).

In general, the Upper Ouémé catchment is dominated by ferruginous soils which are classified as Acrisols or Lixisols according to the World Reference Base (FAO-ISRIC-ISSS 1998). Ferralsols, Plinthosols, Gleysols and Vertisols also occur. Figure 2.12 illustrates a simplified version of the soil map for the Upper Ouémé catchment. The soil maps of Benin were elaborated by French researchers from ORSTOM (now IRD) at the scale 1:200000 in the 1970s; soil types were distinguished according to the French soil classification system CPCS. The main soil types and their properties will be described in detail in Chapter 6.

Overall, the Upper Ouémé catchment forms a not very heterogeneous land area with respect to its geology and its distribution of dominant soil types. However, soil variation along the toposequences is high and often exceeds the variation between different regions in the catchment. Vegetation and land use are adapted to this variability.

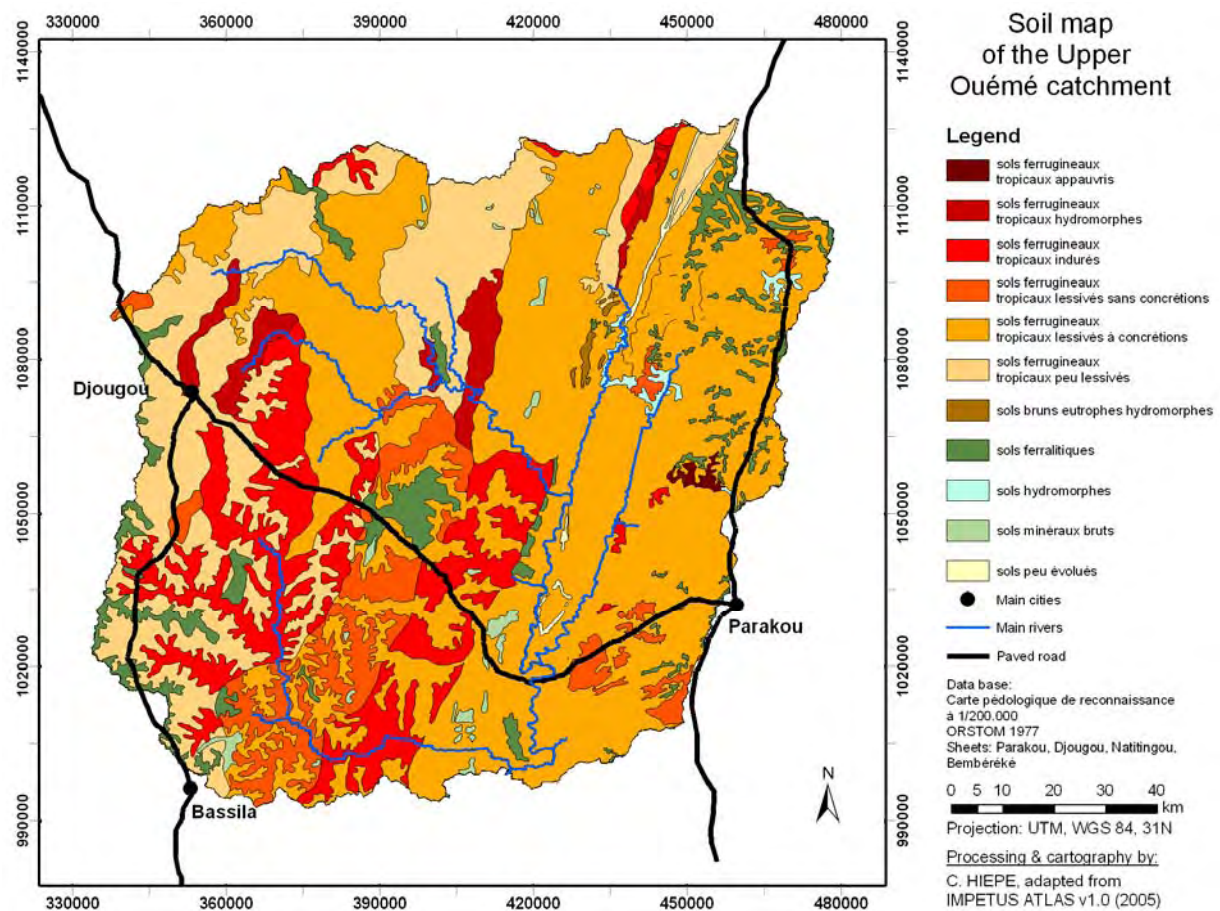


Fig. 2.12 Simplified soil map of the Upper Ouémé catchment, modified from ORSTOM (Dubroeuq, 1977a/b; Faure, 1977a/b; Viennot, 1978).

2.5. Vegetation and land use

The West African savannah can be divided from South to North into the Guinea zone, the Sudan zone, and the Sahel zone (Chevalier 1990). The Upper Ouémé catchment belongs to the Northern Guinea zone (wet Savannah zone). The potential natural vegetation in this area is dry deciduous forest (Anhuf 1994). Brush and grass savannah are naturally conditioned only in depressions and inland valleys with long periods of water impoundments or on land with extremely nutrient-poor soils (Reiff 1998). Today, the Upper Ouémé catchment is characterized by a mosaic pattern of different savannah types consisting of substitute societies or succession stages. This pattern is a consequence of agricultural land use, particularly fallow systems and shifting cultivation, cattle grazing, and selective logging (Williams & Balling 1996). The recent vegetation types in the region can be classified into seven

types according to the definition of the Yangambi Conference (Table 2.2). This classification is based on the physiognomic aspects of vegetation.

Table 2.2 Types of vegetation in the research area (modified from Meurer, 1998; Sturm, 1993; Reiff, 1998; Orthmann, 2005).

Vegetation type	Description	Tree cover
<i>Forêt galerie</i> (Gallery forest)	Closed forest along rivers	>75%
<i>Forêt dense</i> (Dense forest)	Mixed forest, mostly deciduous trees in the upper layer, not influenced by fire, dominant tree: <i>Anogeissus leiocarpus</i>	>75%
<i>Forêt claire</i> (Open forest)	Small or medium-sized trees, more or less touching the canopy, sparse grass and herb layer, influenced by fire; often on small lateritic hilltops	50–75%
<i>Savane boisée</i> (Woodland savannah)	Trees and shrubs form an open canopy; often on large lateritic sites	25–50%
<i>Savane arborée</i> (Tree savannah)	Grass savannah with scattered trees and shrubs	2–25%
<i>Savane arbustive</i> (Brush savannah)	Grass savannah with scattered shrubs	Trees <2% Shrubs:<5%
<i>Savane herbeuse</i> (Grass savannah)	No trees and shrubs, herb layer is dominated by grass; in depressions (inland valleys) and on shallow lateritic sites	<2%

The land use map of the Upper Ouémé catchment was derived by Thamm et al. (2005) from a Landsat-TM satellite scene from 26.10.2000 (Fig. 2.13). The map classifies 14% of the catchment as cropland, 29% as forest and woodland savannah, and 56% as brush and grass savannah. The highest fractions of cropland are concentrated around the cities of Djougou and Parakou and along main roads. In contrast, the cropland area in the southern and central parts of the catchment is significantly lower. The central part is dominated by a protected forest (*Fôret classée de l’Ouémé supérieur*).

Agriculture is the primary economic sector of Benin. Local farming systems are characterized by non-mechanized low-input agriculture; tillage is carried out manually with hoe and blade. Few farmers use ox-ploughing, most of whom living in the northern part of the catchment. Fallow systems are dominant and migrants practice shifting cultivation. In the north-western part of the catchment, land is scarce and therefore fallow periods were shortened and fields become more permanent (Mulindabigwi 2006).

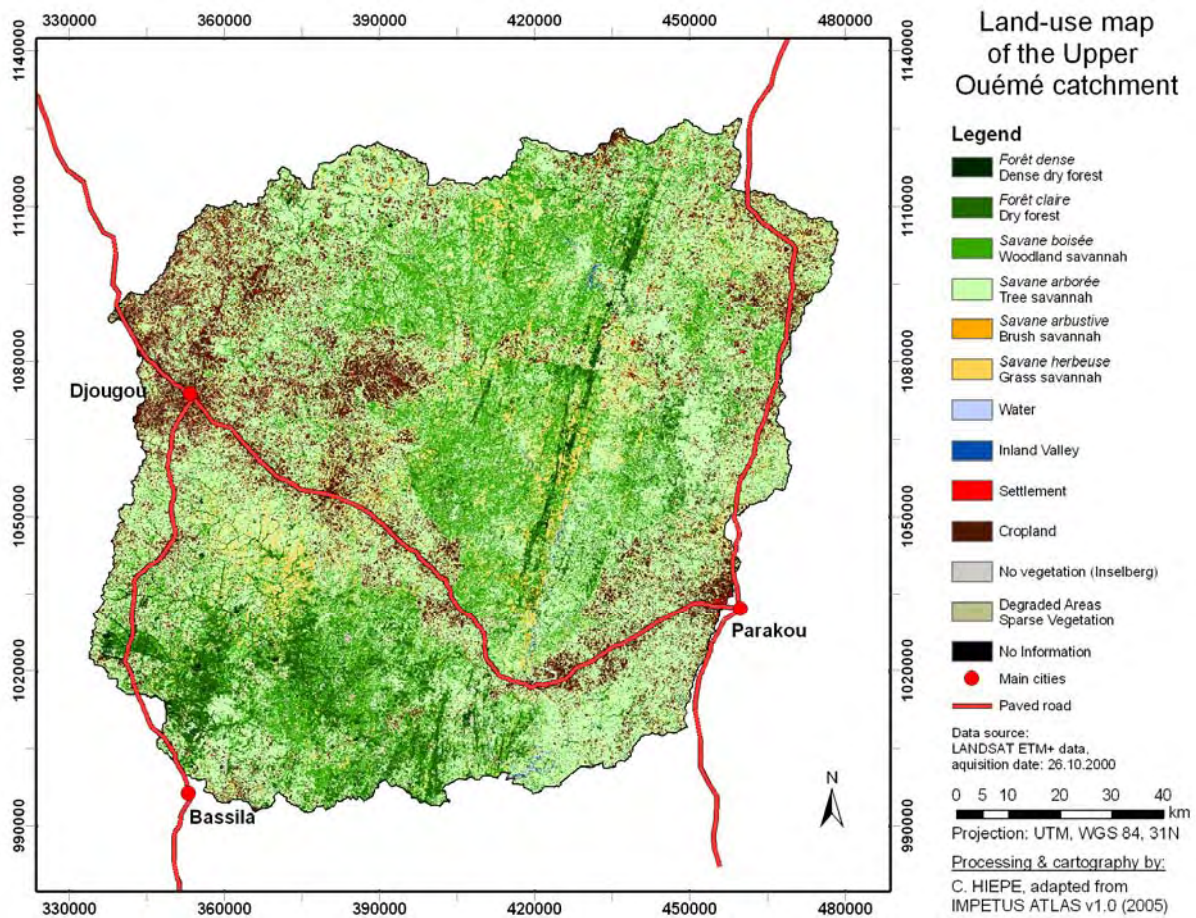


Fig. 2.13 Land use map of the Upper Ouémé catchment derived from Landsat-TM data by Thamm et al. (2005).

The principal crop in the catchment is yam (species *Dioscorea cayanensis* and *Dioscorea rotundata*). A large number of yam varieties are cultivated. Other important crops include cassava, sorghum, maize, cashew, groundnut, and cotton. The growing season typically lasts from May to October. The cultivation of rice in inland valleys is not yet widespread in the Upper Ouémé catchment, but shows a high potential to ensure food security in the future. Drought-resistant, four-month rice varieties are not yet available for farmers (Mulindabigwi 2006). The cashew cash crop is intercropped during the first 4 to 5 years, and later cultivated as monoculture. Only cotton farmers have access to mineral fertiliser, pesticides, and credits, since the government supports this production line (Maliki et al. 2002a). Therefore, the use of chemical fertiliser is limited to the cotton cash crop, and partially to maize fields; organic fertiliser is used only locally. Other efficient techniques to prevent soil erosion and to further improve water management are rarely applied (Mulindabigwi 2006). Rows of plantings 15–25 cm in height and earth mounds 50–150 cm in height for yam and cassava are employed in order to increase the arable soil depth, to loosen the

soil, and to facilitate harvest. The mound density and height varies as a function of the crop variety, soil fertility, and topographic position (Mulindabigwi 2006). Traditionally a 4 to 5 year production cycle is followed by a long-term fallow period of 10 to 15 years (Poss et al. 1997). Due to recent population growth, fallow periods have been shortened to only a few years without modifications in nutrient management. As a consequence, nutrient deficiencies are widespread. Dagbenonbakin (2005) calculated annual losses of 96 kg nitrogen, 11 kg phosphorus, and 119 kg potassium per hectare for a typical yam-cotton-maize-groundnut-sorghum rotation in the Upper Ouémé catchment.

The only ethnic group who traditionally practices animal husbandry are the Fulani herders. Some have been settling in Benin for decades and cultivate food and cash crops. Others, from the Sahelian zone, enter the country during the dry season searching for fertile pasture land. Most herders practice a large transhumance up to 100 km from December to April and a small transhumance up to 20 km from July to October (Meurer 1998).

Over the last decade pronounced land use changes have taken place in the Upper Ouémé catchment (Thamm et al. 2005). Judex (2008) determined annual agriculture area expansion rates of 4.5% to over 15% for the communes in the catchment. For example, the cultivated area increased by 261% in the Tchaourou commune and by 127% in the Bassila commune between 1992 and 2002. This large agricultural expansion in the less densely populated rural municipalities in the southern Upper Ouémé catchment can be explained by high immigration rates (cf. Section 2.6) and extensive low-input agricultural systems. Settlers in the southern part of the catchment clear approximately 1500 ha of savannah and woodland per year in order to cultivate primarily yam (Doevenspeck 2005). But not also migrants, relying on slash and burn agriculture, but also development projects promoting market-orientated cashew and tree plantations, as well as the increasing agricultural activity of women accelerate the expansion of the agricultural area. An annual deforestation rate of 2.5% (2000–2005) was published for Benin in FAO (2005).

Land degradation is accelerated in the north-western part of the catchment. Following the five-phase model of ecological degradation developed by Mulindabigwi (2006) (Fig. 2.14), this part of the catchment has already entered the third stage termed “ecological degradation”. This stage displays a strong degradation of vegetation and soils, a reduced agricultural expansion, increasingly permanent

cropping, high erosion rates, reduced bush fire, a gradual fragmentation of land, land conflicts between families, and forms of migration. In contrast, the situation in the southern Upper Ouémé catchment belongs to the second stage termed “breakdown of ecological equilibrium,” which is characterized by fallow systems, a rapid expansion of agricultural areas, and intensive bush fires. The fourth stage, termed “structural food insecurity,” and the fifth stage, termed “misery and irreversible ecological degradation”, are not present in the Upper Ouémé catchment yet. However, the strong expansion of cashew plantations in the catchment could lead to a direct transition from the second stage to the fourth stage during which fallows disappear before the disappearance of natural vegetation (Mulindabigwi 2006).

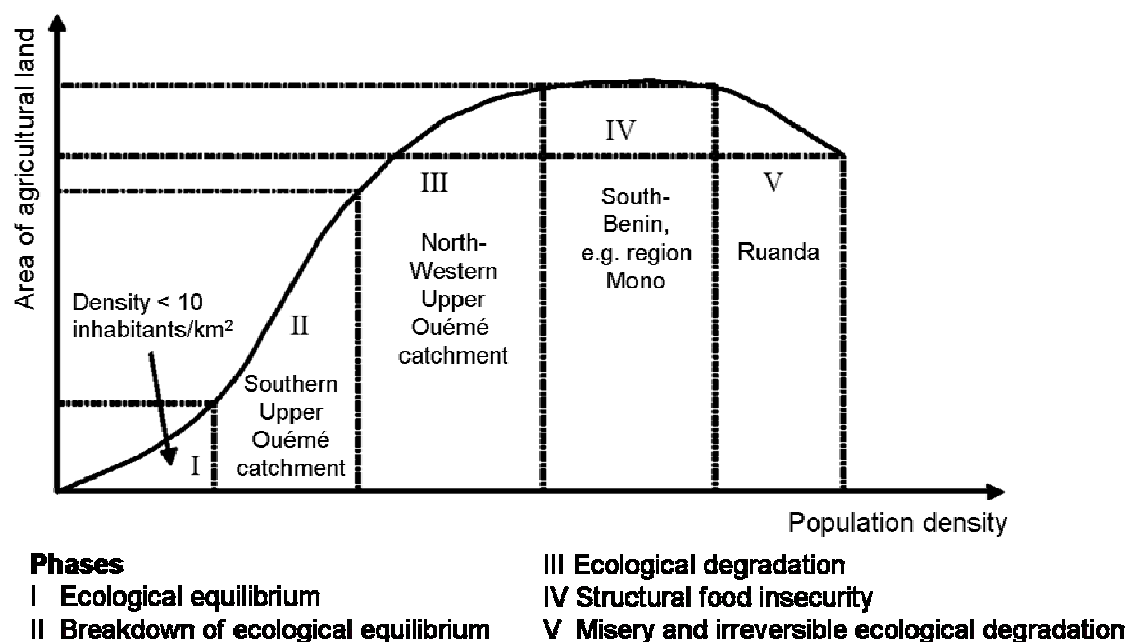


Fig. 2.14 Phase model of ecological degradation developed by Mulindabigwi (2006), modified.

2.6. Population and migration

7.86 million people live in the Republic of Benin. The last census in 2002 recorded a national population growth of 2.9% and an average population density of 60 inhabitants per km² (INSAE 2003). However, the population is irregularly distributed (Fig. 2.15). One fifth of the population lives in the periphery of Cotonou, which equals one percent of the total land area of the country (Doevenspeck 2005). Since the official implementation of the political-administrative decentralisation in 2002, the original six departments have been restructured into twelve. The

communes have received increased responsibility, but to date these new authorities are hypothetical and bureaucratic due to a lack of financial and human capacities. Apart from the commune of Parakou (325 inhabitants/km²) and the commune of Djougou (46 inhabitants/km²), the communes in the Upper Ouémé catchment show population densities below 20 inhabitants per km². However, overall, the population is growing rapidly in the whole country (Fig. 2.15).

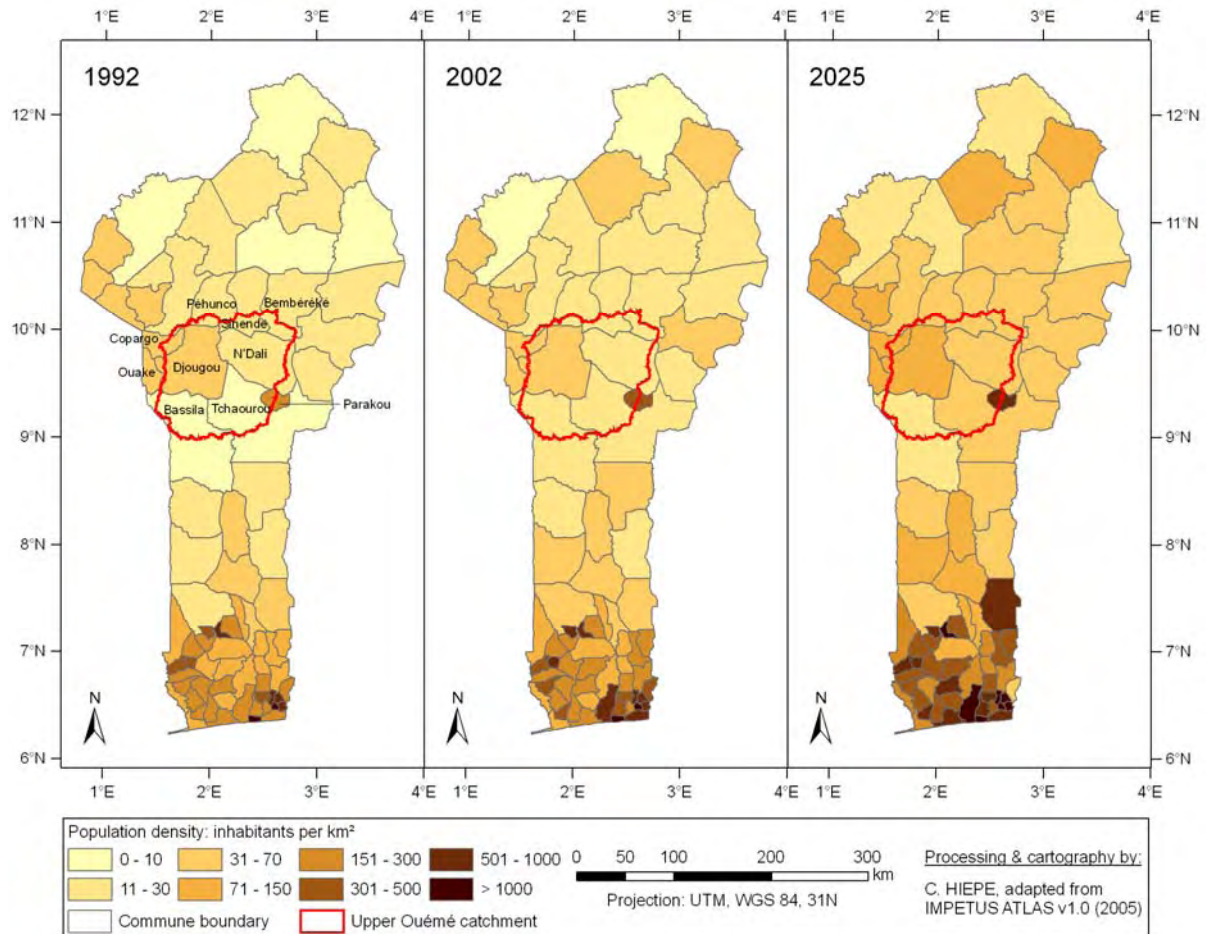


Fig. 2.15 Population densities in the communes of Benin for 1992, 2002, and 2025 based on INSAE data and projections (modified from Doevenspeck (2005)).

The less densely populated communes of Tchaourou and Bassila in the south of the catchment showed population growth rates of 4.9% and 4.8% per year between 1992 and 2002, respectively, due to high immigration rates (INSAE 2003). The Upper Ouémé catchment is part of the transition zone between central and northern Benin, which has been a target area of a multi-ethnic migration movement since the 1970s (Doevenspeck 2005). Most immigrants left their point of origin in the North-West of Benin and the border regions of Togo due to soil degradation, crop yield decline, and

social restraints (Fig. 2.16). Seasonal forms of job migration are often the starting point for later, definitive immigration.

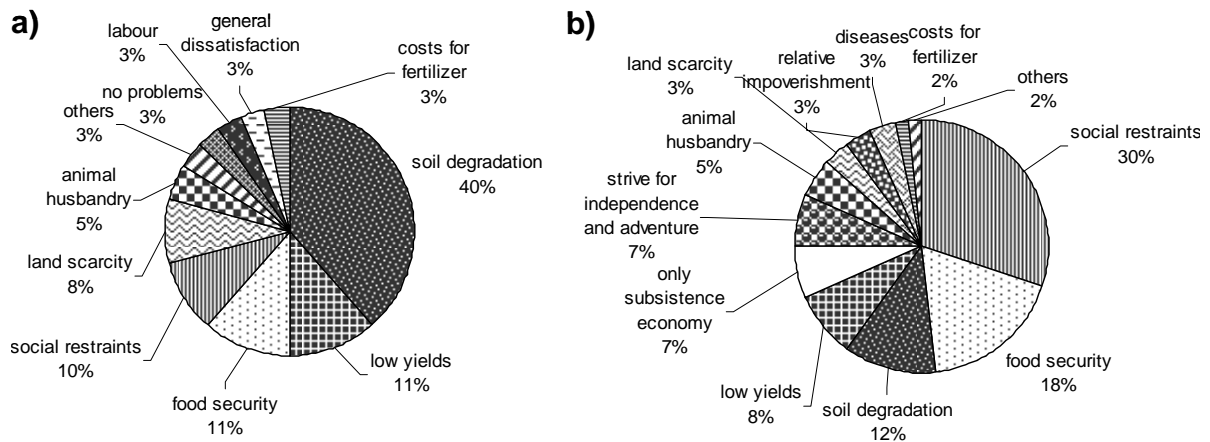


Fig. 2.16 Motivations for migration to the southern Upper Ouémé catchment: a) problems in the home village, b) reasons for transmigration (modified from Doevenspeck (2005)).

Today, migrants form the majority of the population in the southern Borgou department. The most important ethnic groups in the Upper Ouémé catchment are the Yom, Dendi, Bariba, Nagot, and Fulani (*French: Peulh*). According to the projections of Doevenspeck (2005) based on census data from 1992 and 2002, the population in the Upper Ouémé catchment will more than double in the period

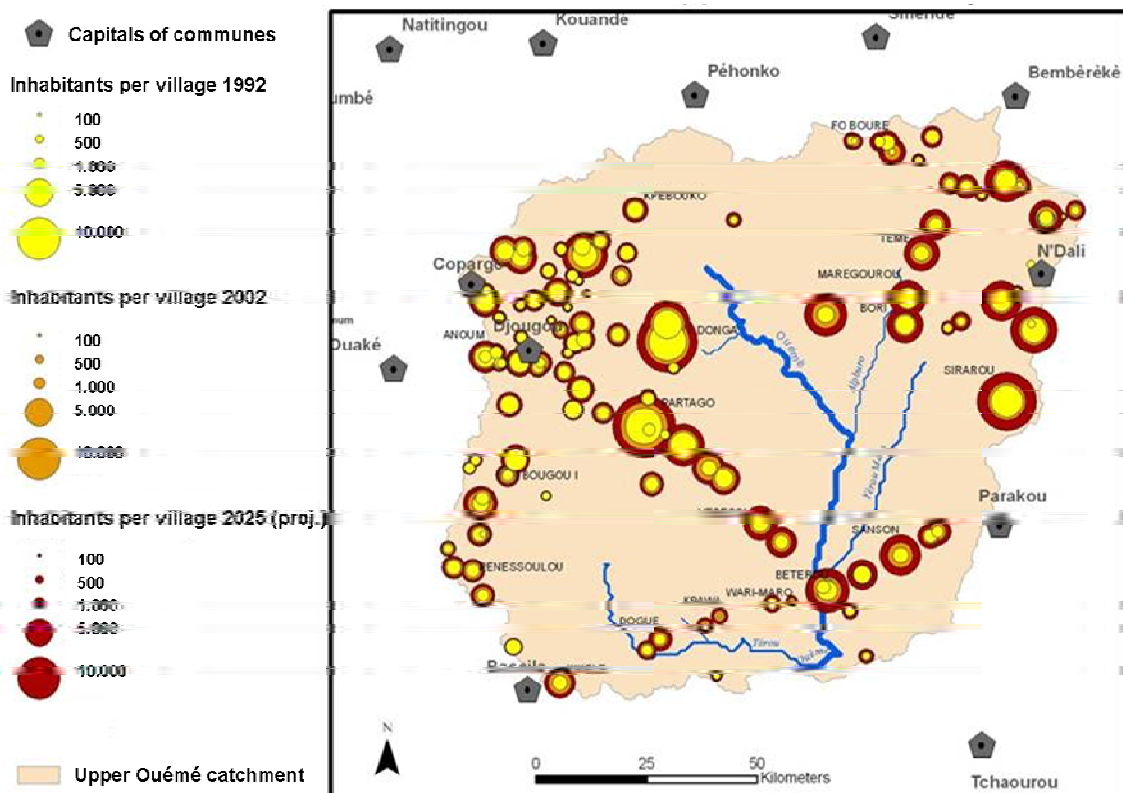


Fig. 2.17 Demographic projections for the Upper Ouémé catchment (from Doevenspeck (2005), business as usual scenario).

between 2002 and 2025 (Fig. 2.17). The settlements along the main roads and in the north-eastern part of the catchment are predicted to grow faster than the settlements in the Djougou region where land is already scarce.

3. HYDROLOGICAL PROCESSES AND SOIL DEGRADATION IN THE TROPICS

This chapter provides an overview of discharge and erosive processes and the characteristics of soil degradation with a special focus on the sub-humid and humid tropics.

3.1. Hydrological Processes in the tropics

Several studies on hydrological processes have been conducted in the West-African wet savannah zone (e.g. Giertz, 2004; Varado et al., 2005; Le Lay & Galle, 2007). A detailed overview of research on hydrological and erosive processes in the humid tropics is provided in the comprehensive reviews of Bonell & Balek (1993), Bonell (1999), and Bonell (2005).

Dominant hydrological processes

Water circulates permanently through atmosphere, biosphere, pedosphere and lithosphere. The principal processes driving the water cycle are precipitation, interception, discharge, and evapotranspiration. *Evapotranspiration* includes all processes by which water at the earth's surface is converted to water vapour, including evaporation from the plant canopy, transpiration, and evaporation from the soil. A fraction of rainfall is stored in the canopy (*interception*). Interception affects infiltration, surface runoff, and evapotranspiration, and reduces the erosive energy of rain drops.

Total discharge is fed by overland flow and subsurface flow. Overland flows can be created by three mechanisms (Fig. 3.1, ABF). Overland flow can be induced by an infiltration excess (*Hortonian overland flow*), and this mechanism is generally dominant if high intensity rainfalls hit soils with low infiltration capacities. Overland flows can also be caused by saturation excess. This process is often observed in saturated, flat areas at the foot slope and on soils with low water holding capacity or subsoils with low permeability. The third mechanism is called *return flow*. In this case, overland flow is created due to a decreased permeability at the lower slope or specific slope morphologies that favour the emergence of subsurface flow on the

surface. Under natural forests, Hortonian overland flow typically does not appear in the humid tropics, even for extreme rainfall intensities, because macropores increase the saturated conductivity of the topsoil (Bonell 1999).

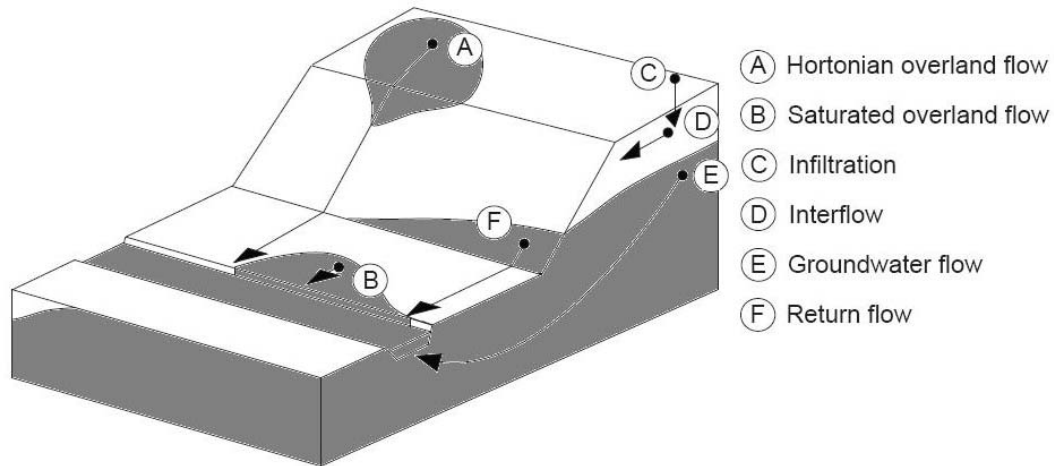


Fig. 3.1 Runoff generation mechanisms (modified from Anderson & Burt (2005)).

If the permeability of the soil is reduced, e.g. due to compaction or the destruction of the macro-porosity after converting natural vegetation into agricultural land, Hortonian overland flow becomes more dominant (Fig. 3.2, b). In contrast, overland flow due to saturation excess is an important mechanism for runoff generation under natural vegetation, in particular at the bottom of the slope (Fig. 3.2, a). Often subsurface storm flow is a major contributor to the development of saturation excess overland flow at the lower slope and in convergent areas (Douglas & Guyot 2005). The lateral movement of water in the shallow subsurface, the so-called interflow, is also a major runoff pathway in the soils of the West African savannah region (Bonell 1999; Giertz 2004). Acrisols and Lixisols with subsoils with low permeabilities or plinthic horizons along the slope promote interflow. At the lower slope, this water often ex-filtrates from the Plinthosols and re-infiltrates in the sandy Gleysols at the border of the inland valleys as long as they are not saturated (Giertz 2004). Interflow may also transport significant amounts of sediment in macropores and pipes, but this phenomenon has not yet been well investigated (Douglas & Guyot 2005).

Infiltration and the movement of water in the unsaturated zone are complex processes, which are influenced by various factors, including catchment characteristics such as soil texture, hydraulic conductivity, land use, and land morphology, all of which are independent of the rainfall event. In contrast, rainfall

intensity, initial soil water content, and groundwater level vary between different events.

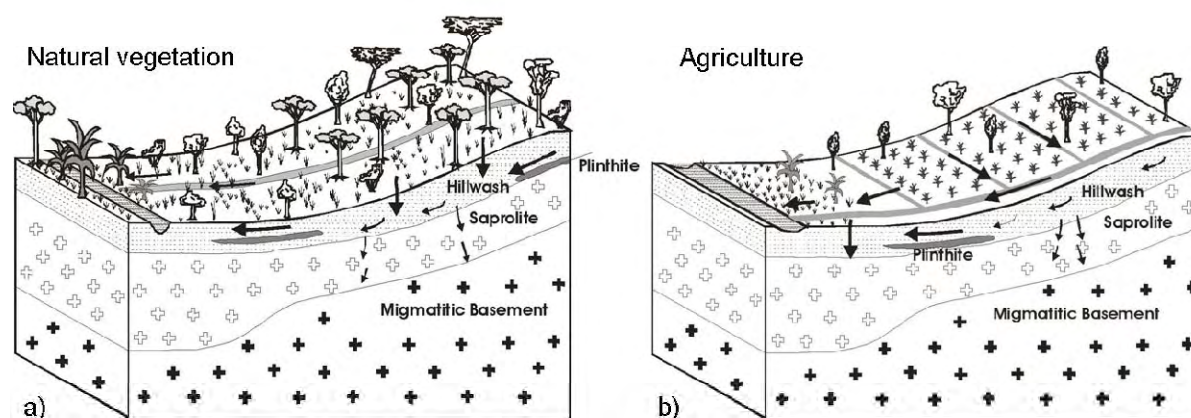


Fig. 3.2 Prevalent runoff generation processes under natural vegetation and agriculture (modified from Giertz (2004)).

Macropores, which were created by earthworms, termites, and ants, provide preferential flow paths and allow for a fast contribution to groundwater flow, especially during heavy rainfalls. However, in dry soils the macropores are not well connected, and the water infiltrates into the soil matrix. Giertz (2004) observed mean saturated hydraulic conductivities of 11.2 to 41.6 cm per day for the loamy-sandy topsoils in the Aguima subcatchment in Central Benin, depending on the degree of land use. Permeabilities in uncultivated soils were 3.7 times higher than in cultivated soils. The inter-annual soil water dynamics are primarily restricted to the two upper meters above the saprolitic weathering material.

Water that percolates through the unsaturated zone into the saturated zone contributes to the groundwater flow. Most hydrological models in the tropics distinguish a shallow and a deep aquifer representing a saprolitic aquifer over a fractured aquifer. Water from the shallow aquifer can still return to the surface (*return flow*) or can re-enter the unsaturated zone by evapotranspiration from deep rooted plants. Water that enters the deep aquifer (*deep recharge*) is often assumed to be lost from the system.

Giertz (2004) emphasized the important role of inland valleys in small catchments in the humid tropics. However, the effects of inland valleys on discharge peaks are a topic of on-going debate in the literature. Many authors have stated that inland valleys smoothen discharge peaks due to the high water holding capacity of clay-rich soils and reduce surface runoff due to dense grass vegetation. In contrast, some

authors have observed higher discharge peaks and amounts of overland flow due to saturation excess (e.g. Balak & Perry, 1973). However, as the size of inland valleys is seldom greater than a few hectares and their occurrences are generally connected to first-order streams, their influence on the hydrology of catchments with a size of several thousand square kilometres remains limited.

3.2. Erosion Processes

Erosion and sedimentation processes take place on the slopes and in the river beds of a catchment. Soil erosion by water on the slope is directly linked to overland flow. Therefore, the occurrence of soil erosion is strongly connected to the hydrological processes mentioned in the previous section.

Dominant erosion processes

Soil erosion by water can be defined as the detachment of soil particles and their subsequent transport (Schachtschabel et al. 1998). Cohesive soils, typically heavy textured or clayey soils, have a more cohesive force and require more energy for detachment. On the other hand, clayey soil particles are easier to transport. Thus, transport-limited conditions have to be distinguished from detachment-limited conditions.

Table 3.1 characterizes the different types of erosion forms. Splash erosion describes the process by which rain drops hit the ground and detach soil particles. The intensity of the splash effect is directly linked to the vegetation height and ground and canopy coverages. Splash erosion decreases exponentially with increasing ground coverage (Lal 1990). Sheet erosion denominates the removal of a thin and fairly uniform layer of soil from the land surface by runoff water. Although soil detachment by splash proceeds transport by sheet flow, both processes may occur simultaneously during a rainfall event. Linear erosion forms are created by turbulent discharges. Depending on their deepness, they can be classified as rills or gullies. Shallow erosion rills, with a depth of up to 10 cm, and deep erosion rills, with a depth of up to 30 cm, are primarily created on sandy soils because of their low shear strength (Richter 1998). While splash and sheet erosion are caused by raindrop impact with and without overland flow, channel flow is crucial for detachment and transport during rill erosion (Lal 1990). The flow velocity in the channel is highly

influenced by the slope steepness. Gully erosion denotes the process during which water flowing at high speed gouges out gullies or deep depressions. The defined minimum depth of a gully varies between 30 and 50 cm in the literature (e.g. Sirvio et al., 2004; Richter, 1998).

Table. 3.1 Classification of erosion forms (composition from Sirvio et al., 2004; Richter, 1998; Auerswald, 1993).

Process	Limits	Characteristics
splash erosion	on the surface, locally	only detachment, no long transport
sheet erosion (low, moderate)	on the surface	laminar, often underestimated
sheet erosion (severe)	on the surface	laminar, tree root exposure, severe crusting
rill erosion (shallow)	2–10 cm deep, < 50 cm wide	frequent on sandy soils, high density
rill erosion (deep)	10–30 cm deep, > 50 cm wide	entire topsoil concerned
gully erosion	> 30 cm deep	permanent
tunnel erosion	< 200 cm wide	seldom, mainly in arid zones; caused by inter-flow over unstable subsoil
crusting	on the surface	favoured by compaction and sheet erosion

Rill and gully erosion frequently take place along foot paths and roads. In the tropics, large rills and gullies often lead to the exposure of nutrient-depleted subsoil (Hashim et al. 1998).

Crusting describes the phenomena by which soil particles silt upward leading to a decline in infiltration

rates and a sealing of the surface. Structural crusts are directly related to the splash impact of raindrops, while depositional crusts result from the settling of fine particles carried in suspension by runoff. Tropical Lixisols are particularly prone to crusting and surface sealing. With continuous mechanized cultivation, the infiltration rate of some Lixisols may decline by several orders of magnitude in only three or four years. Crusting and surface sealing are among the major causes of high runoff rates on tropical soils (Lal 1990). All erosion processes are driven by various factors.

Factors affecting soil erosion by water

The main factors affecting soil erosion are soil properties, rainfall intensity, land use, and land morphology (Fig. 3.3). Rainfall intensity is especially high in tropical regions since precipitation is generally not created by cyclones or front effects, but rather by convection leading to a high proportion of torrential rains with locally limited, high intensity peaks (see Section 2.1). Richter (1998) has considered rainfall with intensities higher than 5 mm per 30 minutes to be erosive.

Soil properties play an important role in erosion because they determine the resisting force of the soil. The erodibility of a soil is a function of physical, chemical, and biological soil properties, but also is affected by climate and the management

system. Dynamic changes in soil erodibility during a rainfall event are not yet well understood (Lal et al. 1998). In general, soils with a high percentage of bonding material, organic matter, and clay contents have a high aggregate stability (Richter 1998) and a high water retention capacity, and thus reduce the extent of water erosion. In contrast, soils with silty or very fine sandy textured topsoils, low infiltration rates, and low organic carbon contents are easily erodible. Morphology, in particular inclination and slope length, heavily influence the flow characteristics and the type of erosion.

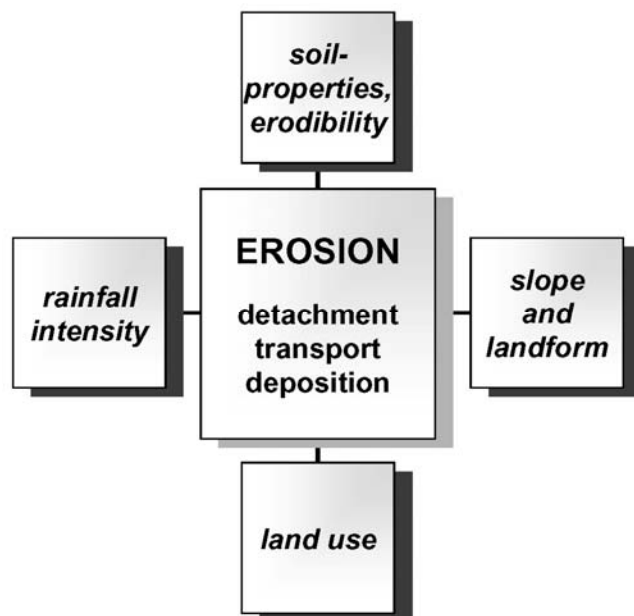


Fig. 3.3 Main factors affecting soil erosion.

The effects of land use change on the hydrological and erosive processes in the tropics were investigated by several authors (e.g. Lal, 1981; Giertz, 2004; Calder, 1992). They attributed the observable increases in surface runoff and sediment yield after deforestation to the following three processes: (i) a decrease of interception, (ii) a lower transpiration leading to higher soil moisture and percolation, (iii) changes of soil

properties due to land use change. Lal (1981) studied the influence of different deforestation techniques and types of land use conversion on surface runoff and soil erosion in southern Nigeria. He recorded the highest surface runoff amounts, up to 250 mm/yr, after mechanical clearing with subsequent agricultural use. The effects of forest clearance are especially severe in the Sahelo-Sudano Zone where agricultural land use rapidly leads to a de-structuring of the top soil layer (Mahé et al. 2005). While increases in the total water yield due to selective logging are modest, suspended sediment fluxes can increase by a factor 2 to 50 (Warren et al. 2003).

In general, a decreasing erosion risk of different land use types can be defined by the following sequence: bare fallow > arable land > perennial crops > grass cover > natural vegetation (Lal 1990).

Sediment delivery

Generally, only a small portion of the eroded material at the hillslope reaches the main river channel. The remaining material is deposited at the foot-slopes and in the flood plains. The fraction of the eroded material divided by the sediment entering the main channel is called sediment delivery ratio (SDR). The SDR varies for different climate and catchment characteristics (soil, rocks, morphology, land use, anthropogenic activities). The SDR decreases with the size of the area, which can be explained by an increase of the time of concentration, hysteretic effects, and an increased chance of sedimentation (Van Noordwijk et al. 1998). Since the SDR is difficult to quantify, simple extrapolations of soil erosion amounts from plot-orientated erosion research to the regional scale are not possible. Catchments with sizes up to 10,000 km² generally have SDR values below 0.2 (Van Noordwijk et al. 1998), i.e. less than 20% of the eroded material reaches the channel.

The majority of sediment is transported in suspension. The sediment which is transported near or on the riverbed, termed the bed load, is difficult to measure. However, in most cases it contributes less than 10% to the total sediment yield (Gregory & Walling 1973 in Malmer et al. 2005). Bank erosion, often undermining fallen riparian trees, can significantly change the morphology of the river bed (Douglas & Guyot 2005).

In general, sediment flows are largely scattered and show high intra-seasonal variability. The relationships between discharge and suspended sediment concentrations (SSC) vary significantly between storm periods. The suspended sediment concentrations are often larger during the rising stage than during the falling stage (Douglas & Guyot 2005). The degree of impact of a rainfall event on the SSC depends on the antecedent conditions, the sediment availability, and the actual pattern of rainfall intensity during individual storms (Douglas & Guyot 2005). For example, the effects of storm flow on the sediment yield can be aggravated by water-saturated soils due to an earlier event, active bank erosion, or the displacement of accumulated sediment from past erosive events (Douglas & Guyot 2005). The majority of sediment is transported during a few extreme rainfall events over the year.

Nutrient depletion

Nutrient depletion describes the process of diminishing nutrient contents in soil. Soil erosion is a major cause of nutrient depletion. Other causes include natural

weathering, wash-out, frequent burning, and removal of crops without compensation from organic or mineral fertilisers or crop residues (Donovan & Casey 1998). The macro-nutrients nitrogen (N), phosphorus (P), and potassium (K) are essential for plants, as they are required to produce proteins, set up fruits and seeds, take up nutrients, and facilitate respiration and transpiration (Mulder 2000). Nutrients occur in the soil in four different forms: (i) plant available nutrients in the soil solution from the mineralisation of soil organic matter (SOM) and mineral weathering, (ii) nutrients in the SOM, (iii) nutrient reserves in minerals, and (iv) nutrients that are absorbed by minerals and SOM, and which are available under favourable soil characteristics (Mulder 2000). SOM is the most important nutrient storage in traditional low input agricultural systems (Donovan & Casey 1998). Water percolating through the unsaturated zone reduces only the nutrient content in the soil solution. In contrast, soil erosion removes nutrients from the soil solution and nutrients bound to SOM and mineral soil particles.

During the transport of the eroded material, the coarse aggregates deposit more rapidly. Thus, the transported material becomes finer and the nutrient content is increased relative to the original soil material. This nutrient enrichment associated with the suspended sediment load is described with the Enrichment Ratio (ER) and can be used for calculating the nutrient loss associated with soil erosion. However, like the sediment delivery, the ER is a complex and dynamic variable that depends on factors such as the soil type, the erosion mechanism, the scale, the biological activity, and the ground cover. On long slopes, the ER increases due to selective deposition and decreases due to entrainment. For clayey soils with limited fertiliser application, the relationship between soil and nutrient loss is closer than for soils of lighter texture for which the ER is much higher (Rose & Yu 1998).

In summary, soil erosion and nutrient loss are often closely linked processes that lead to soil degradation.

3.3. Soil degradation in the tropics

Soil degradation defines a situation in which the deterioration of biological, physical, and chemical soil properties leads to a loss of economical and ecological functions of the soil (Steiner 1994). Physical, chemical, and biological degradation are distinguished depending on the affected soil properties. All three types of degradation

are strongly connected and show feedback mechanisms. The two most important processes that lead to soil degradation are soil erosion and nutrient depletion. Both processes can appear separately, but often aggravate each other in the sub-humid tropics, as the erosion of topsoil implies a loss of SOM and the associated nutrients. On the other hand, nutrient depletion can also be a causative factor for soil erosion because it reduces biomass and ground coverage (Hashim et al. 1998). Soil erosion affects physical, chemical, and biological soil properties. The loss of topsoil, preferably of fine, nutrient-rich particles, directly decreases rooting depths and water holding capacity. Other effects such as compaction, crusting, water-logging, and a decrease of biological activity are indirect consequences of the loss of SOM.

Severity of soil degradation in the tropics

While processes such as nutrient depletion, loss of SOM, and soil acidification are generally reversible, soil erosion is usually an irreversible process (Greenland 1994). The severity of erosion and its consequences depend on the absolute quantity of soil eroded and the depth and quality of soil remaining. The rate of erosion may not be necessarily greater in the tropics than in temperate regions, but the resulting productivity decline is often more drastic due to the harsh climate, low soil fertility, the poor quality of the subsoil (Lal 1990), or unstable soil properties (Steiner 1994). Harsh climatic conditions, high rainfall intensities, prolonged dry seasons, extensive drought periods, high population growth, and an excessive use of resources, have made tropical ecosystems particularly vulnerable to soil erosion and erosion-induced soil degradation.

Several researchers have tried to define soil loss tolerances for specific soil types and environments; a threshold of 12 t/ha/yr is cited in the literature for tropical soils (Lal 1998). However, Lal (1985) measured a soil loss tolerance of only 1 t/ha/yr for shallow Alfisols, with a root restrictive layer at 20 to 30 cm in depth. Lal (1990) underlined that not all soils of the tropics are shallow, fragile, or structurally unstable. However, in many tropical soils, fertility is restricted to the SOM in the topsoil because the dominant clay mineral, kaolinite, has a very low potential cation exchange capacity (Ahn 1970). In the tropics, SOM contents under natural vegetation are not necessarily lower than in the temperate zone, but under cultivation, SOM declines about five times faster (Steiner 1994). Lal (2001) reported an SOM depletion of 70% within 10 years of cultivation in tropical regions.

Africa faces the greatest challenge of breaking the cycle of erosion-induced soil degradation and the resulting decline in crop productivity (Fig. 3.4). As a consequence, increasingly marginal lands are being cultivated (Lal 1990). Traditional resource-poor farming systems become unsustainable as natural fallow periods have to be shortened due to population growth. An intensification of agriculture is needed in order to stop soil depletion and to increase crop yields. On the other hand, very intense land use systems with high fertiliser inputs and monocultures should be avoided.

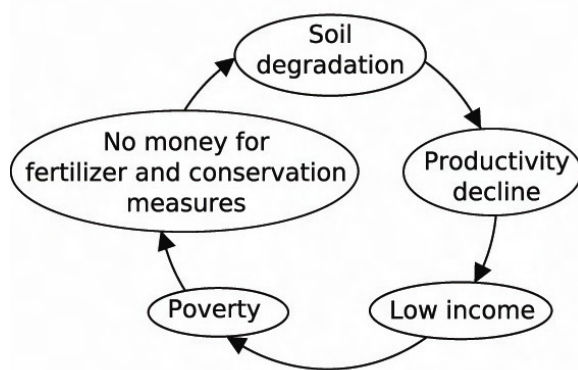


Fig. 3.4 Schematic circle of poverty and soil degradation.

Regular burning contributes significantly to soil degradation in the African savannah regions, destroying biomass, litter, and crop residues. Savannah fires destroy three times more biomass than forest fires (Levine 1994). Fires at the end of the dry season are the most harmful, because the soil is left uncovered during the first heavy rainfalls. As a consequence, soil erosion

and crust formation are facilitated. Burning is a crucial factor for SOM destruction and emissions of greenhouse gases due to volatilisation. About half of the nitrogen and phosphorus in the burning biomass is released to the soil. Furthermore, higher soil temperatures accelerate the mineralization of SOM. Both processes provide a high nutrient availability for one to two years of crop production (Donovan & Casey 1998), but weaken soil fertility without long fallow periods or external inputs.

Productivity losses due to soil erosion can be significant (e.g. Mantel & Van Engelen, 1999; Lal et al, 2000; Jakeman et al., 1998). Lal (1995) reported yield reductions in Africa from 2–40% due to soil erosion, which can be even higher on shallow soils. However, reliable quantifications of productivity losses due to soil erosion are scarce in the literature. The comparability of erosion studies is hampered due to missing information on regional land characteristics and climate conditions, non-standardized methods, poor design, short experimental periods, a lack of scaling procedures, and the complexity of prevailing weather conditions (Lal, 1998; Lal, 2000). Moreover, improved agricultural technologies often compensate for the adverse effects of soil erosion and decline in soil quality.

Causes and effects of soil degradation

Direct and indirect causes, as well as on-site and off-site effects of soil degradation on physical, chemical, and biological soil properties can be distinguished (Fig. 3.5). The on-site effects are more directly relevant, leading over time to a decline in soil fertility and harvest yields if nutrient losses are not compensated for. In contrast, negative short-term on-site effects on agronomic productivity due to the damage of seeds and individual plants, and off-site effects on water quality and infrastructure, are of minor importance in low-input agriculture areas without steep slopes. While the effects of soil erosion are generally negative, soil deposition at the bottom slope can be beneficial over time, and provides the basis for paddy rice fields and fertile flood plains (Van Noordwijk et al. 1998). On the other hand, nutrient-enriched colluvial materials often show hydromorphic properties, a low mechanical resilience, and a high degree of erodibility due to a well sorted grain size and an unsuitable soil structure.

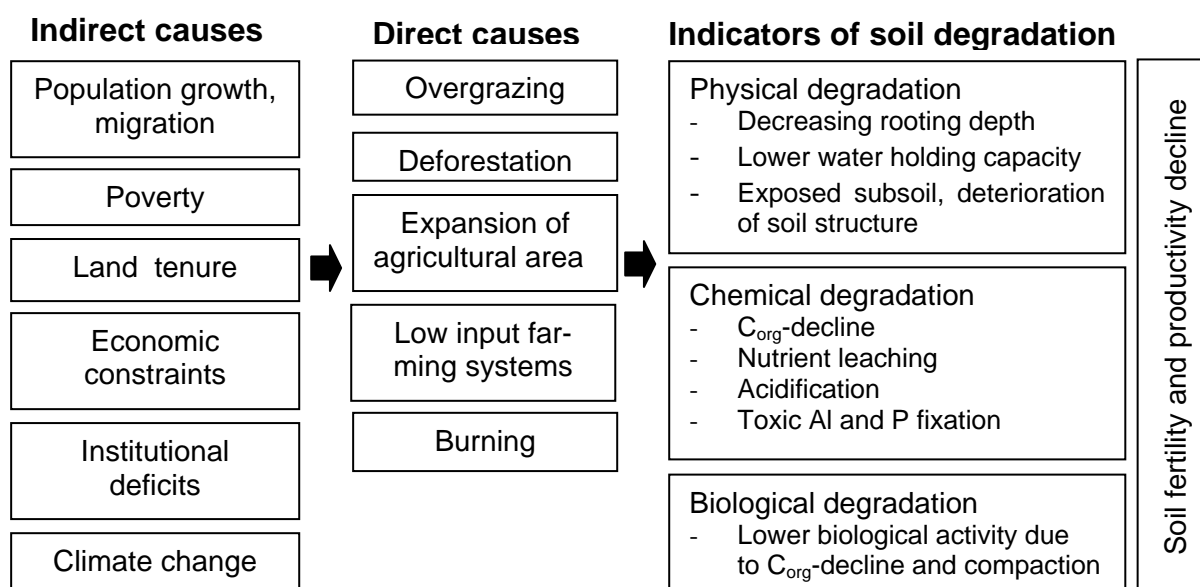


Fig. 3.5 Causes and on-site indicators of soil degradation in Sub-Saharan Africa (composition from Steiner, 1994; FAO, 2001b; Oldeman et al., 1991; Lal, 1998).

The most important direct causes of soil degradation in Sub-Saharan Africa are overgrazing by cattle, regular burning, deforestation, agricultural expansion, and low-input farming systems with shortened fallow periods. The driving forces behind these problems are complex. Country-specific socioeconomic factors, such as poverty, insecure land tenure, institutional deficits, population growth, and migration, are aggravated by international economic conditions and climate change. For Benin, the

national action plan to combat desertification (MEHU 1999) and the national action plan for sustainable management of natural resources and soil fertility (MAEP 2004) provide certain country-specific details. Both reports emphasize the lack of regulated exploitation of forest resources, which has led to an uncontrolled, rapid deforestation of tree savannah and dry forests for yam, cotton, and charcoal production in central and northern Benin over the past decades. Agricultural expansion and an increasing number of transhumant cattle-breeders from neighbouring countries also increase the pressure on pasture resources. In addition, the action plans mention climate change, and in particular, a reduction in rainfall amounts by 20% since the 1970s in the most affected regions in northern Benin. Both reports cite the restrictive international commercial policy, dumping imports, and high foreign debts forcing the national government to reduce fertiliser purchases and food subsidies as constraints for trade and market development. Institutional deficits and land tenure issues in Benin will be discussed in Section 9.2.

Soil fertility management and erosion measures in Sub-Saharan Africa

Many authors have discussed management options for Sub-Saharan Africa in order to reduce erosion and increase soil fertility (e.g. Donovan & Casey, 1998; Lal, 1995; Greenland, 1981; Lal, 1990; Syers & Rimmer, 1994; Lal, 2000; Roose & Barthés, 2001). Several have focused on specific countries such as Tanzania (Dejene et al. 1997), Benin (Saidou et al. 2004), Ghana (ICRA 2000), Kenya (Wamuongo 1997), and Nigeria (Igwe 1999). In 1998, the World Bank, the FAO, and several other partners launched the Soil Fertility Initiative for Sub-Saharan Africa (Donovan & Casey 1998) in order to strengthen management efforts. Integrated fertility management, the use of mineral fertilisers, altered farming systems, and investments in land improvement and efficient water use have been proposed as the dominant strategies to increase food production in sub-Saharan Africa (FAO 2001a). Apart from the application of mineral fertiliser, two main categories of technologies and management practices exist in order to combat soil erosion. Structural technologies, such as contour furrows, ridging, terracing, stone walls, cut-off drains, waterways (to discharge runoff), gully control measures, and contour tillage (Donovan & Casey 1998) aid primarily in reduction of surface runoff. In contrast, organic technologies improve the soil characteristics that resist erosion and increase biomass production and ground coverage. For example, the incorporation of organic

sources improves biological activity, nutrient and water holding capacity, and the physical structure of the soil. The organic technologies include mulching, cover crops, mixed or serial cropping, strip-cropping, contour hedgerows, and the use of deep-rooted species to recycle nutrients (Donovan & Casey 1998). In most parts of central Benin, structural technologies are less efficient in preventing soil degradation than biologic measures due to the slightly undulating terrain and mean annual rainfall totals above 800 mm (Walling 1996).

Traditional measures for addressing the loss of SOM in low-input systems in Benin include fallowing, crop rotations, the application of animal manure, various forms of inter-cropping, and reduced tillage. However, the most frequent solution for farmers in Benin to combat soil fertility decline remains the clearing of new land, i.e. agricultural expansion. The challenges for an effective soil fertility management in Benin are discussed in Section 9.2.

As mentioned above, soil fertility management goes far beyond the application of mineral fertiliser in order to meet plant requirements. Organic sources are applied in order to restore nutrient deficiencies and SOM leading to higher efficiency mineral fertilisers. Legumes, i.e. nitrogen-fixing plants, tapping residual soil moisture and nutrients with their long roots, are important components of soil fertility management. Many legumes also reduce the incidence of pests and diseases. The amount of nitrogen returned from legume rotations depends on whether the legume is harvested for seed and forage, or incorporated as green manure. Depending on the soil type, the quantity and quality of SOM, and the fertility status, organic technologies can have substantial effects on crop yields within one or two years (Donovan & Casey 1998). However, since organic sources alone often enable only limited yield increases, a combination of organic and mineral fertiliser is increasingly promoted, termed Integrated Nutrient Management. Furthermore, the integration of crops and livestock is desirable in order to use animal manure to increase soil fertility.

4. EROSION MODELS AND THEIR APPLICATION IN THE TROPICS

This chapter provides an overview of fundamental aspects of environmental modelling and the state of the art in modelling erosive processes at the catchment scale. Special attention is given to applications of the model SWAT (Soil Water Assessment Tool) and to modelling studies in tropical catchments.

4.1. Fundamental aspects of hydrological modelling

Models are simplified representations of complex systems. They are valuable tools for better understanding environmental processes and supporting decision-making. However, all environmental models deal with problems arising from the complexity of nature and limitations in measurements, process understanding and computational power. As regards spatially distributed hydrological models, Beven (2001) mentions the problems of non-linearity, scale and uncertainty. The problems of scale and non-linearity refer to the fact that many natural phenomena act at different spatial and temporal scales, in different media and with complex interactions (Jakeman et al. 1998). Indeed, observations at the local scale often cannot be directly transferred to the regional scale because different processes become dominant. Scale-specific process descriptions and measurement techniques are needed but are not always available. For example, local measurements of soil erosion with splash-cups, erosion nails, runoff plots or sediment traps may be appropriate for parameterising an erosion model at the field scale (Lal 1990), but these measurements cannot be extrapolated to large catchments because sedimentation then becomes more important. At the regional and macro-scale, measurements of runoff and sediment in rivers are adequate for validating erosion models. Finally, information about erosion processes at multiple scales is needed in order to derive conclusions regarding land management.

The problem of uncertainty addresses the difficulties of obtaining adequate data as model input and for model calibration and validation (see Chapter 8). It is a challenge to obtain representative measurements that reflect the spatial heterogeneity of the medium. Since modelling assumptions are also an important source of uncertainty,

choosing an appropriate model for the considered scale and purpose is crucial. According to the spatio-temporal resolution and the type of equations they are based on, we distinguish different types of hydrological models (Fig. 4.1).

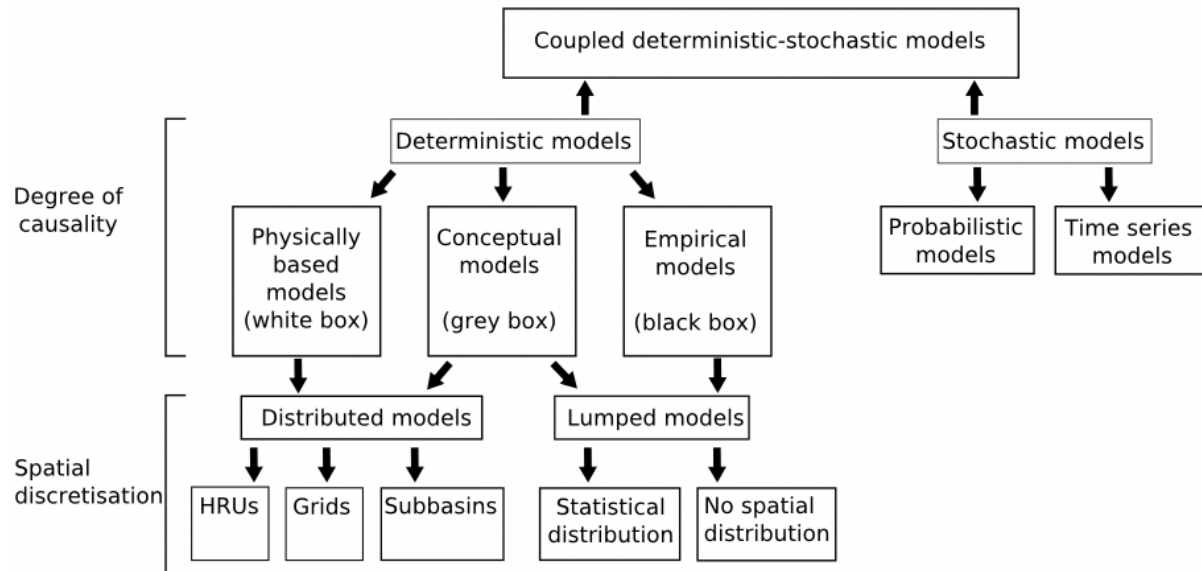


Fig. 4.1 Classification of hydrological models (modified from Dyck & Peschke (1995)).

There exist deterministic and stochastic hydrological models. Deterministic models can be physically-based, conceptual or empirical, depending on the degree of understanding of the processes involved in the equations. Conceptual models are theory-driven, while empirical models, e.g., regression models, are only based on observations and experiments. Although physically-based models contain the highest degree of process understanding, they often include empirical process descriptions, like Darcy's law or the roughness-velocity relationship of Mannings (De Roo 1993). Hydrological models are termed distributed, if the spatial distribution of input variables like land use or soil parameters is taken into account. In contrast, lumped models assume homogeneous input parameters. Many regional hydrological models deal with subbasins and hydrological response units (HRUs), i.e. homogeneous combinations of land use and soil information. In most cases, HRUs have no spatial representation. Such models are termed semi-distributed because the spatial heterogeneity is only captured to a certain extent. On the other hand, these models are computationally more efficient than grid-based models. Distributed models are often criticized for their high numbers of parameters, leading to large uncertainties and difficulties in handling of the model. In contrast, lumped models are simple, robust and require only a few parameters. However, if the purpose of the modelling is

to gain insight into the spatio-temporal pattern of hydrological processes, to ensure transferability in space and time and to perform long-term simulations and scenario analysis, complex models are indispensable. Finally, hydrological models can be time-continuous or event-based. Event-based models represent single runoff events without considering periods without runoff.

4.2. Soil erosion models

Soil erosion modelling emerged with the empirical universal soil loss equation (USLE). The USLE was developed at the US Department of Agriculture (USDA) in 1965 and updated and republished in Wischmeier & Smith (1978). The equation is based on small plot studies in the eastern Rocky Mountains and delivers long-term estimates of average annual sheet erosion. The USLE is widely applied throughout the world. However, the equation has several deficiencies, due to its empirical character and lack of integration of deposition and wind and gully erosion. Therefore, sediment yield can only be calculated indirectly by multiplication with the sediment delivery ratio. Furthermore, the USLE is not suitable for single events or single years (Dickinson & Collins 1998) and often underestimates soil loss, especially for extreme events. Some limitations have been overcome by replacing the rainfall erosivity factor by more complex terms (e.g., MUSLE, RUSLE). For example, De Roo (1998) combined the wetness index, the stream power and the sediment transport capacity with the USLE to estimate erosion risk.

The SLEMSLA model, which is an adaptation of the USLE to South African conditions, considers the seasonal rainfall energy, intercepted rainfall energy, soil erodibility, slope length and slope to estimate soil loss from sheet erosion between contour ridges (Dickinson & Collins 1998). The MUSLE is a common component of semi-physically based erosion models like CREAMS/GLEAMS, HSPF, SEDNET, EPIC, SWRRB and SWAT (see Table 4.1). In the last 15 years, a new generation of erosion models like WEPP and MEDALUS/MEDRUSH have evolved, completely replacing the USLE and its modifications with physically-based process descriptions. However, such models are very parameter-intensive.

Most time-continuous erosion models run on a daily time-step and are applicable to hillslopes or small catchments (see Table 4.1). Only a few models, namely SWRRB,

SWAT and Medrush, are also applicable to large catchments. Continuous simulations are essential for long-term studies focusing on sediment yields and the effects on crop yield. Therefore, event-based models are not shown in Table 4.1, but are listed for completeness: ANSWERS/MODANSW, KINEROS2, EROSION3D, EUROSEM, EUROWISE (LISEM-gullies), WASCH, SMODERP, GUEST and PEPP. Merrit et al. (2003), De Roo (1998) and Borah & Bera (2004) reviewed the most common erosion models.

Table 4.1 Overview of time-continuous, (semi-)physically-based erosion models (composition from Merrit et al. (2003), De Roo (1998), Bronstert & Plate (1997)).

Erosion model	Application	Time scale	Spatial scale	Sediment
SWAT (Soil and Water Assessment Tool)	Hydrology, sediment, nutrients and pesticides	Continuous; daily/subdaily	Catchment; HRUs	MUSLE
SWRRB (Simulator for Water Resources in Rural Basins)	Water balance and hydrology and sedimentation	Event or continuous; daily	Catchment, HRUs	MUSLE
MEDRUSH	Hydrology, erosion	Continuous; daily/hourly	Catchment	mainly physically-based
WEPP (Water Erosion Prediction Project)	Hydrology, erosion	Event or continuous; daily	Hillslope, catchment; grid	mainly physically-based
LISEM (Limburg Soil Erosion Model)	Hydrology, erosion	Event or continuous	Small catchment; grid	mainly physically-based
HILLFLOW 3-D	Hydrology, erosion	Continuous; daily/subdaily	Hillslope, small catchment	mainly physically-based
OPUS	Hydrology, erosion	Event or continuous, daily/subdaily	Hillslope	MUSLE or physically-based
AGNPS (Agricultural Non-point Source Pollution)	Hydrology, erosion, nutrients and pesticides	Event or continuous; daily	Field; grid/HRUs	RUSLE, HUSLE for delivery ratio, deposition
CREAMS (Chemical, Runoff and Erosion from Agricultural Management Systems)	Hydrology, erosion, nutrients and pesticides	Event or continuous; daily/subdaily	Hillslope	USLE, sediment transport capacity
EPIC (Erosion-Productivity Impact Calculator)	Hydrology, erosion, nutrients, crop/soil management, economics	Event or continuous; daily	Field	USLE, MUSLE

4.3. Application of erosion models in the tropics

Erosion modelling studies in the tropics are limited. Most model applications in developing countries use modifications of the empirical USLE combined with a GIS approach to identify hotspots of soil erosion (e.g., Dickinson & Collins, 1998; Igwe, 1999; Gobin et al., 1999; Fistikoglu & Harmancioglu, 2002). Only a few authors have

applied more complex erosion models like SWAT (e.g., Tripathi et al., 2003; Jayakrishnan, 2005) or WEPP (e.g., Leon, 2005; Larose et al., 2004).

Applications of SWAT

In the following, a broad overview of applications of the SWAT model dealing with hydrological and sediment processes and/or climate and land use change is provided. The focus is not restricted to applications in the tropics, as studies in this area are rare and often limited. Gassman et al. (2006) and Gassman et al. (2007) presented comprehensive overviews of the complete body of SWAT applications. More specific reviews can be found in Arnold & Fohrer (2005) and Jayakrishnan (2005).

Gassman et al. (2007) have classified more than 250 peer-reviewed published SWAT-related articles into the categories of hydrologic assessments, climate and land use change studies, pollutant load assessments, model comparison, model interface, sensitivity analysis and calibration techniques. Beyond these, SWAT has been applied to a wide variety of very specific questions, including, for example, canal irrigation, grazing studies, flood retarding structures and models coupled with groundwater, as well as economic and ecological models. The number of SWAT applications worldwide has been growing quickly over the last years due to the numerous advantages of the model (see Section 5.3). Nevertheless, most applications are limited to hydrological studies of catchments in temperate climate regions of the United States and Europe. In Europe, many applications are related to water quantity and water quality issues in the context of the EU water framework directive (e.g., Van Griensven & Bauwens, 2005; Krysanova et al., 2005). In the last decade, several projects of the EU, like CHESSE, EUROHARP and tempQsim, applied the SWAT model (Gassman et al. 2007). In the United States, the major focus is the impact of best management practices on sediment and nitrogen losses (e.g., Chaplot et al., 2004; Vache et al., 2002; Gitau et al., 2004; Kirsch et al., 2002; Atwood, 2001; Santhi et al., 2006; Bracmort et al., 2006). Although the majority of SWAT applications only consider stream flow, sediment flows have also been studied in the United States (e.g., Rosenthal & Hoffman, 2000; Srinivasan et al., 1998; Saleh et al., 2000; Santhi et al., 2001; Benaman & Shoemaker, 2005; White & Chaubey, 2005; Cotter et al., 2003; Hanratty & Stefan, 1998; Kirsch et al., 2002; Muleta & Nicklow, 2005) and in India (Tripathi et al., 2003; Tripathi et al., 2005). Most

of these studies confirmed the robustness of SWAT in predicting stream and sediment flows at different catchment scales (Gassman et al. 2007). However, some difficulties in representing stream and sediment flows were reported (e.g., Benaman & Shoemaker, 2005; Muleta & Nicklow, 2005). Benaman & Shoemaker (2005) explained the strong underestimation of sediment loads in the winter by limitations in SWAT for simulating erosion caused by snowmelt. Muleta & Nicklow (2005) attributed their rather poor results for model validation to a relatively short calibration period of less than three years. The high uncertainties in sediment prediction were reflected by the wide 95% confidence limits, with the upper bound exceeding the lower bound by a factor six (Muleta & Nicklow, 2005).

Many authors have also addressed climate or land use changes. Climatic inputs are derived from historical climate trends, downscaled GCM projections (e.g., Limaye et al., 2001; Krysanova et al., 2005; Hanratty & Stefan, 1998; Takle et al., 2005; Thomson et al., 2003; Varanou et al., 2004) or nested regional climate models (e.g., Stone et al., 2001; Giorgi et al., 1998). Only a few climate change studies have focused on sediment flows (e.g., Nearing et al., 2005; Hanratty & Stefan, 1998; Boorman, 2003; Varanou et al., 2004; Sintondji, 2005). Spatially explicit scenarios of future land use change have mainly been performed in Germany (e.g., Fohrer et al., 2001; Fohrer et al., 2005; Hattermann et al., 2003; Haverkamp, 2000; Volk & Schmidt, 2003; Krysanova et al., 2005).

Several authors have investigated the effects of spatial discretisation and the quality of input data on the model output. In most studies, flow predictions are insensitive to the spatial discretisation. In contrast, sediment yield is often sensitive (e.g., Bingner et al., 1997; Manguerra & Engel, 1999; Fitzhugh & Mackay, 2000; Jha et al., 2004; Chen & Mackay, 2004). Jha et al. (2004) and Haverkamp et al. (2002) established a procedure to determine an appropriate number of subcatchments so as to reduce this effect. Chaubey et al. (2005), Cotter et al. (2003) and Di Luzio et al. (2002) identified the resolution of the digital elevation model as the most critical input parameter, followed by land use and soil data. High sensitivities to climate inputs were reported by Moon et al. (2004) and Hernandez et al. (2000). King et al. (1999) indicated a high sensitivity of model performance to the applied surface runoff estimation technique.

SWAT applications in the tropics

Only a few peer-reviewed articles about SWAT applications in developing countries have been published (e.g., Govender & Everson, 2005; Tripathi et al., 2003; Jayakrishnan et al., 2005; Schuol & Abbaspour, 2006; Tripathi et al., 2005), although many applications have been presented in conference proceedings (see Table 4.2).

Table 4.2 Overview of SWAT applications in tropical developing countries; * peer-reviewed articles, ME Coefficient of Model Efficiency, R^2 coefficient of determination, WY water yield, SY sediment yield

Author(s)	Catchment(s)	Characteristics	Area [km ²]	Calibration			Validation		WY [mm/yr]	SY [t/ha/yr]
				timestep	R ²	ME	R ²	ME		
only stream flow										
KIM et al. (2003)	a:Yongdam, b:Bocheong (Korea)	mountainous; forest and rice, rainfall 1100-1200 mm	a: 930 b: 348	daily	0.77 0.65	0.77 0.65	0.75 0.55	0.76 0.50	691 653	-
GOVENDER & EVERSON (2005)	2 experimental catchments (South Africa)	a:grassland, b:pine forest; rainfall 1300- 1400 mm, slopes 0.25 m/m	a: 0.68 b: 1.95	daily	0.86		0.65		a: 496 b: 230	-
MUTHUWATTA (2004)	Lake Naivasha (Kenya)	mountainous, 640- 1500 mm rainfall	3200	monthly	0.66	0.54				-
SCHUOL & ABBASPOUR (2006)*	West-Africa (Niger, Volta, Senegal)		4000000	monthly		-1.16 to 0.82		-0.63 to 0.54		-
stream and sediment flow										
BARSANTI et al. (2006)	a:Taquarizinho b:Aquidauana (Brazil)	wetland with gullies, a:intensive land use, b:more natural; rainfall a:1350 mm, b:1250 mm	a: 1500, b: 15200	monthly, SY partially estimated	a:0.79 b:0.82 SY b: 0.84	a:0.61 b:0.58			a:133 b:239	a:0.19- 0.63 b:0.03- 0.07
JAYAKRISH- NAN et al. (2005)*	Sondu (W-Kenya)	mountainous, intense dairy farming	3050	monthly, only flow		-0.69		-0.08	144	
JACOBS & SRINIVASAN (2006)	Upper Tana (Kenya)	mountainous, mean annual rainfall <700- 1800 mm, sub- humid	10000	none, relative mode	-	-	-	-	-	-
NDOMBA (2006)	Simiyu (N-Tanzania)	flat terrain, 1100- 2000 m a.s.l., rainfall 1000 mm, pasture and fields	10659	daily, only flow		0.58			78	0.52
LAWAL et al. (2004)	Zagbo (S-Benin)	rainfall 1000 mm, plateau, mainly fields and fallows	56	none	-	-	-	-		0.6-2.7
MACHADO & VETTORAZZI (2003)	Ribeirao dos Marins (Brazil)	pasture and fields	60	monthly, only sediment	0.92	0.83				0.02-17 per subbasin
SINTONDI (2005)	Terou (N-Benin)	lowlands, mainly savannah, sub- humid, 1150 mm	2336	monthly (weekly), only flow	0.73 (0.66)	0.7 (0.62)	0.70	0.60	245	4.3
TRIPATHI et al. (2003)*, TRIPATHI et al. (2005)*	Nagwan (E-India)	1300 mm rainfall; rice and grassland, mean slope 2.3%, sub-humid	90	daily			0.91, SY 0.89	0.87, SY 0.89	144 to 468 per subbasin	4; 1.7 to 19 per subbasin

Many studies must be considered as preliminary and often show severe limitations or unsatisfying simulation results due to limited data availability. For example, some authors report using only one uniform soil type for the whole catchment (e.g., Ndomba, 2006) or a lack of sediment data (e.g., Jayakrishnan et al., 2005;

Ndomba, 2006) and stream flow data for model calibration and validation (e.g., Jacobs & Srinivasan, 2006). A coarse 1 km-DEM (e.g., Jayakrishnan et al., 2005; Ndomba, 2006) and very limited rain gauge data (e.g., Jayakrishnan et al., 2005; Muttuwatha, 2004) are common. As a consequence, many authors only focus on monthly and yearly model output (see Table 4.2). Most applications in developing countries focus on large river catchments of 300 to 10000 km², although a few studies deal with catchments smaller than 100 km² (e.g., Machado & Vettorazzi, 2003; Lawal et al., 2004; Govender & Everson, 2005; Tripathi et al., 2003).

While some authors only consider streamflow, most authors also address sediment flows (e.g., Jacobs & Srinivasan, 2006; Ndomba, 2006; Lawal et al., 2004; Machado & Vettorazzi, 2003; Sintondji, 2005; Barsanti et al., 2003; Tripathi et al., 2003). However, calibration and validation of the sediment budget have been conducted only by Machado & Vettorazzi (2003), Tripathi et al. (2003), and Barsanti et al. (2003).

Identification of erosion-prone subbasins so as to implement the best management practices was the major focus of several studies (e.g., Tripathi et al., 2003; Lawal et al., 2004; Sintondji, 2005; Ndomba, 2006). In contrast to many European and North American studies, the main indicator is not the water quality itself, but the sediment yield as a measure of the degradation of soil and land resources. Therefore, so-called soil loss tolerances play an important role in many studies. Studies of land use change often refer to the past, since spatial information about future land use is lacking (e.g., Barsanti et al., 2003; Lawal et al., 2004). Other authors conduct reforestation scenarios (e.g., Jacobs & Srinivasan, 2006) or plant management scenarios (e.g., Kim et al., 2003; Tripathi et al., 2005) in order to reduce surface runoff and sediment yield. For example, Tripathi et al. (2005) obtained reductions in sediment yield up to 20% in the sub-humid Nagwan watershed in East India for management scenarios combining zero tillage and chemical fertiliser compared to conventional ploughing. Jacobs & Srinivasan (2006) simulated reductions of the sediment yield up to 7% in the Masinga reservoir supplied by the Upper Tana catchment in Kenya after full reforestation up to 1850 m above sea level.

Climate and land use changes have been addressed together only by Sintondji (2005) and Busche (2005) in the framework of the IMPETUS project. Their scenario calculations in the Terou-Igbomakoro catchment in Benin are based on results from the regional climate model REMO and the land use/land cover change

model CLUE-S. Climate change impact studies with the SWAT model remain rare in developing countries.

Except for Jayakrishnan et al. (2005) and Schuol & Abbaspour (2006), model results were satisfactory for all the above-mentioned studies. However, runoff peaks are not always well matched (e.g., Ndomba 2006). Govender & Everson (2005) reported better model performance in dry years than in wet years and difficulties in adequately simulating the growth of mature pine plantations.

Most applications of the SWAT model have so far been conducted in the United States and Europe. However, the user community in developing countries is evolving quickly, in particular in China and India. Although many of these applications have not yet appeared in peer-reviewed journals, they can be frequently found in the proceedings of SWAT conferences (e.g., Yang et al., 2006; Jirayoot & Trung, 2006; Hao et al., 2006; Sen & Banerjee, 2005; Lee et al., 2006). In the long run, this development will hopefully lead to an improved understanding of the capabilities of the SWAT model in regions with scarce and low-quality data and to an extension of the SWAT user databases to tropical soils and land use types.

5. METHODS

This chapter summarizes the methodologies applied in this study. Special attention is given to soil investigations and the modelling procedure. Figure 5.1 shows the different components of this study and their interactions.

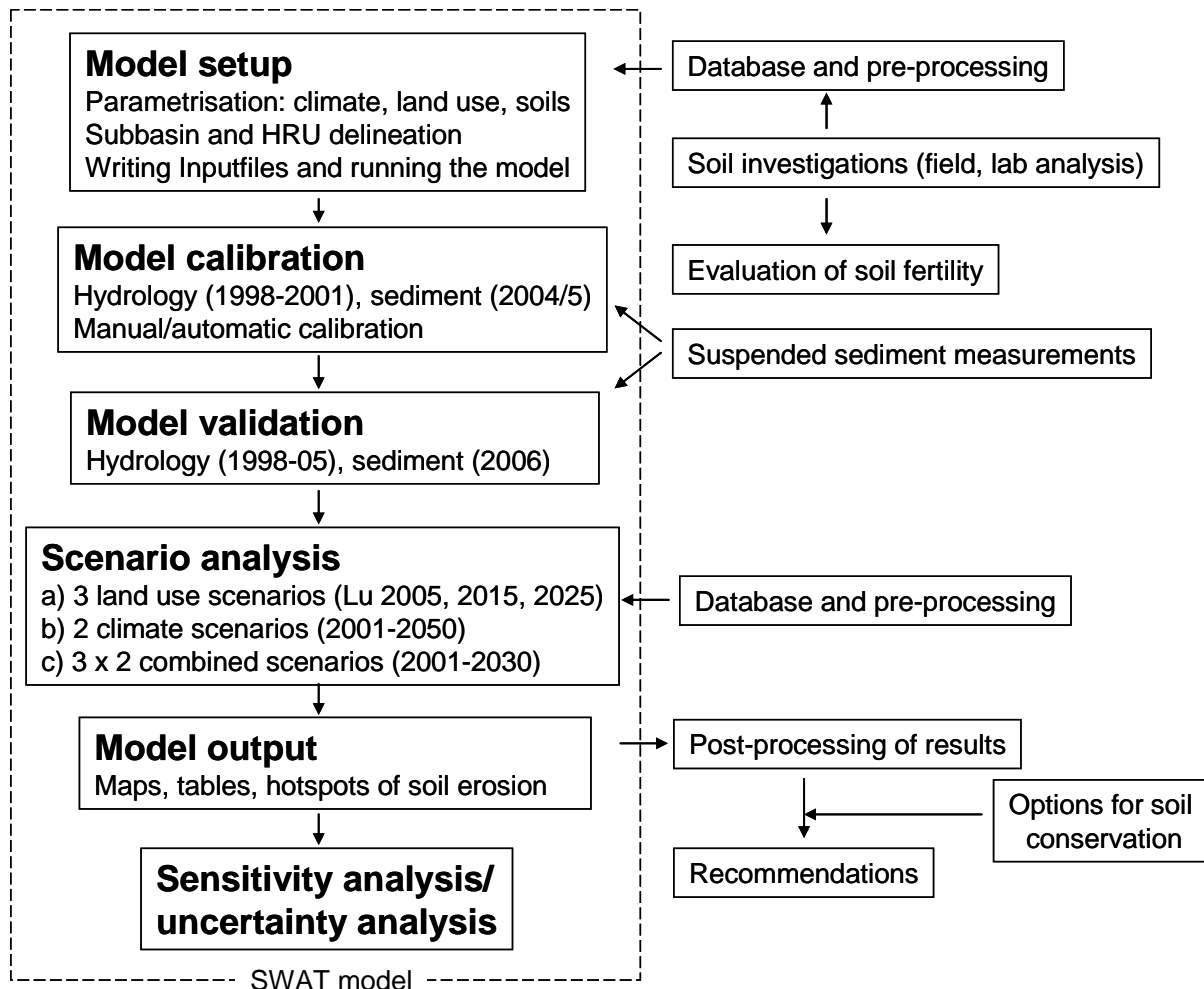


Fig. 5.1 Flowchart of the components of this study and their interactions.

The modelling procedure, namely model setup, model calibration and validation and the scenario analysis, form the central part of the methodology. However, field investigations were necessary for three purposes: (1) soil investigations to parameterise the soil map, (2) measurements of suspended sediment concentration for model calibration and validation and (3) a study of soil conservation activities in Benin to facilitate recommendations in combination with modelling results.

5.1. Soil investigations

A soil survey was conducted in the Upper Ouémé catchment because physical and chemical soil properties for the soil units of the French soil map (Dubroeuq, 1977a/b; Faure, 1977a/b; Viennot, 1978) were only partially available. Sintondji (2005) and Junge (2004) have provided soil properties for the western part of the research area, the subcatchments Terou-Wanou and Aguima. Representative profiles for the remaining 19 soil units were investigated in the framework of this study.

Soil descriptions in the field

Several augerings were performed in each soil unit along a topo-sequence in order to identify a representative profile. All augerings were described according to the Guidelines for Soil Description (FAO 1990) and the German Soil Mapping Tutorial (AG Boden 1994). Mixed soil samples were taken from each horizon. Subsequently, one representative profile for each topo-sequence was derived, and, in these locations, soil profiles of 1.20 to 1.80 meter depth were excavated. After a detailed description of the profiles, soil samples were taken from each horizon.

Figure 5.2 indicates the locations of all 34 representative profiles in the Upper Ouémé catchment. Due to poor infrastructure, most profiles are located close to main roads. Details of the characteristics of the soil units are provided in Chapter 6 including a list of the names and fractions of the soil units displayed in Fig. 5.2. Photos of the 19 representative profiles can be found in Fig. A.2 in Appendix A. Except for soil units 3 and 62, all profiles were derived from 3 to 7 augerings along the topo-sequence. Transect investigations by Sintondji (2005) were not included in Fig. 5.2 because only the representative profiles are documented.

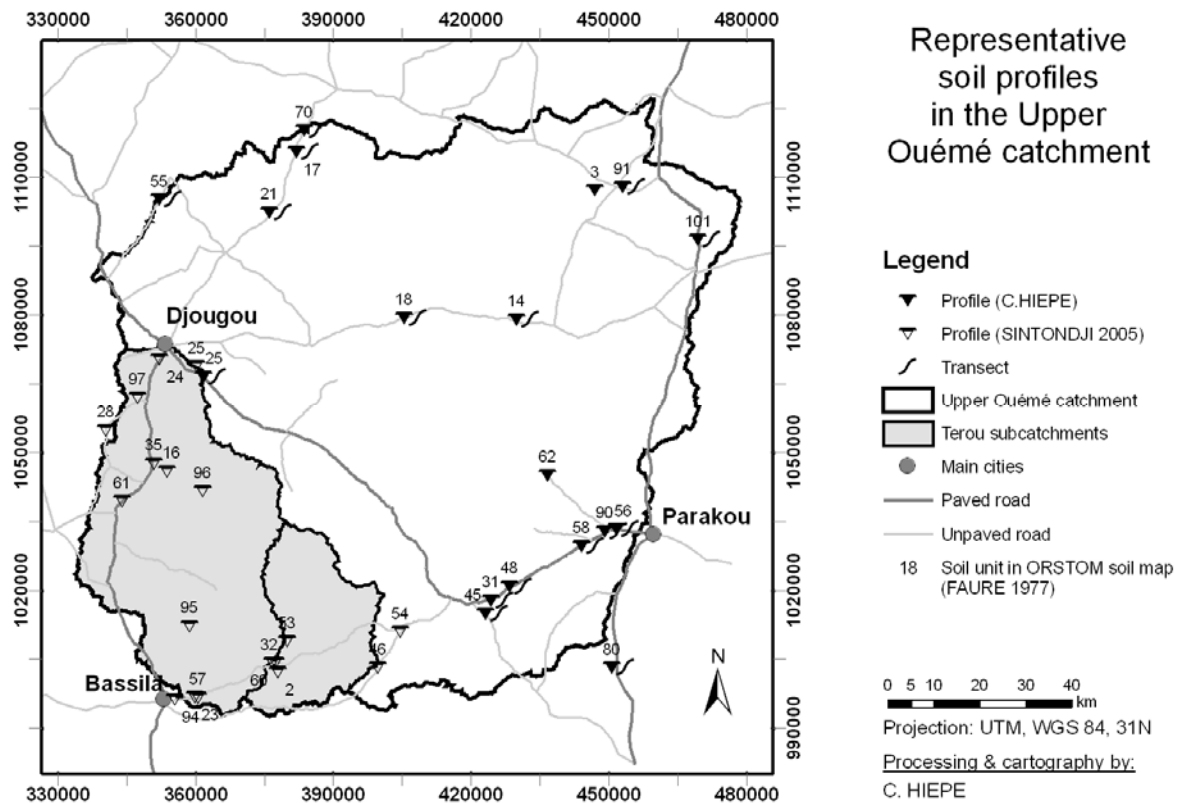


Fig. 5.2 Locations of investigated transects and representative profiles.

Laboratory analysis

The soil samples were oven-dried at 105°C and sieved with a 2 mm sieve to separate coarse and fine soil fractions. The samples were analysed at the Institute of Geography in Bonn (Germany) following the Procedures for Soil Analysis (Van Reeuwijk 1995) to classify the soils according to the World Reference Base for Soil Resources (FAO-ISRIC-ISSS 1998) and to guarantee comparability with earlier investigations from Junge (2004) and Sintondji (2005).

During the laboratory analysis, the following parameters were determined: organic carbon (C_{org}), soil texture, pH, organic nitrogen, cations (K, Ca, Na, Mg), base saturation (BS) and potential cation exchange capacity (CEC_{pot}). Laboratory methods are listed in Table 5.1. Because the inorganic carbon and nitrogen contents were of minor importance, the C/N-ratio was calculated as the quotient of organic carbon and organic nitrogen content. A comparative laboratory analysis of Junge (2004) showed good agreement between the calculated C/N-ratios and the analysis results via C/N-analyser.

Table 5.1 Determined parameters and applied laboratory methods.

Parameter	Laboratory method
C_{org}	Ashing according to LICHTERFELD: 2g soil treated with Potassium-Bi-Chromate
pH	Potentiometric measurement in a solution of 10g soil and 25ml 0.01 M $CaCl_2$
Texture	If $C_{org} > 3\%$ destruction with H_2O_2 , dispersion with $Na_4P_2O_7$, wet-sieving and pipette analysis (Koehn procedure)
Organic Nitrogen	According to KJIELDAHL
Cations (Na,K,Mg,Ca)	a) Ammonium Acetate Method (AA): 5g soil with 100ml 1 M NH_4 -OAc percolated at pH 7 (according to THOMAS) b) Mehlich: 10g soil with 100 ml $BaCl_2$ percolated at pH 8.1 Subsequently, measurements of cation concentrations in the percolate via Atom Absorption Spectrometer (AAS)
CEC_{pot}	a) AA: Following the extraction of basic cations re-exchange with 200ml 0.9 M Na-Acetate/0.1 M NaCl solution and Ethanol (80%), spectral-photometric measurement of the NH_4 -concentration in the extract (according to KEENEY and NELSON) b) Mehlich: Following the extraction of basic cations re-exchange with $MgCl_2$ -solution and measurement of the Ba-concentration in the extract via AAS

The base saturation BS as a percentage of the sum of exchangeable bases of CEC_{pot} was derived as follows:

$$BS [\%] = \frac{\Sigma Ca + Mg + K + Na [cmol_c kg^{-1} soil]}{CEC_{pot} [cmol_c kg^{-1} soil]} \cdot 100$$

CEC_{pot} values were determined by the percolation procedure of the Ammonium Acetate Method (Van Reeuwijk 1995). A comparative analysis with the German standard method (Mehlich) was performed (see Excursus 5.1). The obtained CEC_{pot} values were referred to the clay content of the soil, as this parameter is needed for classification according to the World Reference Base (Eq. 5.1). In order to eliminate the portion of organic carbon from the measured cation exchange capacity, the CEC_{pot} value was further reduced by 3.5 $cmol_c$ per percent C_{org} according to Klamt & Sombroek (1988) (Eq. 5.2-5.4).

$$CEC_{pot} [cmol_c kg^{-1} clay] = \frac{CEC_{pot} [cmol_c kg^{-1} soil]}{clay [\%]} \cdot 100 \quad (5.1)$$

$$CEC_{potsoil (clay fraction)} = CEC_{potsoil} - CEC_{potsoil (C_{org} fraction)} \quad (5.2)$$

$$CEC_{potsoil (C_{org} fraction)} = 3.5 \cdot C_{org} [\%] \quad (5.3)$$

Excursus 5.1: Comparison between Mehlich Method and Ammonium Acetate Method (AA) for determining CEC_{pot} , cations and BS

Many methods exist for measuring cation exchange capacity. Some methods use buffered solutions such as Ammonium Acetate at $pH = 7$ (Ammonium Acetate Method) or Barium chloride at $pH = 8.2$ (Mehlich Method). Iron and aluminium oxides, kaolinitic clays and organic matter have variable charges that depend on the pH and ionic strength of the reagent. Therefore, measured CEC values may be highly sensitive to the method (Ciesielski 1997). This can severely affect fertiliser recommendations from different soil-testing programs (Wang et al. 2004). Although the AA Method is widely used internationally and also recommended by Van Reeuwijk (1995), the buffered pH value of the method is often inappropriate, e.g. for acid soils (Ciesielski 1997). In this study, the German standard method (Mehlich Method) was compared with the Ammonium Acetate Method according to Van Reeuwijk (1995). For the AA method, the official percolation procedure was slightly modified in order to simplify handling and speed up the procedure. Instead of a percolation tube, a hopper was filled with wadding and quartz sand (Fig. 5.3).

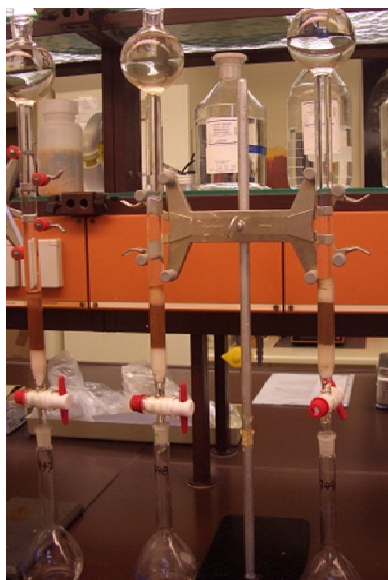


Fig. 5.3 Percolation tube.

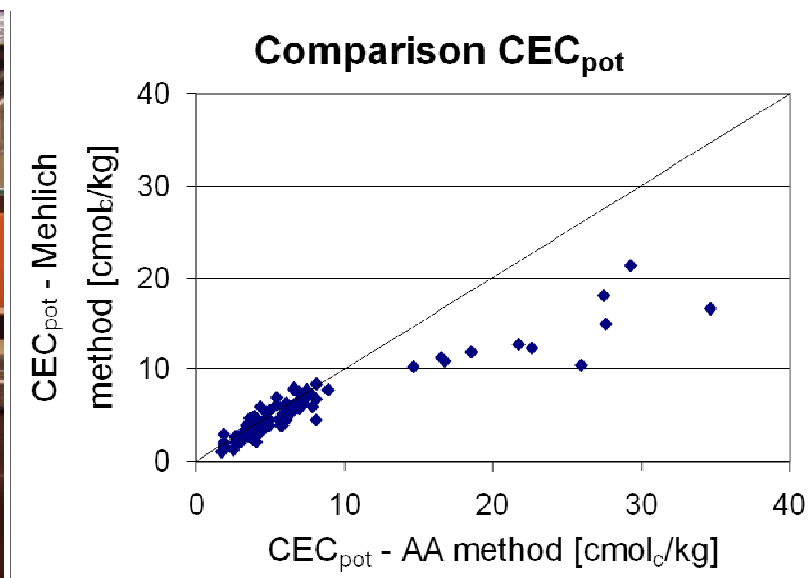


Fig. 5.4 Comparison of Mehlich and AA methods for CEC_{pot} .

First attempts with lake sand led to errors in potassium measurements because lake sand contains high amounts of potassium. Quartz sand only causes problems with sodium, which is negligible for the analysed soils. Samples with high clay contents caused no problems due to the loosening effect of the sand. For the Mehlich method,

calcium measurements were corrected if extracted non-exchangeable cations caused base saturations higher than 100%. Figure 5.4 shows the result of the comparison. For 27 out of 35 samples, CEC_{pot} values for both methods correlate quite well (R^2 0.79, deviations +/-20%). However, for the eight clay-rich samples with CEC_{pot} values higher than 10 $cmol_c$ per kg, Mehlich delivers much lower values. This difference was even stronger if samples were centrifuged instead of percolated for the AA method. The AA method is probably more efficient in extraction due to the loosening effect of the sand. It is well known that the Mehlich method has difficulties in treating clay-rich soils. The comparison of Junge (2004) supports this explanation. For 21 sand-rich soil samples, slightly higher values were obtained with the Mehlich method (+20%). For two samples, one of them clay-rich, Junge (2004) received much lower values with the Mehlich method. Figure A.3 in Appendix A shows the comparison for the cations K, Na, Ca and Mg. For sodium and magnesium, both methods correlate well with slightly higher values for the AA method. Calcium samples with CEC_{pot} values lower than 10 $cmol_c$ per kg also correlate well. However, calcium values for clay-rich samples after correction of the base saturation to 100% are more than doubled for the AA method. For potassium, the AA method underestimates Mehlich values. A systematic error during the measurements is unlikely because measurements were performed independently by two different persons. As illustrated in Chapter 6 most representative profiles show CEC_{pot} values lower than 10 $cmol_c$ per kg. Clay-rich samples with CEC_{pot} higher than 10 $cmol_c/kg$ only appear for soil profiles 21 and 29. Thus, CEC_{pot} and calcium values for these two profiles are subject to larger uncertainties than for the other profiles.

$$CEC_{pot\text{clay}(corr.)} [cmol_c kg^{-1} clay] = \frac{CEC_{pot\text{soil}(clay\ fraction)}}{clay [\%]} \cdot 100 \quad (5.4)$$

Derivation of further soil parameters

Soil erodibility K was determined using an empirical equation recommended in Wischmeier & Smith (1978) that considers soil texture, organic matter, permeability class and aggregate class:

$$K = 2.77 \cdot \frac{M^{1.14}}{10^6} \cdot (12 - S_{org}) + 0.043 \cdot (A - 2) + 0.033 \cdot (4 - D) \quad (5.5a)$$

$$M = (U + ffS) \cdot U \cdot S \quad (5.5b)$$

where

K	soil erodibility, USLE K factor [t m ² h / m ³ t cm]
U	silt [%]
S	sand [%]
ffS	very fine sand [%]
S_{org}	organic matter [%]
A	aggregate class [-]
D	permeability class [-]

Physical soil properties, namely saturated hydraulic conductivity (K_{sat}) and available water capacity, were determined with the pedo-transfer function of Rawls & Brakensiek (1995). This function requires the bulk density as input. As measurements were not available, bulk densities were estimated by a regression model derived from measured soil data from Giertz (2004) and Sintondji (2005). The parameters clay (T), silt (U), sand (S), rock fragment, C_{org} and their quadratic and cubic terms were considered as predictors. Best results for the bulk density were obtained by a stepwise, multiple, linear regression as a function of C_{org} , silt and rock fractions (Eq. 5.6). Splitting the dataset according to different soil type did not improve results.

$$Bd = 1.1712 - 0.106 \cdot C_{org} - 0.005 \cdot U + 0.005 \cdot rock \quad R^2 = 0.405 \quad \alpha < 0.01 \quad (5.6)$$

where

Bd	bulk density [cm ³ /cm ³]
C_{org}	organic carbon [%]
U	silt [%]
$rock$	rock fragment [%]

Furthermore, SWAT requires the hydrologic group according to the US Natural Resources Conservation Service (NRCS) as an input parameter to attribute the curve number. The SWAT user manual (Neitsch et al. 2000a) contains a table for deriving the hydrologic group depending on infiltration rates, profile depths and K_{sat} . In order to avoid reproducing errors in the estimation of hydraulic conductivity, in this study the hydrologic group was attributed only according to soil texture, effective soil depth

and shrink-swell potential. Table 5.2 summarizes the attribution and the selection criteria.

Table 5.2 Definition of the input parameter hydrologic group.

Hydrologic group	Infiltration rate	Applied criteria	Unit in the soil map
A	High	Sandy topsoil (Ss)	80
B	Moderate	Soil texture: Su2, Sl2, Sl3, St2	14, 16, 23, 25, 29, 31, 32, 45, 46, 48, 53-57, 62, 90, 94, 95, 96, 97
C	Slow	Soil texture: Su3, Su4, Sl4, St3, Loam Or effective soil depth < 50 cm	2, 3, 17,18, 24, 28, 35, 58, 60, 61, 70, 91, 101
D	Very slow	Soil texture: Clay	21

5.2. Measurements of suspended sediment

Suspended sediment concentrations can be measured by filtering water samples. However, this method does not allow a high temporal resolution with manageable effort. On the other hand, simple discharge-sediment relationships are problematic as they are often inaccurate due to hysteretic effects (Van Noordwijk et al. 1998). Turbidimeters seem to be a good alternative for continuously measuring sediment flows. The turbidity refers to the ability of particles to scatter incoming light, i.e., the reduction of the transparency of water caused by the presence of fine dispersive, suspended particles.

The sediment load depends on various factors, including the belowground geology, the land use and the structure of the catchment. The main sources of suspended sediment are soil particles. These are directly delivered by soil erosion or remobilised from sediment. The turbidity is also influenced by the nutrient situation in the water body regulating the development of algae or the presence of organic particles. As a consequence of this complexity, site-specific relationships between turbidity and suspended sediment concentration must be derived from filtered water samples. However, robust relationships cannot always be identified (e.g. Riley 1997).

In the present study, three multi-parameter probes type YSI 600-04, including a turbidity sensor YSI 6136 with wipers, were installed at three outlets in the Upper Ouémé catchment in April 2004 (Fig. B.1, Appendix B). Two were installed at the outlets of the Terou-Igbomakoro and the Donga-Pont subcatchments, while the third

was mounted at the Lower Aguima outlet. In 2006, the turbidity probe from the Lower Aguima was moved to Donga-Kolonkonde because permanently low water levels and sedimentation processes in the river bed complicated measurements. The Donga-Kolonkonde subcatchment (105 km²) was of special interest because it covers one of the most degraded areas in the Upper Ouémé catchment.



Fig. 5.5 Turbidity probe after installation in the river bed

Turbidity, electrical conductivity, water temperature and water level were recorded automatically each 30 minutes at outlets Terou-Igbomakoro, Donga-Pont, Lower Aguima and Donga-Kolonkonde. Once a month the probes were cleaned, batteries were changed and if necessary, the heights of the probes were adjusted. In order to avoid accumulating stones and mud in the probe cages, the instruments were covered by cages.

For each gauged site, a specific relationship between turbidity and suspended sediment concentration (SSC) was determined via linear regression analysis (see Chapter 7, Fig 7.3). Between 69 and 87 1.5 litre water samples were taken at each site for gravimetric determination of SSC values using a fluted filter with a diameter of 110 mm. In addition, suspended sediment concentrations were measured daily at the river Ouémé in Beterou by manual water sampling and subsequent filtration of the water samples.

5.3. Erosion modelling with SWAT and scenario analysis

For this study, the model SWAT (Soil Water Assessment Tool) was chosen. SWAT fulfils the following criteria:

- time-continuous, also suitable for long simulation periods
- spatially differentiated (semi-distributed)
- applicable to large-scale catchments (regional scale >10.000 km²)
- GIS interface
- manageable demand of input parameters
- freely available, widespread user group, sufficient documentation and support
- partly process-based, not completely empirical

Most descriptions of erosion processes in SWAT are based on empirical relationships like the USLE factors. However, real process-based erosion models like WEPP or Erosion3D are not yet applicable for large-scale catchments. In this study, the model version SWAT2005 was used in combination with the User Interface AVSWATX.

5.3.1. Model description

The SWAT model was developed at the United States Department of Agriculture (USDA) for studying long-term impacts of climate, land use and agricultural management on water quality and quantity (Arnold et al. 1998). It includes elements of several other models, like CREAMS (hydrology), GLEAMS (pesticides), EPIC (crop growth), ROTO (routing) and QUAL2E (in-stream kinetics) (Gassman et al. 2007). The SWAT model allows the simultaneous simulation of hundreds of subbasins. It includes databases for plant growth, tillage, pesticides, fertiliser, urban areas and soils, mainly for North American conditions. Conservation practices like terracing, strip-cropping, contouring and conservation tillage can also be considered in the model. Furthermore, SWAT contains a daily and sub-daily weather generator (WXGEN). Like the models AGNPS and ANSWERS, SWAT is loosely coupled to a GIS via an ArcView User interface (De Roo 1998). As mentioned above, the model has several advantages: SWAT is a computationally efficient, semi-distributed, time-continuous model that is applicable to large catchments. The SWAT model is a very flexible and robust tool that can be used to simulate a variety of catchment problems (Gassman et al. 2006).

Gassman et al. (2006) summarized various adaptations of the SWAT model to provide an improved simulation of specific processes. Among them are ESWAT (Van Griensven & Bauwens 2005) with enhanced in-stream kinetics, SWIM (Krysanova et al. 2005), and SWAT-G (e.g. Lenhart et al. (2005)) with several modifications for low mountains catchments. Moreover, several interface tools have been developed; first SWAT/GRASS, later ArcView-SWAT (AVSWAT) for SWAT2000 and AVSWATX for SWAT2005 and recently an ArcGIS interface (ArcSWAT) and a MapWindow Interface (MWSWAT). Further interface tools, like AGWA (www.tucson.ars.ag.gov/agwa/), IOSWAT (Haverkamp 2005), i-SWAT (Gassman et

al. 2003) and VizSWAT, have been developed to support input generation, output mapping and execution of SWAT simulations.

The main new features of SWAT2005 compared to SWAT2000 are a sub-daily precipitation generator, automatic calibration, uncertainty analysis and tree growth.

SWAT consists of seven model components: hydrology, weather, sedimentation, soil temperature, crop growth, nutrients and pesticides. Table 5.3 provides a brief overview of the process descriptions of the model components of hydrology, sedimentation, crop growth and channel routing.

In the following, the descriptions of the components hydrology and sediment in the SWAT Theory Manual (Neitsch et al. 2002b) are summarized, as they are of particular importance for this model application.

Hydrology component

Figure 5.6 illustrates the components of the hydrologic cycle. The hydrology component of SWAT is based on the water balance equation (Eq. 5.7a/b). Runoff amounts are predicted for each subbasin and then routed to the channel.

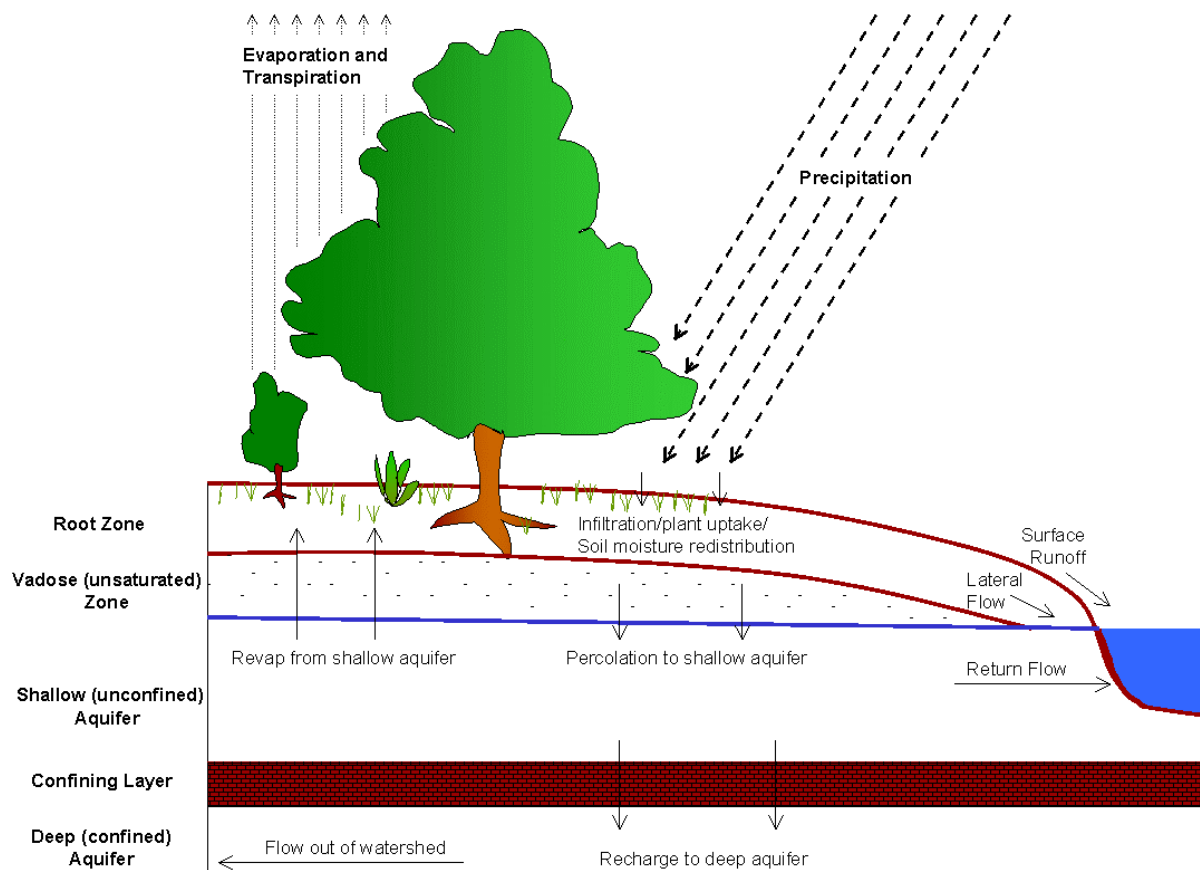


Fig. 5.6 Schematic representation of the hydrologic cycle in SWAT (Neitsch et al., 2002b).

$$R = ET_a + Q_{surf} + Q_{lat} + Q_{base} + \Delta s \quad (5.7a)$$

$$Q_{base} = \text{Recharge} - \text{revap} - \text{return flow} - \text{water use} - \text{deep recharge} \quad (5.7b)$$

where

R rainfall [mm]

ET_a actual evapotranspiration [mm]

Q_{surf} surface runoff (e.g. Hortonian, saturated, ex-filtration) [mm]

Q_{lat} lateral flow [mm]

Q_{base} baseflow, shallow aquifer storage [mm]

Δs storage, change in soil water content [mm]

Surface runoff

SWAT provides two methods for estimating surface runoff: the SCS curve number procedure (Soil Conservation Service 1972) and the Green & Ampt infiltration method (Green & Ampt 1911). The Green & Ampt method requires hourly rainfall data.

In this study, the SCS curve number method was chosen. As a result, Q_{surf} is estimated as a function of daily rainfall, initial abstractions and a retention parameter:

$$Q_{surf} = \frac{(R_{day} - I_a)^2}{(R_{day} - I_a + S)} \quad (5.8)$$

where

Q_{surf} surface runoff [mm]

R_{day} daily rainfall [mm]

S retention parameter [mm]

I_a initial abstractions [mm] (surface storage, infiltration prior to runoff, canopy interception), commonly approximated as 20% of S .

The retention parameter S is a function of the daily curve number CN (Eq. 5.9). Neitsch et al. (2002b) provide an overview of curve numbers for specific land use and soil characteristics. SWAT adjusts the daily curve number according to the antecedent soil moisture conditions. A default slope of 5% is assumed.

$$S = 25.4 \cdot \left(\frac{1000}{CN} - 10 \right) \quad (5.9)$$

Table 5.3 Main components of the SWAT model, process description and factors considered in the model (cursive, if not applied).

SWAT component	Process description	Considered factors
Hydrology		
Surface runoff	SCS-CN equation, <i>Green & Ampt infiltration method</i>	<i>Hourly</i> or daily rainfall, soil and land use properties
Percolation	Storage routing, travel time, up and downward flow	Available water capacity, hydraulic conductivity
Lateral flow	Kinematic storage model, up and downward flow	Slope, porosity, flow length, soil water
Groundwater flow	Linear storage model, shallow and deep aquifer	
Potential evapotranspiration	<i>Priestley-Taylor</i> , Penman-Monteith or <i>Hargreaves</i>	Minimum and maximum air temperature, solar radiation, relative humidity, wind velocity
Actual evapotranspiration	Soil evaporation	Soil depth, water content
	Plant transpiration	ET _{pot} , LAI
Transmission	Lane's method	Channel dimensions, flow duration
Sediment/crop growth		
Sedimentation	MUSLE	USLE-factors, surface runoff, peak flow rate, rock fragment
Soil temperature	per soil layer	damping depth, surface and mean annual air temperature
Crop growth	Heat units concept, potential biomass	LAI as a function of heat units and biomass, water and temperature stress adjustments, harvest index
Nitrogen	Simplified N-cycle in the soil, enrichment ratio for loading function	
Phosphor	Partitioning insoluble and sediment phase, loading function similar to nitrogen	
Agricultural management	Effects on biomass and nutrient cycle	Tillage operations, fertiliser, grazing
Channel routing		
Flood routing	Manning's equation, continuity equation	Travel time, flow rate, transmission and evaporation losses
Sediment routing	Stokes Law fall velocity, SDR for each particle size	<i>River bed degradation</i> (optional)

SWAT calculates the peak runoff rate, the time of concentration for overland and channel flow, the surface runoff lag and the runoff volume for each HRU and subbasin separately. The peak runoff rate is the maximum runoff flow rate that occurs within a given rainfall event. It is an indicator of the erosive power of a storm

and can be used to predict sediment loss. The peak runoff rate is calculated using the modified rational method as a function of surface runoff, subbasin area, time of concentration and the fraction of daily rainfall during time of concentration:

$$q_{peak} = C \cdot i \cdot \frac{Area}{3.6} = \frac{Q_{surf}}{R_{day}} \cdot \frac{R_{tc}}{t_{conc}} \cdot \frac{Area}{3.6} = \frac{\alpha_{tc} \cdot Q_{surf} \cdot Area}{3.6 \cdot t_{conc}} \quad (5.10)$$

where

q_{peak} peak runoff rate [m^3/s]

C runoff coefficient [-], quotient of Q_{surf} and R_{day}

i rainfall intensity [mm/h], quotient of R_{tc} and t_{conc}

$Area$ subbasin area [km^2]

R_{tc} rainfall during time of concentration [mm]

R_{day} daily rainfall [mm]

t_{conc} time of concentration for the subbasin [h]

α_{tc} fraction of daily rainfall that occurs during the time of concentration [-]

Q_{surf} surface runoff [mm].

The time of concentration is the amount of time from the beginning of a rainfall event until the entire subbasin area contributes to flow at the outlet. It is calculated as a function of subbasin slope length, average flow channel length, overland flow velocity and the average channel velocity estimated from Manning's n. For large subbasins with a time of concentration greater than one day, SWAT incorporates a surface runoff storage feature to lag a portion of the surface runoff release to the main channel (Eq. 5.11).

$$Q_{surf} = (Q'_{surf} + Q_{stor,i-1}) \cdot \left(1 - e^{-\frac{-surlag}{t_{conc}}} \right) \quad (5.11)$$

where

Q_{surf} surface runoff discharged to the main channel on a day [mm]

Q'_{surf} generated surface runoff in the subbasin on a day [mm]

$Q_{stor,i-1}$	surface runoff stored or lagged from the previous day [mm]
$surlag$	surface runoff lag coefficient [-]
t_{conc}	time of concentration for the subbasin [h]

As $surlag$ decreases, more water is held in storage. As a consequence, the simulated stream flow hydrograph is smoothed. The peak runoff rate is corrected by transmission losses in the ephemeral channel.

Potential and actual evapotranspiration according to Penman & Monteith

SWAT offers three evapotranspiration models: the Penman-Monteith method (Monteith, 1965; Allen et al., 1989), the Priestley-Taylor method (Priestley & Taylor 1972) and the Hargreaves method (Hargreaves et al. 1985). SWAT can also read in daily ET_{pot} values if the user prefers to apply a different method. In general, ET_{pot} describes the amount of water transpired by a short green crop, completely shading the ground, of uniform height and no shortage of water. As reference crop for ET_{pot} according to Penman-Monteith, the SWAT model uses alfalfa at a height of 40 cm with a minimum leaf resistance of 100 seconds per meter. The Penman-Monteith equation is:

$$\lambda E = \frac{\Delta \cdot (H_{net} - G) + \rho_{air} \cdot c_p \cdot |e_z^0 - e_z| / r_a}{\Delta + \gamma \cdot (1 + r_c / r_a)} \quad (5.12)$$

where

λE	latent heat flux density [MJ/m ² /d]
E	depth rate of evaporation [mm/d]
Δ	slope of the saturation vapour pressure-temperature curve, de/dT [kPa/°C]
H_{net}	net radiation [MJ/m ² /d]
G	heat flux density to the ground [MJ/m ² /d]
ρ_{air}	air density [kg/m ³]
c_p	specific heat at constant pressure [MJ/kg/°C],
e_z^0	saturation vapour pressure of air at height z [kPa]
e_z	water vapour pressure of air at height z [kPa]
γ	psychrometric constant [kPa/°C]

SWAT assumes that the daily soil heat flux G is equal to zero. The aerodynamic resistance is calculated as a function of the height of wind, humidity and temperature. Furthermore, the wind speed and roughness length are considered for momentum and vapour transfer. Taking into account the reference crop, the equation for aerodynamic resistance simplifies to:

$$r_a = \frac{114}{u_z} \quad (5.13)$$

where

$$r_a \quad \text{aerodynamic resistance [s/m]}$$

$$u_z \quad \text{wind speed [m/s]}$$

The canopy resistance r_c for a well-watered reference crop can be estimated as the quotient of the minimum surface resistance for a single leaf and one-half of the canopy leaf area index:

$$r_c = r_1 \cdot (0.5 \cdot LAI) \quad (5.14)$$

where

$$r_c \quad \text{canopy resistance [s/m]}$$

$$r_1 \quad \text{minimum effective stomata resistance of a single leaf [s/m]}$$

$$LAI \quad \text{leaf area index of the canopy [-]}$$

Actual Evapotranspiration

When precipitation falls, SWAT first fills the canopy storage before any water is allowed to reach the ground. The maximum storage capacity varies as a function of LAI. SWAT first evaporates any rainfall intercepted by the plant canopy. Next, SWAT separately calculates the maximum amount of transpiration and soil evaporation using a modified approach of Ritchie (1972). Transpiration is determined as a function of LAI and ET_{pot} using equations 5.12 to 5.14. Maximum transpiration is calculated as a function of ET_{pot} , aboveground biomass, residue and two terms defining the upper and lower limits. The upper limit is defined as 80% of the plant-available water on a given day. If an evaporation demand for soil water exists, SWAT first partitions the evaporative demand between the different layers. SWAT does not allow a different layer to compensate for the inability of another layer to meet its

evaporative demand. The depth distribution used to determine the maximum amount of water allowed to be evaporated is:

$$E_{soil,z} = E_s^{ll} \cdot \frac{z}{z + \exp(2.374 - 0.00713 \cdot z)} \quad (5.15)$$

where

- $E_{soil,z}$ evaporative demand at depth z [mm]
- E_s^{ll} maximum soil water evaporation on a given day [mm]
- z depth below the surface [mm]

The coefficients in Eq. 5.15 were chosen so that 50% of the evaporative demand is extracted from the top 10 mm of soil and 95% from the top 100 mm of soil. This assumption can be modified by the soil evaporation compensation coefficient (ESCO). As the value of the ESCO is reduced, the model can extract more of the evaporative demand from lower levels.

The actual amount of transpiration in a day equals the plant water uptake for the day, which depends on the amount of water required by the plant for transpiration and the amount of water available in the soil. The depth distribution used to determine the maximum amount of water uptake from the soil surface to a depth z is:

$$w_{up,z} = \frac{E_t}{[1 - \exp(-\beta_w)]} \cdot \left[1 - \exp\left(-\beta_w \cdot \frac{z}{z_{root}}\right) \right] \quad (5.16)$$

where

- $w_{up,z}$ potential water uptake from the soil surface to a depth z [mm]
- E_t maximum plant transpiration on a given day [mm]
- z depth below the surface [mm], z_{root} rooting depth [mm]
- β_w water use distribution parameter [-]

As default, β_w is set to 10, so that 50% of water uptake will occur in the upper 6% of the root zone. This assumption can be modified by the plant uptake compensation coefficient (EPCO). As the value of the EPCO is increased, the model allows more of the water uptake demand to be met by lower layers in the soil.

Percolation

Water can flow in the soil under saturated or unsaturated conditions. SWAT records the water contents of the different soil layers but assumes that the water is uniformly distributed within a given layer. Unsaturated flow between layers is indirectly modelled with the depth distribution of plant water uptake and that of soil water evaporation (Eq. 5.15). Water is allowed to percolate if the water content of a soil layer exceeds the field capacity of the layer. The amount of water that moves from one layer to the underlying layer is calculated using the storage routing technique (Eq. 5.17).

$$w_{perc,ly} = SW_{ly,excess} \left(1 - e^{\frac{-\Delta t}{TT_{perc}}} \right) = SW_{ly,excess} \left(1 - e^{\frac{-\Delta t \cdot K_{sat}}{SAT_{ly} - FC_{ly}}} \right) \quad (5.17)$$

where

$w_{perc,ly}$	amount of water percolating to the underlying soil layer [mm]
$SW_{ly,excess}$	drainable volume of water in the soil layer [mm]
Δt	length of time step [h]
TT_{perc}	travel time for percolation [h]
SAT_{ly}	amount of water in the soil layer when completely saturated [mm]
FC_{ly}	water content of the soil layer at field capacity [mm]
K_{sat}	saturated hydraulic conductivity for the layer [mm/h]

If infiltration is explicitly modelled using the Green-Ampt approach, a crack-flow model allows bypass flow to be considered.

Lateral flow

SWAT uses a kinematic storage technique to compute subsurface flow as a function of drainable volume of water, saturated hydraulic conductivity, soil slope, hill slope length and drainable porosity, as follows:

$$q_{lat} = 24 \cdot H_0 \cdot v_{lat} = 0.024 \cdot \left[\frac{2 \cdot SW \cdot K_{sat} \cdot slp}{\phi_d \cdot L_{hill}} \right] \quad (5.18)$$

where

q_{lat}	lateral flow [mm/d]
H_0	saturated thickness normal to the hillslope at the outlet expressed as a fraction of total thickness [mm/mm]
v_{lat}	velocity of flow at the outlet [mm/h]
24	conversion factor hours to days
SW	drainable volume of soil water [mm]
slp	slope [m/m]
ϕ_d	drainable porosity [mm/mm]
K_{sat}	vertical saturated hydraulic conductivity [mm/h]
L_{hill}	hill slope length [m]

For times of concentration greater than one day, SWAT incorporates a lateral flow storage feature to lag a portion of lateral flow release to the main channel.

Groundwater flow

In each subbasin, SWAT simulates an unconfined aquifer that contributes to the flow in the main channel (shallow aquifer) and a confined, deep aquifer. Water that enters the deep aquifer is assumed to contribute to stream flow somewhere outside the catchment. Water leaves groundwater storage either by discharge into rivers and lakes, by upward movement from the water table into the capillary fringe or by seepage to the deep aquifer. Equation 5.19a shows the daily water balance for the shallow aquifer. The shallow aquifer storage is recharged by percolation from the unsaturated zone and reduced by baseflow, deep aquifer recharge, upward flows into the soil zone and withdrawal. Baseflow is implemented as a linear storage with a specific recession coefficient (cf. Eq. 5.19b).

$$aq_{sh,i} = aq_{sh,i-1} + w_{rchrg} - Q_{gw} - w_{revap} - w_{deep} - wu_{sa} \quad (5.19a)$$

$$Q_{gw,i} = Q_{gw,i} \cdot e^{-\alpha \Delta t} + w_{rchrg} (1 - e^{-\alpha \Delta t}) \quad (5.19b)$$

where

$aq_{sh,i}$	shallow aquifer storage on the day i [mm]
$aq_{sh,i-1}$	shallow aquifer storage the day before [mm]

W_{rchrg}	recharge entering the aquifer [mm]
Q_{gw}	groundwater flow or baseflow into the main channel [mm]
W_{revap}	amount of water moving into the soil zone as response to water deficiencies [mm]
W_{deep}	amount of water percolating from the shallow aquifer into the deep aquifer [mm]
WU_{sa}	water use from the shallow aquifer [mm]
α	base flow recession constant [-], describes the lag flow from the aquifer, estimation by baseflow filter techniques

Besides several specific groundwater coefficients, SWAT defines minimum thresholds for the shallow aquifer for the occurrence of return flow and water flow to the unsaturated zone or deep aquifer.

Sedimentation component

The sedimentation component of the SWAT model is based on the Modified Universal Soil Loss Equation (MUSLE). The MUSLE is a revision of the USLE where the rainfall energy factor is replaced by a runoff factor. This improves sediment yield prediction and eliminates the need for delivery ratios because the runoff factor represents the energy for detaching and transporting sediment. Furthermore, the equation can be applied to individual storm events. The equation is:

$$SY = 11.8 \cdot (Q_{surf} \cdot q_{peak} \cdot area_{hru})^{0.56} \cdot K_{USLE} \cdot C_{USLE} \cdot P_{USLE} \cdot LS_{USLE} \cdot CFRG \quad (5.20a)$$

$$CFRG = e^{(-0.053rock)} \quad (5.20b)$$

where

SY	sediment yield [t/ha]
Q_{surf}	surface runoff [mm]
q_{peak}	peak runoff rate [m ³ /s]
K_{USLE}	USLE erodibility factor [0.013 t m ² h/m ³ t cm]
C_{USLE}	USLE crop management factor [-]
P_{USLE}	USLE erosion control factor [-]

LS_{USLE}	USLE slope length factor [-]
$CFRG$	coarse fragment factor [-]
$rock$	rock fragments in the first soil layer [%]

SWAT also computes the USLE for comparison purposes. Calculations of surface runoff and peak runoff rate have already been reviewed in Eqs. 5.8 to 5.11. In the following, a short definition of the USLE factors is given.

Erodibility factor K_{USLE}

Details regarding the calculation of the K_{USLE} factor can be found in Section 5.1 and Neitsch et al. (2002a).

Cover and management factor C_{USLE}

The USLE cover and management factor C_{USLE} is defined as the ratio of soil loss from land cropped under specified conditions to the corresponding loss from a clean-tilled, continuous fallow. This factor represents the reducing effects of plant canopy and plant residue on soil erosion. Because the plant cover varies during the growth cycle of the plant, SWAT updates C_{USLE} daily using Eqs. 5.21a and 5.21b.

$$C_{USLE} = \exp\left(\ln(0.8) - \ln(C_{USLE,mm})\right) \cdot \exp\left[-0.00115 \cdot rsd_{surf}\right] + \ln\left[C_{USLE,mm}\right] \quad (5.21a)$$

$$C_{USLE,mm} = 1.463 \cdot \ln\left[C_{USLE,aa}\right] + 0.1034 \quad (5.21b)$$

where

$C_{USLE,mm}$	minimum value for C_{USLE} for the land cover [-]
$C_{USLE,aa}$	average annual value for C_{USLE} for the land cover [-]
rsd_{surf}	amount of residue on the soil surface [kg/ha]

Support practice factor P_{USLE}

The support practice factor P_{USLE} is defined as the ratio of soil loss with a specific support practice to the corresponding soil loss with up- and down-slope culture. Support practices include contour tillage, contour strip-cropping and terrace systems.

For example, values of P_{USLE} for contouring range from 0.5 to 0.6 for slopes lower than 12% and from 0.7 to 0.9 for slopes up to 25% (Wischmeier & Smith 1978).

Topographic factor LS_{USLE}

The topographic factor LS_{USLE} is the expected ratio of soil loss per unit area from a field slope to the soil loss from a 22.1 m long, 9% slope under otherwise identical conditions. The topographic factor is calculated as follows:

$$LS_{USLE} = \left(\frac{L_{hill}}{22.1} \right)^m \cdot (65.41 \cdot \sin^2(\alpha_{hill}) + 4.56 \cdot \sin \alpha_{hill} + 0.065) \quad (5.22a)$$

$$m = 0.6 \cdot (1 - e^{[-35.835 \cdot slp]}) = 0.6 \cdot (1 - e^{[35.835 \cdot \tan \alpha_{hill}]}) \quad (5.22b)$$

where

LS_{USLE}	USLE slope length factor [-]
L_{hill}	slope length [m]
m	exponential term [-]
α_{hill}	angle of the slope [-]
slp	slope of the HRU expressed as rise over run [m/m]

5.3.2. Modelling procedure

The general modelling procedure applied in this study was presented earlier (Fig. 5.1). Detailed information about each step is given in Chapter 7.

Effort was spent during model parameterisation to prepare climate and soil data (field survey, laboratory analysis, estimation of physical properties, determination of additional model parameters like erodibility and hydrologic group). Land use types from the land use map were referred to existing land use types in the SWAT crop database. Vegetation dynamics were adapted to local conditions by modifying several parameters.

After the model was set up, it was manually calibrated at two outlets (Terou-Igbomakoro, Donga-Pont). First, hydrology was calibrated at yearly and weekly time steps using daily discharge measurements, separated into slow and fast components using the baseflow filter from Arnold & Allen (1999). Then, sediment yield was calibrated at weekly and daily time steps using daily values of suspended sediment

concentration derived from turbidity measurements (see Chapter 7). Figure 5.7 shows the applied manual calibration procedure and the criteria for model evaluation. Model performance was analysed visually and with statistical measures like the coefficient of determination (R^2) and the coefficient of Model Efficiency (ME) (see Section 5.5). Explanations of the calibration parameters can be found in Section 7.1 and Neitsch et al. (2002a). The different scenarios for the scenario analysis are described in Section 7.2.

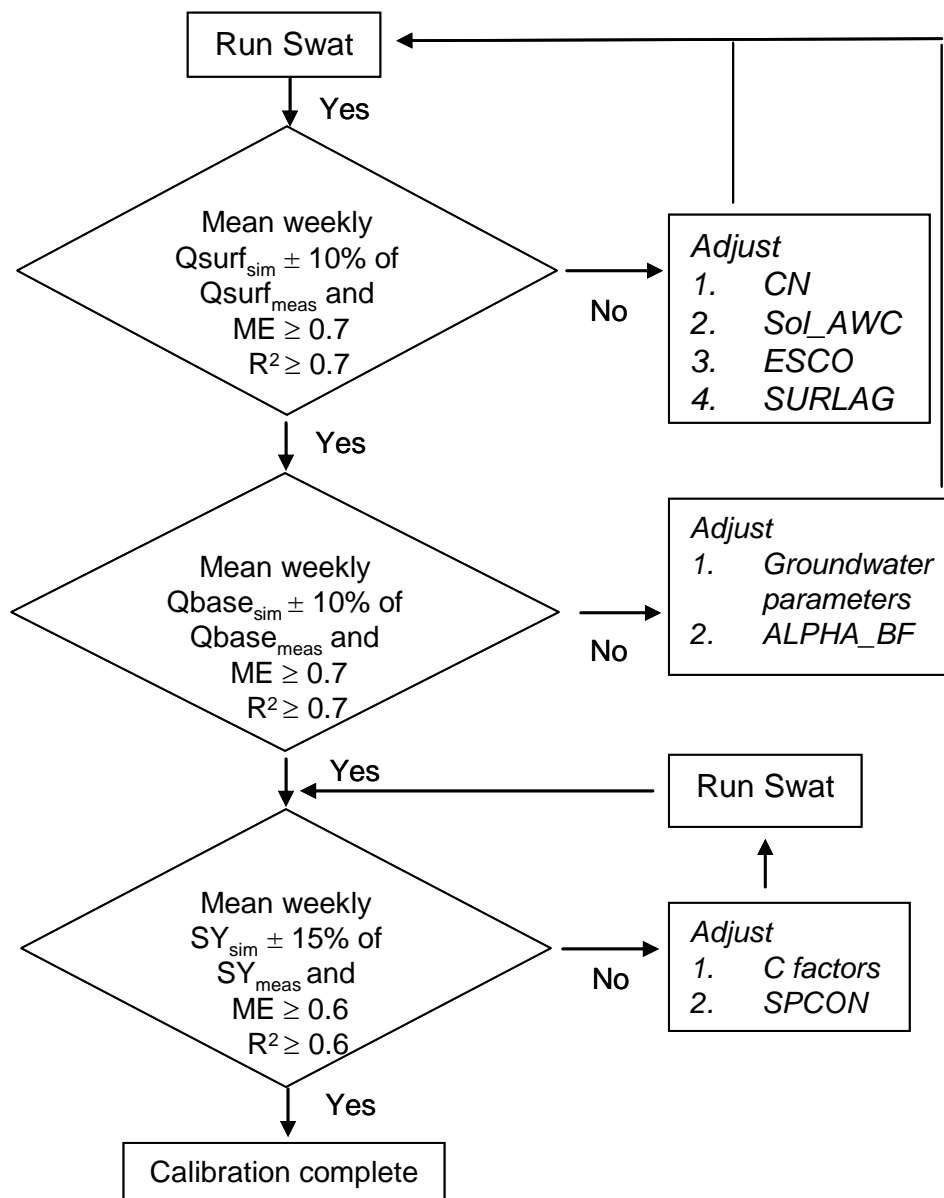


Fig. 5.7 Applied procedures for manual calibration of hydrology and sediment budget.

5.4. Sensitivity and uncertainty analyses and automatic calibration

The following explanations of the SWAT algorithms for the automatic calibration and the sensitivity and uncertainty analyses were taken from Huisman et al. (2004). The algorithms were implemented in SWAT2005 by Ann van Griensven (UNESCO-IHE, Delft).

5.4.1. Sensitivity analysis

The algorithm used in SWAT for the sensitivity analysis is called the *Latin Hypercube One-factor-At-a-Time design* (LH-OAT) and was proposed by Morris (1991). The LH-OAT sensitivity analysis combines the strengths of global and local sensitivity analysis methods. *Latin Hypercube* (LH) sampling for Monte Carlo analysis is robust and efficient. It replaces random sampling from the input distributions by a stratified sampling that better covers the sampling hypercube with fewer samples. For LH sampling, the distribution of each parameter is divided into m ranges, each with a probability of occurrence of $1/m$. Parameter tuples are then randomly generated, ensuring that each range is sampled only once (Fig. 5.8). The model is run m times with these parameter sets. The results are typically analysed with multivariate linear regression methods.

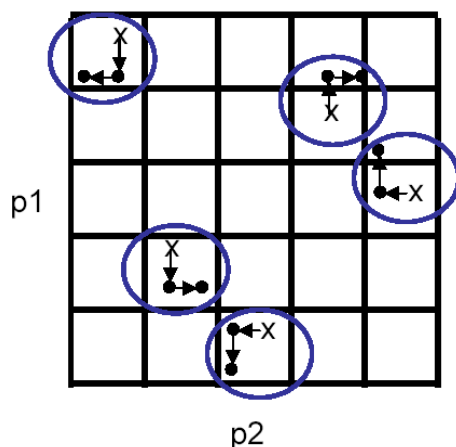


Fig. 5.8 LH-OAT sampling for a two parameter set. Initial parameters of the LH sampling (x) and the OAT points (•) are shown (from Huisman et al. 2004).

The main limitations of LH sensitivity analysis are: i) the assumption of linearity in the multivariate regression analysis, and ii) the ambiguous attribution of changes in output to individual parameters, as all parameters are changed simultaneously. The latter limitation is overcome by the *One-factor-At-a-Time* (OAT) sensitivity analysis. Using this method, each parameter is sequentially changed so that only one parameter is changed per model run. The disadvantage of the OAT design is that it measures only local sensitivities since the

sensitivity of the model output to a parameter may depend on the values of other model parameters (*partial sensitivity*). In the LH-OAT sensitivity analysis, the OAT method is repeated for each LH sampling point (Fig. 5.8). Finally, the *global sensitivity* is calculated as the average of the local sensitivities. The variance of this set provides a measure of the uniformity of the sensitivity over the entire parameter space. Thus, the LH-OAT sensitivity analysis method combines robust, efficient LH sampling, ensuring complete sampling of the parameter space, with the precision of an OAT design, allowing unambiguous attribution of changes in the output in each model run to a specific model parameter.

5.4.2. Automatic calibration

The automatic calibration algorithm in SWAT is based on the *Shuffled Complex Evolution* algorithm developed at the University of Arizona (SCE-UA).

SCE-UA is a global search algorithm that minimizes a single objective function of up to 16 model parameters. It combines the direct search method of the simplex algorithm with a controlled random search, a systematic evolution of points directed to global improvement, competitive evolution and the concept of complex shuffling. In the first step, SCE-UA selects an initial parameter set by random sampling of the parameter space. The feasible parameter range is determined by user-defined upper and lower bounds for each model parameter. After random sampling, the parameter sets are divided into several *complexes*. Each *complex* is evolved independently using the simplex algorithm. The *complexes* are periodically shuffled to form new *complexes* in order to share information gained. In this way, SCE-UA searches the entire parameter space and finds the global optimum with a high success rate. A large number of applications of the SCE-UA in calibrating hydrological models confirm the robustness, effectiveness and efficiency of the algorithm.

The results of the automatic calibration normally depend on the choice of objective function. SWAT2005 currently offers two types of objective functions: i) the sum of squared residuals (SSQ) and ii) the sum of squares of the difference between the measured and simulated values after ranking (SSQR).

The equations are:

$$SSQ = \sum_{i=1,n} (x_{i,measured} - x_{i,simulated})^2$$

$$SSQR = \sum_{j=1,n} (x_{j,measured} - x_{j,simulated})^2$$

where

n	number of pairs of measured and simulated variables (i=1 to n)
j	rank
$x_{measured}$	measured variable
$x_{simulated}$	simulated variable.

Typically, SSQ is chosen in the optimization procedure. However, this objective function focuses on matching the peaks and neglects accurate matches of lower values. In contrast, the SSQR method aims to fit the frequency distribution of the measured and simulated time series. It does not consider the time of occurrence of a given value of a variable.

5.4.3. Uncertainty analysis

The uncertainty analysis in SWAT2005 addresses the uncertainty in the calibration parameters. It uses the model runs from the automatic model calibration instead of re-running the model for a range of parameter values, as is commonly done in other algorithms for uncertainty analyses. First, the simulations are divided into 'good' and 'bad' simulations based on a threshold value c for the objective function. All simulations with a value of the objective function below this threshold are accepted as 'good' simulations. The threshold value is calculated using χ^2 -statistics. The formula for a single objective calibration using the sum of squared residuals (SSQ) is

$$c = OF(\Theta^*) \cdot \left(1 + \frac{\chi^2_{p,0.95}}{n - p} \right)$$

where

c	threshold value for the objective function
n	number of parameters

- p number of free parameters
- Θ^* optimal parameter set consisting of p free parameters ($\Theta_1^*, \dots, \Theta_p^*$)
- $OF(\Theta^*)$ minimum of the SSQ.

The parameter uncertainty can then be calculated by analyzing the properties of the accepted parameter sets.

5.5. Soil evaluation

The terms land and soil evaluation are often used in the same sense, since most land evaluation schemes focus on soil evaluation without considering socioeconomic and political components (Dorransoro 2002). Rossiter (1994) provided an overview of land evaluation methods. In general, capability and suitability classifications can be distinguished. While capability refers to a general kind of land use rather than specific land use systems, suitability includes the needs of specific crops (Rossiter 1994). Capability classifications focus primarily on determining the maximum intensity of land use consistent with low erosion risks and sustained productivity (Landon 1984). The most common capability classifications include the USDA land classification system and the Fertility Capability Soil Classification System (FCC). The FAO framework for Land Evaluation provides the basis for various evaluation schemes with a strong focus on socioeconomic conditions. Soil and terrain databases (SOTER) often form the basis for assessing land qualities. For example, Igué (2000) applied the SWEAP model (a SOTER-based program for assessing water erosion hazard) to central Benin. The semi-quantitative parametric FAO/ITC Ghent method, modified by Sys (1993), is commonly used in the tropics and sub-tropics to calculate land suitabilities for specific crops (Dorransoro 2002). Graef (1999) applied this method to south-western Niger, and Weller (2002) to southern Benin.

The Fertility Capability Classification (Sanchez et al. 2003) was applied in the framework of this study. The FCC is a technical soil classification system that groups soils according to main fertility-related soil constraints, which can be interpreted in relation to specific farming systems or land utilization types (Sanchez et al. 2003). The classification is based on topsoil and subsoil parameters. An FCC code consists of three components: (1) type, (2) substrata type (optional) and (3) modifiers

(optional) (see Table A.5, Appendix A). The FCC type describes the general texture of the surface layer (0-20 cm). The FCC subtype is used to distinguish marked textural changes between the topsoil and subsoil. Type and subtype can include a prime (') symbol to denote 15-35% gravel, or a double prime (") to denote >35% gravel. The modifiers are 13 lower-case letters, which can be used alone or in combination. They are determined from one or more diagnostic land characteristic. For example, the modifier *e* indicates a low cation exchange capacity. To obtain this modifier, a soil profile must fulfil at least one of the following criteria: (1) effective CEC <4 meq/100g soil, (2) sum of cations at pH7 < 7 meq/100g soil or (3) sum of cations, Al and H ions at pH 8.2 <10 meq/100g soil. Figure 5.9 provides an example.

The FCC code "Lehk" summarizes the following soil characteristics:

good water-holding capacity (L throughout, no primes), medium infiltration capacity (L), low ability to retain nutrients for plants (Le), deficient in bases (hk); applications of bases and N should be splitted to avoid leaching (Le), requires liming for Al-sensitive crops (h), potential danger of over-liming leading to unavailability of micronutrients (e), low ability to supply K (k) so that K-fertilizers will be required for plants needing high levels of K.

Fig. 5.9 Example of the Fertility Capability Classification (FCC).

The system has been criticized for some of its specific class limits, e.g. for the prime modifier, and the generality, which does not allow specific fertility management recommendations. Rossiter (1994) criticized the inconsistent structure of the code, where, e.g., different modifiers (*a*, *h*) are used for two intensities of the same phenomenon (soil acidity).

Nevertheless, the FCC classification can provide a lot of information about the land quality indicator 'susceptibility to erosion': the FCC classes *C_i*, *C_x* and *L_x* indicate low susceptibility due to high permeabilities, and the modifiers *v* and *bv* characterize highly-erosive soil materials. Soils with a textural change to clayey subsoils (e.g., *SC*, *LC*) or to rock (e.g., *SR* or *LR*) can degrade easily due to erosion and are susceptible to erosion if the finer-textured surface layer saturates. However, due to the general nature of the FCC classes, usually only two or three severity levels can be separated by the FCC code (Rossiter 1994).

The individual chemical and physical soil properties of the representative profiles have been evaluated according to the classification of Landon (1984). Table A.4 in Appendix A lists the different classes and thresholds.

5.6. Statistical analysis

More than one statistical test should be implemented to evaluate model performance. The coefficients of determination (r^2) and Model Efficiency (ME) are often used as statistical tests to analyse stream flow, as it is easy to compare these values with a fixed ideal reference value of one. In this study, the following indices are applied:

- Pearson coefficient of correlation (r) or coefficient of determination (r^2)
- Coefficient of Model Efficiency (ME) according to Nash & Sutcliffe (1970)
- Index of Agreement (IA) according to Willmott (1981).

The coefficient of correlation r describes the linear dependency between measured and simulated values within the range -1 to 1 (see Eq. 5.24). The index is strongly influenced by the mean value. A model that systematically over- or underpredicts will still result in good r and r^2 values.

$$r = \frac{n \cdot \left(\sum_{i=1}^n x_i \cdot x'_i \right) - \left(\sum_{i=1}^n x_i \right) \cdot \left(\sum_{i=1}^n x'_i \right)}{\sqrt{n \cdot \sum_{i=1}^n x_i^2 - \left(\sum_{i=1}^n x_i \right)^2} \cdot \sqrt{n \cdot \sum_{i=1}^n x_i'^2 - \left(\sum_{i=1}^n x'_i \right)^2}} \quad (5.24)$$

n number of variables

x_i measured variable

x'_i simulated variable

The Coefficient of Model Efficiency (ME) describes the degree of agreement between observed and simulated values (see Eq. 5.25). The ME has a range of values between $-\infty$ to 1. Negative values indicate that the goodness of the model results is lower than the mean of the observed data (Krause et al. 2005). A disadvantage of the Coefficient of Model Efficiency is the high dependency on the mean and the consideration of differences between observed and predicted values as squared values. As a consequence, larger values in a time series significantly influence the outcome. Similar to r^2 , the coefficient is not very sensitive to systematic model over- or underprediction, especially during low flow periods (Krause et al. 2005).

$$ME = \frac{\sum_{i=1}^n (x_i - \bar{x}_i)^2 - \sum_{i=1}^n (x'_i - x_i)^2}{\sum_{i=1}^n (x_i - \bar{x}_i)^2} \quad (5.25)$$

- n number of variables
 x_i measured variable
 x'_i simulated variable
 \bar{x}_i arithmetic mean of x_i ($i = 1, \dots, n$)

In general, model results with a Model Efficiency larger than 0.5 are considered satisfactory. The model yields good results for values between 0.8 and 0.9. Results are very good for values higher than 0.9 (Takle et al. 2005).

The Index of Agreement evaluates the performance of temporal characteristics of the discharge curves (see Eq. 5.26). Therefore, small time lags in observed versus simulated flow result in a significantly lower Index of Agreement (Coffey et al. 2004). The index covers a range of 0 to 1. A value of 1 indicates complete agreement between measured and simulated values.

$$IA = 1 - \frac{\sum_{i=1}^n (x_i - x'_i)^2}{\sum_{i=1}^n (|x_i - \bar{x}| + |x'_i - \bar{x}'|)^2} \quad (5.26)$$

- n number of compared values
 x_i measured variable
 \bar{x} arithmetic mean of x_i ($i = 1, \dots, n$)
 x'_i simulated variable
 \bar{x}'_i arithmetic mean of x'_i ($i = 1, \dots, n$)

6. SOIL DISTRIBUTION AND DEGRADATION IN THE UPPER OUÉMÉ CATCHMENT

In this chapter, dominant soil types in the Upper Ouémé catchment are characterized and evaluated according to their fertility. Furthermore, special attention is given to the soils in inland valleys. The extent of soil degradation in the catchment is illustrated by the results of an interdisciplinary survey and the characterisation of typical erosion forms and degraded fields.

6.1. Soil characteristics in the Upper Ouémé catchment

The soil maps of Benin from ORSTOM delineate 38 soil units in the Upper Ouémé catchment (see Chapter 2, Fig. 2.12). The explanatory notes of the soil maps describe one characteristic profile for each unit. Detailed quantitative data regarding physical and chemical soil properties are not always available. In order to get complete and current descriptions of representative profiles, soil investigations were performed in the framework of this study complementing investigations by Sintondji (2005).

6.1.1. Properties of the representative profiles

In this work, 19 representative profiles have been studied in September 2004. The corresponding soil units cover 77% of the Upper Ouémé catchment; the remaining 23% are covered by soil units that were studied by Sintondji (2005). His representative profiles were used for modelling but are not discussed in this chapter. All profiles were taken on savannah land and old fallows. The majority of studied profiles (16) are fersialitic, while two profiles, types 90 and 91, are ferralitic, and soil type 101 is hydromorphic. The texture of the soil horizons varies from sandy sand to loamy clay, with generally low silt contents (Fig. 6.1). Almost all topsoils have a loamy-sandy texture, usually classified as loamy sands (SI2, SI3) according to the German soil classification, or as loamy sand (LS)/sandy loam (SL) according to the USDA classification. Only the topsoils of soil types 17, 18 and 21 have a loamy texture. In the second horizon, sandy textures also dominate. However, soil types 17,

21 and 48 show clay contents higher than 20%. In the fourth horizon, the majority of profiles feature loams and clays, with clay contents varying between 20 and 55%. Only soil types 31, 74 and 80 have lower clay contents. The third horizon shows a wide range of textures, including typical soil textures for the second and fourth horizon.

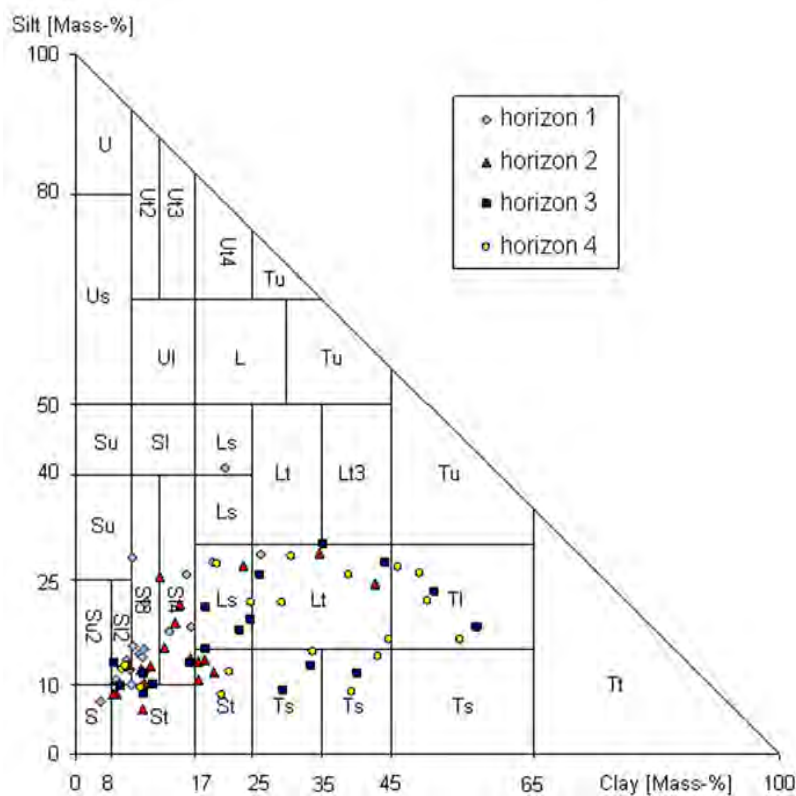


Fig. 6.1 Soil texture of the representative profiles for horizon 1 to 4.

The 19 representative profiles were classified according to the French CPCS classification system and the World Reference Base (WRB) (see Table 6.1). The classification systems are not directly comparable. For example, the CPCS class *sols ferralitiques* covers Ferralsols as well as Ferric Acrisols. The fersialitic soils (*sols ferrugineux tropicaux*) have been classified as

Acrisols, Lixisols, Plinthosols or Arenosols.

In the following, we summarise and evaluate the soil properties of the topsoils according to Landon (1984) (Tables 6.2, 6.3; for evaluation criteria, see Table A.3 in Appendix A). Knowing the topsoil properties is crucial in order to determine the erodibility and fertility of the soils. The depth of the first horizon varies between 5 and 23 cm. Ten of 19 soil types have topsoils with gravel contents higher than 23%, with a maximum of 43% recorded for hydromorphic soil 101. Estimated bulk densities vary between 1.41 and 1.65 g/cm³. The estimated available water capacities (AWC) range from 9 to 18%, which is rather low. The estimated saturated hydraulic conductivities (K_{sat}) lie between 6 and 141 mm/h for the topsoils. Except for the Vertisol, these K_{sat} values are significantly higher than the ex-situ measured K_{sat} values of Giertz (2004) and Sintondji (2005), but they correspond well with the

median K_{sat} values from in-situ measurements by Giertz (2004) on savannah/fallow land.

Table 6.1 Representative profiles – Classification according to the World Reference Base (WRB) and the French soil classification system (CPCS). (g – granite, gn – gneiss, ggn – granitogneiss)

Soil	CPCS classification			WRB classification	Soil map [%]
	Soil type	Characteristics	Parent material		
3	Sols peu évolués		sur quartzite du socle	Orthi-Dystric Leptosol	0.01
14	Sol bruns	eutrophes hydromorph		Ferralsi-Plinthic Cambisol (Endoskeletal)	0.73
17	Sols ferrugineux tropicaux		ggn with biotite	Humic Lixisol	2.20
18	<i>peu lessivés</i>		gn ferro-magnesian	Ferri-Endostagnic Acrisol (Endoskeletal)	3.31
21			sur roche basique	Hypereutric Vertisol	3.53
25		kaolinitic horizon	ggn with biotite	Endoskeleti-Albic Acrisol	3.92
29			basic	Eutric Gleysol or Gleyic Lixisol	0.78
31	<i>lessivés sans concrétions</i>		g, acid	Arenosol	1.70
45	<i>lessivés à concrétions</i>		embrechite	Haplic Acrisol	18.78
48			g, gn with two micas	Profondic Lixisol	5.15
55		kaolinitic horizon	gn, with muscovite and two micas	Haplic Lixisol	1.66
56		kaolinitic horizon	g	Plinthic Acrisol (Hyperochric)	20.84
58		kaolinitic horizon	g, gn calco-alkaline	Humic Lixisol	7.34
62	<i>lessivés induré</i>		ggn, with two micas	Albi-Petric Plinthosol (stagnic, endoeutric)	0.90
70		kaolinitic horizon	gn ferro-magnesian	Albi-Petric Plinthosol	1.47
80	<i>appauvris sans concrétions</i>		g, calco-alkaline with biotite	Plinthic Arenosol	0.73
90	Sols ferralitiques	weak desaturation	ggn, acid	Acric Ferralsol or Ferric Acrisol	1.98
91		young, weak developed	gn, with muscovite and two micas	Plinthic Ferralsol (Lixic)	0.14
101	Sols hydromorphes	gleyey	alluvio-colluvial fluvatile material	Eutric Gleysol	1.95

Eleven soil types belong to Hydrologic group C (slow infiltration rates), seven to Group B (moderate infiltration rates), and only the Vertisol is classified as Group D (very slow infiltration rates).

The erodibility factors (K_{USLE}) are slightly lower than the values obtained by Junge (2004) and Van Campen (1978) for erosion plots in the Aguima subcatchment and near Parakou, respectively. According to the classification of Bolinne & Rosseau (1978) (Table A.4 in Appendix A), most topsoils are sufficiently resistant to erosion due to very low fractions of easily erodible very fine sand and silt. However, soil type 21 (the Vertisol) contains 41% silt and is classified as medium resistant to erosion. Investigations by Junge (2004) showed that K_{USLE} can be significantly higher on cropland and hydromorphic soils at the bottoms of inland valleys.

Organic carbon contents range from 0.2 to 2.4% (Table 6.3). Except for soils 17 and 101, they are classified as very low. The nitrogen contents are low and within the range reported by Swoboda (1994) for soils in the commune Péhunco. The C/N-ratios are between 10 and 25.

Table 6.2 Physical properties of the topsoils.

Soil type	Depth [cm]	Clay [%]	Silt [%]	Sand [%]	Gravel [%]	Texture ¹ [-]	Texture ² [-]	Bd* [g/cm ³]	AWC* [mm/mm]	K _{sat} * [mm/h]	Hydrol. Group	K _{USLE} * [-]
3	10	10	15	75	39	SI3	SL	1.54	0.11	97	B	0.09
14	11	10	22	68	12	SI3	SL	1.48	0.13	68	C	0.14
17	21	26	28	45	28	Lts	L	1.41	0.15	11	C	0.16
18	8	19	27	53	27	Ls4	SL	1.51	0.14	15	C	0.20
21	13	21	41	38	24	Ls2	L	1.44	0.18	6	D	0.30
25	10	9	14	77	26	SI3	SL	1.58	0.10	86	B	0.08
29	20	8	15	76	7	SI3	SL	1.65	0.10	56	C	0.17
31	15	6	10	84	0	SI2	LS	1.58	0.10	138	B	0.06
45	20	8	10	82	24	SI2	LS	1.60	0.10	130	B	0.05
48	13	10	12	79	5	SI3	SL	1.54	0.10	141	B	0.06
55	8	9	14	77	27	SI3	SL	1.63	0.10	74	C	0.11
56	21	6	10	84	13	SI2	LS	1.68	0.09	78	C	0.07
58	23	16	18	66	25	SI4	SL	1.49	0.12	60	C	0.07
62	18	7	13	79	3	SI2	LS	1.61	0.10	82	C	0.09
70	5	8	28	64	14	Su3	SL	1.49	0.15	47	C	0.21
80	15	3	8	89	7	Ss	S	1.67	0.09	113	B	0.03
90	12	8	12	80	18	SI2	LS	1.64	0.09	81	B	0.07
91	5	13	17	69	24	SI4	SL	1.57	0.11	51	C	0.11
101	5	16	26	59	43	SI4	SL	1.41	0.14	49	C	0.13
Mean	13	11	18	71	19	-	-	1.55	0.12	73	-	0.12
Min	5	3	8	38	0	-	-	1.41	0.09	6	-	0.03
Max	23	26	41	89	43	-	-	1.68	0.18	141	-	0.30

* estimated

¹ AG Boden (1994)² USDA (1993)

For ratios higher than 20, nitrogen availability is very limited, and straw residues increase the C/N ratio, while legumes decrease it (Landon 1984). The pH value of the topsoils is low to medium, ranging from 4.5 to 6.3. The cation contents in the topsoil are generally low to medium. Sodium and potassium contents are low for all soil types except for soils 17 and 58. Calcium contents are high for soils 17, 21 and 101, leading to a base saturation of 100%. The cation exchange capacity varies between 1.2 and 12 cmol_c/kg. While CEC_{pot} values are low to very low, base saturation is high for almost all soil types. Only profiles 3, 18, 29 and 56 show a medium base saturation.

Appendix A provides detailed information about the location and properties of all representative profiles, including a photo of each profile (see Appendix A, Figs. A.1, A.2, Table A.2). In the following, we describe four important soil types in the catchment in detail. Soil types 56, 45, 58 and 48 together cover about 52% of the catchment area and are all classified as *sols ferrugineaux tropicaux lessivés à concrétions* (clay eluviated soils with nodules) according to the CPCS classification. However, soils 56 and 58 show a kaolinitic horizon over a nutrient-poor granitic substratum and/or nutrient-rich calco-alkaline granito-gneiss. Soils 45 and 48 occur directly over embrechite (nutrient-rich) and granite/granitic gneiss, respectively.

Table 6.3 Chemical properties of the topsoils.

Soil type	C _{org} [%]	N [%]	C/N [-]	pH [-]	K [cmolc/kg]	Na [cmolc/kg]	Mg [cmolc/kg]	Ca [cmolc/kg]	CEC _{pot} [cmolc/kg]	BS [%]
3	1.6	0.09	19	5.0	0.04	0.01	0.8	3.1	6.9	57
14	1.7	0.08	20	5.9	0.13	0.01	1.2	4.0	6.2	87
17	2.1	0.14	15	6.2	0.36	0.01	1.6	17.6	10.8	100*
18	1.2	0.07	16	5.9	0.12	0.02	1.0	2.9	6.9	58
21	1.2	0.05	25	5.6	0.08	0.08	3.4	12.2	12.0	100*
25	1.1	0.08	14	5.8	0.08	0.01	0.8	3.4	4.6	96
29	0.2	0.02	10	4.5	0.01	0.03	0.4	0.7	2.0	54
31	1.0	-	-	-	-	-	-	-	-	-
45	1.1	0.07	15	5.7	0.09	0.02	0.9	4.3	6.0	87
48	1.4	0.09	16	5.8	0.15	0.01	1.0	5.1	7.9	79
55	0.7	0.04	15	5.3	0.05	0.01	0.5	2.4	4.0	74
56	0.2	0.01	11	4.6	0.03	0.01	0.1	0.3	1.2	37
58	1.8	0.11	17	5.7	0.52	0.02	1.4	8.6	10.3	100*
62	0.6	0.04	17	4.7	0.13	0.02	0.4	2.2	4.4	63
70	1.2	0.08	15	5.6	0.16	0.02	1.0	3.1	5.4	79
80	0.4	0.02	17	5.2	0.07	0.01	0.4	1.1	2.0	75
90	0.5	0.04	15	5.2	0.05	0.02	0.4	1.2	2.7	61
91	1.1	0.08	14	5.5	0.10	0.01	1.0	4.4	7.0	79
101	2.4	0.19	13	6.3	0.19	0.01	1.8	10.2	11.2	100*
Mean	1.1	0.07	16	5.5	0.13	0.02	1.0	4.8	6.2	77
Min	0.2	0.01	10	4.5	0.01	0.01	0.1	0.3	1.2	37
Max	2.4	0.19	25	6.3	0.52	0.08	3.4	17.6	12.0	100

*after Calcium correction

The study sites of the representative profiles 45, 56 and 58 are characterised by undulated pediplaine relief, a position at the mid-slope with an inclination of about 2° and the occurrence of sheet erosion. In contrast, profile 48 is positioned at the upper slope with an inclination of 2.5°. The sites are covered by *savane herbeuse* (profiles 45, 56), *savane arbustive* (profile 48) or *savane arborée* (profile 58).

Soil type 56 – Plinthic Acrisol (Hyperochric)

The representative profile for soil type 56 is classified as Plinthic Acrisol due to the occurrence of a clay-eluviated and a skeletal horizon. In addition, the profile is called hyperochric due to the very pale topsoil (Fig. 6.2). A brown, sandy topsoil overlies a yellowish brown B-horizon of loamy sand and a brown, sandy loam, both with a high content of gravel and large ferro-magnesium nodules. Below 81 cm, there is a multicoloured kaolinitic horizon. Traces of light mica have been found in all B-horizons; horizons 3 and 4 were indurated.



Fig. 6.2 Soil type 56 – representative profile (west of Parakou).

Very fine roots and biogenous pores were only visible in the two upper horizons. As illustrated in Figure 6.3, clay and silt contents increase significantly with depth. PH values between 4.6 and 5.2 indicate an acidic environment. Organic carbon contents are very low (<0.3%) throughout the profile. Nitrogen contents are low to very low, and the low C/N ratios of 10 to 14 indicate strongly limited nitrogen availability for plants. Cation exchange capacity increases with depth from 1.2 to 4.4 cmol_e/kg but remains very low. Clay contents are generally low, and base saturation varies between 30 and 43%. Thus, the profile shows several physical and chemical constraints, including high leaching potential, low nutrient reserves and high gravel content (see next section).

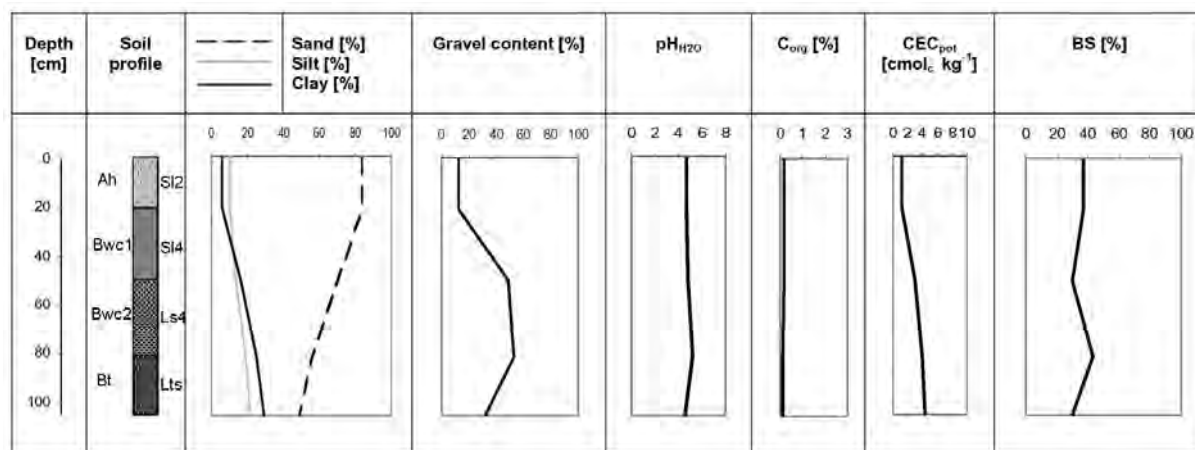


Fig. 6.3 Physical and chemical properties of soil type 56 (representative profile).

Figure 6.4 schematically shows a soil catena along an approximately 1200 m long topo-sequence with five augerings that was studied west of Parakou in order to choose the location for a representative profile for soil type 56. Except for the the 1st

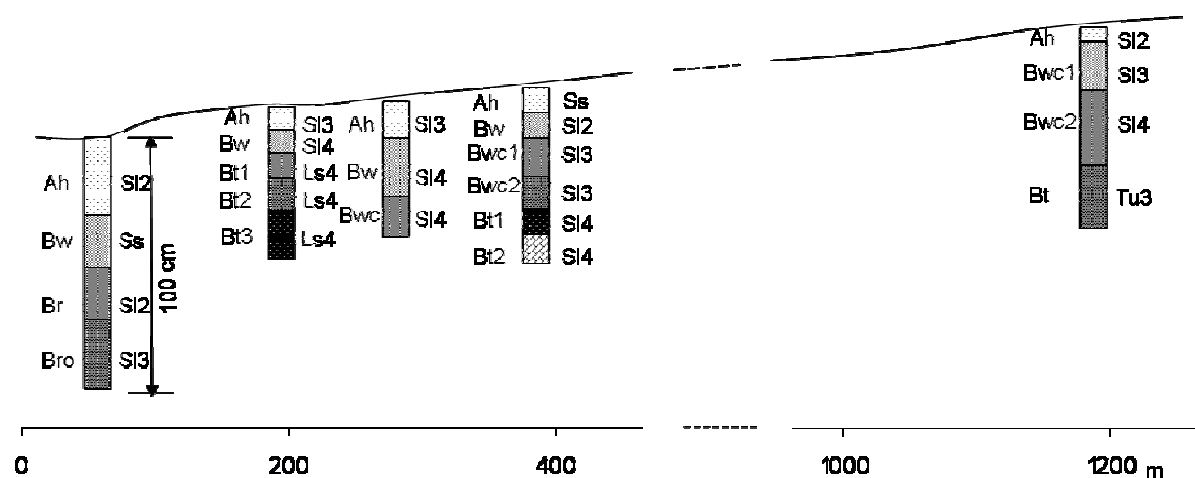


Fig. 6.4 Soil catena in soil unit 56.

augering at the inland-valley fringe, the 3rd to 5th augerings showed a similar sequence of diagnostic horizons and soil textures as the representative profile, for which a position was selected between augerings 3 and 4. Augering 2 did not exhibit a skeletal horizon. In contrast to the representative profile, topsoils of all augerings were very dark brown, not pale. Due to the occurrence of plinthic horizons below a depth of 6 to 20 cm, drilling was only possible to a depth of 54 to 80 cm. As is typical for the sub-humid savannah, gravel content was high, especially on the slope summit. Laboratory analysis of the soil properties of augerings 2 and 4 revealed higher soil fertility for these than for the representative profile due to higher C_{org} contents in all horizons, in particular the topsoil, and higher clay content in the topsoil of augering 2. As a consequence, C/N ratios are also more favourable for crop cultivation for these augerings. Values for pH were very similar. The subsoil gravel contents in augering 4 reached up to 86% (by weight), which was significantly higher than for the representative profile. In contrast to the other augerings and the profile, augering 1 at the inland-valley fringe described a hydromorphic soil with very low gravel contents, sandy textures and subsoil colours indicating reducing and oxidising conditions.

To summarise, the augerings along the soil transect reflect the large heterogeneity of soil properties along the slope, which cannot be captured by one single profile. Nevertheless, the profile can be considered acceptably representative, although the pale topsoil was not identified as typical.

Soil type 45 – Haplic Acrisol

This profile is a typical Acrisol. A very dark brown, humus-rich, sandy A-horizon overlies a dark brown, sandy B-horizon with 49% gravel (mainly small ferric nodules). Underneath, the soil texture changes abruptly to dark yellowish brown, sandy clay that overlies brown, sandy clay; both with gravel contents below 9%. In the 5th horizon, the gravel content is extremely high (84%), and ochre mottles occur. The transitions between the horizons are clear, but irregular. The degree of root penetration and biogenous porosity is slightly higher than for profile 56. The pH remains nearly constant between 5.4 and 5.7, reflecting medium acidity. Organic



Fig. 6.5 Soil type 45 – representative profile (near Beterou).

carbon content drops from 1.1% in the topsoil to about 0.3% in the rest of the profile (Fig. 6.6). The nitrogen content is very low throughout the profile. The C/N ratios decrease from 15 to 9 with increasing depth.

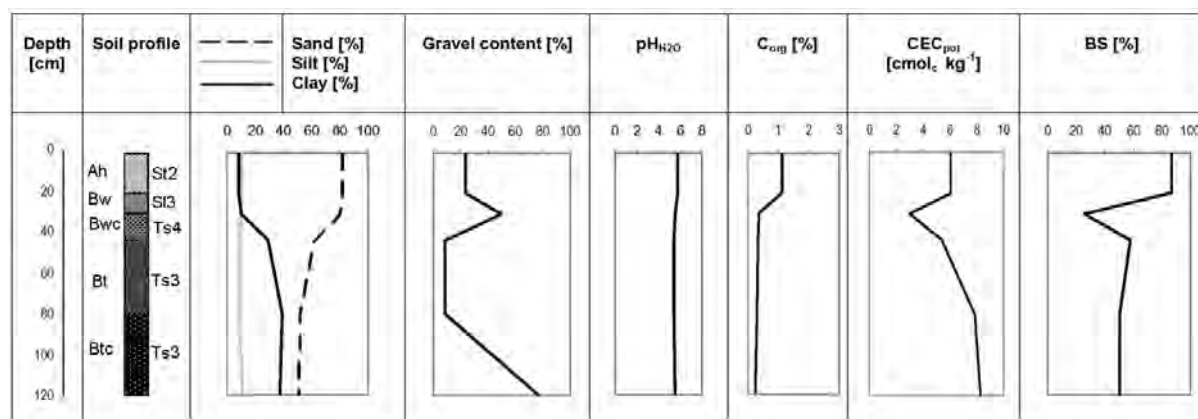


Fig. 6.6 Physical and chemical properties of soil type 45 (representative profile).

The cation contents, CEC_{pot} and base saturation are lowest in the second horizon. Base saturation is high in the topsoil but drops in the subsoil to medium values. The main constraints with regard to agricultural production are the high gravel content in the 2nd and 5th horizons and a high erosion risk due to abrupt textural changes (see next section). No detailed soil transect along the slope was studied for this soil unit, but the representativeness was checked by comparing it with the typical characteristics for this soil unit presented in the descriptions of the soil map of Benin.

Soil type 58 – Humic Lixisol

The representative profile for soil type 58 is classified as a Humic Lixisol due to the occurrence of a thin argic horizon (B_t) and a very humus-rich, very dark grey topsoil with 1.8% organic carbon. The loamy-sandy topsoil overlies a dark brown loamy sand and a dark yellowish brown sandy loam with red clay mottles and 47% gravel content. Underneath, a colourful saprolitic horizon with a sand-rich clay texture and abundant mica occurs. Transitions between the horizons are generally abrupt, but gradual and irregular for the 3rd horizon. Penetration by fine and medium size roots and biological activity is relatively high in the upper horizons. Except for the peak in the 3rd horizon, gravel content is about



Fig. 6.7 Soil type 58 – representative profile (west of Parakou).

20% (Fig. 6.8). The pH ranges from 5.1 to 5.7. Organic carbon contents decrease with depth from 1.8 to 0.2%. The nitrogen content is low in the topsoil and very low in the subsoil (<0.03%).

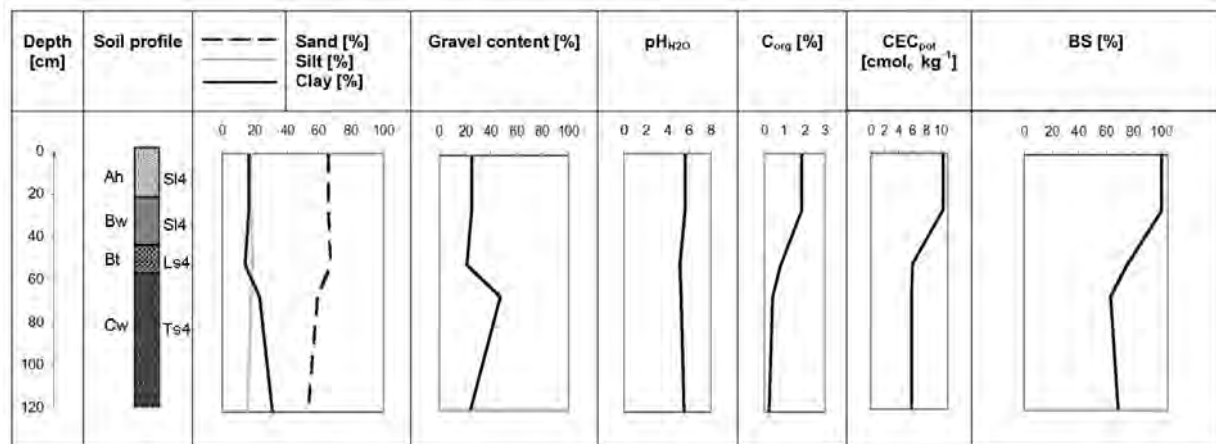


Fig. 6.8 Physical and chemical properties of soil type 58 (representative profile).

The C/N ratios have values of 16 to 24, which are more favourable for crop cultivation than for soil types 45 and 56. CEC_{pot} is also significantly higher, ranging from 6 to 10 cmol_c/kg soil. Base saturation is high throughout the profile. Thus, soil type 58 has a higher chemical fertility than the Acrisols discussed previously. However, water-logging could be a problem due to the clay-rich 4th horizon.

Figure 6.9 schematically shows the corresponding soil transect for soil type 58 along a topo-sequence with five augerings that was studied west of Parakou near the road to Beterou and from which the location for the representative soil profile was chosen at the middle slope between augerings 2 and 3. In this transect, the depth and soil texture of the horizons vary less among the augerings than in the catena for soil

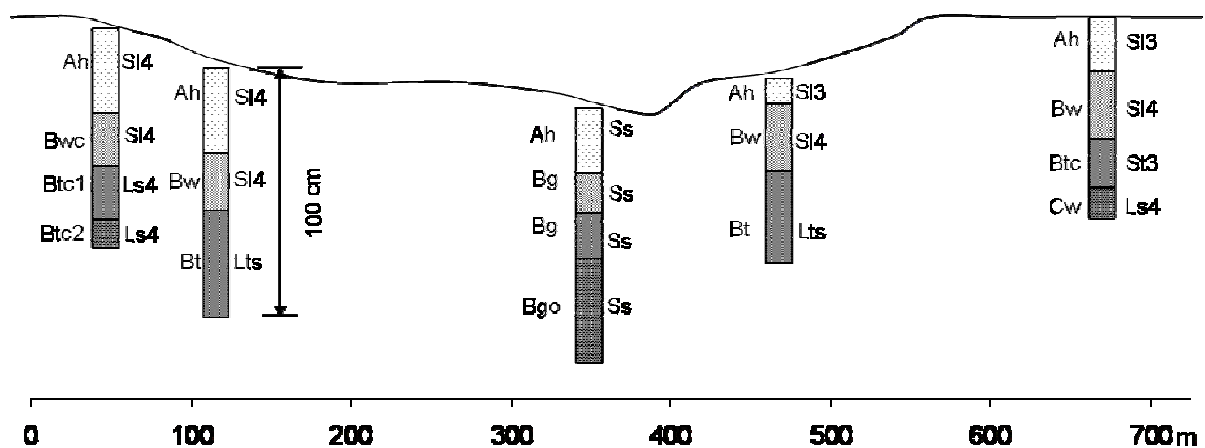


Fig. 6.9 Soil catena in soil unit 58.

type 56. Except augering 3, all augerings and the profile exhibit red mottles in the subsoil, comparatively high organic carbon contents of 0.7 to 2.8% in the topsoil, and rather low pH values between 5 and 5.7. With regards to the topsoils, the depth is very similar among augerings and the profile, but significantly lower for augering 4. The topsoil C_{org} and nitrogen content of the profile lie in the upper range obtained for the augerings, and the clay content is slightly higher than for all augerings. As a consequence, soil fertility of the representative profile is slightly higher than for most augerings. Except for augering 3, all augerings exhibit an argic horizon below 36 to 55 cm depth, like the representative profile. For augerings 1 and 5 positioned near or on the summits, subsoils show significantly elevated gravel contents of 37 to 66%. However, augering 2, which was located close to the profile, did not show any horizon with extreme gravel content, as observed also in the representative profile. A saprolitic horizon with quartz pieces, as identified for the representative profile below 58 cm, was only exhibited by augering 5. For all other augerings, no saprolitic horizon was encountered within a depth of 1m. Augering 3 represents the hydromorphic soils at the fringe of an inland valley and is characterized by nearly pure sands without gravel which were wet below 50 cm depth and show pronounced features of oxidation below 60 cm.

In a nutshell, some soil properties, like gravel content and organic carbon content vary considerably along the hillslope but the chosen profile can be considered as acceptably representative.

Soil type 48 – Haplic Lixisol

The representative profile is classified as Haplic Lixisol due to the occurrence of an argic horizon (B_t).

A thin, very dark greyish brown, sandy topsoil overlays two dark brown sandy B-horizons and a brown, argic horizon (Fig. 6.10). Underneath, a brown, loamy sandy horizon occurs. Little pieces of quartz can be found throughout the profile. For most horizons, transitions are gradual and regular or irregular. Penetration by fine roots and biological activity is high in the upper three horizons. While gravel content is low in the topsoil, horizons 3 to 5 have extremely high gravel contents of 72 to 87%. Values for pH range from 5.2 to 5.8



Fig. 6.10 Soil type 48 – representative profile (near Beterou).

(Fig. 6.11). Organic carbon contents decrease from 1.8 to 0.2% with increasing depth. Nitrogen contents are very low in the entire profile; the C/N ratios range from 14 to 18. CEC_{pot} is lower than for profile 58 with values between 4 and 8 $cmol_c$ per kg soil.

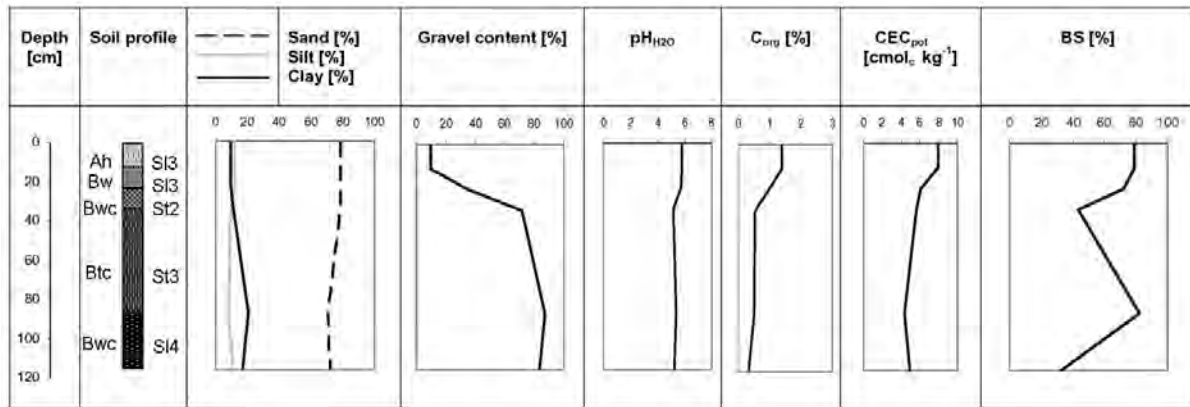


Fig. 6.11 Physical and chemical properties of soil type 48 (representative profile).

Cation contents are more elevated than in the previous profiles but still are classified as low (K, Na) or low to medium (Ca, Mg). Base saturation is generally high, but medium for horizon 3 and 5. The profile is chemically comparatively fertile but shows severe limitations through the extreme gravel contents in the subsoil.

Figure 6.12 schematically visualizes the corresponding soil transect with five augerings for soil type 48 along a topo-sequence which was studied near Beterou and from which the location for the representative soil profile was chosen at the upper slope. Slopes were very long and only slightly inclined; therefore and due to difficult access no augerings were performed at the lower slope and valley bottom. As shown in Fig. 6.12, the depth of the horizons varies considerably among the augerings. Topsoil depths range from 7 to 35 cm with lowest values on the summit.

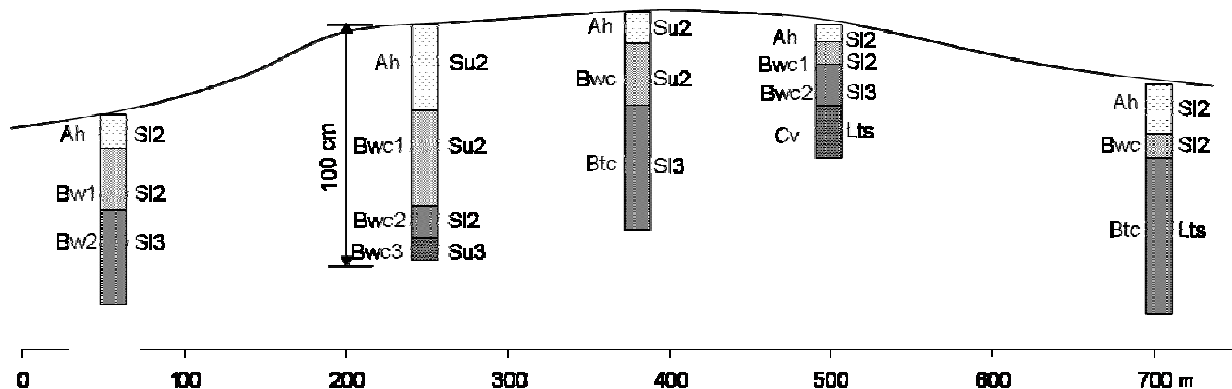


Fig. 6.12 Soil catena in soil unit 48.

C_{org} contents in topsoils are similar as for the profile but significantly higher in augering 3. Except for augering 1, subsoils in the augerings and the profile contain extremely high gravel contents and mica and quartz pieces. Soil colours of horizons vary considerably among the augerings. Augerings 3 and 5 exhibit argic horizons as the representative profile. Augerings 1 and 4 showed slight increases in clay content with depth which may justify argic horizons but would require a laboratory analysis of the soil textures. Comparing the soil samples from augering 2 and 3 with the profile values, pH, C_{org} and nitrogen are very similar within one meter depth. However, while clay contents in the representative profile are between 9 and 21%, they are below 10% in augerings 2 and 3.

In summary, some soil properties like topsoil depth and soil colour vary considerably along the studied hillslope and clay-rich subsoils forming argic horizons as in the case of the representative profile are not always found in the first meter depth. However, the chosen profile reflects well the average soil properties along the slope.

6.1.2. Evaluation of soil quality

In the following, we evaluate the quality of the profiles according to the Fertility Capability Classification (Table 6.4, see criterias in Table A.5, Appendix A).

For most profiles, the physiological deepness is medium to deep. Soil types 17, 25 and 29 are very deep but show several physical and chemical constraints. Except for soils 29, 45, 48, 55 and 70, all soils are limited by low nutrient reserves (modifier *k*). Due to the dominance of nutrient-poor kaolinitic clays, organic matter is the main contributor to soil fertility. However, organic carbon contents are significantly lower than 2% for most soils and decline rapidly under agricultural land use. Soil types 3, 14, 25, 56, 80, 90 and 91 are prone to intensive leaching of nutrients (modifier *e*). Furthermore, some soils show a low pH, further limiting the availability of important nutrients like phosphorus. Without vegetation, such soils degrade easily and irreversibly due to acidification, leading to the release of aluminium and fixation of phosphorus (Stocking 2003). A high erosion risk due to abrupt textural changes was identified for soil types 18, 21, 45, 56 and 90. Gravel contents higher than 35% in at least one horizon are a constraint in all soils except for types 21, 31, 45, 58 and 80. Water-logging limits agricultural use in areas with soil types 58 and 90. Soil 3 (Leptosol) is not suitable for agricultural land use due to many constraints.

Phosphorus contents have not been determined, but phosphorus is a limiting factor in many soils in the region.

Table 6.4 Evaluation of the representative profiles according to the Fertility Capability Classification (FCC) (Sanchez et al. 2003).

Soil	WRB soil group	FCC unit	Interpretation
3	Orthi-dystric Leptosol	L"d+ehk	high leaching potential, low nutrient reserves, gravel content >35%, too dry to grow a crop without irrigation
14	Ferralsi-Plinthic Cambisol	L"ehk	high leaching potential, low nutrient reserves, gravel content >35%
17	Humic Lixisol	L'L"k	low nutrient reserves, gravel content >35% in second horizon, 15-35% gravel in first horizon
18	Ferri-Endostagnic Acrisol	L'C"hk	low nutrient reserves, gravel content >35% in first and second horizon, high erosion risk due to abrupt textural change
21	Hypereutric Vertisol	L'C'k	low nutrient reserves, gravel content 10-35%, high erosion risk due to abrupt textural change
25	Endoskeleti-Albic Acrisol	L'ek	high leaching potential, low nutrient reserves, gravel content >35%
29	Eutric Gleysol (Gleyic Lixisol)	LL"	gravel content >35% in second horizon
31	Arenosol	S	
45	Haplic Acrisol	S'L'	gravel content 10-35%, high erosion risk due to abrupt textural change
48	Haplic Lixisol	LL"	gravel content >35% in second horizon
55	Haplic Lixisol	L"	gravel content >35%
56	Plinthic Acrisol	SL"ehk	high leaching potential, low nutrient reserves, high erosion risk due to abrupt textural change
58	Humic Lixisol	L'g+k	prolonged water logging, low nutrient reserves
62	Albi-Petric Plinthosol	LL"k	low nutrient reserves, gravel content >35% in second horizon
70	Albi-Petric Plinthosol	L'L"	gravel content >35% in second horizon, 15-35% gravel in first horizon
80	Plinthic Arenosol	Sehk	high leaching potential, low nutrient reserves
90	Acrif Ferralsol (Ferric Acrisol)	S"L"eghk	high leaching potential, water logging, low nutrient reserves, gravel content >35%, high erosion risk due to abrupt textural change
91	Plinthic Ferralsol	L'ek	high leaching potential, low nutrient reserves, gravel content >35%
101	Eutric Gleysol	L"L'k	low nutrient reserves, gravel content >35% in first horizon, 15-35% gravel in second horizon

The soils with the highest fertility and the lowest number of restrictions are the Lixisols and Cambisols. However, most Lixisols and Cambisols in the catchment show high gravel contents in the second horizon. If we tried to define a coarse sequence of soil types according to their soil fertility, the order would be: Cambisol > Lixisol > Acrisol > Gleysol > Plinthosol > Arenosol > Leptosol. Vertisols appear only locally in the catchment and show a number of physical constraints for cultivation. The Upper Ouémé catchment is dominated by Acrisols and Lixisols, i.e., soils that

are chemically more fertile than many soils in Southern Benin, but with rooting depths constrained by high gravel contents in the subsoil.

Hydromorphic soils in the inland valleys are characteristic for the Upper Ouémé catchment and are very important for the hydrological cycle, but they were not chosen as representative profile due to their limited occurrence.

6.2. Soil characteristics in inland valleys

Investigations of inland valleys in the small Aguima subcatchment by Giertz (2004) and Junge (2004) revealed common properties of the soils, a typical geomorphologic form and a position above a first order stream. The topsoils in the inland valleys showed higher organic carbon contents than did those at the slope due to the reduced litter decomposition under wet conditions (Schachtschabel et al. 1998). The soils in the centre of the inland valleys had a loamy texture, whereas those at the border of the inland valleys were characterised by loamy sands (Junge 2004). This clay enrichment can be explained by the accumulation of clay particles that were transported along the slope by surface runoff and interflow (Faure & Volkoff 1998).

These local observations led to the question of if these patterns were valid for the entire Upper Ouémé catchment and if it might be possible to include the hydromorphic inland valley soils in the French soil map for hydrological and erosion modelling. Besides knowledge about the properties of inland valley soils, this would require an efficient method to determine the distribution of inland valleys in the Upper Ouémé catchment based on field observations, aerial photographs or remote sensing.



Fig. 6.13 Inland valley near Parakou (October 2004).

Field observations within this study in 2004 and by the inventory of Giertz & Steup in cooperation with the Inland Valley Consortium (IVC) of Benin in 2006 showed that the majority of inland valleys in the catchment are only a few hectares in size and are slightly

concave. Forty-eight percent of inland valleys counted were positioned above a first order stream, 25% at the union of two streams, 20% along a stream and 7% downstream. All 521 inland valleys listed cover a total of 35 km² of the catchment (14500 km²). On average, an area of 3.4 km² is discharging into an inland valley (Schönbrodt 2007).

Classifying inland valleys using Landsat data is extremely difficult, as individual trees or shrubs at the borders of small inland-valleys or agricultural use change the signal at the satellite image. The fact that classified inland valleys are scarce in the Djougou region can be explained by the higher degree of cultivation of inland valleys in this region. Furthermore, the Landsat image was taken on 26.10.2000, when several inland valleys may have been already dry, leading to a classification of inland valleys as grass savannah (*savane herbeuse*). Field observations revealed that the land use classification only correctly classifies large inland valleys. Small classified inland valleys often did not correspond to inland valleys in the field and vice versa. Aerial photographs taken in 2003 by the PAMF project covering a corridor between Dogué and Djougou seem to allow a better delineation of smaller inland valleys but do not capture the whole catchment.

Soil properties of five inland valleys were studied in March 2004 in order to examine the degree of heterogeneity between inland valleys in the Upper Ouémé catchment. A detailed field study of the soil characteristics of representative inland valleys was not feasible due to time and labour constraints. In the following, we discuss some general findings and the physical and chemical properties of the topsoils. Appendix A summarises the transect locations near Dogué (S-HVO), Boko (E-HVO) and Sérrou (W-HVO) (Table A.5, Appendix A) and the characteristics of all studied soil profiles in the inland valleys (Table A.7, Appendix A). For each transect, 5 to 11 augerings of 1 m depth were conducted.

Soil textures varied considerably between and within the inland valleys (Fig. 6.15). Two transects (*Boko1*, *Sérrou2*) showed only sandy textures (Fig 6.14), while *Sérrou1* displayed only loamy and clayey textures. The two inland valleys near Dogué are characterised by loamy sands above 70 cm depth and sandy loams or sandy clays at the fringes (*Dogué1 and 2*) and valley bottoms (*Dogué2*) (Fig. 6.16). Two profiles of transect *Dogué2* were Fluvisols with topsoils significantly richer in silt and organic carbon and higher pH values. The profiles at the valley bottom of *Dogué1* display loams over the whole first metre.

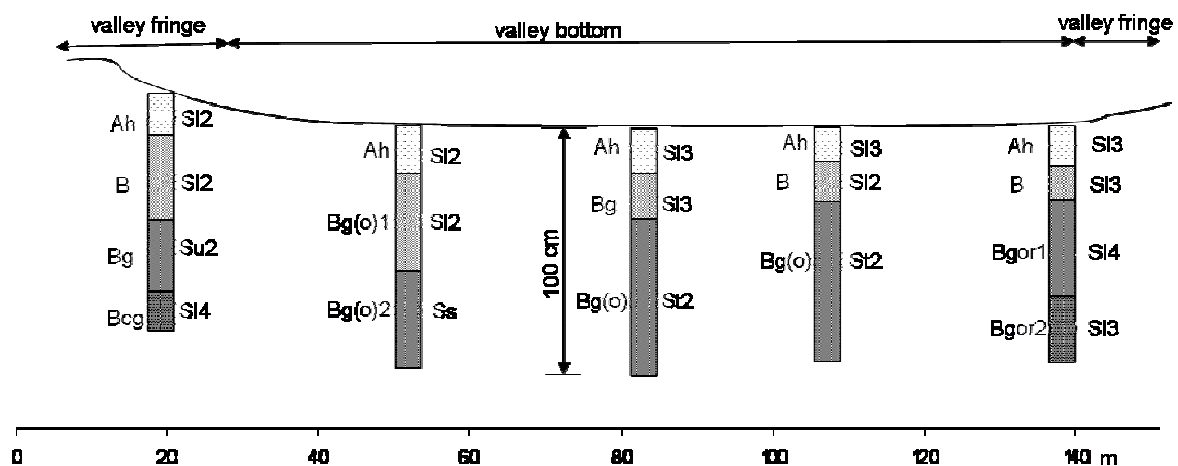


Fig. 6.14 Soil catena in inland-valley *Boko1*.

Nevertheless, the studied inland valley soils in the Upper Ouémé catchment have the following common physical properties: (1) vertical differences in soil texture from top to subsoil with increasing clay content and decreasing silt content, (2) a dominance of loamy sands (SI2, SI3) in topsoils and loams (Lts) and sandy clays (Ts) in the subsoil (Fig. 6.15), (3) changes in the sand fraction from fine sand to coarse sand, and (4) low pH values and in general, low gravel contents (0-15%) increasing with depth.

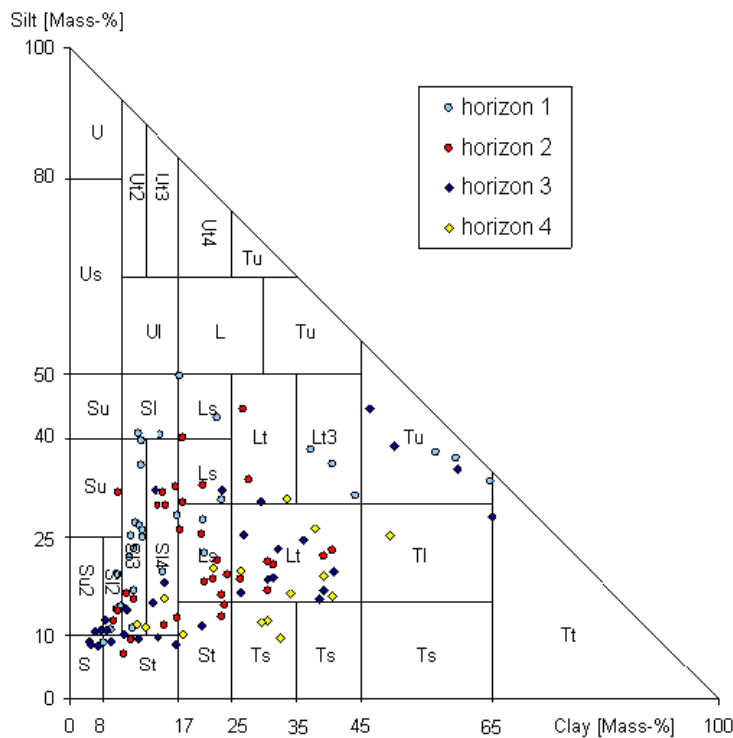


Fig. 6.15 Soil texture of inland-valley profiles, horizon 1 to 4.

The subsoil horizons are usually influenced by oxidation (Bgo horizon) and/or reduction (Bgr horizon). While the soils of transects *Dogué1*, *Dogué2* and *Sérou1* show pronounced gleyic properties, this is less obvious for transects *Boko1* and *Sérou2*. Indurated plinthic horizons have not been found. In addition, saprolite was rarely encountered within the first metre. This corresponds to observations by Schönbrodt (2007) and Junge (2004)

that saprolite occurs in most cases below 1.5 to 2 metres depth.

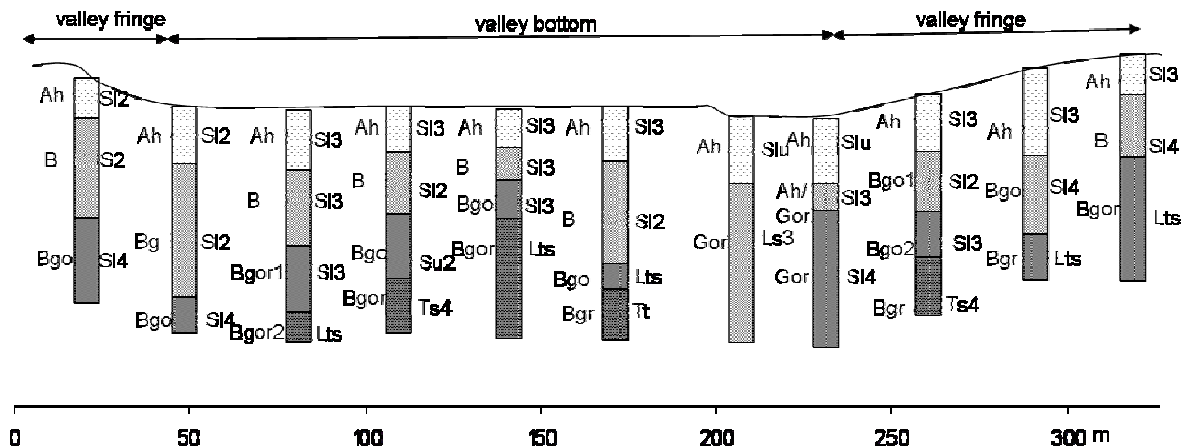


Fig. 6.16 Soil catena in inland-valley *Dogué2*.

The mean physical and chemical properties of the topsoils in the inland valleys are shown in Table 6.5. The results are compared with findings by Schönbrodt (2007), who studied 13 inland valleys of 1 to 10 ha size representative of 3 regions in the Upper Ouémé catchment that were defined for the survey of Giertz and Steup in cooperation with IVC Benin based on their positions at the river, their geomorphology and the changes in water height and surface during water saturation.

Table 6.5 Topsoil characteristics of studied inland-valleys.

Inland-valley	Depth [cm]	Sand [%]	Silt [%]	Clay [%]	Gravel [%]	Text. [-]	C _{org} [%]	N [%]	C/N [%]	pH [-]	CEC _{pot} [cmol _c /kg]	K ~	Na ~	Mg ~	Ca ~	BS [%]
<i>Dogué1</i> fringe	28	61	25	14	0.0	SI4	1.0	0.06	18	4.5	5.1	0.09	0.04	0.4	1.5	39
<i>Dogué1</i> bottom	25	44	35	21	0.0	Ls3	1.3	0.08	16	4.8	7.7	0.12	0.07	1.0	3.3	59
<i>Dogué2</i> fringe	24	66	24	10	0.0	SI3	1.0	0.05	19	5.1	5.4	0.09	0.04	1.1	2.4	62
<i>Dogué2</i> bottom	22	57	33	10	0.0	SI3	1.2	0.06	19	4.8	6.0	0.08	0.09	0.8	2.5	59
<i>Boko</i> fringe	17	83	11	6	2.6	SI2	0.6	0.03	18	5.7	3.4	0.04	0.04	0.3	2.4	81
<i>Boko</i> bottom	18	76	16	9	10.5	SI3	0.7	0.04	15	4.6	3.3	0.08	0.06	0.3	1.2	50
<i>Sérou1</i> bottom	15	14	36	50	0.4	Tu2	2.1	0.14	15	4.4	13.2	0.14	0.13	1.4	4.3	46
<i>Sérou2</i> bottom	30	82	12	6	6.9	SI2	0.6	0.03	22	4.9	3.4	0.06	0.05	0.2	1.9	60

The depth of the A-horizon varies between 9 and 36 cm, with a mean of 23 cm, which is significantly higher than for the representative profiles (mean 13 cm, see Table 6.2). The organic carbon content of all sampled topsoils varies from 0.3 to 2.8%, with a mean of 1.3% for the inland valley bottom and 0.9% at the fringe, which is nearly identical to the values found by Schönbrodt (2007). Thus, in general, the organic carbon content is higher than on the hillslopes but still very low according to the classification of Landon (1984). Inland valley *Sérou1* is an exception, with organic carbon contents of 1.4 to 2.8% and significantly higher clay content in the topsoil, leading to a significantly higher CEC_{pot} and above-average contents of calcium and

magnesium. The mean C/N ratios for the inland valleys are between 15 and 22, i.e., higher than the mean ratios of 13 to 16 obtained by Schönbrodt (2007) and the mean of 17 obtained by Mund (2004) for the savannah zone in the Cote d'Ivoire. Mean C/N ratios tend to be higher at the fringe than at the bottom (see also Schönbrodt, 2007). Smaling et al. (1985) considered narrow C/N ratios of 10 to 15 to be favourable with regards to nitrogen availability in the inland valleys of the Nigerian Guinea savannah zone. CEC_{pot} values of topsoils are low (*Dogué1/2*, *Sérou1*) or very low (*Boko*, *Sérou2*), and base saturation is medium to high. Contents of cations are low (sodium, potassium) or low to medium (calcium, magnesium) in all topsoils. In general, soil chemical characteristics are more favourable on the sites that were recently under rice cultivation, i.e., *Dogué1/2* and *Sérou1*.

To conclude, the studied soils in the inland valleys of the Upper Ouémé catchment show a number of common characteristics but also large heterogeneity among them and within each site. Schönbrodt (2007) could not identify significant differences in soil properties of the inland valley soils among the North/East, West/Central and South/South-east regions of the catchment.

Finally, integrating inland valleys into the SWAT model does not seem feasible due to their small size, highly variable soil properties and difficulty in determining the distribution of inland valleys without conducting a costly and time-consuming field survey. Although a field survey has been conducted by Giertz & Steup in cooperation with the IVC in the meantime and produced a map of inland valleys (Fig. 6.17), methodological problems remain for their consideration in a regional-scale erosion model. First, the actual number of inland valleys in the catchment is significantly higher than the inventoried 521, as the survey captured only accessible inland valleys close to villages and roads (Fig. 6.17). Second, the typical scattered distribution of small inland valleys in the catchment is hard to incorporate into a regional, semi-distributed model with a coarse soil map at the scale 1:200000.

Nevertheless, inland valleys are very important for hydrology at the local scale and agriculture due to the higher soil fertility and water availability. Knowing their hydrological and pedological properties is crucial for efficient, sustainable management. Of the 521 inventoried inland valleys in the Upper Ouémé catchment, 69% were used for agriculture, and 2.5% had sophisticated water regulation. Of the 110 inland valleys captured by the earlier national inventory, only 11% were used for agriculture.

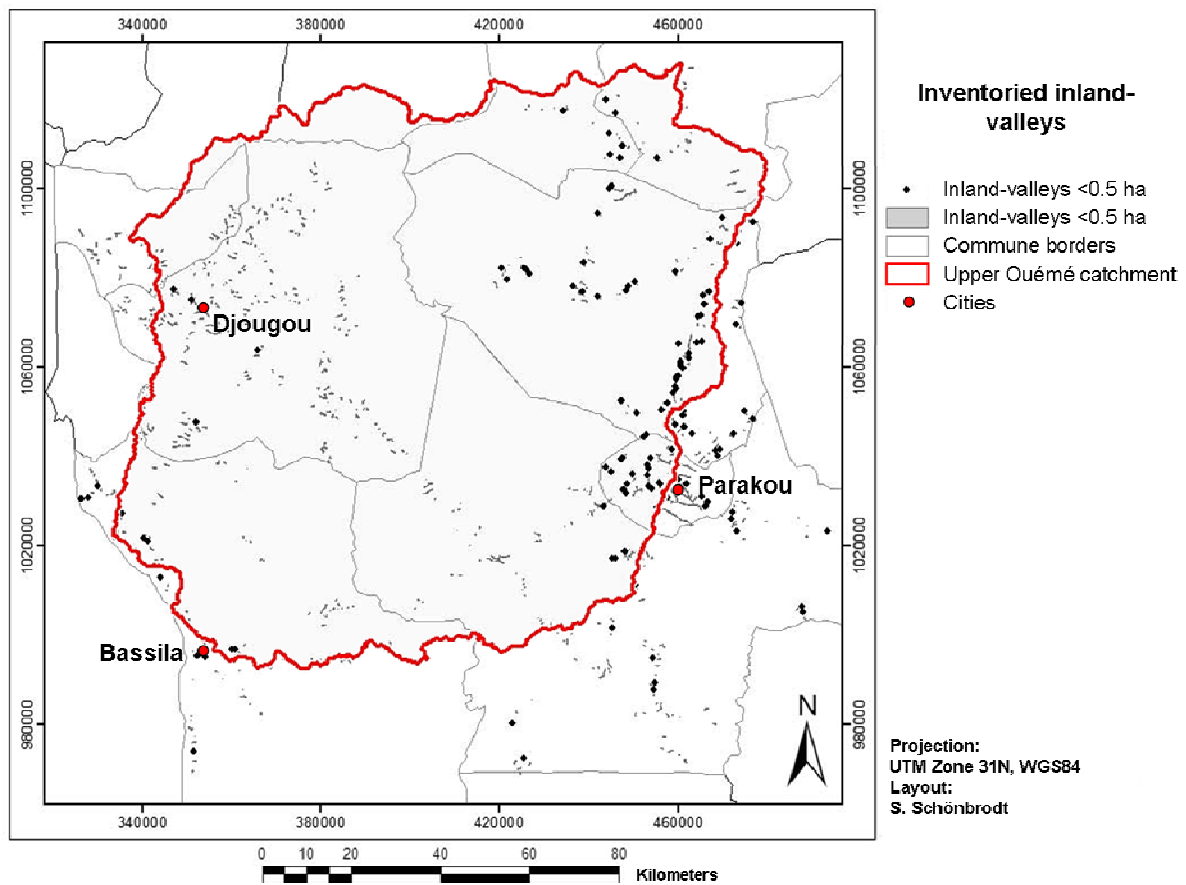


Fig. 6.17 Inventoried inland valleys from the study of Giertz & Steup (unpublished) in cooperation with the IVC Benin (from Schönbrodt 2007, modified).

6.3. Soil degradation in the Upper Ouémé catchment

The Upper Ouémé catchment is one of the less intensively used regions in Benin, with a younger settling history than South Benin or the regions around Ouaké and Boukombé. As a consequence, most of the area can be described as slightly or non-degraded. However, around the cities Parakou and Djougou and in the north-western part of the area, soil degradation is moderate to severe.

Interdisciplinary survey in the Upper Ouémé catchment

The representative, interdisciplinary survey conducted by IMPETUS researchers in 2005 in the Upper Ouémé catchment also includes information about the degree of soil degradation and the distribution of soil conservation measures in the area. For example, 38% of the 434 interviewed farmers considered their land to be degraded.

Although the sample size at the communal level is not large enough to allow representative conclusions at this level, a spatial analysis of the results gives some hints. As expected, soil degradation is often cited as a problem in the communes Copargo (82%), Ouaké (70%), Parakou (66%) and Djougou (63%); i.e., in areas with dense populations and long settlement histories (Fig. 6.18). In contrast, in all other communes, less than 30% of the farmers perceive soil degradation as a problem; with the lowest value obtained for the commune Ndali (7%). In several villages in the commune Ouaké and in the district Banikani of Parakou, all 20 interviewed farmers are facing soil degradation. Overexploitation and a shortage of fallow periods are cited as the main reasons, although land scarcity and permanent cultivation are also mentioned by several farmers.

Questions about the colour and texture of the topsoils of the dominant soil also provide hints about the degree of soil degradation. While in the commune Bassila humus-rich topsoils dominate (44%) with a dark colour (79%), the fraction of humus-rich topsoils is below 15% in the communes Copargo and Ouaké. In these degraded areas, grey sandy (60-70%) and gravel-rich topsoils (20-25%) are mostly cited. Technologies applied to improve and sustain the soil quality include crop rotation as the dominant strategy (35%), followed by burning (14%), erosion measures (13%) and other technologies (25%, mainly mineral and organic fertiliser, drainage) (Fig. 6.19).

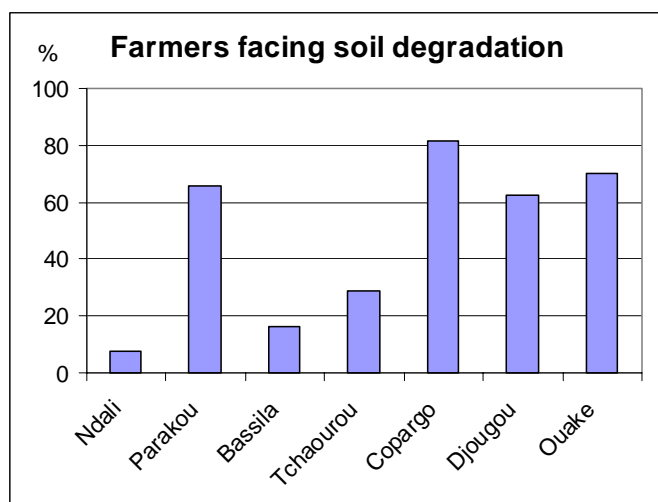


Fig. 6.18 Percentage of farmers facing degraded soils in the HVO based on data from HVO-Survey (2005).

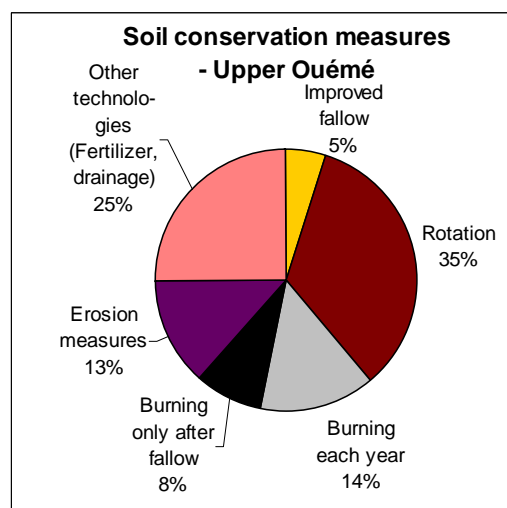


Fig. 6.19 Applied technologies to improve soil quality based on data from HVO-Survey (2005).

On the communal level, it becomes obvious that erosion measures are mainly mentioned in the communes Bassila, Ouaké and Tchaourou, especially in villages

with contacts with development projects. Improved fallow is most frequently cited in the commune Ndali (Fig. 6.20). In the more degraded communes Copargo, Djougou and Ouaké, the category of other technologies (especially fertiliser) becomes more important. Although traditional non-mechanised soil tillage with axe and hoe dominates in the whole catchment, ox-ploughing is practiced by about 15% of the interviewed farmers in the communes Ndali and Tchaourou (Fig. 6.21). Tractors are only used in the commercial plantations around the city Parakou.

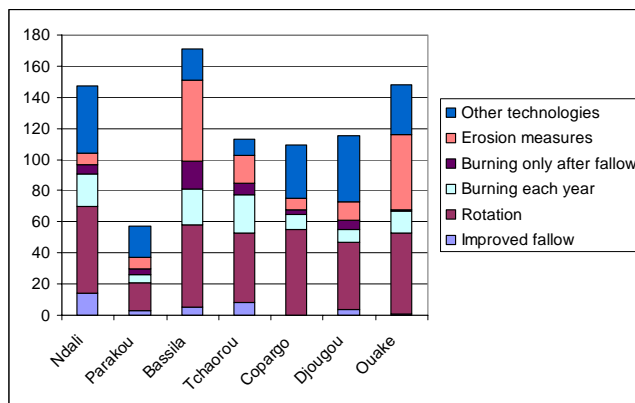


Fig. 6.20 Applied technologies for improvement of soil quality by commune based on data from HVO-Survey (2005).

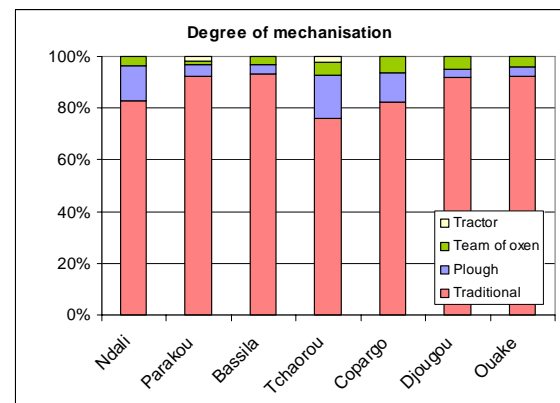


Fig. 6.21 Degree of mechanisation in the communes of the Upper Ouémé catchment based on data from HVO-Survey (2005).

Erosion forms in the Upper Ouémé catchment

Junge (2004) quantified net erosion losses from a footpath and a small unpaved road in the Aguima subcatchment. On the regional scale, such investigations are not feasible. In addition, the use of remote sensing techniques and air photographs is very limited in this sub-humid region with dense vegetation and a dominance of sheet and rill erosion. Therefore, erosion forms in the Upper Ouémé catchment were studied more generally to identify characteristic features of typical erosion forms and roughly validate the simulated spatial pattern of sediment yield. Special attention was paid to the regions with the highest calculated soil loss rates (see Chapter 7), i.e., the subcatchments around Djougou and Parakou. The elevated occurrence of erosion forms in these regions was confirmed during field observations. Sheet and rill erosion on fields and rill erosion along paths and roads were identified as the dominant erosion forms in the catchment (Fig. 6.22). Gullies can be found not only along large unpaved roads in the countryside but also in Parakou city (Fig. 6.23). However, these gullies are not only created by runoff, but they also often serve as channels and are mechanically deepened by engineering activities.



Petit mil field near Moné



Petit mil/soybean field near Djougou



Rice field near Alayomdé

Fig. 6.22 Sheet and rill erosion on fields.

Such establishment and maintenance of roads can lead to a heavy surface sealing of the adjoining slopes (Fig. 6.24). De Haan (1998) observed gully erosion at the beginning of the rainy season or along steep slopes, roads and rivers in the northern Borgou department. In general, the ground is covered by vegetation in the rainy season. However, bare soil is exposed on urban land, roads, paths and former sand excavation sites.



Road near Kolonkondé (a)



Road near Igbomakoro (a)



Road near Moné (b)

Fig. 6.23 Rill erosion (a) and gully erosion (b) along paths and roads.

On former sand excavation sites, which frequently occur along the main roads, part of the soil profile was removed, and the soil hardened due to heavy vehicles, leading to enhanced soil erosion and crusts several metres in width (Fig. 6.25). Exposed roots of plants and trees are typical for these sites.



During heavy rainfalls



One day after heavy rainfall

Fig. 6.24 Surface runoff on crusted surface next to road.

As a consequence of relief inversion, crusts are also frequently exposed on summits (Fig. 6.27). In the most degraded areas, topsoil erosion and tillage have led to the exposure of the gravel-rich, reddish subsoil (Fig. 6.26).



Fig. 6.25 Crusting and soil erosion in former sand excavation sites.

Table 6.6 provides typical characteristics of the studied observed erosion forms (3 to 4 sites each) in the Upper Ouémé catchment. Although not statistically representative, the studied sites capture the variety and dimensions of erosion forms encountered during the field investigations. The locations and general characteristics of the 13 studied sites are summarised in Table A.8 in Appendix A.

Most studied sites with erosion forms displayed low vegetation cover, a position at the lower or mid slope, a high gravel content on the surface and different degrees of surface sealing. Gullies were rarely found, with a maximum depth of two metres.

Slight sheet erosion is hardly visible, but it takes place on most single-cropped fields as vegetation cover is not dense and cover crops are rarely used. However, on some fields sheet erosion is moderate to severe and leads to visible reductions in crop performance.



Fig. 6.26 Gravel accumulation on yam field near Barei.



Fig. 6.27 Crusting on summits.

Although they are closely associated with erosion forms, accumulation forms were not studied as they are less critical for soil quality and plant growth in the catchment.

Table 6.6 Typical characteristics of observable erosion forms in the Upper Ouémé catchment.

Erosion form	Land use	Slope [%]	Slope position	Width x Length [m x m]	Depth [m]	Vegetation cover [%]	Surface gravel [%]	Sealing
Sheet	agricultural fields, sometimes reduced crop performance	2	mid	av. 100x150 m	< 0.02	variable	variable	none or slight, siltation on surface
Rills	path/roads	2-4	mid/low	deep rills av. 0.5 x 50 m, shallow rills up to 1 km long	0.05 - 0.4	~10	variable	partially
Gully	next to roads	3-4	mid/low	av. 2x150 m, up to 1 km long	0.6 - 2	< 10	< 10	very frequent
Surface sealing	mainly former sand excavation sites (5-10 years old)	1-2, at side slopes 4-6	low	excavation sites av. 70x300 m, crusts up to 5x5 m	-	< 30	30-85	massive; mosaic of crusts, sheet/rill erosion and accumulation

Characterisation of degraded fields

Besides soil erosion by water, topsoil deterioration due to regular burning and nutrient mining belong to the major soil degradation processes in the Upper Ouémé catchment leading to less productive, exhausted soils. In the catchment, exhausted fields were visually recognised by a number of indicators, including poor yield performance, occurrence of crusts, surface gravel or erosion forms, exposure of subsoil, low vegetation cover, increased pest infestations, and absence or occurrence of location-specific indicator plants. However, to avoid incorrect

interpretation due to other dominant factors (e.g., adverse weather, pests and diseases), visual observations were complemented with farmer interviews and soil augerings of 1 m depth. Only all three sources combined allow a full understanding of the degradation status of an agricultural field and possible options to improve it. Ideally, reference soil data should be used either from an earlier point in time (chronosequential sampling) or from a nearby non-degraded site (paired sampling).

We performed soil augerings on 20 visually degraded, agricultural fields and 5 nearby non-degraded sites as reference. Farmer interviews were conducted at 16 of the 20 sites plus 5 additional sites without soil investigations. Most studied sites are positioned on the middle and upper slopes. Fields on marginal land at the lower slope with near-surface indurated soil horizons were not considered. Visually, the exhausted fields are characterised by high contents of surface gravel/crust debris (max. 95% cover, mean 40%) of small ($\varnothing < 0.5$ cm) or medium to large size (1 to 30 cm), reduced vegetation cover (min $< 10\%$ cover, mean 35%), and occurrence of sheet and rill erosion. Often, crop performance is reduced and crops are planted in the direction parallel to the slope (see details in Table A.8, Appendix A). However, farmer interviews and soil investigations revealed that not all of these sites are characterised by low productivity. Two soil profiles with extremely high surface gravel contents (sites F9, Pr2) are chemically very fertile and deliver good yields if an appropriate crop is chosen. The farmer interviews provided information about the land use history of the sampled fields, including crop cycles, duration of the fallow period, plant management and perceived problems with regard to rainfall, soil properties and crop yield (see details in Table A.9, Appendix A). As pointed out earlier, farmers are well aware of soil degradation (see Excursus 6.1).

The interviewed farmers cultivate the fields for 3 to 7 years (mean 4.2 years) followed by a fallow period of 2 to 5 years (mean 2.9 years). Farmers report fallow periods of 6 to 20 years in the past. On the study sites, farmers were in the 3rd to 5th years of cultivation, i.e., towards the end of the cropping cycle, and were encountering difficulties in maintaining good yields without fertiliser input.

The farmers consider the current fallow periods insufficient to restore soil fertility. They adjust their cropping cycle accordingly, alternating between tubers and cereals or cereals and legumes (Mulindabigwi 2006), and include legumes such as groundnut (60% of interviewed farmers), niebe and soy bean.

Excursus 6.1: Farmer's knowledge about soil types and soil degradation

Most African farmers are aware of various forms of soil degradation on their farms (Dejene et al. 1997). Various local soil classifications exist which reflect soil properties and degree of degradation. Farmers in Central Benin classify their soils as a function of topography, surface material, easiness of soil tillage and production capacity (Junge, 2004; Agossou & Igué, 2003): a) stony soils on summits and ridges; b) gravel rich soils in the valleys, c) inland-valley soils (Gandonou 2000). Local indicators of soil degradation in Benin include the colour of the topsoil ("*terre noire*" = arable land, rich in organic matter, "*terre rouge*" = exposed subsoil), location-specific indicator plants and a specific smell and taste (Agossou & Igué, 2003; Gantoli, 1997). Farmers in Tanzania mention as indicators, for example, rill and gully erosion, increased run-off, the exposure of roots, decreases in crop yield, change in colour of crop leaves, stunted crops, the emergence of weeds and unpalatable species and the disappearance of termite mounds and grass or herb layer (Dejene et al. 1997).

About 7% of the cropping area in the Upper Ouémé catchment is covered by legumes, in particular in the north and west (Mulindabigwi 2006). Most farmers cultivate cassava at the end of the cropping cycle due to its low water and soil fertility demands, high litter production (pseudo-fallow) and easy conservation (see also Mulindabigwi, 2006; Saidou et al. 2004). Yam is only cultivated on newly reclaimed land far away from the villages or on long-term fallows (> 6 years). Three of the interviewed farmers were motivated by development projects to apply laborious soil conservation measures such as yam cultivation on short-term fallows in combination with dung or *Gliricidia* or installation of *Vetiver* hedges to prevent soil erosion. In addition, several farmers cite cultivation perpendicular to the slope as a practised measure for soil conservation; however, 50% of the sampled fields are cultivated in rows parallel to the slope. In general, spontaneous fallow and inclusion of groundnut in the crop cycle are the dominant strategy for restoring soil fertility; active soil fertility management is rare (Floquet et al. 2002). Crop residues are generally left on the field but often subject to burning. Five farmers reported burning the field annually, while six farmers try to protect the field through fire bands. About half of the farmers cultivate cotton and therefore have access to chemical fertiliser, which they use for cotton and maize. Only one farmer applies chemical fertiliser to groundnut and rice as well. Nearly no farmers are applying organic manure outside the homestead, but they allow Fulani herders to let their cattle graze after harvest. Only one farmer buys

organic manure. The interviewed farmers consider the soils on the studied fields to be generally fertile but exhausted due to overexploitation. In general, no significant differences in the responses between autochthonous and allochthonous interviewed farmers were observed.

Table 6.7 compares the mean physical and chemical topsoil properties of the 16 exhausted fields with the mean properties of the 19 representative profiles and the two profiles on sacred land. The properties of all studied profiles are summarised in Table A.10, Appendix A).

Table 6.7 Comparison of mean topsoil soil properties of exhausted fields, fallow and sacred land in the Upper Ouémé catchment.

Sites	# Pro- files	Depth	Sand	Silt	Clay	Gravel	C _{org}	N	C/N	pH	CEC _{pot}	K	Na	Mg	Ca	BS
		[cm]	[%]	[%]	[%]	[%]	[%]	[%]	[%]	[-]	[cmol _c /kg]	~	~	~	~	[%]
exhausted fields	16	11	78	13	8	22	0.9	0.04	22	5.3	2.7	0.12	0.01	0.8	2.7	72
fallow/savannah (repr profiles)	19	13	71	18	11	19	1.1	0.07	16	5.5	6.2	0.13	0.02	1.0	4.8	77
sacred land	2	9	75	14	11	25	2.6	0.18	15	6.1	12.2	0.37	0.01	1.4	9.4	62

Table 6.7 clearly shows the pronounced decrease in chemical soil fertility of the topsoils from the sacred to the fallow land and the exhausted fields. As soil texture and gravel content are similar among the three categories, the significant decrease in cation contents and CEC_{pot} can be mainly attributed to the lower organic carbon content. Although C_{org} on the exhausted fields is 20% lower than on the fallows and 65% lower than on the sacred land, values are still much higher than on the highly degraded fields in Ouaké (not shown here). There, the studied soils had only 0.2 to 0.3% C_{org} and base saturations as low as 15%. Data from Igué (published in Floquet et al. (2002)) show similar values for the *terre de barre* region in Southern Benin comparing sacred forest (C_{org} 5.7%, CEC_{pot} 16.2 cmol_c/kg, BS 100%, pH 7.3) and fields after 1-2 years cultivation (C_{org} 2.8%, CEC_{pot} 6.6 cmol_c/kg, BS 77%, pH 6.1) and long term cultivation (C_{org} 0.8%, CEC_{pot} 3.9 cmol_c/kg, BS 21%, pH 4.2). Nye & Greenland (1960, cited in Mulindabigwi (2006)) reported a 45% loss of C_{org} in a four year fallow system, while Hölscher et al. (2005) cite 20 to 40% loss of base cations in slash and burn agriculture through volatilisation and ash particle transport. Organic carbon or organic matter is often considered a very important indicator of soil degradation, besides nutrient levels and physical conditions (Greenland 1994). However, Mulindabigwi (2006) questions this indicator for the Upper Ouémé catchment because almost the entire catchment is subject to regular burning.

In the following, two examples of exhausted fields with reference sites are discussed to illustrate variations in soil properties in more detail: Figure 6.28 shows a cassava

field in Serou in the western Upper Ouémé catchment; the background is the border of a sacred forest that was taken as reference.



Fig. 6.28 Exhausted cassava field (soil augering Pr8) and sacred forest (soil augering Pr7) in Serou.



Fig. 6.29 Sorghum field with high variability of plant growth near Copargo (soil augerings Pr10, Pr11).

While the reference showed no surface gravel, 80% vegetation cover and a thick litter layer, the cassava plot was covered by 40% medium-size gravel and only 50% vegetation. Surface crusts were visible, and soils were reported to be shallow. Cassava was planted in slope-parallel rows with 30 cm high earth mounds following a one year fallow in the crop cycle sorghum – fallow – cassava (2 years) – sorghum. Due to the hardened subsoil, soil augerings in the cassava field and the sacred forest reached only 35 and 61 cm, respectively. Both augerings exhibited a similar sequence of three horizons with 26 to 40% gravel, mainly of ferric nodules. The third horizon was red and showed saprolitic characteristics. However, the depths of the horizons for the field augering are a bit smaller than for the forest, and topsoil contents of clay, organic carbon and nitrogen were more than twice as much on the forest site (see Table A.10, Appendix A). Organic carbon content was 4.4%, which is very high compared to the 0.9% C_{org} on the cassava field. Consequently, CEC_{pot} , cations and base saturation were also substantially higher in the topsoil as well as in the subsoil. The CEC_{pot} of 21.7 $cmol_e/kg$ in the topsoil is about 3.5 times higher than the average CEC_{pot} obtained for the representative profiles. PH values were also significantly higher in the forest. Although the C/N ratio is more favourable for crop cultivation on the cassava field, overall soil fertility is significantly higher at the reference site.

The second example is a sorghum field near Copargo in the north-western Upper Ouémé catchment with 80% large surface gravel, 50% vegetation cover and very poor plant growth. Planting rows run parallel to the slope. As a reference, an augering was conducted a few metres to the back of the field, where sorghum grows more than twice as high, according to the farmer due to a cut tree causing locally higher soil fertility. There, surface was covered by only 30% gravel and 40% vegetation. In both cases, the auger did not reach the first metre depth due to hardened subsoil. However, while the augering covers 77 cm including an A-horizon 16 cm thick for the reference, for the less fertile plot only the first 50 cm was accessible, and the A-horizon was only 4 cm thin. Below 41 and 44 cm, respectively, both augerings exhibit a dark red, mottled horizon with high bulk density. Soil augerings confirmed the higher soil fertility of the reference resulting from significantly elevated C_{org} contents in the topsoil and higher pH, nitrogen, cations and clay contents and lower gravel contents (in particular ferric nodules and quartz) throughout the entire profile (Table A.10, Appendix A). The high potassium and magnesium contents are striking.

In summary, the descriptions of the soil characteristics in the Upper Ouémé catchment revealed that the catchment is dominated by Acrisols and Lixisols. Although these soils are chemically more fertile than many soils in Southern Benin, nutrient availability is often limited, and physical restrictions due to high gravel contents and indurated horizons in the subsoil are high. Examples of transect studies illustrate the high variability of soil properties along the slope that can only partially be captured by the representative profiles for the dominant soil types. In particular, hydromorphic soils in the inland valleys are typical for the catchment but not dominant and therefore not considered in the representative profiles and the French soil map. Including the inland valleys in the soil map was not feasible due to their small dimensions and heterogeneous soil properties. Information about the degree of soil degradation in the Upper Ouémé catchment from an interdisciplinary survey, observations of erosion forms and a characterisation of degraded fields by farmer interviews and soil sampling showed that soil erosion and nutrient depletion are considerable problems in the western part of the catchment and near Parakou. In many parts of the catchment, nutrient depletion due to shortened fallow periods, low inputs and regular burning is more critical than the actual loss of topsoil. However, creeping soil erosion is dangerous due to its irreversibility, the important role of the

humus-rich topsoil for soil fertility and the potential exposure of unfavourable subsoils. Farmers are aware of the various forms of soil degradation but rely on fallow periods, crop rotation, and, if accessible, mineral fertiliser to maintain soil fertility. Regular burning and further expansion of cropland is widely practiced, while active soil management is rare. Rill erosion along paths and roads and sheet erosion on the fields are the dominant erosion forms in the catchment. Thus, gully formation and extensive surface sealing do not need to be considered in erosion modelling in the catchment.

7. EROSION MODELLING IN THE UPPER OUÉMÉ CATCHMENT

This chapter presents the results of erosion modelling with SWAT. First, the results of the calibration and validation of the SWAT model and then the findings of the analysis of climate and land use scenarios with SWAT are presented. Each part is introduced with a brief overview about the underlying databases and pre-processing steps.

7.1. Model setup 1998-2005, calibration and validation

This section presents the databases used to set up the SWAT model for the time period 1998-2005 and the results of model calibration and validation with regard to hydrology and the sediment budget. The influence of spatial discretisation on the model performance is also analysed. Finally, the model results for the period 1998-2005 are discussed.

7.1.1. Databases and pre-processing

The input data for the model setup originate from various sources (see Table 7.1).

Table. 7.1 Model input data and corresponding data sources.

	Variables	x	t	Period	Source
Climate data	min/max-temperature [°C], solar radiation [W/m ²], wind velocity [m/s], relative humidity [%]	2 stations	daily	1998-2005	DMN, IMPETUS
	precipitation [mm]	13 stations	daily	1998-2005	DMN, CATCH, IMPETUS
Soil data	soil map	5 sheets		1977	Dubroeuq, 1977a/b; Faure, 1977a/b; Viennot, 1978
	soil properties	representative profiles		2003/04	IMPETUS, own measurements
Discharge data	total discharge [m ³ /s]	8 outlets	daily	1998-2005	CATCH, IMPETUS
	total discharge [m ³ /s]	3 outlets	hourly, half-hourly	1998-2005	CATCH, IMPETUS
Turbidity measurements	turbidity [NTU], electric conductivity [mS/cm], water level [cm], water temperature [°C]	3 outlets	30 min	2004-2006	own measurements
	suspended sediment concentration [mg/l]	1 outlet: Beterou	daily	2004-2006	own measurements
Land use map	12 land use types	28.5 m-grid	26.10.2000		IMPETUS
DEM	elevation [m a.s.l.]	90 m-grid	February 2000		NASA SRTM

Whereas land use and soil data mainly originate from the IMPETUS project, discharge measurements were provided by the French research project AMMA/CATCH and IMPETUS. The climate data were recorded by the National Directorate of Meteorology (DMN) in Benin.

Land use data

The land use and land cover classification for the Upper Ouémé catchment was provided by Thamm et al. (2005) and Judex (2008), based on Landsat 7 ETM+-data from the years 2000 and 2001 (26.10.2000, 29.10.2001). The derived land use map (see Fig 2.13, Section 2.4) distinguishes two types of forests (*forêt claire*, *forêt dense*), four savannah types (*savane arborée*, *savane boisée*, *savane herbeuse*, *savane saxicole*), fields and two settlement classes. The classification follows the French nomenclature of land use types according to the Yangambi Conference (Sturm 1993). Furthermore, the classification includes the class ‘fallow,’ which describes degraded areas, frequent in the north-western part of the catchment. Fallows, in the original sense, are classified as different savannah types depending on their age. The original classes of land use were attributed to land use classes in the database of the SWAT model (Table 7.2).

Table 7.2 Attribution of the classes of land use for the Upper Ouémé catchment to the SWAT land use types.

Land use map	SWAT land use type	SWAT_Code	Portion [%]
cropland	agriculture - generic	AGRL	13.75
<i>forêt claire</i>	forest deciduous	FRSD	8.75
<i>forêt dense</i>	forest evergreen	FRSE	1.29
inland valley	wetlands non-forested	WETN	1.83
<i>savane arborée</i> , <i>savane arbustive</i>	range brush	RRGB	45.33
<i>savane boisée</i>	forest mixed	FRST	19.18
<i>savane herbeuse</i> , degraded fallows	range grasses	RNGE	8.26
<i>savane saxicole</i>	Juniperus grass	JHGR	0.43
settlement - high density	urban medium/low density	URML	0.02
settlement - low density	urban low density	URLD	0.43
water	forest evergreen	FRSE	0.16
no vegetation (inselberg)	urban institutional	UINS	0.57

To define hydrological response units (HRUs), i.e. homogeneous soil and land use combinations, a threshold of 10% for land and soil use was defined to avoid too many small HRUs. As a consequence, the number of land use types decreased from 12 to 6. Special attention was given to a similar percentage of agricultural land before

and after HRU delineation (see Table 7.3), because a small deviation can heavily affect modelling results. However, the fractions of *savane arborée/arbustive* and *savane boisée* were significantly increased at the cost of *forêt claire*, *savane herbeuse* and inland valleys.

Table 7.3 Distribution of land use types before and after establishing a threshold of 10% for the definition of hydrological response units (HRUs).

Land use type	SWAT code	Portion before [%]	Portion after HRU definition [%]	Deviation [Δ%]
<i>savane arborée, savane arbustive</i>	RNGB	45.33	52.60	16.04
<i>savane boisée</i>	FRST	19.18	20.44	6.57
cropland	AGRL	13.75	14.16	2.98
<i>forêt claire</i>	FRSD	8.75	7.82	-10.63
<i>savane herbeuse, fallows</i>	RNGE	8.26	4.91	-40.56
inland valley	WETN	1.83	0.06	-96.72

The land use types were adjusted to local conditions in Benin by modifying plant heights and the parameters determining the annual development of the leaf area index according to Mulindabigwi (2006). During parameterisation of the rangeland class in SWAT (RNGB, RNGE), a problem of unlimited biomass growth appeared. In order to allow a correct representation of biomass growth, a new land use class SAVA with similar properties was created. Values for the USLE crop factor C were taken from Junge (2004), Sintondji (2005) and Roose (1977).

Soil data

A digitised version of the soil maps for Benin was taken from ORSTOM (Dubroeuq, 1977a/b; Faure, 1977a/b; Viennot, 1978), and measurements of soil properties from Sintondji (2005) and studied representative profiles in 2004 (see Section 6.1) were used. Available water capacity and saturated hydraulic conductivity were estimated with the pedotransfer function of Rawls & Brakensiek (1995).

Digital elevation model (SRTM)

A digital elevation model from February 2000 with a resolution of 3 arc-seconds (~90 meters) was downloaded from the NASA Shuttle Radar Topography Mission (SRTM) (<http://www2.jpl.nasa.gov/srtm/>, accessed on 10.12.2004). Before using this DEM, missing pixels at inselbergs resulting from clouds were filled with data from topographic maps 1:200,000.

Parameterisation of climate data

Data from two climate stations (Parakou 1998-2000, Dogué savannah 2001-2005) and 13 pluviometric stations were considered in the model (Fig. 7.2). Thus, the climate parameters of wind velocity, air temperature, solar radiation and relative humidity and therefore also ET_{pot} were assumed to be constant in the whole catchment. This simplification can be justified by the flat relief and homogeneity of the research area. Because wind velocities at the station Dogué savannah were clearly underestimated due to dense vegetation, this parameter was taken from the nearby climate station Dogué Mt. de Gaulle. Daily values for solar radiation before 2001 had to be estimated from sunshine duration. The 13 pluviometric stations were chosen from about 38 stations in the Upper Ouémé catchment considering the completeness of the datasets for the period 1998-2005 and a regular distribution over the catchment. Missing values were filled with values from the closest neighbouring pluviometric station. The values for the parameterization of the SWAT weather generator were taken from Sintondji (2005), based on climate data for the stations Parakou and Dogué for the years 1962-2001 and 1993-2002. However, since gaps in observed climate data were filled, use of a weather generator was not required.

Model setup via AVSWAT interface

After preparing all input datasets and adding them into the SWAT user databases, a new SWAT project was created with the ArcView User Interface.

The main steps of the procedure included delineating subbasins and HRUs and writing all input files (Fig. 7.1).

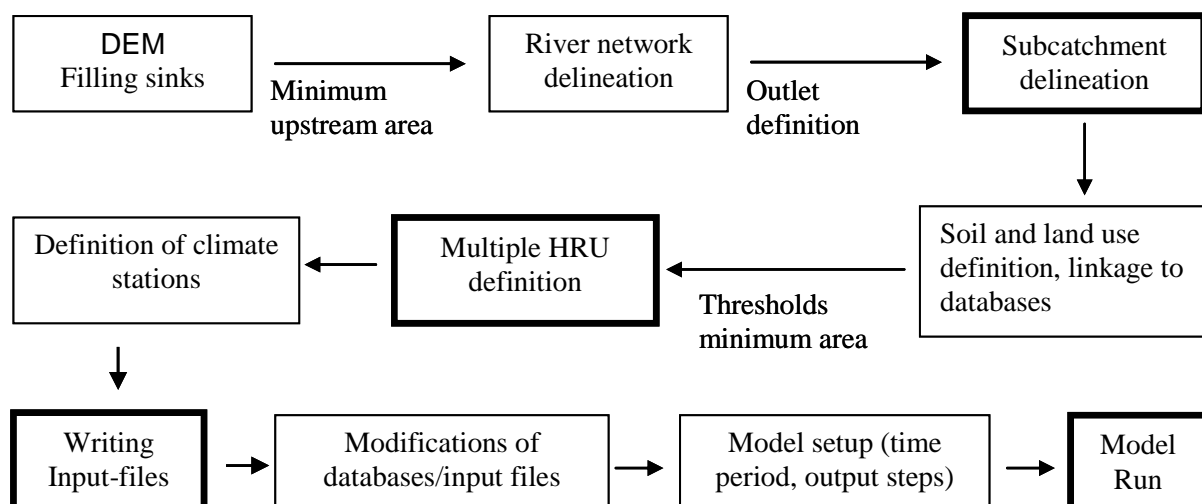


Fig. 7.1 Steps for setting up a new SWAT project with the ArcView User Interface.

Thresholds of 6000 ha for the minimum upstream area and 10% for the delineation of HRUs were chosen so as to balance the number of subbasins with the spatial resolution of the input data and to allow an adequate representation of the main land use and soil types. This configuration led to 121 subbasins and 926 HRUs in the Upper Ouémé catchment (Fig. 7.2).

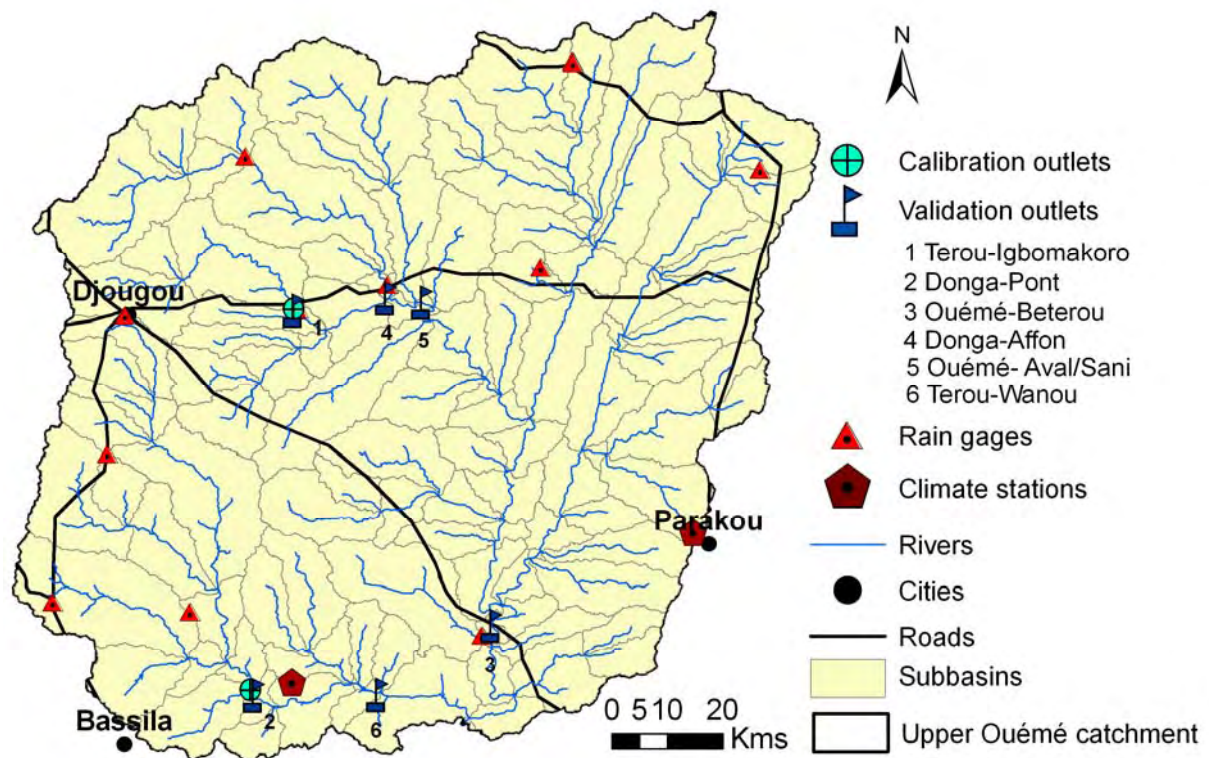


Fig. 7.2 Delineated subcatchments, considered climate stations and locations of calibration and validation outlets.

Suspended sediment concentration

For all gauged sites, i.e. Terou-Igbomakoro, Donga-Pont, Lower Aguima and Donga-Kolonkonde, a specific relationship between turbidity and suspended sediment concentration (SSC) was determined. Water sampling was performed in the period 2004-2006 during the rainy season. Water sampling after large discharge events in 2005 and 2006 significantly improved the quality of the relationship obtained with measurements in 2004. For Donga-Kolonkonde, water sampling started in 2006. Finally, for each curve, between 69 and 87 water samples were considered to gravimetrically determine the SSC. The SSC values were then plotted against the turbidity values, and the linear regression line and coefficient of determination (R^2) were determined for the outlets Terou-Igbomakoro, Donga-Pont, Lower Aguima and

Donga-Kolonkonde (Fig. 7.3). In order to avoid negative turbidities for very low SSC values, the relationship between both variables was assumed to be directly proportional ($y = a \cdot x$) below the lowest sampled SSC value. The coefficients of determination (R^2) ranged from 0.55 and 0.78. These values can be considered satisfactory and lie within the lower and mid ranges published by other authors for catchments in Germany (e.g., Pfannkuche & Schmidt, 2003), the United States (e.g., Gray et al. 2003; Inamdar, 2004; Dana et al., 2004) and Nepal (Brasington & Richards 2000).

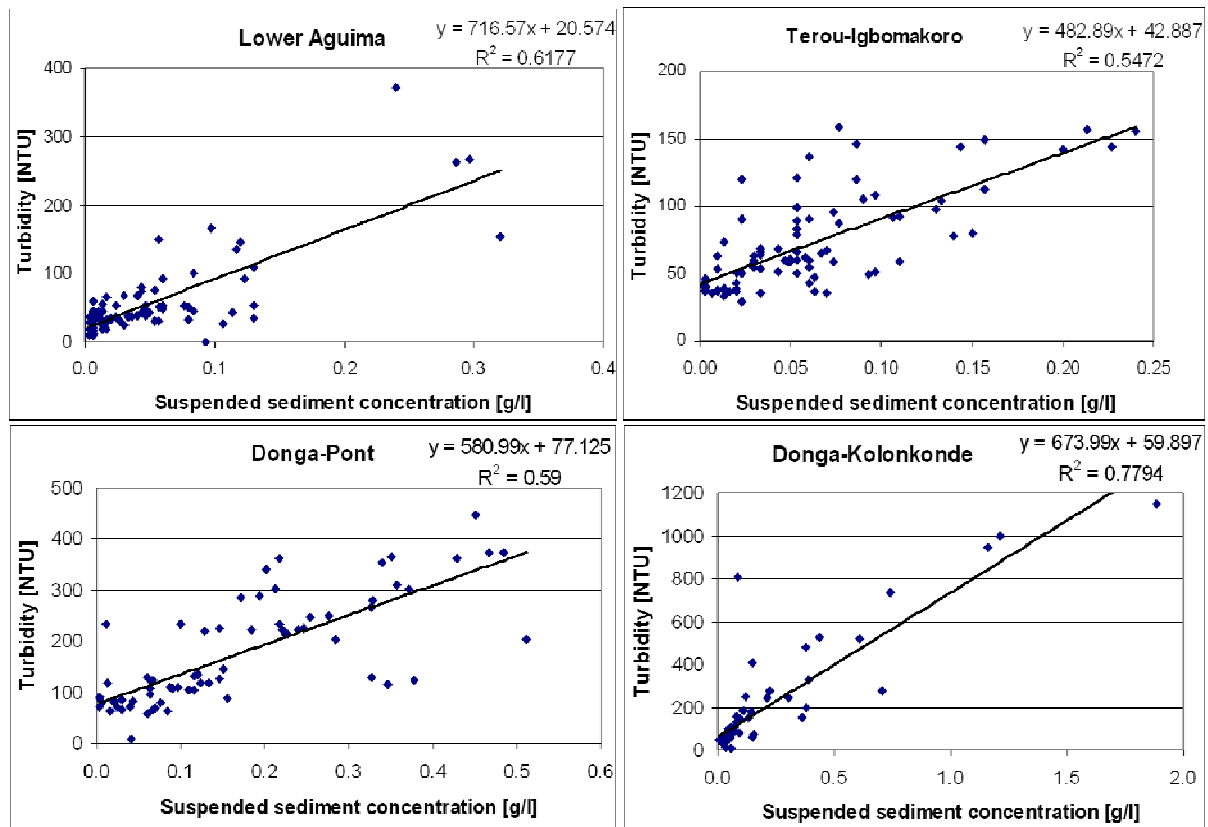


Fig. 7.3 Site-specific relationships between turbidity and suspended sediment concentration.

The sediment curves were calculated for the outlets by combining the suspended sediment concentrations with hourly and half-hourly discharge data. For example, Figure 7.4 shows the sediment curve for the Terou-Igbomakoro and Donga-Pont catchments for the year 2005 with an hourly time step. The graphs indicate highest discharge and sediment peaks in mid-July. Although the Donga-Pont catchment is only one-fourth the size of the Terou-Igbomakoro catchment, the transported sediment loads in 2005 amount to almost 50% of those at the Terou-Igbomakoro outlet. One extreme discharge event on the 14th and 15th of July at Donga-Pont carried extremely high sediment loads, up to 456 tons per hour. Several sediment

peaks accompanied the discharge event, the highest recorded three hours after the discharge maxima.

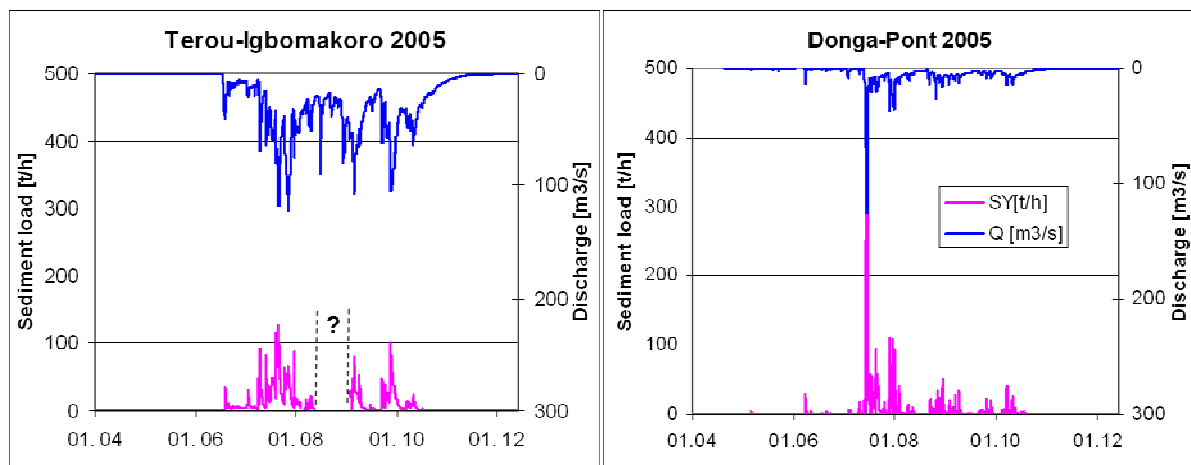


Fig. 7.4 Sediment and discharge curves in 2005 at the outlets Terou-Igbomakoro and Donga-Pont derived from measurements.

The sediment curves for the other outlets and the year 2004 are shown in Subsection 7.1.3, which deals with model calibration of the sediment budget. Calculation of annual sediment loads was hampered by several gaps in the data records, e.g., for the period 12.08-1.09.2005 at the Terou-Igbomakoro outlet. Therefore, the derived annual sediment yields should be considered as minimum values (see Table 7.4).

Table 7.4 Minimum annual sediment loads derived from turbidity measurements (Donga-Pont, Terou-Igbomakoro, Lower Aguima), and daily water sampling (Ouémé-Beterou).

	Turbidity _{max} [NTU]	SSC _{max} [g/l]	SY 2004 [t/ha/yr]	SY 2005 [t/ha/yr]
Donga-Pont	700 (800)	1.22	>> 0.05	0.41
Terou-Igbomakoro	248 (566)	1.08	> 0.07	>0.17
Lower Aguima	500 (756)	0.17	0.02	0.17
Ouémé-Beterou	-	1.03	0.05	0.22

The calculated sediment yields lie in the typical range of reported values for African rivers. For example, Walling et al. (2001) obtained an-

annual sediment yields between 0.15 and 0.26 t/ha/yr for the Upper Kaleya catchment (63 km²) in South Zambia. The authors also listed literature values for many African rivers, all less than 1 t/ha/yr. In Asian catchments, suspended sediment yields are often significantly higher due to steep slopes, silty soils and intense land use (e.g., Chappell et al. (2004), Douglas & Guyot 2005). The recorded maxima of suspended sediment concentrations from turbidity measurements also agree with those reported in the literature, ranging from 0.04 to 5 g/l (e.g., Gray et al., 2003; Inamdar, 2004; Pfannkuche & Schmidt, 2003; Lewis, 1996; TetraTech, 2004).

Baseflow separation

In order to learn about the fractions of discharge components in the measured total flow, the digital filter technique of Arnold & Allen (1999) was applied. This method was originally used in signal analysis and processing. The equation is:

$$Q_{surf}(t) = \beta \cdot Q_{surf}(t-1) + (1 + \beta) / 2 \cdot (Q_{tot}(t) - Q_{tot}(t-1))$$

where

Q_{surf}	filtered surface runoff (quick response)
Q_{tot}	total streamflow
β	filter parameter (set to 0.925)

Several studies have shown that the results of the digital baseflow filter compare well with manual baseflow separation techniques (Arnold & Allen 1999). The filter program delivers three baseflow curves for different climate zones. The second curve is most suitable for humid areas.

Moreover, measurements of electric conductivity in 30 minute intervals at the Terou-Igbomakoro and Donga-Pont outlets allowed baseflow separation for several events in 2004 and 2005. Based on the assumption that each discharge component shows a typical specific electric conductivity, and considering the mass balance equation, the fraction of surface runoff could be derived as follows:

$$Q_{surf} = (EC_{Q_{tot}} - EC_{Q_{base}}) \cdot Q_{tot} / (EC_{rain} - EC_{base}) \quad (7.1)$$

where

Q_{surf}	surface runoff [l/s]
Q_{tot}	total runoff [l/s]
$EC_{Q_{tot}}$	electric conductivity of total runoff [$\mu\text{s/cm}$]
$EC_{Q_{base}}$	electric conductivity of baseflow [$\mu\text{s/cm}$]
EC_{rain}	electric conductivity of rainfall [$\mu\text{s/cm}$], estimated as 13.7

Figure 7.5 shows typical curves after a rainfall event. As discharge increases, the electrical conductivity is reduced. The reduction is assumed to be proportional to the

fraction of fast discharge components, since rainwater has only a short contact with the ion-rich soil.

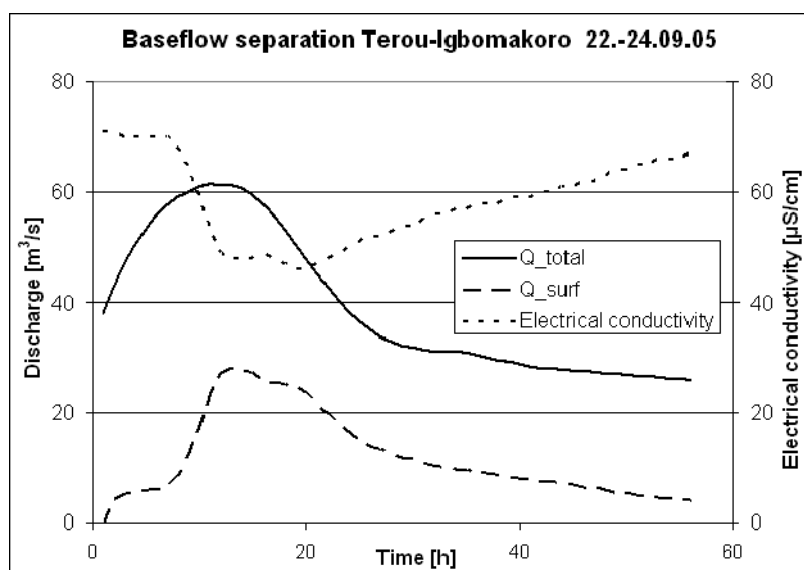


Fig. 7.5 Baseflow separation based on discharge measurements for an event at Terou-Igbomakoro outlet.

lower values for the baseflow, in particular at the end of the rainy season. Furthermore, the filter-based baseflow curve is smoothed compared to the curve of conductivity measurements.

A comparison of the curve with the baseflow curve derived from measurements of electrical conductivity at the Terou-Igbomakoro and Donga-Pont outlets in 2004 and 2005 showed satisfactory agreement between both curves (Fig. 7.6). However, the baseflow filter delivered slightly

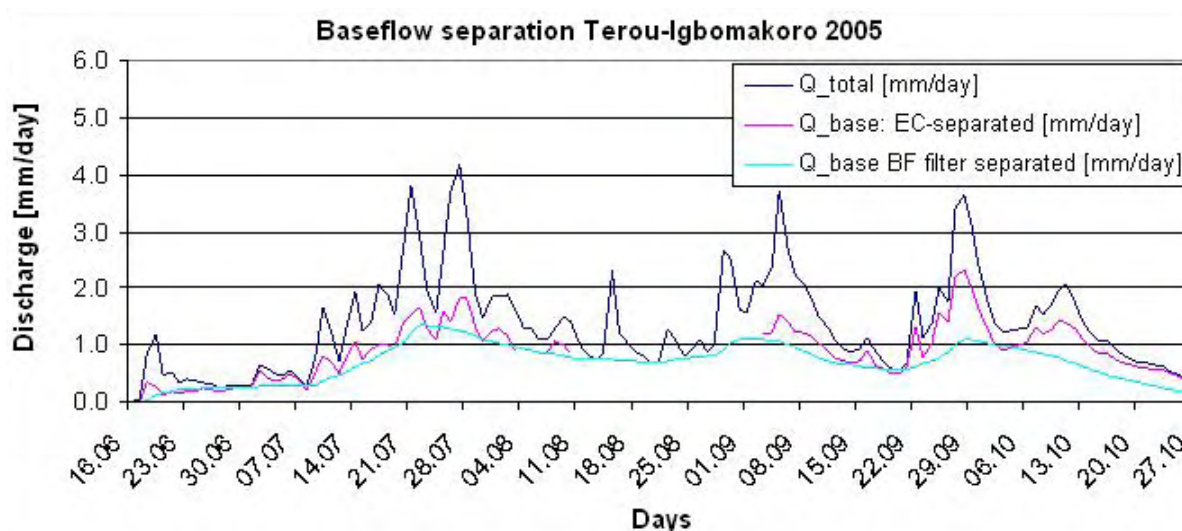


Fig. 7.6 Comparison of baseflow separation according to the baseflow filter program of Arnold & Allen (1999) with separation based on measurements of electrical conductivity and equation 7.1.

A scatter plot of 17 and 12 analysed rainfall events of the years 2004 and 2005 in the Terou-Igbomakoro and Donga-Pont catchments illustrates the good correlation between surface runoff, which was separated based on measurements of electrical conductivity, and total discharge (Fig. 7.7). A linear regression delivers an average

fraction of surface runoff of 28% and 30% in the Donga-Pont and Terou-Igbomakoro subcatchments, respectively.

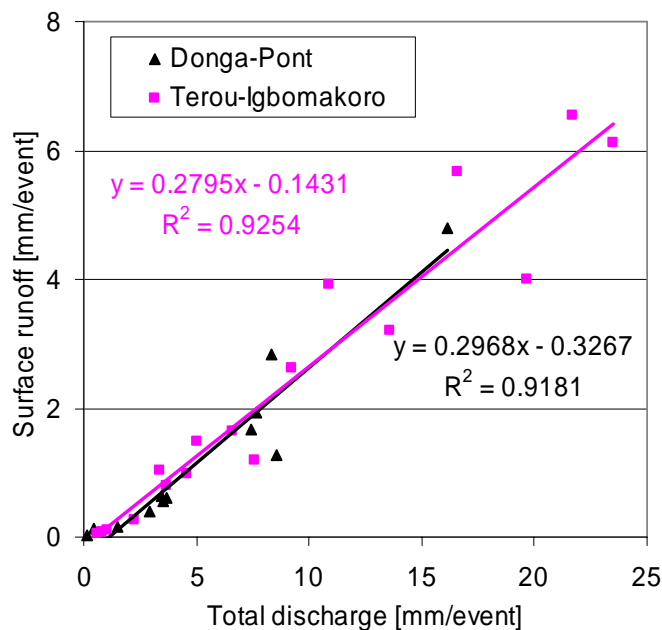


Fig. 7.7 Fraction of surface runoff derived from measurements of electrical conductivity.

The fraction of surface runoff is significantly higher for large events. From conductivity measurements, the average fraction of surface runoff is only slightly higher in the more intensively used Donga-Pont catchment. The separation of baseflow from measured discharge with the digital filter revealed a more significant difference between the two subcatchments. With a fraction of surface runoff of about 55% in the period 1998-2005, the Donga-Pont subcatchment exceeded the mean value of 43% for the Terou-Igbomakoro subcatchments. Giertz (2004) obtained for two gauges in the small Aguima subcatchment 40% and 34% of total discharge as fast discharge components from electrical conductivity measurements.

To sum up, although there are differences, the baseflow derived from the digital baseflow filter seems to be suitable for calibrating the discharge components.

7.1.2. Model calibration/validation - Hydrology

Model calibration - Hydrology

Model calibration was performed simultaneously at the Terou-Igbomakoro and Donga-Pont outlets following the calibration procedure illustrated in Fig. 5.1, Chapter 5. Table 7.5 summarizes the calibration parameters for the hydrological calibration. The calibration parameters for the Terou-Igbomakoro subcatchment were taken from Sintondji (2005) as a starting point but had to be modified due to differences in the databases. Moreover, the SCS curve numbers were split into one to four curve numbers per land use according to the hydrologic group, considering soil properties. The baseflow recession constants at the Donga-Pont and Terou-

Igbomakoro outlets were estimated with the baseflow filter program of Arnold & Allen (1999) for discharge data from 1998 to 2005. Subsequently, one averaged recession constant was assumed for the whole Upper Ouémé catchment. Automatic calibration was performed after extensive manual calibration and did not substantially change the results of manual calibration.

In the default modus, SWAT heavily overestimated runoff. This was mainly due to low simulated values for actual evapotranspiration compared to values obtained by other authors working in this region (e.g., Varado et al., 2005; Le Lay & Galle, 2007). If the Priestley-Taylor method was used, ET_{pot} values were even lower than for Penman-Monteith.

Table 7.5 Calibrated parameters for hydrological calibration, comparison with default values and assumptions by Sintondji (2005); (# value did not appear, - measured values).

Parameter	Definition	SWAT Default	SINTONDJI (2005)	This study			
				Hydrol. group			
				A	B	C	D
CN_AGRL	SCS curve number [-]	77	78	#	76	78	81
CN_FRST	SCS curve number [-]	78	60	55	59	62	64
CN_FRSD	SCS curve number [-]	79	66	54	58	61	#
CN_RNGE	SCS curve number [-]	66	69	58	62	65	67
CN_RNGB	SCS curve number [-]	69	69	58	62	65	67
CN_WETN/PAST	SCS curve number [-]	60	79	#	67	#	#
SURLAG	Surface runoff lag coefficient [-]	4	0.2887	0.2887			
ALPHA_BF	Base flow recession constant [-]	0.048	0.0336	0.1			
GWQMN	Threshold depth of water in shallow aquifer for return flow [mm]	0	7	20			
GW_REVAP	Groundwater revap coefficient [-]	0.02	0.19	0.3			
REVAPMN	Threshold depth of water in shallow aquifer for revap or percolation to deep aquifer	1	0.02	0			
RCHRG_DP	Fraction of deep aquifer percolation [-]	0.05	0.03	0.4			
LAI_INIT	Initial leaf area index [-]	0	3	3			
CH_K2	Channel hydraulic conductivity [mm/h]	0	7.1359	0			
ESCO	Soil evaporation compensation factor [-]	0.95	0.1	0.1			
SOL_AWC(layer)	Available water capacity of the soil layer [mm/mm]	-	+12.5%	+25%			
SOL_Z	Total depth of soil profile [mm]	-	-	+30%			
SOL_K(layer)	Saturated hydraulic conductivity of the soil layer [mm/h]	-	-	Values < 5 set to 5			

In order to reduce the overestimation of runoff, groundwater parameters and the soil evaporation compensation factor (ESCO) were adjusted so as to maximise actual evapotranspiration and increase the fraction of deep aquifer recharge. Moreover, physical soil properties were modified, resulting in increased soil percolation and reduced surface runoff. The estimated saturated hydraulic conductivities (K_{sat} or SOL_K) were very low for clay-rich subsoils, causing water-logging in some profiles. In order to avoid this, all K_{sat} values smaller than 5 mm per hour were set to 5 mm

per hour. This seems more realistic, considering the frequent occurrence of biopores and preferential flow paths in the humid and sub-humid tropics. In contrast with Sintondji (2005), the channel hydraulic conductivity CH_K2 was not modified. Thus, water loss through the channel bed was considered insignificant. Soil investigations in the river beds revealed a wide range of soil textures, from sands to clays. Increasing CH_K2 did not improve the calibration results.

As a result of hydrological calibration, yearly amounts of total discharge agreed well, in particular for the Terou-Igbomakoro subcatchment (Fig. 7.8). The mean annual discharge for the calibration period was slightly overestimated, by 3% and 8% for the Donga-Pont and Terou-Igbomakoro subcatchments, respectively (see Table 7.6). In addition, in 1999, discharge was significantly overestimated in the Donga-Pont subcatchment. Looking at the weekly curves (Fig. 7.9) and the daily data, this can be attributed to an underestimation of the discharge peaks at the end of August and beginning of October resulting from rainfall peaks. It is not clear if actual rainfall was higher or if the weak response of the SWAT model is responsible for the mismatch.

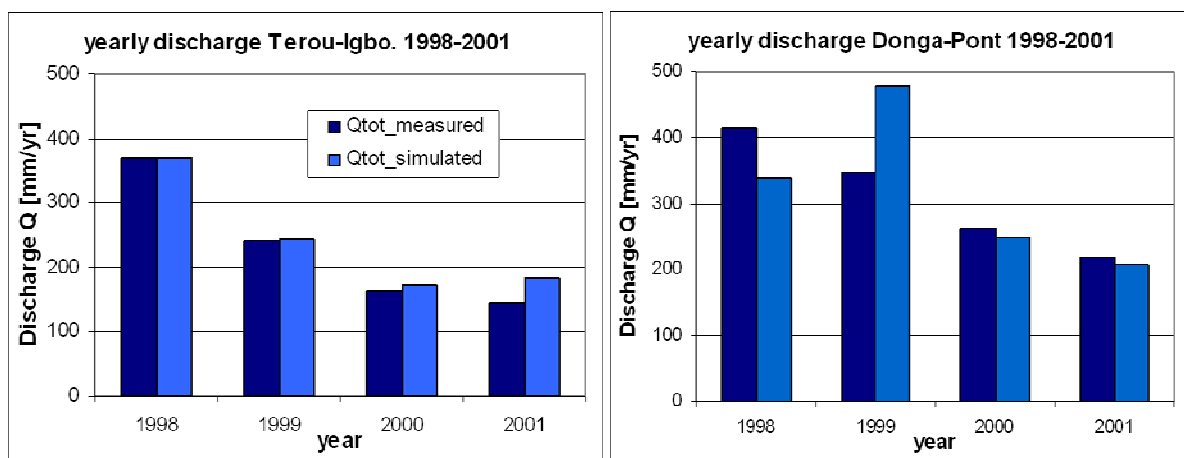


Fig. 7.8 Comparison of simulated and measured annual discharge for the calibration period: Terou-Igbomakoro and Donga-Pont outlets.

The temporal characteristics were optimised by modifying SURLAG, ALPHA_BF, GW_DELAY, GWQMN and REVAPMN. Finally, satisfactory measures of performance were obtained for weekly time steps in the Terou-Igbomakoro subcatchment (ME 0.85, R^2 0.87, IoA 0.96) and the Donga-Pont subcatchment (ME 0.81, R^2 0.81, IoA 0.95). Figure 7.9 illustrates the temporal characteristics for simulated and measured discharge. In general, the beginning and end of the discharge period are well captured. However, at the beginning of the rainy season in 1999 and 2001, discharge was significantly overestimated in the Donga-Pont

subcatchment. Most peaks of the hydrograph are well reproduced. In the Terou-Igbomakoro subcatchment, the simulated and measured discharge curves fit quite well. Nevertheless, the discharge curve for Terou-Igbomakoro is slightly biased at the end of the rainy season.

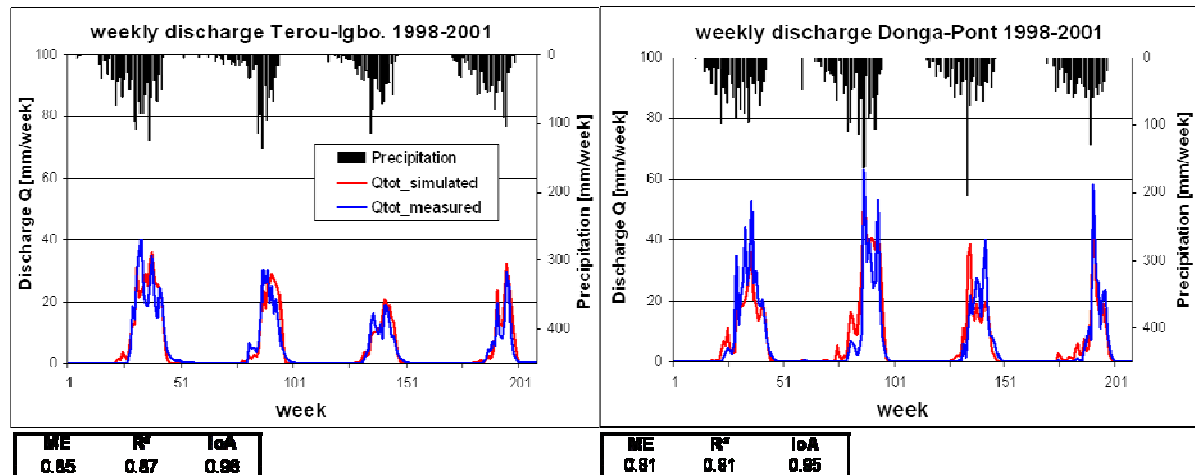


Fig. 7.9 Comparison of simulated and measured weekly discharge for the calibration period: Terou-Igbomakoro and Donga-Pont outlets, measures of performance.

A comparison of the temporal characteristics of the discharge fractions revealed that this bias is probably due to a retardation of the baseflow (Fig. 7.10). A further reduction of GW_DELAY to force the groundwater flow to appear earlier was not feasible because it caused significantly increased runoff amounts. However, despite a slight overestimation of surface runoff, the total amounts of the measured discharge components were well reproduced (see Table 7.6).

Table 7.6 Comparison of mean simulated and measured discharge components for the calibration period at the Terou-Igbomakoro and Donga-Pont outlets. Baseflow here includes lateral flow and shallow aquifer recharge. Measured baseflow was derived with a digital baseflow filter.

	Simulated			Measured			WY_sim/ WY_meas	Q _{surf_sim} / Q _{surf_meas}	Q _{base_sim} / Q _{base_meas}
	WY [mm/yr]	Q _{surf} [mm/yr]	Q _{base} [mm/yr]	WY [mm/yr]	Q _{surf} [mm/yr]	Q _{base} [mm/yr]	[%]	[%]	[%]
Donga-Pont	320	181	139	311	176	135	103	103	103
Terou-Igbo.	247	110	137	229	103	126	108	107	109

The scatter plots and flow duration curves in Figs. 7.11 and 7.12 confirm the correct representation of weekly rainfall sums over the calibration period in both catchments. For the Terou-Igbomakoro catchment, the regression line between simulated and measured weekly discharge almost covers the 1:1 line. Discharge between 5 and 20 mm per week is slightly underrepresented, whereas that between 1 and 5 mm is more frequently simulated than measured. For the Donga-Pont subcatchment, a small bias of the model towards lower values can be observed. The reproduction of

the frequency distribution is satisfying. However, discharge between 15 and 20 mm per week is significantly overestimated.

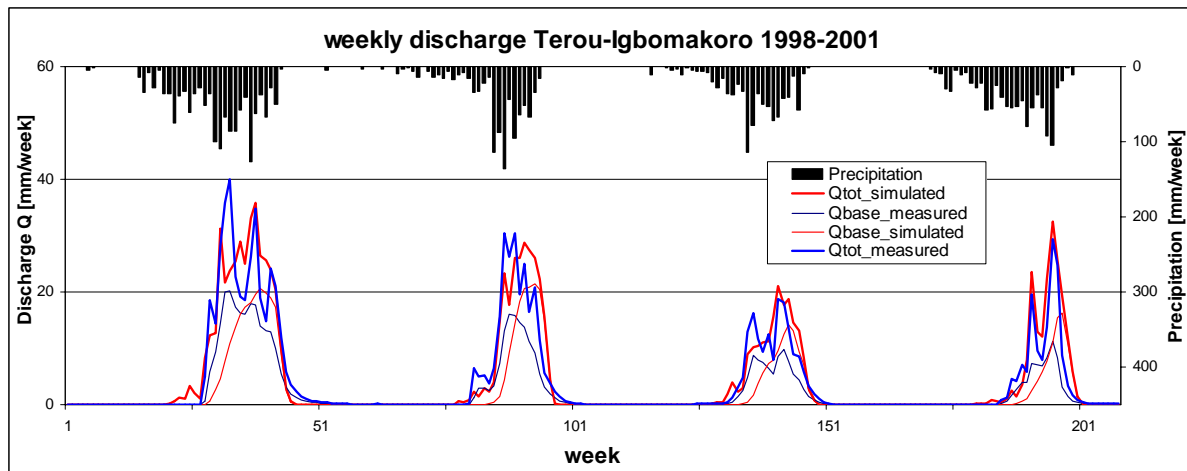


Fig. 7.10 Discharge components: baseflow fraction from measured and simulated discharge data in the Terou-Igbomakoro subcatchment.

Looking at the mean annual soil water balance for the two subcatchments and the Upper Ouémé catchment in the calibration period (see Table 7.7), it becomes clear that rainfall in the Donga-Pont subcatchment is significantly higher than in the rest of the catchment. Therefore, all variables of the water balance are also provided as the fraction of mean annual rainfall.

Table 7.7 Mean simulated annual soil water balance in the Donga-Pont, Terou-Igbomakoro and Upper Ouémé catchments in the calibration period (1998-2001).

	Donga-Pont	Terou-Igbo.	Upper Ouémé	Donga-Pont	Terou-Igbo.	Upper Ouémé
Precipitation [mm/yr]	1279	1095	1158	100%	100%	100%
Surface runoff [mm/yr]	181	110	112	14%	10%	10%
Baseflow [mm/yr]	141	137	127	11%	12%	11%
Shallow aquifer recharge [mm/yr]	360	337	325	28%	31%	28%
Deep aquifer recharge [mm/yr]	126	118	114	10%	11%	10%
Actual evapotranspiration [mm/yr]	733	635	710	57%	58%	61%
Potential evapotranspiration [mm/yr]	1634	1635	1635	128%	149%	141%
Change in soil water storage [mm/yr]	67	47	54	5%	4%	5%

As expected from the land use distribution, the highest fraction of surface runoff, 15% of mean annual rainfall, is obtained in the Donga-Pont subcatchment. In the Terou-Igbomakoro and the Upper Ouémé catchments only about 10% of mean annual rainfall run off superficially. In contrast to modelling studies by Giertz (2004), who found a mean fraction of interflow of 55% in the Aguiema subcatchment (30 km²), the SWAT model finds only an average of 3-6% of the total flow to be lateral flow. Problems with the SWAT model in the representation of interflow in lowland areas

have been reported by several authors (e.g., Busche, 2005; Sintondji, 2005; Eckhardt et al., 2002). Therefore, lateral flow and shallow aquifer recharge have been aggregated as baseflow in Tables 7.6 and 7.7. As a consequence of the lower rainfall, the absolute values for actual evapotranspiration in the Terou-Igbomakoro subcatchment are 75-100 mm lower than in the other two catchments.

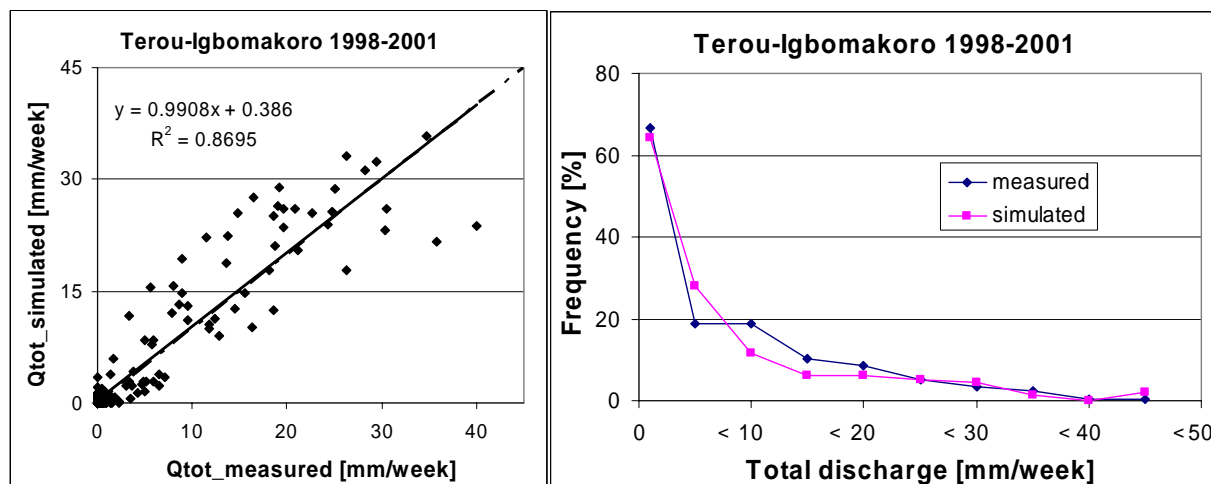


Fig. 7.11 Scatter plot and frequency distribution for measured and simulated weekly discharge at the Terou-Igbomakoro outlet in the calibration period.

Moreover, the plausibility of the mean annual water balance was checked for the hydrological response units. The results were consistent, showing higher actual evapotranspiration and higher leaf area index and biomass in forest areas than on savannah and agricultural land. In comparison, agricultural land was characterized by the highest amounts of total water yield and surface runoff, while soil water percolation and baseflow were significantly lower. For the inland valleys, soil water

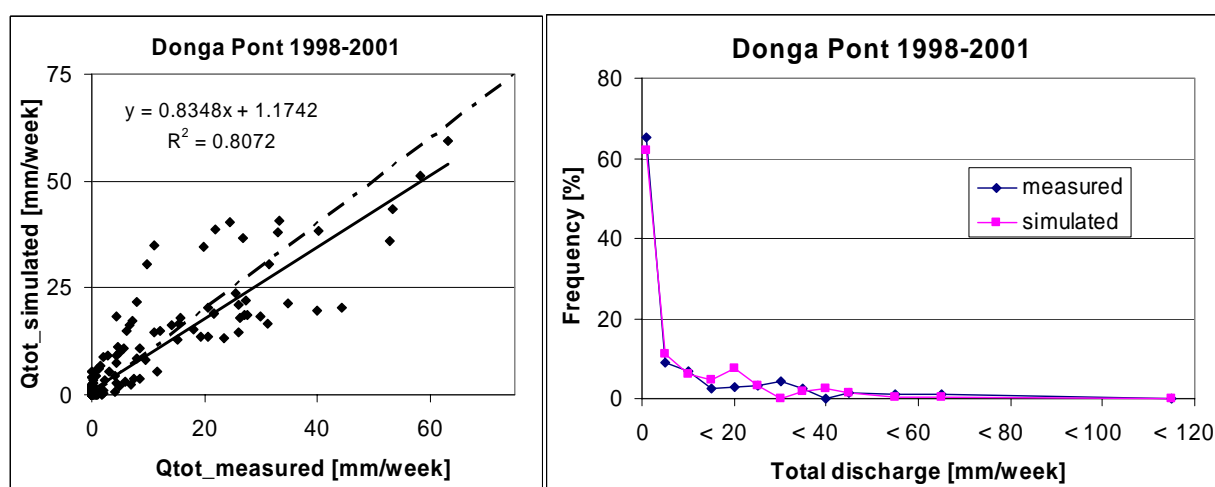


Fig. 7.12 Scatter plot and frequency distribution for measured and simulated weekly discharge values at the Donga-Pont outlet in the calibration period.

percolation and groundwater recharge were even lower than for agricultural land. The transmission losses in the channel through evaporation were smaller than 2 mm per year, and therefore were negligible.

Model validation - Hydrology

In order to validate the hydrological model component, the model parameterisation after calibration at the Terou-Igbomakoro and Donga-Pont outlets was applied to another time period (split sample test) as well as to other subbasins in the Upper Ouémé catchment (proxy basin test).

a) Temporal validation of hydrology (2002-2005)

The application of the calibrated model to the validation period (2002 to 2005) led to satisfactory results. Total runoff amounts were very well reproduced for the Terou-Igbomakoro subcatchment (Table 7.8). For the Donga-Pont subcatchment, total runoff amounts were overestimated by about 28%, in particular concerning surface runoff (Fig. 7.13).

Table 7.8 Comparison of mean simulated and measured discharge components for the validation period at the Terou-Igbomakoro and Donga-Pont outlets.

	Simulated			Measured			WY_sim/	Q _{surf_sim} /	Q _{base_sim} /
	WY	Q _{surf}	Q _{base}	WY	Q _{surf}	Q _{base}	WY_meas	Q _{surf_meas}	Q _{base_meas}
	[mm/yr]	[mm/yr]	[mm/yr]	[mm/yr]	[mm/yr]	[mm/yr]	[%]	[%]	[%]
Donga-Pont	275	168	101	214	124	91	128	135	111
Terou-Igbo.	178	82	91	187	86	101	95	95	90

The temporal characteristics between the measured and simulated discharge curves agreed very well (Fig. 7.14) and led to similar performance measures as those in the calibration period. For the Donga-Pont subcatchment, the performance was slightly better than for the calibration period.

The overestimation of total discharge at the Donga-Pont outlet can be attributed to two discharge peaks in 2003 and 2005, for which the model overreacts to underlying extreme rainfall amounts of 150-200 mm per week. However, such events are always difficult to capture with semi-physically-based hydrological models using the SCS curve number approach.

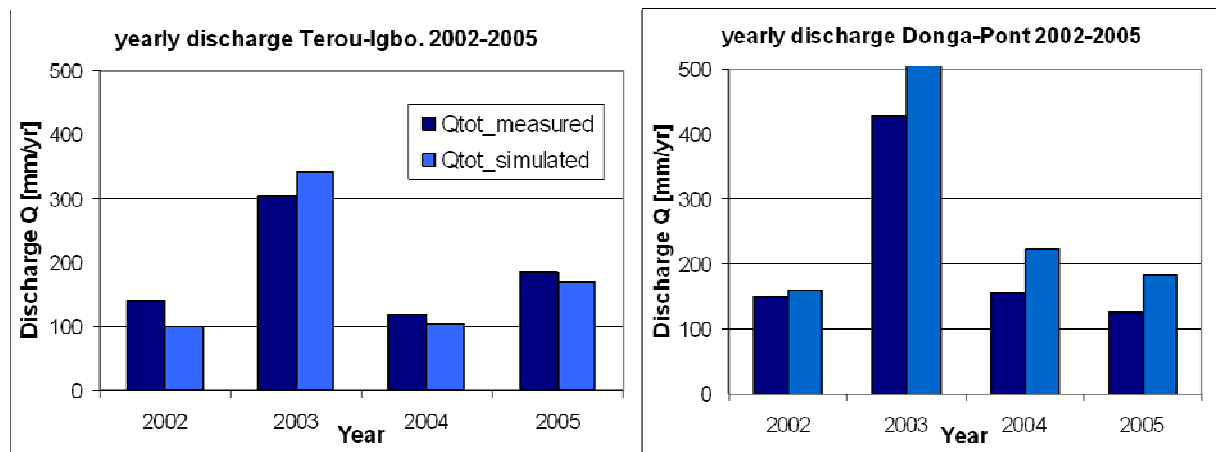


Fig. 7.13 Comparison of simulated and measured annual discharge for the validation period: Terou-Igbo and Donga-Pont outlets.

Furthermore, a high degree of uncertainty remains in the rainfall pattern due to the high spatial and temporal rainfall variability in the Upper Ouémé catchment (see Chapter 8).

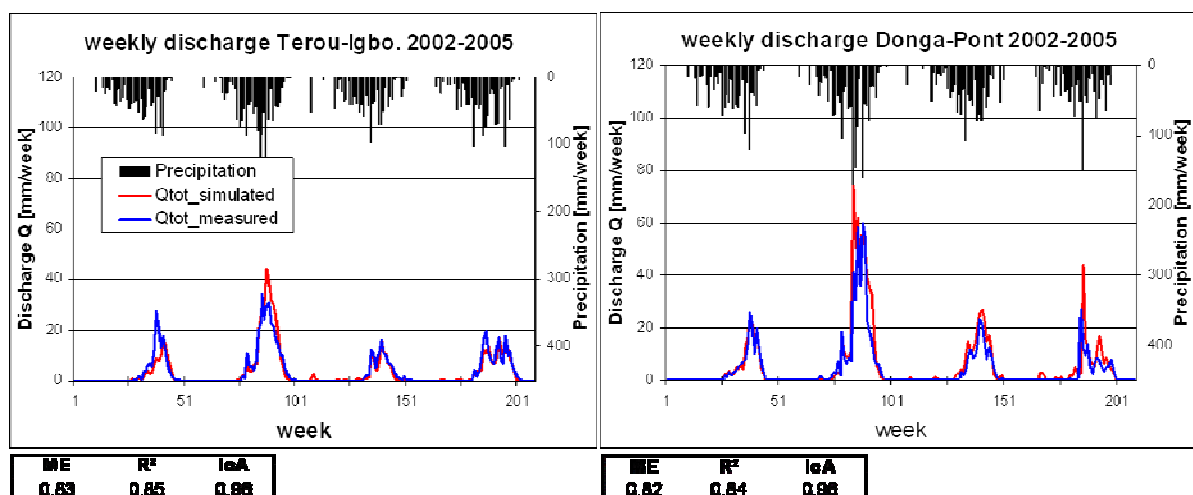


Fig. 7.14 Comparison of measured and simulated weekly discharge for the validation period: Terou-Igbo and Donga-Pont outlets, measures of performance.

Table 7.9 summarizes the mean annual soil water balance in the two subcatchments and the Upper Ouémé catchment. Compared to the water balance from the calibration period (Table 7.7), the rainfall amounts are higher, in particular in the Terou-Igbo subcatchment. As a consequence, biomass growth and evapotranspiration increase significantly. In contrast, absolute and relative values for surface and groundwater flow are significantly lower than in the calibration period. While the mean fraction of surface runoff remains almost constant for the Donga-Pont and the Upper Ouémé catchments, surface runoff in the Terou-Igbo subcatchment drops from 10 to 7% of the mean annual rainfall.

Table 7.9 Mean simulated annual soil water balance in the Donga-Pont, Terou-Igbomakoro, and Upper Ouémé catchments for the validation period (2002-2005).

	Donga-Pont	Terou-Igbo.	Upper Ouémé	Donga-Pont	Terou-Igbo.	Upper Ouémé
Precipitation [mm/yr]	1308	1219	1209	100%	100%	100%
Surface runoff [mm/yr]	168	82	103	13%	7%	9%
Baseflow [mm/yr]	108	97	102	8%	8%	8%
Shallow aquifer recharge [mm/yr]	315	287	296	24%	24%	25%
Deep aquifer recharge [mm/yr]	110	101	104	8%	8%	9%
Actual evapotranspiration [mm/yr]	812	829	789	62%	68%	65%
Potential evapotranspiration [mm/yr]	1478	1479	1479	113%	121%	122%
Change in soil water storage [mm/yr]	62	34	42	5%	3%	3%

b) Spatial validation of hydrology

Besides the validation of the calibrated model at the Donga-Pont and Terou-Igbomakoro outlets for the period 2002-2005 (see previous section), the model performance was evaluated at further validation outlets in the Upper Ouémé catchment (Fig. 7.2 and Fig. 2.7). If discharge data was available, the whole period 1998-2005 was considered. Table 7.10 summarizes the performance measures and the discharge balance for the considered outlets. For the Donga and Terou subcatchments, model efficiencies lie between 0.77-0.83 and can be considered as satisfactory to good. Average discharge is overestimated by 10% for the Donga-Pont and Donga-Affon outlets, and is underestimated by 10 to 14% for the Terou-Igbomakoro and Terou-Wanou outlets. This reflects the difficulties encountered during model calibration to simultaneously calibrate two quite different subcatchments with the same parameter set. For the Ouémé-Aval/Sani and Ouémé-Beterou subcatchments, model efficiencies are significantly lower but still satisfying considering the size and position of the catchments. However, discharge is heavily overestimated in these subcatchments.

Table 7.10 Validation of discharge at several outlets in the Upper Ouémé catchment.

	Catchment Area [km ²]	Simulation period	Model Efficiency	r ²	IoA	Discharge balance Q _{sim} /Q _{meas} [%]
Donga-Pont	586	2002-2005	0.82	0.84	0.96	111
Donga-Affon	1308	1998-2005	0.77	0.84	0.78	109
Terou-Igbomakoro	2324	2002-2005	0.83	0.85	0.96	90
Terou-Wanou	3136	1998-2002	0.77	0.77	0.70	86
Ouémé-Aval/Sani	3506	1999-2005	0.47	0.91	0.85	156
Ouémé-Beterou	10085	1998-2005	0.59	0.89	0.82	146

Figure B.2 in Appendix B shows the weekly discharge curves of the additional validation outlets beyond Donga-Pont and Terou-Igbomakoro.

Bormann & Diekkrüger (2004) obtained similar performance measures during validation of the conceptual UHP model for the Upper Ouémé catchment. Similarly, they obtained model efficiencies of 0.76 to 0.83 for the Terou and Donga subcatchments and 0.54 for the Ouémé-Beterou subcatchment.

7.1.3. Model calibration/validation - Sediment budget

After a successful calibration and validation of the hydrological model component, the sediment budget could be studied in detail.

Calibration and validation of the sediment budget referred to the sediment loadings of the HRUs that reach the channel as suspended sediment. Instream sediment deposition and bank erosion were not considered due to insufficient knowledge about these processes in the Upper Ouémé catchment. Thus, the dynamic geomorphology of the natural river beds in the catchment was not addressed.

Model calibration - Sediment

In order to calibrate the sediment budget, only the USLE crop practice factors and a parameter in the sediment transport equation (SPCON) were adjusted (Table 7.11). The USLE crop management factor (P_USLE) was kept as 1 because soil conserving tillage measures are only locally applied in the catchment. The derived average slope length of 91.463 m and the average slope steepness of 3 to 22% per subbasin were not modified.

Table 7.11 Calibrated parameters for sediment calibration, comparison with default values, and assumptions used by Sintondji (2005).

Parameter	Definition	SWAT Default	Sintondji (2005)	This study
C_USLE: AGRL	USLE crop practice factor [-]	0.2	0.4	0.18
C_USLE: WETN	USLE crop practice factor [-]	0.003	-	0.005
C_USLE: RNGE	USLE crop practice factor [-]	0.005	0.05	0.005
C_USLE: RNGB	USLE crop practice factor [-]	0.005	0.05	0.005
C_USLE: FRST	USLE crop practice factor [-]	0.001	0.01	0.003
C_USLE: FRSD	USLE crop practice factor [-]	0.001	0.001	0.001
SPCON	Linear parameter in channel sediment routing [-]	0.0001	0.0001	0.0005

The default values of the USLE crop practice factors were kept for forest (FRSD) and the savannah types RNGB and RNGE. The C-factor was slightly increased for inland

valleys and woodland savannah. For cropland, the reduction of the C-factor from 0.2 to 0.18 delivered the best agreement with the sediment yield derived from the turbidity measurements. The SPCON factor determines the maximum amount of sediment that can be transported in the channel during an event. For the default value of 0.0001, 43% of the sediment entering the channel in the Donga-Pont subcatchment remained in the channel through severe transport limitations in one subbasin. For Terou-Igbomakoro, the difference between sediment entering and leaving the channel was 24% for the period 1998-2005. The adjustment of SPCON to 0.0005 significantly improved the calibration of the sediment budget for both subcatchments. Otherwise, successful simultaneous calibration of both catchments would not have been feasible. After calibration, 8%, 18%, and 3% of the sediment load remained in the channel for the Terou-Igbomakoro, Donga-Pont, and Upper Ouémé (sub-)catchments, respectively.

Total amounts of sediment yield were compared for the days when discharge and suspended sediment measurements were available. Thus, the values in Table 7.12 have to be considered as minimum values for the years 2004 and 2005. The simulated sediment amounts in the Donga-Pont subcatchment were overestimated by about 60% due to an overestimation of discharge by 30% in the period with valid measurements. In the Terou-Igbomakoro subcatchment, sediment yields and discharge were underestimated by about 10-15% in the period with valid measurements in 2004 and 2005 (Table 7.12).

Table 7.12 Comparison of cumulative sediment and water yields in 2004 and 2005 for days with valid measurements in the Donga-Pont and the Terou-Igbomakoro subcatchments.

	year	# days considered	WY_meas [mm]	SY_meas [t/ha]	WY_sim [mm]	SY_sim [t/ha]	WY_sim/WY_meas [%]	SY_sim/SY_meas [%]
Donga-Pont	2004	45	37	0.047	48	0.079	130	167
	2005	118	124	0.414	162	0.658	131	159
Terou-Igbomakoro	2004	160	82	0.066	67	0.056	83	85
	2005	176	157	0.165	141	0.145	89	88

However, the temporal characteristics of the simulated sediment curve were reproduced quite well, in particular for the Donga-Pont subcatchment (Fig. 7.15). For the Terou-Igbomakoro subcatchment, several sediment peaks were not correctly matched in 2005 due to inadequately simulated discharge peaks.

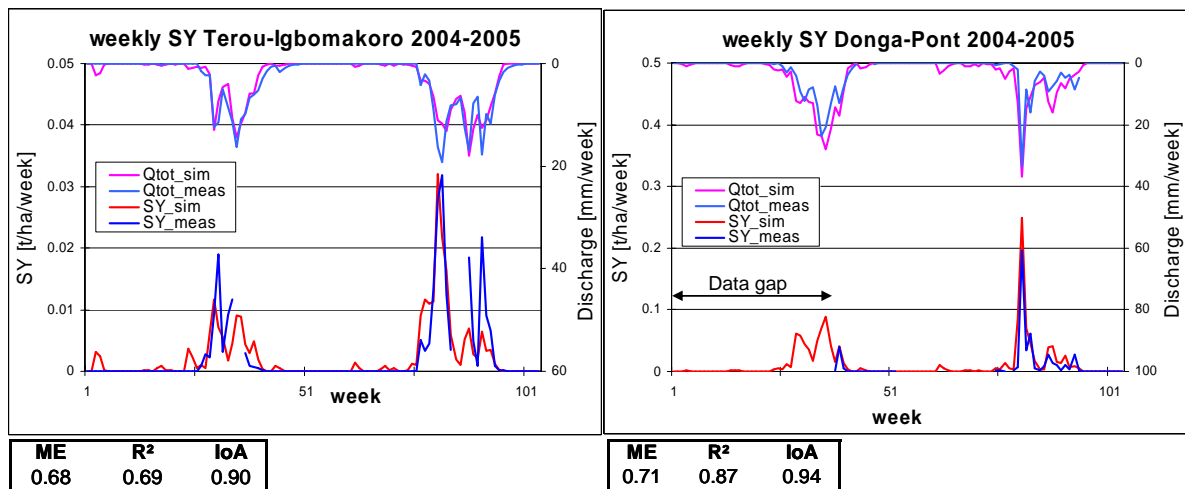


Fig. 7.15 Comparison of measured and simulated weekly discharge and sediment yield for 2004 and 2005 at the Terou-Igbomakoro and the Donga-Pont outlets.

The measurements of model performance for the weeks with valid measurements were satisfactory for the Terou-Igbomakoro subcatchment (ME 0.68, R^2 0.69, IoA 0.90) and the Donga-Pont subcatchment (ME 0.71, R^2 0.87, IoA 0.94).

The scatter plots for the weekly values reveal an underestimation of large sediment events at the Terou-Igbomakoro outlet and an overestimation of sediment yields at the Donga-Pont outlet (Fig. 7.16).

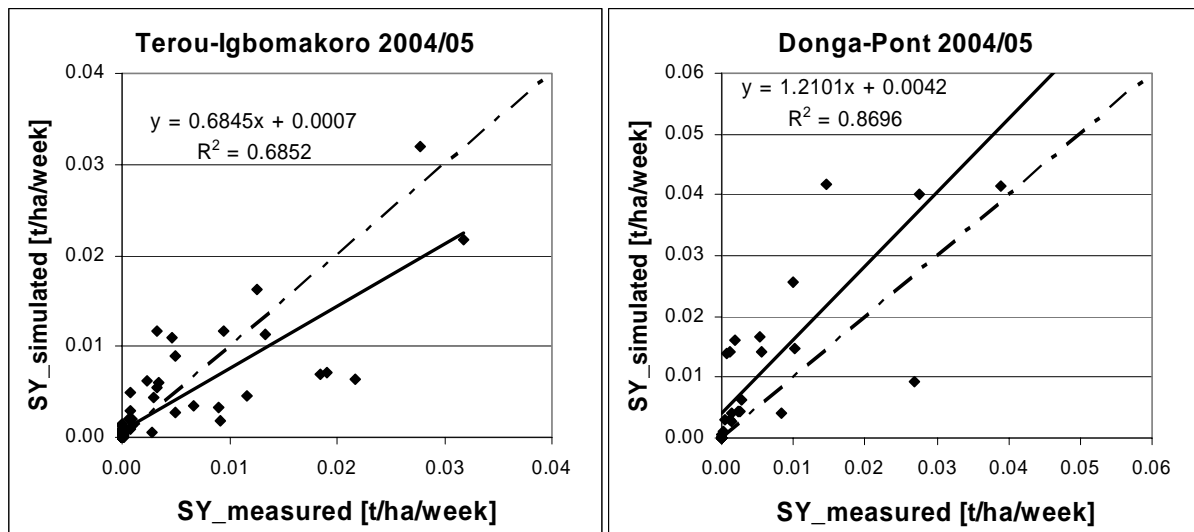


Fig. 7.16 Scatter plots for measured and simulated weekly sediment yields at the Donga-Pont and the Terou-Igbomakoro outlets in the calibration period 2004/2005.

Figure 7.17 shows the daily temporal characteristics of discharge and sediment yield for both subcatchments. Clearly, most over- and underpredictions of the sediment yield are linked to inaccurate reproduction of the discharge events. For example, in August 2004 a measured discharge event in the Terou-Igbomakoro subcatchment is

not captured at all, which leads to a missing sediment peak at the same time. In this case, the missing discharge peak corresponds to an uncaptured rainfall event in the rainfall data. In contrast, the mismatch of sediment peaks at the beginning of the 2005 rainy season can be attributed to an overestimation of discharge peaks. The extreme event in mid-July 2005 in the Donga-Pont subcatchment led to a sediment peak that is more than ten times higher than the highest sediment peak in the Terou-Igbomakoro subcatchment. The large differences in the magnitude of the sediment yield between both subcatchments are also reflected by a factor of ten between the y-axis scales in Figs. 7.15 and 7.17.

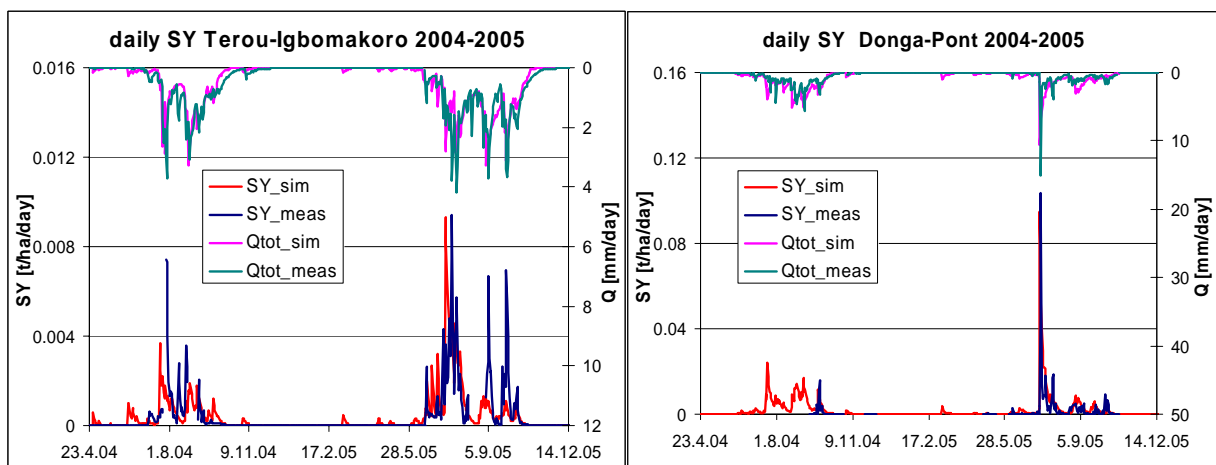


Fig. 7.17 Measured and simulated daily sediment yield and total discharge at the Terou-Igbomakoro and the Donga-Pont outlets in the calibration period 2004/2005.

In summary, the agreement between the measured and simulated sediment yields in the calibration period is quite satisfactory taking into account the various sources of uncertainty (see Chapter 8).

Model validation – Sediment budget

The spatial validation of the sediment budget at the Beterou outlet achieved satisfactory results only for the year 2005 (Fig 7.18). For 2004, the simulated sediment yields are almost 5 times higher than the measured values (Table 7.13).

Table 7.13 Comparison of cumulative sediment yields and discharge values in 2004 and 2005 for days with valid measurements in the Ouémé-Beterou subcatchment.

year	# days considered	Q_{tot_meas} [mm]	SY_meas [t/ha]	Q_{tot_sim} [mm]	SY_sim [t/ha]	Q_{tot_sim}/Q_{tot_meas} [%]	SY_sim/SY_meas [%]
2004	186	175	0.04	215	0.21	123	478
2005	179	120	0.11	153	0.17	128	158

The 23% overestimation of discharge is not sufficient to explain this large difference in sediment yield. The measured sediment yields for 2004 are probably also subject to handling errors in the water sampling and the filtration in the first year of investigation (for details, see Chapter 8). Temporal validation for 2006 at the Terou-Igbomakoro and the Donga-Pont outlets could not be performed because the rainfall data for 2006 was not yet available.

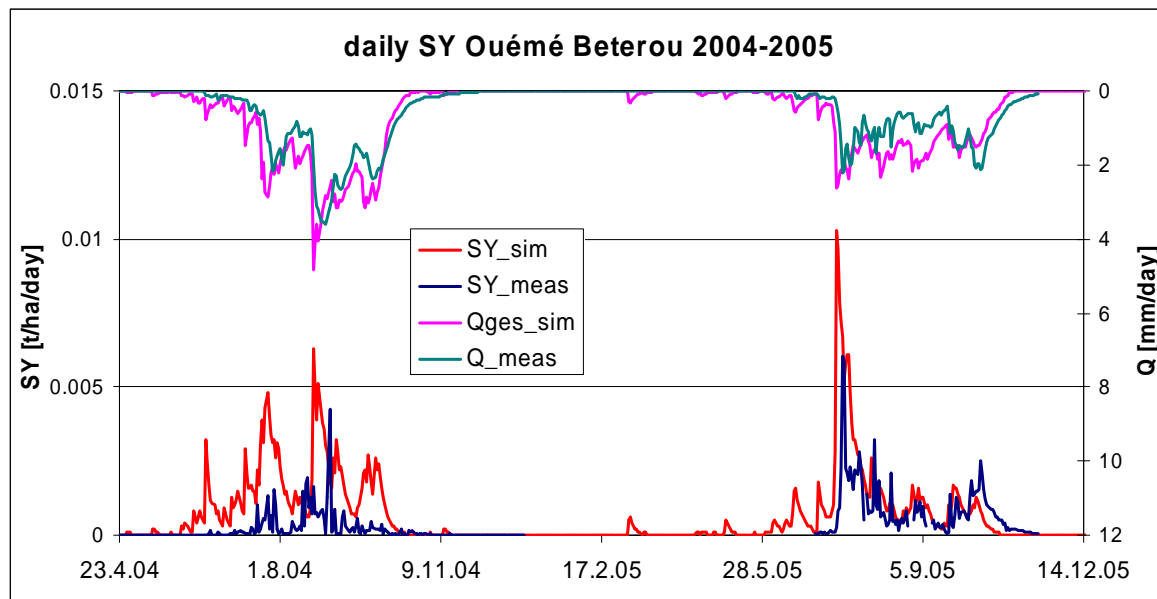


Fig. 7.18 Comparison of daily measured and simulated total discharge and sediment yield for 2004 and 2005 at the Ouémé-Beterou outlet.

7.1.4. Influence of spatial discretisation on model performance

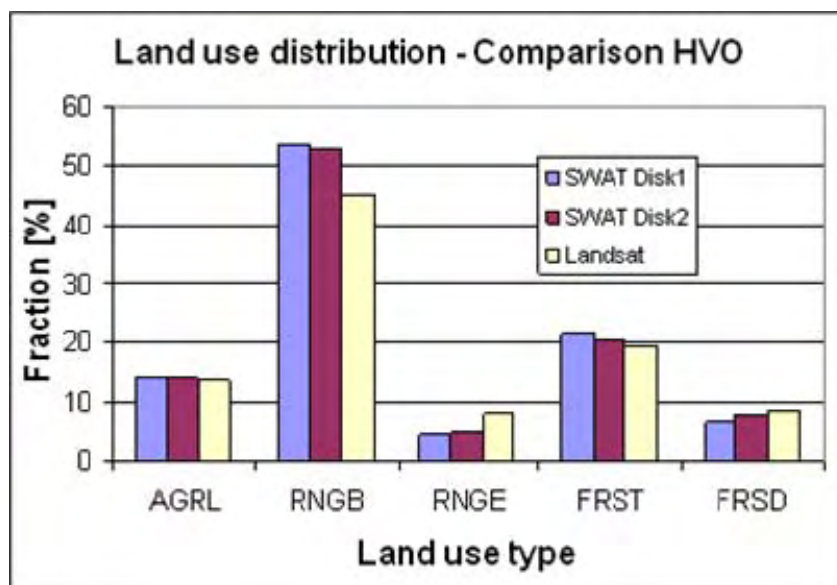
Several authors have reported that model results from SWAT can be very sensitive to the spatial discretisation of the model because the thresholds for subbasin and HRU delineation affect land use and soil distribution as well as the number of considered climate stations (e.g., Bingner et al., 1997; Manguerra & Engel, 1999; Fitzhugh & Mackay, 2000; Jha et al., 2004; Chen & Mackay, 2004; see also Section 4.2).

In this study, model calibration was performed for two different discretisations (Table 7.14). So far, we have discussed the results of discretisation 2. For

Table 7.14 Comparison of model performance for the period 1998-2001 for two different discretisations.

	Discretisation 1						Discretisation 2					
	# sub-basins	# HRUs	Q_sim [mm/yr]	Q_sim/Q_meas [%]	ME	R ²	# sub-basins	# HRUs	Q_sim [mm/yr]	Q_sim/Q_meas [%]	ME	R ²
Donga-Pont	1	11	324	104	0.78	0.82	3	21	320	102	0.78	0.81
Terou-Igbo.	9	72	263	115	0.82	0.83	15	117	247	106	0.87	0.87
Upper Ouémé	55	462	245	-	-	-	121	926	236	-	-	-

discretisation 2, the threshold for subbasin delineation for discretisation 1 was reduced from 15000 ha to 6000 ha. As a result, the number of subbasins increased from 55 to 121 and one additional pluviometric station was considered. Furthermore, all fractions of land use types for the Upper Ouémé catchment were better represented, except for a very slight increase in the deviation for agricultural land (Fig. 7.19). However, the overestimation of cropland in the Donga-Pont subcatchment increased from 15 to 22%. The model performance in the calibration period 1998-2001 could be significantly improved for the Terou-Igbomakoro subcatchment and remained similar for the Donga-Pont subcatchment (Tab 7.14).



In the Donga-Pont subcatchment, simulated runoff peaks were smoothed due to the division of the subbasin into three subbasins with two different rain gauges. Therefore, the model performance improved significantly in the validation period 2002-2005. The Model

Fig. 7.19 Comparison of the land use distribution in the Upper Ouémé catchment for two different discretisations with the original distribution from the Landsat classification.

Efficiency increased from 0.75 to 0.88 for the Donga-Pont subcatchment (Fig. 7.20).

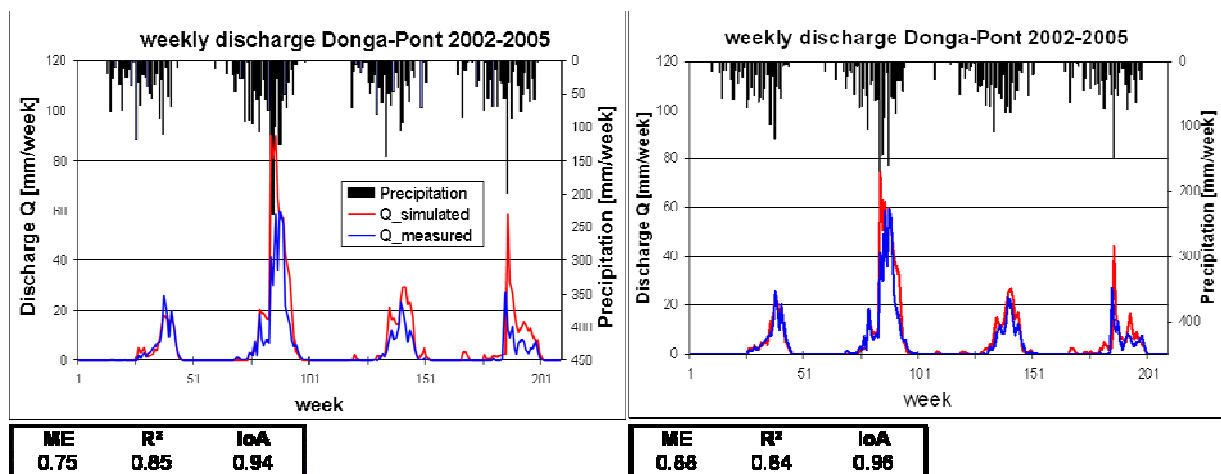


Fig. 7.20 Comparison of measured and simulated weekly discharge for the period 2002-2005 at the Donga-Pont outlet for discretisation 1 (left) and discretisation 2 (right).

7.1.5. Discussion of modelling results 1998-2005

In this section, we present the simulation results for the whole period 1998-2005 and address the temporal and spatial dynamics of rainfall, water yield and sediment yield. The mean simulated total discharge in the period 1998-2005 amounts to 219 mm/yr with about 107 mm surface runoff per year (see Table 7.15). Total discharge and surface runoff are substantially higher in the Donga-Pont subcatchment. The mean annual sediment loss of 0.22 t/ha/yr in the whole Upper Ouémé catchment lies between the values for the Donga-Pont and the Terou-Igbomakoro subcatchments.

Table 7.15 Land use and hydrological characteristics of Donga-Pont and Terou-Igbomakoro subcatchments and the whole Upper Ouémé catchment derived from modelling results 1998-2005, mean values and standard deviations.

	Field [%]	Savannah [%]	Forest [%]	Rainfall [mm/yr]	WY [mm/yr]	Q _{surf} [mm/yr]	SY [t/ha/yr]
Donga-Pont	39	61	0	1294 +/- 201	297 +/- 142	174 +/- 78	0.85 +/- 0.47
Terou-Igbomakoro	11	72	17	1157 +/- 170	213 +/- 103	96 +/- 41	0.14 +/- 0.06
Upper Ouémé	14	78	8	1184 +/- 121	219 +/- 68	107 +/- 28	0.22 +/- 0.06

The mean annual sediment yield in the Donga-Pont subcatchment is about six times higher than for the Terou-Igbomakoro subcatchment, reflecting a higher portion of cropland (factor 3.5) and higher rainfall amounts and intensities in this region. Standard deviations for daily precipitation are high in the small Donga-Pont subcatchment. Sintondji (2005) simulated significantly higher sediment yields for the Terou-Igbomakoro subcatchment. He obtained as mean sediment yield 4.72 t/ha/yr for the period 1998-2003. However, he did not calibrate or validate the sediment budget.

Apart from surface runoff and actual evapotranspiration, the relative water balance is quite similar in the two subcatchments and the whole Upper Ouémé catchment (see Table 7.16). Surface runoff accounts for 13% of annual rainfall in the Donga-Pont subcatchment. In the Terou-Igbomakoro subcatchment, only 8% of annual rainfall runs off superficially. As in the calibration and validation periods, the high values for actual evapotranspiration in the Donga-Pont subcatchment are a consequence of the higher rainfall. Relative to the rainfall sums, actual evapotranspiration is higher in the Terou-Igbomakoro subcatchment and the Upper Ouémé catchment. If we compare the USLE factors for the Terou-Igbomakoro, Donga-Pont and Upper Ouémé catchments, we learn more about their contributions to the differences in sediment yield. As Table 7.17 shows, the USLE C factor, which represents land use, shows the

highest variation between catchments with a maximum in the intensively used Donga-Pont subcatchment. The sediment yield, which SWAT simulates according to the MUSLE, equals about one-third of the sediment yield according to the USLE (see Table 7.17).

Table 7.16 Mean water balance for the period 1998-2005 in the Donga-Pont and Terou-Igbomakoro subcatchments and the whole Upper Ouémé catchment.

	Donga-Pont	Terou-Igbo.	Upper Ouémé	Donga-Pont	Terou-Igbo.	Upper Ouémé
Precipitation [mm/yr]	1294	1157	1184	100%	100%	100%
Surface runoff [mm/yr]	174	96	107	13%	8%	9%
Baseflow [mm/yr]	125	117	114	10%	10%	10%
Shallow aquifer recharge [mm/yr]	337	312	310	26%	27%	26%
Deep aquifer recharge [mm/yr]	118	109	109	9%	9%	9%
Actual evapotranspiration [mm/yr]	772	732	749	60%	63%	63%
Potential evapotranspiration [mm/yr]	1556	1557	1557	120%	135%	132%
Change in soil water storage [mm/yr]	64	41	48	5%	4%	4%

Looking at the sources of sediment loads by land use (see Table 7.18), it becomes obvious that cropland is by far the main contributor in the Upper Ouémé catchment (96.9%), followed by brush and grass savannah (2.4%) and woodland and tree savannah (0.5%). The average sediment yields for cropland, inland valleys and brush and grass savannah are 2.13 t/ha/yr, 0.46 t/ha/yr and 0.13 t/ha/yr, respectively. Thus, the mean sediment yield for inland valleys is significantly higher than for other savannah types but less important for the total sediment load due to its very limited occurrence (0.06%).

Table 7.17 USLE factors and mean simulated soil loss rates for the Terou-Igbomakoro, Donga-Pont and Upper Ouémé catchments in the period 1998-2001.

	Mean USLE_K	Mean USLE_LS	Mean USLE_C	Mean USLE_P	Mean soil loss MUSLE [t/ha/yr]	Mean soil loss USLE [t/ha/yr]
Donga-Pont	0.08 (0.03-0.12)	0.42 (0.34-0.56)	0.07	1	0.85	2.40
Terou-Igbo.	0.08 (0.03-0.17)	0.39 (0.36-0.42)	0.02	1	0.14	0.40
Upper Ouémé	0.08 (0.03-0.30)	0.41 (0.27-0.86)	0.03	1	0.22	0.65

The simulated annual sediment yields of 0.06-0.26 t/ha/yr for the whole catchment lie within the lower range of values reported in the literature for similar catchments. For example, Walling et al. (2001) simulated sediment yields of 0.15-0.26 t/ha/yr in a small catchment in Zambia, and Wiese (1997) reported a natural soil loss rate on flat wet savannah land of about 0.9 t/ha/yr that increased after clearing to 14 t/ha/yr. Dickinson & Collins (1998) obtained sediment yields between 0.1 and 1.2 t/ha/yr for the Mgeni catchment in South Africa (4000 km²) using the Calsite Model.

Table 7.18 Average sediment loadings in % and total sediment loads and sediment yields per land use in the Upper Ouémé catchment.

Land use	SWAT Code	Sediment load [t/yr]	Sediment load [%]	Sediment yield [t/ha/yr]
Cropland	AGRL	432623	96.87	2.132
Dry forest	FRSD	370	0.08	0.003
Woodland and tree savannah	FRST	2342	0.52	0.008
Brush and grass savannah	SAVA	10849	2.43	0.013
Inland valleys	WETN	403	0.09	0.462

Donovan and Casey (1998) reported an annual topsoil loss of 0.3 to 0.7 mm in Mali. Junge (2004) determined an average annual topsoil loss of 0.4 to 0.6 mm in the Aguima subcatchment from differences in topsoil depth of agricultural soil and soils under savannah vegetation.

Considering an average bulk density of the topsoil of 1.51 g/cm^3 (Giertz 2004), the simulated sediment yield of 0.22 t/ha/yr for the Upper Ouémé catchment equals an average topsoil loss of only 0.015 mm/yr. However, since large parts of the catchment are covered by forest or savannah, which contribute less than 4% to the total sediment load at the catchment outlet, it is more useful to calculate the topsoil loss for the cropland. The simulated sediment yield of 2.13 t/ha/yr on cropland equals an average annual topsoil loss on fields of 0.14 mm. Due to the higher amounts and intensities of rainfall, the sediment yield for agricultural land is higher in the Donga-Pont subcatchment, leading to an estimated topsoil loss of 0.19 mm per year. Thus, the estimated topsoil loss on agricultural land in the Upper Ouémé catchment from SWAT is about 3 to 5 times lower than the estimate by Junge (2004) in the Aguima catchment. This reflects the fact that only a small portion of the eroded material reaches the channel (see Section 3.2). According to Van Noordwijk et al. (1998), generally less than 20% of the eroded material reaches the channel in catchments up to 10000 km² in size.

Likewise, the measured amounts of suspended sediment at the regional scale are one or two orders of magnitude lower than the soil loss rates of 12-120 t/ha/yr on fields and 3.8 t/ha/yr on savannah land obtained by Junge (2004) on small erosion plots in the catchment.

Figure 7.21 shows the spatial pattern of the mean simulated sediment yield. The highest sediment yields, with a maximum of 2.21 t/ha/yr, were obtained in the subbasins around Djougou.

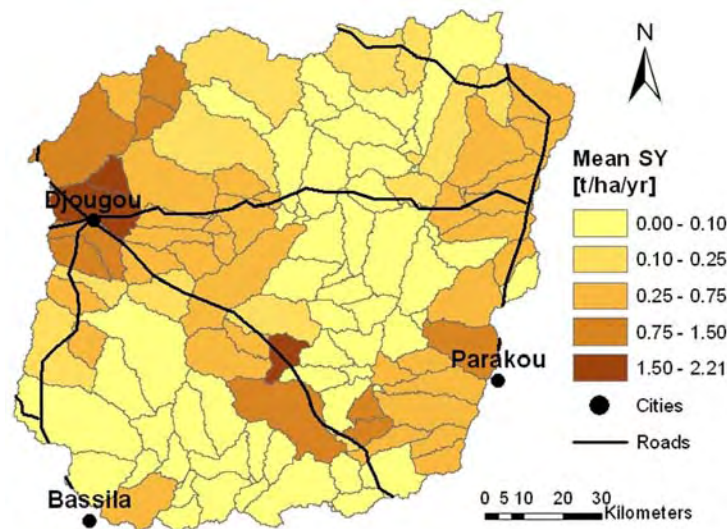


Fig. 7.21 Spatial distribution of the mean simulated sediment yield in the Upper Ouémé catchment (1998-2005).

Furthermore, the sediment yield is elevated in the north-western part of the catchment, along the road south-east of Djougou, on the Parakou plateau, and at the north-eastern edge of the catchment. Sediment yields lower than 0.1 t/ha/yr are simulated in most subbasins of the Terou-

Igbomakoro subcatchment, as well as in the central and

northern parts of the catchment. As erosion and sediment transport are directly linked to surface runoff, their spatial patterns are very similar (Fig. 7.22). Clearly, surface runoff is also significantly higher in the Djougou region than in the rest of the catchment. This is due to high rainfall amounts, high rainfall intensities and a high fraction of cropland in this region. The fraction of cropland in the subbasins around Djougou varies between 28 and 48%. In the north-eastern region, high runoff is mainly caused by high rainfall. In the Parakou region, the high fraction of cropland leads to high

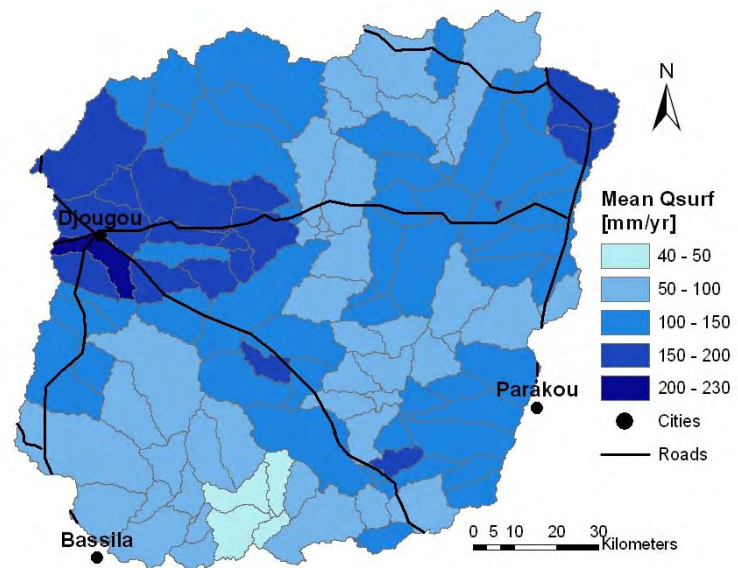


Fig. 7.22 Spatial distribution of the mean simulated surface runoff in the Upper Ouémé catchment (1998-2005).

surface runoff. The rainfall sums are comparatively low in the Parakou region, resulting in a rather low total water yield (see Appendix B, Fig. B.3). Variations in annual water and sediment yields are high (Fig. 7.23). The highest total water and sediment yields were simulated in 1998, 1999 and 2003. The highest monthly rainfall and water and sediment yield occur in August and September (Fig. 7.24).

However, annual variations in both months are high, in particular for the sediment yield. Suspended sediment concentrations are very high at the beginning of the rainy season, in June and July, but their contribution to the annual sediment yield remains small due to the low water yields in these months.

Daily sediment flows are triggered by the occurrence of erosive rainfalls, which are usually defined

as rainfalls of more than 10 mm per hour. To simplify, we consider all daily rainfalls of more than 10 mm as erosive (see also Junge (2004) and Segalen & Van Diepen (1984)). Then, the average number of days with erosive rainfall varies

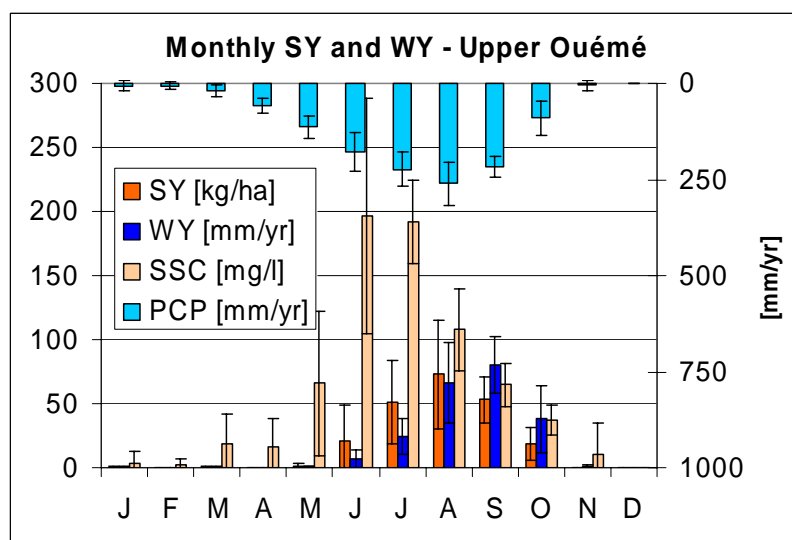


Fig. 7.24 Mean monthly values and standard deviation for sediment and water yields, suspended sediment concentration and precipitation in the Upper Ouémé catchment (1998-2005).

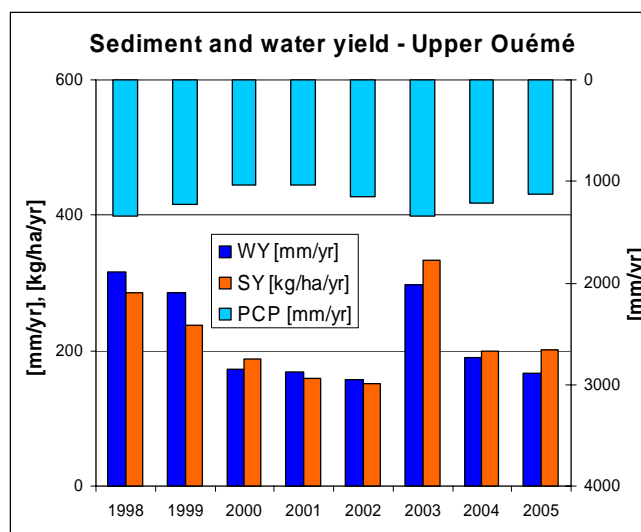


Fig. 7.23 Annual precipitation, sediment and water yields in the Upper Ouémé catchment (1998-2005).

between 35 and 44 days per year depending on the pluviometric station. The corresponding standard deviation varies between 4 and 9 days. The highest number of erosive rainfalls was counted in the north-western part of the catchment (stations Djougou, Tebou, Penessoulou), and the

lowest number was counted at stations Parakou and Saramanga. The number of erosive rainfalls was particularly high in 1998, 2002 and 2003. In accordance with Junge (2004), the highest number of erosive rainfalls was recorded in August and September, explaining the high sediment concentrations in these months. In two out of three rainy days, rainfall exceeds 10 mm for at least one station. On all these days, 81% of the total sediment in the Upper Ouémé catchment was transported.

A cumulative distribution of daily sediment yield for all rainy days shows that a few rainy days/rainfall events are responsible for the major sediment transport in the Upper Ouémé catchment (Fig. 7.25). For example, at point A in Fig. 7.25, 50% of the total sediment was transported in only 12% of all rainy days caused by 28% of total rainfall.

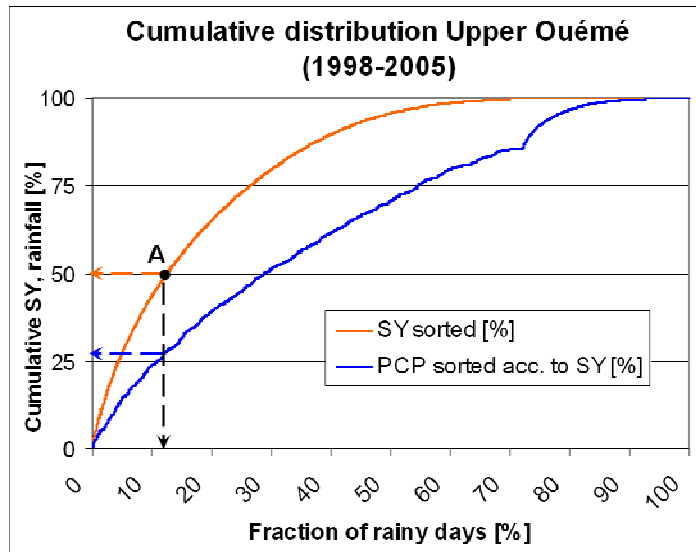


Fig. 7.25 Cumulative distribution of sediment yield and rainfall in the Upper Ouémé catchment (1998-2005).

However, depending on the prior conditions, not all days with high rainfall caused high sediment yields. About 28% of all rainy days did not contribute to the sediment yield.

As the daily sediment yield at the catchment outlet shows a superposition of several erosion events, it is not possible to distinguish individual erosion events.

7.1.6. Conclusions

Water and sediment budgets of the SWAT model were successfully calibrated and validated for the Upper Ouémé catchment. The model reproduced recent water and sediment dynamics satisfactorily. Water balances were reasonable. The model performed well under a wide range of conditions, including different land uses and climatic conditions. Thus, the model can be used for scenario analysis.

A finer discretisation significantly improved the modelling results. The spatial pattern of sediment and water yield for the period 1998 to 2005 agreed well with field observations. Current hotspots of soil erosion have been identified in the north-western part of the catchment, along the road Djougou-Parakou, on the Parakou plateau. At the north-eastern edge of the catchment sediment yields are also elevated. In 1998-2005, about 28% of total rainfall was responsible for 50% of the sediment load. Suspended sediment concentrations reached a maximum in June/July, while rainfall, sediment and water yield peaked in August/September. The mean sediment yield of 0.22 t/ha/yr in the Upper Ouémé catchment equals an average topsoil loss of about 0.14 mm per year on agricultural land. The topsoil loss

is significantly higher in the Donga-Pont subcatchment. The simulated sediment yields lie in the lower range reported in the literature for similar catchments. However, in the future, sediment yield may increase significantly because cropland is expanding rapidly.

7.2. Scenario analysis 2001-2050

After successful calibration and validation of the SWAT model, various scenarios for climate and land use changes could be calculated. Before presenting the results of the scenario analysis, the origin, characteristics, and pre-processing of the input data will be discussed.

7.2.1. Databases and pre-processing

The input data for the land use and climate change scenarios were mainly based on results of the regional climate model REMO and the land use and land cover model CLUE-S (Table 7.19). Future land use maps for the Upper Ouémé catchment were available for the years 2000 to 2025. REMO delivered daily climate data from 2001 to 2050 and for the historic period 1960 to 2000.

Table 7.19 Model input data for scenarios.

	Variables	x	t	Period	Source	Author	Model
Climate data	Min/Max-temperature, solar radiation, wind velocity, relative humidity	13 stations	daily	1960-2000	IMPETUS	Paeth et al. (2008)	REMO
	Min/Max-temperature, solar radiation, wind velocity, relative humidity	13 stations	daily	2001-2050	IMPETUS	Paeth et al. (2008)	REMO A1B scenario
	Min/Max-temperature, solar radiation, wind velocity, relative humidity	13 stations	daily	2001-2050	IMPETUS	Paeth et al. (2008)	REMO B1 scenario
Land use data	Land use map	250 m grid	yearly	2000-2025	IMPETUS	Judex (2008)	CLUE-S

Land use change data

The annual land use maps for the period 2000-2025 were generated by Judex (2008) with a spatial resolution of 250 meters using the land use/land cover change model CLUE-S (Verburg et al. 2002). CLUE-S is an integrative, spatially explicit, dynamic simulation model that identifies the yearly demand for each land use type and

distributes it iteratively over all raster cells according to their occurrence probability and some decision rules. The occurrence probability for each land use type was calculated with a logistic regression model including predictors such as distance to roads, settlements and markets, population density, relief position, and protected areas. Starting from a Landsat classification of the year 1991, the model could satisfactorily reproduce total changes and the spatial pattern of the land use classification for the year 2000.

For the land use scenarios, the demand for each land use type was modelled following the assumptions of socioeconomic scenarios B1 “Economic growth and decentralisation”, B2 “Economic stagnation and institutional insecurity”, and B3 “Business as usual” developed in the IMPETUS project (IMPETUS 2006). Three corresponding land use scenarios, here referred to as L1, L2, and L3, were calculated with the CLUE-S model. The main assumptions for these scenarios with regard to population growth, crop production, and protected areas are summarized in Table 7.20. The differences between the population projections for the three IMPETUS scenarios are rather low. The most distinguishing factor between the scenarios is the degree of intensification in agriculture regulating the per capita demand of cropland. For scenario L1, i.e., under economic growth and decentralisation, increased use of fertiliser leads to a significant reduction in the per capita cropland area (-15% in 2025). In contrast, the demand of per capita cropland remains constant for scenario L2. For scenario L3, it is assumed that the per capita cropland area decreases with increasing population density but without significant intensification. The scenarios differ also in the degree of conservation of protected forests. While strong institutions are assumed to stop the encroachment of cropland into the forest for scenario L1, this is only the case for scenario L3 as long as land

Table 7.20 Definition of land use scenarios L1, L2, and L3 according to Judex (2008).

	L1 "Economic growth and decentralisation"	L2 "Economic stagnation and institutional insecurity"	L3 "Business as usual"
Population growth	slower than in the period 1992-2002	faster than in the period 1992-2002	as in the period 1992-2002
Agricultural production	Increased fertilizer use reduces cropland demand per capita (minus 15% in 2025)	constant cropland demand per capita	decreasing cropland demand per capita with increasing population density
Protected areas	no agricultural use	agricultural use	agricultural use as a function of land pressure

use intensity remains below a threshold. In contrast, for scenario L2 land use conversion is possible in the central part of the catchment (*Forêt classée de l'Ouémé Supérieur*) since governmental institutions are considered to be very weak and development agencies have left the area.

Figure 7.26 compares the land use map of the year 2001 with the map for 2025 according to the “Business as usual” scenario” (L3) originating from CLUE-S model. For this scenario, the land use class “Cropland (>20%)” increases by 80% until 2025. For scenarios L1 and L2, this class increases by 56% and 119%, respectively. Judex (2008) resampled the original land use classification from 2000 for CLUE-S from 30 to 250 meters in order to reduce the computational demand and to achieve robust relationships during the regression analysis. As a consequence, the number of land use classes was reduced and the classes were re-defined according to thresholds. For example, the new land use class “Cropland (>20%)” characterizes grid cells containing 20-100% cropland. .

This re-definition of land use classes is not suitable for erosion modelling where a correct representation of land use, in particular of cropland, is crucial. Since some cells classified as “Cropland” may actually be covered only by 20% cropland, a direct application of the maps would significantly overestimate surface runoff and sediment yield. In order to avoid this, a simple disaggregation scheme was applied to transform

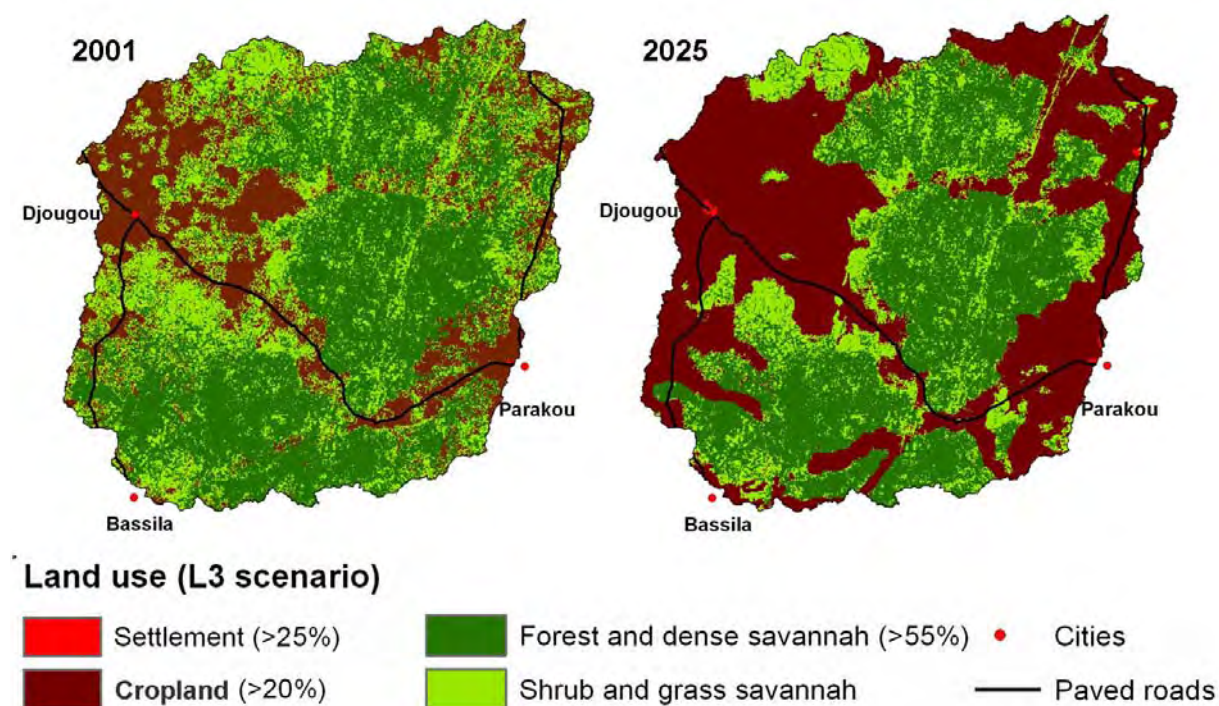


Fig. 7.26 Land use maps for 2001 and 2025 for scenario L3 (Business as usual) from the CLUE-S model.

the 250 meter grids of the CLUE-S land use maps into 25 meter grids with differentiated land use. First, a comparison of the CLUE-S map for the year 2000 with the original land use map for 2000 delivered the average distribution of land use types in each 250 meter grid cell (Table 7.21).

Table 7.21 Percentages for the disaggregation of the CLUE-S land use map.

		Land use classes CLUE-S			
		Cropland (>20%)	Forest and woodland savannah	Tree, brush and grass savannah	Settlement
Land use classes SWAT	Cropland	43%	1%	8%	26%
	Forest and woodland savannah	4%	53%	14%	0%
	Tree, brush and grass savannah	52%	46%	78%	6%
	Settlement	1%	0%	0%	67%

For example, a grid cell of “Cropland (>20%)” contained on average 43% “Cropland”, 4% “Forest and woodland savannah”, 52% “Other savannah types”, and 1% “Settlement” (Table 7.21, first column). Second, for each CLUE-S map, the 250 meter grid cells were divided into one hundred 25 meter grid cells and filled with the different land use types according to the distribution in Table 7.21. Figure 7.27 illustrates the scheme for a 250 meter grid cell with the land use class “Cropland (>20%)”. A regular pattern was chosen in order to keep the same pattern for grid cells without land use changes.

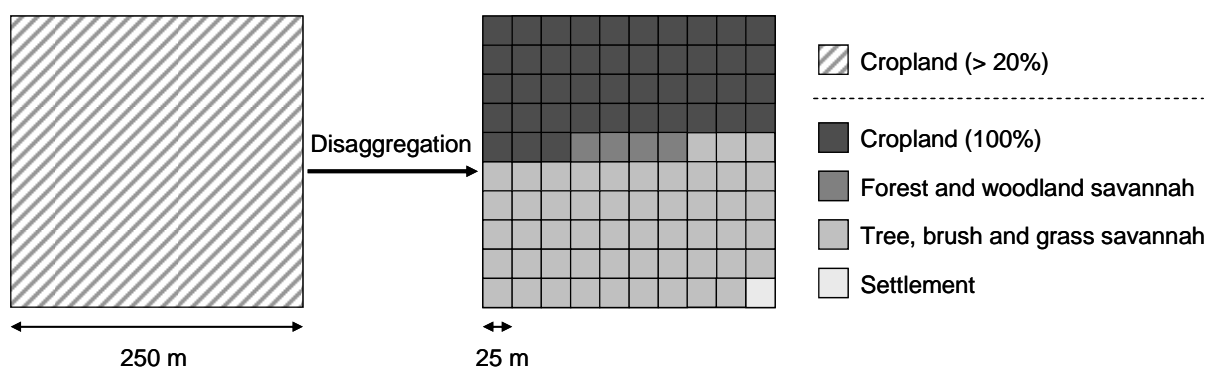


Fig. 7.27 Disaggregation scheme for the CLUE-S land use maps: Example is for the land use class “Cropland (>20%)”.

The percentages in Table 7.21 were derived as an average for the entire Upper Ouémé catchment. Nevertheless, the fraction of cropland in the disaggregated land use map for 2000 is also similar to that of the original map for the Terou-Igbomakoro and Donga-Pont subcatchments (cp. first and fourth columns in Fig. 7.28).

Thus, the disaggregation scheme produces reasonable results for the year 2000 and could be applied to all maps of the land use scenarios. Since the integration of new land use maps requires a new setup of the SWAT model, not all land use maps from CLUE-S for the period 2001-2025 were used. Essentially, the land use scenarios were only performed for the land use maps for the years 2005, 2015, and 2025. After disaggregation, the increases in field area until 2025 ranged from 51% to 108% for the land use scenarios.

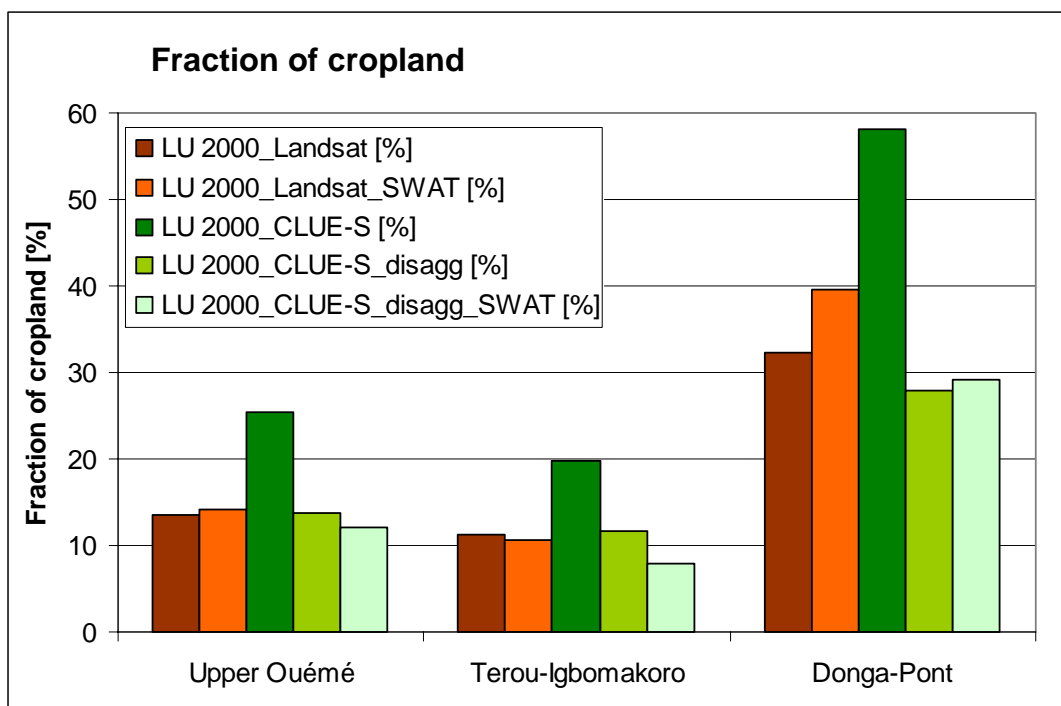


Fig. 7.28 Fractions of cropland in the original model, after aggregation for CLUE-S, and after disaggregation and HRU delineation.

It has been shown that the disaggregated CLUE-S map for the year 2000 satisfactorily represents the land use distribution of the original land use classification. However, the fraction of land use types in the SWAT model is also influenced by the applied HRU threshold of 10%. For the model with the disaggregated CLUE-S map (Lu00 model), the threshold leads to an underestimation of the fraction of cropland in the Upper Ouémé catchment by 11%, with substantial differences between the two subcatchments (see last two columns in Fig. 7.28). For the land use scenarios, the threshold reduces the cropland area by 10%, 5%, and 1.5% for the Lu05, Lu15, and Lu25 models, respectively (Fig. 7.29). Clearly, the influence of the threshold decreases with increasing cropland area.

Table 7.22 summarizes the effects of the disaggregation and the HRU threshold on the cropland area in the land use scenarios. It is clear that the disaggregation leads to a significant decrease in the relative changes in cropland.

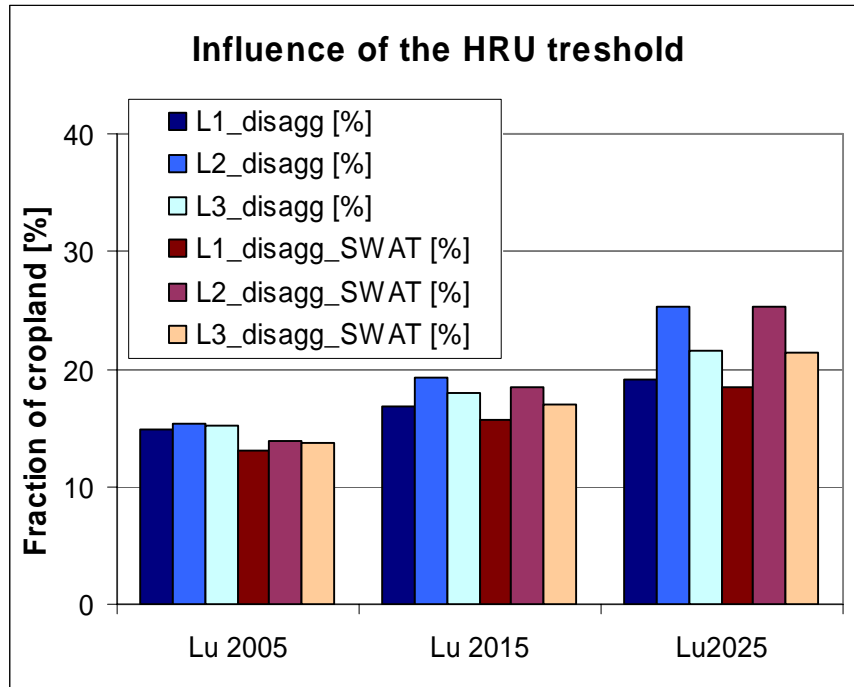


Fig. 7.29 Fraction of cropland for the land use scenarios before and after HRU delineation in the SWAT model.

However, the HRU threshold nearly compensates for this reduction. The remaining slight underestimation of the cropland area is even more realistic if we consider that the use of the Lu00 model as a reference instead of the original model leads to a relative overestimation of the

cropland area of the land use scenarios.

Thus, the final pattern of cropland areas adequately represents the pattern originating from the CLUE-S model. This allows a meaningful scenario analysis.

Table 7.22 Land use scenarios: change of fraction of cropland according to CLUE-S results before and after implementation in the SWAT model.

Land use map Δcropland [Δ%]*	2005			2015			2025		
	L1	L2	L3	L1	L2	L3	L1	L2	L3
1. CLUE-S	+12	+17	+15	+31	+57	+44	+56	+119	+80
2. CLUE-S_disagg	+9	+12	+10	+22	+41	+31	+40	+85	+57
3. SWAT	+7	+14	+12	+29	+51	+40	+51	+108	+75

* reference year 2000 (Lu00 model)

Climate Change Data

The input parameters for the climate scenarios were provided by Paeth et al. (2008) using the regional climate model REMO driven by the IPCC SRES scenarios A1B and B1. REMO is a regional climate model that is nested in the global circulation model ECHAM5/MPI-OM (Paeth et al. 2008). The advantages of the new set of REMO simulations are: (1) a comparatively high resolution of 0.5°, (2) the

consideration of spatial patterns of future land use change, and (3) a transient forcing from 1960 to 2000 and three ensemble runs for two scenarios from 2001 to 2050, reflecting the uncertainties due to unknown initial conditions (Paeth et al., 2008).

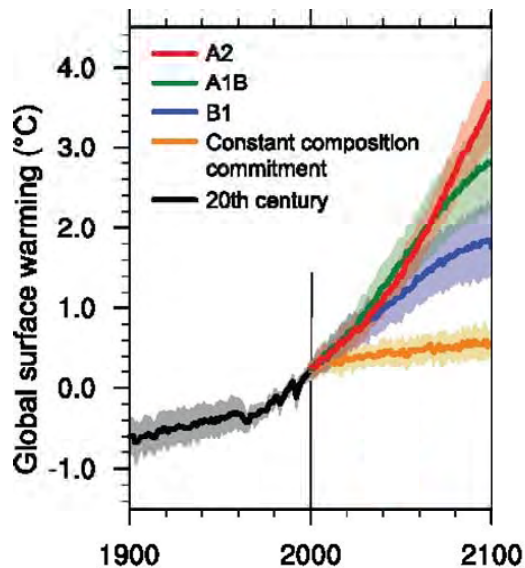


Fig. 7.30 IPCC SRES scenarios: Increase of air temperature until 2100 (IPCC 2001).

the introduction of clean, sustainable technologies. Consequently, the predicted CO₂ emissions and temperature increases are lower than for the A1B scenario (Fig. 7.30). Both scenarios are rather optimistic compared to the whole SRES scenario family. The SRES scenarios do not consider additional climate initiatives like the emission targets of the Kyoto Protocol.

Current climate models cannot correctly represent the climatology of rainfall, but they are more reliable in terms of atmospheric circulation and thermodynamics (Paeth et al. 2008). Therefore, the model results cannot be directly fed into hydrological models. In the case of REMO, the model systematically underestimated the amount and variability of rainfall over West Africa including a shift in rainfall distribution towards more weak events and fewer extremes (Paeth, in preparation).

To address this, so-called Model Output Statistics (MOS) are applied in order to adjust the rainfall data using other near-surface parameters such as temperature and sea level pressure wind components (Paeth et al. 2008). A cross-validated multiple regression analysis was used in order to adjust monthly data to the CRU observational dataset (CRU dataset) (Paeth et al. 2008). After post-processing the REMO data with the MOS algorithm, the monthly distribution of rainfall and the potential evapotranspiration were correctly represented. For example, at the station Parakou the simulated and measured rainfall data for the period 1960-2000 agreed very well (Fig. 7.31, left). The mean monthly potential evapotranspiration according to

Penman-Monteith also shows a very good accordance in the rainy season (Fig. 7.31, right). Thus, the MOS algorithm could be extrapolated to the entire time period 1960-2050.

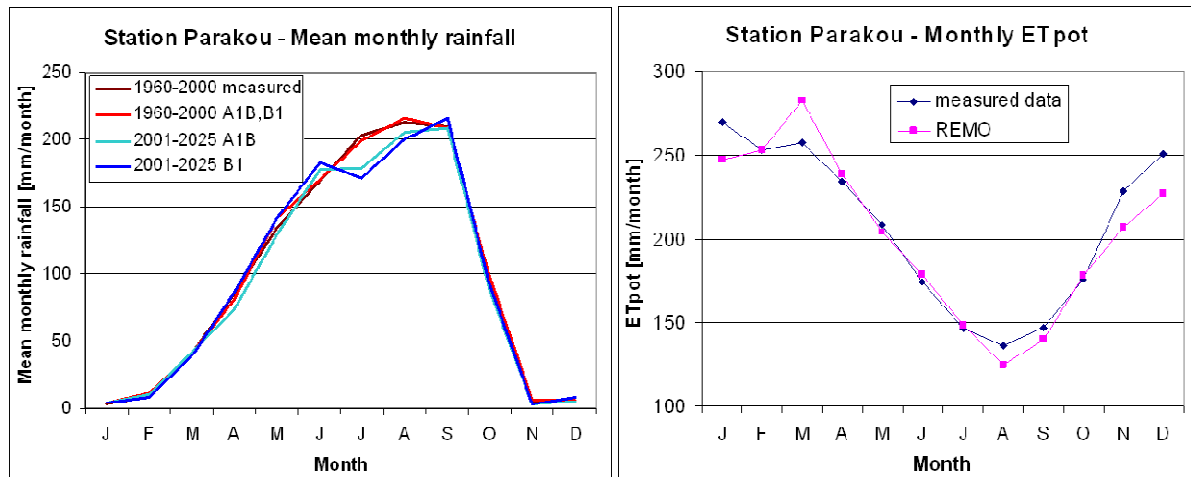


Fig. 7.31 Comparison of measured and simulated climate data for the period 1960 to 2000 at the station Parakou: monthly rainfall (left), calculated monthly ET_{pot} according to Penman-Monteith (right).

However, the averaged values of rainfall for 0.5° grid cells were still not suitable for hydrological modelling where rainfall data from individual stations is used. The smoothed daily rainfall distribution shifted towards weaker events of REMO would have led to significant underestimations of surface runoff and soil erosion.

Therefore, the gridded rainfall data from REMO was attributed to virtual station data derived from simulated present-day and future precipitation in the corresponding grid box plus an orographic term and a stochastic term (Paeth et al., 2008). After this second statistical post-processing, the daily rainfall was correctly reproduced, including the frequency distribution of site-specific events and the magnitude of extreme events (Fig. 7.32). For the station Parakou, low intensity rainfalls (< 50 mm/day) were slightly overestimated, while high intensity rainfalls (50-200 mm/day) slightly underestimated.

With regard to the monthly distribution, the rainfall amounts are slightly higher at the beginning of the rainy season and slightly lower in the middle of the rainy season. Table 7.23 summarizes the changes in the rainfall characteristics for the periods 2001-2025 and 2026-2050 for the Upper Ouémé catchment and the Donga-Pont and Terou-Igbomakoro subcatchments. Compared to the mean simulated rainfall for 1960-2000 the mean rainfall decreases by 4 to 10% depending on the scenario. The relative changes for the Upper Ouémé catchment and the two subcatchments are similar.

The comparison to the measured mean rainfall for 1998-2005 leads to very similar results for the whole Upper Ouémé catchment, with decreases in rainfall between 3 and 8%. However, since Donga-Pont subcatchment received above average rainfall amounts and Terou-Igbomakoro subcatchment received lower amounts in the period 1998-2005 (cp. Section 2.1, Table 2.1), the relative changes show opposite trends. Compared to this period, reductions in the rainfall reach up to 14% in the Donga-Pont catchment. Nevertheless, the period 1998-2005 was taken as the baseline because the model was parameterized, calibrated, and validated for this

Table 7.23 Changes in simulated rainfall (PCP) for the Upper Ouémé catchment and the two subcatchments compared to the original model for the period 1998-2005.

	Original	Original	A1B		B1	
	1960-2000	1998-2005	2001-2025	2026-2050	2001-2025	2026-2050
	PCP [mm]	PCP [mm]	Δ PCP [%]	Δ PCP [%]	Δ PCP [%]	Δ PCP [%]
Upper Ouémé	1196	1184	-4	-8	-3	-5
Donga-Pont	1236	1294	-10	-14	-9	-12
Terou-Igbomakoro	1260	1157	2	-2	4	1

period.

While Table 7.23 showed the changes in annual rainfall as averages for the ensemble runs and for specific time periods, Fig. 7.33 shows the temporal variation of annual rainfall in time and between the ensemble runs. Compared to the period 1960-2000, the mean rainfall amounts, as well as the maxima and minima, are shifted towards lower values. In particular, for the period 2026-2050 almost all mean

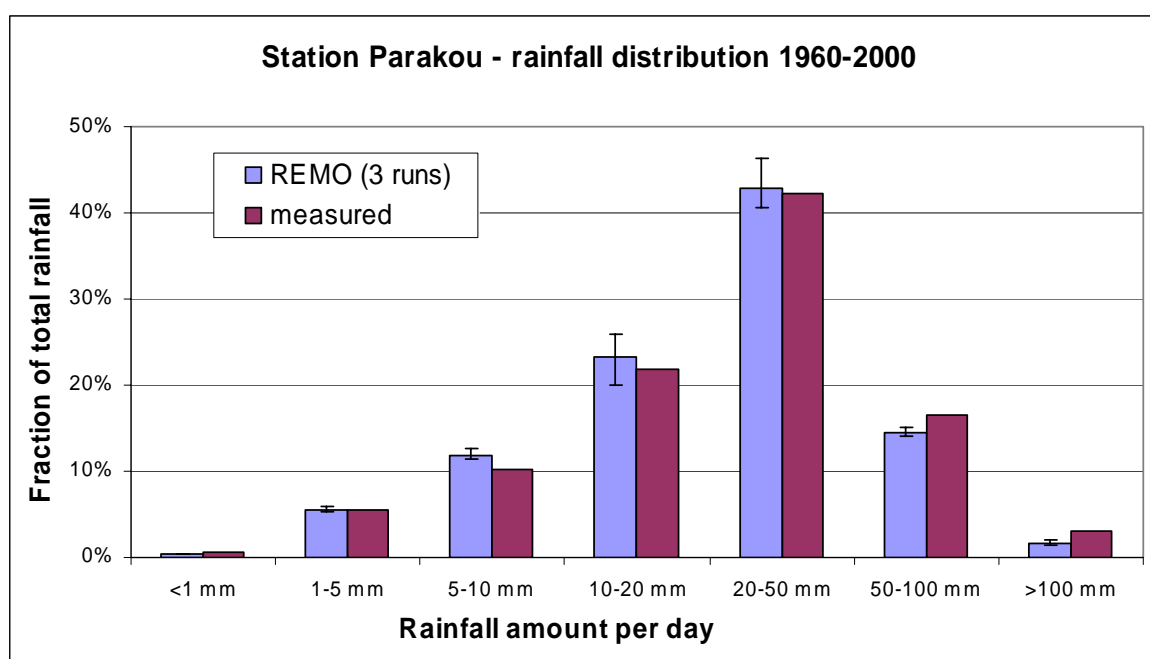


Fig. 7.32 Comparison of measured and simulated daily rainfall distribution for the period 1960 to 2000 at the station Parakou; the bars reflect the total range of the ensemble runs.

annual rainfalls for both scenarios lie below the averages for 1960-2000 and 1998-2005, as indicated by the black horizontal lines. Furthermore, the diagram illustrates the large variations in rainfall among years and ensemble runs.

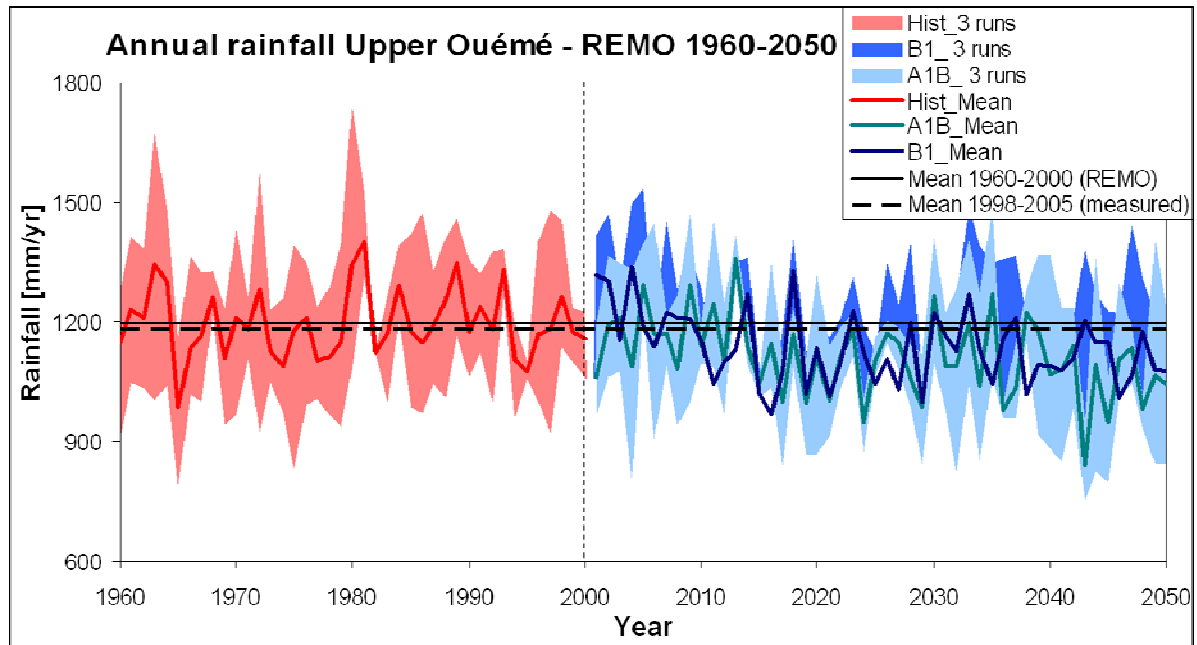


Fig. 7.33 Simulated annual rainfall in the Upper Ouémé catchment for 1960-2050 from the REMO model. The mean of all three ensemble runs for each scenario (historic, A1B, B1) and the range covered by the ensemble runs are shown. The black horizontal lines show the mean simulated rainfall for 1960-2000 (—) and the mean measured rainfall for 1998-2005 (---).

Overview of the simulation runs for the scenario analysis

After pre-processing the input data for the scenario analysis and testing the validity of the baseline scenarios, multiple simulation runs were performed for the scenario analysis. Figure 7.34 summarizes the different scenario runs and their denomination as they will appear in the following descriptions of the results. Each climate scenario required three model runs, representing the three ensemble runs from REMO. The use of the ensembles allowed studying of the influence of the uncertainties in the initial conditions of the climate model on the results of the erosion model. Averaging the three ensemble runs before the application would have implied a loss of information and a smoothing of climatic extremes. The choice of one representative run of the ensemble was also impossible since each ensemble run has its own characteristic behaviour resulting from differences in the initial conditions. After applying all three ensemble runs in the SWAT model, the results could be averaged. Then, the results of the climate scenarios were compared to the original model for 1998-2005, as was presented in Section 7.1. Each CLUE-S land use scenario (L1 to

L3) was performed for the land use maps for 2005, 2015, and 2025. The simulation period was kept as in the original model, i.e., from 1998-2005. The results of the land use scenarios were compared to the so-called Lu00 model, which is a modified version of the original model with the disaggregated CLUE-S land use map for 2000.

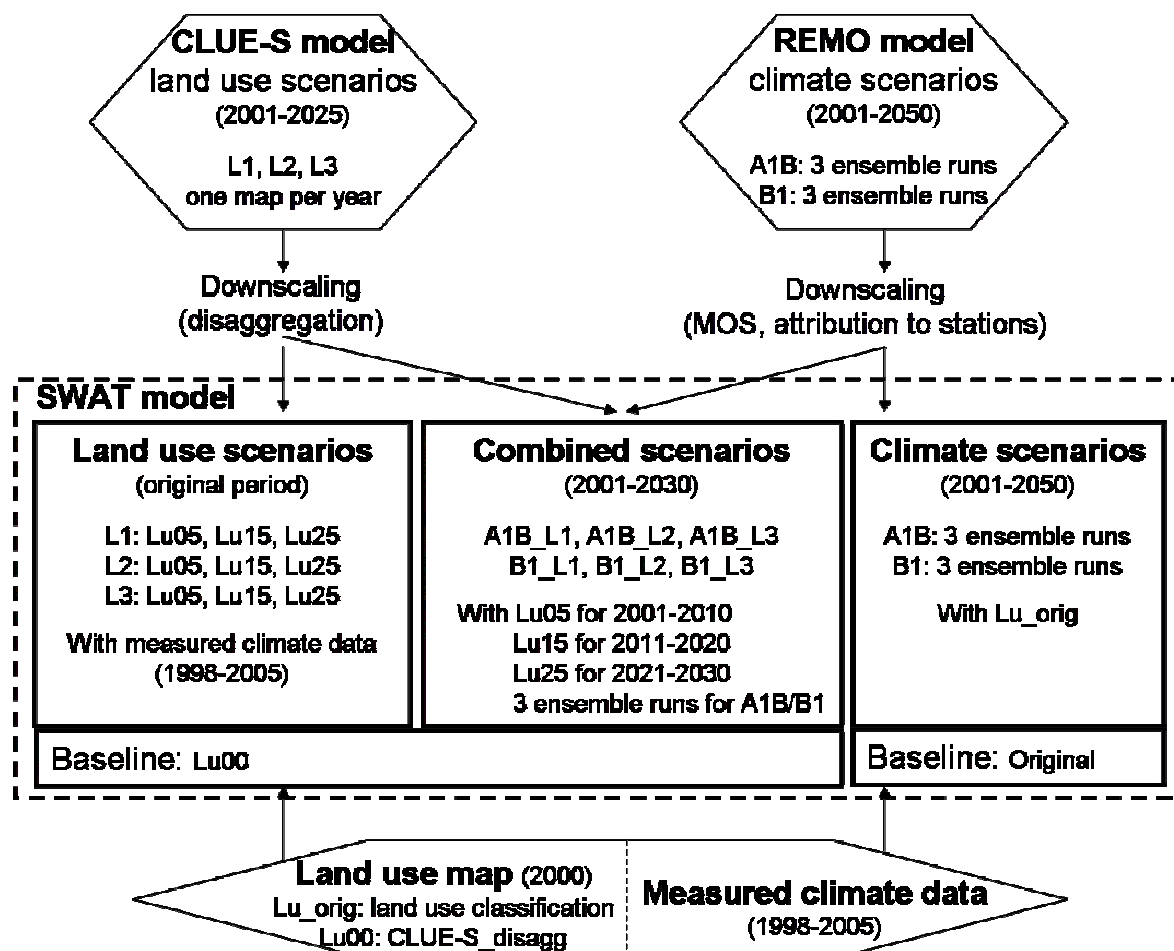


Fig. 7.34 Denomination of the SWAT simulation runs based on the land use and climate scenarios from the CLUE-S and REMO models.

In the combined climate and land use change scenarios, each of the three land use maps (2005, 2015, and 2025) was used for one decade of climate data in the period 2001-2030. The results of the combined scenarios were compared to the results of the Lu00 model. In summary, the climate and land use scenarios each required 9 model runs. For the combined scenarios, 9 SWAT projects and 54 model runs were performed.

7.2.2. Land use change scenarios

Before comparing the land use scenarios to the reference scenario Lu00, the plausibility of the Lu00 model was intensively checked. Therefore, the model results of the Lu00 model were compared with the results of the original model.

Comparison of the original model with the Lu00 model

A good agreement of the yearly water and sediment yields was obtained for the whole catchment and the Terou-Igbomakoro and Donga-Pont subcatchments (Fig. 7.35). However, the Lu00 model underestimates water and sediment yields as a result of a lower fraction of cropland (see previous section). For the whole catchment, mean annual discharge and sediment yield decrease by 1.2% and 11.3%,

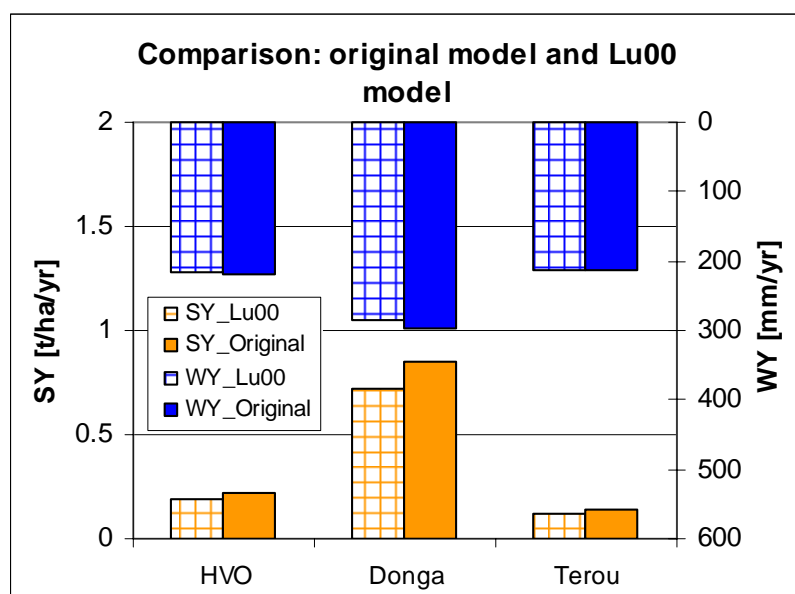


Fig. 7.35 Simulated annual water yield (WY) and sediment yield (SY) for the original model and the Lu00 model.

respectively. For the Donga-Pont subcatchment, both variables are reduced by 15.7% and 4.7%. For the Terou-Igbomakoro catchment, sediment and water yield are 11.2% and 0.5% lower for the Lu00 model than for the original model. The mean annual surface runoff in the Upper Ouémé catchment

is underestimated by 3.7% (Fig. 7.36).

The mean monthly values of the water yield and evapotranspiration are very similar in both models. The 11% underestimation of the monthly sediment yield is regularly distributed over the whole rainy season (Fig. 7.37). In May, the overestimation amounts to 20%, which is not of great importance due to the low absolute values.

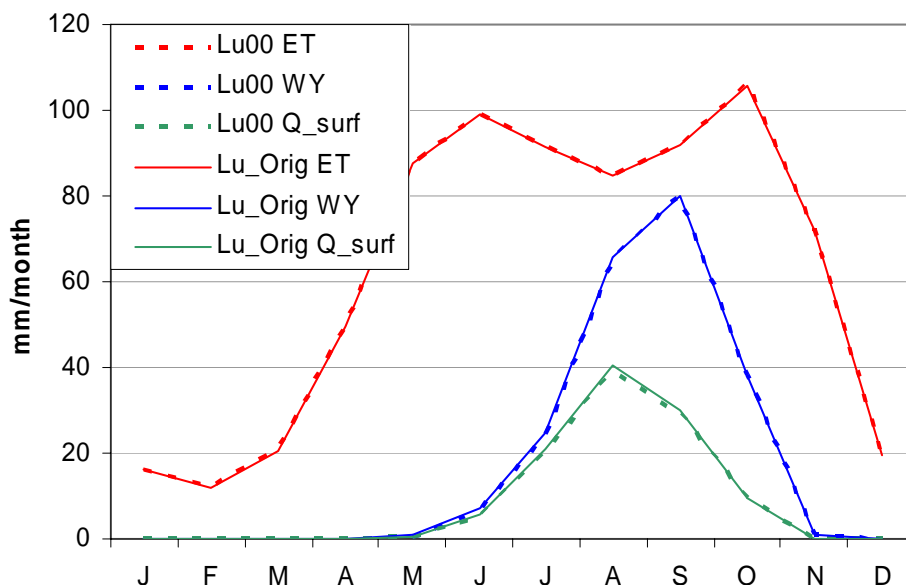


Fig. 7.36 Simulated monthly water yield (WY), Q_{surf} , and ET in the Upper Ouémé catchment for the original model and the Lu00 model.

In conclusion, the results of the Lu00 model are comparable to those of the original model. Consequently, the Lu00 model can be used as baseline scenario for the land use scenarios.

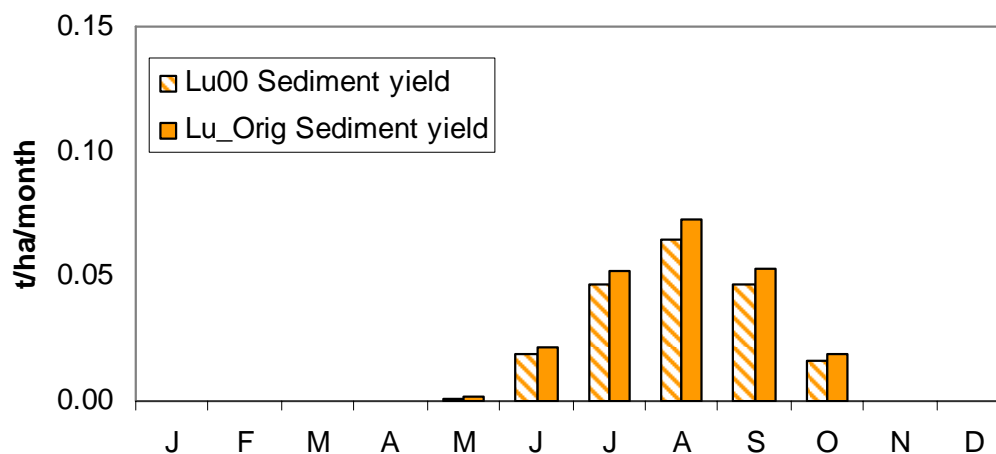


Fig. 7.37 Simulated monthly sediment yield in the Upper Ouémé catchment for the original model and the Lu00 model.

Comparison of the land use scenarios with the Lu00 model

The mean annual sediment and water yields of the land use scenarios were compared with those of the Lu00 model (Fig. 7.38). While the increases in the total water yield are rather small, the increases of the sediment yield are more pronounced. As expected, the L2 scenario “economic stagnation and institutional insecurity” leads to the highest increase in sediment yield.

Until 2025, water and sediment yields increase by 7% and 95% for this scenario, resulting from an increase of cropland area of 108% (Table 7.24).

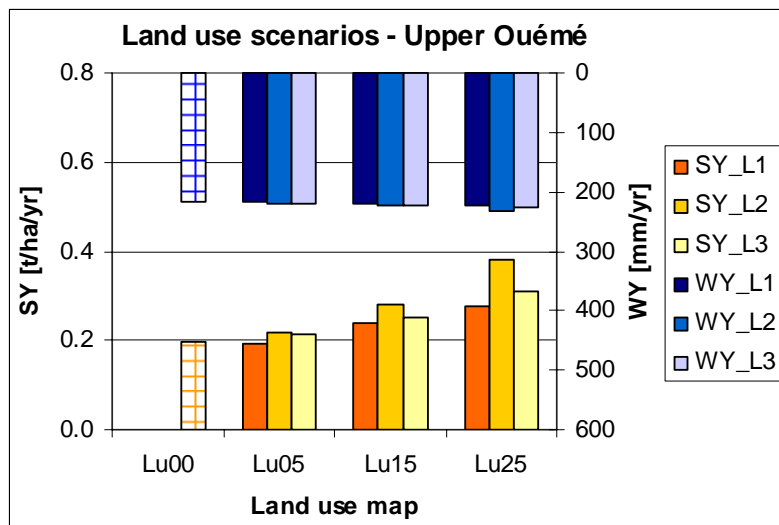


Fig. 7.38 Simulated water and sediment yields for the land use scenarios L1, L2, L3 compared to the Lu00 model

For the L1 scenario, assuming an intensification of crop production, the relative increase in the sediment yield until 2015 and 2025 is only half as large as for the L2 scenario. For 2005, sediment yield even decreases by 0.7% despite a slight increase in the cropland area.

Several subbasins in the central part of the catchment show decreasing sediment yields for this scenario. In these subbasins without cropland, sediment yields are so low, that small shifts from shrub and grass savannah to forest and dense savannah or slightly different HRUs after pre-processing of the land use maps can lead to decreases in sediment yield. As agricultural expansion increases, these effects become negligible. The results for the “Business as usual” scenario L3 lie between the results for scenarios L1 and L2. Until 2025, water and sediment yields increase for L3 by 2% and 60%, respectively.

Table 7.24 Mean simulated annual sediment yield (SY) and water yield (WY) for the period 1998-2005 for the land use scenarios L1, L2, L3 compared to the Lu00 model.

	Cropland [%]	SY [t/ha/yr]	WY [mm/yr]	Q _{surf} [mm/yr]	Compared to LU00			
					ΔCropland [%]	ΔSY [%]	ΔWY [%]	ΔQ _{surf} [%]
Lu00	12.18	0.19	217	104	-	-	-	-
L1_Lu05	13.04	0.19	218	106	7	-0.67	0.47	1.54
L2_Lu05	13.94	0.22	219	107	14	11.28	0.98	3.08
L3_Lu05	13.68	0.21	218	107	12	9.18	0.86	2.64
L1_Lu15	15.73	0.24	220	110	29	22.05	1.82	6.00
L2_Lu15	18.43	0.28	224	115	51	44.97	3.35	10.68
L3_Lu15	17.04	0.25	222	113	40	29.74	2.65	8.35
L1_Lu25	18.39	0.28	224	115	51	42.41	3.35	10.68
L2_Lu25	25.35	0.38	232	128	108	95.33	7.32	22.70
L3_Lu25	21.36	0.31	227	120	75	59.85	4.97	15.68

In summary, the mean sediment yield of 0.19 t/ha/yr for the Lu00 model increases to 0.28 - 0.38 t/ha/yr by 2025. The mean annual surface runoff increases from

104 mm/yr to 115 - 128 mm/yr depending on the scenario. The total water yield increases slightly by 3 to 7%.

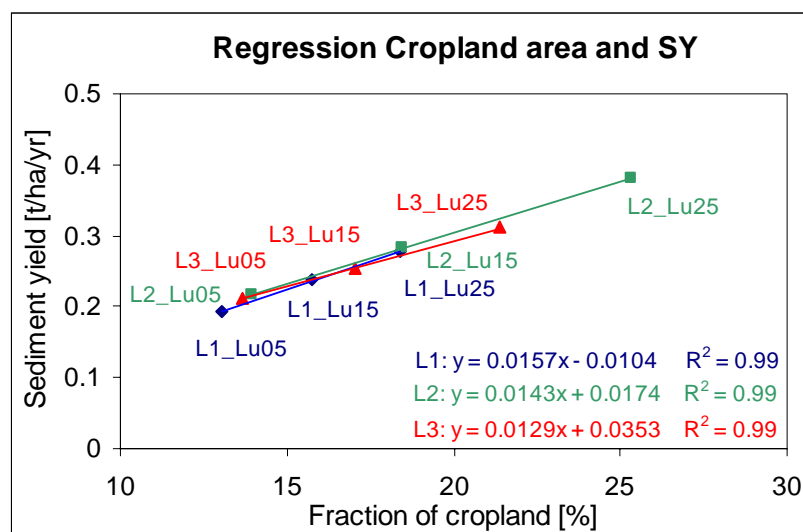


Fig. 7.39 Regression between the field fraction and the sediment yield for the land use scenarios L1 to L3.

If the sediment yield is plotted against the fraction of cropland for all scenarios, one obtains an almost linear relationship for the three land use scenarios L1, L2, and L3 ($R^2=0.99$) (Fig. 7.39). This linear relationship was also observed by Busche (2005) for the Terou-Igbomakoro sub-

catchment. As shown in Table 7.24, relative changes in cropland area lead to slightly smaller relative changes in sediment yield.

Figures 7.40 and 7.41 compare the maps of the mean sediment yield and the mean surface runoff for the scenarios L1_Lu25, L2_Lu25, and L3_Lu25 with the

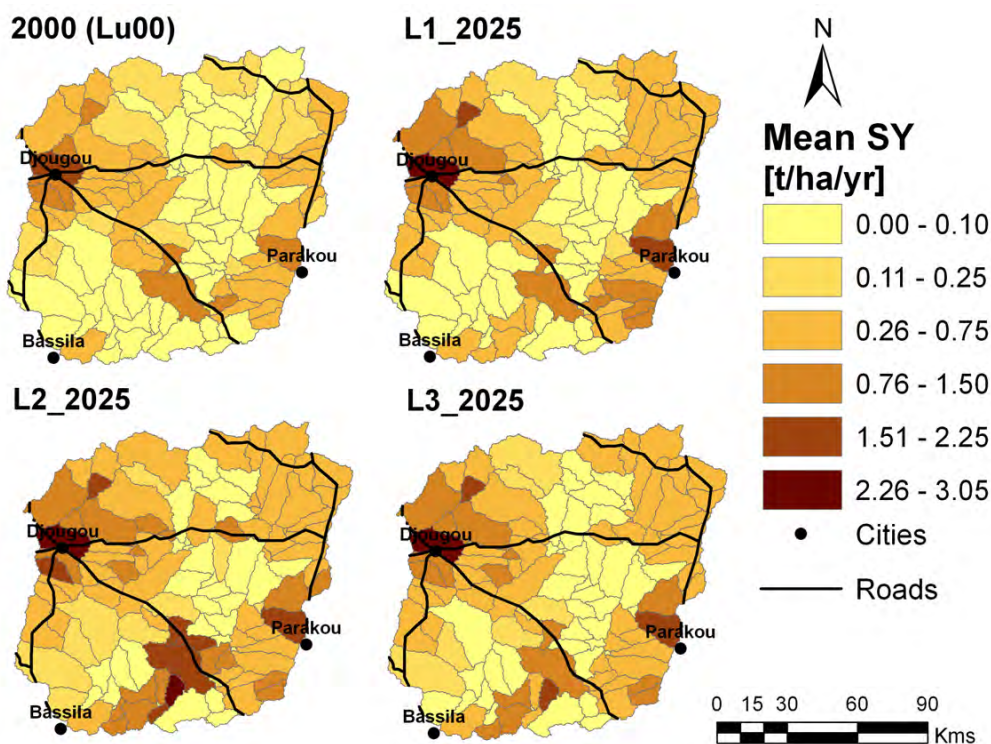


Fig. 7.40 Comparison of the mean annual simulated sediment yield (1998-2005) for the Lu00 model and the Lu25 model for the land use scenarios L1 to L3.

Lu00 model. At first glance, we see an increase of the sediment yield in the NW and SE of the catchment. The spatial pattern of the three scenarios for 2025 seems to be quite similar, but a closer look at the maps reveals differences. For example, the increases in the SW and the SE of the catchment are more pronounced for the L2 scenario than for the other scenarios.

In general, the spatial pattern with high sediment yields and high surface runoff in the NW, SE, and NE of the catchment remains similar by 2025. However, the scenarios exhibit a further hotspot of soil erosion in the southern part of the catchment. Except for the L2 scenario, the sediment yields in the central part of the catchment remain very low (<0.1 t/ha/yr) resulting from the assumption that the protected forest (*Fôret classée de l'Ouémé supérieur*) is not converted into cropland. For some of these subbasins, the land use scenarios deliver a slight reduction of the sediment yield. This negative bias is caused by the pre-processing of the land use data and can significantly influence the results in subbasins with a very low fraction of crop land. For the L2 scenario, the borders of the protected forest are subject to a rapid expansion of the cropland area, leading to the highest relative and absolute growth rates in surface runoff and sediment yield in the catchment (Fig. 7.40-41). While in

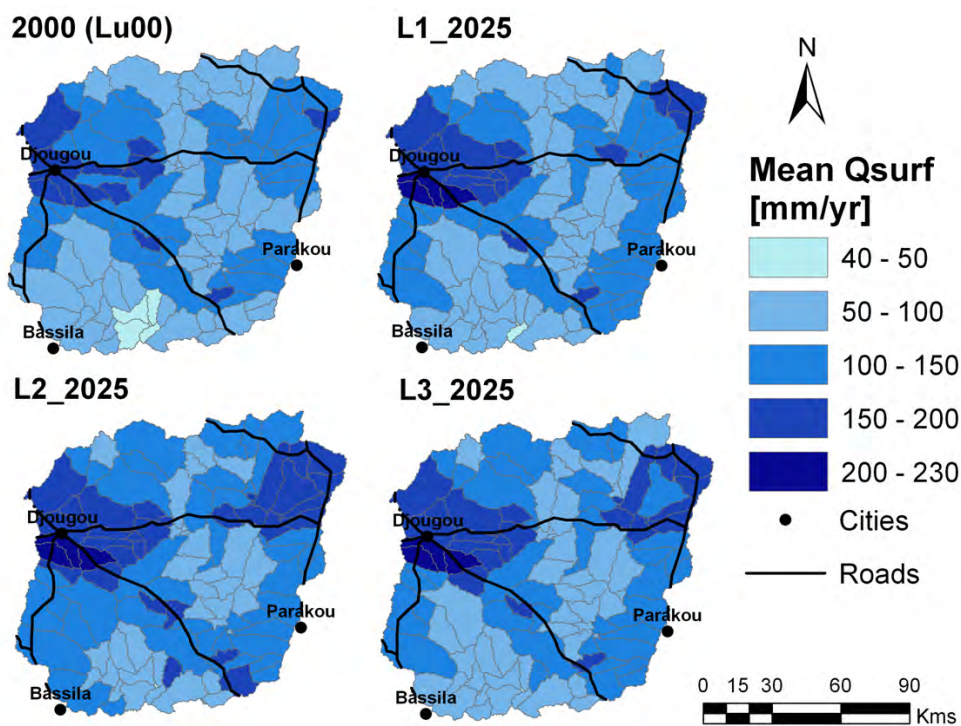


Fig. 7.41 Comparison of the mean annual simulated surface runoff (1998-2005) for the Lu00 model and the Lu25 model for the land use scenarios L1 to L3.

most subbasins the mean sediment yield increases by less than 1.2 t/ha/yr, the increase in the southern border areas of the protected forest reaches up to 3 t/ha/yr. For the Terou-Igbomakoro (SW) and Donga-Pont (NW) subcatchments, the maps in Fig. 7.40 indicate an increase in the sediment yield for all scenarios. The relative increase of the sediment yield in most subbasins of the Terou-Igbomakoro subcatchment is high. In some subbasins, the sediment yield in 2025 is 20 to 40 times higher than in 2000. Nevertheless, the absolute increases in the Terou-Igbomakoro catchment still remain lower than in the intensively used Donga-Pont subcatchment. In the subbasins of the Donga-Pont subcatchment, the sediment yield increases by 30 to 95%. The small differences between the three land use scenarios L1-L3 in this subcatchment are not visible in Figs. 7.40 and 7.41.

In the following, the results for the two subcatchments are presented in detail. The bar charts in Figs. 7.42 and 7.43 show sediment and water yields for all land use scenarios using different y-axes for the sediment yield due to the large differences between the two subcatchments.

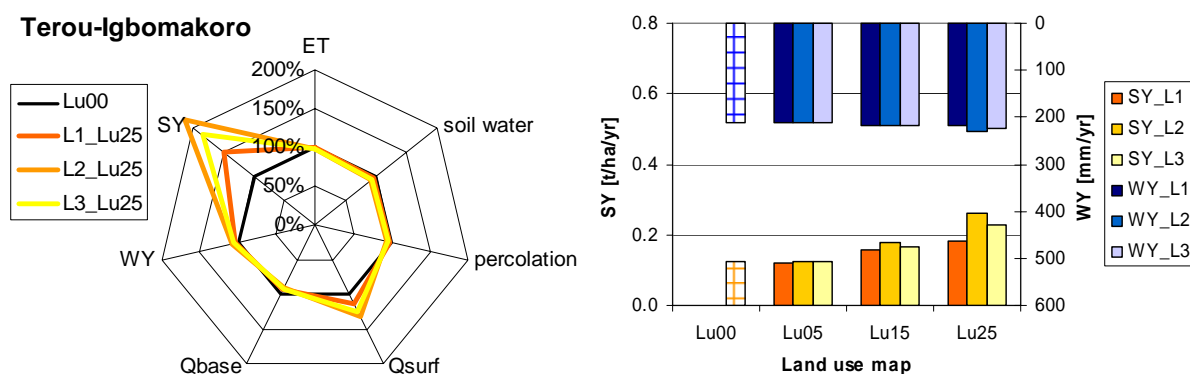


Fig. 7.42 Relative comparison of the components of the water balance in the Terou-Igbomakoro subcatchment: land use scenarios Lu00 (black), Lu25-L1 (orange), Lu25-L2 (ochre), Lu25-L3 (yellow); mean annual sediment and water yields in the Terou-Igbomakoro subcatchment.

For all land use scenarios, the sediment yield increases. This trend is more pronounced for the Terou-Igbomakoro subcatchment than for the Donga-Pont subcatchment. In contrast, total water yields increase only slightly. The differences between the three scenarios L1-L3 are significantly higher for the Terou-Igbomakoro subcatchment. For the intensively used Donga-Pont subcatchment, these differences are almost negligible.

The net diagrams in Figs. 7.42-7.44 reveal the underlying changes in the components of the water balance. It is obvious that changes in surface runoff are the main driving force for changes in sediment yield besides the empirical USLE factors. For the 2025 land use maps, the increase in surface runoff ranges from 15 to 32% for the Terou-Igbomakoro subcatchment, depending on the land use scenario.

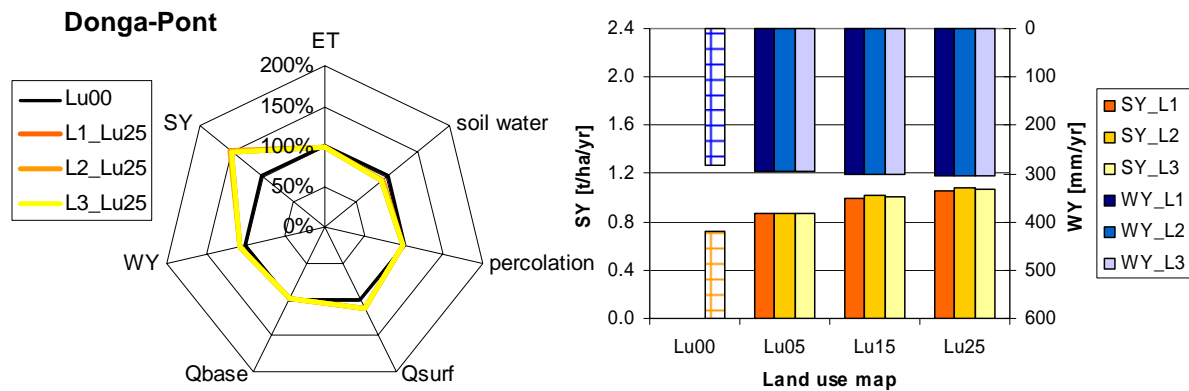


Fig. 7.43 Relative comparison of the components of the water balance in the Donga-Pont subcatchment: land use scenarios Lu00 (black), Lu25-L1 (orange), Lu25-L2 (ochre), Lu25-L3 (yellow); mean annual sediment and water yields in the Donga-Pont subcatchment.

For Donga-Pont, surface runoff in 2025 is about 13% higher than in the Lu00 model. All other components of the water balance, namely baseflow, soil water, and evapotranspiration, remain nearly constant in the two subcatchments. Precipitation was not included in the diagrams since it is equal for all land use scenarios.

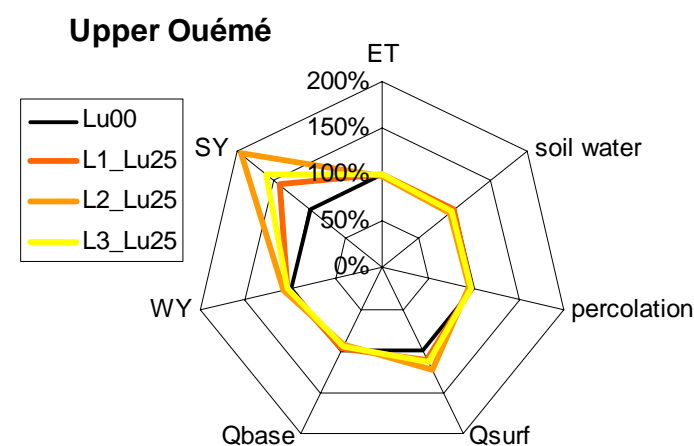


Fig. 7.44 Relative comparison of the components of the water balance in the Upper Ouémé catchment: land use scenarios Lu00 (black), Lu25-L1 (orange), Lu25-L2 (ochre), Lu25-L3 (yellow).

The net diagram for the whole Upper Ouémé catchment is very similar to the one for the Terou-Igbomakoro subcatchment; the increases in surface runoff and sediment yield are slightly lower. Looking at the monthly results of the Lu25 models for the Upper Ouémé catchment, negligible changes in actual evapotranspiration and total runoff and a significant increase in surface runoff become visible (e.g., Fig. 7.45).

The increases in surface runoff and sediment yield are regularly distributed over the whole rainy period (Figs. 7.45, 7.46). The monthly increases in sediment yield in the

period June to October for 2025 range between 36 to 53%, 84 to 113%, and 52 to 73% for the three land use scenarios L1, L2, and L3.

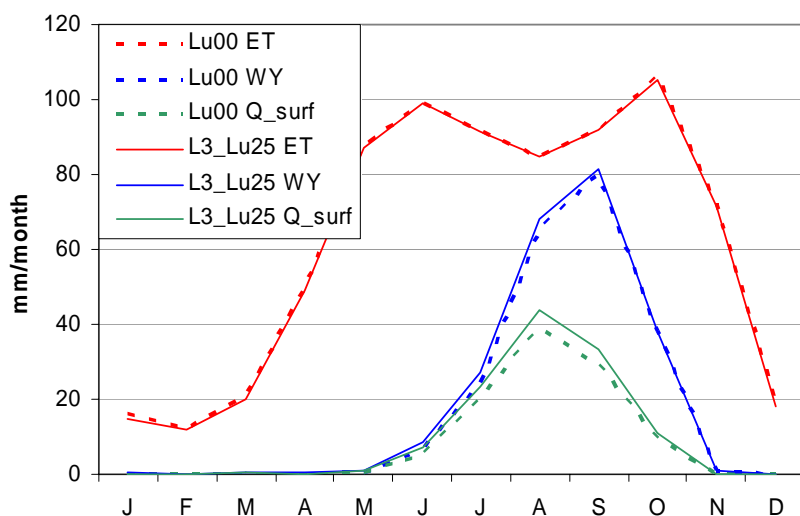


Fig. 7.45 Comparison of the mean monthly evapotranspiration, water yield and surface runoff in the Upper Ouémé catchment for scenario L3_Lu25.

By 2025, sediment yields increase by 42%, 95%, and 60% for land use scenarios L1, L2, and L3, respectively. However, the spatial pattern with high sediment yields in the NW, SE, and NE areas of the catchment changes only slightly. In particular for the L2 scenario, soil erosion is additionally aggravated in the south portion of the catchment. With regard to the Terou-Igbomakoro and Donga-Pont subcatchments, surface runoff and sediment yield increase enormously in the Terou-Igbomakoro subcatchment but do not reach the high erosion rates in the Donga-Pont subcatchment.

In conclusion, all land use scenarios lead to significantly increased surface runoff and sediment yield while changes in total water yield and all other components of the water balance are negligible.

By 2025, sediment yields increase by

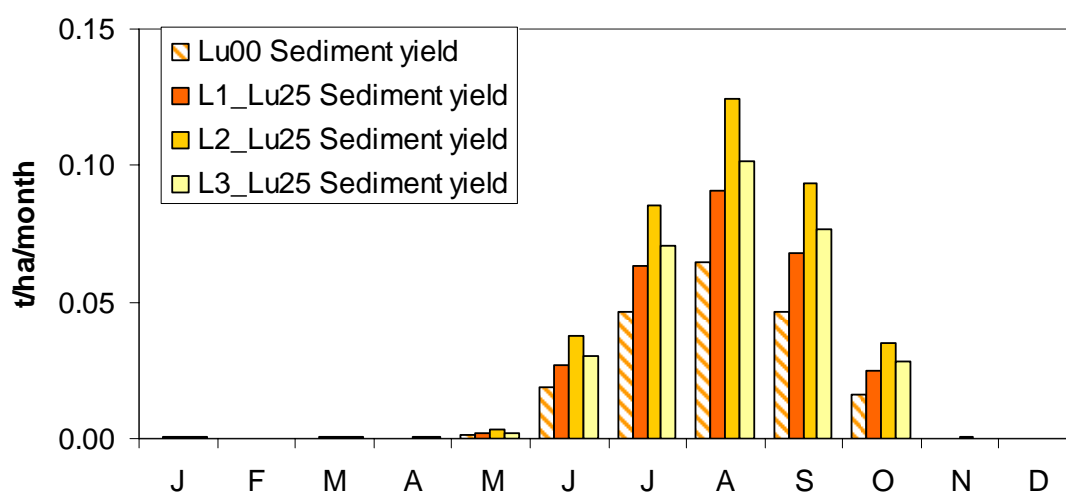


Fig. 7.46 Comparison of the mean monthly sediment yields in the Upper Ouémé catchment for the Lu25 models and the Lu00 model.

7.2.3. Climate change scenarios

The results of the climate scenarios will be presented for the whole catchment and two subcatchments to point out regional variations (Table 7.25). The results of each climate scenario are averaged for the three runs with the SWAT model referring to the three ensemble runs from the climate model REMO. In order to allow for comparisons with land use scenarios, the results are presented for the two periods 2001-2025 and 2026-2050.

Table 7.25 Mean simulated annual values of rainfall (PCP), sediment yield (SY), and water yield (WY) of the three ensemble runs for the climate scenarios A1B and B1, change in % from the original model (1998-2005).

	1998-2005 Original			2001-2025 A1B			2026-2050 A1B			2001-2025 B1			2026-2050 B1		
	PCP [mm/yr]	WY [mm/yr]	SY [t/ha/yr]	PCP [Δ%]	WY [Δ%]	SY [Δ%]	PCP [Δ%]	WY [Δ%]	SY [Δ%]	PCP [Δ%]	WY [Δ%]	SY [Δ%]	PCP [Δ%]	WY [Δ%]	SY [Δ%]
Upper Ouémé	1184	219	0.22	-4	-12	-14	-8	-23	-27	-3	-6	-5	-5	-12	-17
Donga-Pont	1294	297	0.85	-10	-23	-27	-14	-33	-35	-9	-18	-19	-12	-25	-28
Terou-Igbo.	1157	213	0.14	2	1	-5	-2	-11	-21	4	10	7	1	3	-7

Compared to the period 1998-2005, mean annual rainfall is reduced by 2 to 8% in the Upper Ouémé catchment and by 9 to 14% in the Donga-Pont subcatchment. As a consequence of the reduced rainfall and slightly increased evapotranspiration the mean water and sediment yields decrease in the periods 2001-2025 and 2026-2050 in both catchments for at least five of six runs. For the Upper Ouémé catchment, mean water yields decrease by 6 to 23% and sediment yields decrease by 5 to 27%. For individual ensemble runs, reductions of up to 38% for water yield and 41% for sediment yield are obtained (second ensemble run, A1B, 2026-2050). However, standard deviations of the mean values for the ensemble runs are considerably high, in particular for the period 2026-2050 reaching up to 17%.

For the Donga-Pont subcatchment, the reductions in water and sediment yields are more drastic than for the whole Upper Ouémé catchment. For example, water and sediment yields decrease on average by 18 to 33% and 19 to 35%, depending on the scenario and the considered time period. For the second ensemble run, water and sediment yields for the period 2026-2050 decrease by 47% and 50% compared to 1998-2005. However, one has to keep in mind that rainfall in the Donga-Pont subcatchment in 1998-2005 was significantly above the long-term average, including several very extreme events that caused very high surface runoff and sediment yields. Consequently, the relative changes tend to be overestimated. However, the

negative trend also remains if the results are compared with the model results for 1960-2000 based on climate data from the REMO model.

For the Terou-Igbomakoro subcatchment, the effects of climate changes are less clear. The average annual rainfall changes only slightly by -2 to +4%, leading to various responses of mean water and sediment yields. While the sediment yield decreases for all ensemble runs of the A1B scenario, the water yield decreases only for two of three ensemble runs. On average, sediment yield differs by -5% and -21% and water yield changes by +1% and -11% for the two periods (Table 7.25). For the B1 scenario, the mean water and sediment yields increase by 10% and 7% in the Terou-Igbomakoro subcatchment in the period 2001-2025. In 2026-2050, the mean annual water yield is 3% higher and the sediment yield 7% lower than in the original model (1998-2005). However, the ensemble runs deliver water yields in 2026-2050 ranging from -10% to +19%, and sediment yields from -21 to +18% in both periods. In conclusion, for the Upper Ouémé catchment both scenarios lead, on average, to reduced water and sediment yields. This effect is particularly pronounced for scenario A1B and the time period 2026-2050. While these trends are even more apparent for the Donga-Pont subcatchment, no clear trend was observed for the Terou-Igbomakoro subcatchment.

So far, the time periods 2001-2025 and 2026-2050 have been compared to the time period 1998-2005. Figures 7.47 and 7.48 show the precipitation and potential evapotranspiration as well as the resulting water and sediment yields in five year intervals for the Upper Ouémé catchment. Potential evapotranspiration increases over the whole period for both scenarios, resulting from rising average temperatures.

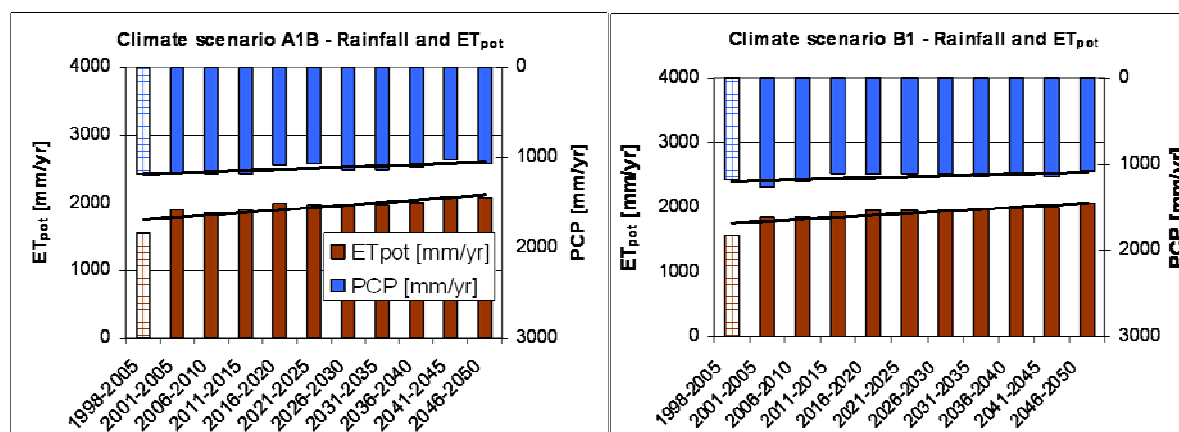


Fig. 7.47 Mean simulated annual values of ET_{pot} and precipitation (PCP) of the three ensemble runs for climate scenarios A1B and B1 for the period 2001-2050 for the Upper Ouémé catchment.

However, actual evapotranspiration remains nearly constant.

Mean annual rainfall tends to decrease but is subject to temporal variation, which

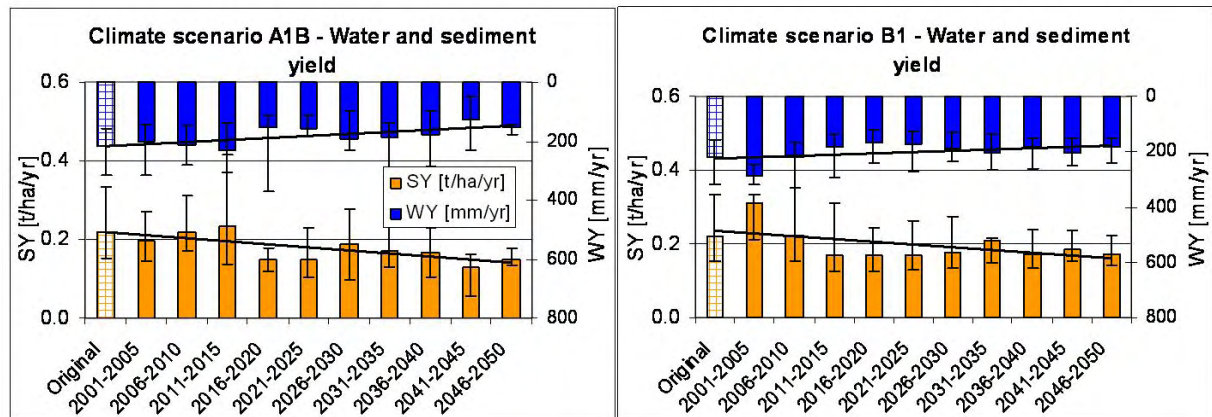


Fig. 7.48 Mean simulated annual values of sediment yield (SY) and water yield (WY) of the three ensemble runs for the climate scenarios A1B and B1 for the period 2001-2050 for the Upper Ouémé catchment.

triggers the temporal dynamics of sediment and water yields (Fig. 7.48). The “error” bars in Fig. 7.48 do not reflect the mean square values but the range of results for the ensemble runs. Although the variation between the ensemble runs can be very large, a tendency towards decreased water and sediment yields can be observed, particularly for scenario A1B.

While the period 2001-2010 (for A1B until 2015) shows comparatively high water and sediment yields, the following semi-decades until 2050 show mean water and sediment yields below the average for the reference period 1998-2005. The spatial maps for sediment yield (Fig. 7.49) show a similar pattern as for the reference period. The differences between the time periods 2001-2025 and 2026-2050 appear to be larger than the differences between the two scenarios. Until 2050, some subbasins in the region around Djougou and in the NE of the catchment experience a visible decrease in the sediment yield compared to the period 1998-2005. As mentioned before, the decrease of sediment yield in the Djougou region is smaller compared with the results for 1960-2000 based on climate data simulated by REMO. Correspondingly, the spatial pattern of surface runoff and water yield change towards lower values (Fig. 7.50 and Fig. B.5, Appendix B). Since the land use is kept constant, changes in total water yield drive the changes in surface runoff and sediment yield.

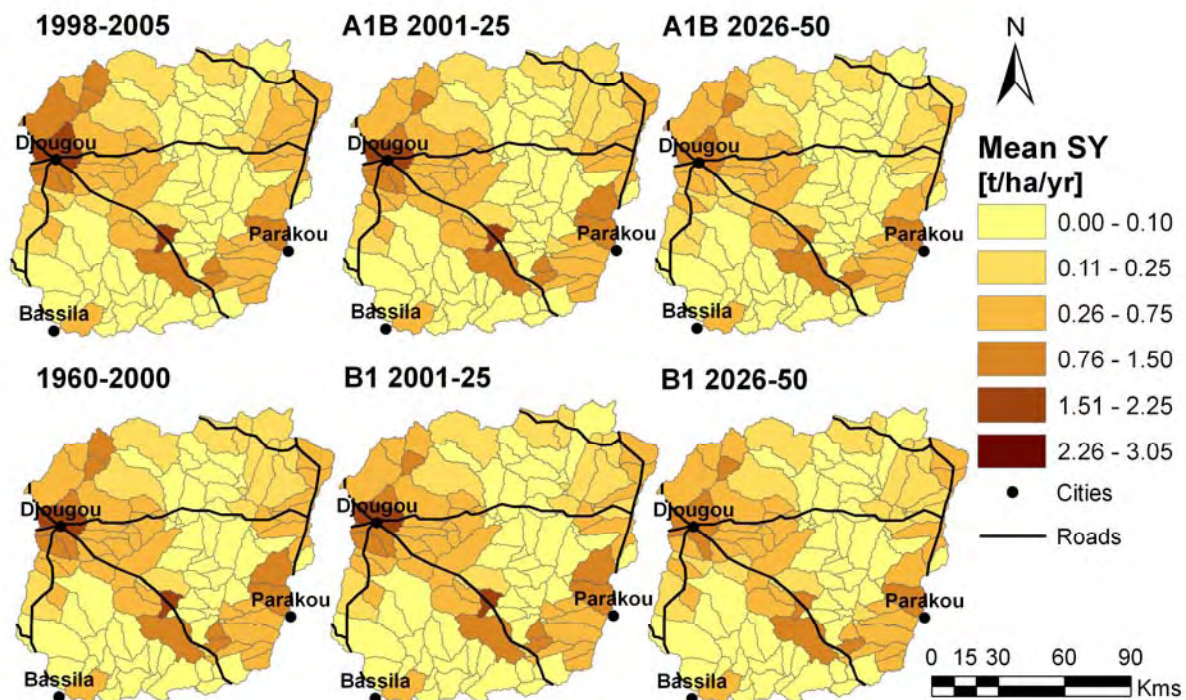


Fig. 7.49 Mean spatial distribution of sediment yield for the climate scenarios A1B and B1 for the periods 2001-2025 and 2026-2050 compared to the original model (1998-2005) and the model with REMO climate data for 1960-2000.

The decreases of surface runoff and water yield in the NW, NE, and SE of the catchment are more pronounced for the A1B scenario and the period 2026-2050. The increase of surface runoff and water yield in the S/SW of the catchment (Terou-

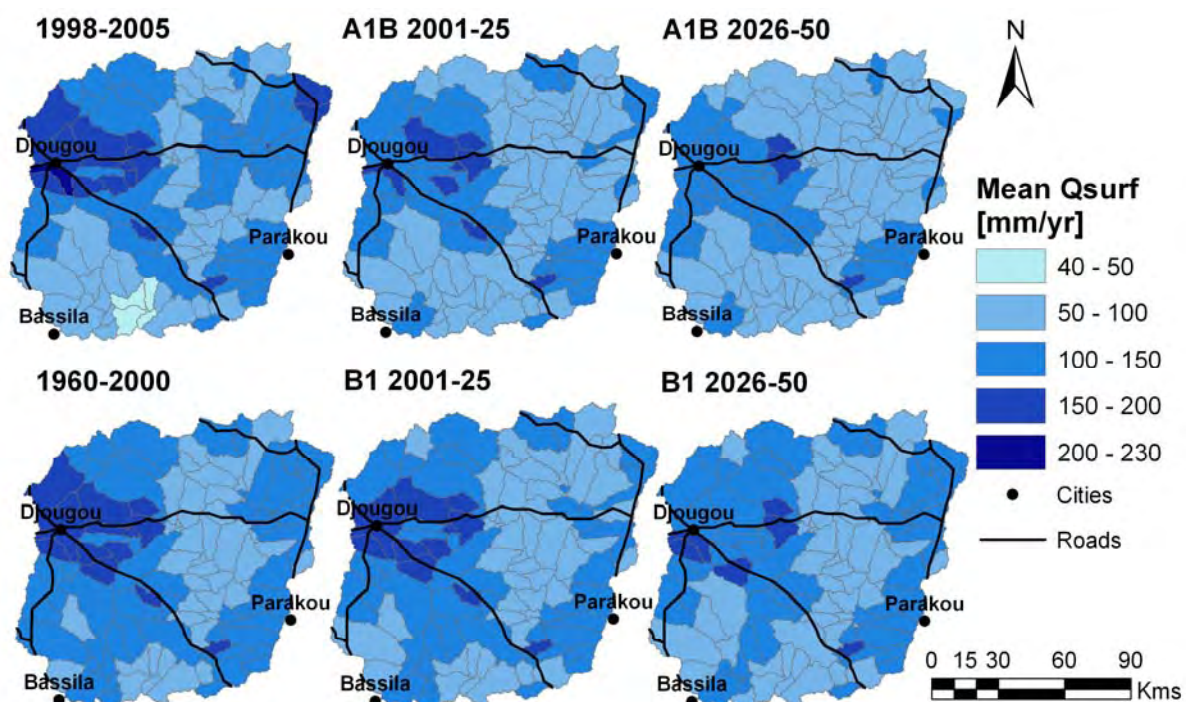


Fig. 7.50 Mean spatial distribution of surface runoff for climate scenarios A1B and B1 for the periods 2001-2025 and 2026-2050 compared to the original model (1998-2005) and the model with REMO climate data for 1960-2000.

Igbomakoro) appears only in comparison to the period 1998-2005. Compared to the period 1960-2000, driven by REMO climate data, surface runoff also decreases in this part of the catchment. The results for 1960-2000 may be more representative since they cover a longer time period. However, the model for 1998-2005 is kept as the main reference because it is based on measured climate data and was intensively validated in space and time.

In the following, the results for the Terou-Igbomakoro and Donga-Pont subcatchments are discussed in more detail. Figures 7.51 and 7.52 illustrate the changes in the water and sediment yields in five year increments using different y-axes for the sediment yield due to the large differences between the two subcatchments.

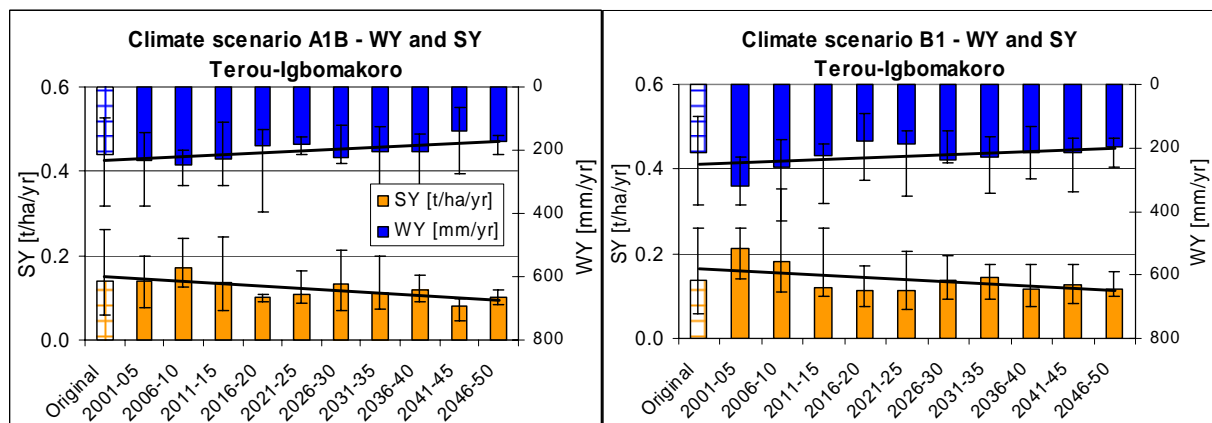


Fig. 7.51 Mean simulated annual values of sediment yield (SY) and water yield (WY) of the three ensemble runs for climate scenarios A1B and B1 for the period 2001-2050 in the Terou-Igbomakoro subcatchment.

The temporal variation of water and sediment yields for the Terou-Igbomakoro subcatchment equals the variation for the Upper Ouémé catchment in Fig. 7.48. Likewise, all semi-decades after 2010 show mean sediment yields below the reference value for 1998-2005. However, the absolute values for the semi-decades are about 19-42% lower than for the whole Upper Ouémé catchment. For the Donga-Pont subcatchment, the negative trend for water and sediment yields is more pronounced than for the whole catchment. However, the variation between the ensemble runs is high (see large bars in Fig. 7.52). As discussed earlier, the unusually high water and sediment yields in the Donga-Pont subcatchment in 1998-2005 compared to all other semi-decades can be partially explained by the misrepresentative, above average rainfalls in the Djougou region in this period. This may exaggerate the negative linear trends for water and sediment yields in 1998-

2050 seen in Fig. 7.52. However, the trends remain similar, if the period 1998-2005 is not considered.

Relative to the period 1998-2005, potential evapotranspiration, rainfall, and water and sediment yields decrease for the Upper Ouémé catchment and the Donga-Pont subcatchment (Figs. 7.53 (right), 7.54). The relative decreases in baseflow are stronger than the decreases in surface runoff. Evaporation remains nearly constant.

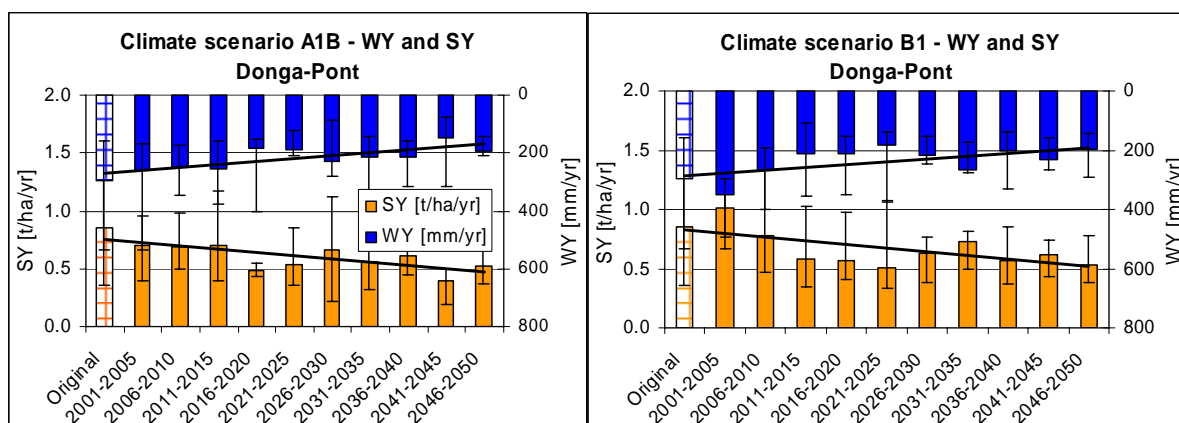


Fig. 7.52 Mean simulated annual values of sediment yield (SY) and water yield (WY) of the three ensemble runs for climate scenarios A1B and B1 for the period 2001-2050 in the Donga-Pont subcatchment.

The extreme relative increase in soil water compared to 1998-2005 for the Donga-Pont subcatchment is caused by the extremely low value in this period, which seems to not be representative for this subcatchment.

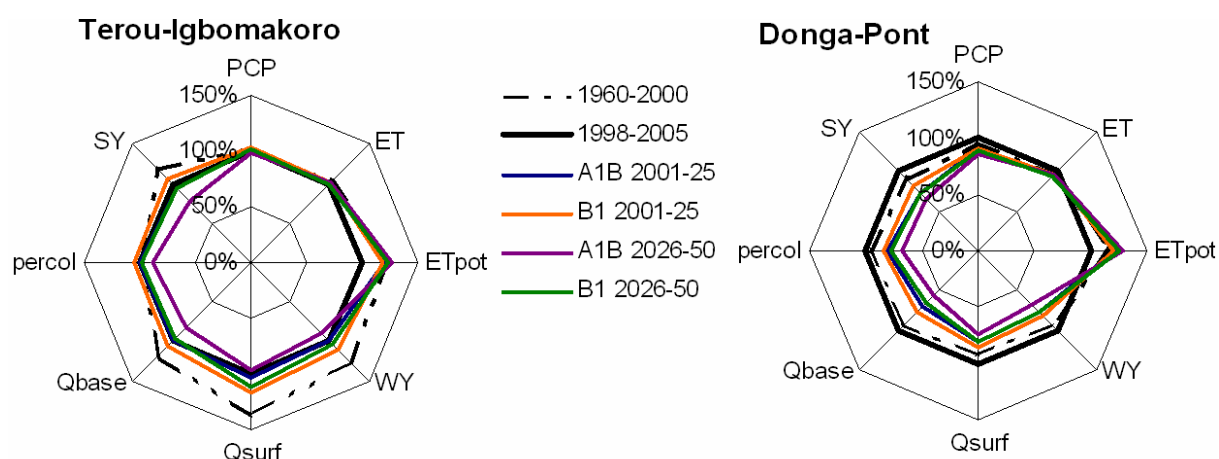


Fig. 7.53 Components of the water balance in the Terou-Igbomakoro and Donga-Pont subcatchments for the climate scenarios relative to the original model (1998-2005).

The interpretation of the net diagram for the Terou-Igbomakoro subcatchment also strongly depends on the choice of the reference (Fig. 7.53, left). Compared to the values in the period 1960-2000 water yield, surface runoff, baseflow, and sediment

yield decrease in 2001-2025 and 2026-2050. However, compared to the original model (1998-2005), these output variables increase for some of the scenario periods.

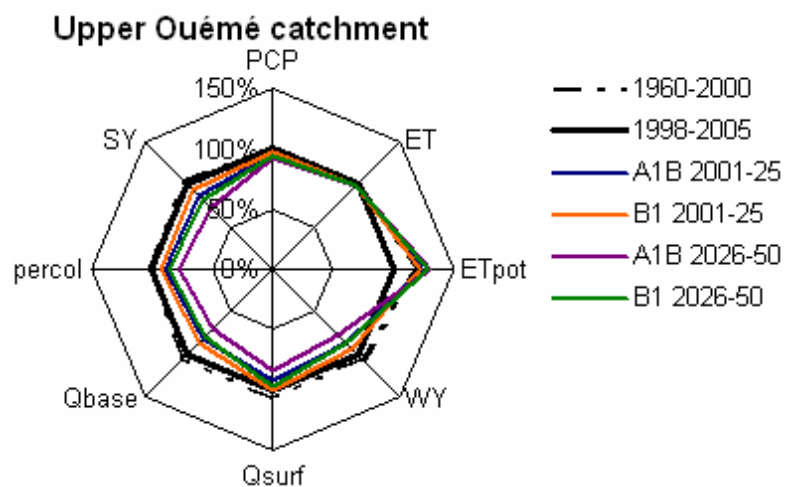


Fig. 7.54 Components of the water balance in the Upper Ouémé catchment for the climate scenarios relative to the original model (1998-2005).

The monthly distributions of sediment and water yields in the Upper Ouémé catchment differ between the climate scenarios, resulting from large reductions in monthly rainfall and slight changes in monthly potential and actual evapotranspiration. In the middle of the rainy season, actual evapotranspiration is slightly higher than in the reference period, but at the end of the rainy season it is slightly lower (not shown). The differences are greater for the A1B scenario than for the B1 scenario. Monthly rainfall is strongly reduced over the whole rainy season for scenario A1B compared to the reference period (1998-2005). In contrast, rainfall is higher for the B1 scenario from March to May and is lower in June to August.

Figure 7.55 shows the monthly distribution for water and sediment yields. In May, the sediment yields for all scenarios lie above the values for 1998-2005 but are below the values for 1960-2000. At the end of the rainy season (Sept.-Nov.) all scenarios behave similar. However, in July and August the sediment yields for the scenarios are significantly lower than in the two reference periods, in particular for scenario A1B 2026-2050. The sediment yield in June varies greatly between the two considered time periods. While the average sediment yield in 2001-2025 slightly exceeds the values of the reference periods, the average sediment yield in 2026-2050 is significantly lower than in the periods 1998-2005 and 1960-2000. The reductions in monthly water yield are regularly distributed over the whole period of June to September. In contrast, the monthly water yield increases in May and

For example, sediment yield for scenario B1 in 2001-2025 is 7% higher than in the period 1998-2005. This is caused by a 10% higher total water yield and a 17% higher amount of surface runoff. Evapotranspiration, percolation and soil water change only slightly.

October. The temporal pattern for the different scenarios and periods is similar but the absolute values differ greatly in the middle of the rainy season.

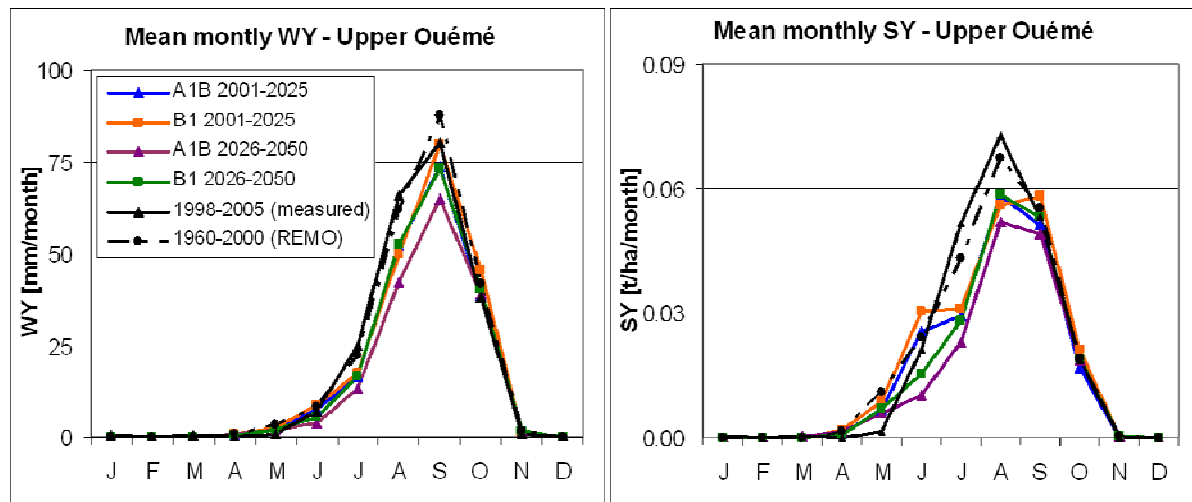


Fig. 7.55 Mean monthly water and sediment yields for climate scenarios A1B and B1 for the periods 2001-2025 and 2026-2050 compared to the period 1960-2000 (REMO climate data) and 1998-2005 (measured climate data).

In summary, water and sediment yields show a negative trend in most parts of the catchment, resulting from reduced rainfall and slightly increased actual evapotranspiration for the climate scenarios. For the Upper Ouémé catchment, the mean water and sediment yields decrease by 6 to 23% and 5 to 27%, respectively. The negative trend is more pronounced for scenario A1B than for scenario B1, and is more apparent in the period 2026-2050 than in 2001-2025. The reduction appears mainly in the middle of the rainy season, i.e., in August and September. The spatial pattern of high sediment and water yields remains similar but the NW (including the Donga-Pont subcatchment) and the NE of the catchment experience a visible decrease of sediment yield. In the Donga-Pont subcatchment, the decreases in water and sediment yields are more drastic than in the whole catchment. For the Teroulgbomakoro subcatchment, the direction of the trend depends on the chosen reference period. Compared to the period 1998-2005, surface runoff and water and sediment yields in this subcatchment slightly increase for most climate scenarios. In contrast, the three variables decrease if the results for 1960-2000, based on REMO climate data, are taken as reference. All other components of the water balance, like evapotranspiration, percolation, and soil water change differ only slightly among the climate scenarios.

7.2.4. Combined scenarios of land use and climate changes

In this subsection, the results of the combined scenarios of land use and climate changes will be presented. For these scenarios, land use maps for 2005, 2015, and 2025 from CLUE-S model were attributed to the decades within the period 2001-2030 and then combined with the corresponding climate data from the REMO model (see Section 2.1, Fig. 7.34). For each combined scenario, the decades had to be calculated separately, but will be visualised in one diagram. The results of the three ensemble runs for each scenario are averaged.

The scenario results for the Upper Ouémé catchment for the period 2001 to 2030 unite the effects of reduced water and sediment yields resulting from climate change with increased surface runoff and sediment yield caused by land use change. For comparison with the separate land use and climate change scenarios, Table 7.26 considers only the period 2001-2025.

Table 7.26 Mean simulated annual values of sediment yield (SY), water yield (WY), and surface runoff (Q_{surf}) of the combined land use and climate change scenarios in the Upper Ouémé catchment. The results are averages of three ensemble runs for each climate scenario. Absolute values and change in % from the baseline scenario Lu00 (1998-2005) are shown.

	2001-2025	A1B			B1			A1B			B1		
		SY [t/ha/yr]	WY [mm/yr]	Q_{surf} [mm/yr]	SY [t/ha/yr]	WY [mm/yr]	Q_{surf} [mm/yr]	SY [Δ%]	WY [Δ%]	Q_{surf} [Δ%]	SY [Δ%]	WY [Δ%]	Q_{surf} [Δ%]
Upper Ouémé	L1	0.19	193	103	0.21	207	108	-2	-11	-4	+7	-4	+1
	L2	0.24	196	108	0.26	210	114	+21	-10	+1	+31	-3	+6
	L3	0.21	194	105	0.23	208	111	+8	-10	-2	+18	-4	+4

Because of the greater reduction in rainfall, climate scenario A1B combined with land use scenarios L1 to L3 shows a greater reduction in water yield (-10%) than scenario B1 combined with L1 to L3 (WY -4%). For climate scenario B1 combined with land use scenarios L1 to L3, surface runoff increases by 1 to 6%. Thus, decreases in surface runoff due to climate change are overcompensated for by increases due to land use change. For the A1B scenarios, the trend varies. Surface runoff increases slightly for A1B_L2 while it decreases by 2 to 4% for the other scenarios. Sediment yields are heavily influenced by both land use and climate changes. Compared to the Lu00 model, sediment yields increase for all scenarios except for A1B_L1 (Table 7.26). As a consequence of the smaller reduction in water yield, the increase in sediment yield is greater for B1 scenarios than for the A1B scenarios. For B1 combined with L1 to L3, sediment yield differs by +7 to +31%, while for A1B combined with L1 to L3 it varies by -2 to +21% compared to the reference period 1998-2005. As in the pure land use scenarios (see Subsection 7.2.2), the

L2 scenarios lead to the highest increases in sediment yield. In most scenarios, increases in sediment yield due to land use change, mainly the expansion of cropland area, exceed the reductions in sediment yield resulting from climate change.

The diagrams in Fig. 7.56 show the results for the Upper Ouémé catchment for 2001 to 2030 in semi-decades, including linear trends and the variation between the

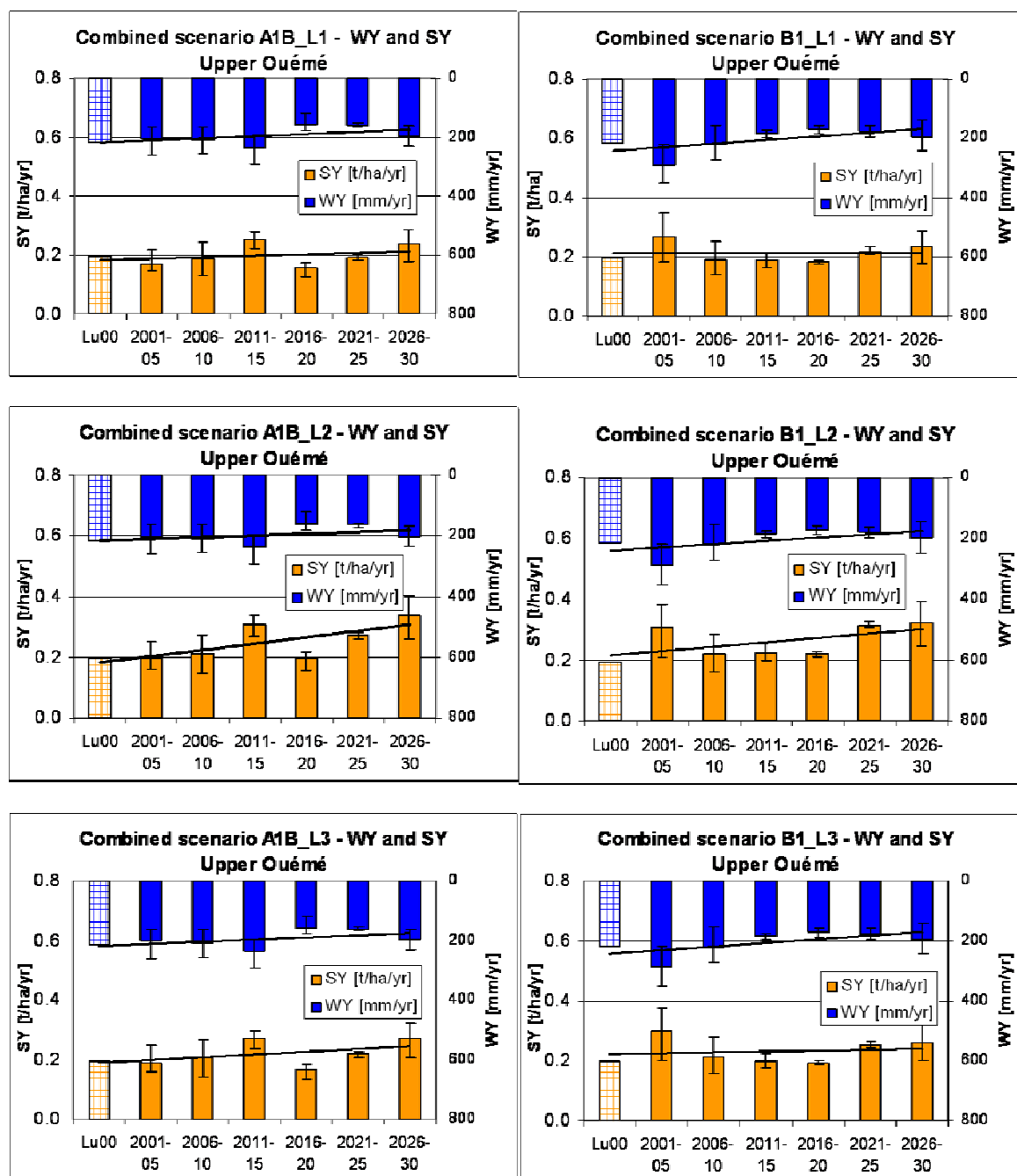


Fig. 7.56 Mean simulated annual values of sediment yield (SY), and water yield (WY) for combinations of land use scenarios L1, L2, and L3 with climate change scenarios A1B and B1 for the period 2001 to 2030. The presented results are averages of three ensemble runs for each climate scenario.

ensemble runs (bars). As already mentioned, the water and sediment yields show opposite trends. However, for scenarios A1B_L1 and B1_L1 no clear trend for the sediment yield was observed. In general, climate variability between the semi-decades can be very high and mask the effects of land use change on sediment yield. For example, the large differences in water and sediment yields for the second decade of the A1B scenarios and the first decade of the B1 scenarios are caused mainly by large differences in rainfall, while land use remained constant. Potential evapotranspiration differed only slightly in these two periods.

Likewise, for the pure climate scenarios (see Subsection 7.2.3), the variation between the ensemble runs for the B1 scenarios is greater than for the A1B scenarios. Standard deviations of the mean values for the ensemble runs for the semi-decades vary between 0.6 and 9%.

From the maps in Fig. 7.57, the spatial pattern of the sediment yield appears similar to the one for the pure land use scenarios (see Subsection 7.2.2, Fig. 7.40). Compared to the Lu00 model (1998-2005), sediment yield increases for all scenarios

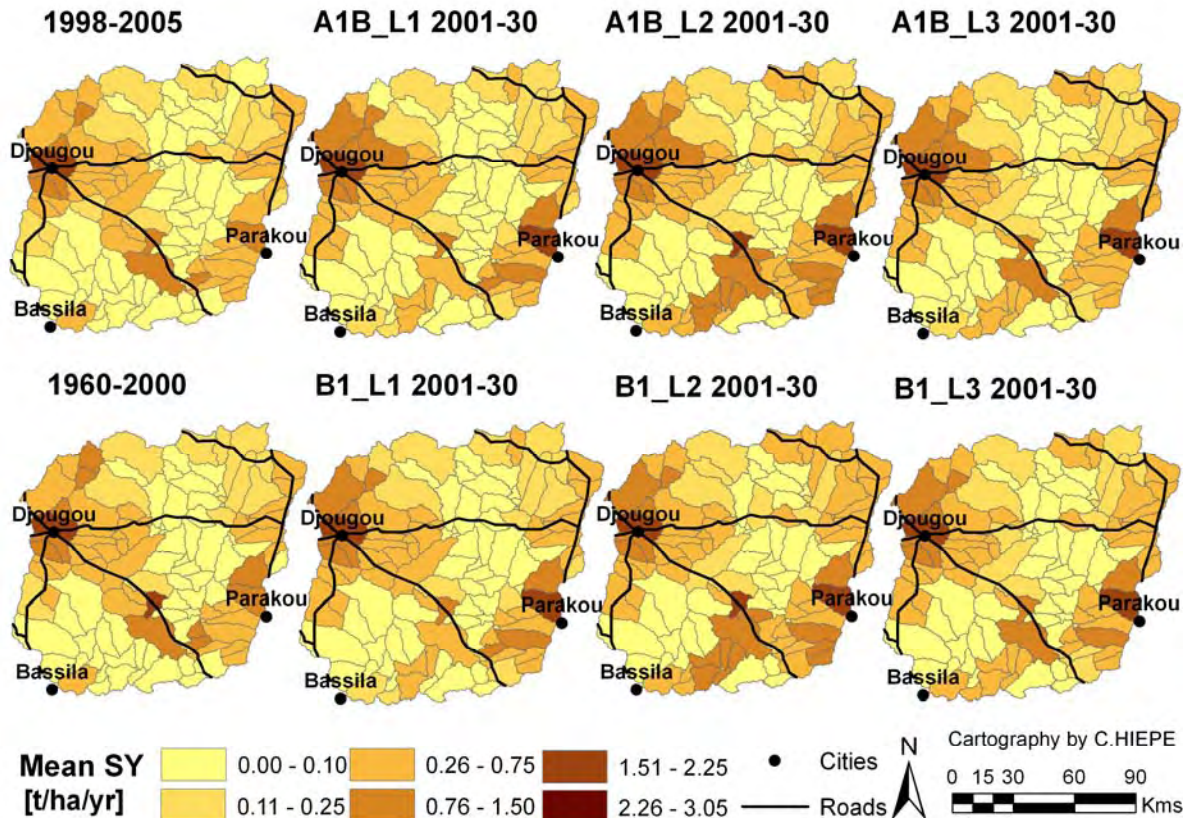


Fig. 7.57 Mean spatial distribution of sediment yield for the combinations of climate scenarios A1B and B1 with land use scenarios L1-L3 for the period 2001-2030 compared to Lu00 model (1998-2005) and the model with REMO climate data for 1960-2000.

in the regions around Djougou and Parakou as well as in the southern and north-eastern part of the catchment. The very low sediment yields in the central part of the catchment are slightly reduced due to shifts between the observed and modelled savannah and forest vegetation resulting from the pre-processing of the land use maps.

For direct comparison, Fig. 7.57 uses the same legend as Fig. 7.40 in Subsection 7.2.2 for the land use scenarios. The maximum sediment yield per subbasin for the combined scenarios is only 1.91 t/ha/yr, compared with the maximum of 3.05 t/ha/yr for the pure land use scenarios. Upward shifts in the six sediment yield classes are, for example, visible in the southern part of the catchment, in particular for the A1B_L2 and B1_L2 scenarios. Visible changes in the Djougou region occur mainly among the A1B and B1 scenarios independent of the chosen land use scenario.

The strongest absolute increases of sediment yield occur in the Parakou region and in the South of the catchment. In the Djougou region, the strong absolute increases in surface runoff and sediment yield resulting from land use change are weakened due to reductions in water yield resulting from climate change (Figs. 7.57 and 7.58 and Fig. B.8, Appendix B). In relative terms, the largest increases in sediment yield are obtained in the southern and south-western parts of the catchment. If the REMO model 1960-2000 is taken as a reference, the changes in the spatial patterns remain similar. However, the relative increases in sediment yield are then slightly lower around Djougou and Parakou, as well as in the southern part of the catchment, and slightly higher in some subbasins in the North-East of the catchment.

Compared to 1998-2005, surface runoff increases strongly in the south-western part of the catchment, in particular for the B1 scenarios (Fig. 7.58). Compared to 1960-2000, the increase in surface runoff in the South-West is less obvious. For scenarios A1B_L2 and B1_L2, surface runoff increased significantly in the South of the catchment independent of the chosen reference.

In the following, the results for the Terou-Igbomakoro and Donga-Pont subcatchments are discussed (Table 7.27). In the Terou-Igbomakoro subcatchment, water and sediment yields, as well as surface runoff, increase for all scenarios compared to the reference period (1998-2005). The increases range from 2 to 13% for water yield, 14 to 32% for surface runoff, and 7 to 40% for sediment yield.

Although both climate and land use changes trigger the variation in sediment yield among the scenarios, the effects of land use change are dominant.

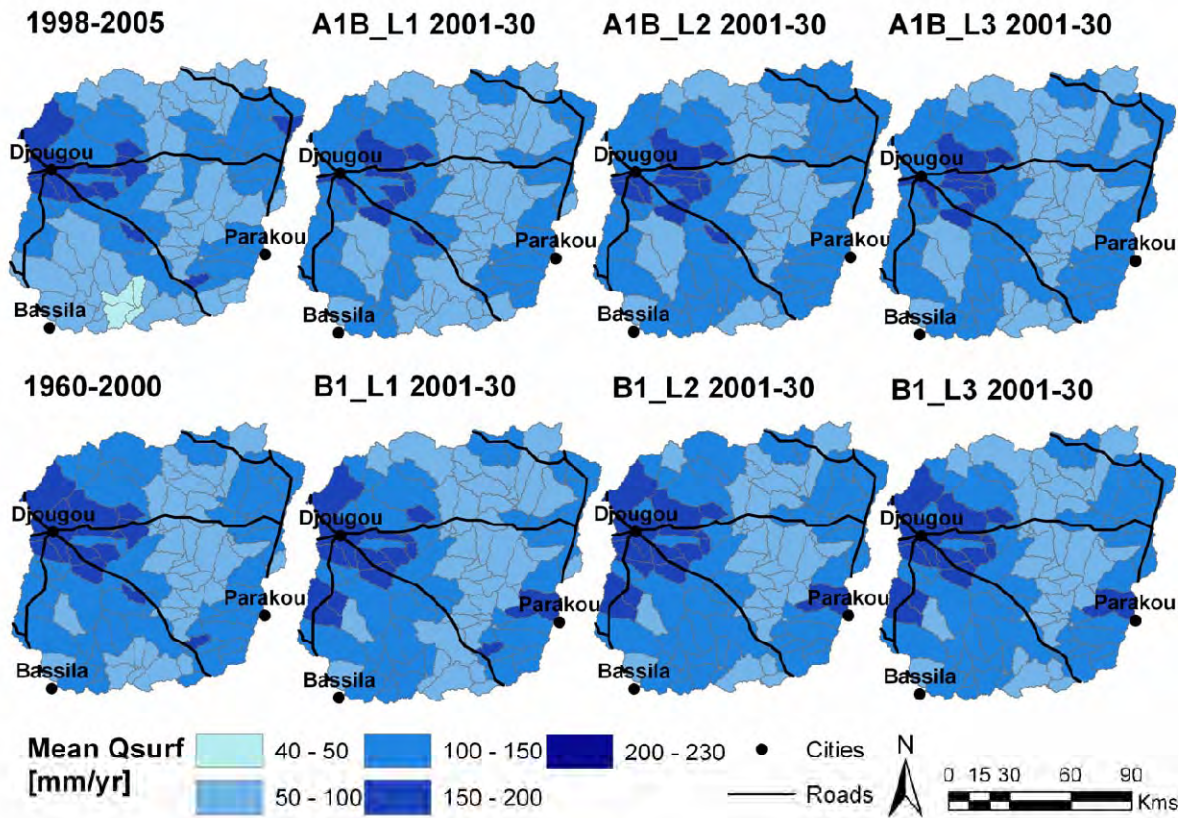


Fig. 7.58 Mean spatial distribution of surface runoff for the combinations of climate scenarios A1B and B1 with land use scenarios L1-L3 for the period 2001-2030 compared to the Lu00 model (1998-2005) and the model with REMO climate data for 1960-2000.

In contrast, changes in water and sediment yields in the Donga-Pont subcatchment result mainly from changes in climate variables leading to reductions in water yield and surface runoff. Since the Donga-Pont subcatchment is already extensively used for agriculture, the expansion of cropland is limited. Therefore, the variation between the land use scenarios L1 to L3 is rather small. For the A1B scenarios, mean water yields decrease by 19%, mean surface runoff by 11%, and sediment yields by 4 to 5% compared to 1998-2005. For the B1 scenarios, mean water yields decrease by 13% and surface runoff by 7%, while sediment yield increases by 5 to 6%. The opposite trends for mean surface runoff and sediment yield for the B1 scenarios result from temporal variations between and within the ensemble runs.

Figure 7.59 shows the water and sediment yields by semi-decade for the two subcatchments, including linear trends for the period 2001 to 2030 for the combinations of land use scenario L3 (“Business as usual”) with climate scenarios A1B and B1. The diagrams for all other combined scenarios can be found in

Appendix B (Figs. B.6, B.7). For the Terou-Igbomakoro subcatchment, an increasing trend in sediment yield is confirmed for all scenarios, while the trend in water yields is less clear. Although the mean water yield for 2001-2025 exceeds the value for 1998-2005 by 2 to 13% (Table 7.27), visualisation of the data indicates a negative trend within this period for the B1 scenarios.

Table 7.27 Mean simulated annual values of sediment yield (SY), water yield (WY), and surface runoff (Q_{surf}) of combined land use and climate change scenarios in the Terou-Igbomakoro and Donga-Pont subcatchments. The results are averages of the three ensemble runs for each climate scenario. Absolute values and change in % from baseline scenario Lu00 (1998-2005) are presented.

	2001-2025	A1B			B1			A1B			B1		
		SY [t/ha/yr]	WY [mm/yr]	Q_{surf} [mm/yr]	SY [t/ha/yr]	WY [mm/yr]	Q_{surf} [mm/yr]	SY [t/ha/yr]	WY [mm/yr]	Q_{surf} [mm/yr]	SY [t/ha/yr]	WY [mm/yr]	Q_{surf} [mm/yr]
Terou-Igbo.	L1	0.13	215	107	0.15	236	118	+7	+2	+14	+20	+12	+25
	L2	0.15	217	113	0.17	238	124	+25	+3	+20	+40	+13	+32
	L3	0.14	216	111	0.16	237	121	+16	+2	+18	+30	+12	+29
Donga-Pont	L1	0.68	229	143	0.76	246	150	-5	-19	-11	+5	-13	-7
	L2	0.69	230	144	0.76	247	151	-4	-19	-11	+6	-13	-7
	L3	0.68	229	144	0.76	247	150	-5	-19	-11	+5	-13	-7

For the Donga-Pont subcatchment, a negative trend in water yield is confirmed for all scenarios. The trend for the sediment yield is less clear, in particular for the

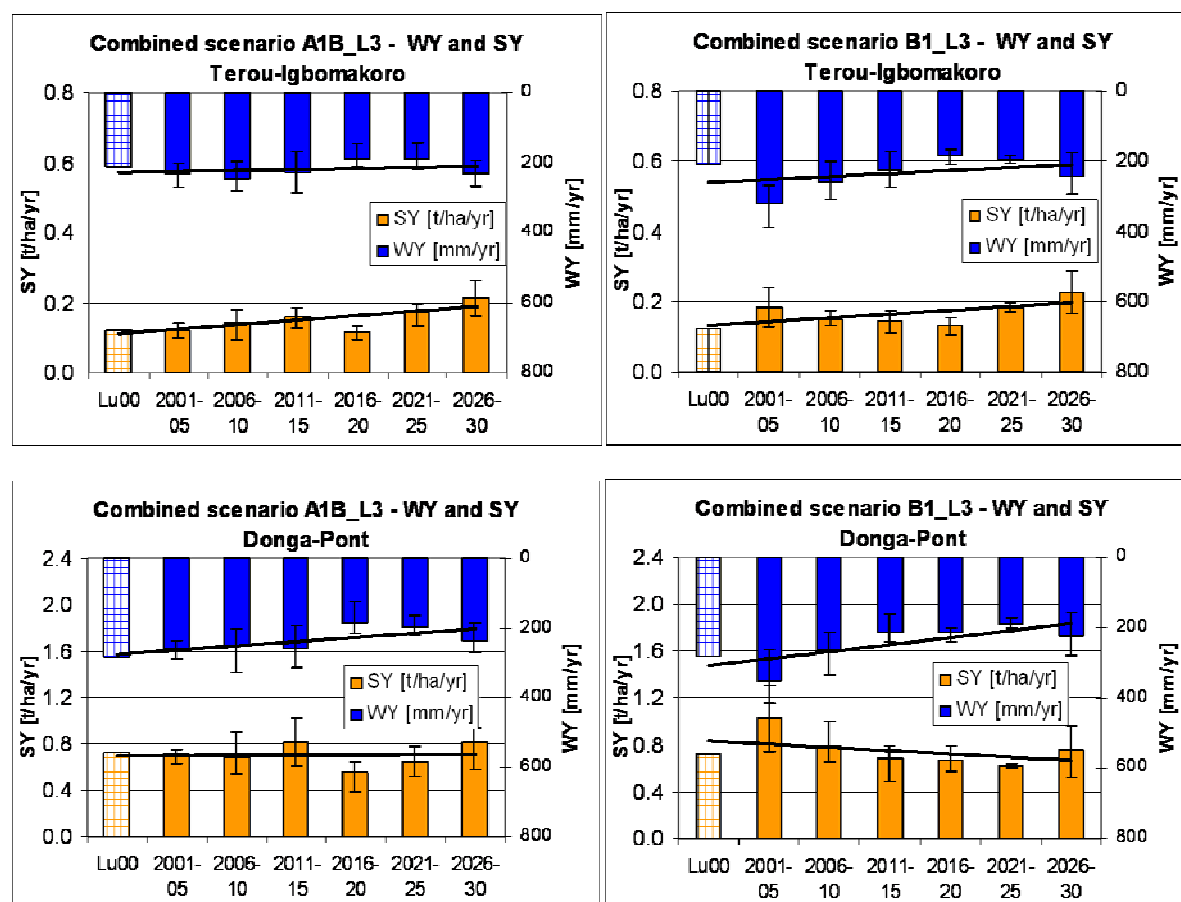


Fig. 7.59 Mean simulated annual values of sediment yield (SY), and water yield (WY) for the combination of land use scenario L3 with the climate change scenarios for the period 2001 to 2030 for the Terou-Igbomakoro and Donga-Pont subcatchments. The presented results are averages of three ensemble runs for each climate scenario.

A1B scenarios. Although the sediment yield for 2001-2025 for the B1 scenarios exceeds the value for 1998-2005 by 5-6% (Tab 7.27), the trend by semi-decade is negative and is closely related to the negative trend in water yield.

Net diagrams show the relative changes of the main components of the water balance (Fig. 7.60). For the Terou-Igbomakoro subcatchment, changes in rainfall, evapotranspiration, and percolation differ less than 4% from the values for 1998-2005. The increase in water yield corresponds to a strong increase in surface runoff (up to 32%) for all scenarios. For the Terou-Igbomakoro subcatchment, changes in rainfall, evapotranspiration, and percolation differ less than 4% from the values for 1998-2005. The increase in water yield corresponds to a strong increase in surface runoff (up to 32%) for all scenarios. Baseflow differs by only +1% to -6% depending on the scenario. Soil water increases significantly. Compared to 1960-2000, the pattern looks different: Soil water increases only slightly and water yield, surface runoff, and baseflow decrease for all scenarios. Sediment yields change by -15 to +15% depending on the scenario.

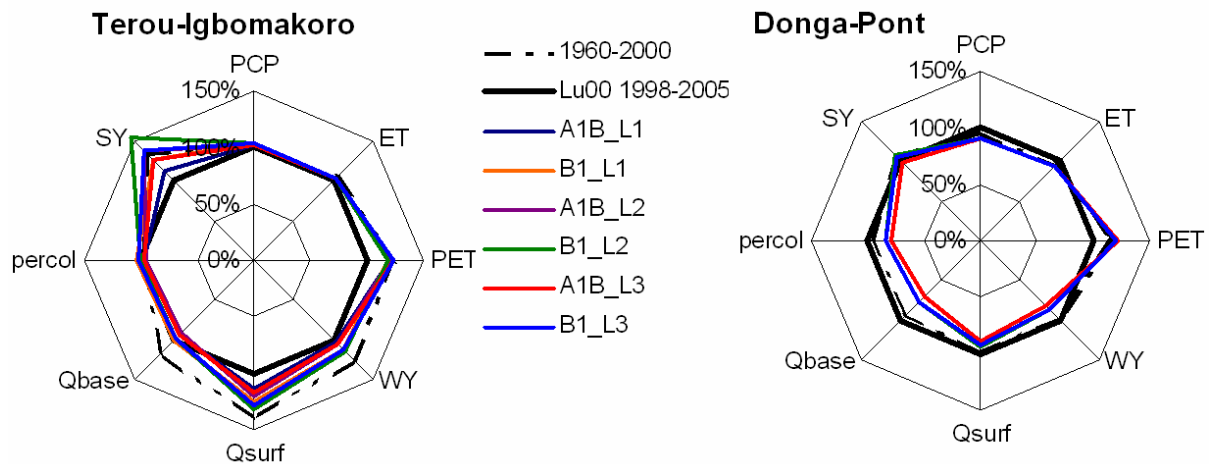


Fig. 7.60 Components of the water balance in the Terou-Igbomakoro and Donga-Pont subcatchments for the combined scenarios relative to the Lu00 model (1998-2005).

For the Donga-Pont subcatchment, the net diagram is similar to the one from the pure climate scenarios (Fig. 7.53). However, reductions in surface runoff and sediment yield are less drastic and sediment yield even increases slightly for the B1 scenarios. As discussed for the pure climate scenarios, baseflow and percolation are strongly reduced while percolation increases greatly compared to the period 1998-2005. These trends are much less drastic if 1960-2000 is taken as a reference. For the Upper Ouémé catchment (Fig. 7.61), the effects of the two subcatchments are combined. Sediment yield and soil water increase strongly for all scenarios, while

percolation and baseflow are strongly reduced. Although total water flow decreases

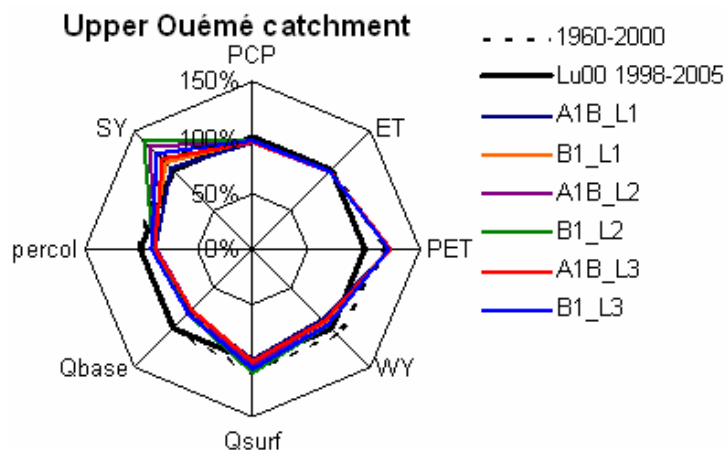


Fig. 7.61 Components of the water balance in the Upper Ouémé catchment relative to the Lu00 model (1998-2005).

for all scenarios, surface runoff increases slightly for most scenarios. Evapotranspiration remains nearly constant.

The monthly distributions of water and sediment yields for the combined scenarios are similar to those of the pure climate scenarios, reflecting the shifts in the monthly rainfall

distribution. A presentation of the monthly distributions as differences from the values for the original model (Fig. 7.62) makes the changes more visible.

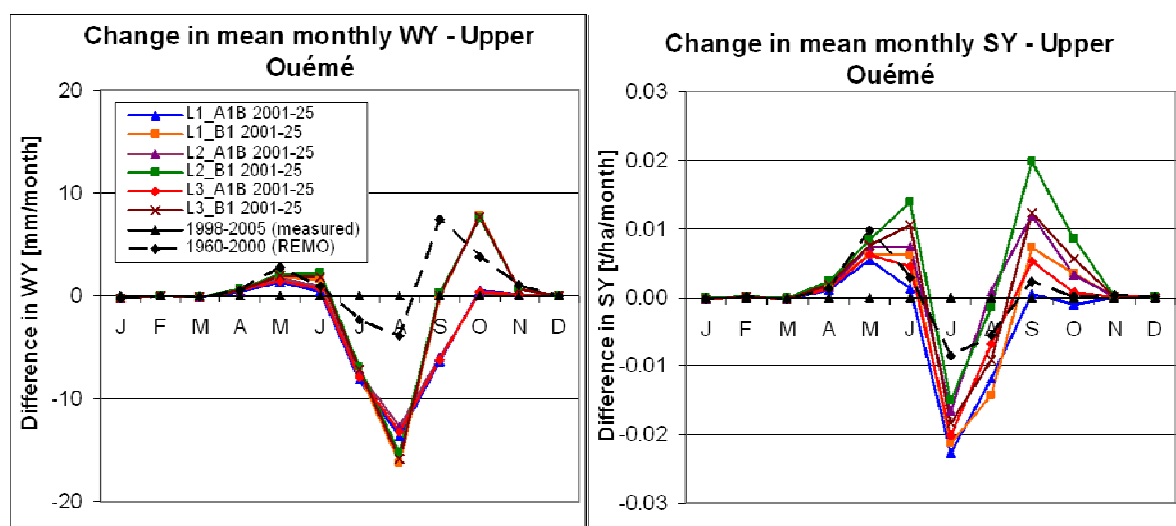


Fig. 7.62 Deviation of mean monthly water and sediment yields for the combined scenarios for the periods 2001-2025 and 1960-2000 (REMO climate data) from the results for 1998-2005 (measured climate data).

While monthly water yields are significantly reduced by up to 13 to 16 mm (20 to 25%) in the middle of the rainy season compared to the original model (1998-2005), values in April to June and October/November are up to 2 mm and 8 mm higher, respectively. While the water yields for all combined scenarios lie in a narrow range from January to August, differences among the scenarios are more pronounced in September/October, with much higher water yields for the B1 scenarios than for the A1B scenarios. Variations among the scenarios for the sediment yield are higher but the temporal pattern of the deviations is similar to that for the water yield, with two positive peaks at the beginning and end of the rainy season and a larger negative

peak in the middle of the rainy season. The largest differences at the beginning and end of the rainy season are simulated for scenario L2_B1 with +0.014 t/ha (+65%) in June and +0.020 t/ha (+37%) in September. The largest monthly decrease in sediment yield shows scenario L1_A1B with -0.023 t/ha, corresponding to -44%.

In conclusion, all combined scenarios show a reduction in mean water yield in the Upper Ouémé catchment compared to the period 1998-2005. Mean surface runoff showed a slightly positive trend for the B1 scenarios and slightly positive and negative trends for the A1B scenarios. Baseflow and percolation were strongly reduced. Mean sediment yield increased significantly (7-31%) for all scenarios except for scenario A1B_L1. Thus, in general the increases in sediment yield due to land use change exceeded the reductions in sediment yield resulting from climate change. Mean sediment yield increased above all in the regions around Djougou and Parakou, as well as in the southern and the north-eastern part of the catchment. The greatest absolute increases of sediment yield occurred in the Parakou region and in the South, while the greatest relative increases were in the south and south-western parts of the catchment. For the Terou-Igbomakoro subcatchment, the results were mainly triggered by changes in land use leading to positive trends in surface runoff and sediment yield for all scenarios. Baseflow and percolation changed only slightly. For the Donga-Pont subcatchment, changes in climate were dominant, causing negative trends for water yield and surface runoff. Furthermore, percolation and baseflow were strongly reduced in the Donga-Pont subcatchment. Mean sediment yields in this subcatchment decreased or increased slightly, depending on the scenario. Monthly water yields in the Upper Ouémé catchment were reduced over the June to September period and increased in May and October without significant differences between the scenarios. Mean monthly sediment yields increased over the whole rainy season except for a significant decrease in August. While monthly sediment yields for the reference scenario and A1B scenarios peaked in August, the maximum for the B1 scenarios was reached in September.

7.2.5. Scenario analysis - Conclusions

In the following, the effects of the land use, climate change, and combined scenarios for the Upper Ouémé catchment and the Terou-Igbomakoro and Donga-Pont subcatchments will be summarized and compared to the results of similar studies.

The pure land use scenarios for 2001-2025 increase sediment yield and surface runoff significantly in the Upper Ouémé catchment and the two subcatchments for all scenarios L1 to L3 (see 1st block in Table 7.28). In contrast, the climate scenarios and combined scenarios lead to a more differentiated picture between the scenarios and catchments (see 2nd and 3rd block in Table 7.28).

The climate scenarios reduce water yield and sediment yields in the Upper Ouémé catchment due to decreases in rainfall. Potential evapotranspiration increases significantly due to higher temperatures, but actual evapotranspiration remains nearly constant. Surface runoff decreases for the A1B scenarios and remains nearly constant for the B1 scenarios.

In the combined scenarios, the negative trend for water yield due to climate change is weakened due to land use change, but remains dominant. In contrast, sediment yields increase for all combined scenarios except for L1_A1B, showing the dominance of land use change for this variable. Surface runoff decreases slightly for the A1B_L1 to L3 scenarios but increases for the B1_L1 to L3 scenarios.

Table 7.28 Comparison of effects of land use, climate, and combined scenarios on rainfall (PCP), water yield (WY), sediment yield (SY), and surface runoff (Q_{surf}) in the Upper Ouémé catchment and the Terou-Igbomakoro and Donga-Pont subcatchments for the period 2001-2025 compared to the original model.

		Orig			A1B				B1			
		SY [Δ%]	WY [Δ%]	Q_{surf} [Δ%]	PCP [%]	SY [Δ%]	WY [Δ%]	Q_{surf} [Δ%]	PCP [%]	SY [Δ%]	WY [Δ%]	Q_{surf} [Δ%]
Upper Ouémé	Orig	/	/	/	-	---	---	--	-	-	--	0
	L1	++++	+	++	-	-	---	-	-	++	-	0
	L2	++++	+	+++	-	++++	--	0	-	++++	-	++
	L3	++++	+	++	-	++	---	-	-	+++	-	+
Terou-Igbo.	Orig	/	/	/	+	-	0	+	+	++	++	+++
	L1	+++	+	++	+	++	+	+++	+	+++	++	++++
	L2	++++	+	+++	+	++++	+	+++	+	++++	++	++++
	L3	++++	+	+++	+	+++	+	+++	+	++++	++	++++
Donga-Pont	Orig	/	/	/	--	----	----	---	--	---	---	---
	L1	++++	0	++	--	-	---	---	-	+	--	--
	L2	++++	+	+++	--	-	---	---	-	++	--	--
	L3	+++	0	++	--	-	---	---	-	+	--	--

Legend + 1 to 5% ++ 5 to 10% +++ 10 to 20% ++++ > 20%
 0 < +/- 1% - -1 to -5% -- -5 to -10% --- -10 to -20% ---- >-20%

The intensively used and comparably wet Donga-Pont subcatchment (39% cropland) and the less intensively used Terou-Igbomakoro subcatchment (11% cropland) behave differently and cover the wide range of possible responses within the Upper Ouémé catchment (14% cropland). While surface runoff and water yields in the Donga-Pont subcatchment decrease strongly for all climatic and combined scenarios,

both parameters increase strongly in the Terou-Igbomakoro subcatchment. Likewise, for most scenarios sediment yields decline in the Donga-Pont subcatchment and increase in the Terou-Igbomakoro subcatchment. However, for the B1_L1 to L3 scenarios sediment yield also increases in the Donga-Pont subcatchment. This results from the high variation in rainfall trends between the ensemble runs.

A comparison of the results with the scenario analysis performed by Busche (2005) based on the parameterised SWAT model from Sintondji (2005) for the Terou-Igbomakoro subcatchment is not directly possible due to differences in model parameterisation and input data for model calibration and scenario analysis. However, simulated relative increases in surface runoff and sediment yield for the land use scenario (Business as usual) were very similar. In contrast, the climate scenarios from Busche (2005) based on 5 year time slices of REMO for the B2 scenario and the combined scenarios indicated opposite effects on surface runoff, water and sediment yield than those simulated in this work. This is mainly due to the different rainfall signal given by the more recent, time-continuous REMO simulations. The scenario analysis for the Upper Ouémé catchment indicates increasing sediment yields and decreasing water yields for the period 2001-2025 over a wide range of scenarios. Trends in surface runoff depend strongly on the chosen scenario. However, the variability within the Upper Ouémé catchment is large. In subbasins with a high potential of cropland expansion (e.g., Terou-Igbomakoro subcatchment), future sediment yields will be driven by land use changes and may therefore strongly increase. In subbasins with low potential of cropland expansion and strong reductions in rainfall (e.g., Djougou region including Donga-Pont subcatchment), future sediment yields may strongly decrease. While agricultural expansion in the entire Upper Ouémé catchment will probably slow down in the next decades, climate change impacts will increase with time. The simulated climate scenarios until 2050 show that the effects on water and sediment yields cannot simply be extrapolated and that, after 2025, differences between climate scenarios will increase.

In general, the spatial patterns of sediment yield and surface runoff for the “business as usual” scenario remain similar (Fig. 7.63, Fig. B.10 in Appendix B). In addition to the current hotspots of soil erosion in the Djougou and Parakou regions, as well as along the main roads Djougou-Beterou-Parakou, new hotspots arise in the southern and north-eastern parts of the catchment.

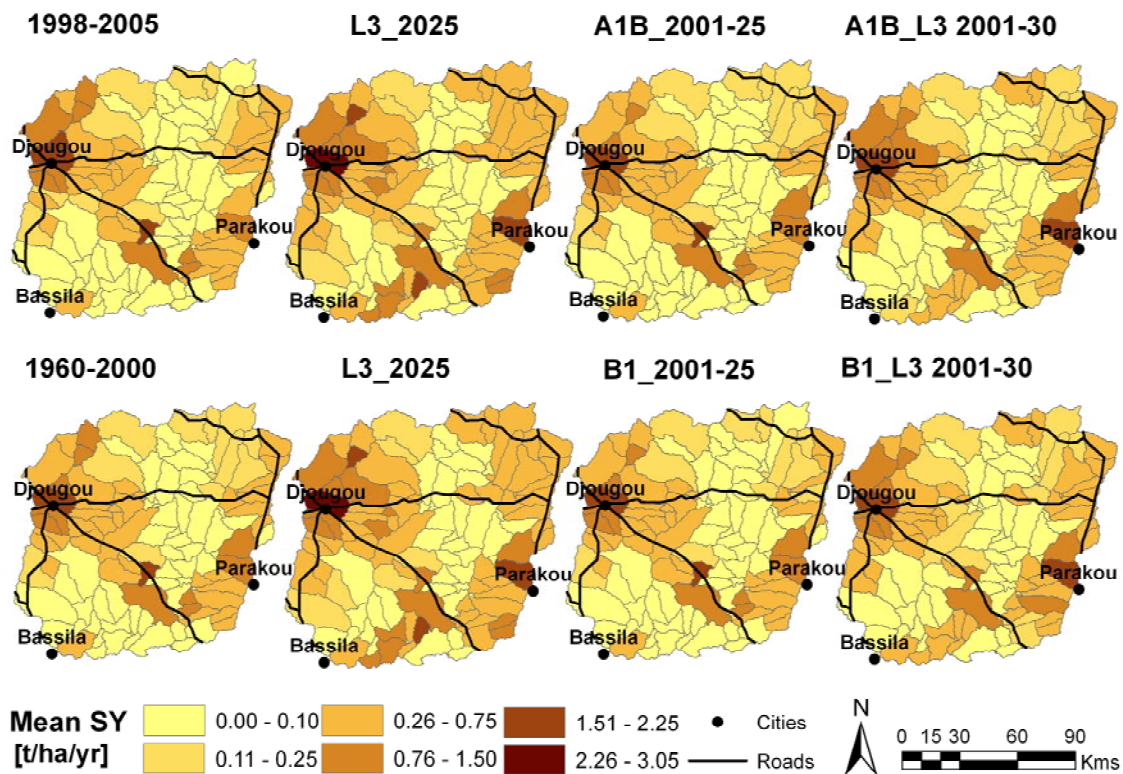


Fig. 7.63 Mean spatial distribution of sediment yield for the land use, climate, and combined scenarios compared to the Lu00 model (1998-2005) and the model with REMO climate data for 1960-2000.

8. UNCERTAINTIES IN THE MODELLING PROCESS

The presented research results are subject to various kinds of uncertainties. In this chapter, the most important sources of uncertainty in the modelling process are discussed and evaluated. Uncertainties can be associated with model input data, model structure, calibration parameters and data used for model calibration and validation.

8.1. Uncertainties in the model input data

Relief

The resolution of approximately 90 meters of the digital elevation model (DEM) is rather low. However, considering the flat topography, the large size of the catchment and the coarse resolution of the other input maps, this resolution seems to be adequate. Since SWAT is not a raster-based but a semi-distributed model, the uncertainties in relief can be considered low. Nevertheless, a DEM with a higher resolution would improve the delineation of the river network and the subcatchments.

Land use

Land use classifications in the sub-humid tropics are a challenge due to high interannual vegetation dynamics, small field sizes, the heterogeneous landscape and strong atmospheric interferences (Thamm et al. 2005). However, the land use map for the year 2000 is of high quality, as it was extensively validated in the field. The agreement of the ground data and the classified data was 80.3% (Judex 2008). However, the central part and some other areas of the Upper Ouémé catchment are difficult to reach for field validation. Furthermore, the small inland valleys and gallery forests cannot be distinguished accurately from grass savannah and dense forests (*forêt dense*), respectively.

Another constraint concerning the land use data was the limited adjustment of the parameters in the SWAT land use database to the conditions in Benin. Only the plant height, the maximum leaf area index and the parameters determining the length of the growing period were modified using measured data for the Upper Ouémé catchment from Orthmann (2005), Mulindabigwi (2006) and Dagbenonbakin (2005).

However, despite too high biomass values, the dynamics of biomass and leaf area index were correctly represented. In general, discharge and sediment yield showed a low sensitivity to changes in plant parameters during the calibration process (see sensitivity analysis in Section 8.2).

Modelling future land use and land cover is difficult, particularly in developing countries where geospatial data is scarce. The land use maps used for the years 2001-2025 from the model CLUE-S are unusual for Africa and are built on comparatively good databases provided by IMPETUS and its partners for the Upper Ouémé catchment. The CLUE-S model represents the land use dynamics in the period 1991-2000 well (Judex 2008). The agreement between the simulated land use map and the land use classification from the Landsat scene for 2000 was 86% (Judex 2008). Nevertheless, the scenario maps contain significant uncertainties due to the coarse representation of the driving forces and simplified assumptions concerning the demand for agricultural land without using economic and agricultural production models. Intervention scenarios with CLUE-S showed that the construction of additional roads would significantly change the simulated pattern of cropland expansion.

Another important source of uncertainty was the disaggregation of the CLUE-S land use maps for SWAT. As discussed in Subsection 7.2.1, this can lead to significant changes in the land use distribution. However, in the land use maps for 2005, 2015 and 2025, the deviations are acceptable. In general, the disaggregation scheme tends to underestimate the total fraction of cropland. This is because the scheme assumes constant percentages for the land use distribution in each 250 meter grid cell as derived for the year 2000 for the whole catchment. As the catchment is characterized by cropland expansion, the actual fraction of cropland in a 250 meter grid cell "Cropland >20%" will probably not remain constant but increase during the period 2001-2025. Furthermore, the disaggregation scheme was homogeneously applied to the whole Upper Ouémé catchment without considering heterogeneities in land use intensity. A derivation and application of specific disaggregation schemes for intensively used areas, protected forests and the rest of the catchment might be more appropriate. However, the underestimation of cropland in the intensively used areas and the overestimation in the protected forest are partially compensated by applying a minimum threshold of 10% in HRU definition in SWAT.

All other uncertainties concerning land use scenarios are of minor importance. They concern, among other things, projections of population growth. The projections at the department level had to be disaggregated to the commune and village levels, leading to an underestimation of population growth in the Upper Ouémé catchment (Judex 2008).

Soil data

Uncertainties in soil data are related to the low resolution of the soil map, the determination of representative profiles and the analysis of soil samples.

The soil map was elaborated by ORSTOM at the scale 1:200.000. The polygon size ranges from 0.1 to 833 km² with an average of 32 km². The soil map only shows the dominant soil types. Therefore, the high variability of tropical soils along the toposequences (see Section 6.1) cannot be incorporated. As a consequence, the fraction of hydromorphic and indurated soils in the catchment is underestimated. Since these soil types favour surface runoff, sediment yield is underestimated.

Each representative profile was chosen after studying one transect along the toposequence and consulting the descriptions in the explanatory notes of the soil maps. One soil sample was taken from each horizon. However, the significant small scale variability of chemical and physical properties was only partially captured. As a consequence, there are high uncertainties in the chemical soil properties of nitrogen content, CEC_{pot}, BS and cations. Mixed samples from larger plots would probably reduce these uncertainties, but since these properties were not used as model parameters, this study focused rather on complete, consistent descriptions of individual representative profiles.

Recently, Igué (2007) completed a soil map for the Upper Ouémé catchment based on the SOTER approach (see Section 5.5). In the SOTER map, a set of 1 to 6 soil profiles corresponds to each spatial terrain unit representing the soil variability along the toposequence. Each terrain unit was determined exclusively from the physiographic landform, the slope class and the relief intensity, not taking into account the geology. Consequently, the average size of the 31 polygons in the SOTER soil map is even larger than in the French soil map. On the other hand, non-spatial information about the fraction of different soil types within the units is provided. It would be interesting to determine if this SOTER map can improve the modelling results of this study. In order to do that, the soil units would have to be

randomly distributed in the terrain units, because SWAT only includes a splitting routine for land use maps. In addition, using the SOTER map would probably require a new calibration of the SWAT model.

The error ranges during laboratory analysis of the soil samples should be in the usual range of no more than 5 to 10%. The determination of soil texture was complicated by high clay, mica and iron contents in the soils. Especially for red, ferralitic soil probes, the measured clay content can vary enormously for different intensities of pre-treatment due to a lack of dispersion of clay minerals (Wiechmann 1991). During CEC_{pot} determination, photometric measurements of the re-exchange (Ammonium Acetate method) and measurements of barium using an atom absorption spectrometer (Mehlich method) required special attention. A further potential source of error was the determination of the physical soil parameters in conjunction with a multiple linear regression for the bulk density and a pedotransfer function (PTF) for the saturated hydraulic conductivity (K_{sat}) and the available water capacity of the soil (SoI_{awc}). The applied PTF did not account for high gravel contents and macropores, which can heavily influence K_{sat} in the catchment (Giertz 2004). Nevertheless, a correction factor for the gravel content was not applied because the estimated K_{sat} values in the subsoil were already low compared to measurements from Giertz (2004). A correction factor would have further reduced the K_{sat} values. In order to avoid water-logging in many profiles, all K_{sat} values smaller than 5 mm/hr were set to 5 mm/hr. Giertz (2004) obtained good agreement of total discharge and discharge components between the topsoil parameterisation with the K_{sat} value from the PTF from Rawls & Brakensiek (1995) and the parameterisation with the mean K_{sat} value from in-situ measurements in the Aguima subcatchment. Tietje & Hennings (1996) found in a comparison of six pedotransfer functions with K_{sat} measurements in Northern Germany that the PTF from Brakensiek underestimated K_{sat} for silt and clay soils. All PTFs performed best for loamy sands in their study.

Climate data

The climate data for the period 1998-2005 were taken from the IMPETUS climate station Dogué savannah and the synoptic station Parakou. Giertz (2004) concluded after comparing three IMPETUS climate stations near Dogué that the uncertainties for the climate parameters of humidity, air temperature, wind velocity and solar radiation are fairly low in this area. However, transferring the parameter values to the

whole Upper Ouémé catchment produces uncertainties. Furthermore, for the years 1998-2000, solar radiation had to be estimated from sunshine duration.

One general problem is the high variability of rainfall in the sub-humid zone, which is only poorly captured by a meteorological network. The implementation of 14, regularly distributed, pluviometric stations in the model is satisfactory. Additional stations have been used to fill gaps. In particular, in the period 1998-2000, gaps of several weeks were frequent for the stations Pelebina, Sonomoun, Tebou, Wewe and Saramanga. Some missing discharge peaks in the model results can probably be attributed to rainfall events not captured in the pluviometric data (e.g., on 14.08.2004 at Terou-Igbomakoro outlet). The results for the two different discretisations (see Subsection 7.1.4) confirm that an additional pluviometric station can significantly increase performance measures and matching of discharge peaks. Bormann & Diekkrüger (2003) and Sintondji (2005) also obtained improved measures of performance for the Terou-Igbomakoro subcatchment when they increased the number of pluviometric stations considered in the model.

Earlier scenario studies in the Terou-Igbomakoro subcatchment (Busche, 2005; Sintondji, 2005) had to build on REMO simulations for 5-year time slices in the period 2001-2025 for the SRES scenario B2. The availability of continuous REMO simulations for this study significantly reduced uncertainties in the climate scenarios, and the ensemble runs allowed the influence of the initial conditions to be studied. The main uncertainties derived from the climate data for the period 2001-2050 for the climate change scenarios can be attributed to weaknesses of the regional climate model REMO and to the spatial resolution of the REMO data. As discussed in Subsection 7.2.1, standard post-processing with a statistical algorithm (MOS) was applied to the rainfall simulations. Afterwards, the simulated monthly rainfall distribution and the derived daily ET_{pot} agreed quite well with the measured data in the period 1960-2000. However, REMO rainfall data needed a second post-processing step in order to adequately represent the spatio-temporal distribution of daily rainfall. Therefore, the gridded rainfall data was attributed to historic frequency distributions at individual stations. The two post-processings, the second in particular, are a high source of uncertainty and led to a loss of information about future rainfall patterns.

Although REMO considers feedbacks between vegetation and the atmosphere, biosphere dynamics are yet poorly represented in climate modelling. The ensemble

runs reflect the uncertainties in the initial conditions of the climate model. It was shown in Section 7.2 that the simulated sediment and water yield can vary enormously between ensemble runs. Last but not least, the IPCC (2007) stated that global circulation models (GCMs) show quite different rainfall trends for West Africa. REMO follows the physical parameterisation of the GCM ECHAM4. Nesting REMO into another GCM, using another regional climate model (e.g., MM5) or using other SRES scenarios could have led to significantly different results with regard to future runoff and soil erosion in the Upper Ouémé catchment. This must be kept in mind when drawing conclusions from the model results and defining adaptation strategies.

8.2. Uncertainties in the model assumptions

The uncertainties in the model assumptions cover the model structure, the parameter uncertainty and uncertainties due to the spatial discretisation of the model affecting the representation of land use and soils. The largest weaknesses in the model structure occur in the calculation of ET_{pot} , the SCS curve number approach and the neglect of channel degradation. The uncertainties in the initial conditions were compensated for by including a three-year warm-up period in each model run. A spatio-temporal validation of the model beyond discharge and sediment yield would have been desirable in order to examine the correct representation of all relevant processes. However, at the regional scale, collecting such data was not feasible.

Correctly determining potential evapotranspiration is a general problem in most hydrological models. A comparison of the Priestley-Taylor and Penman-Monteith methods for calculating ET_{pot} with the SWAT model revealed differences of 15%. Even for the Penman-Monteith method, ET_{pot} can differ significantly depending on the chosen reference crop. SWAT uses alfalfa as reference crop in contrast to other models that use short green grass.

Despite its empirical nature, the SCS curve number approach seems to be appropriate for the regional scale where detailed spatio-temporal information about soil properties, rainfall variability and land use is missing (Arnold et al. 1998). If hourly rainfall data is available, the Green Ampt approach could be applied. However, using the Green Ampt approach instead of the SCS curve number approach does not

necessarily improve modelling results (e.g., King et al. 1999). Bormann & Diekkrüger (2003) and Sintondji (2005) also obtained good representations of discharge in the Terou-Igbomakoro subcatchment with the SCS-CN approach.

Moreover, the channel degradation routine of SWAT was not activated in this application due to a lack of information about erosion and sedimentation processes in the channel. As the rivers in the catchment are heavily affected by channel deposition and degradation, this simplification can contribute significantly to the uncertainty of the modelling results. Adjusting the SPCON factor, which determines the maximum amount of sediment that can be transported in the channel, could compensate for unrealistic assumptions regarding the channel morphology. However, site-specific knowledge about channel morphology and processes could improve the sediment modelling.

Several authors report limitations of the SWAT model. First, the model does not include an alteration of inherent soil properties due to soil erosion or agricultural management, which leads in the long-term to an underestimation of sediment loss in the Upper Ouémé catchment. Second, SWAT does not allow flows between hydrological response units (HRUs). Thus, the position of the land use types within a subbasin does not influence the water and sediment yields. Third, the interflow is not well represented (see Chapter 7). Fourth, the sediment routing is simplified and does not account for sediment size effects. Suspended sediment and bed load are not distinguished. Improvements of the sediment routines and the SCS curve number approach in SWAT are currently being developed (Gassman et al. 2007).

An additional source of uncertainty is the influence of spatial discretisation on the modelling results. Several authors have shown that the thresholds for the subbasin and HRU delineation can significantly influence sediment results (see Section 4.5). A comparison of two discretisation scenarios in this application confirmed this phenomenon for the Upper Ouémé catchment (see Subsection 7.1.4). However, the main improvement in model performance for the finer discretisation was attributed to one additional climate station; the land use distribution in the whole catchment was only slightly better represented. The range of slopes in the HRUs remained nearly constant. As all 14 climate stations are considered in the finer discretisation, a further increase in the number of subbasins will probably produce only minor improvements of the modelling results.

The land use distribution is modified by applying a minimum threshold in HRU delineation. For the original model, the chosen HRU thresholds of 10% for land use and soil enabled a good representation of the original fraction of agricultural land. However, the fractions of grass savannah and forest were underestimated, while tree and brush savannah increased. The implementation of a new land use map, i.e. each land use scenario, in SWAT required a new HRU delineation. Thus, the land use distribution of the disaggregated CLUE-S maps was modified by the HRU threshold. As mentioned before, this effect partially compensated for the underestimation of cropland due to the disaggregation scheme. In order to avoid the distorting effect of the HRU threshold, Jha et al. (2004) recommended defining only one HRU per subbasin. However, this approach would have required a significantly higher number of subbasins and therefore much longer computation time in order to adequately represent the future expansion of scattered field areas in the Upper Ouémé catchment. The new ArcSWAT interface can reduce this effort because it includes a splitting routine for land use which allows different thresholds to be defined for different land use types.

Sensitivity analysis

The LH-OAT (Latin Hypercube - One Factor at a Time) sensitivity analysis was performed for the whole Upper Ouémé catchment for the calibration period 1998-2001.

In a first step, the sensitivity analysis referred to the mean daily discharge and sediment yield without using measurements. Tables 8.1 and 8.2 list the nine most

Table 8.1 Most sensitive model parameters for the mean daily discharge for the Upper Ouémé catchment (1998-2001), Categories: >1 very high, >0.1 high.

Parameter		Rank_Q	Mean sensitivity	Category
CN2	SCS curve number [-]	1	3.98	very high
ALPHA_BF	Baseflow alpha factor [days]	2	1.85	very high
SOL_AWC	Soil available water capacity [mm H ₂ O/mm soil]	3	1.20	very high
GWQMN	Threshold water depth in the shallow aquifer for flow [mm]	4	0.87	high
RCHRG_DP	Fraction of deep recharge [-]	5	0.45	high
CANMX	Maximum canopy storage [mm]	6	0.25	high
GW_REVAP	Groundwater "revap" coefficient [-]	7	0.20	high
ESCO	Soil evaporation compensation factor [-]	8	0.19	high
SOL_Z	Soil depth [mm]	9	0.19	high

sensitive parameters. For both output variables, the SCS curve number is by far the most sensitive. The discharge and sediment yields are very sensitive to changes in the baseflow recession constant (ALPHA_BF) and the available water capacity of the soil (SOL_AWC). Discharge is also highly sensitive to the groundwater parameters GWQMN, RCHRG_DP and GW_REVAP.

Table 8.2 Most sensitive model parameters for the mean daily sediment yield for the Upper Ouémé catchment (1998-2001), Categories: >1 very high, >0.1 high.

Parameter		Rank_SY	Mean sensitivity	Category
CN2	SCS curve number [-]	1	6.82	very high
SPCON	Linear re-entrainment parameter for channel sediment routing [-]	2	1.60	very high
ALPHA_BF	Baseflow alpha factor [days]	3	1.46	very high
SLOPE	Average slope steepness [m/m]	4	1.42	very high
SURLAG	Surface runoff lag time [days]	5	1.30	very high
SOL_AWC	Soil available water capacity [mm H ₂ O/mm soil]	6	0.86	high
CH_K2	Channel effective hydraulic conductivity [mm/hr]	7	0.76	high
USLE_P	USLE erosion control factor [-]	8	0.68	high
USLE_C	USLE crop management factor [-]	9	0.64	high

Additional parameters to which sediment yield is highly sensitive are the SPCON factor, the average slope steepness (SLOPE) and the surface runoff lag time (SURLAG).

In a second step, a new sensitivity analysis was performed against discharge measurements from 1998-2001 at the Terou-Igbomakoro outlet (see Table 8.3). Due

Table 8.3 Most sensitive model parameters for daily discharge; relative to measurements at the Terou-Igbomakoro outlet; categories: >1 very high, >0.1 high.

Parameter		Rank_Q	Mean sensitivity	Category
CN2	SCS curve number [-]	1	8.25	very high
ALPHA_BF	Baseflow alpha factor [days]	2	2.14	very high
SOL_AWC	Soil available water capacity [mm H ₂ O/mm soil]	3	2.00	very high
SURLAG	Surface runoff lag time [days]	4	1.99	very high
CH_K2	Channel effective hydraulic conductivity [mm/hr]	5	1.79	very high
GWQMN	Threshold water depth in the shallow aquifer for flow [mm]	6	1.22	very high
SOL_Z	Soil depth [mm]	7	1.14	very high
RCHRG_DP	Fraction of deep recharge [-]	8	1.05	very high
CH_N	Mannings'n value for the main channel	9	0.62	high

to the consideration of measured discharge data, the rank of the surface runoff lag time and the channel parameters CH_K2 and CH_N increased by ten. This can be explained by the fact that daily discharge values are being considered instead of the mean value. Except for ESCO and CANMX, the mean sensitivity increased for all very sensitive parameters. Except for Mannings', the most sensitive parameters for discharge are identical with those obtained by Sintondji (2005) for the Terou-Igbomakoro subcatchment. However, the rankings of the parameters vary.

In contrast to other studies (e.g., Spruill et al. 2000), K_{sat} is not one of the most sensitive parameters, since the SCS curve number approach does not consider this parameter in the calculation of surface runoff. To sum up, the results of the sensitivity analysis confirm the high sensitivity of the SWAT model to changes of the curve number, the available soil water capacity and the groundwater parameters, as reported in the literature (e.g., Sintondji, 2005; Arnold et al, 2000).

In order to evaluate the effects of uncertainties in the parameter values, 1000 simulations with different parameters sets were performed. The parameter sets were determined by sampling meaningful parameters ranges of the most sensitive calibration parameters (see Table 8.4) according to the Monte-Carlo Latin-Hypercube procedure.

Table 8.4 Parameter ranges for the uncertainty analysis.

	CN2	SOL_AWC	ALPHA_BF	SURLAG	CH_K2	GWQMN	RCHRG_DP	ESCO
Min value	-10%*	-25%*	0	0.1	0	0	0.02	0
Max value	+10%*	+25%*	0.1	0.5	50	40	0.35	0.2

* increase or decrease % of initial value

After running the SWAT model, the parameters were plotted against water yield, sediment yield and model efficiency for the Terou-Igbomakoro and Donga-Pont subcatchments (Figs. 8.1-8.5 and Figs. B.11-B.13, App. B).

Because of the high sensitivity of the chosen parameters, the mean values for discharge and model efficiency vary considerably among the realizations (Figs. 8.1-8.4). The mean annual discharge of all realizations is 292 mm/yr for Terou-Igbomakoro and 372 mm/yr for Donga-Pont, which is significantly higher than the 213 and 297 mm/yr in the original model. This reflects the effort to reduce simulated discharge during calibration. During the uncertainty analysis, only 4 of the 8 parameters, namely ALPHA_BF, RCHRG_DP, CN2, SOL_AWC, show clear trends for mean annual discharge. For ALPHA_BF, values smaller than 0.01 mean discharge drops dramatically in both subcatchments (see Fig. 8.1). This is due to the

extreme delay in the occurrence of base flow, leading to increased capillary rise and evapotranspiration. Model efficiency tends to increase with increasing ALPHA_BF. The decrease in discharge with increasing RCHRG_DP is evident since the deep recharge is considered to be lost from the system (Fig. 8.2). Model efficiencies are scattered over the whole parameter range, with a tendency to increase with increasing deep recharge.

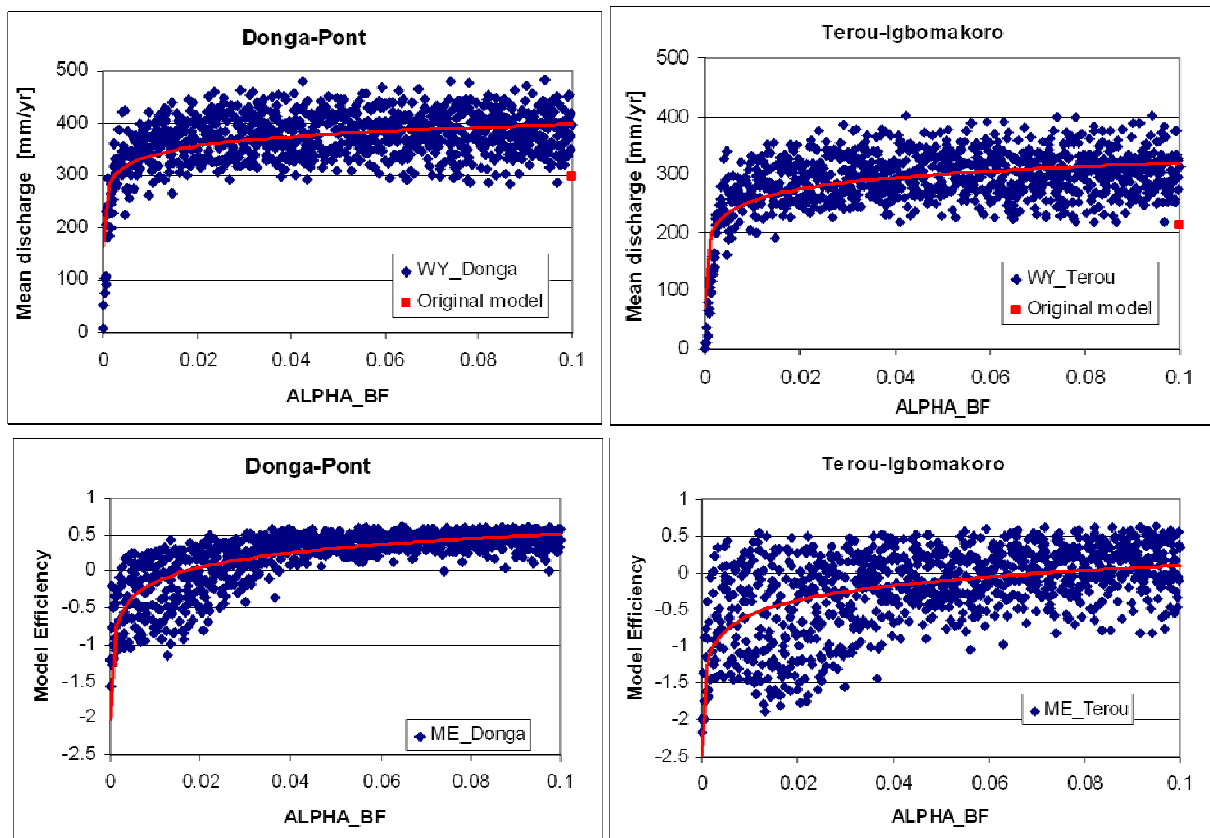


Fig. 8.1 Sensitivity of mean annual discharge and model efficiency to changes of the parameter ALPHA_BF (red dot: parameter value and simulated mean discharge for the period 1998-2001, red line: logarithmic regression).

For changes in curve number, mean discharge and model efficiency are widely scattered. Both tend to increase over the whole parameter range (Fig. 8.3). Mean annual discharge tends to decrease with increasing SOL_AWC, but the effect on model efficiency is not clear. In contrast to findings from Busche (2005) and Sintondji (2005), for the Terou-Igbomakoro subcatchment, reductions in SOL_AWC tend to increase mean annual discharge. All other parameters, namely SURLAG, CH_K2, ESCO and GWQMN, show no clear trends for mean annual discharge in the considered parameter ranges (Figs. B.11, B.12). However, model efficiency shows a

negative trend with increasing values of CH_K2 and GWQMN. This confirms the choice of the lower limit for CH_K2 during model calibration.

For all considered parameters, model efficiency is more widely scattered for the Terou-Igbomakoro subcatchment than for the Donga-Pont subcatchment.

The mean annual sediment yields also vary considerably among the realizations along the parameter ranges. The mean annual sediment yield of all realizations is 0.12 t/ha/yr for Terou-Igbomakoro and 0.79 t/ha/yr for Donga-Pont, which is only slightly less than the values from the original model (0.14 and 0.85 t/ha/yr, respectively).

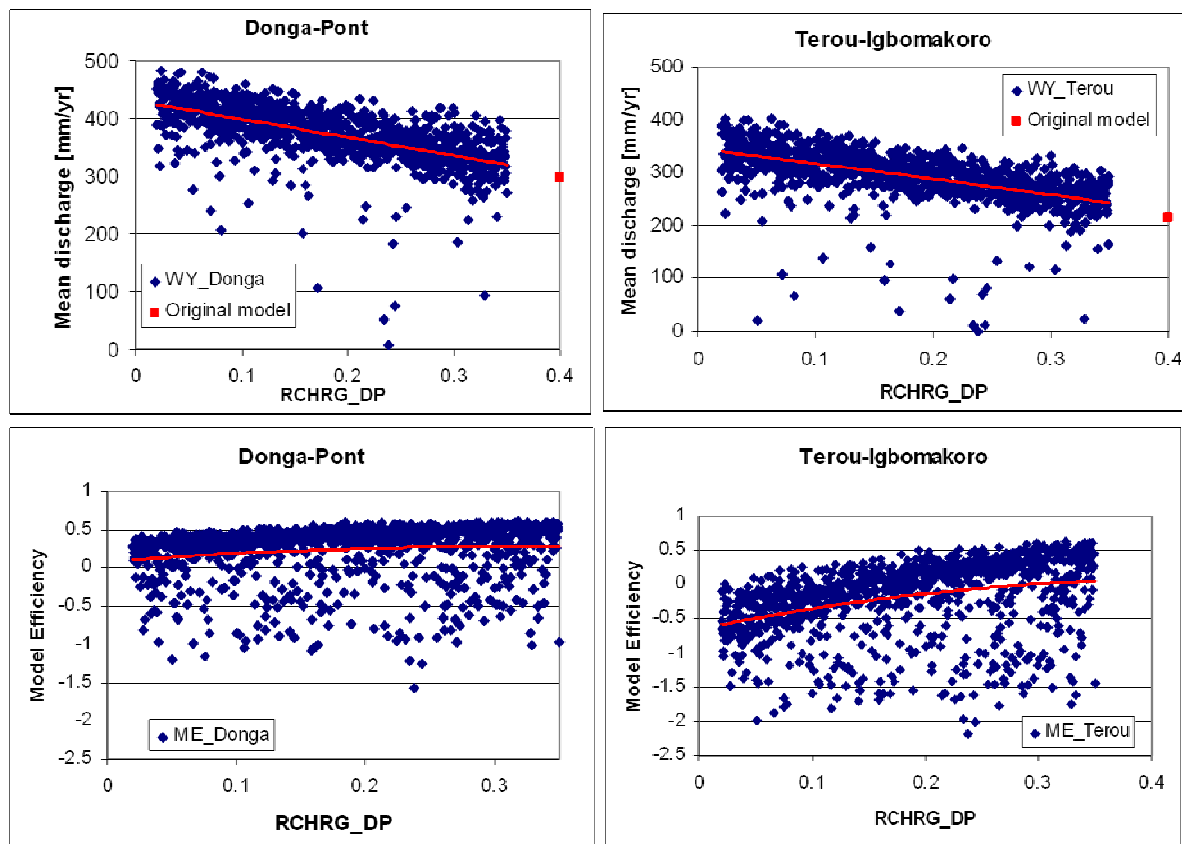


Fig. 8.2 Sensitivity of mean annual discharge and model efficiency to changes of the parameter RCHRG_DP (red dot: parameter value and simulated mean discharge for the period 1998-2001, red line: polynomial regression).

As expected, sediment yields are highly sensitive to the curve number (CN2). With increased CN2, sediment yield increases considerably in both subcatchments as a result of increased surface runoff (Fig. 8.4), and variations among the realizations for a certain CN2 value are much lower than for all other parameters. SURLAG and ALPHA_BF show slightly positive trends (Fig. 8.4-5). The drop in discharge for very small ALPHA_BF values is reflected by significantly lower sediment yields.

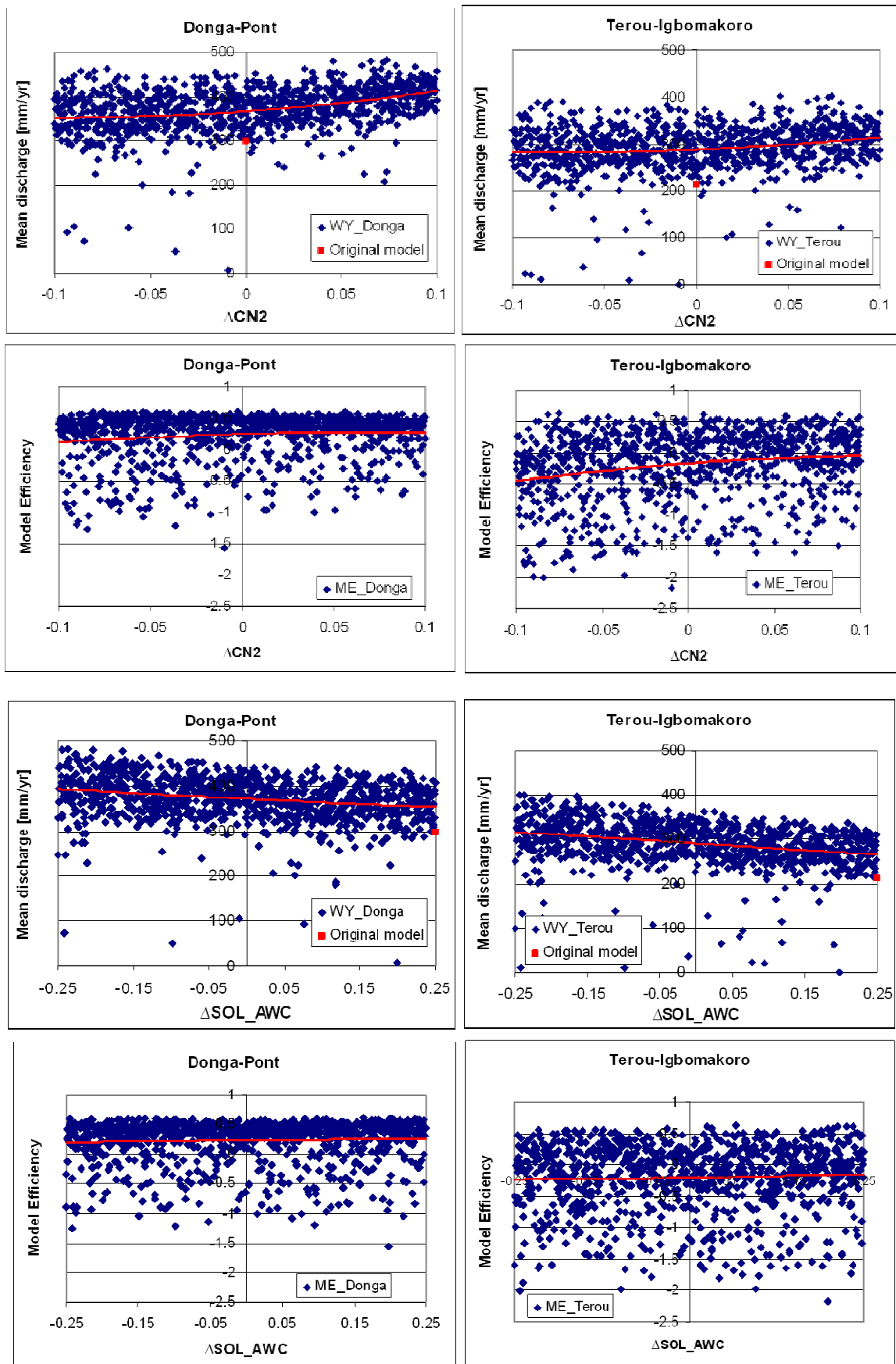


Fig. 8.3 Sensitivity of mean annual discharge and model efficiency to changes of parameters $CN2$ and SOL_AWC (red dot: parameter value and simulated mean discharge for the period 1998-2001, red line: polynomial regression).

A slightly negative trend for the sediment yield can be observed for CH_K2 (Fig. 8.5). The figures for all other parameters contain no clear patterns (see Fig. B.13, Appendix B).

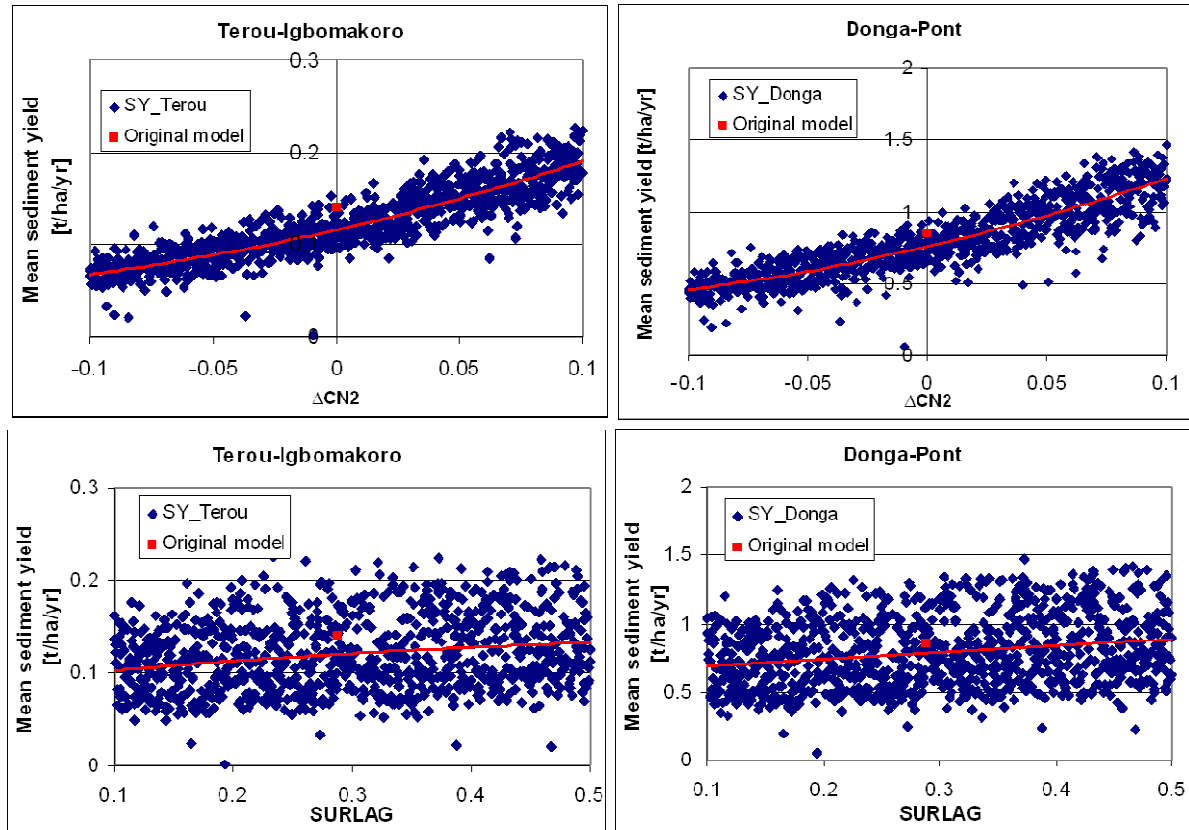


Fig. 8.4 Sensitivity of mean annual sediment yield to changes of parameters CN2 and SURLAG (red dot: parameter value and simulated mean sediment yield for the period 1998-2001, red line: polynomial regression).

The mean weekly curves for total discharge and sediment yield for all realizations of Terou-Igbomakoro and Donga-Pont and the 90% confidence interval are shown in Figs. 8.6 and 8.7. The width of the confidence interval for discharge is larger in the middle and the end than at the beginning of the rainy seasons. In the middle of the rainy season, the interval is shifted towards lower discharge values.

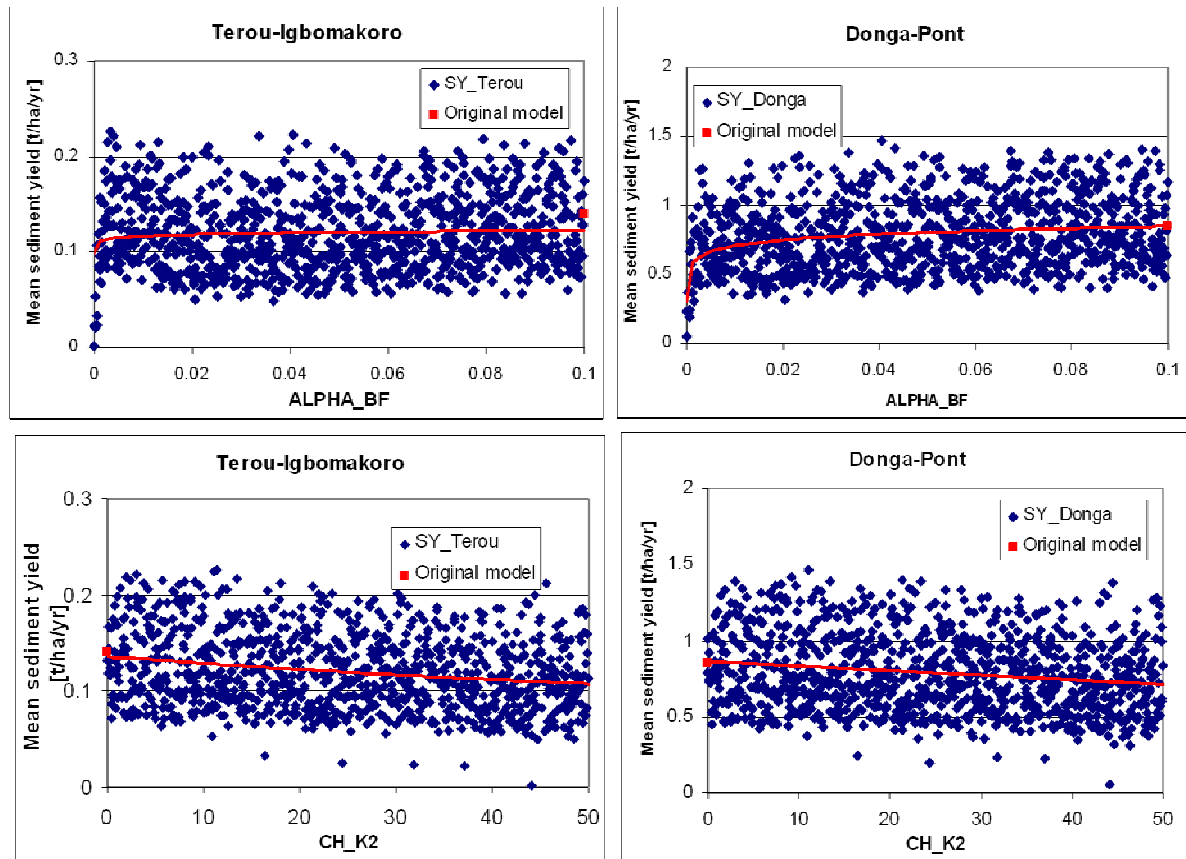


Fig. 8.5: Sensitivity of mean annual sediment yield to changes of parameters ALPHA_BF and CH_K2 (red dot: parameter value and simulated mean sediment yield for the period 1998-2001, red line: polynomial regression, for ALPHA_BF: logarithmic regression).

In contrast, the uncertainties in sediment yield are mainly related to individual sediment peaks, with high upper bounds of the confidence interval. This is even more obvious in the daily graphs showing the confidence intervals (see Fig. B.14, Appendix B).

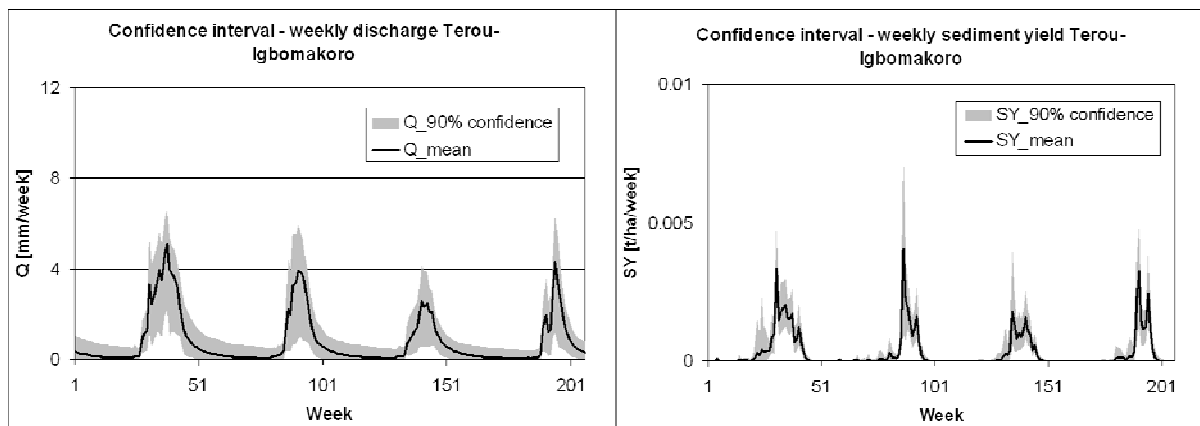


Fig. 8.6 Confidence interval (90%) for mean weekly discharge and sediment yield at the Terou-Igbomakoro outlet.

Large uncertainties in the sediment peaks are also triggered by uncertainties in the fraction of surface runoff, which are not visible in the graph for total discharge. At the

beginning and end of the rainy season, the confidence interval for the sediment yield is very small.

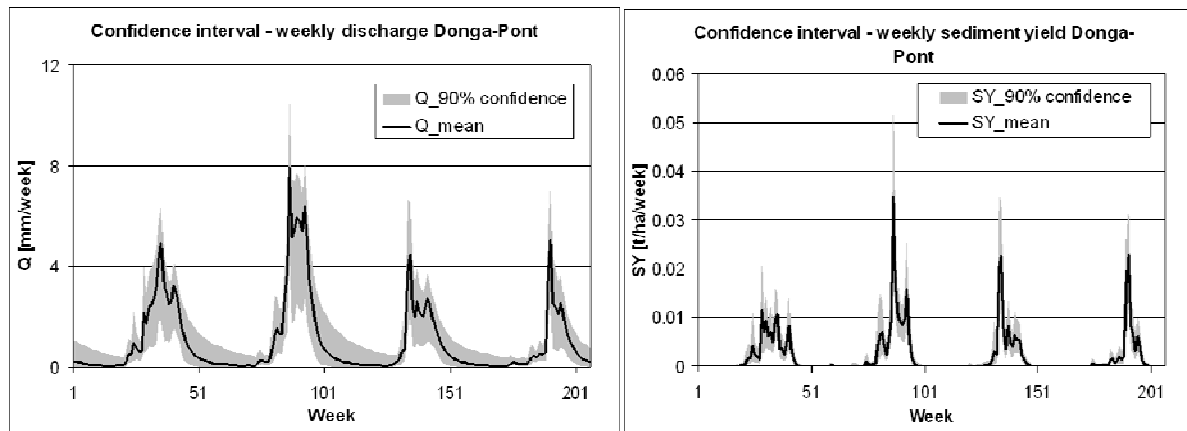


Fig. 8.7 Confidence interval (90%) for mean weekly discharge and sediment yield at the Donga-Pont outlet.

8.3. Uncertainties in observed data for model calibration and validation

Uncertainties in the measurements for model calibration can be very large and can heavily affect calibration results. In the following, the uncertainties related to the discharge and suspended sediment curves are discussed.

Discharge curves

The discharge data were derived from continuous water level records at gauging stations via site-specific water level (H) – discharge relationships (Q). Before 2000, the water level at Terou-Igbomakoro outlet was only recorded daily from a batten gauge. In general, H-Q relationships include high uncertainties; in natural tropical rivers in particular, erosion and sedimentation processes in the river bed and seasonal growth of bank vegetation lead to highly dynamic cross-sections. One large discharge event can completely change the H-Q relationship. As determining the relationship requires a great deal of effort, the curves are often not updated for several years.

For example, at the Aguima outlet, a large discharge event in September 2003 completely changed the H-Q relationship. In 2005, a new relationship was determined. Using the old relationship would have changed the discharge amounts by a factor of two (oral comm. Giertz).



Fig. 8.8 Stagnant water around the turbidity probe at the Terou-Igbomakoro outlet (11/2005).

For the considered outlets in the Upper Ouémé catchment, the H-Q relationships were determined about every 3 to 10 years by the French research project CATCH/AMMA and the General Directorate of Water (DGEau Benin). For example, for Terou-Igbomakoro outlet, one H-Q relationship was used for the period 1993-2003. Moreover, the measurements of extreme discharge events often include large uncertainties due to flooding of riparian zones and rare corresponding measurements in the H-Q relationship. The high uncertainties in the measured discharge peaks hamper the evaluation of the model results

because the model efficiency is very sensitive to extreme events. Furthermore, the geomorphology of the river bed limits discharge measurements at the beginning and end of the rainy season. For example, at the Terou-Igbomakoro outlet, discharge flow at the position of the limnigraph stops days to weeks earlier than in other parts of the river bed at the same cross-section (Fig. 8.8). As a consequence, measured annual discharge is underestimated.

Baseflow separation with a digital filter programme and measurements of the electrical conductivity allow only a rough estimation of the discharge components. However, both methods lead to similar results. Thus, the digital filter programme seemed suitable for evaluating the simulated discharge components on an annual basis.

Suspended sediment curves

Uncertainties in the suspended sediment curves can be attributed to the turbidity recordings, water sampling and gravimetric determination of suspended sediment concentrations. In particular, in the year 2004, large gaps in the measurements hampered the calculation of annual sediment yields and the quality of sediment calibration. The high uncertainties in the turbidity records are related to pollution of the optical sensor during extreme events and periods with extremely low water levels. In periods with low water levels, the position of the turbidity sensor was lowered to a minimum distance of 20 cm above the river bed in order to capture small

events. However, after large discharge events at the beginning of the rainy season, the probe was often covered by mud or leaves and the wiper could not properly clean the optical sensor before the next measurement. In some cases, the turbidity values remained extremely high for several days until the next discharge event cleaned the optic. Although such artificially high turbidity values were removed from the dataset, it was difficult to choose a suitable threshold as the problem occurred mostly after large events. The turbidity measurements were plotted against the discharge measurements in order to identify an appropriate threshold; a maximum threshold for turbidity of 800 NTU (nephelometric units) seemed reasonable for the Donga-Pont, Terou-Igbomakoro and Aguima subcatchments. In the small and very intensively used Donga-Kolonkonde subcatchment, higher values seemed reasonable. However, the threshold can significantly influence the turbidity and SSC relationship as well as the sediment curves, because it defines the highest suspended sediment peaks. A threshold of 400 NTU would have reduced the annual sediment load at Donga-Pont outlet by a factor 2.5. For the other two outlets, this threshold would have caused only minor changes. Similar problems have been reported in the literature.

At three of the four installation points of turbidity probes, short-term measurements were taken at a higher temporal resolution in order to study the influence of the resolution. In all cases, the 30-minute interval for turbidity measurements was sufficient to capture the temporal pattern of turbidity (Fig. 8.9). However, during extreme events, single peaks of sediment load may be missed. According to Hasenpusch (1995), turbidity probes generally underestimate high concentrations of suspended sediment. The turbidity – suspended sediment relationship at an outlet may also vary during the year depending on different sediment sources. In this study, the different components of suspended sediment were not analysed, but as a rough indicator for the different sources, the colour of the filtered sediment was recorded. Gray, dark grey or black were dominant at all four sampling outlets, followed by brown sediment. At Donga-Kolonkonde outlet, red sediment also appeared. No clear relationship between sediment colour and date or sediment amount could be identified.

The uncertainties in water sampling are rather low. Repeated measurements revealed that a time lag of a few minutes and a horizontal distance of a few meters

between the limnigraph and the sampling point did not produce large differences in the determined suspended sediment concentration.

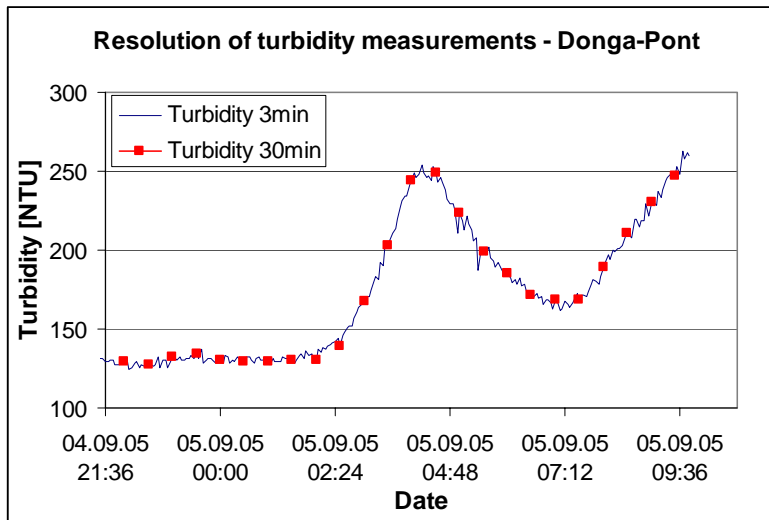


Fig. 8.9 Temporal resolution of turbidity measurements: comparison of a 3-minute and 30-minute interval at the Donga-Pont outlet.

While water sampling was restricted to near-surface water, the turbidity measurements were recorded at greater depths. However, it was assumed that turbulent flow conditions lead to a fairly homogeneous vertical distribution of suspended sediment concentration at the main outlets.

The most important source of uncertainty in the gravimetric determination of suspended sediment concentration was the air humidity of 40 to 100%, since no exsiccator was available. In order to minimize the falsifying effect of air humidity, the filters were weighed before and after filtration at the same air humidity. Furthermore, an optimal cooling time of 30 to 60 minutes was determined to guarantee equilibrium of the humidity of the filter with the surrounding air. In addition, reference filters were treated in the same manner as the other filters in order to survey accuracy. Following this procedure, the difference in determined suspended sediment concentrations due to slight differences in the humidity of the filters was lower than 0.01 g per litre. Handling errors in the gravimetric determination were higher in the first year of sampling (2004). Blind filtration tests with distilled water confirmed the cleanness of the filter paper. For water samples with very low sediment concentrations, the accuracy of the balance of 0.005 gram was a limiting factor.

The model was calibrated against suspended sediment yields. This implies an underestimation of the total sediment yield, since the bed load was not considered. Sintondji (2005) measured bed loads of 45.7 tons from September 2003 to January 2004 at the Terou-Igbomakoro outlet. However, his method implied high uncertainties and was not applicable to the middle discharge period with water heights above two meters. Beyond this, no data were available for the catchment regarding the annual fraction of bed load.

8.4. Evaluation of uncertainties in the modelling process

As noted, a wide range of uncertainties must be considered when interpreting the modelling results of this study. Table 8.5 evaluates the various sources of uncertainty. The uncertainties in input and calibration data are major contributors. For the input data, soil and rainfall data show the highest uncertainties, while of the calibration and validation data, the sediment measurements have higher uncertainty than the discharge data. The accuracy and completeness of the suspended sediment measurements could be significantly improved by more frequent surveillance of the turbidity probes, the use of an exsiccator for gravimetric determination, and improved discharge – SSC curves via additional water sampling during stormflow events.

The uncertainties due to the model structure are difficult to quantify. Future studies should address channel degradation.

The sensitivity analysis identified as the most sensitive calibration parameters: CN2, ALPHA_BF, SOL_AWC, SURLAG, CH_K2, GWQMN, RCHRG_DP and SPCON. Additional efforts to determine these parameters could significantly reduce parameter uncertainty. In particular, more detailed knowledge regarding the groundwater parameters (GWQMN, RCHRG_DP) and the physical soil parameters (SOL_AWC, CH_K2) should be acquired for the Upper Ouémé catchment.

The uncertainties in the scenario results are significantly higher than in the modelling results for the period 1998-2005. This is due to higher uncertainties in the climate and land use data, partially caused by limited computational power and insufficient process understanding. According to Mahe et al. (2005), an increase in computer

Table 8.5 Evaluation of the different sources of uncertainty in the modelling results.

	Model setup 1998-2005	Scenario analysis 2001-2025/50
Input data		
Relief	-	-
Land use map	+/-	++
Vegetation parameters	(+)	(+)
Soil	+	+
Climate	+	++
Model assumptions		
Discretisation	+/-	+
Surface runoff	+/-	+/-
Groundwater	+	+
Sediment	+/-	+/-
Calibration/Validation data		
Discharge data	+	xxx
Sediment data	++	xxx
Baseflow separation	+/-	xxx

++ very high uncertainty
 + high uncertainty
 +/- mean uncertainty
 - low uncertainty
 (+) high uncertainty, but low sensitivity
 xxx input parameter not necessary

power in the upcoming years will significantly improve climate models by allowing the consideration of land surface feedbacks and atmospheric aerosols. A spatially differentiated algorithm for pre-processing land use maps could improve the scenario analysis. However, the input data for model calibration and validation and scenario analysis were very good compared to the data availability for most large African catchments.

9. OPTIONS FOR SUSTAINABLE LAND USE

In this chapter, possible options and priority areas for soil management in the Upper Ouémé catchment are explored based on the field investigations (Chapter 6), modelling results (Chapter 7) and existing experiences with soil management in Central Benin (Section 9.2). Therefore, modelling results are synthesized and simplified in a way that facilitates their communication to decision makers and integration into a decision-support system for stakeholders in Benin. By re-connecting the biophysical research results to the socioeconomic and institutional context more specific recommendations can be derived for policy makers and development workers in Benin.

9.1. Hotspots of soil erosion in the Upper Ouémé catchment

Current and future hotspots of soil erosion have been identified in the modelling process (see Chapter 7). In the following some of the maps of Chapter 7 illustrating the spatial pattern of sediment yields will be presented again but with communal borders replacing the subbasin borders as these are more relevant for most stakeholders in Benin. However, only the parts of the communes within the catchment are considered. For the recent period 1998-2005 hotspots of soil erosion occur in the communes Djougou, Copargo and Parakou (Fig. 9.1). Surface runoff is also elevated in the commune Ndali and in the small part of the commune Sinende which lies in the Upper Ouémé catchment. As already discussed in Chapter 7, the hotspots result from high land use intensities (communes Copargo, Djougou, Parakou) and harsh climatic conditions (communes Copargo, Djougou, Ndali, Sinende).

The absolute values of sediment yield have not been translated into qualitative categories such as low, medium and high, as such an evaluation would require additional knowledge about acceptable soil loss tolerances based on thresholds for productivity loss and expert knowledge in the country. However, the qualitative categories of the national action plan for desertification control (Table 9.1) and the map of soil degradation for Benin (Fig. 9.2) from MEHU (2003) give an idea how the quantitative values can be interpreted in the national context of Benin. The table and

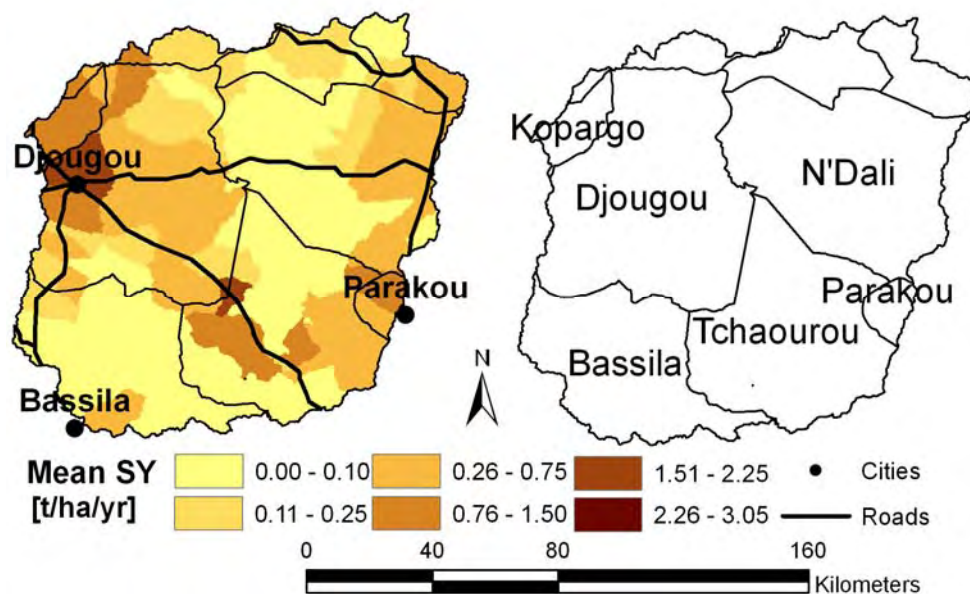


Fig. 9.1 Mean sediment yield for 1998-2005 in the Upper Ouémé catchment (left), communal borders within the Upper Ouémé catchment (right).

the map show that the Upper Ouémé catchment covers the whole spectrum of the country with regard to soil degradation ranging from large protected forests to highly degraded areas in the north-western part of the catchment (communes Djougou and Copargo). The latter belongs to the regions which are strongly affected by desertification in its wider sense, whereas the Ndali region in the north-eastern part of the catchment is moderately affected (Table 9.1). The main part of the catchment (communes Bassila, Tchaourou, Parakou) is considered as not affected by desertification processes. Except for Parakou, this is consistent with the findings from the field investigations and modelling of this study.

Table 9.1 Zones of severity of desertification in Benin according to MEHU (1999).

Intensity of desertification	Region
Strongly affected	Boukoubé-Cobly-Matéri-Tanguieta, Ouaké-Djougou-Copargo, Karimama-Malanville-Kandi-Banikoara-Ségbana
Moderately affected	Cotton regions: Kouandé, Kérou, Kalalé, Bembéréké, Sinendé, Ndali, Nikki
Slightly affected	Zou-Sud, l'Atlantique, parts of Ouémé, Couffo and Mono
Not affected	All other communes

Figure 9.2 provides additional details with regard to the dominant type of soil degradation and the resulting extent of productivity loss in Benin. It shows that the most degraded areas in north-western Benin are characterised by sheet and rill erosion by water and wind erosion, as well as by strong nutrient depletion, which is

the major degradation type in Southern Benin. The estimated extent of productivity loss varies within the Upper Ouémé catchment.

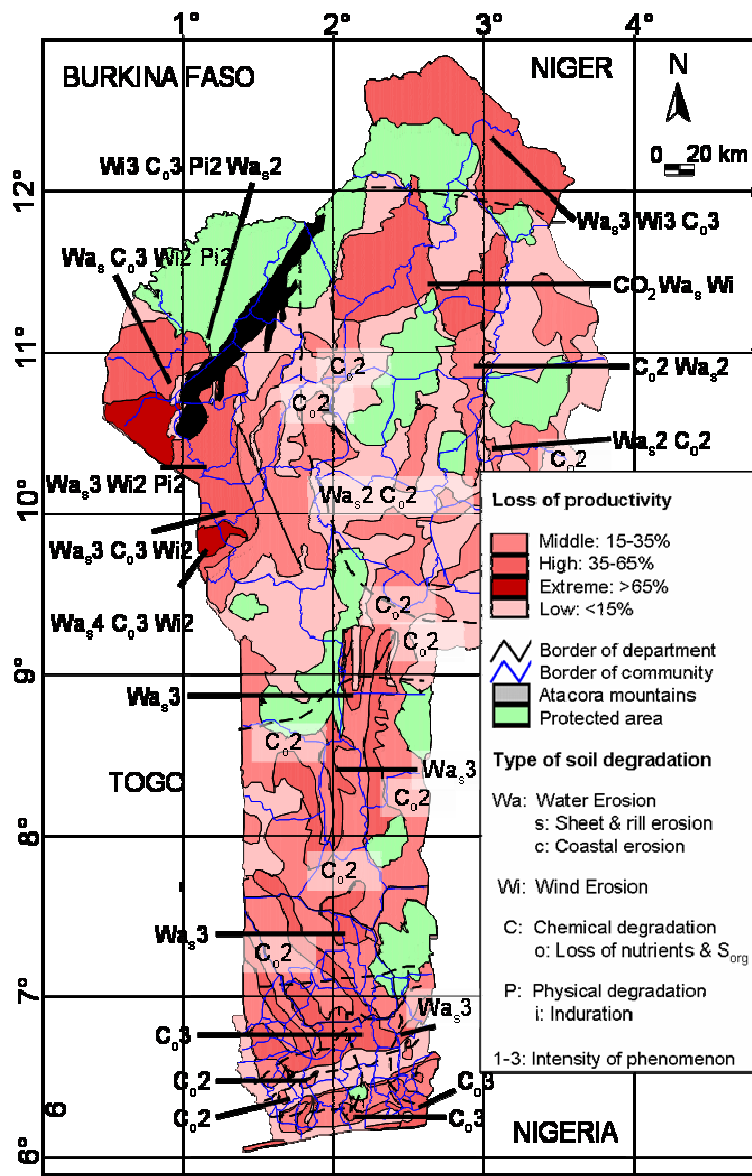


Fig. 9.2 Map of soil degradation in Benin (modified from MEHU 2003).

use, climate change and combined scenarios, similar to Fig. 7.63 in Chapter 7. However, while Fig. 7.63 shows only the results for the “business as usual” scenario, Fig 9.3 presents scenarios L1 and L2 to cover the entire range of simulated future sediment yields. As discussed previously, increases in sediment yield are most drastic for the land use scenario L2_2025, for which the fraction of cropland more than doubles in the Upper Ouémé catchment due to increased population growth and a constant cropland demand per capita. This scenario assumes economic stagnation and that institutional insecurity is leading to a massive encroachment of cropland into protected forest areas in the communes Bassila, Tchaourou and Ndali. For this

In summary, whereas a small part of the Upper Ouémé catchment belongs to regions of the country that are most affected by soil degradation, other parts are still covered by protected forests and not degraded. In comparison to the entire country, the population density and the fraction of cropland are still rather low in most of the Upper Ouémé catchment. However, this is changing. The impacts of land use and climate changes on the amounts of soil loss and future hotspots of soil erosion have been identified in Chapter 7. Figure 9.3 shows the spatial pattern of sediment yield for the land

scenario, sediment yield strongly increases in all communes of the Upper Ouémé catchment; in particular, a new hotspot is evolving in the southern part of the catchment, affecting the communes of Tchaourou and Bassila. In contrast, increases in sediment yield are moderate for scenario L1_2025, which assumes an intensification of agricultural production triggered by economic growth and successful decentralisation, leading to an expansion of the cropping area by “only” 51%. As a consequence of reductions in rainfall by 3% and 4%, the climate scenarios lead to a decrease in sediment yield by 5% and 14% for scenarios B1 and A1B, respectively. Differences in the spatial distribution of sediment yield between the two scenarios are not visible in Fig. 9.3. Sediment yield is in particular reduced in the commune Djougou, but also increases in some communes (e.g., Parakou, Bassila).

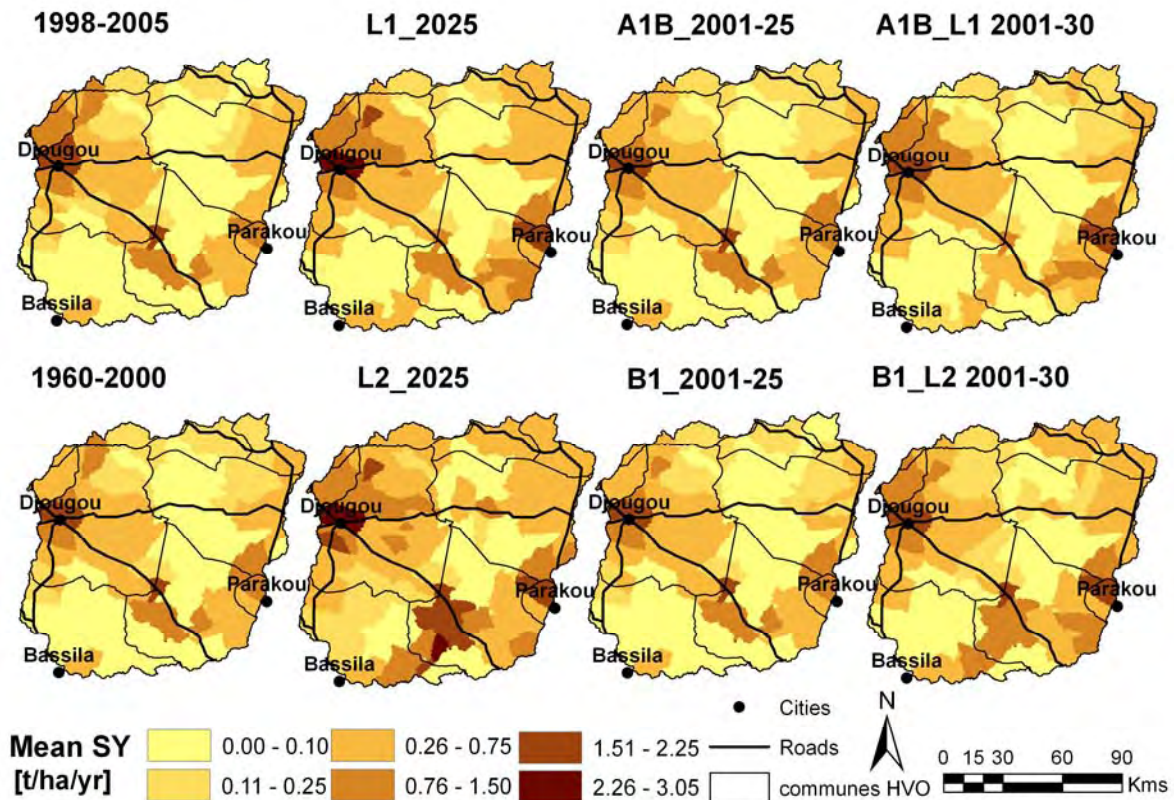


Fig. 9.3 Mean sediment yield for the range of climate, land use and combined scenarios in the Upper Ouémé catchment compared to the original model (1998-2005) and the model with REMO data for 1960-2000.

The combined scenarios A1B_L1 and B1_L2 for 2001 to 2030 combine the effects of climate and land use change. As a consequence of this interaction and the consideration of the land use maps for 2000, 2010, and 2020, and not only 2025, increases in sediment yield appear to be less drastic. The strong increase in sediment yield in the commune Djougou resulting from land use change is weakened

by decreases in sediment yield due to climate change. For the commune Bassila, slight relative increases in sediment yield due to climate change combine with strong relative increases due to land use change, but the absolute increase is still too small to be seen in Fig. 9.3. For the whole range of combined scenarios, sediment yield increases significantly in the southern and north-eastern parts of the catchment.

To summarise, current hotspots of soil erosion in the Upper Ouémé in the communes Djougou, Copargo and Parakou are expected to become aggravated within the next two decades due to massive cropland expansion. The north-eastern corner of the catchments with already elevated sediment yields will develop into a hotspot (parts of communes Ndali, Sinende, Bembéréké). A new hotspot of soil erosion is expected to occur in the southern part of the catchment (parts of communes Bassila and Tchaourou). As a consequence of reduced rainfall, simulated by the climate model REMO, the increase in sediment yield could be weakened in some parts of the catchment, in particular the commune Djougou.

However, the results of the climate scenarios must be interpreted carefully, since current climate models provide different signals for future rainfall trends in West-Africa (IPCC 2007). Although the REMO simulations follow the observed trends of reduced rainfall in the Upper Ouémé catchment, rainfall may also increase in the coming decades, and, combined with increased rainfall variability accelerate rather than reduce annual sediment yield. Due to these uncertainties, decision makers may identify future hotspots of soil erosion from the maps for the land use scenarios rather than for the combined scenarios. However, decision makers should also keep in mind that the socioeconomic scenarios behind the land use scenarios do not capture all possible interventions. For example, the construction of new roads or asphalt coatings of existing earth roads in the Upper Ouémé catchment could significantly influence the spatial pattern of land use (see intervention scenario by Judex 2008) and would hence modify the sediment yield maps presented in this work.

Furthermore, the results of the climate scenarios for the Upper Ouémé catchment should not be misinterpreted, in the sense that less rainfall means less erosion and that climate change could therefore be beneficial in terms of combating soil degradation. First, changes in rainfall play out differently within the catchment, and decreases in absolute rainfall amounts do not necessarily mean less erosion due to increased rainfall variability. Second, decreases in the water yield due to reduced

rainfall have a number of negative consequences, including reduced growth of natural vegetation and crops, which, in turn, would reduce vegetation cover and enhance surface runoff and soil erosion by water. Third, in the long run, increasing temperatures will increase C_{org} losses in the topsoil through enhanced decomposition and more frequent and intense fires, and they will reduce vegetation cover through increased heat stress of the plants, thus also enhancing soil erosion by water.

The modelling results identified current and future hotspots of soil erosion in the Upper Ouémé catchment. These investigations at the catchment scale complement the detailed local studies from Junge (2004) about soil erosion rates for specific farming systems in the Aguima subcatchment. Knowledge about soil erosion processes at multiple scales is required to derive recommendations regarding suitable soil management measures at the catchment scale. Sustainable soil management measures not only enhance soil fertility and crop yield but also contribute to climate change adaptation and mitigation. Activities to improve soil management should build on the wide range of existing, but often very local, experiences in Central Benin.

9.2. Soil conservation in Central Benin – Status quo

The roots of soil erosion management lie in the farming system, as soil erosion decreases exponentially with an increase of vegetal cover (Lal 1990). Therefore, soil erosion prevention goes far beyond structural measures and includes a wide range of plant and soil management activities in order to maintain soil fertility and the productive capacity of the soil. Before discussing the soil conservation measures that have been promoted in Benin, the national institutional framework related to resources management and agricultural production will be presented, as it is crucial for the long-term sustainability of development activities.

9.2.1. The institutional framework

The institutional landscape in Benin is complex and dynamic. Therefore, it is impossible to present a complete overview of the institutional landscape related to natural resources management and agricultural production in Benin. In development

cooperation, various donors act in the country and have built parallel structures to the public system. Although the coordination and coherence of their activities has improved in the last year, in particular in the health and education sectors, it remains insufficient (MEHU 2005). Furthermore, institutional structures are changing due to the ongoing decentralisation process and the new government in 2005. Figure 9.4 provides an overview of the main actors in the sustainable management of soil resources in Benin.

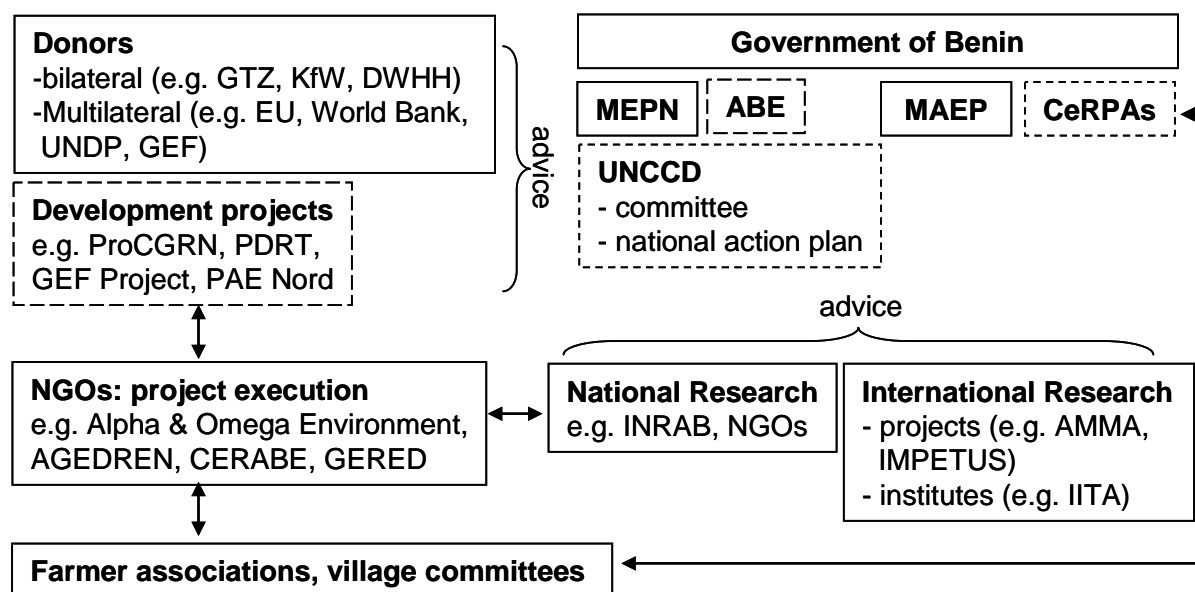


Fig. 9.4 Actors in the field of sustainable management of soil resources in Benin.

Development projects

In the seventies, soil conservation projects were initiated in Benin after several severe droughts, for example in the Atacora region. This region, which is strongly affected by soil degradation, has a long history of soil conservation activities. From 1963 to 1969, the project SEDAGRI¹ promoted the construction of terraces (*banquettes*) and walls (*diguettes*), and later chemical fertiliser for groundnut, composting and tree plantations with Acacia, Eucalyptus and Sienna. In the eighties, development aid focused on developing sustainable agricultural systems, but no significant progress was achieved. The UNSO project intensively promoted reforestation in the commune Ouaké from 1985 to 1990 (GTZ-AFD 2004).

¹ The names of the projects are explained at the Abbreviation Section, page xxiv. More details about the projects can be found in Table C.1 in Appendix C.

In the nineties, several resources management projects, like PGRN (1984-1989), PGTRN (1999-2005) and a project to combat bush fire (1986-1990), followed. Since that time, more attention has been given to participatory approaches. For example, PGTRN elaborated local land use codes (*code local*) in the framework of land management plans (*Plan de Gestion de Terroir*). Land management plans were developed for 99 villages and 13 village-associations within this project (GTZ-AFD 2004). Furthermore, several unions for resources management with the status of NGO were formed. The project PPEA, which started in 1983 as an animal health project in the Atacora region, changed its focus to adapting production patterns and established common land use planning between farmers and livestock keepers (Kirk 1996). In 2004, GTZ launched the programme ProCGRN with the objective of promoting sustainable land use considering the new institutional setting accompanying the decentralisation process. One major focus is to integrate participatory land use planning at the village level into communal development plans. The target regions of this programme are the departments of Cotonou, Atlantique, Donga and Atacora. The programme integrates several former GTZ projects including PGTRN, PPEFB and PRRF. In the Upper Ouémé catchment, resource management activities are mostly focused on managing the protected forest in the south (e.g., GTZ project PRRF) or on the densely populated areas in the west. The sequence of GTZ projects PGRN-PGTRN-ProCGRN covered only four villages in the Upper Ouémé catchment, namely Anum, Gondessar, Bandessar and Dangoussar in the Barei district (GTZ-AFD 2004).

In the last decade, development aid has focused mainly on infrastructure, micro credits, decentralisation and diversification of agricultural production. Very few agricultural development projects address the unsustainable cultivation of the main food crops (Singer 2005). One exception is the project PDRT, which propagates cassava and other tubers as alternatives to cotton and promotes sustainable production methods in the whole country. In the Upper Ouémé catchment, PDRT works with several environmental NGOs and covers up to ten villages per commune (e.g., Manigri, Kikilé, Gaouga, Alafiarou, Fo-Bouré, Sonnomoun, Bori). In 2007, a large GEF-financed project (Forests and adjacent land management project, FAML) was launched. The project acts in 16 forests in northern and central Benin, including the *Fôret classée* in the central Upper Ouémé catchment. The project focuses on community-based forest management and promotes, in cooperation with the

extension services (CeRPAs), improved agricultural techniques and agro-forestry in order to combat soil degradation (World Bank 2006). The ongoing projects concerning soil conservation, acting partially in the Upper Ouémé catchment, are summarized in Table 9.2. Besides field projects, international donors also perform national policy consultations, e.g., at the Ministry of Agriculture (MAEP) and the Ministry of Environment (MEPN), and support agricultural research. However, responsibilities are unclear due to the decentralisation process, and the weak capacities of the agricultural extension services hamper the effectiveness of project interventions.

Table 9.2 Ongoing projects concerning soil conservation acting partially in the Upper Ouémé catchment (Sources: SINGER, 2005; MEHU, 2005; own investigations).

Project name	Donors	Period	Intervention zone	Commune HVO	Objectives	Related NGOs in HVO
PDRT	IFAD, BOAD	2001-2008	Whole country	all	Manioc production, sustainable agriculture	GERED, Alpha & Omega, Vie & environnement, CoVADES Benin*
FALMP	GEF, World Bank	2007-2011	16 forests in Central/ North Benin	Tchaourou, Ndali	Community-based forest management	in process
ProCGRN	GTZ, KFW, World Bank, AFD, BAD	2004-2014	Atacora, Donga, Cotonou, Atlantique	Djougou	Sustainable resource management	Alpha & Omega
PAEB Nord	DWHH, DED, EU	2007-2009	Borgou, Donga	Bassila, Ndali	Sustainable agriculture, resource management	GERED, CERABE, AGEDREN
Millenium villages	DWHH	2007-2010	village Manigri	Bassila	Agroforestry, micro credits, water sector	AGEDREN

* complete list: <http://www.pdrt.info>.

Non-Governmental Organisations (NGOs)

In the nineties, international donors strengthened the private sector and civil society in order to compensate for the negative effects of the structural adjustment programmes (Singer 2005). Today, most donors prefer to cooperate with private and civil entities and try to avoid involving governmental agencies in project implementation. Only in the education and health sectors close cooperation with governmental agencies still exists. In 2003, more than 3000 NGOs were registered in Benin (DED 2003). Among them are 77 environmental NGOs, most addressing

environmental education. In recent years, a trend towards fusion of NGOs can be observed (oral comm. Zanou 2005, MEPN). The study of Singer (2005) in southern Borgou showed that most NGOs have almost no budget or are financially completely dependant on donors and therefore widely reproduce the donors' agenda. NGOs are often closely linked to one donor who created or pushed this NGO in the past and continues this involvement for many years (cf. Table 9.2). For example, the NGO Alpha & Omega Environment works mainly for the GTZ project ProCGRN, while the NGOs AGEDREN, GERED and CERABE are financed mainly by PAEB North. Alpha & Omega Environment covers a wide spectrum of activities from watershed management, land use planning, land tenure, water sanitation and improved fire places to environmental education (GTZ-AFD 2004).

Research institutions

In the nineties, the focus of research switched from anti-erosive structures to soil fertility and the agricultural production system itself. Beninese studies on local soil erosion were performed in Alafiarou and Cotonou by the National Centre of Agro-Pedology (CENAP) until 1998. In 1995/1996, the FAO supported national erosion research. On-farm soil fertility research was promoted from 1986 to 1999 through a German collaborative research centre at the University of Hohenheim (SFB 308). Since 2002, soil fertility research is mainly conducted at the National Institute for Agricultural Research (INRAB) in Savé, and partly also in Bohicon and Kandi. The INRAB section in Niaouli and the International Institute for Tropical Agriculture (IITA) in Cotonou focus on seed and genetic research. National research depends highly on external resources.

Governmental structures and policies

The Ministry of Agriculture (MAEP) and Ministry of Environment (MEPN) are of particular interest for soil resource management. Until 2006, the Directorate of Forests and Natural Resources of the MEPN (DFRN) was part of the MAEP. This institutional change is expected to improve communication in environmental policies. The MAEP partially finances agricultural research and agricultural consultancy (CeRPAs). Another important institution is the Beninese Agency of Environment (ABE), which is linked to the MEPN and supported by several donors (MAEP 2004). For example, ABE orders research studies on soil fertility at the INRAB and prepares

them for the ministries. Despite the severity of the problem, soil degradation and desertification are not prior topics of governmental policies. Nevertheless, there exist several initiatives to put this important topic on the agenda: In 2002, an operational plan and a strategy for sustainable soil fertility management were elaborated. Two years later, an action plan for sustainably managing natural resources and soil fertility was released (MAEP 2004). The costs for implementing the plan for integrated soil fertility management are estimated at 10.7 billions FCFA (16.3 million euro). The plan emphasises the role of participation, necessary changes in the legislative and institutional frameworks, the need to improve technology transfer and the distribution of inputs incorporating the private sector. DIFOV, INRAB, DFRN, CeRPA and the private sector are mentioned as acting institutions. The government is highly dependent on development aid. In 2002, payments of bi-national and multinational donors contributed 68.7% to the national income (République du Bénin 2002).

Producer organisations (*groupement villageois*) and regional centres for rural development (CARDERs) were founded in the eighties in order to organize cotton production. The CARDERs (now CeRPAs) supply the producer organisations with input, give advices and buy cotton from the producer organisations. Ox-ploughing and agrarian credits were introduced. In the nineties, structural adjustment programmes weakened the national agencies considerably. Today, the CeRPAs promote above all the production of individual crops and monocultures instead of general sustainable production methods (MAEP 2004).

UNCCD structures

The Republic of Benin signed and ratified the United Nations convention to combat desertification (UNCCD) in 1994 and 1996. The ten-year national action plan to combat desertification (PAN/LCD) was approved in 1999 (MEHU 1999). The plan identified eight prior intervention topics, among them the efficient management of water resources and land tenure and land management issues. An inter-sectoral and multidisciplinary national committee (CNLD) was established with a permanent secretary at the MEPN (MEHU 2005). The participation of the civil society is warranted by a hierarchic participation of NGOs. In 1997, three NGOs (Friends of the Earth, Benin21, ACED) formed a national network, called RIOD Benin, which is now supported by the three founder NGOs plus six further NGOs as representatives for the twelve departments. In the Upper Ouémé catchment, the development

association ADD Ndali and the NGO CJEBBS represent the NGOs in the departments Borgou/Alibori and Atacora/Donga (oral comm. ZANOUE). An evaluation report (MEHU 2005) identified several constraints of the PAN/LCD. First, the programme was formulated without a logical framework defining the objectives, indicators and the evaluation procedure. Second, there is a lack of coordination between the sector-specific interventions in different sectors and most executed projects are not directly initiated by the PAN/LCD. Furthermore, financing from the national budget, international funds and NGOs is insufficient.

9.2.2. Promoted soil conservations measures

A large variety of soil conservation measures has been promoted in Benin during the last several decades. The advantages and disadvantages of each measure are summarized in Table C.2 in Appendix C. In the following, the measures are described within the categories of cultural technology and soil tillage, plant management, fertiliser and general conditions. Further details about soil conservation measures in Benin can be found in De Haan (1998), Gandonou (2000), FAO (2001a), GTZ-AFD (2004), GTZ-AFD (2003), Fadohan (2004), Gantoli (1997), and INRAB (2001, 2002).

Cultural technology and soil tillage

Field limitations of earth, stone walls or bushes and tillage directions perpendicular to the slope were promoted by several projects, including UNSO and PGTRN (GTZ-AFD 2004). Figure 9.8 illustrates two promoted tillage directions: perpendicular to the slope and shifted earth mounds for yam cultivation (*en quinconce*). Although most farmers in the Upper Ouémé catchment are aware of the relationship between tillage direction and erosion, many prefer a slope direction parallel to the slope to improve drainage in order to avoid water stagnation around the crop, which could lead to yield losses (Mulindabigwi 2006). In order to prevent erosion and a loss of soil humidity from the bare yam mounds at the beginning of the rainy season, some ethnic groups cover the tops of the mounds with mulch or mud (see Fig. 9.5a).

Due to the absence of mechanisation, tillage is quite reduced. Ox-ploughing is only widespread in the northern Borgou department, where it was introduced by UNDP and the World Bank in the seventies for cotton production (De Haan 1998). In the

Upper Ouémé catchment, ox-ploughing is only relevant in the northern part. Studies on erosion plots in Alafiarou in the south-eastern part of the catchment showed positive effects of ox-ploughing resulting from increased infiltration rates (oral comm. Azontonde, CENAP). However, many environmental experts consider zero tillage with crop residues as mulch as a better option than ploughing.

As mentioned in Chapter 3, massive anti-erosive structures were widely promoted in the seventies and eighties but were only adopted in areas with steep slopes and stony soils, like the Atacora Mountains. Gandonou (2000) mentioned as traditional anti-erosive measures for medium and steep slopes in this region stone strips (*Cordons pierreux*), honeycomb structures (*Nids d'abeilles*) and partitioned fields (*Billonage cloisonné*).



Fig. 9.5 Promoted tillage directions on fields: (a) yam mounds *en quinconce*, (b) tillage direction perpendicular to the slope.

In inland valleys, hedgerows (*Haies de pourghère*), earth mounds and stone dams (*Micro-barrages en pieux*) are constructed to protect yam fields. However, these measures alone cannot stop soil erosion; changes in plant management are essential.

Plant management

Activities in the seventies focused on appropriate crops, improved varieties, diversification and the use of mineral fertiliser. In the eighties, in-situ production of biomass as organic fertiliser became more important. *Stylosanthes*, manuring and composted straw were promoted (Floquet et al. 2002). In the nineties, agricultural research and development projects in Benin put effort into establishing legumes as cover crops or components of agro-forestry systems in order to improve soil fertility and minimise erosion. Thus, integrated management of soil fertility was propagated.

National and international research institutes like INRAB, IITA and SFB Hohenheim tested the efficiency of several legumes on research stations in southern Benin and later in on-farm experiments. The legumes *Mucuna pruriens*, *Gliricidia sepium*, *Leucaena leucocephala* and *Cajanus cajan* were identified as most suitable. Other legumes, like the cover crop *Pueraria javanica* or the woody legume *Morengas sp.*, were rejected because they were less efficient in preventing soil erosion and soil fertility decline or led to strong crop yield losses (oral comm. Azontonde). Although alley-cropping experiments with *Leucaena leucocephala* in South Benin showed enormous increases in maize yield (oral comm. Azontonde), introduction at the farm level failed due to high labour and space requirements. Insufficient maintenance led to competition between hedges and crops and did not significantly increase the carbon levels of the soil (Wallace et al. 2005). *Cajanus cajan*, *Mucuna sp.* and *Leucaena leucocephala* were also promoted by several development projects like PGTRN, PPEA and PBEBE. Besides agro-forestry, the project PPEA propagated composting, excrement from animals, crop rotation, associations (e.g., maize/sorghum with groundnut, niebe/yam with gombo, maize with cowpea) and the distribution of crop residues after harvest or herbaceous biomass during the cropping season to maintain humidity and prevent erosion. Today, most farmers in northern Benin use the deep-rooted, drought-resistant legume groundnut in crop rotation to improve soil fertility. In the Upper Ouémé catchment, crop rotation also follows an alternating pattern of soil-degrading and soil-conserving crops (Mulindabigwi 2006). *Mucuna pruriens var. utilis* (see Fig. 9.6) was tested in 1983 by CENAP researchers as a very efficient, fast-growing cover crop that is sown 45 days after maize and completely covers the soil after maize harvest (Donovan & Casey 1998). *Mucuna*



Fig. 9.6 Cover crops in association with Maize: *Niebe sp.*



Mucuna sp.

reaches maturity in 150 to 200 days. Afterwards, it is slashed and left as a mat of decomposing leaves and stalks, into which the next crop is planted directly. The on-farm research project RAMR tested *Mucuna* in the Adja plateau in South Benin with 20 farmers in 1986/87 and observed spontaneous adoption by 103 farmers in the neighbourhood in 1989 (UNDP 2002). The main reason was the effective suppression of weeds (*Imperata*) through *Mucuna*. Because of this success, *Mucuna* was widely promoted in southern Benin and later also in northern Benin. The NGO Sasakawa Global 2000 promoted *Mucuna* through the extension services (CARDERS) and reached more than 40.000 Beninese farmers by 1997 (UNDP 2002). Although adoption rates were still high after 5 years (67%), many farmers finally abandoned the technology due to various constraints (see Table C.2 in Appendix C) (Floquet et al. 2002). In 2001, only 24% of the farmers in the villages where RAMR introduced *Mucuna* in 1986/87 were still applying the technology (UNDP 2002). Land scarcity in South Benin and high labour demand were the main reasons for this (FAO 2001a). Today, the cover crop niebe (see Fig. 9.6) is gaining popularity. Traditionally cultivated for consumption in the Couffo region, the new niebe variety *Vohounvo* is as effective as *Mucuna* as a cover crop and offers additional short-term benefits. When the first crop (maize or groundnut) grows between March and August, niebe follows as second crop from August to October (oral comm. Azontonde).

The fast-growing bushy legume *Gliricidia* was introduced by INRAB and SFB Hohenheim in 1985/1986 because legume trees needed high phosphorus contents and shaded too much. *Gliricidia* is planted in rows, and the regularly-cut



Fig. 9.7 Agro-Forestry: *Cajanus cajan*.



Gliricidia sepium.

branches and leaves are used as mulch to fertilise the soil (see Fig. 9.7). After two years of establishment, *Gliricidia* allows a settled cultivation of yam. The yam should alternate with maize or groundnut/niebe to prevent parasites (Maliki et al. 2002a). The project PGTRN promoted the *Gliricidia*-yam based cropping system from 2001 to 2003, reaching 168 farmers in the commune Ouaké. One of the target villages, Bandessar near Djougou, is part of the Upper Ouémé catchment. However, auto-diffusion was not achieved because the purchase of plants from nurseries was too expensive and direct seeding did not work well (GTZ-AFD 2004).

Vetiver hedges were introduced in 1995 by the IITA (see Fig. 9.8). Although propagated in the whole country, e.g., by the project PGTRN, adoption by farmers was only successful in a few cases. Nevertheless, *Vetiver* hedges are still promoted by projects like ProCGRN and PDRT in northern Benin.



Fig. 9.8 *Vetiver* hedges near Barei.

Several projects also promoted planting trees in the field (improved fallow). During the fallow period, these trees improve the soil properties and offer the benefits of valuable wood, natural essences or food. Some trees like *Azelia Africana* are cut after each fallow period (oral comm. Loconon, AGEDREN). The project PAEB North encouraged farmers in the forest region Bassila to keep trees or to plant young trees (up to 40 trees/ha) like *Acacia auriculiformis*, *Azelia africana*, *Milicia excelsa*, *Pseudocedrela kotchyi*, and *Khaya senegalensis* in their fields. *Acacia* fallow was also promoted for firewood production by the *Projet de Bois de Feu* between 1986 and 1995. In this period, more than 4000 Beninese farmers implemented *Acacia* fallow as forest or as fallow (Floquet et al. 2002). The managed tree fallows were well accepted by farmers as they directly refer to their traditional understanding of soil fertility management.

Development projects that tried to sensitize the population to the negative effects of regular burning often had great difficulty in convincing farmers, because they burn for multiple purposes like hunting, prevention of snake infestations, a better view of the terrain, a quick release of nutrients, facilitation of land preparation, reduction of pests and diseases and re-growth of young cattle forage. Demonstration plots showing the negative impact of bush fires on soil and vegetation and the fertilizing effects of crop residues only produced to action in land-scarce regions, like the commune Ouaké. In several communes in the Borgou, bush fires are prohibited, but farmers often continue burning (De Haan 1998). Therefore, many projects (e.g., PAEB North) at least recommend early fires in November/December and promote honey production in order to indirectly achieve protection of natural resources (oral comm. Loconon).

Last but not least, the use of organic and mineral fertiliser is propagated over the whole country. Several research studies in Benin (e.g., Dagbenonbakin 2005) showed that the use of mineral fertiliser, or even more efficiently, the combination of mineral and organic fertiliser, can significantly increase crop yields, especially for maize. Unfortunately, most research studies are too short to observe differences in chemical soil properties. Most agronomists recommend the use of mineral fertiliser despite the negative effects on base saturation and soil acidity in the long run. However, fertiliser use in the Upper Ouémé catchment is restricted to cotton and maize because of economic constraints such as high prices, low income of farmers and difficult access to fertilisers and credits. Moreover, fertiliser recommendations are often inadequate and many farmers do not use improved seeds that are much more sensitive to mineral fertiliser. Organic fertiliser from animal husbandry is also difficult for most farmers to access and requires enormous labour effort. Many farmers allow herders to graze their field after harvest, but trading of manure is very uncommon. Semi-sedentary Fulani herders often practice mobile parking of cattle on their fields but more seldom cooperate with farmers (Maliki et al. 2002b). Projects like PGRN, PGTRN and ProCGRN have had some success in promoting composting.

To sum up, a broad variety of measures has been tested on research stations and farmers' fields and promoted for wider replication in Benin. From the point of view of farmers and herders, each measure has several advantages and constraints (see Table C.2 in Appendix C) that can differ enormously between regions, farmers and herders or ethnic groups.

9.2.3. Challenges in implementing soil conservation measures

In Benin, adoption rates for soil conservation measures are often low, although many have been promoted for decades. Most introduced measures are only applied very locally and by a small percentage of farmers in the region. Measures do not spread easily to neighbouring regions. Experiences in other African countries have been similar. It is not easy to find examples of comprehensive success from which to learn lessons. Effective soil conservation is a complex task that requires developing profitable techniques, spreading knowledge, policy alignment and continuous monitoring (Donovan & Casey 1998). In Benin, the technologically most efficient measures against soil degradation often show the lowest adoption rates because of the high labour demand and the lack of short-term benefits. One must keep in mind that agro-forestry systems need to be well managed to achieve potential benefits. Except for groundnut and *niebe*, most legumes did not provide short-term benefits like wood, fruits, essences, food, fodder and weed control. However, a few measures have been widely adopted. Among them are chemical fertilisation of maize fields and composting in the Boukoumbé region (Gandonou 2000), diversification of crops and the use of groundnut in crop rotation. Furthermore, the interventions improved the motivation of farmers to adapt endogenous methods.

Many explanations for the failure of soil conservation projects in Sub-Saharan Africa are discussed in the literature (e.g., Steiner, 1994; Bergsma, 2004; Gandonou, 2000; Penning de Vries et al., 1998; ICRA, 2003). They often refer to socio-economic factors, such as availability of labour and capital, security of tenure and institutional deficits that determine farmers' responses to technological solutions presented by researchers. For example, knowledge about local land tenure is essential for the success of development projects promoting reforestation, agro-forestry or cashew plantations (see Excursus 9.1). However, only very few projects, like PAMF and PGTRN explicitly addressed land tenure issues (Singer 2005). The project PGTRN introduced land tenure plans and a simplified land register for rural areas.

In the following, the main obstacles at the farmer, project and national levels are discussed in the case of Benin (see Table 9.3).

Excursus 9.1: Land tenure situation in the Upper Ouémé catchment

In the Upper Ouémé catchment dominates the traditional land tenure system, the official registration is often not known in the rural areas. Traditionally, land is a collective, spiritual, non-saleable resource, hold in trust by the earth-priest who distributes the land and mediates land-related conflicts. Most marginalised groups in the land tenure system are the non-owners, in particular tenants, pastoralists and women (Neef 1999). Women receive land from male family members. Allochthonous can ask the earth-priest for leasing a portion of land for a symbolic rent, often natural products for the lineage or a collective of landowners. In times of increasing land scarcity different forms of rent (cash, natural products, labour) become more important (Doevenspeck 2005). The usage rights for pasture land are based on a common law system and are not specified. As a consequence of large agricultural expansion forced by migration, the land tenure situation for allochthonous in the Upper Ouémé catchment has been deteriorated steadily during the last 10 to 20 years (Singer 2005). Despite a still high potential for extensive agricultural land in the southern Borgou department a shortage of land resources can be observed resulting in a monetarisation and higher restrictions of land usage rights for allochthonous groups depending on date of settlement (Singer 2005). Traditionally, allochthonous are not allowed to plant trees because this would automatically guarantee their land usage rights (Schneider 1997; Adjei-Nsiah et al. 2006). Nowadays, immigrants in many villages get less fertile lands and have to pay higher tributes in form of man power. The land tenure system fosters the land intensive, unsustainable yam-cropping system by migrants and the establishment of cashew plantations by local farmers because the cultivation of land secures the land property rights (Doevenspeck 2005). While In South Benin and parts of Central Benin land scarcity leads to an increase of conflicts about land sales, border lines and rent modalities, this is not yet the case in the Upper Ouémé catchment. Here, land conflicts refer mainly to traditional conflicts between farmers and herders. Farmers often perceive that livestock destroys their fields and herders see their pastures and traditional trails endangered through the enormous expansion of agricultural land (Gantoli 1997).

Farmer level

Development projects, NGOs and the extension services do not reach all farmers in Benin. However, even in the intervention areas of development projects, long-term adoption rates of soil conservation measures are usually low (Gandonou 2000). Obviously, the management practices were not profitable from the farmer's point of view. During the last 10-15 years, the analysis of factors for non-adoption and the

political conditions have become a major focus of applied agricultural research in Benin. Several authors have systematically assessed positive factors and constraints with regards to the adoption of soil conservation measures from the farmer's point of view (e.g., Floquet et al., 2006; Gantoli, 1997; Fadohan, 2004).

Table 9.3 Institutional obstacles for the sustainability of development projects dealing with soil conservation in Benin (various sources: ¹Singer, 2005; ²oral comm. Azontonde; ³Doevenspeck, 2005; ⁴GTZ-AFD, 2003).

Principles for sustainability	Obstacles in Benin
Participation & ownership	Exclusion of farmers in project design and evaluation
Continuous capacity building	Weak agricultural research and extension service, low personal and financial capacities of NGOs, development projects cannot replace continuous agricultural consultancy ² , lack of capacities at the village level ⁴
Accordance to government policies	Soil management no priority, no comprehensive national strategy
Financial independence after project end	Difficult to achieve due to low capacities
Management, avoid parallel structures	Parallel structures exist, lack of coordination among donors and with government
Social conditions, Understanding local decision-making	Local political structures not adequately considered (exclusion of some groups like migrants, profit of male and female elites) ¹
Adapted technologies	Agricultural research not applied enough, insufficient incorporation of endogenous knowledge; insufficient cooperation between donors, NGOs, researchers and extension service
Farmer's needs	Response to degradation often migration ³ , focus on short-term needs, additional labour-demand vs. non-mechanized agriculture, insecure land tenure
Positive environmental effects	Also negative effects ¹ , e.g. indirect promotion of agricultural expansion
Realistic duration	Only a few long-term projects, lack of follow up activities

An assessment of soil conservation activities in the region revealed that the highest adoption rates were obtained for measures with large immediate, additional benefits, minimal costs and limited labour efforts. In general, all farmers tried to minimize labour, accepting lower efficiency (oral comm. Loconon; Gandonou, 2000). In fact, labour limitations at the beginning of the growing season are a widespread phenomenon among poor farming households, frequently leading to poor yield by late planting or untimely weeding (Donovan & Casey 1998). As a consequence, agro-forestry systems were adopted in lower densities (oral. comm. Loconon, Floquet et al. (2006)). For example, the legume *Gliricidia* was planted scattered on the field instead of the prescribed planting in dense rows (Fadohan 2004).

For the same reason, stone walls were only established on stony fields and organic fertiliser use was usually restricted to home fields in the Atacora region (Gandonou 2000). Floquet et al. (2006) investigated the adoption rates of soil conservation measures promoted by the SFB Hohenheim (1994-1999). By 1998, 20% of the farmers who took part in the experiments had transferred at least one technology to further plots. In 2005, 65% of participating farmers in southern Benin still applied the *Acacia* fallow. All other techniques, i.e. alley-farming with *Gliricidia sepium*, live fences with *Senna siamea*, *Cajanus cajan* as a short fallow and *Mucuna utilis* as a cover crop, had been rejected after the end of the project. The *Acacia* fallow remained attractive due the easy handling and high benefits by marketing the wood at nearby markets. In Central Benin, a modification of the yam-based alley-cropping system showed the highest adoption rates. Farmers had reduced the shrub density and NGO researchers had added a cover crop. The adoption rates at the sites in Central Benin were lower than in the South but had not yet reached a plateau.

It is often argued that soil conservation measures are only widely adopted if they offer short-term economic benefits or if the problem of soil degradation is already severe. This also seems to be true for Central Benin. Experiences in the northern Borgou showed that conservation measures had little success because the final solution to environmental degradation for most people was to migrate to colonization areas in the region (De Haan, 1998; Doevenspeck, 2005). It is difficult to judge if farmers in Central Benin are unwilling to invest in the long-term fertility of their land as long as land resources are available in neighbouring regions, or if a farmer's behaviour is only a consequence of wrong project design and a lack of understanding of the farmer's perceptions of soil degradation and the farming system. It is important to consider that risk minimisation, not necessarily yield maximisation, is the dominant strategy of most farmers as long as no alternative income is available. Therefore, farmers rely on long distances between fields, crop diversification, and mixed cropping, and do not invest in fertiliser.

In the strongly degraded regions in South and Central Benin, like the Adja plateau or the commune Dassa Zoumé, farmers more frequently adopted soil conservation measures. Unfortunately, in these areas, fallow periods are already very short or completely gone so that many measures, like improved fallows or other space-demanding measures, are no longer applicable. Furthermore, the organic carbon

content of degraded soils is so weak that mineral fertiliser is less effective (Maliki et al. 2002a). Maliki et al. (2003) emphasized that the profitability and therefore adoption success depends not only on the degree of land degradation but also on the exploitation type, the age and the land tenure status of the farmer (see Fig. 9.9). Whereas traditional farmers were interested in soil conservation measures as long as they were not too labour-intensive, migrants were less interested due to their cash orientation and difficult land tenure status. Farmers who already practiced an integration of agriculture and animal husbandry were clearly less interested in agroforestry and cover crops. Adult men had the highest adoption potential for agroforestry, while young men preferred mineral fertiliser. Old men, women and migrants allochthonous had the lowest adoption potential for agroforestry (Maliki et al. 2001).

Project level

Many early projects failed due to deficiencies in the participation process. To a certain degree, this situation in Benin has improved during the last fifteen years due to more participative and multi-sectorial development and research projects, the stronger role of local NGOs and an added focus on accompanying short-term benefits for farmers. Furthermore, activities have shifted from massive anti-erosion structures to low-tech improvements of agricultural systems. Nevertheless, several deficiencies in project design still exist.

Floquet et al. (2002) identified an insufficient focus on the different clients and a lack

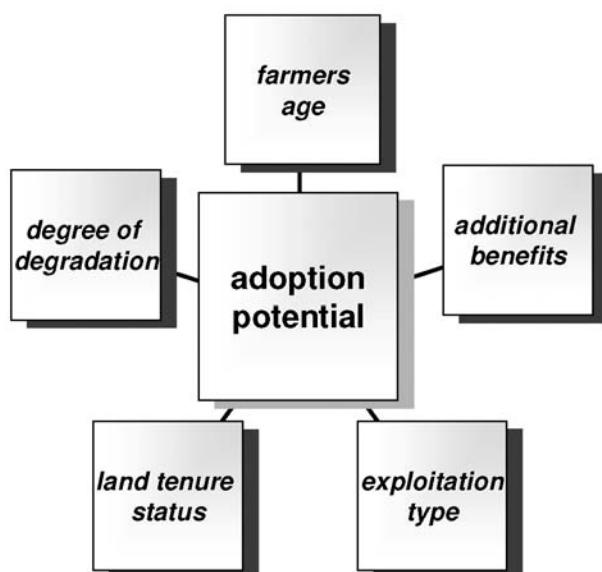


Fig. 9.9 Factors influencing the adoption potential for soil conservation measures.

of adaptation of technologies to different degrees of soil degradation and soil types as the main reasons for the low adoption rates in the heavily degraded *terre de barre* region in South Benin. Singer (2005) stated that the current resource management projects in the Upper Ouémé catchment will not be able to initiate sustainable land use in the area. He argues that the current emphasis of development aid on socio-economic infrastructure and income generation through diversification and

micro-credits for women indirectly enhances the expansion of unsustainable production methods. He outlines how micro-credits promote agricultural production by women and enhance cashew plantations. Furthermore, timber logging is a common source of financial contributions to projects in times of village financial difficulty due to low cotton production. The unsustainable production of cotton and the exhaustive cultivation of yam as a cash crop and charcoal by migrants are not addressed by development projects. As a positive exception, Singer (2005) mentions the GTZ project sequence PGRN-PGTRN-ProCGRN, which introduced a settled yam cultivation system with *Gliricidia*. On the other hand, Singer (2005) admits that the recent priorities result from the failed implementation of sustainable production methods in the eighties when farmers gave no priority to this topic following risk minimisation strategies. Until now, agricultural consultancy has not been attractive to the private sector because farmers are used to free consultancies and free provision of new technical equipment.

National level

The sustainable use of land resources requires appropriate policies and institutional arrangements to encourage the intensification of smallholder farming systems (Dejene et al. 1997). The dysfunction of the agricultural extension services (CeRPAs) is one of the main obstacles to effective implementation of integrated soil fertility management in Benin. Extension services cannot be replaced by development projects with short durations and limited intervention areas or by NGOs who are financially completely dependent on projects. Fortunately, the CeRPAs are currently receiving increased attention and substantial additional financial resources to extend their staff and improve their services.

The absence of a comprehensive national programme for integrated soil fertility management is an additional constraint. In addition, the communication between research institutions and NGOs is insufficient. Local NGOs often adapt and translate the instruction manuals for soil fertility management published by INRAB, including farmers' needs (oral comm. Loconon). Unfortunately, their knowledge about local adoption preferences is often not transferred to national research institutions and other NGOs. Last but not least, efforts against soil degradation are also hampered by gaps in agricultural research knowledge and an insufficient funding of the national action plan to combat desertification.

The analysis of the adoption constraints during the last 10-15 years also reveals that the direct promotion of measures by individual model farmers cannot initiate a large scale extension of technologies in Benin (Floquet et al. 2002). Therefore, three new extension strategies are currently being tested (Amadji et al. 2003). The new approaches employed by CeRPA agents or NGOs include the formation of pairs of farmers, educating students in schools who can communicate the technical dossiers to their parents and engaging voluntary farmers as examples. Strong effort is being put into improving and completing appropriate technical material by INRAB and several NGOs. These promising approaches to increase sustainable land management activities are supported by various actors like ABE, GTZ, ILRI, INRAB and PADSE.

9.3. Recommendations

As illustrated in the previous section, effective soil conservation is a complex task that requires not only extensive knowledge about the farming systems but also a deep understanding of the socioeconomic and institutional settings in a country. Many long term measures must be taken at different levels to widely improve soil and plant management in Benin, which is crucial for sustainable land use, poverty reduction, food security and adaptation to climate change. For example, Bokonon-Ganta et al. (2003) estimates crop yield losses in the department of Collines due to climate change to be 6-30% by 2025 depending on the crop type using the DSSAT model. Socioeconomic scenarios lead to a potential crop yield decrease of 10-40%. Current trends of decreasing yields for the main crops of yam, sorghum and cassava in some parts of Benin, like the Atacora region (Gantoli 1997), can only be reversed if the problem of soil degradation is addressed. In the face of rapid expansion of cropping areas and climate change, this is becoming even more urgent. Based on the findings presented in this work and discussions with various stakeholders in Benin, we provide several recommendations for the different actors.

Government agencies

Improving the institutional framework conditions is crucial for sustainable soil management. The national extension services (CeRPAs) must be strengthened through substantial investments (as is currently being done) and capacity building,

and focus on general sustainable production methods instead of individual crops, such as cotton. Furthermore, a participative modernisation of traditional land tenure and temporary incentives for soil water conservation measures via fertiliser subsidies or micro-credits and farmer field schools are required.

A national strategy for sustainable land management and a comprehensive program for integrated fertility management are needed. Cooperation between donors, CeRPAs, INRAB, NGOs and the private sector in promoting improved agricultural technologies needs to be strengthened and better address farmers' needs. The success of soil conservation activities should be continuously monitored using indicators like adoption rates, rates of soil erosion and crop yields. Soil conservation activities should be extended and better coordinated with the national UNCCD structures and efforts to adapt to climate change. The National Adaptation Programme of Action (NAPA) of Benin, which was published in January 2008, includes a project proposal for improved water resources management in Central and Northern Benin, mainly focusing on education and stabilisation and reforestation of slopes and riparian zones. Efforts to combat soil degradation and adapt to climate change need to go beyond this and also address soil and plant management in the fields.

Aid donors

Donors should support the governmental institutions (e.g., MAEP, MEPN, ABE, INRAB) in formulating and implementing a comprehensive strategy for managing soil fertility in Benin and must make long term financial commitments for funding research and development projects to address soil fertility management. Development projects should foster stronger linkages between national research institutions and their counterparts, as well as NGOs, to improve coordination of soil fertility management research and technology development. Development projects should strengthen existing institutions (e.g., CeRPAs) and enable them to scale up soil conservation activities.

At the project level, migrants should be explicitly addressed as a target group because many of them practice slash-and-burn agriculture for commercial yam-cropping and charcoal production, which has strong negative environmental effects. The settled yam-based cropping system with *Gliricidia* promoted by ProCGRN could address this problem if the security of land tenure is improved. Although the adoption

potential for soil conservation measures is higher in regions where land is scarce and soils are already severely degraded, activities should not be restricted to these areas. Measures in not yet intensively used regions, like large parts of the Upper Ouémé catchment, can successfully prevent a deterioration of the physical soil properties and be attractive for farmers if they offer additional short-term benefits and require limited labour. Thus, activities to promote soil conservation should be increased in the entire catchment, but in particular in the north-western part of the Upper Ouémé catchment and around Parakou, because these areas are current and future hotspots of soil degradation in the catchment. For example, the project ProCGRN acting in the departments Atacora and Donga could extend its activities to the north-western part of the catchment (communes Copargo and Djougou). Previous efforts to support the government in establishing land use planning at the national and communal levels should be enhanced.

Research

Research must address soil erosion, nutrient depletion and land management practices in an integrated way. To achieve increased use of organic and mineral fertilisers by farmers, a key element for sustainable soil management in Africa, agricultural research in Benin may focus on the following areas: i) improving methods for an integrated management of soil fertility, e.g. the combination of mineral fertiliser with *Acacia* or *Mucuna* (Floquet et al. 2002), ii) stronger participation of farmers in identifying and evaluating soil conservation measures, iii) developing profitable technologies for different target groups, e.g., the transformation of *Mucuna* as fodder or the test of fire-resistant cover plants (Floquet et al. 2002) and iv) using crop models to model crop growth, nutrient flows and the effectiveness of fertiliser.

With regard to soil erosion, similar studies should be conducted in other parts of Benin using efficient and robust models with relatively low data requirements to quantify sediment yields and identify hotspots at the catchment scale. Since most policy makers are more interested in effects on crop production rather than soil erosion per se, crop models must be used to link erosion to productivity loss and analyse the effects of different soil and plant management strategies on sediment and crop yields. Ideally, soil loss tolerances could be derived by building on the extensive knowledge of changes in soil properties and associated production losses from national research.

In the framework of IMPETUS, the crop model EPIC has been used to simulate crop yields in the Upper Ouémé catchment using the same spatial discretisation and land use and climate change scenarios as in this work (see Gaiser et al. 2006). Based on the results from the SWAT and EPIC models for the Upper Ouémé catchment, a common spatial decision support system (SDSS) called PEDRO (*Protection du sol et durabilité des ressources agricoles dans le bassin versant de l'Ouémé*) has been developed and discussed with various stakeholders in Benin (see Gaiser et al., 2008; IMPETUS, 2008). The SDSS quantifies changes in river discharge, sediment yield, crop yield, agricultural production and the balance of food demand and food production for the presented climate and land use change scenarios. Furthermore, the effects of user-defined crop management practices on crop production and food security can be evaluated at the regional scale (Gaiser et al. 2008). Such spatially explicit decision support systems are still in their infancy but can, if designed in close collaboration with the target audience, be very powerful tools to communicate complex, spatially explicit research results to decisions makers and support them in planning. Although the application potential of SDSSs such as PEDRO for decision makers in Benin may be limited due to the barely existing land use planning, they enhance their understanding of modelling studies and scenario analyses and help to improve knowledge sharing between science and policy.

10. Literature

Adjei-Nsiah, S., A. Saidou, D. Kossou, O. Sakyi-Dawson & T. W. Kuyper (2006). Tenure security and soil fertility management: Case studies in Ghana and Benin. Colloque international "Les frontières de la question foncière - At the frontier of land issues, Montpellier. http://www.mpl.ird.fr/colloque_foncier/Communications/PDF/Adjei%20Nsiah.pdf (accessed: 30.06.2008)

AG Boden (1994). Bodenkundliche Kartieranleitung, 4.Auflage. Bundesanstalt für Geowissenschaften und Rohstoffe und Geologische Landesämter. Stuttgart, Schweizerbart'sche Verlagsbuchhandlung. 392 Seiten.

Agossou, V. & M. Igue (2003). Caractérisations paysanne et scientifique des sols des sites d'expérimentation agricole de la région centrale du Bénin. In: Actes 1 de l'Atelier Scientifique Centre du Benin du 18 au 19 décembre 2002, Dassa, INRAB.

Ahn, P. (1970). West African Soils. Oxford (UK), Oxford University Press. 332pp.

Allen, R. G., M. E. Jensen, J. L. Wright & R. D. Burman (1989). "Operational estimates of evapotranspiration." Agronomy Journal 81: 650-662.

Amadji, F., I. Adje, R. Maliki & M. Roesch (2003). Gestion durable des terres avec des légumineuses herbacées: approches techniques et méthodologiques en vue de l'adoption des technologies. In: Actes 1 de l'Atelier Scientifique Centre du Benin du 18 au 19 décembre 2002, Dassa, INRAB.

Anhuf, D. (1994). Satellitengestützte Vegetationsklassifikation der Côte d'Ivoire. Mannheimer Geographische Arbeiten. 45: 190 Seiten.

Arnold, J. G., R. Srinivasan, R. S. Muttiah & J. R. Williams (1998). "Large area hydrologic modeling and assessment part I: model development." Journal of the American Water Resources Association 34(1): 73-89.

Arnold, J.G. & P. M. Allen (1999). "Validation of automated methods for estimating baseflow and groundwater recharge from stream flow records." Journal of the American Water Resources Association 35 (2): 411-424.

Arnold, J. G., R. S. Muttiah, R. Srinivasan & P. M. Allen (2000). "Regional estimation of base flow and groundwater recharge in the Upper Mississippi river basin." Journal of Hydrology 227: 21-40.

Atwood, J. D. (2001). Simulated nitrogen loading from corn, sorghum and soybean production in the Upper Mississippi Valley. In: Sustaining the Global Farm. Selected papers from 10th ISCO meeting. D. E. Stott, R. H. Mohtar and G. C. Steinhardt: 344-348. <http://topsoil.nserl.purdue.edu/nserlweb/isco99/pdf/ISCOdisc/SustainingTheGlobalFarm/P133-Atwood.pdf> (accessed: 30.06.2008)

Auerswald, K. (1993). Bodeneigenschaften und Bodenerosion. Berlin, Gebrüder Borntraeger Verlag. 208 Seiten.

Balek, J. & J.E. Perry (1973): "Hydrology of seasonally inundated African headwater swamps." Journal of Hydrology 19: 227 – 249.

Barsanti, P., L. Disperati, P. Marri & A. Mione (2003). Soil erosion evaluation and multitemporal analysis in two Brazilian basins. In: Proceedings of the 2nd International SWAT conference. 266: 117-130.
<http://www.brc.tamus.edu/swat/conferences.html>

Benaman, J. & C. A. Shoemaker (2005). "An analysis of high-flow sediment event data for evaluating model performance." Hydrological Processes 19: 605-620.

Beven, K. J. (2001). Rainfall-Runoff Modelling. The Primer. Chichester, Wiley. 360pp.

Bingner, R. L., J. Garbrecht, J. G. Arnold & R. Srinivasan (1997). "Effect of watershed subdivision on simulation runoff and fine sediment yield." Transactions of the American Society of Agricultural Engineers 40(5): 1329-1335.

Bokonon-Ganta, B. E., E. Ogouwale & M. Fakorede (2003). Vulnérabilité de l'agriculture aux changements climatiques dans la région des Collines (Centre du Bénin): Quelles stratégies d'adaptation? In: Actes 1 de l'Atelier Scientifique Centre du Bénin du 18 au 19 décembre 2002, Dassa, INRAB.

Bollinne, A & Rosseau, P. (1978). Erodibilité des sols de moyenne et haute Belgique. Utilisation d'une méthode de calcul du facteur K de l'équation universelle de perte en terre. – Bull. Soc. Géogr. de Liège 14: 127-140.

Bonell, M. (1999). "Tropical forest hydrology and the role of the UNESCO." International Hydrological Programme. Hydrology and Earth System Sciences 3(4): 451-461.

Bonell, M. (2005). Forests, water, and people in the humid tropics. Past, present, and future hydrological research for integrated land and water management. Cambridge, Cambridge University Press. 958pp.

Bonnell, M. & J. Balek (1993). Recent Scientific Developments and Research Needs in Hydrological Processes of the Humid Tropics. In: Hydrology and Water Management in the Humid Tropics. M. BONELL, M. M. HUFSCHMIDT and J. S. GLADWELL: 167 – 260.

Boorman, D. B. (2003). "Climate, Hydrochemistry and Economics of Surface-water Systems (CHESS): adding a European dimension to the catchment modelling experience developed under LOIS." Science of the Total Environment 314: 411-437.

Borah, D. K. & M. Bera (2004). "Watershed-scale hydrologic and nonpoint-source pollution models: Review of applications." Transactions of the ASAE 47(3): 789-803.

Bormann, H. & B. Diekkrüger (2003). "Possibilities and limitations of regional hydrological models applied within an environmental change study in Benin (West Africa)." Physics and Chemistry of the Earth, 28(33-36): 1323 – 1332.

Bormann, H. & B. Diekkrüger (2004). "A conceptual, regional hydrological model for Benin (West Africa): Validation, uncertainty assessment and assessment of applicability for environmental change analyses." Physics and Chemistry of the Earth, 29(11-12): 759 – 768.

Bracmort, K. S., M. Arabi, J. R. Frankenberger, B. A. Engel & J. G. Arnold (2006). "Modeling long-term water quality impact of structural BMPs." Transactions of the ASABE 49(2): 367-374.

Brasington, J. & K. Richards (2000). "Turbidity and suspended sediment dynamics in small catchments in the Nepal Middle Hills." Hydrological Processes 14: 2559-2574.

Bremer, H. (1995). Boden und Relief in den Tropen. Berlin-Stuttgart. Gebrueder Borntraeger. 324 Seiten.

Bronstert, A. & E. J. Plate (1997). "Modelling of runoff generation and soil moisture for hillslopes and micro-catchments." Journal of Hydrology 198: 177-195.

Busche, H. (2005). Modellierung hydrologischer und erosiver Prozesse im Terou-Einzugsgebiet (Benin) unter der Annahme von Landnutzungs- und Klimaänderung. Geographisches Institut. Bonn, Universität Bonn. Examensarbeit. 113pp.

Calder, I. R. (1992). Hydrologic effects of land use change. Handbook of Hydrology. D. R. Maidment. New York, McGraw-Hill: 13.1 – 13.50.

Chaplot, V., A. Saleh, D. B. Jaynes & J. Arnold (2004). "Predicting water, sediment and NO₃-N loads under scenarios of land-use and management practices in a flat watershed." Water, Air and Soil Pollution 154: 271-293.

Chappell, N. A., I. Douglas, J. M. Hanapi & W. Tych (2004). "Sources of suspended sediment within a tropical catchment recovering from selective logging." Hydrological Processes 18(4): 685-701.

Chaubey, I., A. S. Cotter, T. A. Costello & T. S. Soerens (2005). "Effect of DEM data resolution on SWAT output uncertainty." Hydrological Processes 19: 621-628.

Chen, E. & D. S. Mackay (2004). "Effects of distribution-based parameter aggregation on a spatially distributed agricultural nonpoint source pollution model." Journal of Hydrology 295(1-4): 211-224.

Chevalier, A. (1990). "Les zones et les provinces botaniques de l'Afrique occidentale française." C.R. Acad. Sci.: 1205-1208.

Ciesielski (1997). "A comparison between three methods for the determination of cation exchange capacity and exchangeable cations in soils." Agronomie 17: 9-16.

Coffey, M. E., S. R. Workman, J. L. Taraba & A. W. Fogle (2004). "Statistical procedures for evaluating daily and monthly hydrologic model predictions." Transactions of the ASAE 47(1): 59-68.

Cotter, A.S., Chaubey, I., T. A. Costello, T. S. Soerens & M.A. Nelson (2003). "Water quality model output uncertainty as affected by spatial resolution of input data". Journal of the American Water Resources Association 39 (4): 977-986.

Dagbenonbakin, G. (2005). Productivity and water use efficiency of important crops in the Upper Oueme Catchment - influence of nutrient limitations, nutrient balances and soil fertility. Bonn, University of Bonn. Dissertation. 165pp.

[http://hss.ulb.uni-](http://hss.ulb.uni-bonn.de/diss_online/landw_fak/2005/dagbenonbakin_gustave/0634.pdf)

[bonn.de/diss_online/landw_fak/2005/dagbenonbakin_gustave/0634.pdf](http://hss.ulb.uni-bonn.de/diss_online/landw_fak/2005/dagbenonbakin_gustave/0634.pdf)

Dana, G. L., A. K. Panorska, R. B. Susfalk, D. McGraw, W. A. McKay & M. Dornoo (2004). Suspended sediment and turbidity patterns in the Middle Truckee River, California for the period 2002-2003: 82pp.

<http://www.truckee.dri.edu/tmdl/SedimentPatternsMiddleTruckeeDRI2004.pdf>

(accessed: 30.06.2008)

De Haan, L. (1998). Gestion de Terroir at the Frontier: village land management including both peasants and pastoralists in Benin. In: The Arid Frontier. Interactive Management of Environment and Development. H. J. BRUINS and H. LITHWICK Boston, Kluwer Academic Publishers: 209-277.

De Roo, A. J. (1993). Modelling surface runoff and soil erosion in catchments using geographical information systems; Validity and applicability of the "ANSWERS" model in two catchments in the loess area of South Limburg. Geography. Utrecht, Rijks-University of Utrecht. 157: 304pp.

De Roo, A. J. (1998). "Modelling runoff and sediment transport in catchments using GIS." Hydrological Processes 12: 905-922.

DED (2003). EO-Bericht 2003. Förderung entwicklungspolitisch relevanter Einheimischer Organisationen (EO) und Selbsthilfe-Initiativen (SHI). Deutscher Entwicklungsdienst (DED).

http://www.ded.de/cipp/ded/lib/all/lob/return_download,ticket,g_u_e_s_t/bid,1437/no_mime_type,0/~/eo_bericht2003a.pdf (accessed 30.06.2008)

Dejene, A., E. K. Shishira, P. Z. Yanda & F. J. Johnson (1997). Land degradation in Tanzania: perception from the village. World Bank Technical Paper: 370. Washington, D.C., World Bank. 79pp. http://lada.virtualcentre.org/eims/download.asp?pub_id=93841 (accessed 30.06.2008)

Di Luzio, M., R. Srinivasan & J. Arnold (2002). ArcView Interface for SWAT2000-Users Guide. Temple, Blackland Research Center. <http://www.brc.tamus.edu/swat/downloads/doc/swatav2000.pdf> (accessed 30.06.2008)

Dickinson, A. & R. Collins (1998). Predicting Erosion and Sediment Yield at the Catchment Scale. In: Soil erosion at multiple scales. Principles and methods for

assessing causes and impacts. Edited by F. W. T. PENNING DE VRIES, F. AGUS and J. KERR. Wallingford, UK, CABI Publishing: 317-342.

Doevenspeck, M. (2005). Migration im ländlichen Benin. Sozialgeographische Untersuchungen an einer afrikanischen Frontier. Fakultät für Biologie, Chemie und Geowissenschaften. Bayreuth, Universität Bayreuth. Dissertation. 282 Seiten.

Donovan, G. & F. Casey (1998). Soil Fertility Management in Sub-Saharan Africa. Word Bank Technical Paper 408. Washington, D.C., World Bank. 60pp.
http://www-wds.worldbank.org/servlet/WDSContentServer/WDSP/IB/1998/06/01/000009265_3980716172552/Rendered/PDF/multi_page.pdf

Dorronsoró, C. (2002). Soil evaluation. The role of soil science in land evaluation. Sustainable use and management of soils in arid and semiarid regions. In: SUMASS 2002. Cartagena 1. Quaderna Editorial. A. FAZ, R. ORITZ, A. R. MERMUT and M. 106-128. Murcia.

Douglas & Guyot (2005). Erosion and sediment yield in the humid tropics. In: Forests, Water and People in the Humid Tropics. M. BONELL and L. A. BRUIJNZEEL. Cambridge, Cambridge University Press: 407-421.

Dubroeuq, D. (1977a). Carte pédologique de reconnaissance de la République Populaire du Bénin à 1/200.000. Feuille de Save. Note explicative No. 66 (3). Paris, ORSTOM: 45pp.

Dubroeuq, D. (1977b). Carte pédologique de reconnaissance de la République Populaire du Bénin à 1/200.000. Feuille de Parakou. Note explicative No. 66 (5). Paris, ORSTOM: 45pp.

Dyck, S. & G. Peschke (1995). Grundlagen der Hydrologie. Berlin, Verlag für Bauwesen.

Eckhardt K., S. Haverkamp, N. Fohrer & H.-G. Frede, 2002. SWAT-G, a version of SWAT99.2 modified for application to low mountain range catchments. Physics and Chemistry of the Earth 27: 641-644.

El Fahem, T. (2008). Hydrogeological conceptualisation of a tropical river catchment in crystalline basement area and transfer into a numerical groundwater flow model - Case study for the Upper Ouémé catchment in Benin. Institute of Geology. Bonn, University of Bonn. Dissertation. 156 Seiten. http://hss.ulb.uni-bonn.de/diss_online/math_nat_fak/2008/el-fahem_tobias/el-fahem.htm

Fadohan (2004). Analyse technique et économique des systèmes agroforestiers diffusés par le projet de gestion des terroirs et des ressources naturelles (PGTRN) dans la commune de Ouesse (Département des collines): Cas de *Cajanus cajan* (LINN.) et de *Gliricida sepium* (jack) Walp. Ecole polytechnique d'Abomey-Calavi. Department des techniques d'aménagement et protection de l'environnement. Abomey-Calavi, Université d'Abomey-Calavi. Mémoire de fin de formation.

FAO-ISRIC-ISSS (1998). World Reference Base for Soil Resources. World Soil Resources Reports 84. FAO, Rome. 88pp.

FAO (1990). "Guidelines for soil profile description." Third edition (revised). FAO, Rome. 75pp.

FAO (2001a). The economics of soil productivity in sub-Saharan Africa. FAO, Rome. 58pp. <ftp://ftp.fao.org/agl/agll/docs/ecsoilpr.pdf> (accessed: 30.06.2008)

FAO (2001b). Soil fertility management in support of food security in Sub-Saharan Africa. FAO, Rome. 55pp. <ftp://ftp.fao.org/agl/agll/docs/foodsec.pdf> (accessed: 30.06.2008)

FAO (2005). Global Forest Resources Assessment 2005. Progress towards sustainable forest management. FAO Forestry Paper 147, 320pp. <http://www.fao.org/DOCREP/008/a0400e/a0400e00.htm> (accessed: 30.06.2008)

FAO (2006). The State of Food Insecurity in the World 2006. Eradicating world hunger - taking stock ten years after the World Food Summit. Rome, FAO: 40pp. <http://www.fao.org/docrep/009/a0750e/a0750e00.HTM> (accessed: 30.06.2008)

Fass, T. (2004). Hydrogeologie im Aguima Einzugsgebiet in Benin/Westafrika. Institute of Geology. Bonn, University of Bonn. Dissertation. 137 Seiten. http://hss.ulb.uni-bonn.de/diss_online/math_nat_fak/2004/fass_thorsten

Faure, P. (1977a). Carte pédologique de Reconnaissance de la République Populaire du Bénin à 1 : 200,000 : Feuille Djougou. Notice explicative 66 (4). Paris, ORSTOM: 49pp.

Faure, P. (1977b). Carte pédologique de Reconnaissance de la République Populaire du Bénin à 1 : 200,000 : Feuille Natitingou et Porga. Note explicative No. 66 (6+8). Paris, ORSTOM: 49pp.

Faure, P. & B. Volkoff (1998). "Some factors affecting regional differentiation of the soils in the Republic of Benin (West Africa)." Catena 32: 281-306.

Fink, A. H., D. G. Vincent & V. Ermert (2006). "Rainfall Types in the West African Sudanian Zone during the Summer Monsoon 2002." American Meteorological Society 134: 2143-2163.

Fistikoglu, O. & N. B. Harmancioglu (2002). "Integration of GIS with USLE in Assessment of Soil Erosion." Water Resources Management 16: 447-467.

FitzHugh, T. W. & D. S. Mackay (2000). "Impacts of input parameter spatial aggregation on an agricultural nonpoint source pollution model." Journal of Hydrology 236(1-2): 35-53.

Floquet, A., G. Amadji, M. Igue, R. Mongbo & J. Dahdovonon (2002). Le point sur les contraintes socio-économiques et agro-techniques à l'adoption des innovations de gestion de la fertilité des sols sur terres de barre: Synthèse de travaux réalisée par

un groupe de travail de l'initiative ERICA. In: Actes 2 de l'Atelier Scientifique Sud et Centre du Benin du 12 au 13 décembre 2001, Niaouli, INRAB.

Floquet, A., R. Maliki & Y. Cakpo (2006). Seven Years after the SFB 308 - Adoption Patterns of Agroforestry Systems in Benin. In: Proceedings of the Tropentag 2006 - Conference on International Agricultural Research for Development, Bonn. <http://www.tropentag.de/2006/proceedings/proceedings.pdf>

Fohrer, N., S. Haverkamp, K. Eckhardt & H.-G. Frede (2001). "Hydrologic Response to Land Use Changes on the Catchment Scale." Physics and Chemistry of the Earth 26(7-8): 577-582.

Fohrer, N., S. Haverkamp & H.-G. Frede (2005). "Assessment of the effects of land use patterns on hydrologic landscape functions: development of sustainable land use concepts for low mountain range areas." Hydrological Processes 19: 659-672.

Fölster, H., (1983). Bodenkunde - Westafrika (Nigeria-Kamerun). Afrika-Kartenwerk Beiheft W4. Berlin, Borntraeger. 102 Seiten.

Gaiser, T., H. Weippert, A.M. Igue & K. Stahr (2006). Application of the land resources information system SLISYS in the Oueme basin of Benin (West Africa). In: Proceedings of the Tropentag 2006 - Conference on International Agricultural Research for Development. <http://www.tropentag.de/2006/abstracts/full/183.pdf>

Gandonou, E. (2000). Lutte anti-érosive et gestion de la fertilité des sols dans la région Boukoumbé.

Gantoli, G.Y. (1997). Approche participative pour une meilleure gestion de la fertilité des sols. Expériences du Projet Promotion de l'Élevage dans l'Atacora. In: Proceedings of the workshop on erosion induced loss in soil productivity in Ghana 8-11 December, 1997. Edited by RACIM, S.A. QUANASAH, C. & R.D. ASIAMA. Nairobi, FAO Regional Office for Africa.

Gassman, P. W., T. Campbell, S. Secchi, M. Jha & J. Arnold (2003). The i SWAT Software Package: A tool for Supporting SWAT Watershed Applications. In: Proceedings of the 2nd International SWAT Conference: 229-234. <http://www.brc.tamus.edu/swat/conferences.html>

Gassman, P. W., M. R. Reyes, C. H. Green & J. G. Arnold (2006). SWAT Peer-Reviewed literature - A Review. In: Proceedings of the 3rd International SWAT conference, July 11-15, Zurich, Zurich, EAWAG. <http://www.brc.tamus.edu/swat/conferences.html>

Gassman, P. W., M. R. Reyes, C. H. Green & J. G. Arnold (2007). "The Soil and Water Assessment Tool: Historical development, applications, and future research directions." Transactions of the ASABE 50(4): 1211-1250.

Giertz, S. (2004). Analyse der hydrologischen Prozesse in den sub-humiden Tropen Westafrikas unter besonderer Berücksichtigung der Landnutzung am Beispiel des

Aguima-Einzugsgebietes in Benin. Institute of Geography. Bonn, University of Bonn. Dissertation. 233 Seiten.

http://hss.ulb.uni-bonn.de/diss_online/math_nat_fak/2004/Giertz_simone/

Giertz, S & G. Steup (unpublished). Inventarisation of inland valleys in the Upper Ouémé catchment, Benin. Field survey in 2006 in cooperation with Inland Valley Consortium Benin. Inland valley survey. Unpublished.

Giorgi, F., L. O. Mearns, C. Shields & L. McDaniel (1998). "Regional nested model simulations of present day and 2 x CO₂ climate over the central plains of the US." Climatic Change 40(3-4): 457-493.

Gitau, M. W., T. L. Veith & W. J. Gburek (2004). "Farm-level optimization of BMP placement for cost-effective pollution reduction." Transactions of the ASAE 47(6): 1923-1931.

Gobin, A. M., P. Campling, J. A. Deckers, J. Poesen & J. Feyen (1999). "Soil erosion assessment at the Udi-Nsukka Cuesta (Southeastern Nigeria)." Land Degradation & Development 10: 141-160.

Godjo, T., F. Amadji & I. Adjé (2003). Analyse du besoin et Etude des équipements existants pour le Fauchage du Mucuna utilis et de l'Aeschynomene histrix. In: Actes 1 de l'Atelier Scientifique Centre du Benin du 18 au 19 décembre 2002, Dassa, INRAB.

Govender, M. & C. S. Everson (2005). "Modelling streamflow from two small South African experimental catchments using the SWAT model." Hydrological Processes 19: 683-692.

Graef, F. (1999). Evaluation of Agricultural Potentials in Semi-arid SW-Niger – A Soil and Terrain (NiSOTER) Study. In: Hohenheimer Bodenkundliche Hefte 54. E. KANDELER, M. KAUPENJOHANN and K. STAHR. Stuttgart, Universität Hohenheim Institut für Bodenkunde und Standortslehre. 217pp.

Gray, J. R., T. S. Melis, E. Patino, M. C. Larsen, D. J. Topping, P. P. Rasmussen & C. Figueroa-Alamo (2003). U.S. Geological Survey Research on Surrogate Measurements for Suspended Sediment: 6pp.

<http://www.tucson.ars.ag.gov/icrw/Proceedings/Gray.pdf> (accessed: 30.06.2008)

Green, W. & G. Ampt (1911). "Studies on soil physics, 1. The flow of air and water through soils." Journal of Agricultural Sciences 4: 11-24.

Greenland, D. J. (Editor) (1981). Characterization of soils in relation to their classification and management for crop production: examples from some areas of the humid tropics. Clarendon Press, Oxford, England.

Greenland, D. J. (1994). Soil Science and Sustainable Land Management. In: Soil science and sustainable land management in the tropics. J. K. SYERS and D. L. RIMMER. Wallingford, CABI: 1-15

GTZ-AFD (2003). PGTRN-Ouake Rapport de fin de phase (1999-2003). Natitingou (Republique du Bénin).

GTZ-AFD (2004). PGTRN. Rapport de fin de phase (1998-2003). Cotonou (Republique du Bénin).

Hanratty, M. P. & H. G. Stefan (1998). "Simulation climate change effects in a Minnesota agricultural watershed." Journal of Environmental Quality 27: 1524-1532.

Hargreaves, G. L., G. H. Hargreaves & J. P. Riley (1985). "Agricultural benefits for Senegal River Basin." Journal of Irrigation and Drainage Engineering. 111(2): 113-124.

Hasenpusch, K. (1995). Nährstoffeinträge und Nährstofftransport in den Vorfluter zweier landwirtschaftlich genutzter Gewässereinzugsgebiete. Wissenschaftliche Mitteilungen der Bundesforschungsanstalt für Landwirtschaft. Sonderheft 158. Braunschweig-Vökenrode, Bundesforschungsanstalt für Landwirtschaft: 216 Seiten.

Hashim, G. M., K. J. Coughlan & J. K. Syers (1998). On-site Nutrient Depletion: An Effect and a Cause for soil erosion. In: Soil erosion at multiple scales. Principles and methods for assessing causes and impacts. F. W. T. PENNING DE VRIES, F. AGUS and J. KERR. Wallingford, UK, CABI Publishing: 207-222.

Hattermann, F., V. Krysanova & F. Wechsung (2003). Propagation of Uncertainty in Large Scale Ecohydrological Modeling. In: Proceedings of the 2nd International SWAT conference: 224-227. <http://www.brc.tamus.edu/swat/conferences.html>

Haverkamp, S. (2000). "Methodenentwicklung zur GIS-gestützten Modellierung des Landschaftswasserhaushaltes." Boden und Landschaft - Schriftenreihe zur Bodenkunde, Landeskultur und Landschaftsökologie 29. Dissertation.151 Seiten.

Haverkamp, S., Fohrer, N. & H.-G. Frede (2005). "Assessment of the effect of land use patterns on hydrologic landscape functions: a comprehensive GIS-based tool to minimize model uncertainty resulting from spatial aggregation." Hydrological Processes 19: 715-727.

Haverkamp, S., R. Srinivasan, H. G. Frede & C. Santhi (2002). "Subwatershed spatial analysis tool: discretization of a distributed hydrologic model by statistical criteria." Journal of the American Water Resources Association 38(6): 1723-1733.

Hernandez, M, S. C. Miller, D. C. Goodrich, B. F. Goff, W. G. Kepner, C. M. Edmonds & K.B. Jones (2000) "Modelling runoff response to land cover and rainfall spatial variability in semi-arid watersheds." Environmental Monitoring & Assessment 64(1): 285-298.

Hölscher, D, J. Mackensen & J.M. Robert (2005). „Forest recovery in the humid tropics: Changes in vegetation structure, nutrient pools and the hydrological cycle. In: Forests, Water and People in the Humid Tropics. M. BONELL and L. A. BRUIJNZEEL. Cambridge, Cambridge University Press: 598-621.

Huisman, S., A. Van Griensven, R. Srinivasan & L. Breuer (2004). European SWAT Summerschool 2004, Advanced Course. Coursebook. Giessen, University of Giessen: 112pp.

Hulme, M., R. Doherty, T. Ngara, M. New & D. Lister (2001). "African climate change: 1900-2100." Climate Research 17: 145-168.

ICRA (2000). Towards sustainable agricultural development. Research & development options for improved water management for agriculture of the Upper East Region of Ghana. Working Document Series 85. ICRA.

ICRA (2003). Diffusion des stratégies de gestion intégrée de la fertilité des sols dans le Zoundwéogo - Burkina Faso. Working Document Series 112. ICRA.

Igué, A. M. (2000). The Use of a Soil and Terrain Database for Land Evaluation Procedures - Case Study of Central Benin. Faculty of Agronomy. Hohenheimer Bodenkundliche Hefte (58). Stuttgart, University of Hohenheim. Dissertation: 235pp.

Igué, A. M. (2007). D 15: Soil information system for the Oueme basin. In: Report of the RIVERTWIN project. www.rivertwin.de/Publications&Reports.htm (accessed on 10.10.2007, not accessible anymore)

Igwe, C. A. (1999). "Land use and soil conservation strategies for potentially highly erodible soils of central-eastern Nigeria." Land Degradation and Development 10: 425-434.

IMPETUS (1999). Band 1. Unveröffentlichter Projektantrag. Integratives Management-Projekt für einen effizienten und tragfähigen Umgang mit Süßwasser in Westafrika. Universitäten zu Köln and Bonn. <http://www.impetus.uni-koeln.de/veroeffentlichungen/projektberichte.html>

IMPETUS (2001). Erster Zwischenbericht. Integratives Management-Projekt für einen effizienten und tragfähigen Umgang mit Süßwasser in Westafrika: Fallstudien für ausgewählte Flußeinzugsgebiete in unterschiedlichen Klimazonen. Universitäten zu Köln and Bonn.

<http://www.impetus.uni-koeln.de/veroeffentlichungen/projektberichte.html>

IMPETUS (2002). Zweiter Zwischenbericht. Integratives Management-Projekt für einen effizienten und tragfähigen Umgang mit Süßwasser in Westafrika: Fallstudien für ausgewählte Flußeinzugsgebiete in unterschiedlichen Klimazonen. Universitäten zu Köln and Bonn.

<http://www.impetus.uni-koeln.de/veroeffentlichungen/projektberichte.html>

IMPETUS (2003). Dritter Zwischenbericht. Integratives Management-Projekt für einen effizienten und tragfähigen Umgang mit Süßwasser in Westafrika: Fallstudien für ausgewählte Flußeinzugsgebiete in unterschiedlichen Klimazonen. Universitäten zu Köln and Bonn.

<http://www.impetus.uni-koeln.de/veroeffentlichungen/projektberichte.html>

IMPETUS (2006). Second Final Report. An Integrated Approach to the Efficient Management of Scarce Water Resources in West Africa: Case studies for selected

river catchments in different climatic zones. Cologne, Universities of Cologne and Bonn: 286pp.

<http://www.impetus.uni-koeln.de/veroeffentlichungen/projektberichte.html>

IMPETUS (2008). Achter Zwischenbericht. Integratives Management-Projekt für einen effizienten und tragfähigen Umgang mit Süßwasser in Westafrika: Fallstudien für ausgewählte Flusseinzugsgebiete in unterschiedlichen Klimazonen. Universitäten zu Köln and Bonn.

<http://www.impetus.uni-koeln.de/veroeffentlichungen/projektberichte.html>

IMPETUS Atlas v1.0 (2005). Interactive IMPETUS Digital Atlas. Edited by Thamm, H.-P., P. Recha, M. Christoph & O. Schütz, Remote Sensing Research Group, University of Bonn, Bonn.

Inamdar, S. (2004). Assessment of modelling tools and data needs for developing the sediment portion of the TMDL plan for a mixed landuse watershed. Buffalo, New York, Great Lakes Center. 39pp. http://www.glc.org/basin/pubs/projects/ny_AsModTI_%20pub1.pdf (accessed: 30.06.2008)

INRAB (2001). Actes de l'Atelier scientifique 1, Niaouli 11-12 janvier 2001. Recherche agricole pour le développement. Edited by B. P. AGBO, D. Y. ARODKOUN, K. AIHOU and A. MATTHESS, Institute National de la Recherche Agricole au Benin (INRAB).

INRAB (2002). Actes de l'Atelier scientifique 3, Niaouli 11-12 décembre 2002. Recherche agricole pour le développement. Edited by I. GBÉGO, A. ADJANOHOUN, B. BANKOLÉ et al., Institute National de la Recherche Agricole au Benin (INRAB).

INSAE (2003). Recensement général de la population et de l'habitation de février 2002. Résultats Provisoires, Institut National de la Statistique et de l'Analyse Economique Benin.

IPCC (2001). Climate Change 2001. Third Assessment Report (TAR), Intergovernmental Panel on Climate Change. <http://www.ipcc.ch>

IPCC (2007). Climate Change 2007. Fourth Assessment Report (AR4), Intergovernmental Panel on Climate Change. <http://www.ipcc.ch>

Jacobs, J. H. & R. Srinivasan (2006). Application of SWAT in Developing Countries using Readily Available Data. In: Proceedings of the 3rd International SWAT conference, Zurich, EAWAG.

<http://www.brc.tamus.edu/swat/conferences.html>

Jakeman, A. J., T. R. Green, L. Zhang, S. G. Beavis, J. P. Evans, C. R. Dietrich & B. Barnes (1998). Modelling Catchment Erosion, Sediment and Nutrient Transport in Large Basins. In: Soil erosion at multiple scales. Principles and methods for assessing causes and impacts. F. W. T. PENNING DE VRIES, F. AGUS and J. KERR. Wallingford (UK), CABI: 343-356

Jayakrishnan, R., R. Srinivasan, C. Santhi & J. G. Arnold (2005). "Advances in the application of the SWAT model for water resources management." Hydrological Processes 19: 749-762.

Jha, M., P.W. Gassman, S. Secchi, R. Gu & J. Arnold (2004). "Effect of watershed subdivision on SWAT flow, sediment and nutrient predictions." Journal of the American Water Resources Association 40 (3): 811-825.

Jirayoot, K. & L. D. Trung (2006). Application of SWAT Model to the Decision Support Framework of the Mekong River Commission. In: Proceedings of the 3rd International SWAT Conference: 320-329. Zurich, EAWAG.
<http://www.brc.tamus.edu/swat/conferences.html>

Judex, M. (2008). Modellierung der Landnutzungsdynamik in Zentralbenin mit dem XULU-Framework. Geographisches Institut. Bonn, Universität Bonn. Dissertation. 166 Seiten. http://hss.ulb.uni-bonn.de/diss_online/math_nat_fak/2008/Judex_michael

Junge, B. (2004). Die Böden des oberen Ouémé-Einzugsgebietes in Benin/Westafrika - Pedologie, Klassifizierung, Nutzung und Degradierung. Institut für Bodenkunde. Bonn, Universität Bonn. Dissertation. 217 Seiten.
http://hss.ulb.uni-bonn.de/diss_online/landw_fak/2004/Junge_birte/

Kim, C., H. Kim, C. Jang, S. Shin & N. Kim (2003). SWAT application to the Yongdam and Bocheong watersheds in Korea for daily stream flow estimation. In: Proceedings of the 2nd International SWAT conference: 283-292.
<http://www.brc.tamus.edu/swat/conferences.html>

King, K. W., J. G. Arnold & R. L. Binger (1999). "Comparison of Green-Ampt and curve number methods on Goodwin Creek Watershed using SWAT." Transactions of the American Society of Agricultural Engineers (ASAE) 42(4): 919-925.

Kirk (1996). The Role of Land Tenure and Property Rights in Sustainable Resource Use: The Case of Benin. Guiding Principles: Land Tenure in Development Cooperation. GTZ. Eschborn.
http://www.mekonginfo.org/mrc/html/kirk_ben/kib_inh.htm (accessed: 30.06.2008)

Kirsch, K., A. Kirsch & J. G. Arnold (2002). "Predicting sediment and phosphorus loads in the Rock River Basin using SWAT." Transactions of the American Society of Agricultural Engineers (ASAE) 45(3): 1757-1769.

Klamt, E. & W. G. Sombroek (1988). Contribution of Organic Matter to Exchange Properties of Oxisols. In: Proceedings of the Eight International Soil Classification Workshop. Classification, Characterization and Utilization of Oxisols, Rio de Janeiro, Brasil.

Krause, P., D. P. Boyle & P. Bäse (2005). "Comparison of different efficiency criteria for hydrological model assessment." Advances in Geoscience 5: 89-97.

Krysanova, V., F. Hattermann & F. Wechsung (2005). "Development of the ecohydrological model SWIM for regional impact studies and vulnerability assessment." Hydrological Processes 19: 763-783.

Lal, R. (1981). Deforestation of Tropical Rainforest and Hydrological Problems. In: Tropical Agricultural Hydrology. R. LAL and E. W. RUSSELL. Chichester, Wiley & Sons: 131-140.

Lal, R. (1985). "Mechanized tillage systems effects on physical properties of an Alfisol in watersheds cropped to maize." Soil & Tillage Research 6: 149-161.

Lal, R. (1990). Soil erosion in the tropics. Principles & Management. New York, McGraw-Hill, Inc. 580pp.

Lal, R. (1995). Sustainable management of soil resources in the humid tropics. Tokyo, United Nations University Press. 146pp.

Lal, R. (1998). Agronomic Consequences of Soil Erosion. In: Soil erosion at multiple scales. Principles and methods for assessing causes and impacts. F. W. T. PENNING DE VRIES, F. AGUS and J. KERR. Wallingford, UK, CABI: 149-160.

Lal, R., W. H. Blum, C. Valentine & B. A. Stewart, Eds. (1998). Methods for assessment of soil degradation. Advances in Soil Science. New York, CRC Press.

Lal, R., M. Ahmadi & R. M. Bajracharya (2000). "Erosional impacts on soil properties and corn yield on alfisols in central Ohio." Land Degradation and Development 11: 575-585.

Lal, R. (2000). "Physical management of soils of the tropics: priorities for the 21st century." Soil Science 165(3): 191-207.

Lal, R. (2001). "Soil degradation by erosion." Land Degradation & Development 12: 519-539.

Landon, J. R. (1984). Booker Tropical Soil Manual. A handbook for soil survey and agricultural land evaluation in the tropics and subtropics. Essex, Booker Agriculture Internat. Ltd.

Larose, M., J. L. Oropeza-Mota, D. Norton, A. Turrent -Fernández, M. Martínez-Menes, J. A. Pedraza-Oropeza & N. Francisco-Nicolás (2004). "Application of the WEPP model to hillside lands in the Tuxtlas, Veracruz, Mexico." Agrociencia 38(2).

Lawal, O., T. Gaiser & K. Stahr (2004). Effect of land use changes on sediment load in the Zagbo River Catchment in Southern Benin. In: Proceedings of the Tropentag 2004 - Conference on International Agricultural Research for Development. <http://www.tropentag.de/2004/proceedings/proceedings.pdf>

Le Lay, M., S. Galle, G.-M. Saulnier & I. Braud (2007). Detecting changes in watershed behavior: a model-based methodology. Application to West African non-stationary conditions. Submitted to Water Resources Research.

- Lee, D. H., N. W. Kim & I. M. Chung (2006). Comparison of Runoff Responses between SWAT and Sequentially Coupled SWAT-MODFLOW Model. In: Proceedings of the 3rd International SWAT Conference: 271-278. Zurich, EAWAG.
- Lenhart, T., A. van Rompaey, A. Steegen, N. Fohrer, H.-G. Frede & G. Govers (2005). "Considering spatial distribution and deposition of sediment in lumped and semi-distributed models." Hydrological Processes 19: 785-794.
- Leon, C. C. R. (2005). A multi-scale approach for erosion assessment in the Andes. Wageningen, University of Wageningen. Dissertation: 147pp.
- Leroux, M. (2001). The Meteorology and Climate of Tropical Africa. London, Springer. 548pp.
- Levine, J. S. (1994). Biomass burning and the production of greenhouse gases. In: Climate Biosphere Interaction: Biogenic Emissions and Environmental Effects of Climate Change. R. G. ZEPP. Athens, Georgia, John Wiley and Sons: 139-159.
- Lewis, J. (1996). "Turbidity-controlled suspended sediment sampling for runoff-event load estimation." Water Resources Research 32(7): 2299-2310.
- Limaye, A. S., T. M. Boyington, J. F. Cruise, A. Bulus & E. Brown (2001). "Macroscale hydrologic modeling for regional climate assessment studies in the southeastern United States." Journal of the American Water Resources Association 37(3): 709-722.
- Machado, R. E. & C. A. Vettorazzi (2003). "Simulacao da producao de sedimentos para a microbacia hidrografia do ribeirao dos marins (SP)." Revista Brasileira de Ciênc do Solo 27: 735-741.
- MAEP (2004). Action plan for the sustainable management of natural resources and soil fertility, Ministère de l'Agriculture, de l'Élevage et de la Pêche (MAEP), Direction de Forêt et Ressources Naturelles.
- Mahé, G., E. Servat & J. Maley (2005). Climatic variability in the tropics. In: Forests, Water and People in the Humid Tropics. M. BONELL and L. A. BRUIJNZEEL. Cambridge, Cambridge University Press: 267-286.
- Maliki, R., F. Amadji & C. Englehart (2001). Quelques options de gestion de la fertilité des sols et de stabilisation des rendements dans la zone des savanes au centre du Bénin: contraintes à leur adoption. In: Actes 1 de l'Atelier Scientifique Sud et Centre du Bénin du 11 au 12 janvier 2001, Niouli, INRAB.
- Maliki, R., F. Amadji, I. Adje, A. Adifon, A. Badou & J. Hounnou (2002a). Identification des conditions d'application du système igname-Gliricidia sepium par les producteurs du Centre-Bénin. In: Actes 2 de l'Atelier Scientifique Sud et Centre du Bénin du 12 au 13 décembre 2001, Niouli, INRAB.
- Maliki, R., F. Amadji, I. Adje, J. Honou & S. Nondichao (2002b). Gestion des espaces agro-pastoraux: conflits entre agriculteurs et éleveurs au Centre du Bénin. In: Actes 2

de l'Atelier Scientifique Sud et Centre du Benin du 12 au 13 décembre 2001, Niaouli, INRAB.

Maliki, R., F. Amadji & I. Adje (2003). Effets comparés de deux méthodes de préparation du sol sur la gestion de la fertilité des terres agricoles au Centre du Bénin. In: Actes 1 de l'Atelier Scientifique Centre du Benin du 18 au 19 décembre 2002, Dassa, INRAB.

Malmer, A., M. Van Noordwijk & L. A. Bruijnzeel (2005). Effects of shifting cultivation and forest fire. In: Forests, Water and People in the Humid Tropics. M. BONELL and L. A. BRUIJNZEEL. Cambridge, Cambridge University Press: 533-560.

Mama, V. C. & J. Oloukoi (2003). Colonisation agricole et dynamique sociale dans la région centrale du Bénin. In: Actes 1 de l'Atelier Scientifique Centre du Benin du 18 au 19 décembre 2002, Dassa, INRAB.

Manguerra, H. B. & B. A. Engel (1999). "Hydrologic parameterisation of watersheds for runoff prediction using SWAT." Journal of the American Water Resources Association 34(5): 1149-1162.

Mantel, S. & V. W. P. van Engelen (1999). "Assessment of the impact of water erosion on productivity of maize in Kenya: an integrated modelling approach." Land Degradation and Development 10: 577-592.

MEHU (1999). National Action Plan for Desertification Control (PAN/LCD), Ministère de l'Environnement, de l'Habitat et de l'Urbanisme (MEHU), République du Bénin. 78pp. http://bch-cbd.naturalsciences.be/benin/implementation/documents/autrepa/desert_en.pdf (accessed 30.06.2008).

MEHU (2003). Aptitudes des sols et leur repartition au Benin: Etat des lieux et perspectives d'aménagement à l'horizon 2025. Cotonou, Ministère de l'Environnement, de l'Habitat et de l'Urbanisme (MEHU), République du Bénin.

MEHU (2005). Rapport d'évaluation de la mise en oeuvre du Programme d'Action National de Lutte Contre la Désertification (PAN/LCD). ASSISTENTS:, H. ONIBON, A. TOSSA and A. TCHABI. Cotonou, Ministère de l'Environnement, de l'Habitat et de l'Urbanisme (MEHU), Direction de l'Environnement.

Merritt, W. S., R. A. Letcher & A. J. Jakeman (2003). "A review of erosion and sediment transport models." Environmental Modelling & Software 18: 761-799.

Meurer, M. (1998). Geo- und weideökologische Untersuchungen in der subhumiden Savannenzzone NW-Benins. Karlsruher Schriften zur Geographie und Geoökologie 1. Universität Karlsruhe. 279 Seiten.

Monteith, J. L. (1965). Evaporation and the environment. In: The state and movement of water in living organisms. XIXth Symposium of the Society of Experimental Biology. Swansea, Cambridge University Press: 205-234.

Moon, J., R. Srinivasan & J. H. J.H. Jacobs (2004). "Streamflow estimation using spatially distributed rainfall in the Trinity River Basin, Texas." Transactions of the ASAE 47(5): 1445-1451.

Morris, M. D. (1991). "Factorial sampling plans for preliminary computational experiments." Technometrics 33(2): 161-174.

Mulder, I. (2000). "Farmers' Perceptions of Soil Fertility in Benin." Working Paper; International Institute for Environment and Development 28.

Muleta, M. K. & J. W. Nicklow (2005). "Sensitivity and uncertainty analysis coupled with automatic calibration for a distributed watershed model." Journal of Hydrology (306): 127–145.

Mulindabigwi, V. (2006). Influence des systèmes agraires sur l'utilisation des terroirs, la séquestration du carbone et la sécurité alimentaire dans le bassin versant de l'Ouémé supérieur au Bénin. Department of Agriculture. Bonn, University of Bonn. Dissertation. 227pp.

http://hss.ulb.uni-bonn.de/diss_online/landw_fak/2006/Mulindabigwi_valens

Mund, J.-P. (2004): Kleinbäuerlicher Nassreisbau in Bas-fonds der Côte d'Ivoire, Westafrika. Dissertation Mainz, Mainzer Geographische Studien, Band 50, 281 Seiten.

Muttuwatha, L. P. (2004). Long term rainfall-runoff-lake modelling of the lake Naivasha basin, Kenya. Enschede (The Netherlands), International institute for geo-information science and earth observation. Dissertation: 71pp.

Nash, J. E. & J. V. Sutcliffe (1970). "River flow forecasting through conceptual models part I – a discussion of principles." Journal of Hydrology (10): 282 – 290.

Ndomba, P. M. (2006). The suitability of SWAT in sediment yield modelling for ungauged catchments: A case of Simiyu river subcatchment in Tanzania. Proceedings of the 3rd International SWAT conference: 61-69, Zurich, EAWAG. <http://www.brc.tamus.edu/swat/conferences.html>

Nearing, M. A., V. Jetten, C. Baffaut, O. Cerdan, A. Couturier, M. Hernandez, Y. Le Bissonnais, M. H. Nichols, J. P. Nunes, C. S. Renschler, V. Souchère & K. van Oost (2005). "Modelling response of soil erosion and runoff to changes in precipitation and cover." Catena 61: 131-154.

Neef, A. (1999). Auswirkungen von Bodenrechtswandel auf Ressourcennutzung und wirtschaftliches Verhalten von Kleinbauern in Niger und Benin. Development economics and policy 12: 265-278.

Neitsch, S. L., J. G. Arnold, J. R. Kiniry, R. Srinivasan & J. R. Williams (2002a). Soil and Water Assessment Tool- User's Manual Version 2000, Chapter 1-21. Temple, Grassland, Soil and Water Research Laboratory, Blackland Research Center. <http://www.brc.tamus.edu/swat/downloads/doc/swatuserman.pdf>

Neitsch, S. L., J. G. Arnold, J. R. Kiniry, J. R. Williams & K. W. King (2002b). Soil and Water Assessment Tool- Theoretical Documentation Version 2000. Temple, Blackland Research Center, Grassland, Soil and Water Research Laboratory. <http://www.brc.tamus.edu/swat/downloads/doc/swat2000theory.pdf>

Office Béninois des Mines (1984). Notice explicative de la carte géologique à 1 : 200 000, feuille Djougou-Parakou-Nikki, République Populaire du Bénin, Ministre des Finances et d'Economie. 39 pp.

Ojo, O., S. Gbuyiro & C. Okoloye (2004). "Implications of climatic variability and climate change for water resources availability and management in West Africa." GeoJournal (61): 111-119.

Oldeman, L. R. (1998). Soil degradation: A threat to food security? Report 98/01. ISRIC. Wageningen (The Netherlands), International Soil Reference and Information Centre. 15pp. http://www.isric.org/isric/webdocs/Docs/ISRIC_Report_1998_01.pdf (accessed on 30.06.2008)

Oldeman, L. R., R. T. A. Hakkeling & W. G. Sombroek (1991). World map of the status of human-induced soil degradation: An Explanatory Note. ISRIC-UNEP report. Wageningen. 35pp. <http://www.isric.org/isric/webdocs/Docs/ExplanNote.pdf>

Orthmann, B. (2005). Vegetation ecology of a woodland-savanna mosaic in central Benin (West Africa): Ecosystem analysis with a focus on the impact of selective logging. Institute of Botany. Rostock, University of Rostock. Dissertation. 116pp. http://www.impetus.uni-koeln.de/fileadmin/content/veroeffentlichungen/publikationsliste/959_Orthmann.pdf

Paeth, H. (In preparation). Statistical postprocessing of simulated precipitation data for hydrological and climatological analysis in West-Africa. 54pp. In preparation.

Paeth, H., K. Born, R. Girmis, R. Podzun & D. Jacob (2008). "Regional climate change in tropical Africa under greenhouse forcing and land use changes." Journal of Climate, in press.

Penning de Vries, F. W. T., F. Agus & J. Kerr, Eds. (1998). Soil erosion at multiple scales. Principles and methods for assessing causes and impacts. Wallingford, UK, CABI Publishing. 390pp.

Pfannkuche, J. & A. Schmidt (2003). "Determination of suspended particulate matter concentration from turbidity measurements: particle size effects and calibration procedures." Hydrological Processes 17: 1951-1963.

Poss, R., J. C. Fardeau & H. Saragoni (1997). "Sustainable agriculture in the tropics: the case of potassium under maize cropping in Togo." Nutrient Cycling in Agroecosystems(46): 205-213.

Priestley, C. H. B. & R. J. Taylor (1972). "On the assessment of surface heat flux and evaporation using large scale parameters." Monthly Weather Review 100: 82 – 92.

Raunet, M. (1985). "Bas-fonds et riziculture en Afrique: Approche structurale comparative." Agronomie Tropicale 40(3): 181-201.

Republique du Benin (2008). Programme d'action national d'adaptation aux changements climatiques du Benin (PANA-Benin). MEPN. Cotonou, Benin.
<http://unfccc.int/resource/docs/napa/ben01f.pdf>

Rawls, W. J. & D. L. Brakensiek (1995). Prediction of soil water properties for hydrological models. In: Proceedings of the symposium watershed management in the eighties, Denver.

Reiff, K. (1998). Das weidewirtschaftliche Nutzungspotential der Savannen Nordwest-Benins aus floristisch-vegetationskundlicher Sicht. In: Geo- und weideökologische Untersuchungen in der subhumiden Savannenzzone NW-Benins. M. MEURER. Karlsruhe, Karlsruher Schriften zur Geographie und Geoökologie. 1: 51-86.

Richter, G., (Hrsg.) (1998). Bodenerosion - Analyse und Bilanz eines Umweltproblems. Darmstadt, Wissenschaftliche Buchhandlung. 264 Seiten.

Riley, S. J. (1997). "The sediment concentration-turbidity relation: its value in monitoring at Ranger Uranium Mine, Northern Territory, Australia." Catena 32: 1-14.

Ritchie, J. (1972). "A model for predicting evaporation from a row crop with incomplete cover." Water Resources Research (8): 1204-1213.

Roose, E. (1977). "Érosion et ruissellement en Afrique de l'ouest. Vingt années de mesures en petites parcelles expérimentales." Travaux et Documents de l'ORSTOM 78: 108pp.

Roose, E. & B. Barthés (2001). "Organic matter management for soil conservation and productivity restoration in Africa: a contribution from Francophone research." Nutrient Cycling in Agroecosystems 61: 159-170.

Rose, C. W. & B. Yu (1998). Dynamic Process Modelling of Hydrology and Soil Erosion. In: Soil erosion at multiple scales. Principles and methods for assessing causes and impacts. F. W. T. PENNING DE VRIES, F. AGUS and J. KERR. Wallingford, UK, CABI: 269-286

Sachs, J. D. (2005). Investing in Development: A Practical Plan to Achieve the Millennium Development Goals. London, Earthscan Publications Ltd.

Saidou, A., T. W. Kuyper, D. K. Kossou, R. Tossou & P. Richards (2004). "Sustainable soil fertility management in Benin: learning from farmers." NJAS - Wageningen Journal of Life Sciences 52(3): 349-369.
<http://library.wur.nl/ojs/index.php/njas/article/viewFile/341/60> (accessed: 30.06.2008)

Saleh, A., J. G. Arnold, P. W. Gassman, L. M. Hauck, W. D. Rosenthal, J. R. Williams & A. M. S. McFarland (2000). "Application of SWAT for the Upper North Bosque

River Watershed." Transactions of the American Society of Agricultural Engineers (ASAE) 43(5): 1077-1087.

Sanchez, P., C. Palm & S. Buol (2003). "Fertility capability soil classification: a tool to help assess soil quality in the tropics." Geoderma (114): 157– 185.

Santhi, J. G., J. R. Arnold, W. A. Williams, R. Dugas, R. Srinivasan & L. M. Hauck (2001). "Validation of the SWAT model on a large river basin with point and nonpoint sources." Journal of the American Water Resources Association 37(5): 1169-1188.

Santhi, C., R. Srinivasan, J. G. Arnold & J. R. Williams (2006). "A modeling approach to evaluate the impacts of water quality management plans implemented in a watershed in Texas." Environmental Modelling & Software 21(8): 1141-1157.

Schachtschabel, P., H.-P. Blume, G. Brümmer, K. H. Hartge & U. Schwertmann (1998). Lehrbuch der Bodenkunde. Stuttgart, Ferdinand Enke Verlag. 491 Seiten.

Schmidt, J. (2000). Application of physically based models. Berlin, Springer Verlag. 318pp.

Schneider, M. (1997). "Leitfaden zur Analyse des Bodenrechts in ländlichen Gebieten Westafrikas." Eschborn, GTZ: 34pp.

Schönbrodt, S. (2007). Inventarisierung und bodenkundliche Charakterisierung von Bas-Fonds in Einzugsgebieten des Oberen Ouéme (West Afrika). Geographisches Institut. Universität Göttingen. Göttingen. Diplomarbeit. 126 Seiten.

School, J. & K. C. Abbaspour (2006). "Calibration and uncertainty issues of a hydrological model (SWAT) applied to West Africa." Advances in Geoscience 3: 137-143.

Segalen, P. & C. A. Van Diepen (1984). "Projects of Soil Classification." Technical Paper - International Soil Reference and Information Centre (ISRIC) 7.

Singer, U. (2005). Entwicklungsprojekte im ländlichen Benin im Kontext von Migration und Ressourcenverknappung. Bayreuth, Universität Bayreuth. Dissertation. 255pp. <http://opus.ub.uni-bayreuth.de/volltexte/2006/209/>

Sintondji, L. O. C. (2005). Modelling the rainfall-runoff process in the Upper Ouémé catchment (Terou in Bénin Republic) in a context of global change: extrapolation from the local to the regional scale. Faculty of Mathematics and Natural Sciences. Bonn, University of Bonn. Dissertation. 205pp.

Sirvio, T., Rebeiro-Hargrave & P. Pellikka (2004). Geoinformation in gully erosion studies in Taita Hills, SE-Kenya, preliminary results. In: Proceedings of the 5th African Association of Remote Sensing of Environment Conference, 17-22 October 2004, Nairobi, Kenya, Nairobi. 7pp.
http://www.helsinki.fi/science/taita/reports/aarse_sirvio.pdf

Smaling, E.M.A., E. Kiestra & W. Andriess (1985): Detailed Soil Survey and Qualitative Land Evaluation of the Echin-Woye and the Kunko Benchmark Sites, Bida area, Niger State, Nigeria. ILRI, Wageningen, The Netherlands.

Soil Conservation Service (1972) Section 4: Hydrology. In: National Engineering Handbook. SCS.

Spruill, C. A., S. R. Workman & J. L. Taraba (2000). "Simulation of Daily and Monthly Stream Discharge from Small Watersheds Using the SWAT Model." Transactions of the ASAE 43(6): 1431-1439.

Srinivasan, R., J. G. Arnold, J. G. Ramanarayanan & S. T. Bednarz (1998). "Large area hydrologic modeling and assessment part II: model application." Journal of the American Water Resources Association 34(1): 91-101.

Steiner, K. (1994). „Ursachen der Bodendegradation und Ansätze für eine Förderung der nachhaltigen Bodennutzung im Rahmen der Entwicklungszusammenarbeit“. Eschborn, GTZ: 148 Seiten.

Stocking, M. A. (2003). "Tropical Soils and Food Security: The Next 50 Years." Science 302.

Stone, M. C., R. H. Hotchkiss, C. M. Hubbard, T. A. Fontaine, L. O. Mearns & J. G. Arnold (2001). "Impacts of climate change on Missouri river basin water yield." Journal of the American Water Resources Association 37(5): 1119-1130.

Stoorvogel, J. J. & E. M. A. Smaling (1990). Assessment of soil nutrient depletion in Sub-Saharan Africa. 1983 - 2000. Report 28. Wageningen (The Netherlands), Winand Staring Centre: 134pp.

Sturm, H.-J. (1993). Produktions- und weideökologische Untersuchungen in der subhumiden Savannenzzone Nordbenins. Karlsruher Schriften zur Geographie und Geoökologie. Band 2: 94pp.

Swoboda, J. (1994). Geoökologische Grundlagen der Bodennutzung und deren Auswirkung auf die Bodenerosion im Grundgebirgsbereich Nord-Benins - ein Beitrag zur Landnutzungsplanung. Frankfurt, Universität Frankfurt. Dissertation. 119 Seiten.

Syers, J. K. & D. L. Rimmer (1994). Soil science and sustainable land management in the tropics. Wallingford, CAB International. 290pp.

Sys, C., E. van Ranst, I. Debaveye & F. Beernaert (1993). Land Evaluation. Part II: Crop requirements. Brussels (Belgium), General administration for development cooperation.

Takle, E. S., M. Jha & C. J. Anderson (2005). "Hydrological cycle in the upper Mississippi River basin: 20th century simulations by multiple GCMs." Geophysical Research Letters 32(18).

TetraTech (2004). Technical support document for establishment of a suspended sediment total maximum daily load for the Pajaro river watershed. San Luis Obispo, California regional water quality control board: 113pp.

Thamm, H.-P., Judex, M. & G. Menz (2005). "Modelling of Land-Use and Land-Cover Change (LUCC) in Western Africa using Remote Sensing." *Zeitschrift für Photogrammetrie* 3/2005: 191-199.

Thomson, A. M., R. A. Brown, N. J. Rosenberg, R. C. Izaurralde, D. M. Legler & R. Srinivasan (2003). "Simulated impacts of El Nino/Southern Oscillation on United States Water Resources." *Journal of the American Water Resources Association* 39(6): 1565-1565.

Tietje, O. & V. Hennings (1996). "Accuracy of the saturated hydraulic conductivity prediction by pedo-transfer functions compared to the variability within FAO textural classes." *Geoderma* 69: 71-84

Tripathi, M. P., R.K. Panda & N.S. Raghuwanshi (2003). "Identification and prioritisation of critical sub-watersheds for soil conservation management using the SWAT model." *Biosystems Engineering* 85(3): 365-379.

Tripathi, M. P., R. K. Panda & N. S. Raghuwanshi (2005). "Development of effective management plan for critical subwatersheds using SWAT model." *Hydrological Processes* 19: 809-826.

UNDP (2002). Mucuna cover cropping: Benin. In: *Sharing innovative experiences 5. Examples of successful initiatives in agriculture and rural development in the south:* 9-23. UNDP, New York.

UNEP (2007). GEO4: Environment for development. *Global Environment Outlook* UNEP. <http://www.unep.org/geo/geo4/media/> (accessed on 30.06.2008)

USDA (1993). Soil Survey Manual. USDA Handbook No. 18. US Government. Print. Office, Washington D.C. 437 pp.

Vache, K. B., J. M. Eilers & M. V. Santelmann (2002). "Water quality modeling of alternative agricultural scenarios in the U.S. Corn Belt." *Journal of American Water Resources Association* 38(2): 773-787.

Van Campen, W (1978): Mesures d'érosion sur un sol ferrugineux tropical, Station Alafiarou, Parakou, Bénin. – *CENAP Etude No 185*, Cotonou, Bénin. 59pp.

Van Griensven, A. & W. Bauwens (2005). "Application and evaluation of ESWAT on the Dender basin and the Wister Lake basin." *Hydrological Processes* 19: 827-838.

Van Noordwijk, M., M. Van Roode, E. L. McCallie & B. Lusiana (1998). Erosion and Sedimentation as Multiscale, Fractal Processes: Implications for Models, Experiments and the Real World. In: *Soil erosion at multiple scales. Principles and methods for assessing causes and impacts.* Edited by F. W. T. PENNING DE VRIES, F. AGUS and J. KERR. Wallingford, UK, CABI Publishing: 223-254.

Van Reeuwijk, L.P. (1995). "Procedures for Soil Analysis." Fifth edition. ISRIC Technical Paper 9. Wageningen, The Netherlands. 105pp.

Van Wambeke, A. (1991). Soils of the tropics. Properties and appraisal. London, McGraw-Hill, 343pp.

Varado, N., I. Braud, S. Galle, M. Le Lay, L. Séguis, B. Kamagate & C. Depraetere (2005). "Multi-criteria assesment of the Representative Elementary Watershed approach on the Donga catchment (Benin) using a downward approach of modeling complexity." Hydrology and Earth System Sciences Discussion 2: 2349-2391.

Varanou, E., M. Pikounis, E. Baltas & M. Mimikou (2004). Application of the SWAT model for the Sensivity Analysis of Runoff to Landuse Change. In: Proceedings of the 2nd International SWAT Conference: 90-93.

<http://www.brc.tamus.edu/swat/conferences.html>

Verburg, P. H., W. Soepboer, A. Veldkamp, R. Limpiada, V. Espaldon & S. S. A. Mastura (2002). "Modeling the Spatial Dynamics of Regional Land Use: The CLUE-S Model." Environmental Management 30(3): 391-405.

Viennot, M. (1978). Carte pédologique de reconnaissance de la République Populaire du Bénin à 1/200.000. Feuille de Bembereke. Note explicative No. 66 (7). Paris, ORSTOM: 43pp.

Volk, M. S. & G. Schmidt (2003). The Model Concept in the Project FLUMAGIS: Scales, Simulation and Integration. In: Proceedings of the 2nd International SWAT Conference: 236-248. <http://www.brc.tamus.edu/swat/conferences.html>

Wallace, J. S., A. Young & C. K. Ong (2005). The potential of agroforestry for sustainable land and water management. In: Forests, Water and People in the Humid Tropics. M. BONELL and L. A. BRUIJNZEEL. Cambridge, Cambridge University Press: 652-670.

Walling, D.E. (1996): Hydrology and Rivers. In: The Physical Geography of Africa. Adams, W.M., Goudie, A.S. & A.R. Orme (Ed.): Oxford University Press: 103 – 121.

Walling, D. E., A. L. Collins, H. M. Sichingabula & G. J. L. Leeks (2001). "Integrated assessment of catchment suspended sediment budgets: A Zambian example." Land Degradation and Development 12: 387-415.

Wamuongo, J. D. (1997). Review of Kenyan Agricultural Research - Vol. 8 Soil Science and Management. Nairobi, KARI.

Wang, J. J., D. L. Harrell, R. E. Henderson & P. F. Bell (2004). "Comparison of Soil-Test Extractants for Phosphorus, Potassium, Calcium, Magnesium, Sodium, Zinc, Copper, Manganese, and Iron in Louisiana Soils." Communications in Soil Science and Plant Analysis 35(1 & 2): 145-160.

Warren, A., H. Osbahr, S. Batterbury & A. Chappell (2003). "Indigenous views of soil erosion at Fandou Béri, Southwestern Niger." Geoderma 111: 439-456.

Weischet, W.&W. Endlicher (2000). Regionale Klimatologie – 2. Die Alte Welt: Europa, Afrika, Asien. Stuttgart, Teubner. 625pp.

Weller, U. (2002). Land evaluation and landuse planning for Southern Benin (West Africa) BENSOTER. Institute for Soil Science. Hohenheim, Hohenheim (Germany): 159pp.

White, K. L. & I. Chaubey (2005). "Sensitivity analysis, calibration, and validations for a multisite and multivariable SWAT model." Journal of the American Water Resources Association 41(5):1077-1089

Wiechmann, H. (1991). "Eigenschaften rezenter Böden aus Saprolit." Mitteilungen der Deutschen Bodenkundlichen Gesellschaft 66: 1193-1196.

Williams, M. A. J. & R. C. Balling (1996). Interactions of Desertification and Climate. London, Arnold.

Willmott, C. J. (1981). "On the validation of models." Physical Geography 2: 184pp.

Windmeijer, P. N. & W. Andriess (1993). Inland Valleys in West Africa: An agro-ecological characterization of rice-growing environments ILRI publication 52. Wageningen (The Netherlands): 160pp.

Wischmeier, W. H. & D. D. Smith (1978). Predicting rainfall erosion losses - A guide to conservation planning. Agricultural Handbook 537. USDA. Washington (DC): 58pp.

World Bank (2006). GEF Project Document on a proposed document in a proposed grant from the Global Environment Facility trust fund in the amount of USD 6.00 Million to the Republic of Benin for a forests and adjacent land management program, World Bank: 89pp.

Yang, J., K. Abbaspour & P. Reichert (2006). Interfacing SWAT with System Analysis Tools: A Generic Platform. In: Proceedings of the 3rd International SWAT Conference. Zurich, EAWAG: 169-178.

<http://www.brc.tamus.edu/swat/conferences.html>

Web sources

Bergsma (2004). The expert and the farmer in development cooperation. Webseminar. <http://www.geocities.com/eswaranpadma/Farmer.html>

République du Benin (2002). Rapport annuel sur la Coopération pour le Développement. http://www.gouv.bj/textes_rapports/rapports/rapport_coop_dev.php (accessed 30.06.2008)

Rossiter, D. G. (1994). "Lecture Notes: Land Evaluation." <http://www.itc.nl/~rossiter/pubs/s494toc.htm>.

11. APPENDIX

Fig. A.1 Geological map of the Upper Ouémé catchment – Sheet Djougou-Parakou-Nikki	255
Fig. A.2 Photos and classification of the representative profiles	257
Fig. A.3 Comparison of Mehlich Method and Ammonium Acetate methods for determination of CEC _{pot}	277
Fig. B.1 Sites of turbidity and discharge measurements: (a) Donga Pont, (b) Lower Aguima, (c) Donga Kolonkonde, (d) Terou-Igbomakoro (Date: September 2004, 2006)	292
Fig. B.2 Spatial validation: Comparison of measured and simulated weekly discharge at the validation outlet	293
Fig. B.3 Spatial distribution of the mean total discharge in the Upper Ouémé catchment for the original model (1998-2005)	294
Fig. B.4 Spatial distribution of the mean total discharge in the Upper Ouémé catchment for the land use scenarios L1 to L3 and the Lu00 model	294
Fig. B.5 Mean spatial distribution of water yield for the climate scenarios A1B and B1 for the periods 2001-2025 and 2026-2050 compared to the original model (1998-2005) and the model with REMO data for 1960-2000	295
Fig. B.6 Mean simulated annual values of rainfall, sediment yield (SY) and water yield (WY) in the Donga-Pont subcatchment for the combination of the land use scenarios L1 and L2 with the climate change scenarios for the period 2000 to 2030. The presented results are averages of three ensemble runs for each climate scenario	295
Fig. B.7 Mean simulated annual values of rainfall, sediment yield (SY) and water yield (WY) in the Terou-Igbomakoro subcatchment for the combination of the land use scenarios L1 and L2 with the climate change scenarios for the period 2000 to 2030. The presented results are averages of three ensemble runs for each climate scenario	296
Fig. B.8 Mean spatial distribution of water yield for the combinations of the climate scenarios A1B and B1 with the land use scenarios L1-L3 for the period 2001-2030 compared to the Lu00 model (1998-2005) and the model with REMO data for 1960-2000	297
Fig. B.9 Mean spatial distribution of water yield for the land use, climate and combined scenarios compared to the Lu00 model (1998-2005) and the model with REMO climate data for 1960-2000	297
Fig. B.10 Mean spatial distribution of surface runoff for the land use, climate and combined scenarios compared to the Lu00 model (1998-2005) and the model with REMO climate data for 1960-2000	298

Fig. B.11 Sensitivity of mean annual discharge and model efficiency to changes of the parameters ESCO and SURLAG (red dot: parameter value and simulated mean discharge for the period 1998-2001, red line: polynomial regression)	299
Fig. B.12 Sensitivity of mean annual discharge to changes of the parameters GWQMN and CH_K2 (red dot: parameter value and simulated mean discharge for the period 1998-2001, red line: polynomial regression)	300
Fig. B.13 Sensitivity of mean annual sediment yield to changes of the parameters ESCO, SURLAG, GWQMN and SOL_AWC (red dot: parameter value and simulated mean discharge for the period 1998-2001, red line: polynomial regression)	301
Fig. B.14 Confidence interval (90%) for mean daily discharge and sediment yield at the Terou-Igbomakoro and Donga-Pont outlets	302
Table A.1 Location of the investigated representative profiles in the Upper Ouémé catchment	256
Table A.2 Physical and chemical soil properties of the representative profiles	259
Table A.3 Evaluation of soil quality according to Landon (1984)	277
Table A.4 Classification of erodibility (K factor in USLE) according to Bolline & Rosseau (1978)....	278
Table A.5 Fertility Capability Classification System (FCC)	278
Table A.6 Location of the investigated inland valleys in the Upper Ouémé catchment	279
Table A.7 Properties of investigated inland valley soils in the Upper Ouémé catchment	280
Table A.8 Location and characteristics of studied degraded fields and reference sites in in the Upper Ouémé catchment and the commune Ouaké	284
Table A.9 Characteristics of studied degraded fields in the Upper Ouémé catchment according to farmer interviews.....	285
Table A.10 Soil characteristics of studied degraded fields and reference sites in the Upper Ouémé catchment	288
Table A.11 Questionnaire for the characterisation of agricultural sites	291
Table A.12 Location of the investigated erosion forms in the Upper Ouémé catchment	291
Table C.1 Main finished and ongoing development projects in Benin concerning soil degradation ..	303
Table C.2 Main soil conservation measures in Benin: Effects, advantages and constraints from the Beninese farmer's point of view	305

Appendix A. Soil investigations

In the following the location and photos of all studied representative profiles are presented. Subsequently, a table for each representative profiles will be shown summarizing the measured soil properties. Each table includes the number of the soil unit and the classification according to the World reference base (WRB) and the French classification system CPCS.

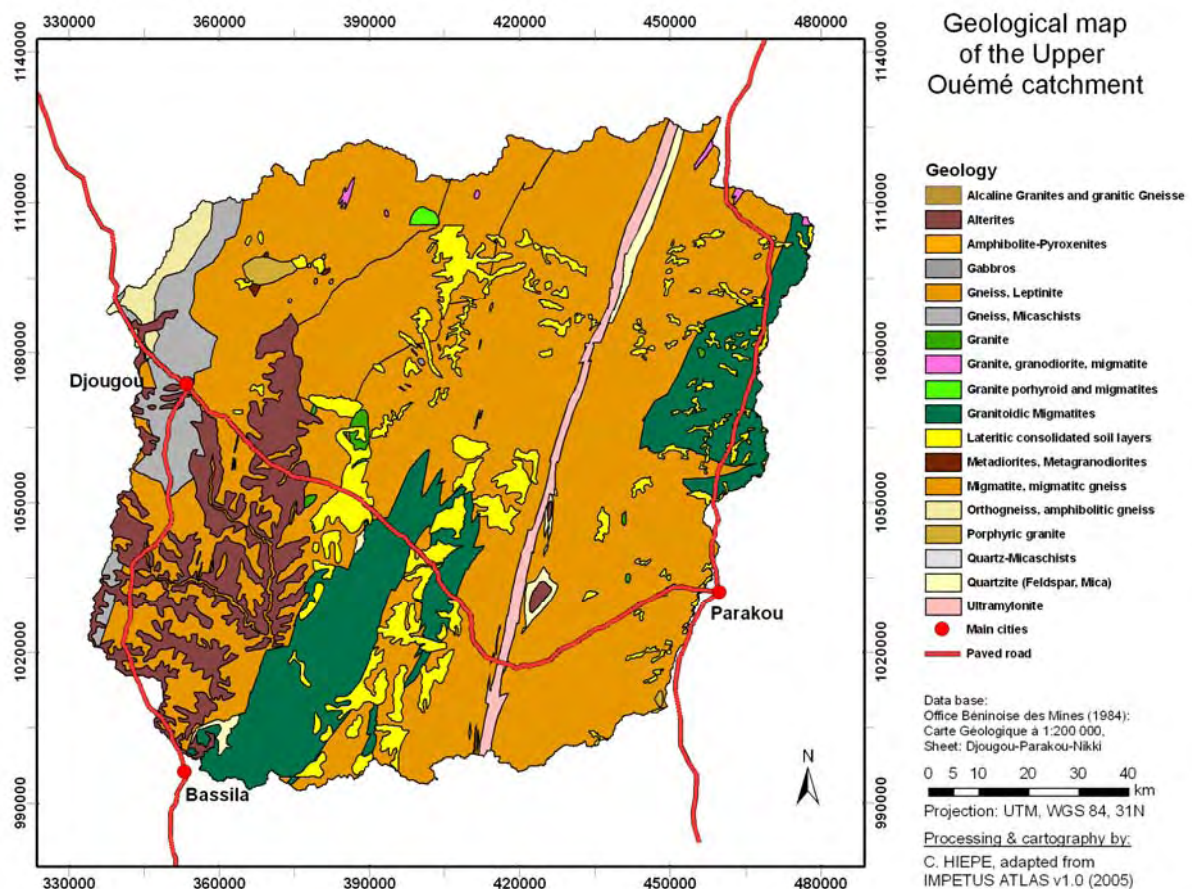


Fig. A.1 Geological map of the Upper Ouémé catchment – Sheet Djougou-Parakou-Nikki (Source: Office Béninois des Mines 1984).

Table A.1 Location of the investigated representative profiles in the Upper Ouémé catchment (Date: 14.09.-23.10. 2004).

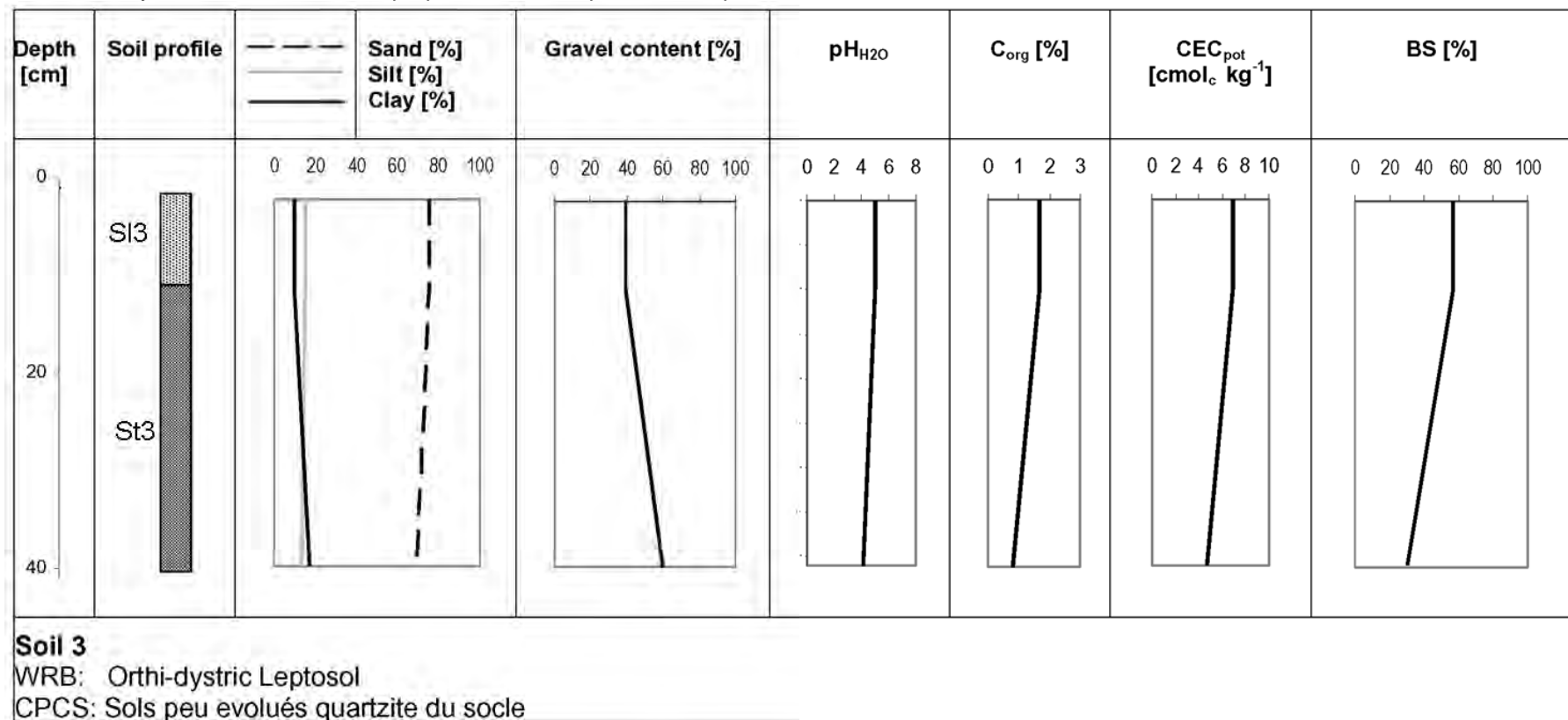
Soil type	x (UTM)	y (UTM)	Profile position	Land use	Location	# augerings	# sampled augerings
3	447013	1107177	Upper slope	<i>savane arbustive</i>	Kandi fault, W of Ndali	0	0
14	429958	1079009	Mid-slope	<i>savane arboree</i>	Bori	4	1
17	382013	1115455	Upper slope	<i>savane arbustive</i>	Kpere	6	1
18	405381	1079353	Upper slope	<i>savane arboree</i>	Sani	4	2
21	376098	1102334	Upper slope	<i>savane arbustive</i>	Kpere	4	4
25	361628	1066550	Upper slope	<i>savane arboree</i>	between Serou and Beterou	5	4
29	352004	107403	Upper slope	<i>savane arboree</i>	Djougou	6	6
31	424326	1017647	Mid-slope		Beterou	0	0
45	423218	1014805	Mid-slope	<i>savane herbeuse</i>	Beterou	0	0
48	428466	1020744	Upper slope	<i>savane arbustive, herbaceous fallow</i>	Beterou	7	5
55	352095	1105139	Summit	<i>savane arboree</i>	N of Copargo	5	2
56	451747	1033111	Mid-slope	<i>savane herbeuse</i>	W of Parakou	5	3
58	444170	1029504	Mid-slope	<i>savane arboree</i>	W of Parakou	6	4
62	436790	1044897	Mid-slope	<i>savane arbustive</i>	NW of Parakou		
70	383732	1120135	Upper slope	<i>savane arboree</i>	Kpere	4	3
80	450812	1003104	Lower slope	<i>savane arbustive, Cashew</i>	S of Parakou	5	3
90	449280	1032748	Upper slope	<i>savane arbustive</i>	W of Parakou	8	6
91	453183	1107826	Upper slope	<i>savane arbustive</i>	NW of Ndali	6	3
101	469505	1096298	Floodplaine	teak plantation	Ndali	5	4

<p>Soil 3</p> 	<p>Soil 14</p> 	<p>Soil 17</p> 	<p>Soil 18</p> 	<p>Soil 21</p> 
<p>WRB: Orthi-dystric Leptosol CPCS: Sols peu evolues sur quartzite du socle</p>	<p>WRB: Ferrali-Plinthic Cambisol [Endoskeletal] CPCS: Sol bruns eutrophes hydromorph</p>	<p>WRB: Humic Lixisol CPCS: Sols ferrugineux tropicaux peu lessivés sur granito-gneiss à biotite</p>	<p>WRB: Ferri-Endostagnic Acrisol [Endoskeletal] CPCS: Sols ferrugineux tropicaux peu lessivés sur gneiss à ferro-magnésiens</p>	<p>WRB: Hypereutric Vertisol CPCS: Sols ferrugineux tropicaux peu lessivés sur roche basique</p>
<p>Soil 25</p> 	<p>Soil 29</p> 	<p>Soil 31</p> 	<p>Soil 45</p> 	<p>Soil 48</p> 
<p>WRB: Endoskeleti-Albic Acrisol CPCS: Sols ferrugineux tropicaux peu lessivés sur matériaux kaolinitiques issu de granito-gneiss à biotite</p>	<p>WRB: Eutric Gleysol [or Gleyic Lixisol] CPCS: Sols ferrugineux tropicaux hydromorph sur roche basique</p>	<p>WRB: Arenosol CPCS: Sols ferrugineux tropicaux lessivés sans concrétions sur granite acide</p>	<p>WRB: Haplic Acrisol CPCS: Sols ferrugineux tropicaux lessivés avec concrétions sur embréchite</p>	<p>WRB: Profondic Lixisol CPCS: Sols ferrugineux tropicaux lessivés à concrétions sur granit et granito-gneiss à deux micas</p>

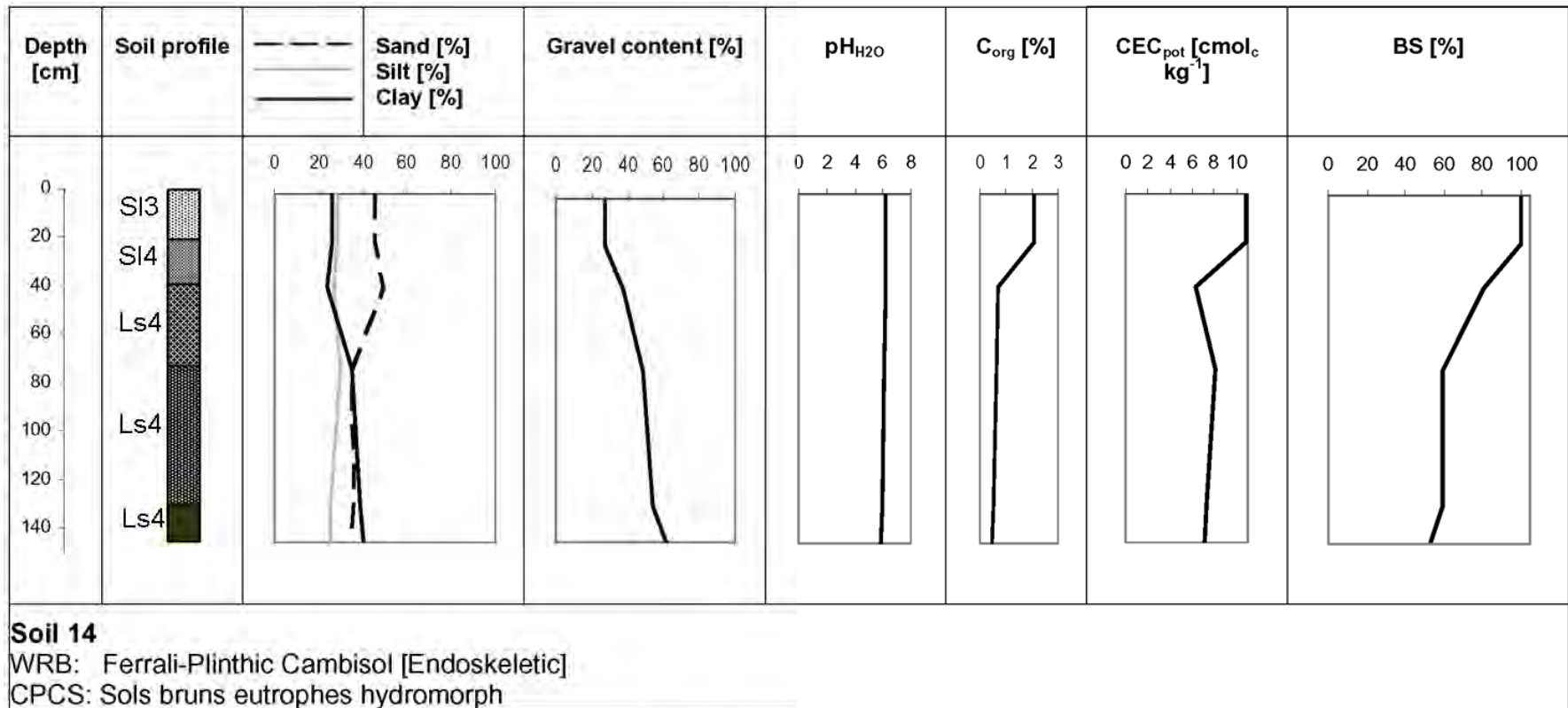
Soil 55	Soil 56	Soil 58	Soil 62	Soil 70
				
WRB: Haplic Lixisol CPCS: Sols ferrugineux tropicaux lessivés avec concrétions sur matériaux kaoliniques issus de gneiss à muscovite et à deux micas	WRB: Plinthic Acrisol [Hyperochric] CPCS: Sols ferrugineux tropicaux lessivés avec concrétions sur matériaux kaoliniques issus de granite acide	WRB: Humic Lixisol CPCS: Sols ferrugineux tropicaux lessivés avec concrétions sur matériaux kaoliniques issus de granite et granito-gneiss à deux micas	WRB: Albi-Petric Plinthosol [stagnic, Endoeutric] CPCS: Sols ferrugineux tropicaux lessivés indurés sur granito-gneiss à deux micas	WRB: Albi-Petric Plinthosol CPCS: Sols ferrugineux tropicaux lessivés indurés sur matériaux kaoliniques issus de gneiss à ferromagnésiens
Soil 80	Soil 90	Soil 91	Soil 101	
				
WRB: Plinthic Arenosol CPCS: Sols ferrugineux tropicaux appauvris sans concrétions sur granite calco-alcalin à biotite	WRB: Acric Ferralsol CPCS: Sols ferralitiques faiblement destrurés sur granito-gneiss acide	WRB: Plinthic Ferralsol CPCS: Sols ferralitiques rajeunis ou pénévulés sur gneiss à muscovite et à deux micas	WRB: Eutric Gleysol CPCS: Sols hydromorphes à gley sur matériau alluvio-colluvial fluvial	

Fig. A.2 Photos and classification of the representative profiles.

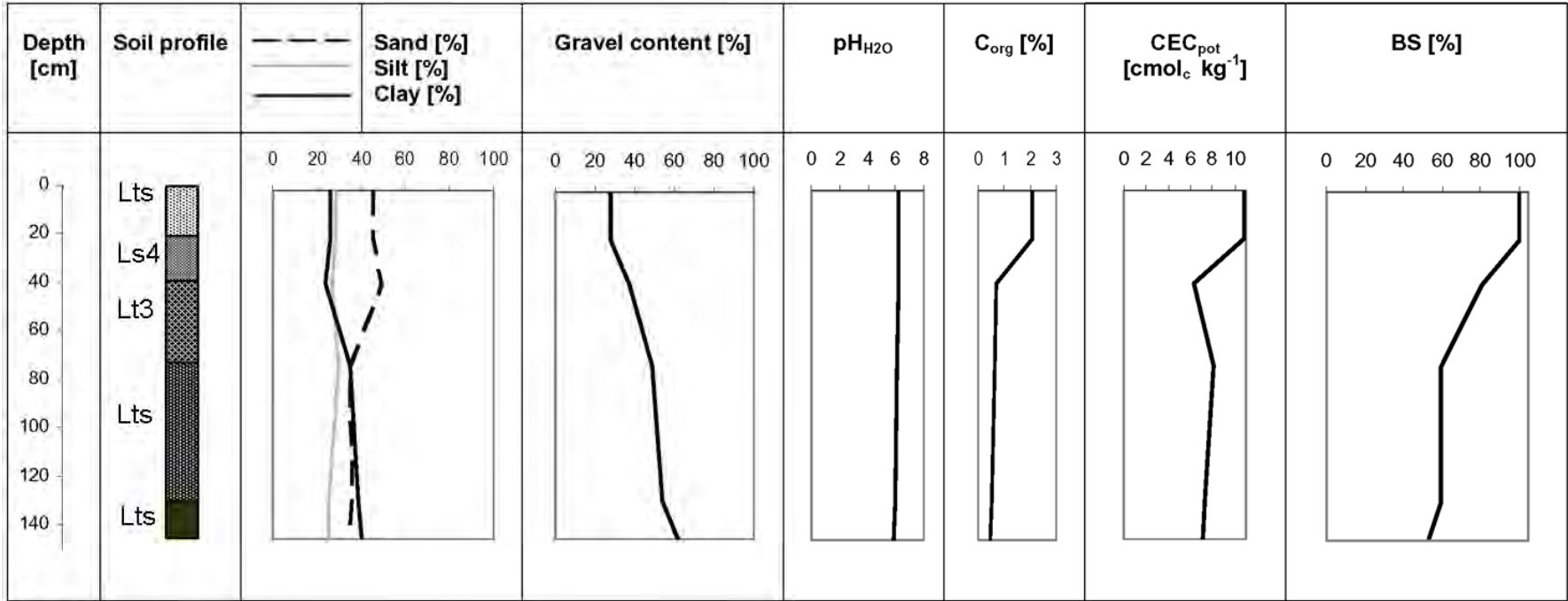
Table A.2 Physical and chemical soil properties of the representative profiles.



Depth [cm]	Sand [%]	Silt [%]	Clay [%]	Colour [-]	Gravel [%]	C _{org} [%]	S _{org} [%]	N [%]	C/N [-]	pH CaCl2	K	Na	Mg	Ca	CEC	CEC	BS [%]	
											cmol _e /kg AAS	cmol _e /kg AAS	cmol _e /kg ICP,AAS	cmol _e /kg ICP,AAS	cmol _e /kg soil	cmol _e /kg clay		
1	10	75.42	14.97	9.61	10YR/3.2	39.40	1.65	2.83	0.09	19	5.01	0.04	0.01	0.79	3.10	6.92	12.03	56.90
2	41	69.37	13.25	17.38	7.5YR/3.4	59.70	0.82	1.42	0.04	19	4.17	0.02	0.01	0.06	1.34	4.76	10.82	30.02



Depth [cm]	Sand [%]	Silt [%]	Clay [%]	Colour [-]	Gravel [%]	C _{org} [%]	S _{org} [%]	N [%]	C/N [-]	pH CaCl ₂	K	Na	Mg	Ca	CEC	CEC	BS [%]	
											cmol _c /kg AAS	cmol _c /kg AAS	cmol _c /kg ICP,AAS	cmol _c /kg ICP,AAS	cmol _c /kg soil	cmol _c /kg clay		
1	11	45.31	28.45	26.25	10YR/3.2	27.95	2.09	3.60	0.14	20	6.17	0.36	0.01	1.62	8.80	10.79	13.21	100.00
2	30	49.35	26.94	23.70	5YR/3.4	37.26	0.72	1.23	0.04	17	6.19	0.09	0.01	0.67	4.31	6.29	15.95	80.87
3	50	34.85	30.00	35.15	5YR/4.4	48.95	0.64	1.11	0.04	18	6.13	0.04	0.02	0.88	3.84	8.05	16.49	59.24
4	60	35.66	25.62	38.73	7.5YR/4.6	54.07	0.51	0.88	0.03	14	6.02	0.13	0.02	1.12	3.09	7.31	14.27	59.59
5	80	34.86	25.08	40.06	7.5YR/5.4	61.31	0.44	0.76	0.02	16	5.82	1.04	0.02	0.38	2.31	7.09	13.81	53.05

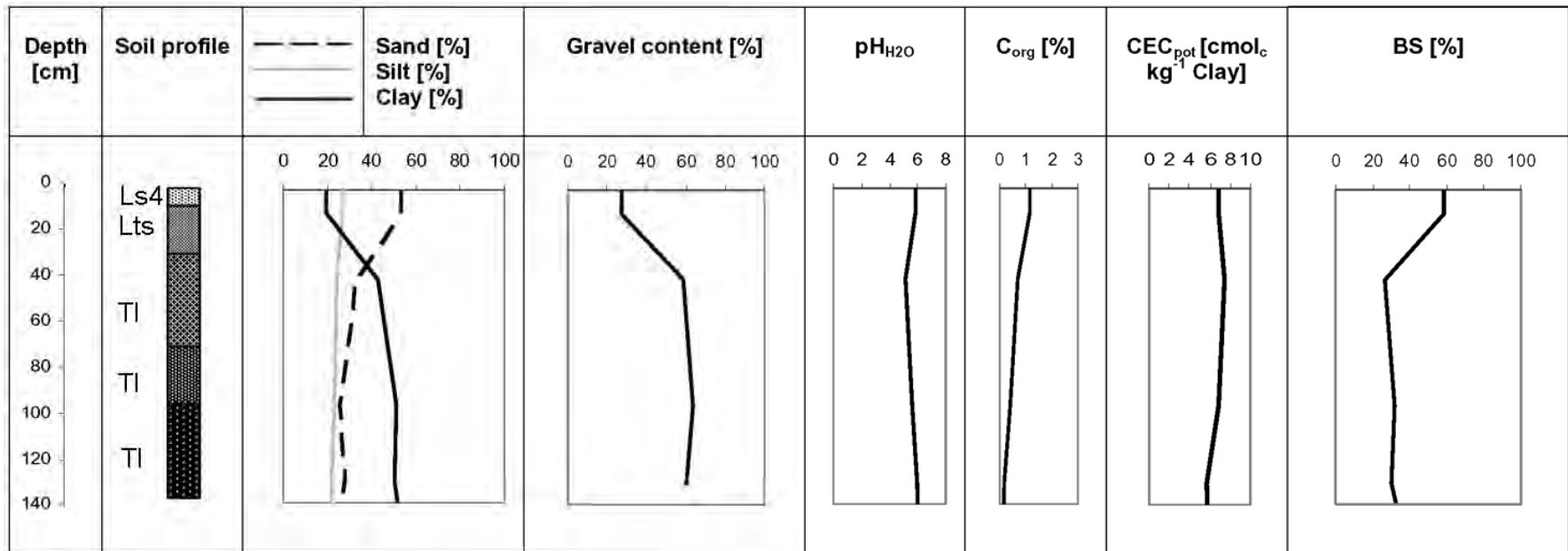


Soil 17

WRB: Humic Lixisol

CPCS: Sols ferrugineux tropicaux peu lessivés sur granito-gneiss a biotite

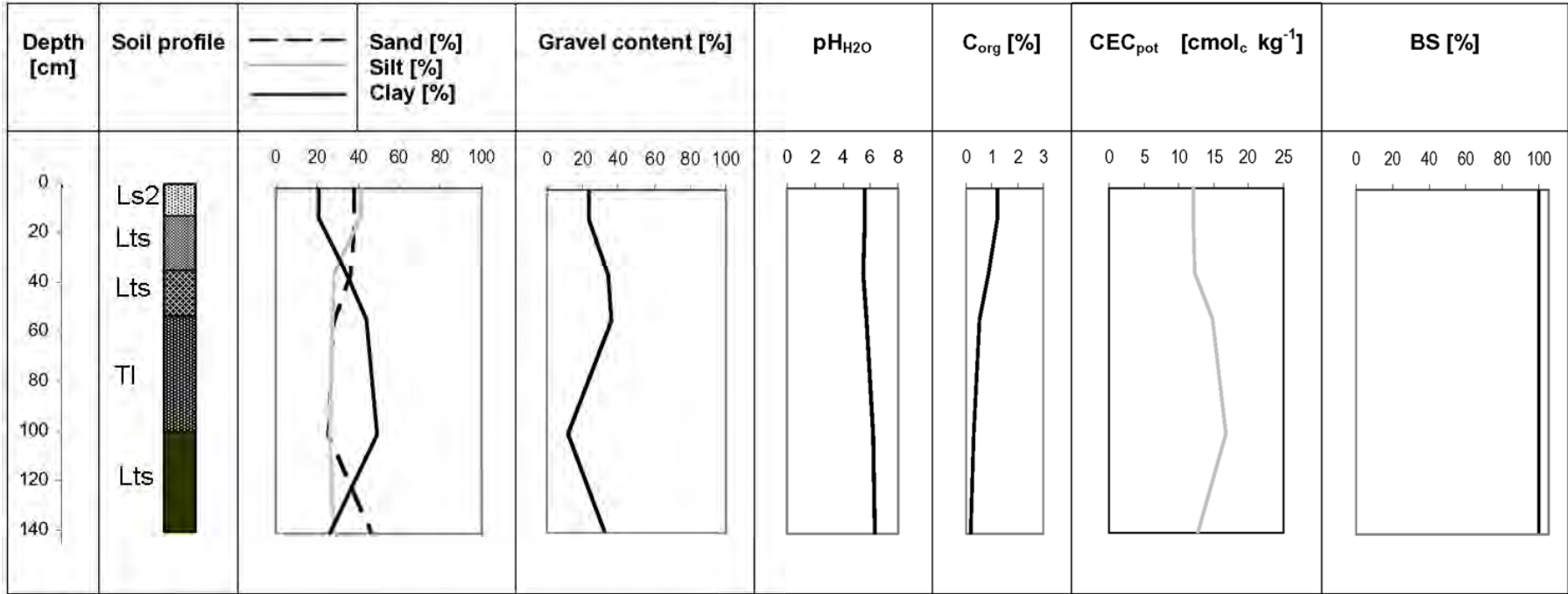
Depth [cm]	Sand [%]	Silt [%]	Clay [%]	Colour [-]	Gravel [%]	C _{org} [%]	S _{org} [%]	N [%]	C/N [-]	pH CaCl2	K	Na	Mg	Ca	CEC	CEC	BS [%]	
											cmol _c /kg AAS	cmol _c /kg AAS	cmol _c /kg ICP,AAS	cmol _c /kg ICP,AAS	cmol _c /kg soil	cmol _c /kg clay		
1	21	45.31	28.45	26.25	10YR/3.3	27.95	2.09	3.60	0.14	15	6.17	0.36	0.01	1.62	8.80	10.79	13.21	100.00
2	40	49.35	26.94	23.70	5YR/4.4	37.26	0.72	1.23	0.04	16	6.19	0.09	0.01	0.67	4.31	6.29	15.95	80.87
3	75	34.85	30.00	35.15	5YR/4.4	48.95	0.64	1.11	0.04	17	6.13	0.04	0.02	0.88	3.84	8.05	16.49	59.24
4	134	35.66	25.62	38.73	5YR/4.4	54.07	0.51	0.88	0.03	18	6.02	0.13	0.02	1.12	3.09	7.31	14.27	59.59
5	150	34.86	25.08	40.06	5YR/4.6	61.31	0.44	0.76	0.02	19	5.82	1.04	0.02	0.38	2.31	7.09	13.81	53.05

**Soil 18**

WRB: Ferri-Endostagnic Acrisol [Endoskeletal]

CPCS: Sols ferrugineux tropicaux peu lessivés sur gneiss a ferro-magnésiens

Depth [cm]	Sand [%]	Silt [%]	Clay [%]	Colour [-]	Gravel [%]	C _{org} [%]	S _{org} [%]	N [%]	C/N [-]	pH CaCl ₂	K	Na	Mg	Ca	CEC	CEC	BS [%]	
											cmol _c /kg AAS	cmol _c /kg AAS	cmol _c /kg ICP,AAS	cmol _c /kg ICP,AAS	cmol _c /kg soil	cmol _c /kg clay		
1	8	53.25	27.35	19.40	7.5YR/4.4	26.90	1.15	1.98	0.07	16	5.88	0.12	0.02	0.98	2.87	6.87	14.59	58.03
2	30	33.05	24.38	42.57	5YR/4.6	58.69	0.67	1.15	0.05	12	5.14	0.08	0.01	0.52	1.39	7.38	11.85	26.94
3	72	25.84	23.10	51.06	5YR/6.6	63.89	0.43	0.73	0.03	12	5.64	0.07	0.01	0.54	1.56	6.79	10.38	32.17
4	98	28.07	21.88	50.05	5YR/5.6	60.13	0.19	0.33	0.01	14	6.00	0.05	0.01	0.51	1.13	5.61	9.87	30.26
5	141	18.50	22.87	58.63	5YR/5.6	46.41	0.13	0.22	0.01	12	6.15	0.04	0.01	0.64	2.04	6.00	9.48	45.63

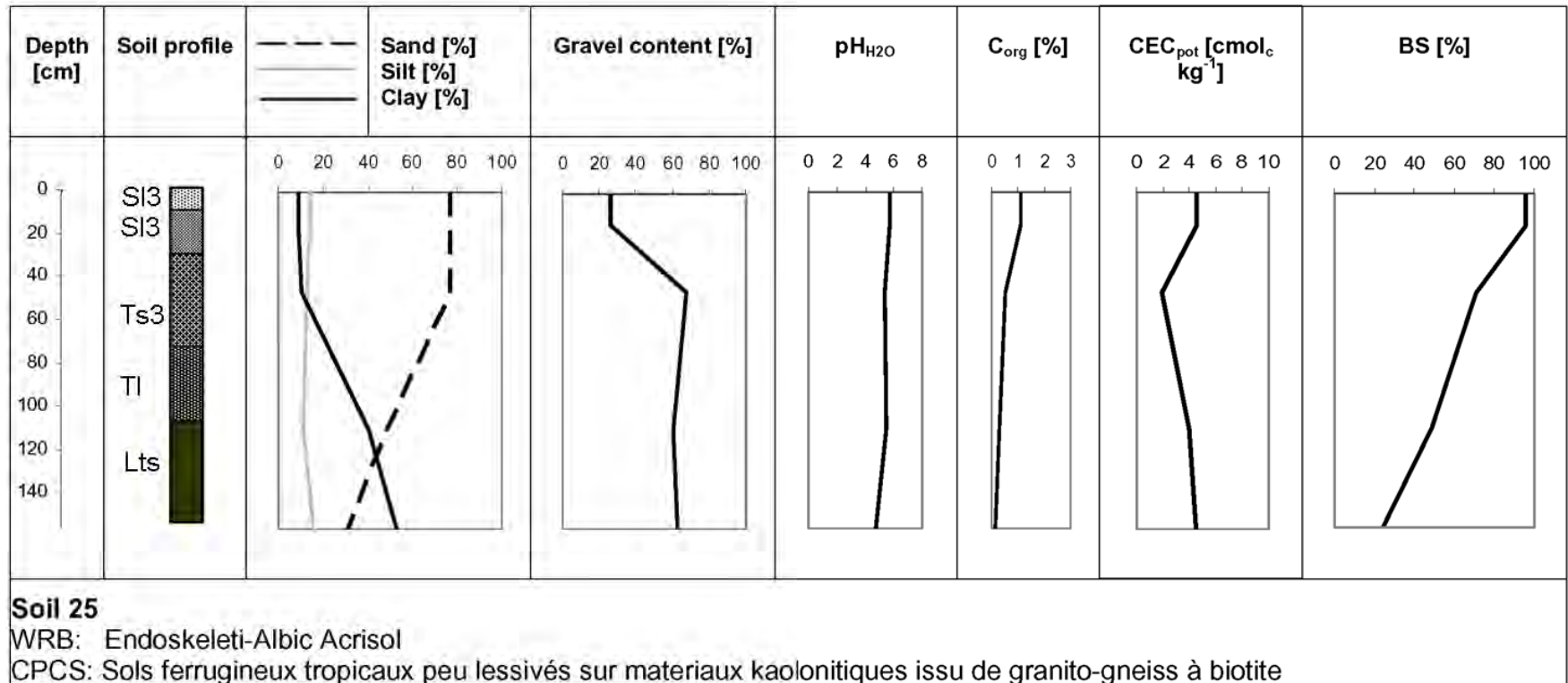


Soil 21

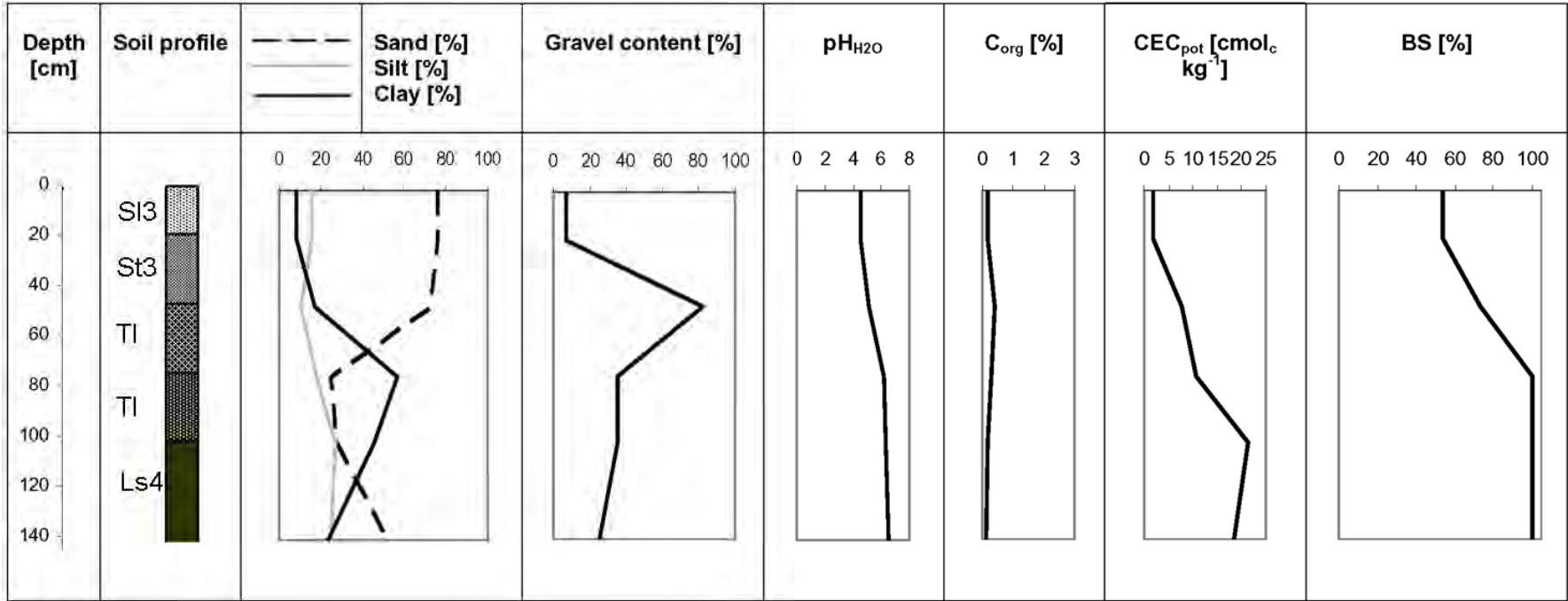
WRB: Hypereutric Vertisol

CPCS: Sols ferrugineux tropicaux peu lessivés sur roche basique

Depth [cm]	Sand [%]	Silt [%]	Clay [%]	Colour [-]	Gravel [%]	C _{org} [%]	S _{org} [%]	N [%]	C/N [-]	pH CaCl ₂	K cmol _c /kg AAS	Na cmol _c /kg AAS	Mg cmol _c /kg ICP,AAS	Ca cmol _c /kg ICP,AAS	CEC cmol _c /kg soil	CEC cmol _c /kg clay	BS [%]
1	13	37.90	40.87	5Y/3.1	23.59	1.22	2.09	0.05	25	5.60	0.08	0.08	3.41	8.41	11.98	36.34	100
2	36	36.78	28.70	5Y/3.1	33.79	0.88	1.51	0.06	15	5.54	0.14	0.10	5.00	14.18	12.24	26.54	100
3	55	28.52	27.40	5Y/4.1	35.71	0.51	0.88	0.04	14	5.72	0.34	0.17	7.69	19.15	14.88	29.71	100
4	103	25.24	25.79	5Y/4.1	11.91	0.31	0.53	0.01	24	6.19	0.48	0.16	10.05	21.08	16.64	31.80	100
5	145	46.01	28.08	10YR/3.1 10YR/5.8 5Y/6.1	32.37	0.15	0.26	0.01	12	6.35	0.23	0.25	8.49	17.19	12.69	46.90	100



Depth [cm]	Sand [%]	Silt [%]	Clay [%]	Colour [-]	Gravel [%]	C _{org} [%]	S _{org} [%]	N [%]	C/N [-]	pH CaCl2	K cmol _c /kg AAS	Na cmol _c /kg AAS	Mg cmol _c /kg ICP,AAS	Ca cmol _c /kg ICP,AAS	CEC soil cmol _c /kg	CEC clay cmol _c /kg	BS [%]	
1	10	76.69	14.29	9.02	10YR/3.1	26.26	1.11	1.90	0.08	14	5.75	0.08	0.01	0.82	3.44	4.55	7.49	95.74
2	31	76.84	12.60	10.56	7.5YR/4.2	67.26	0.54	0.93	0.03	17	5.43	0.07	0.01	0.44	0.86	1.97	0.67	70.67
3	74	48.37	11.54	40.09	5YR/4.6	60.08	0.29	0.49	0.03	11	5.48	0.04	0.00	1.11	0.76	3.94	7.33	48.80
4	109	28.89	16.43	54.67	5YR/5.6	62.86	0.14	0.24	0.01	11	4.71	0.03	0.01	0.38	0.57	4.58	7.48	21.52
5	156	31.85	24.78	43.37	2.5YR/4.8, 7.5YR/5.8, 10YR/6.8	39.88	0.08	0.14	0.01	9	4.61	0.02	0.01	0.16	0.43	3.95	8.45	15.48

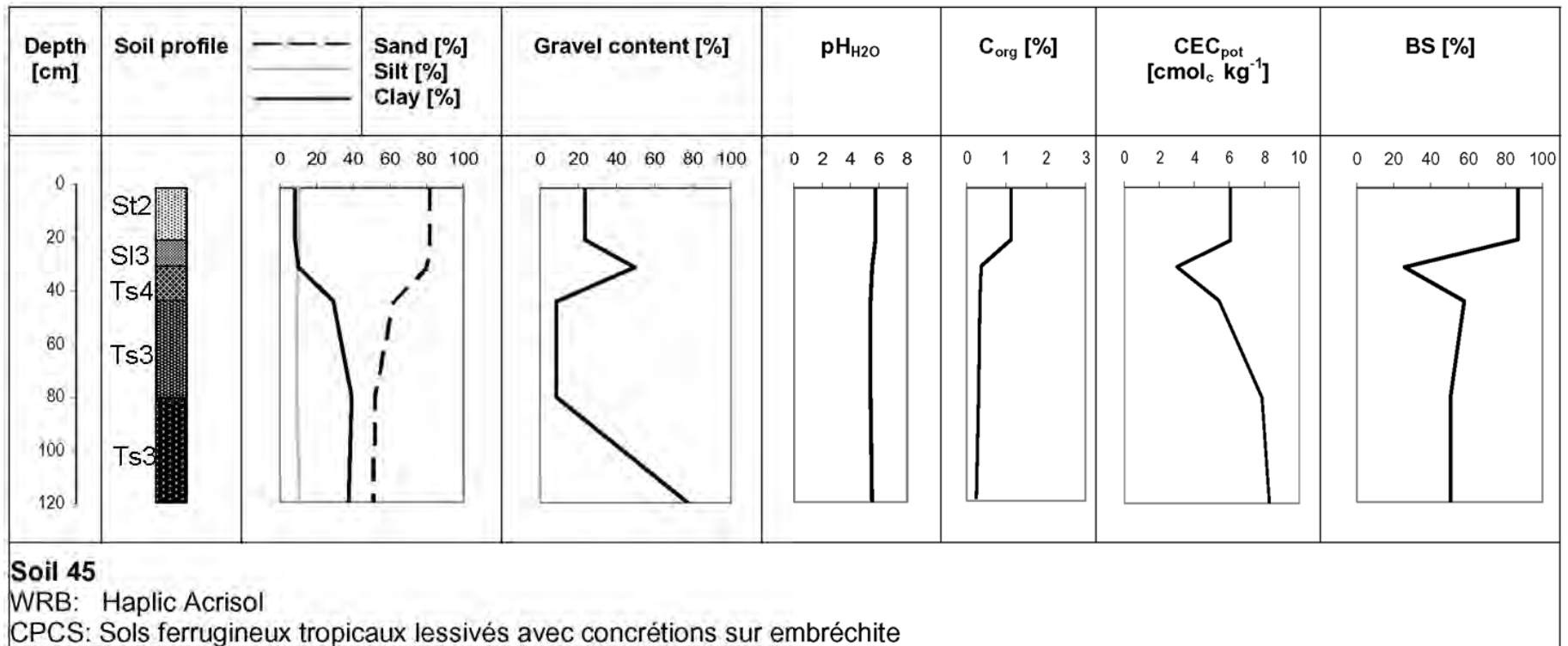


Soil 29

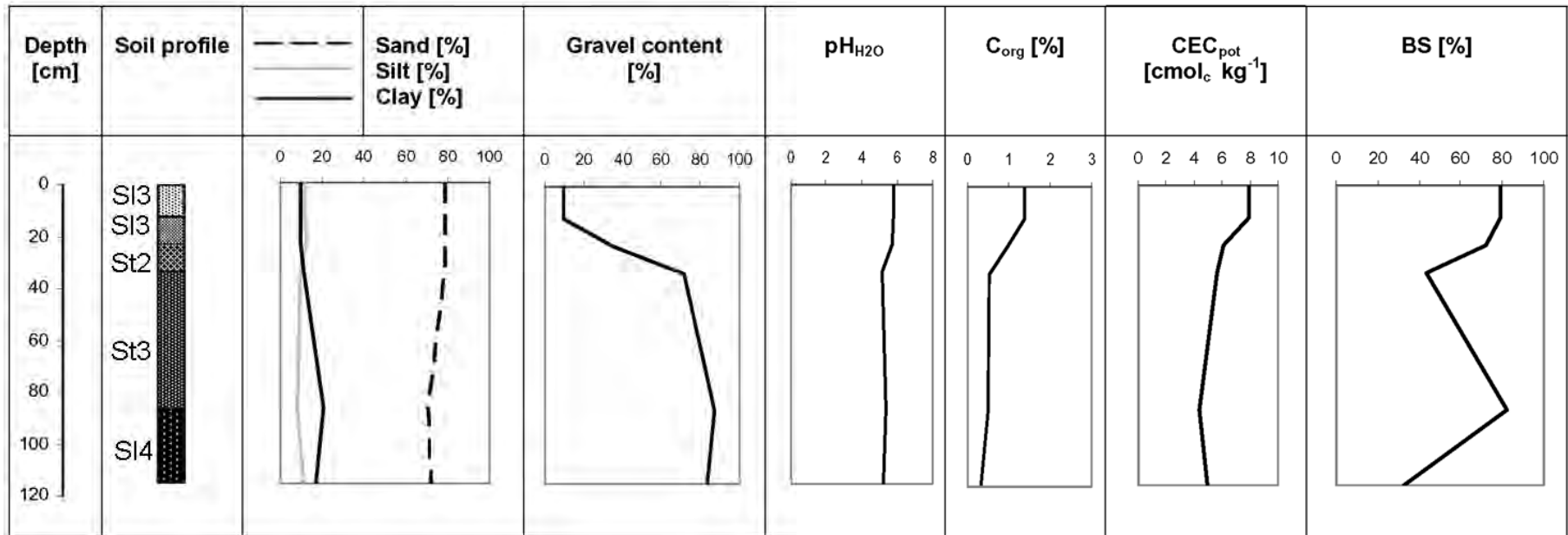
WRB: Eutric Gleysol [or Gleyic Lixisol]

CPCS: Sols ferrugineux tropicaux hydromorph sur roche basique

	Depth [cm]	Sand [%]	Silt [%]	Clay [%]	Colour [-]	Gravel [%]	C _{org} [%]	S _{org} [%]	N [%]	C/N [%]	pH CaCl2	K cmol/kg AAS	Na cmol/kg AAS	Mg cmol/kg ICP,AAS	Ca cmol/kg ICP,AAS	CEC cmol/kg soil	CEC cmol/kg clay	BS [%]
1	20	76.30	15.46	8.24	10YR/4.3	7.37	0.19	0.33	0.02	10	4.48	0.01	0.03	0.36	0.65	1.98	15.94	53.62
2	48	72.11	10.49	17.40	10YR/4.3	82.13	0.41	0.70	0.04	9	5.12	0.05	0.05	2.30	3.16	7.58	35.35	73.35
3	77	24.98	18.06	56.96	5Y/6.1	35.45	0.27	0.46	0.02	13	6.15	0.04	0.19	8.22	2.04	10.49	16.77	100.00
4	105	27.42	26.74	45.84	5Y/6.1	35.22	0.18	0.30	0.01	14	6.38	0.05	0.19	10.93	10.14	21.32	45.15	100.00
5	151	54.96	24.71	20.34	5YR/5.8, 2.5Y/4.0, 5Y/6.1	23.77	0.11	0.19	0.01	19	6.56	0.03	0.19	11.28	6.58	18.09	87.07	100.00



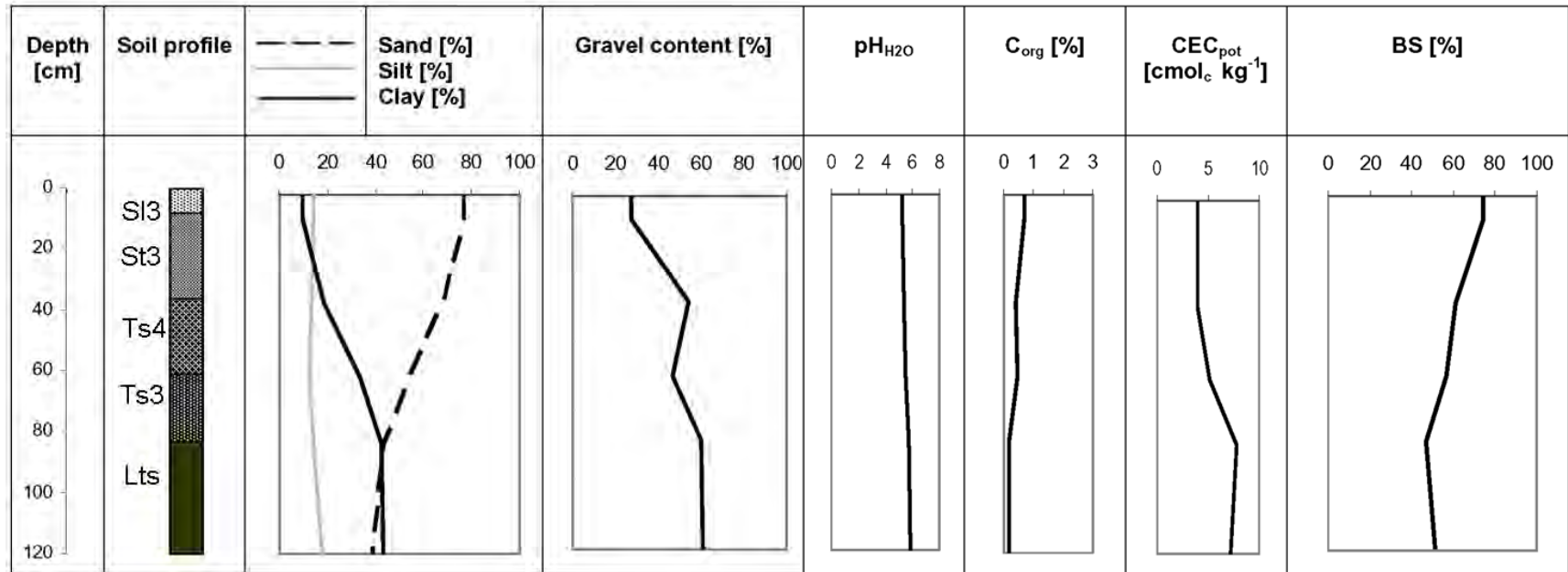
	Depth [cm]	Sand [%]	Silt [%]	Clay [%]	Colour [-]	Gravel [%]	C _{org} [%]	S _{org} [%]	N [%]	C/N [-]	pH CaCl ₂	K cmol _c /kg AAS	Na cmol _c /kg AAS	Mg cmol _c /kg ICP,AAS	Ca cmol _c /kg ICP,AAS	CEC cmol _c /kg soil	CEC cmol _c /kg clay	BS [%]
1	20	82.09	9.95	7.95	10YR/2.2	23.64	1.11	1.91	0.07	15	5.71	0.09	0.02	0.87	4.27	6.04	27.04	87.12
2	30	80.16	10.17	9.67	10YR/3.3	49.13	0.36	0.61	0.02	14	5.49	0.03	0.01	0.40	0.32	2.99	17.99	25.87
3	43	61.49	9.05	29.46	10YR/3.4	8.60	0.34	0.58	0.03	10	5.44	0.10	0.02	0.86	2.18	5.43	14.44	58.06
4	80	51.84	8.88	39.28	7.5YR/4.3	8.53	0.28	0.48	0.03	9	5.46	0.12	0.02	1.01	2.82	7.84	17.46	50.63
5	120	51.23	11.35	37.42	7.5YR/4.3	83.79	0.24	0.41	0.02	10	5.50	0.10	0.03	0.98	3.07	8.36	20.12	50.09

**Soil 48**

WRB: Haplic Lixisol

CPCS: Sols ferrugineux tropicaux lessivés à concrétions sur granite et granito-gneiss à deux micas

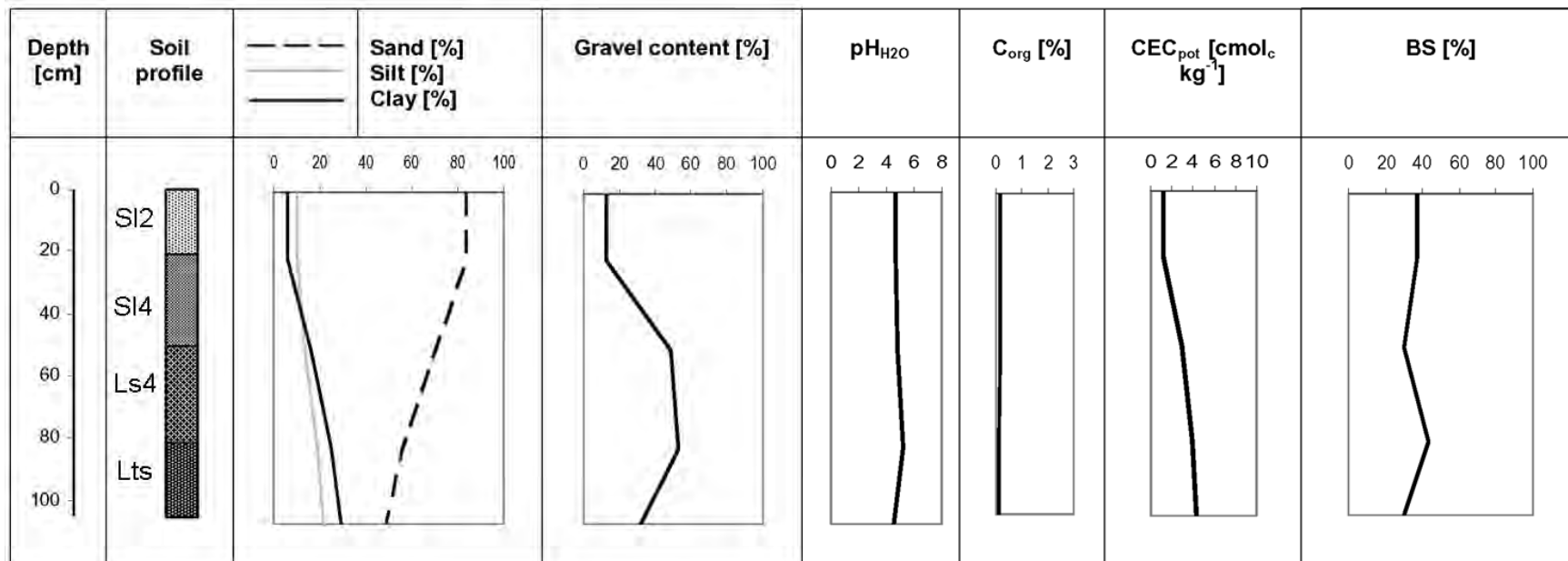
Depth [cm]	Sand [%]	Silt [%]	Clay [%]	Colour [-]	Gravel [%]	C _{org} [%]	S _{org} [%]	N [%]	C/N [-]	pH CaCl2	K	Na	Mg	Ca	CEC	CEC	BS [%]
											cmol _c /kg AAS	cmol _c /kg AAS	cmol _c /kg ICP,AAS	cmol _c /kg ICP,AAS	cmol _c /kg soil	cmol _c /kg clay	
1	13	78.52	11.72	10YR/3.2	<10	1.39	2.39	0.09	16	5.84	0.15	0.01	0.99	5.10	7.88	30.77	79.42
2	24	78.53	12.16	7.5YR/3.2	35.30	0.96	1.66	0.05	18	5.76	0.05	0.02	0.91	3.44	6.10	29.34	72.44
3	35	79.01	9.90	7.5YR/3.3	71.69	0.52	0.89	0.04	14	5.18	0.05	0.01	0.54	1.81	5.59	34.03	43.21
4	90	70.82	8.43	7.5YR/4.4	86.95	0.49	0.84	0.03	14	5.38	0.13	0.16	0.33	2.99	4.38	12.89	82.49
5	120	72.24	11.09	7.5YR/5.4	83.73	0.31	0.54	0.02	17	5.21	0.06	0.02	0.56	0.95	4.89	22.77	32.61

**Soil 55**

WRB: Haplic Lixisol

CPCS: Sols ferrugineux tropicaux lessivés avec concrétions sur matériaux kaoliniques issus d'gneiss à muscovite et à deux micas

Depth [cm]	Sand [%]	Silt [%]	Clay [%]	Colour [-]	Gravel [%]	C _{org} [%]	S _{org} [%]	N [%]	C/N [-]	pH CaCl2	K AAS [cmol _e /kg]	Na AAS [cmol _e /kg]	Mg ICP,AAS [cmol _e /kg]	Ca ICP,AAS [cmol _e /kg]	CEC soil [cmol _e /kg]	CEC clay [cmol _e /kg]	BS [%]	
1	8	76.57	13.94	9.49	10YR/3.2	27.10	0.67	1.16	0.04	15	5.26	0.05	0.01	0.45	2.43	3.97	16.97	74.21
2	36	68.20	13.52	18.29	10YR/4.4	54.11	0.41	0.71	0.03	14	5.41	0.04	0.01	0.27	2.09	3.95	13.68	61.06
3	61	53.81	12.64	33.55	7.5YR/5.4	46.26	0.44	0.75	0.03	15	5.52	0.06	0.01	0.29	2.57	5.20	10.96	56.31
4	83	43.28	13.87	42.84	10YR/5.4	60.40	0.20	0.35	0.02	11	5.68	0.11	0.01	0.58	2.99	7.85	16.67	46.99
5	120	38.94	17.85	43.21	10YR/5.6, 2.5YR/4.6	61.14	0.16	0.27	0.02	10	5.83	0.11	0.01	0.85	2.75	7.26	15.54	51.27

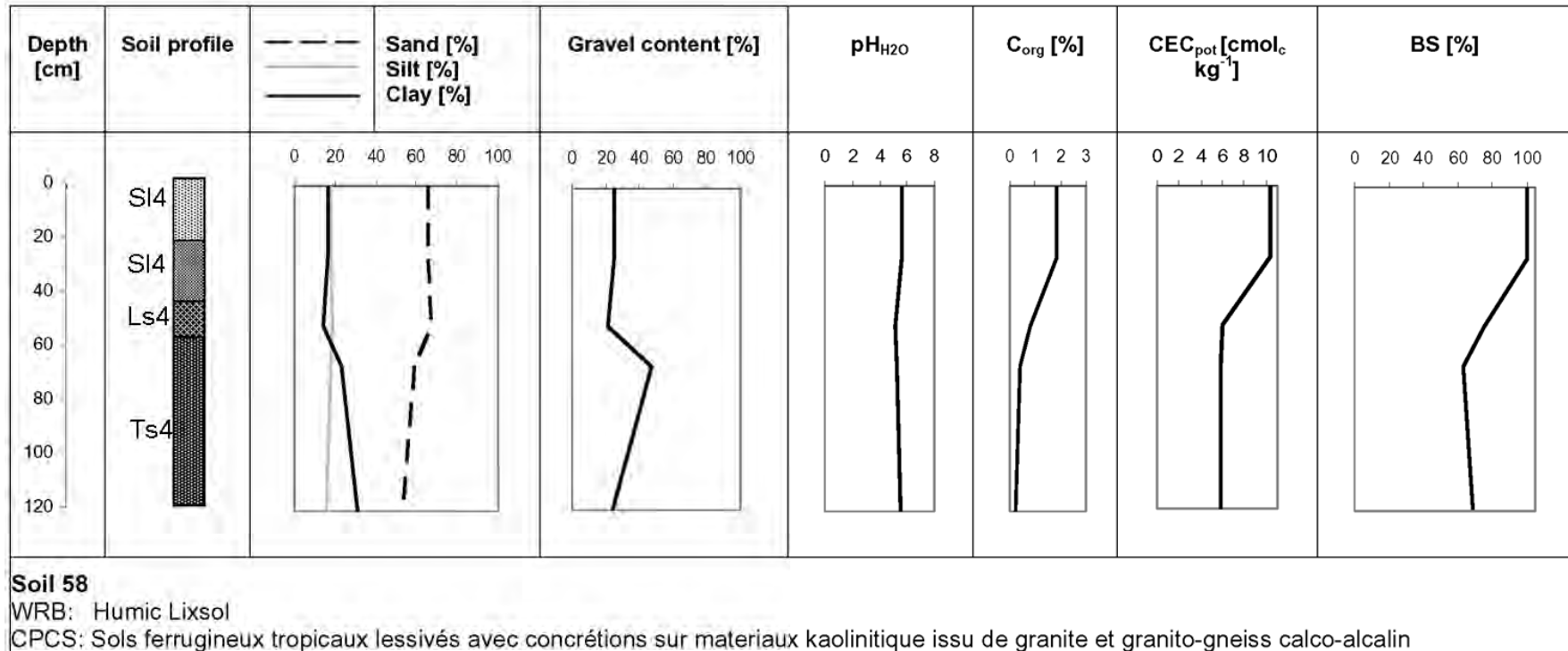


Soil 56

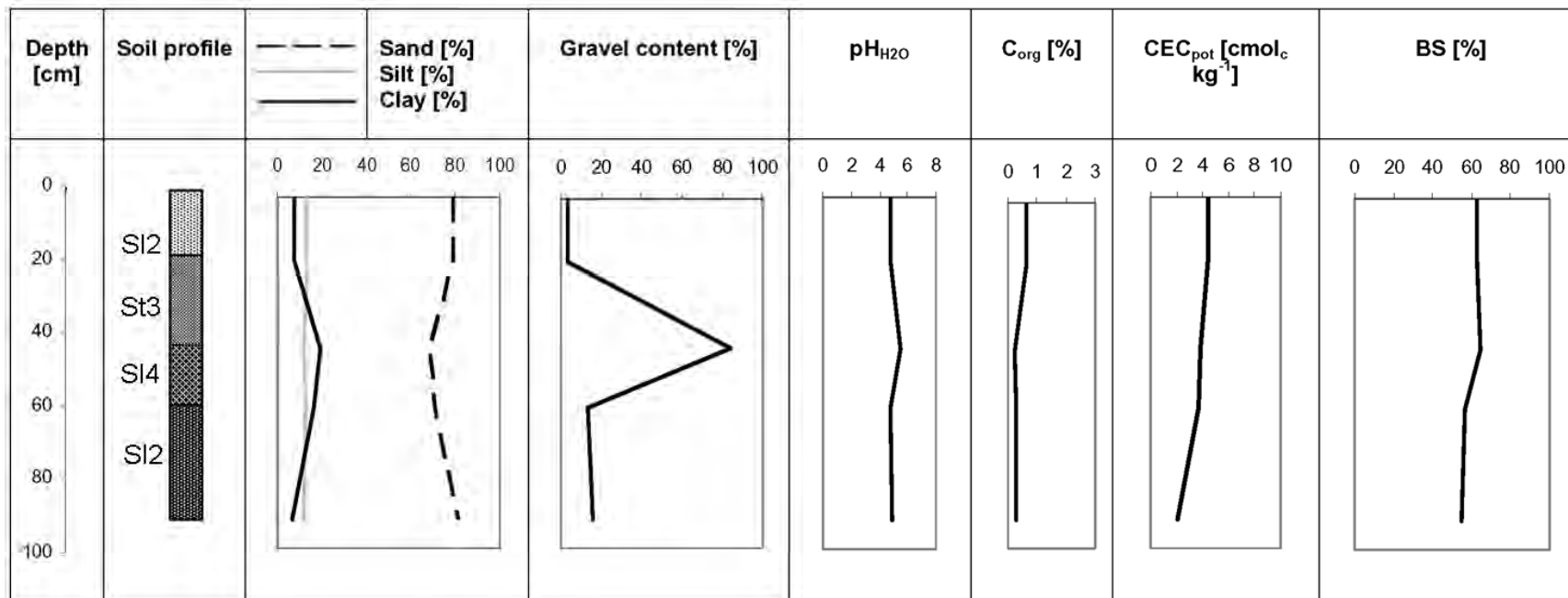
WRB: Plinthic Acrisol [Hyperochric]

CPCS: Sols ferrugineux tropicaux lessivés avec concrétions

Depth [cm]	Sand [%]	Silt [%]	Clay [%]	Colour [-]	Gravel [%]	C _{org} [%]	S _{org} [%]	N [%]	C/N [-]	pH CaCl2	K	Na	Mg	Ca	CEC	CEC	BS [%]	
											cmol _c /kg AAS	cmol _c /kg AAS	cmol _c /kg ICP,AAS	cmol _c /kg ICP,AAS	cmol _c /kg soil	cmol _c /kg clay		
1	21	83.70	10.50	5.80	10YR/4.3	12.97	0.17	0.29	0.01	11	4.63	0.03	0.01	0.12	0.30	1.23	21.92	36.84
2	50	69.94	13.78	16.28	10YR/5.8 2.5YR/4.8,	48.57	0.15	0.26	0.01	13	4.81	0.03	0.01	0.23	0.59	2.86	96.66	30.35
3	81	55.74	19.28	24.98	7.5YR/5.6	52.61	0.10	0.18	0.01	10	5.19	0.05	0.01	0.53	1.12	3.94	110.26	43.38
4	105	49.09	21.56	29.35	2.5YR/4.8, 10YR/7.4, 10YR/6.8	32.00	0.13	0.23	0.01	14	4.58	0.09	0.03	0.51	0.71	4.38	89.81	30.32



	Depth [cm]	Sand [%]	Silt [%]	Clay [%]	Colour [-]	Gravel [%]	C _{org} [%]	S _{org} [%]	N [%]	C/N [-]	pH CaCl ₂	K	Na	Mg	Ca	CEC	CEC	BS [%]
												cmol _c /kg AAS	cmol _c /kg AAS	cmol _c /kg ICP,AAS	cmol _c /kg ICP,AAS	cmol _c /kg soil	cmol _c /kg clay	
1	23	65.59	18.17	16.24	10YR/3.1	24.89	1.83	3.14	0.11	17	5.66	0.52	0.02	1.41	8.33	10.29	23.99	100
2	45	67.18	18.70	14.12	10YR/4.3 2.5YR/4.8	20.99	0.81	1.39	0.03	24	5.14	0.08	0.02	0.37	4.09	6.03	22.64	75.57
3	58	58.84	17.75	23.41	10YR/4.4	46.79	0.39	0.67	0.02	16	5.26	0.12	0.02	0.41	3.14	5.86	19.15	62.95
4	120	51.75	14.64	33.61	7.5YR/4.2, 10YR/6.4, 2.5YR/4.6	16.34	0.18	0.30	<0.01	>18	5.56	0.14	0.03	0.53	3.40	5.79	15.41	70.83

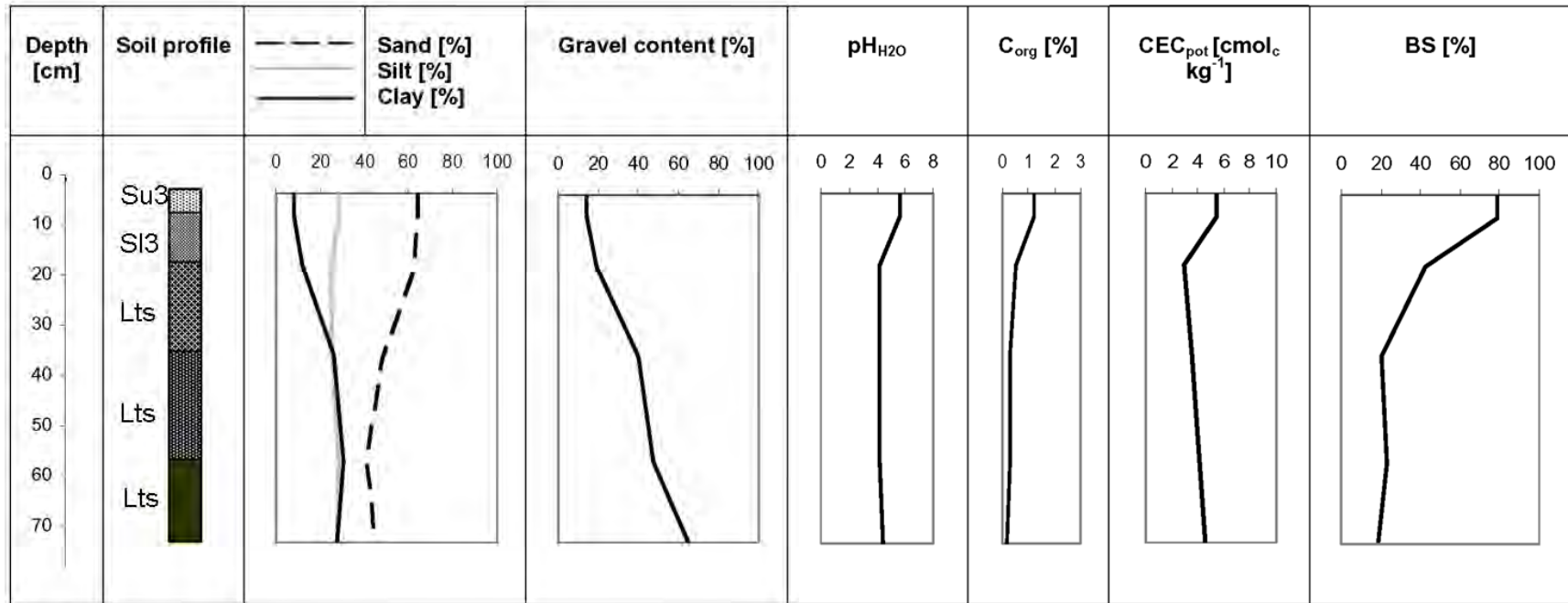


Soil 62

WRB: Albi-Petric Plinthosol [stagnic, endoeutric]

CPCS: Sols ferrugineux tropicaux lessivés indurés sur granito-gneiss à deux micas

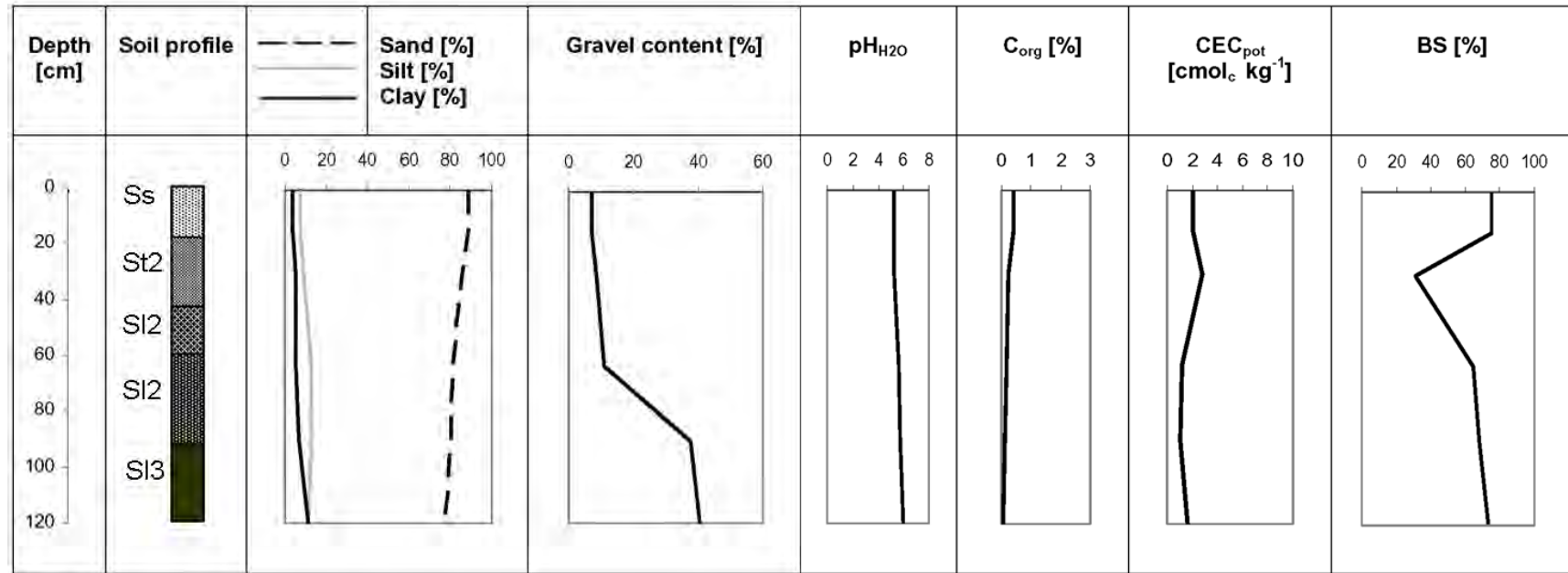
Depth [cm]	Sand [%]	Silt [%]	Clay [%]	Colour [-]	Gravel [%]	C _{org} [%]	S _{org} [%]	N [%]	C/N [-]	pH CaCl2	K cmol _c /kg AAS	Na cmol _c /kg AAS	Mg cmol _c /kg ICP,AAS	Ca cmol _c /kg ICP,AAS	CEC cmol _c /kg soil	CEC cmol _c /kg clay	BS [%]	
1	18	79.22	13.41	7.38	10YR/3.2	3.30	0.65	1.11	0.04	17	4.72	0.13	0.02	0.44	2.18	4.41	29.17	62.64
2	43	68.88	11.62	19.50	10YR/5.3	84.27	0.24	0.40	0.02	10	5.55	0.11	0.02	0.55	1.76	3.79	15.24	64.33
3	60	70.68	12.97	16.34	10YR/6.6	13.47	0.29	0.50	0.03	10	4.82	0.09	0.03	0.36	1.58	3.65	16.18	56.42
4	92	81.13	12.15	6.72	10YR/6.4, 5YR/5.6, 10YR/2.m	15.51	0.27	0.47	0.02	14	4.86	0.06	0.02	0.13	0.92	2.06	16.47	54.99

**Soil 70**

WRB: Albi-Petric Plinthosol

CPCS: Sols ferrugineux tropicaux lessivés indurés sur matériaux kaolinique issu de gneiss à ferro-magnésiens

	Depth [cm]	Sand [%]	Silt [%]	Clay [%]	Colour [-]	Gravel [%]	C _{org} [%]	S _{org} [%]	N [%]	C/N [-]	pH CaCl2	K	Na	Mg	Ca	CEC	CEC	BS [%]
												cmol _c /kg AAS	cmol _c /kg AAS	cmol _c /kg ICP,AAS	cmol _c /kg ICP,AAS	cmol _c /kg soil	cmol _c /kg clay	
1	5	64.04	28.07	7.89	10YR/4.2	13.80	1.23	2.11	0.08	15	5.59	0.16	0.02	1.00	3.07	5.39	13.93	78.79
2	16	62.63	25.45	11.93	10YR/5.3	19.16	0.51	0.87	0.03	19	4.21	0.05	0.02	0.58	0.61	2.96	9.94	42.60
3	36	48.25	25.60	26.15	10YR/5.4	39.73	0.32	0.54	0.03	12	4.12	0.06	0.02	0.22	0.44	3.59	9.51	20.49
4	60	41.14	28.32	30.54	10YR/6.4	47.19	0.30	0.51	0.03	12	4.15	0.07	0.01	0.18	0.68	4.06	9.88	23.13
5	78	44.73	27.66	27.61	2.5YR/4.8, 10YR/6.3	65.34	0.15	0.27	0.02	9	4.37	0.06	0.01	0.12	0.63	4.50	14.33	18.53

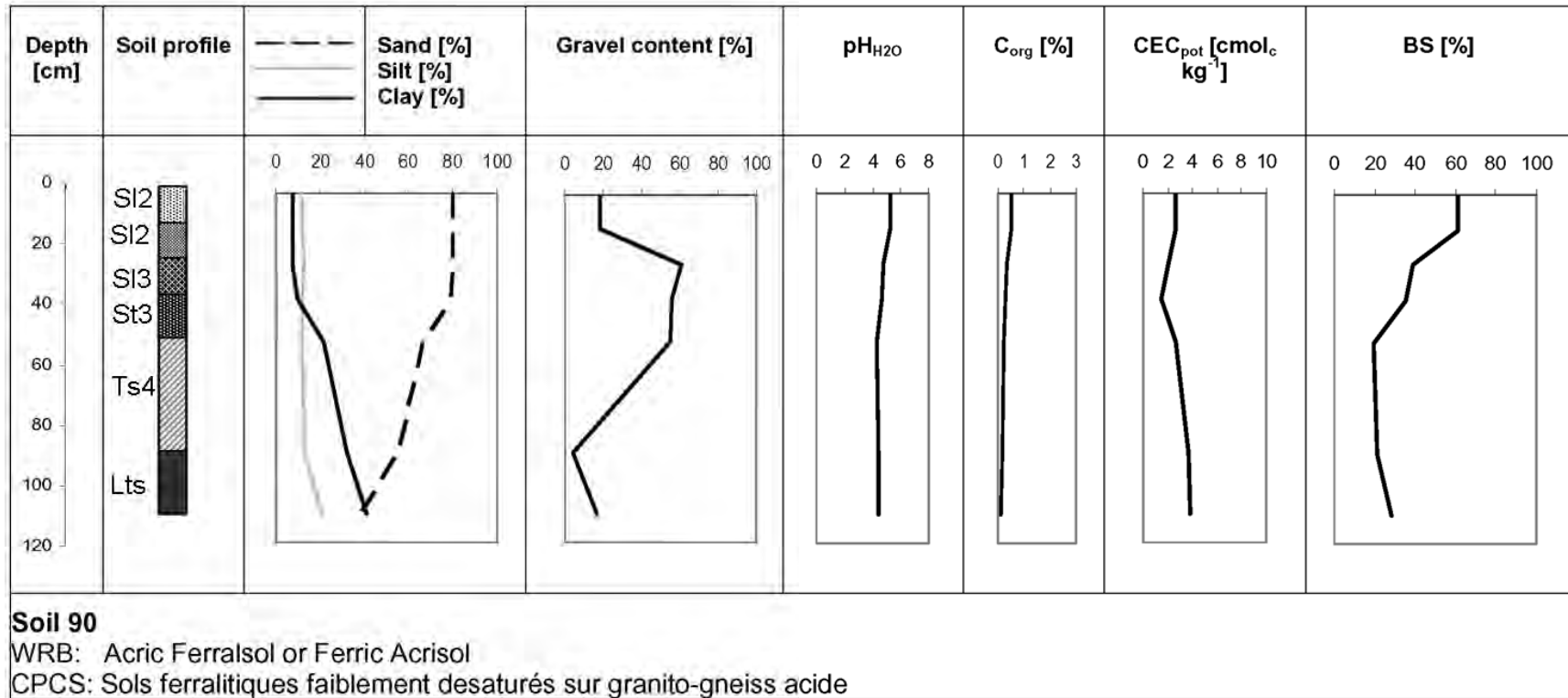


Soil 80

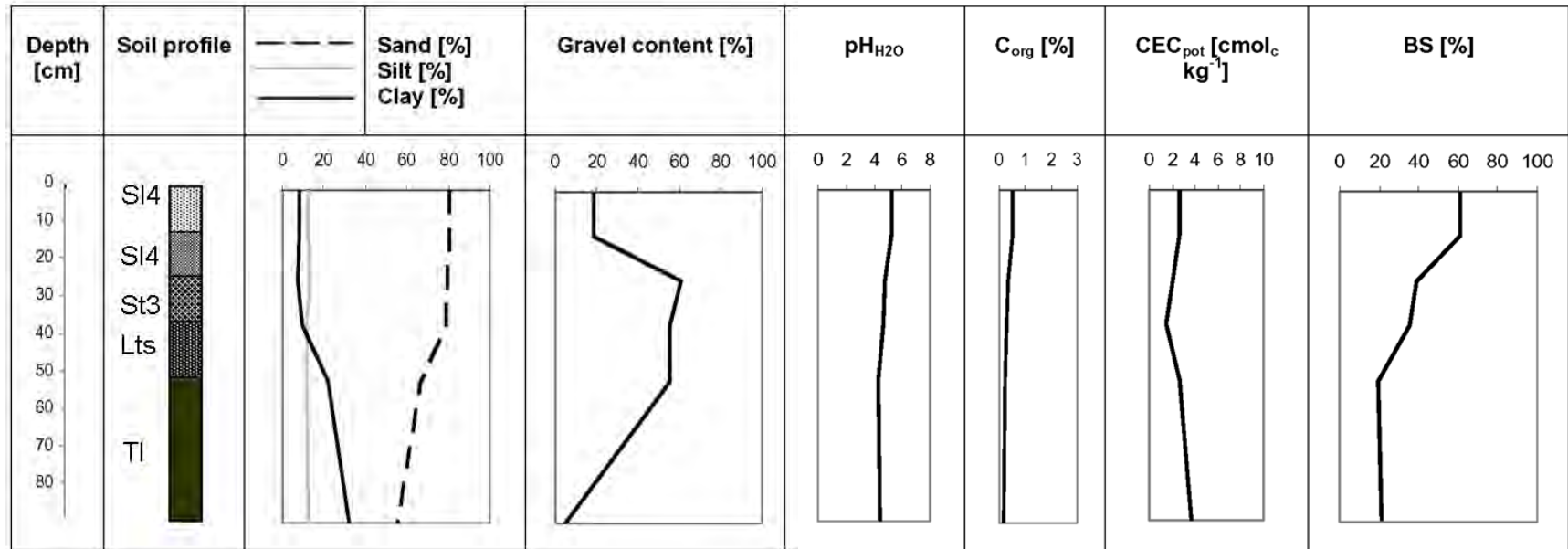
WRB : Plinthic Arenosol [Endoeutric]

CPCS : Sols ferrugineux tropicaux appauvris sans concrétions sur granite calco-alkalin à biotite

	Depth [cm]	Sand [%]	Silt [%]	Clay [%]	Colour [-]	Gravel [%]	C _{org} [%]	S _{org} [%]	N [%]	C/N [-]	pH CaCl2	K cmol _c /kg AAS	Na cmol _c /kg AAS	Mg cmol _c /kg ICP,AAS	Ca cmol _c /kg ICP,AAS	CEC cmol _c /kg soil	CEC cmol _c /kg clay	BS [%]
1	15	89.03	7.51	3.45	10YR/3.2	6.96	0.43	0.74	0.02	17	5.24	0.07	0.01	0.35	1.08	2.02	15.17	74.82
2	30	85.91	8.71	5.38	7.5YR/4.2	8.69	0.24	0.41	0.01	18	5.21	0.08	0.02	0.10	0.69	2.83	37.17	31.03
3	63	81.44	12.96	5.59	7.5YR/5.4	10.85	0.18	0.31	0.01	16	5.57	0.04	0.01	0.08	0.59	1.11	8.56	64.92
4	90	80.20	12.67	7.12	7.5YR/5.4	37.41	0.13	0.23	0.01	20	5.78	0.05	0.01	0.13	0.52	1.04	8.09	68.24
5	120	77.10	11.58	11.33	10YR/5.4	40.56	0.06	0.11	0.01	8	6.00	0.06	0.01	0.22	0.91	1.65	12.60	73.09



	Depth [cm]	Sand [%]	Silt [%]	Clay [%]	Colour [-]	Gravel [%]	C _{org} [%]	S _{org} [%]	N [%]	C/N [-]	pH CaCl2	K cmol _c /kg AAS	Na cmol _c /kg AAS	Mg cmol _c /kg ICP,AAS	Ca cmol _c /kg ICP,AAS	CEC cmol _c /kg soil	CEC cmol _c /kg clay	BS [%]
1	12	80.15	12.18	7.67	10YR/3.2	18.10	0.54	0.93	0.04	15	5.23	0.05	0.02	0.36	1.22	2.69	10.33	61.13
2	24	79.73	12.81	7.46	10YR/4.2	60.64	0.36	0.62	0.02	16	4.80	0.04	0.01	0.16	0.57	2.00	9.90	39.17
3	36	78.80	11.57	9.63	10YR/5.4	55.76	0.26	0.45	0.02	16	4.63	0.04	0.01	0.15	0.33	1.45	5.58	35.80
4	51	66.70	11.59	21.71	2.5YR/5.8, 10YR/6.6	55.23	0.23	0.40	0.02	15	4.29	0.05	0.01	0.18	0.28	2.68	8.59	19.14
5	89	55.21	12.70	32.09	as h4	4.39	0.18	0.31	0.02	11	4.37	0.06	0.02	0.31	0.40	3.72	9.62	21.42
6	110	38.28	20.74	40.99	2.5YR/4.8, 10YR/6.6	16.62	0.13	0.23	0.01	10	4.42	0.10	0.02	0.41	0.56	3.89	3.89	28.01

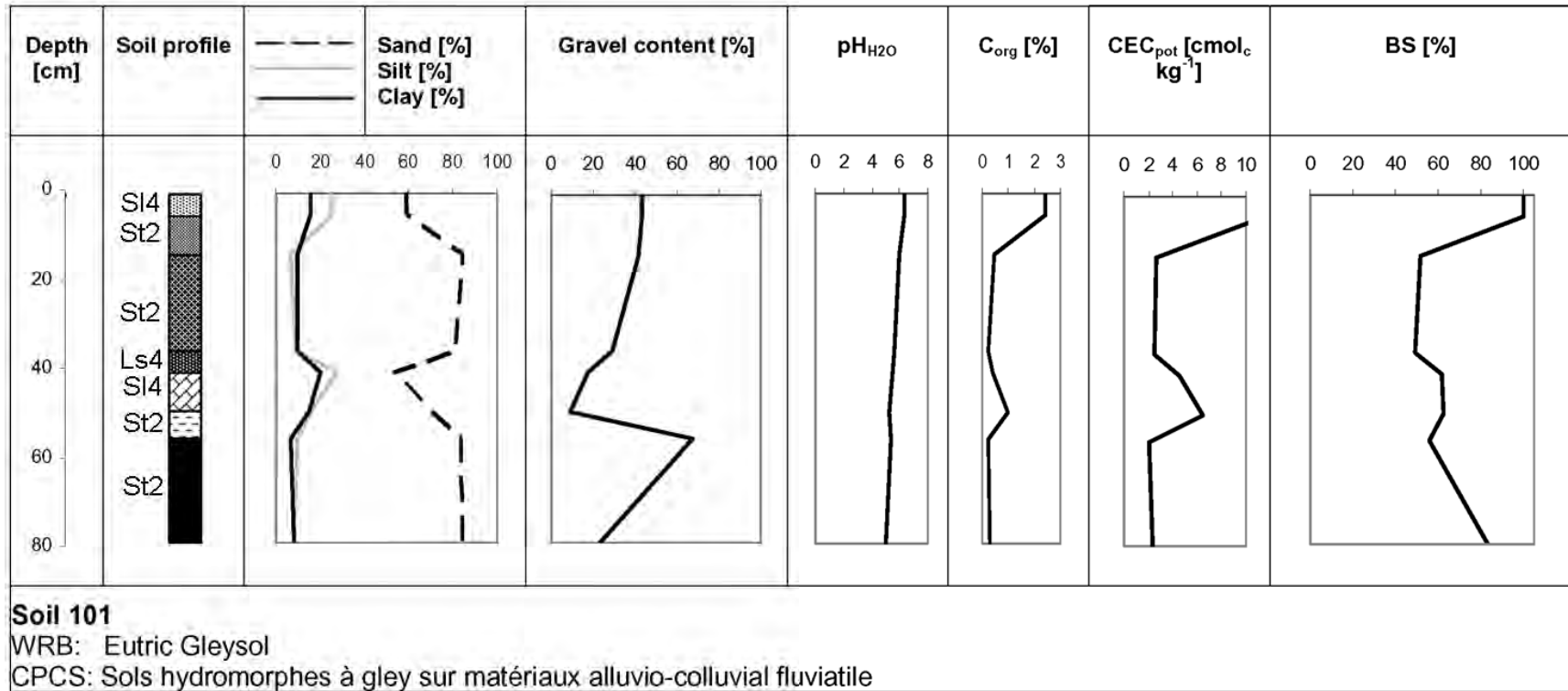


Soil 91

WRB: Plinthic Ferralsol [Lixic]

CPCS: Sols ferrallitiques rajeunis ou pénévlués sur gneiss à muscovite et à deux micas

Depth [cm]	Sand [%]	Silt [%]	Clay [%]	Colour [-]	Gravel [%]	C _{org} [%]	S _{org} [%]	N [%]	C/N [-]	pH CaCl ₂	K cmol _c /kg AAS	Na cmol _c /kg AAS	Mg cmol _c /kg ICP,AAS	Ca cmol _c /kg ICP,AAS	CEC cmol _c /kg soil	CEC cmol _c /kg clay	BS [%]	
1	5	80.15	12.18	7.67	10YR/3.2	18.10	0.54	1.87	0.08	14	5.23	0.10	0.01	1.01	4.45	2.69	10.33	61.13
2	27	79.73	12.81	7.46	10YR/4.4	60.64	0.36	0.86	0.03	16	4.80	0.06	0.02	0.53	1.19	2.00	9.90	39.17
3	48	78.80	11.57	9.63	10YR/4.4	55.76	0.26	0.72	0.03	17	4.63	0.04	0.01	0.69	1.27	1.45	5.58	35.80
4	95	66.70	11.59	21.71	7.5YR/4.6	55.23	0.23	0.67	0.03	14	4.29	0.15	0.01	1.73	1.12	2.68	8.59	19.14
5	110	55.21	12.70	32.09	7.5YR/5.8	4.39	0.18	0.59	0.02	16	4.37	0.21	0.01	1.83	1.36	3.72	9.62	21.42



Depth [cm]	Sand [%]	Silt [%]	Clay [%]	Colour [-]	Gravel [%]	C _{org} [%]	S _{org} [%]	N [%]	C/N [-]	pH CaCl2	K cmol _c /kg AAS	Na cmol _c /kg AAS	Mg cmol _c /kg ICP,AAS	Ca cmol _c /kg ICP,AAS	CEC cmol _c /kg soil	CEC cmol _c /kg clay	BS [%]
1	5	58.72	25.55	10YR/2.2	2.42	43.47	2.42	2.42	13	6.32	0.19	0.01	1.76	9.27	11.23	17.50	100.00
2	14	84.18	6.36	5YR/3.4	0.47	41.94	0.47	0.47	25	5.94	0.09	0.01	0.31	0.97	2.66	10.61	52.04
3	36	81.60	8.63	7.5YR/4.4	0.23	29.34	0.23	0.23	16	5.64	0.06	0.02	0.31	0.84	2.48	17.10	49.20
4	41	52.79	27.25	7.5YR/4.4	0.42	17.59	0.42	0.42	12	5.47	0.11	0.01	0.61	2.10	4.58	15.61	61.92
5	50	69.79	15.53	10YR/3.2	0.96	9.05	0.96	0.96	17	5.23	0.08	0.02	0.71	3.19	6.42	20.87	62.31
6	56	83.30	9.90	5YR/3.4	0.23	67.84	0.23	0.23	17	5.36	0.03	0.01	0.24	0.90	2.12	19.05	55.80
7	80	84.01	8.14	7.5YR/4.4	0.30	23.56	0.30	0.30	18	5.05	0.05	0.01	0.34	1.55	2.35	16.54	83.21

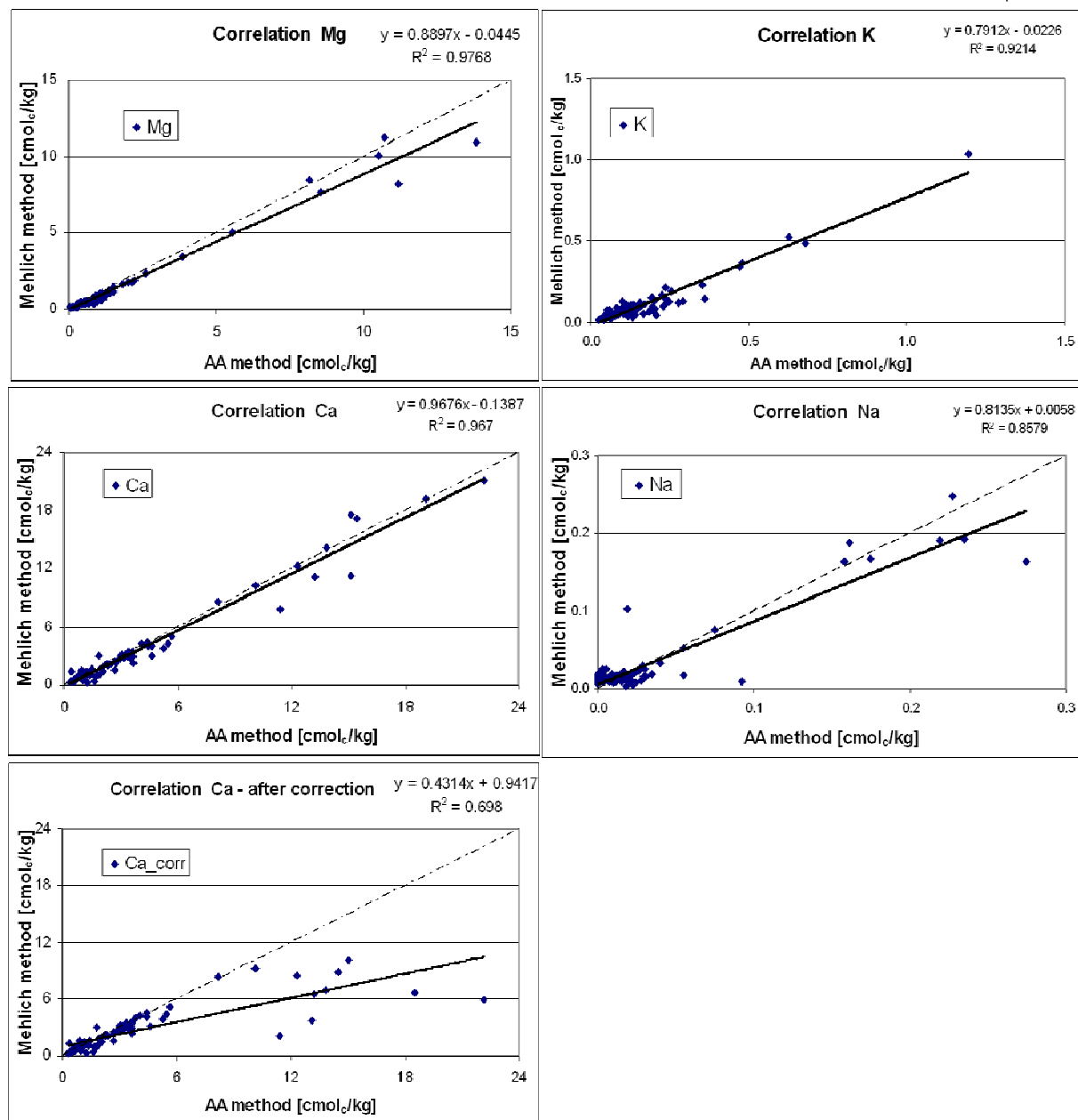
Fig A.3 Comparison of Mehlich and Ammonium Acetate (AA) methods for determination of CEC_{pot} .

Table A.3 Evaluation of soil quality according to Landon (1984).

Physiological deepness [cm]	extreme shallow	very shallow	shallow	medium	deep	very deep
	< 10	10 – 30	30 – 50	50 – 100	100 – 150	> 150
Rooting depth	Limitation					
Very good	no limitation, good structure, 0 – 2% coarse fragment, bulk density 1					
Good	2 – 15% coarse fragment, bulk density 2					
Moderate	unfavourable structure (coarse prismatic, coarse blocky), 14 – 40% coarse fragment, bulk density 3, 4					
Low	Limitation, very unfavourable structure (plattig, very coarse prismatic, very coarse blocky), 40 – > 80% coarse fragment, bulk density 5					

... continued	very low	low	medium	high	very high
Air capacity [Vol.-%]	< 2	2 – < 4	4 – < 12	12 – < 20	> 20
Available field capacity [mm]	very low	low	medium	high	very high
	< 50	50 – 90	90 – 140	140 – 200	> 200
pH (H₂O)		low	medium	high	very high
		< 5.5	5.5 – 7.0	7.0 – 8.5	> 8.5
	very low	low	medium	high	very high
CEC_{pot} [cmol_c/kg soil]	< 5	5 – 15	15 – 25	25 – 40	> 40
C_{org} [%]	< 2	2 – 4	4 – 10	10 – 20	> 20
Nitrogen, total [%]	< 0.1	0.1 – 0.2	0.2 – 0.5	0.5 – 1.0	> 1.0
	low		medium		high
Exchangable Ca [cmol_c/kg]	< 4		4 – 10		> 10
Exchangable Mg [cmol_c/kg]	< 0.5		0.5 – 4		> 4
Exchangable K [cmol_c/kg]	< 0.2		0.2 – 0.6		> 0.6
Exchangable Na [cmol_c/kg]	< 1				> 1
Available P₂O₅ [ppm]	< 15		15 – 50		> 50
Base saturation [%]	< 20		20 – 60		> 60

Table A.4 Classification of erodibility (K factor in USLE) according to Bolline & Rosseau (1978).

Erodibility [t h N ⁻¹ ha ⁻¹]	Classification	
< 0.1	<i>Sols très résistants à l'érosion</i>	very resistant to erosion
0.1 - 0.25	<i>Sols assez résistants à l'érosion</i>	resistant to erosion
0.25 - 0.35	<i>Sols moyennement sensibles à l'érosion</i>	medium resistance to erosion
0.35 - 0.45	<i>Sols assez sensibles à l'érosion</i>	sensitive to erosion
> 0.45	<i>Sols très sensibles à l'érosion</i>	very sensitive to erosion

Table A.5 Fertility Capability Classification System (FCC) (Sanchez et al. 1982).

Type		
S	sandy topsoil:	LS, S (USDA definition)
L	loamy topsoil:	< 35% clay, no LS, S
C	clayey topsoil:	> 35% clay
O	organic soil:	> 30% organic matter to 50 cm depth
Substrate type		
S	sandy subsoil:	LS, S (USDA definition)
L	loamy subsoil:	< 35% clay, no LS, S
C	clayey subsoil:	> 35% clay
R	rock or hart root-restricting layer	
Modifier		
g	gley	Soil or mottles ≤ 2 chroma within 60 cm of the soil surface and below all A horizons, or soil saturated with water for > 60 days in most years
d	dry	ustic, aridic or xeric soil moisture regime (subsoil dry > 90 cumulative days per years within 20-60 cm depth)

e	low CEC	Applies only to plough layer or upper 20 cm if shallower: CEC < 4 meq/100 g soil by Σ bases + KCl-extractable Al (effective CEC), or CEC < 7 meq/100 g soil by sum of cations at pH 7, or CEC < 10 meq/100 g soil by sum of cations, Al and H at pH 8.2
A	Al-toxicity	> 60% Al-saturation of the effective CEC within 50 cm of the soil surface, or > 67% acidity saturation of CEC by Σ cations at pH 7 within 50 cm of the soil surface, or > 87% acidity saturation of CEC by sum of cations at pH 8.2 within 50 cm of the soil surface, or pH < 5 in 1:1 H ₂ O within 50 cm, except in organic soils where pH must be less than 4.7
h	acid	10-60% Al-saturation of the effective CEC within 50 cm of the soil surface, or pH in 1:1 H ₂ O between 5 and 6
i	high P-fixation by iron	% free Fe ₂ O ₃ /% clay > 0.15 and more than 35% clay, or hues of 7.5 YR or redder and granular structure. This modifier is used only in clay (C) types; it applies only to plough layer or upper 20 cm if shallower
x	x-ray amorphous	pH > 10 in 1 N NaF, or positive to field NaF-test, or other indirect evidence of allophone dominance in the clay fraction
v	Vertisol	very sticky plastic clay: > 35% clay and > 50% of 2:1 expanding clays, or severe topsoil shrinking and swelling
k	low K reserves	< 10% weatherable minerals in silt and sand fraction within 50 cm of the soil surface, or exchangeable K < 0.2 meq/100 g, or K < 2% of sum of bases; if bases < 10 meq/100 g
b	basic reaction	free CaCO ₃ within 50 cm of the soil surface (effervescence with HCl), or pH > 7.3
s	salinity	≥ 4 mmhos/cm electrical conductivity or saturated extract at 25° within one meter of the soil surface
n	natric	$\geq 15\%$ N-saturation of CEC within 50 cm of the soil surface
c	Cat clay	pH in 1:1 H ₂ O < 3.5 after drying and jarosite mottles with hues of 2.5 Y or yellower and chromas 6 or more are present within 60 cm of the soil surface
`	gravel	a prime (´) denotes 15-35% gravel or coarser particles (> 2 mm) by volume to any type or substrata type texture; two prime (``) denotes more than 35% gravel or coarser particles (> 2 mm) by volume to any type or substrata type texture

Table A.6 Location of the investigated inland valleys in the Upper Ouémé catchment (Date: March 2004).

Transect	Location	begin		end		# augerings	Remarks
		x	y	x	y		
<i>Dogué1</i>	Dogué	~384000	~1008000	~384000	~1008000	8	after rice cultivation
<i>Dogué2</i>	Dogué	~384000	~1008000	~384000	~1008000	11	after rice cultivation
<i>Sérou1</i>	Sérou	357954	1068716	356959	1068220	8	after rice cultivation, parallel to river
<i>Sérou2</i>	30 km S of Sérou	388161	1050762	388242	1050692	5	
<i>Boko</i>	N of Boko	459129	1054046	459119	1053927	5	near vegetable cultivation

Table A.7 Properties of investigated inland valley soils in the Upper Ouémé catchment (*after Ca correction, ‘-’ not sampled, ¹AG Boden (1994), ²USDA (1993)).

No.	Hor	Hor	Depth	Sand	Silt	Clay	Gravel	Text. ¹	Text. ²	Colour	C _{org}	N	C/N	pH	CEC _{pot}	K	Na	Mg	Ca	BS
			[cm]	[%]	[%]	[%]	[%]	[-]	[-]	[-]	[%]	[%]	[%]	[-]	[cmol _c /kg]	[%]				
BF1	1	Ah	18	63	27	10	0.0	SI3	SL	10YR4/2	1.3	0.06	23	4.7	5.6	0.06	0.04	0.5	2.3	53
BF1	2	B	39	79	14	7	1.3	SI2	LS	10YR6/3	0.4	0.03	14	4.7	2.6	0.05	0.03	0.3	0.9	46
BF1	3	Bgo	51	77	10	14	18.4	St2	LS	10YR5/4	0.3	0.02	16	4.4	3.5	0.06	0.05	0.5	1.1	47
BF1	4	Bgor	100	57	12	31	19.1	Ts4	SCL	2.5Y5/6	0.4	0.03	13	4.6	8.8	0.13	0.10	2.1	3.4	65
BF2	1	Ah	36	34	43	23	0.1	Ls2	L	10YR5/2	1.5	0.10	16	5.0	9.9	0.19	0.09	1.6	4.0	59
BF2	2	Bgo/r	67	46	30	25	0.0	Ls4	L	2.5Y6/4	0.5	0.03	14	4.9	7.3	0.06	0.17	1.5	2.9	64
BF2	3	Bgr(o)	100	48	25	27	0.0	Lts	SCL	2.5Y6/3	0.3	0.02	16	5.1	8.0	0.07	0.33	2.7	4.1	89
BF3	1	Ah	29	46	31	23	0.0	Ls3	L	10YR5/3,5/4	1.2	0.08	16	4.5	7.1	0.09	0.08	0.7	2.9	53
BF3	2	B	67	73	17	10	16.6	SI3	SL	10YR6/3,2.5Y6/4	0.3	0.02	16	5.1	3.1	0.08	0.07	0.5	1.7	74
BF3	3	Bgo	76	50	19	31	19.4	Lts	SCL	2.5Y6/4	0.3	0.03	10	5.1	8.1	0.12	0.12	1.6	5.0	84
BF3	4	Bgr	87	-	-	-	-	SI4	-	10YR6/2	-	-	-	-	-	-	-	-	-	-
BF4	1	Ah	22	56	23	21	0.0	Ls4	SCL	10YR4/4	0.9	0.06	16	5.0	6.6	0.12	0.03	0.9	3.4	68
BF4	2	B	39	55	21	24	1.6	Ls4	SCL	10YR5/4	0.9	0.06	15	4.8	8.0	0.12	0.03	0.9	3.5	56
BF4	3	Btc	71	51	19	31	33.1	Lts	SCL	10YR6/6	0.6	0.05	12	4.8	9.5	0.09	0.05	0.9	3.5	47
BF4	4	Bgo	95	54	20	26	6.0	Lts	SCL	2.5Y6/6	0.3	0.02	11	4.8	8.0	0.08	0.13	1.1	3.0	53
BF5	1	Ah	20	52	27	21	0.0	Ls4	SCL	10YR5/3	1.3	0.08	17	4.9	7.2	0.10	0.07	1.0	3.6	66
BF5	2	Bsq	42	53	19	28	14.7	Lts	SCL	10YR5/4	0.8	0.06	14	4.6	7.3	0.09	0.05	0.9	2.8	53
BF5	3	Bgo	60	44	17	39	18.0	Lts	CL	10YR6/4	0.5	0.04	12	4.9	9.0	0.10	0.10	1.5	3.8	61
BF5	4	Bgor	90	43	16	41	16.2	Lts	C	10YR7/6	0.2	0.03	6	5.0	9.9	0.10	0.12	1.6	3.8	56
BF6	1	Ah	20	33	50	17	0.0	Ls2	SIL	10YR4/2	1.3	0.09	14	4.6	7.5	0.11	0.06	0.6	2.7	47
BF6	2	B	55	38	45	18	0.0	Ls2	L	10YR6/2, 2.5Y7/1	0.6	0.04	15	4.4	4.2	0.11	0.05	0.3	1.2	41
BF6	3	Bgo	70	44	32	24	0.0	Ls3	L	10YR7/3, 2.5Y7/3	0.4	0.04	10	4.3	4.6	0.13	0.08	0.5	1.1	38
BF6	4	Bgor	100	57	20	22	4.1	Ls4	SCL	10YR7/3, 2.5Y7/3	0.2	0.03	6	4.4	4.3	0.12	0.08	0.5	1.0	41
BF7	1	Ah	36	55	28	17	0.0	SI4	SL	10YR5/2	1.0	0.06	16	4.5	5.3	0.12	0.05	0.4	1.4	38
BF7	2	B	76	70	13	18	1.7	St3	SL	10YR6/3	0.4	0.03	14	4.6	4.1	0.08	0.04	0.5	1.2	43
BF7	3	Bg	97	68	11	21	0.0	St3	SCL	10YR6/2	0.4	0.03	16	4.8	4.5	0.09	0.04	0.7	1.5	51
BF8	1	Ah	30	66	20	14	0.0	SI4	SL	10YR5/3	0.8	0.05	17	4.3	4.4	0.09	0.03	0.3	0.7	26
BF8	2	B	47	70	15	15	1.4	SI4	SL	10YR6/2	0.6	0.03	19	4.4	3.6	0.08	0.04	0.3	0.8	34
BF8	3	Bgo1	78	75	9	16	11.8	St2	SL	10YR6/4	0.4	0.02	17	4.6	3.6	0.06	0.03	0.4	1.1	42
BF8	4	Bgo2	95	72	10	18	11.4	St3	SL	10YR6/3	0.3	0.02	14	4.7	3.4	0.06	0.03	0.4	1.1	47
BF9	1	Ah	17	73	19	7	0.0	SI2	SL	10YR5/2	0.7	0.04	18	4.7	3.8	0.07	0.02	0.2	1.2	41
BF9	2	B	59	72	21	7	0.0	SI2	SL	10YR6/1	0.4	0.02	24	4.4	2.0	0.05	0.03	0.1	0.4	29
BF9	3	Bgo	95	67	18	15	0.0	SI4	SL	10YR8/1,2.5Y8/2	0.2	0.01	17	4.4	2.5	0.05	0.04	0.4	0.6	45

... continued

No.	Hor	Hor	Depth	Sand	Silt	Clay	Gravel	Text. ¹	Text. ²	Colour	C _{org}	N	C/N	pH	CEC _{pot}	K	Na	Mg	Ca	BS
		.	[cm]	[%]	[%]	[%]	[%]	[-]	[-]	[-]	[%]	[%]	[%]	[-]	[cmol _e /kg]	[%]				
BF11	1	Ah	25	66	25	9	0.0	SI3	SL	10YR4/2,5/2	0.9	0.05	19	4.9	4.5	0.07	0.03	0.6	2.0	61
BF11	2	B	57	74	18	8	0.1	SI3	SL	10YR6,2	0.5	0.03	16	4.5	2.5	0.06	0.05	0.2	0.7	41
BF11	3	Bgor1	85	77	14	9	0.9	SI3	SL	2.5Y6/3	0.3	0.02	16	4.3	1.8	0.04	0.05	0.2	0.5	42
BF11	4	Bgor2	97	50	16	34	0.0	Lts	SCL	2.5Y7/3	0.2	0.02	14	4.1	7.3	0.08	0.13	2.5	2.1	66
BF12	1	Ah	19	67	23	10	0.0	SI3	SL	10YR4/2,5/2	1.0	0.06	18	4.7	4.7	0.05	0.05	0.5	2.0	54
BF12	2	B	45	78	15	7	0.0	SI2	LS	10YR6/2	0.5	0.02	21	4.7	2.2	0.04	0.04	0.2	0.6	43
BF12	3	Bgo	72	85	11	4	0.8	Su2	LS	10YR7/2,2.5Y7/2	0.2	0.01	27	4.6	1.1	0.02	0.04	0.2	0.3	50
BF12	4	Bgor	95	58	12	30	3.6	Ts4	SCL	10YR8/1,2.5Y8/2	0.2	0.01	20	4.7	7.0	0.08	0.13	2.6	2.7	78
BF13	1	Ah	16	53	36	11	0.0	SI3	SL	10YR5/2	1.0	0.06	16	4.8	5.5	0.08	0.06	0.7	2.1	53
BF13	2	B	30	70	21	8	0.0	SI3	SL	10YRR6/2	0.6	0.03	22	4.7	2.5	0.04	0.06	0.4	1.0	58
BF13	3	Bgo	46	77	14	9	0.5	SI3	SL	10YR7/3	0.3	0.02	16	4.8	2.6	0.04	0.07	0.4	0.9	54
BF13	4	Bgor	96	42	19	39	10.8	Lts	CL	2.5Y6/4	0.4	0.03	14	4.8	12.2	0.16	0.20	4.0	6.2	86
Bf 14	1	Ah	23	49	40	11	0.0	SI3	L	10YR4/2	1.6	0.08	21	4.4	8.1	0.10	0.15	0.8	2.9	49
BF14	2	B	65	76	18	6	3.3	SI2	LS	10YR6/1	0.4	0.02	21	4.5	2.6	0.02	0.06	0.3	0.8	45
BF14	3	Bgo	76	46	16	38	0.0	Lts	SCL		0.2	0.01	20	-	12.1	0.15	0.32	4.7	6.7	97
BF14	4	Bgr	97	-	-	-	-	Tt	C	2.5Y8/1	-	-	-	-	-	-	-	-	-	-
BF15	1	Ah	28	45	41	14	0.0	Slu	L	10YR4/1	2.1	0.13	16	7.2	11.1	0.25	3.40	3.4	4.1	100*
BF15	2	Gor	94	46	33	21	0.0	Ls3	L	10YR5/1	0.8	0.04	22	7.0	8.2	0.11	1.76	3.5	2.8	100*
BF16	1	Ah	27	48	41	11	0.0	Slu	L	10YR4/1	1.5	0.08	19	5.2	7.4	0.09	0.13	1.6	3.7	75
BF16	2	Ah/Gor	38	55	34	11	0.0	SI3	SL	10YR6/1	0.7	0.03	21	5.1	3.5	0.06	0.11	1.1	1.6	82
BF16	3	Gor	95	55	32	13	0.0	SI4	SL	2.5Y6/2	0.4	0.02	18	5.4	4.4	0.05	0.16	1.8	1.6	81
BF17	1	Ah	24	62	27	11	0.0	SI3	SL	10YR4/2	1.3	0.07	19	5.6	7.6	0.12	0.07	1.9	4.0	79
BF17	2	Bgo1	49	71	22	7	0.0	SI2	SL	10YR5/2	0.6	0.03	19	5.3	3.0	0.07	0.05	0.7	1.4	76
BF17	3	Bgo2	68	82	10	8	0.0	SI3	LS	2.5Y7/2	0.2	0.01	19	5.8	1.9	0.03	0.09	0.9	0.8	96
BF17	4	Bgr	92	58	10	33	0.0	Ts4	SCL	10YR7/2	0.2	0.02	15	6.1	10.5	0.11	0.31	6.3	3.8	100*
BF18	1	Ah	36	64	25	11	0.0	SI3	SL	10YR4/2	1.2	0.06	21	5.6	6.3	0.09	0.04	1.7	3.3	83
BF18	2	Bgo	68	64	23	13	0.0	SI4	SL	10YR6/2	0.7	0.03	22	5.4	4.8	0.09	0.10	1.7	2.1	84
BF18	3	Bgr	87	57	17	26	0.0	Lts	SCL	10YR6/2, 2.5Y6/2	0.3	0.01	19	7.5	9.6	0.11	0.49	5.4	4.2	106
BF19	1	Ah	17	63	26	11	0.0	SI3	SL	10YR5/2	0.8	0.05	18	4.4	3.7	0.06	0.04	0.6	1.0	46
BF19	2	B	43	58	26	16	0.0	SI4	SL	10YRR6/3	0.6	0.04	16	4.1	5.0	0.06	0.07	0.9	1.1	41
BF19	3	Bgor	94	40	20	41	0.0	Lts	C	2.5Y6/3	0.3	0.02	16	6.5	13.6	0.18	0.40	6.9	6.2	100*

... continued

No.	Hor	Hor	Depth [cm]	Sand [%]	Silt [%]	Clay [%]	Gravel [%]	Text. ¹ [-]	Text. ² [-]	Colour [-]	C _{org} [%]	N [%]	C/N [%]	pH [-]	CEC _{pot} [cmol _e /kg]	K [cmol _e /kg]	Na [cmol _e /kg]	Mg [cmol _e /kg]	Ca [cmol _e /kg]	BS [%]
BFP1	1	Ah	17	83	11	6	2.6	SI2	LS	10YR5/3	0.6	0.03	18	5.7	3.4	0.04	0.04	0.3	2.4	81
BFP1	2	B	51	84	10	6	5.4	SI2	LS	10YR5/3	0.4	0.02	18	5.5	2.5	0.05	0.04	0.3	1.7	83
BFP1	3	Bg(o)	80	84	11	5	8.9	Su2	LS	10YR6/3	0.2	0.01	14	5.3	1.5	0.03	0.04	0.1	0.8	71
BFP1	4	Bcg	96	70	16	15	27.6	SI4	SL	10YR6/6	0.1	0.01	14	5.5	2.8	0.06	0.06	0.6	1.7	86
BFP2	1	Ah	19	79	14	7	5.5	SI2	LS	10YR4/2	0.7	0.05	15	4.8	3.6	0.06	0.07	0.5	1.8	66
BFP2	2	Bg(o)1	58	76	16	7	17.8	SI2	SL	10YR5/3	0.5	0.03	16	5.0	3.2	0.06	0.09	0.4	1.9	76
BFP2	3	Bg(o)2	97	87	8	4	11.9	Ss	S	10YR5/2	0.2	0.01	16	5.4	1.3	0.03	0.05	0.2	0.7	73
BFP3	1	Ah	18	69	22	9	11.6	SI3	SL	10YR5/2	0.8	0.05	17	4.5	3.4	0.11	0.07	0.4	1.0	47
BFP3	2	Bg	36	72	19	10	11.6	SI3	SL	10YR6/2	0.5	0.03	18	4.7	2.6	0.07	0.06	0.4	0.9	56
BFP3	3	Bg(o)	99	85	9	6	13.7	St2	LS	10YR6/4	0.1	0.01	18	5.2	1.5	0.04	0.05	0.3	0.6	60
BFP5	1	Ah	16	79	11	10	14.3	SI3	SL/LS	10YR5/3	0.5	0.04	13	4.4	2.8	0.07	0.04	0.2	0.7	37
BFP5	2	B	30	77	13	10	7.9	SI3	SL	10YR6/4	0.4	0.03	14	4.5	2.9	0.05	0.04	0.3	0.7	36
BFP5	3	Bgor1	68	72	15	13	14.2	SI4	SL	10YR6/4	0.3	0.02	16	4.5	3.5	0.05	0.04	0.3	0.7	33
BFP5	4	Bgor2	95	77	11	12	12.6	SI3	SL	10YR5/4	0.2	0.01	13	5.0	2.2	0.04	0.05	0.5	0.8	61
C2	1	Ah	14	2	33	64	0.0	Tu2	C	10YR3/2	2.1	0.16	14	4.0	13.4	0.06	0.11	1.1	2.9	31
C2	2	Bg(o)	60	4	30	66	0.0	Tt	C	10YR4/3	1.1	0.08	13	4.2	12.0	0.03	0.10	1.9	4.1	52
C2	3	Bg	98	9	45	46	0.0	Tu2	SIC	2.5Y4/2	0.5	0.03	16	4.4	9.0	0.02	0.13	2.1	4.0	69
C3	1	Ah	10	2	33	65	0.0	Tu2	C	10YR2/2	2.8	0.18	15	4.2	15.7	0.28	0.14	1.2	4.0	36
C3	2	Bgo1	45	2	25	73	0.0	Tt	C	10YR4/3	0.9	0.07	12	4.3	10.2	0.04	0.11	1.9	4.3	61
C3	3	Bgo2	99	7	28	65	0.0	Tl	C	2.5Y4/2	0.7	0.05	13	4.3	9.7	0.02	0.13	2.1	3.6	60
C4	1	Ah	9	3	37	59	0.0	Tu2	C	10YR3/2	2.2	0.15	15	4.5	12.7	0.12	0.15	1.6	5.3	57
C4	2	B	24	4	32	64	0.1	Tu2	C	10YR5/3	0.9	0.07	13	4.6	11.5	0.05	0.13	2.0	4.7	60
C4	3	Bg(o)	50	11	39	50	0.0	Tu2	C	10YR5/3	0.5	0.03	16	4.3	8.8	0.03	0.27	2.8	5.7	100*
C4	4	Bgo	100	-	-	-	-	Tt	C	2.5Y5/2	-	-	-	-	-	-	-	-	-	-
C5	1	Ah	9	6	38	56	0.0	Tu2	C	10YR3/2	2.1	0.14	14	4.4	14.9	0.04	0.34	1.6	3.7	38
C5	2	Bg	29	3	30	67	0.0	Tt	C	10YR4/3	1.1	0.02	62	4.5	12.4	0.03	0.09	2.5	5.8	68
C5	3	Bg(r)	59	5	35	60	0.0	Tu2	C	10YR5/3	0.7	0.05	13	4.3	13.3	0.03	0.16	1.9	3.8	44
C5	4	Bgr	100	-	-	-	-	Tt	C	2.5Y4/2	-	-	-	-	-	-	-	-	-	-
C6	1	Ah1	16	23	36	41	0.0	Lt3	C	10YR3/4	2.5	0.15	17	4.8	11.9	0.17	0.05	1.5	5.2	58
C6	2	Ah2	33	34	33	34	4.8	Lt2	CL	10YR3/4	1.2	0.08	15	4.6	8.8	0.09	0.05	1.1	3.3	52
C6	3	Bgr	65	45	23	32	1.2	Lts	SCL/CL	10YR6/4	0.7	0.05	14	4.4	6.7	0.06	0.05	0.8	2.0	42
C6	4	Bgo	99	36	26	38	10.4	Lts	CL	2.5Y6/2	0.6	0.04	13	4.3	7.4	0.06	0.08	1.0	2.5	49

... continued

No.	Hor	Hor	Depth	Sand	Silt	Clay	Gravel	Text. ¹	Text. ²	Colour	C _{org}	N	C/N	pH	CEC _{pot}	K	Na	Mg	Ca	BS
			[cm]	[%]	[%]	[%]	[%]	[-]	[-]	[-]	[%]	[%]	[%]	[-]	[cmol _e /kg]	[%]				
C7	1	Ah	25	24	38	37	0.7	Lt3	CL	10YR4/3	1.9	0.11	17	4.5	11.2	0.15	0.04	1.2	4.2	49
C7	2	Ah/Bg(o)	40	26	40	34	0.7	Lt2	CL	10YR5/3	1.4	0.09	16	4.5	10.6	0.12	0.04	1.1	3.6	46
C7	3	Bg1	81	40	31	29	1.3	Lt2	CL	10YR6/3	0.6	0.04	14	4.3	6.5	0.07	0.04	0.9	2.2	49
C7	4	Bg2	99	36	31	34	0.0	Lt2	CL	2.5Y6/2	0.4	0.03	13	4.4	6.4	0.07	0.05	1.2	2.6	60
C8	1	Ah1	17	25	31	44	2.4	Lt3	C	10YR4/3	1.4	0.10	14	4.6	13.0	0.13	0.07	1.6	4.6	50
C8	2	Ah2	40	24	32	44	0.0	Lt3	C	10YR4/3	1.3	0.09	15	4.6	13.1	0.13	0.08	1.6	4.3	47
C8	3	Bgr1	73	39	25	36	0.0	Lts	CL	10YR5/4	0.8	0.05	17	4.6	8.7	0.10	0.07	1.3	3.0	51
C8	4	Bgr2	100	26	25	49	0.0	TI	C	2.5Y6/2	0.3	0.02	17	-	11.8	0.15	0.26	3.3	6.0	83
C9	1	Ah	27	78	14	8	17.4	SI2	LS	10YR5/3	0.9	0.04	22	4.5	3.4	0.04	0.07	0.2	1.4	47
C9	2	B1	51	81	12	7	2.8	SI2	LS	10YR6/2	0.4	0.02	20	4.8	2.4	0.03	0.05	0.2	1.0	52
C9	3	B2	95	83	11	6	9.1	SI2	LS	10YR7/2	0.2	0.01	19	5.2	1.4	0.03	0.05	0.1	0.7	63
C10	1	Ah	28	84	10	6	3.0	SI2	LS	10YR5/3	0.3	0.01	23	4.7	2.3	0.01	0.04	0.1	0.9	47
C10	2	B1	55	83	12	5	7.3	Su2	LS	10YR8/3	0.2	0.01	16	4.9	2.1	0.02	0.09	0.1	0.7	45
C10	3	B2	100	88	9	3	5.0	Ss	S	10YR8/3	0.1	0.00	24	5.4	0.8	0.02	0.02	0.1	0.3	62
C11	1	Ah1	29	86	9	5	1.6	St2	LS	10YR5/2	0.4	0.02	21	4.8	3.2	0.07	0.04	0.1	1.0	39
C11	2	Ah2	49	86	9	5	1.2	St2	LS	10YR5/3	0.4	0.02	19	4.8	2.8	0.06	0.03	0.2	1.1	46
C11	3	Bg(o)	62	82	12	6	2.2	SI2	LS	10YR7/2	0.2	0.01	25	5.1	1.8	0.02	0.03	0.1	0.8	53
C11	4	Bgo	100	78	12	10	1.9	SI3	SL	10YR7/2	0.2	0.01	20	5.4	2.5	0.03	0.03	0.2	1.1	57
C12	1	Ah	31	88	9	3	12.1	Ss	S	10YR4/3	0.3	0.02	20	5.1	1.9	0.02	0.03	0.1	1.1	68
C12	2	Bg(r)	58	89	7	4	7.9	Ss	S	10YR5/3	0.2	0.02	14	5.3	1.8	0.04	0.03	0.2	1.0	67
C12	3	Bgor	100	88	9	3	4.4	Ss	S	10YR5/3	0.2	0.01	17	5.5	1.2	0.03	0.02	0.1	0.8	81
C13	1	Ah	33	73	17	10	0.6	SI3	SL	10YR2/3	1.3	0.06	22	5.3	6.2	0.13	0.07	0.6	5.4	100*
C13	2	Bg1	66	68	16	16	0.9	SI4	SL	10YR1.7/1	0.8	0.03	25	5.2	6.7	0.06	0.06	0.9	5.7	100*
C13	3	Bg2	99	80	9	11	9.1	St2	SL	10YR2/3	0.3	0.01	23	5.4	4.7	0.05	0.04	0.6	3.4	85

Table A.8 Location and characteristics of the investigated degraded fields and reference sites (cursive) in the Upper Ouémé catchment and the commune Ouaké (Date 18.09.-02.10.2005).

No.	x, y	Land use	Remarks	Location	Profile position	Inter-view
Pr1	458535, 1040850	Field: Groundnut	10% small gravel, 25% veg.cover, erosion between rows, sand accumulation	N of Parakou	Upper slope	y
Pr2	460729, 1031211	Field: Maize (1 st yr after fallow)	60% large gravel (1-7 cm), 30% veg.cover	Bankani	-	y
Pr3	448425, 1020316	Field: Maize (2 nd yr after fallow)	30% small gravel, 60% veg.cover, low yield, rows along slope, rill erosion	S of Parakou	Upper slope	y
Pr4	357863, 1068455	Sacred fallow (reference)	30% small gravel, 50% veg.cover, erosion along footpath	Sérou	Mid-slope	no
Pr5	357863, 1068455	Fallow 3rd year (reference)	25% medium gravel (0.5->2.5 cm), 40% veg.cover, indicator plants indicating returning soil fertility	Sérou	Mid-slope	no
Pr6	357980, 1068377	Field: beans	80% large gravel (1-8 cm), 10% veg.cover, ploughed, rows along slope, no rotation, sheet erosion, low plant density	Sérou	Upper slope	y
Pr7	357057, 1068350	Sacred forest (reference)	no gravel, 80% veg.cover, thick litter layer	Sérou	Summit	no
Pr8	357110, 1068333	Field: Cassava	1 yr after short fallow, 40% large gravel (1-4.5 cm), 50% veg.cover, surface crusts, shallow soil, mounds 30 cm high	Sérou	Summit	no
Pr10	342188, 1089756	Field: Sorghum, bean, cashew	80% large gravel (1-30 cm), 50% veg.cover, low yield (sorghum < 1 m), rows along slope	Copargo	-	no
Pr11	342188, 1089756	Field: Sorghum, bean, cashew	30% large gravel (1-20 cm), 40% veg.cover, 2x plant height of Pr10 due high local soil fertility	Copargo	-	no
Pr12	344680, 1080790	Field: Sorghum, petit mill	30% small gravel, on mounds 60% gravel, 15% veg.cover, low yield, surface sealing, severe sheet erosion, sand accumulation	Djougon	Upper slope	no
Pr13	325543, 1067319	Field: Groundnut, <i>Gliricidia</i>	no gravel, 60% veg.cover, groundnut not in rows but on ex-yam mounds	Ouaké	Inland valley fringe	y
Pr14	325543, 1067319	Field: Groundnut, <i>Gliricidia</i> (new)	no gravel, 40% veg.cover, accumulation of sand, groundnut not in rows but on ex-yam mounds	Ouaké	Lower slope	no
Pr15	339166, 1066490	Field: Soy bean	70% large gravel (0.5-10 cm), 30% veg.cover, rows parallel to slope	Barei	Mid-slope	y
Pr16	385867, 1073219	Savane boisée	40% small gravel, quartz gravel, <10% veg.cover but 60% leaves, sealed surface, small termite mounds, indurated, clay-rich soil	Donga	Upper slope	no
F1	355381, 1076665	Field: Cassava, (maize,sorghum)	10% small gravel, 40% veg.cover	Djougon	Upper slope	y
F2	384606, 1078031	Field: Sorghum, groundnut	10% small gravel, 85% veg.cover	Gaouga	Upper slope	y
F5	350283, 1075874	Field: Gombo, tomato	60% medium gravel (on mounds 90%), 20% veg.cover, low yield, weeds, crusts along path, rows parallel to slope, sheet erosion	Djougon	Mid-slope	y
F8	347263, 1081331	Field: Groundnut, bean, petit mill	40% small gravel (80% between rows), 30% veg.cover, rows parallel to slope, traces of charcoal	Kparisi	Mid-slope	y
F9	347263, 1081331	Field: Yam, petit mill, (bean)	up to 95% medium/large gravel, 25% veg.cover, mounds "en quinconce" but highly eroded, good yield	Kparisi	Mid-slope	no
F15	374078, 1077907	Field: Petit mill	<10% small gravel, 30% veg.cover, generally poor yield but for petit mill OK, moderate erosion along field borders and rows, >10 cm sand accumulation, indurated subsoil	Moné	Mid-slope	y
F19	374745, 1075859	Field: Sorghum	50% small/medium gravel, 25% veg.cover, maize residues, good yield	Moné	Mid-slope	y
F20b	386442, 1006332	Field: Cassava, maize	20% small/medium gravel, 60% veg.cover (mounds and herbs), low yield, pseudo-fallow	Dogué	Upper slope	y
F21	384806, 1006241	Field: Maize	40% medium gravel, 15% veg.cover, low yield, rows parallel to slope, indurated subsoil	Dogué	Mid-slope	y
F22	382293, 1006909	Field: Cassava	<10% small gravel, 10 to 50% veg.cover, slight sheet erosion, sand accumulation, drought cracks, reduced yield, maize residues/weeds	Dogué	Upper slope	y
E1	341665, 1068595	Field: Cotton (4 th year)	80% large gravel (iron nodules), 20% veg.cover, highly eroded but since 2004 protected by Vetiver hedges, gravel-rich topsoil	Barei	Little hill	y

Table A.9. Characteristics of studied degraded fields in the Upper Ouémé catchment according to farmer interviews.

Soil	Location	Farmer	Crop cycle	Cropping period [years]	Fallow period [years]	Change in fallow period, soil fertility restoration	Chemical fertilizer	Manure	Burning	Soils	Rainfall	Yield	Soil conservation measures
Pr1	Parakou	m	maize - cotton - maize - cotton - etc.; if low soil fertility <u>groundnut</u> alternating with maize/sorghum	when required	2	5 for subsequent yam cultivation; requires fertilizer for good yield	yes (maize, cotton)	yes, peulh cattle allowed to graze after harvest	yes, early	OK, low gravel content but not very fertile due to accumulated sand, 1999 reclaimed from savannah land, since 2002 less fertile	-	-	
Pr2	Parakou-Banikani	m	<u>maize</u> permanent (home field)	3	3-4	sufficient	no	yes, on home fields	no	fertile	2005 less than 2004	-	domestic waste on homefields, tree debris
Pr3	Gouarou	m, migrant from Boukombé	sorghum - maize, sorghum (row) - <u>maize</u> , sorghum (mound)	3 or more	3		no	no	only for land reclamation	"tired"	2005: not enough	-	crop residues
Pr13	Yamala	m	agroforestry with <u>Gliricidia</u> : yam, <u>groundnut</u> , yam, groundnut, yam; before: yam, groundnut, maize, yam	5	2	before 2001 no fallow, in region generally 2-3 years; not enough but improved fallow helps	no, in the past yes	no	-	sandy, low gravel content, in general fertile soils but reduced fertility due to overexploitation	2005 less than 2004, not enough	-	improved fallow with <u>Gliricidia</u> (Legume), b) crop residues
Pr15	Assotè	m	Millet – sorghum – <u>soy bean</u> +beans – cassava	4	2	reduced	no	no	no	OK, but was better before the 90ies	2004: good, 2005: not enough, dryspell in August	-	perpendicular to the slope, crop residues
Pr16	Foyo near Donga	m5	yam – groundnut/maize/cotton – yam – groundnut/maize/cotton; cotton 1 year or more, mixed cropping: e.g. yam + sorghum, yam + cassava (outer belt), yam + beans	??	3	parents used to have 10-15 years; Ok if fertilizer is used, land conflicts	yes, maize and cotton, groundnut & rice (every year)	yes, peulh cattle allowed to graze after harvest	yes, late	fertile, some gravel, sandy with increasing depth also clay	2004: good, 2005: not enough	-	a) perpendicular to the slope, b) soybean & teak on exhausted soils (10-15 years), c) crop residues, distribute leaves on fieldm d) cashew
F1	Djougou	m, Gourmantche, parents from Burkina Faso	cassava - maize - maize - groundnut o. maize/sorghum - <u>cassava</u>	5 or more	0, 2-3	with manure only pseudofallow with cassava, otherwise 2-3 years, in the past 6-20 years; not enough	no	every year bought manure applied	-	no gravel, soil "tired", requires manure	2004: too much, 2005: good	OK	manure, crop residues (groundnut, others burned)

... continued

Soil	Location	Farmer	Crop cycle	Cropping period [years]	Fallow period [years]	Change in fallow period, soil fertility restoration	Chemical fertilizer	Manure	Burning	Soils	Rainfall	Yield	Soil conservation measures
F2	Gaouga	m, old, Lokpa, migrant from Bellefongou	groundnut - cotton - maize - groundnut - <u>groundnut/sorghum</u> - cotton ...; field2: yam/rice - maize/rice - yam (if last harvest was good)	6 or more	0, other fields 3-4	reduced, but still OK	no	-	only after cotton (feb/march)	good, soils "tired" but Ok through crop rotation, even yam possible but weeding is labour-intensive	last year OK, this year dry spell in August	poor due to insect pest	groundnut cultivation
no	Donga	m, old, Peulh, migrant from Bellefongou	yam - maize/sorghum + at the border Petit Mill	2	0, 2, 4	same, enough land, OK	yes, cotton und maize		-	sandy, gravelly, fertile, no erosion	2004: good, 2005: yam suffered from late rainfall this year, no problem for sorghum	OK	-
F5	Sidikparo, near Djougou	f, autochthon, Yom	yam - cotton - sorghum - <u>Gombo/tomato</u>	4	3	not enough, 4 th year already low yields	yes, maize und cotton	yes, peulh cattle allowed to graze after harvest	yes, early	low soil fertility, shallow, gravelly soil which is currently not fertile, mounds heavily reduced due to rainfalls in September	2004: good, 2005: dry spell in August reduces maize harvest	poor (4th year), year1-3 was good	crop residues
F8	near Kparsi	m, Yom, migrant from Kpabegou	a,b) yam - Sorgho - cotton (if profitable) - ...; c) yam-sorghum-cotton- <u>groundnut (+beans, petit mills)</u> -maize-fallow, d) yam-sorghum-fallow; yam on long fallow	2-4	3-4	same as parents, yam only good on old fallows	yes, cotton und maize	yes, peulh cattle allowed to graze after harvest	no (protection), but happens	variable, sandy, partially high gravel content, land available for yam	2005: dryspell August/early Sept, reduces yam harvest	very good	crop residues
F15	Mone	m2, I.Yom,II:Peulh, migrant from Kpassabega	I: yam-sorghum-groundnut-cassava_fallow, yam-sorghum-cotton-maize-fallow, II: yam-maize-groundnut-cashew/cassava-cassava-cashew (tall); yam- <u>PetitMill</u> -fallow; fallow-yam-maize-cashew/cassava-cashew	I. 4, II 4-5, if soil very tired less	4	I: reduced, in the past 6-10 years, now yam already after 4 yrs. Fallow, compromise	I: yes, if cotton then also maize II: no	yes, peulh cattle allowed to graze after harvest	no, anti-fire band 3m	I:sandy soils good for yam, gravelly soil good for sorghum	I: 2004: OK, 2005: onset too late; II: 2004: good, 2005: not good	I:good, II. II:good, but poor for petitmill although less demanding than sorghum	
F19	Mone	f, migrant from Permas (Natitingou)	yam-sorghum/maize-groundnut- <u>sorghum</u> -?	4 or more	about 4		no	yes, peulh cattle allowed to graze after harvest	no, anti-fire band 4m	gravelly, other soil at inland valley fringe sandy	2004/2005: too late onset	good	crop residues, cattle after harvest

... continued

Soil	Location	Farmer	Crop cycle	Cropping period [years]	Fallow period [years]	Change in fallow period, soil fertility restoration	Chemical fertilizer	Manure	Burning	Soils	Rainfall	Yield	Soil conservation measures
F20b	Dogue	m, autochthon, Nagot	cotton-beans-maize-groundnut-maize-fallow-groundnut-cassava-evtI.Cashew; yam-maize-cassava-fallow	3-5	3	10 would be ideal	yes, cotton	yes, peulh cattle allowed to graze after harvest	yes, early	gravelly but deep, little erosion	2004/2005: too late onset		groundnut
F21	Dogue	m, young, autochthon, Nagot	a) cassava/maize-cassava-groundnut-cassava-maize/cassava-fallow, b) cotton-cotton-fallow/cashew-groundnut/beans-maybe beans/maize	3-5	2 (split field),		yes, cotton	yes, peulh cattle allowed to graze after harvest	no, anti-fire band 4m	OK, sandy	2004: good, 2005: too late onset	poor, years before good	
F22	Dogue	m, autochthon, Nagot	fallow lang-yam-cassava-cassava-fallow; yam-sesame-cassava-cassava-maize-Teak	3-5	5		no, in the past for cotton	yes, peulh cattle allowed to graze after harvest	yes, early	sandy, no erosion	2004: good, 2005: too late onset	only this particular field poor	
E1	Barei	m	<u>cotton</u> permanent (4 th year)	-	-		yes, for cotton and Vetiver grass	no	-	extreme gravel content, steep slope	-	-	Vetiver hedges depending on slope, financed from PDRT since 2004
no	near Copargo	m	yam-sorghum/niebe/groundnut/fallow-cassava/beans/maize-sorghum-fallow	2	1-2		no	no	yes, early	Soil 'tired', sorghum would require fertilizer	-	-	crop residues
no	Kpabegou	m	yam-sorghum-cotton/maize	3	3-5		yes, maize und cotton	only if high rainfall	yes, early	sandy, partially gravel	2005: good onset, but than not enough	-	-
no	Kakpala	m2	yam – maize - petit mil/groundnut – beans – maize; house field: maize – millet – petit mil	5	2	same as father	yes, maize, if enough money also groundnut und yam	only house fields	yes, early (home fields and Eukalyptus plantations excluded)	gravelly, soils tired but fertilizer allows good harvest, still land for reclamation available (yam)	2004: too much, 2005: good, dryspell in August not problematic	good due to fertilizer	Gliricidia-yam based system which allows yam cultivation every second year (yam-groundnut-yam-sorghum), sowing better than putting branches
no	Kimkim	m2, migrant from Togo (I)	I: maize – maize – groundnut – sorghum+millet – maize; II: yam - maize –sorghum millet – groundnut + millet maize	permanent	up to 10 (far away)		yes, for maize and groundnut, seldom yam	only house fields	yes, early and late	gravel, indurated, soils less fertile, very old fallows/savannah for yam far away	2004: good, 2005: dry spell of 3 weeks in August	lower field sizes better to manage, give better yield	traditional stone rows too labour intensive; perpendicular to the slope; organic fertilizer before yam cultivation, young migrate to fertile temporarily towards Bassila/Djougou

Table A.10. Soil characteristics of studied degraded fields and reference sites in the Upper Ouémé catchment (- not sampled, ¹AG Boden (1994), ²USDA (1993)).

No.	Hor	Depth [cm]	Sand [%]	Silt [%]	Clay [%]	Gravel [%]	Text. ¹ [-]	Text. ² [-]	Colour [-]	C _{org} [%]	N [%]	C/N [%]	pH [-]	CEC _{pot} [cmol _e /kg]	K [cmol _e /kg]	Na [cmol _e /kg]	Mg [cmol _e /kg]	Ca [cmol _e /kg]	BS [%]
Pr 2-1	1	5	72	19	9	34	SI3	SL	grey	1.7	0.01	73	5.8	7.9	0.30	0.00	1.6	6.1	100
Pr 2-2	2	42	68	20	11	27	SI3	SL	brown	0.6	0.03	67	6.0	4.8	0.10	0.00	0.7	3.0	80
Pr 2-3	3	51	59	21	19	21	Ls4	SL	red	0.4	0.03	15	5.8	2.1	0.10	0.00	0.5	1.1	81
Pr 2-4	4	73	-	-	-	-	Ts2	C	red	-	-	-	-	-	-	-	-	-	-
Pr 3-1	1	20	86	10	4	24	Ss	LS	dark brown	0.3	0.02	9	5.6	1.7	0.12	0.00	0.2	0.6	56
Pr 3-2	2	49	80	12	7	27	SI2	LS	red brown	0.6	0.00	32	4.9	3.2	0.16	0.00	1.1	0.6	61
Pr 3-3	3	66	60	10	30	23	Ts4	SCL	red brown	0.4	0.02	27	4.8	3.5	0.24	0.01	1.1	0.6	56
Pr 3-4	4	90	58	14	28	21	Ts4	SCL	red brown	0.2	0.06	13	4.8	3.2	0.05	0.00	0.4	1.6	64
Pr 4-1	1	8	83	12	5	24	SI2	LS	10YR/3.4	0.8	0.03	15	5.2	2.7	0.02	0.00	0.2	0.5	25
Pr 4-2	2	37	79	13	8	25	SI2	LS	10YR/3.4	0.5	0.02	19	4.4	2.9	0.02	0.01	0.1	0.6	24
Pr 4-3	3	61	70	15	14	35	SI4	LS	10YR/3.3	0.4	0.02	18	4.4	2.8	0.05	0.00	0.1	0.6	27
Pr 4-4	4	67	67	18	16	32	SI4	LS	5YR/4.4	0.3	0.01	15	-	3.5	0.04	0.01	0.2	0.8	30
Pr 5-1	1	13	81	14	6	25	SI2	LS	7.5YR/3.2	1.7	0.01	238	5.3	3.4	0.05	0.00	0.4	1.5	57
Pr 5-2	2	38	79	13	8	26	SI3	LS	7.5YR/4.2	0.8	0.03	137	4.6	4.0	0.04	0.00	0.2	1.1	36
Pr 5-3	3	46	69	16	15	39	SI4	SL	7.5YR/4.4	0.5	0.02	17	-	3.5	0.02	0.00	0.3	1.0	39
Pr 5-4	4	55	67	18	15	34	SI4	SL	5YR/5.4	0.3	0.04	17	-	4.1	0.03	0.00	0.5	1.3	42
Pr 6-1	1	11	78	16	6	37	SI2	LS	10YR/3.4	0.7	0.03	17	5.2	3.5	0.07	0.00	0.6	1.6	66
Pr 6-2	2	18	63	22	15	21	SI4	SL	7.5YR/3.4	0.6	0.03	18	5.0	4.0	0.04	0.00	0.8	1.8	66
Pr 6-3	3	50	-	-	-	-	Ls4	SCL	10YR/3.3	-	-	-	-	-	-	-	-	-	-
Pr 6-4	4	68	53	23	24	22	Ls4	SCL	7.5YR/4.4	0.5	0.01	16	4.7	4.7	0.04	0.00	0.9	1.5	52
Pr 6-5	5	96	45	21	35	24	Lts	CL	7.5YR/5.4	0.4	0.31	73	4.5	4.6	0.03	0.01	0.8	1.6	54
Pr 7-1	1	10	67	16	17	26	SI4	SL	10YR/2.1	4.4	0.07	14	6.9	21.7	0.72	0.01	2.6	18.4	100
Pr 7-2	2	32	76	15	10	40	SI3	SL	10YR/4.1	1.0	0.02	15	6.3	13.6	0.26	0.00	0.8	6.2	53
Pr 7-3	3	61	67	18	15	29	SI4	SL	5YR/4.6	0.3	0.06	16	-	1.3	0.07	0.07	0.7	0.4	100
Pr 8-1	1	7	84	10	6	27	SI2	LS	7.5YR/4.2	0.9	0.04	16	6.0	4.3	0.10	0.00	0.9	2.9	92
Pr 8-2	2	26	80	11	9	36	SI3	LS	7.5YR/4.2	0.7	-	20	5.7	2.7	0.05	0.00	0.2	0.8	37
Pr 8-3	3	35	-	-	-	-	Lts	SCL/CL/C	5YR/4.6	-	-	-	-	-	-	-	-	-	-
Pr 10-1	1	4	75	18	7	20	SI2	SL	10YR/3.1	1.0	0.04	16	5.1	4.6	0.09	0.00	0.5	2.8	74
Pr 10-2	2	25	78	15	8	33	SI2	LS	10YR/5.3	0.8	0.02	18	4.9	4.8	0.09	0.00	0.3	1.9	47
Pr 10-3	3	41	78	12	10	40	SI3	SL	2.5Y/5.2, 2.5YR/4.6	0.4	0.02	15	4.8	3.0	0.12	0.07	0.3	0.7	41
Pr 10-4	4	50	63	17	20	25	Ls4	SL/SCL	2.5YR/3.6	0.3	0.11	14	4.7	5.4	0.14	0.00	0.5	1.1	33

... continued

No.	Hor	Depth	Sand	Silt	Clay	Gravel	Text. ¹	Text. ²	Colour	C _{org}	N	C/N	pH	CEC _{pot}	K	Na	Mg	Ca	BS
		[cm]	[%]	[%]	[%]	[%]	[-]	[-]	[-]	[%]	[%]	[%]	[-]	[cmol _e /kg]	[%]				
Pr 11-1	1	16	73	13	14	13	SI4	SL	10YR/3.1	1.8	0.05	16	6.0	10.1	0.30	0.00	2.5	7.3	100
Pr 11-2	2	44	69	15	16	27	SI4	SL	7.5YR/4.2	0.7	0.03	14	5.7	4.7	0.86	0.00	0.7	2.4	82
Pr 11-3	3	77	72	12	16	27	SI4	SL	2.5Y/5.2, 2.5YR/3.6	0.4	0.03	13	5.3	4.4	0.35	0.00	0.5	1.5	54
Pr 12-1	1	3	79	10	11	7	SI3	SL	10YR/4.3	0.4	0.04	14	5.2	2.9	0.08	0.00	0.4	1.0	50
Pr 12-2	2	17	69	9	23	13	St3	SCL	10YR/4.3	0.6	0.04	14	4.4	5.4	0.08	0.00	0.3	0.8	23
Pr 12-3	3	48	64	10	26	10	Ts4	SCL	7.5YR/5.4	0.6	0.02	15	4.3	4.9	0.09	0.00	0.2	0.7	20
Pr 12-4	4	80	45	15	40	15	Lts	SCL/CL	7.5YR/5.6	0.2	0.02	11	4.5	6.5	0.12	0.01	0.3	0.9	21
Pr 13-1	1	35	84	8	7	13	St2	LS	7.5YR/4.2	0.3	0.02	13	4.6	2.3	0.13	0.00	0.2	0.6	40
Pr 13-2	2	52	80	8	12	14	St2	SL	7.5YR/4.4	0.4	0.02	18	4.4	2.2	0.02	0.00	0.2	0.5	30
Pr 13-3	3	71	77	10	14	9	St2	SL	7.5YR/5.4	0.2	0.03	14	4.4	3.1	0.06	0.00	0.2	0.6	28
Pr 13-4	4	86	64	10	26	12	Ts4	SCL	7.5YR/4.4	0.3	0.02	11	4.4	6.5	0.08	0.00	0.3	1.2	24
Pr 14-1	1	12	89	8	3	5	Ss	S	7.5YR/4.4	0.2	0.01	13	4.5	2.3	0.05	0.00	0.1	0.2	15
Pr 14-2	2	37	85	9	6	2	St2	LS	7.5YR/4.4	0.2	0.01	12	4.4	2.5	0.05	0.00	0.1	0.3	16
Pr 14-3	3	56	78	11	11	6	SI3	SL	7.5YR/5.6	0.2	0.02	16	4.5	2.0	0.12	0.01	0.2	0.8	59
Pr 14-4	4	82	71	12	17	5	St3	SL	7.5YR/5.6	0.2	0.03	10	4.6	4.7	0.08	0.00	0.2	0.7	22
Pr 15-1	1	14	86	8	6	24	St2	LS	7.5YR/4.2	0.4	0.03	14	4.8	3.0	0.06	0.00	0.3	1.0	43
Pr 15-2	2	34	79	12	9	26	SI3	LS	7.5YR/4.2	0.5	0.02	15	4.7	3.6	0.06	0.00	0.4	1.2	44
Pr 15-3	3	52	78	11	11	38	SI3	SL	7.5YR/5.6	0.3	0.03	14	4.8	4.3	0.05	0.00	0.3	0.9	28
Pr 15-4	4	74	66	14	19	38	St3	SL	5YR/4.6	0.4	0.05	14	4.8	6.8	0.06	0.02	0.3	1.1	21
Pr 16-1	1	9	32	18	51	20	TI	C	5YR/(4.4	0.7	0.04	15	5.0	12.6	0.39	0.03	5.0	4.4	78
Pr 16-2	2	29	38	19	43	23	Lts	C	5YR/4.6	0.5	0.02	15	5.3	10.6	0.39	0.03	4.6	3.5	81
Pr 16-3	3	44	46	18	37	26	Lts	SC	2.5YR/4.6	0.3	0.02	13	5.7	8.5	0.26	0.04	3.8	2.7	79
Pr 16-4	4	60	-	-	-	-	Ts2	C	2.5YR/4.6	-	-	-	-	-	-	-	-	-	-
Pr 16-5	5	82	-	-	-	-	Tt	C	2.5YR/4.6	-	-	-	-	-	-	-	-	-	-
F1-1	1	10	83	11	6	16	SI2	LS	10YR/3.3	0.5	0.03	21	4.5	8.0	0.09	0.05	2.3	3.3	72
F1-2	2	23	72	15	13	43	SI4	SL	10YR/5.4	0.5	0.03	19		6.4	0.18	0.02	0.6	1.3	33
F1-3	3	59	36	29	37	34	Lts	CL	5YR/4.6	0.3	0.03	13	5.5	12.1	0.10	0.05	1.9	2.8	40
F1-4	4	71	47	23	30	37	Lts	SCL	5YR/5.8	0.3	0.03	12	5.4	3.8	0.03	0.01	0.6	1.7	62
F2-1	1	25	76	14	10	12	SI3	SL	10YR/3.2	0.8	<0.01	22	4.9	6.1	0.09	0.00	0.5	2.0	41
F2-2	2	36	67	12	21	17	St3	SCL	7.5YR/4.4	0.5	0.05	17	4.6	6.2	0.07	0.01	0.7	2.6	56
F2-3	3	58	52	15	33	19	Ts4	SCL	7.5YR/4.6	0.5	0.03	13	4.3	10.4	0.07	0.00	0.7	1.9	26
F2-4	4	77	44	17	39	34	Lts	CL	7.5YR/4.6	0.4	0.03	11	4.4	5.5	0.07	0.03	0.8	2.2	56
F2-5	5	84	45	20	35	20	Lts	SCL/CL	7.5YR/4.6	0.3	0.02	12	4.5	10.8	0.07	0.00	0.7	2.4	30

Table A.11 Questionnaire for the characterisation of agricultural sites (translated from French to English).

Questionnaire – Exhausted agricultural sites (translated from French)	
1.	What is your name? Were you born here? If not, from where did you come here and why? To which ethnic group do you belong?
2.	Which crops are currently planted on this field?
3.	Which crops have you planted on all your fields this year? Which crops do you normally cultivate?
4.	Which crop rotation are you practicing on this field? What did you cultivate one/two years before? What will you cultivate the next year, and the year after ...?
5.	How many years do you cultivate this field before the fallow period? How long is your fallow period? Was this fallow period the same at your fathers/grandfathers time? If not, why?
6.	Do you use fertiliser for this field or one of your fields? If yes, which fertiliser do you use and for which crops (mineral fertiliser, organic manure ...)?
7.	Which tools do you use to cultivate your fields? Only hoe and axe or something else?
8.	Do you burn your fields regularly? If yes, when do you burn?
9.	What is the soil like at this field? Is it heavy or light, with/without gravels? Is the soil quality good or bad? Is the soil exhausted (<i>fatigué</i>)? Which colour has the soil?
10.	What do you think about the rainfall distribution this year? How was it in the last year?
11.	Do you think this area is suitable for agricultural land use? Which position along the hillslope do you prefer for agricultural production and for which crops?
12.	Have you been satisfied with the harvest this year?
13.	Do you apply soil conservation measures? If yes, which measures do you apply?

Table A.12 Location of studied erosion forms in the Upper Ouémé catchment (Date 12.09.-1.10.2005).

Site	x (UTM)	y (UTM)	Location	Position	Slope [%]	Land use	Erosion form	Degree
ER1	460921	1030944	Parakou-Banikani	Middle slope	3	settlement	deep rill, gully	Moderate
ER2	458535	1040850	N of Parakou	Lower slope	4	former sand excavation site	sheet erosion, rills, crusts	Severe
ER3	458956	1031298	Parakou-Sinahou	Upper slope	4	none	gully	Severe
ER4	341706	1088909	NO of road Copargo-Kpassabega		4	former sand excavation site	rills, crusts	Severe
ER5	453291	1025283	S of Parakou		3	former sand excavation site	sheet, rills, crusts	Severe
ER6	344620	1080781	Ara catchment (W of Djougou), near road	Lower slope	6	former sand excavation site	sheet, rills, crusts	Severe
ER7	340512	1067376	SW of Barei	Middle slope	3	unpaved road (width 5m)	rills along path, crusts	Severe
ER8	357782	1068455	Serou	Middle slope	2	foot path (width 1m)	rills along path	Moderate
ER9	365970	1074589	Barienou	Lower slope, inland valley border	side slopes up to 10	none	rills along path	Moderate
ER10	385448	1009126	Dogué: Lower Aguima	Lower slope	3	foot path	rills along path	Severe
ER11	384806	1006241	Dogué: Upper Aguima	Middle slope	2	unpaved road	sheet erosion, eroded planting rows	Moderate
ER15	369637	1075769	Moné	Lower slope	4	none	gully	Severe
ER16	369661	1075774	Moné	Middle slope	4	none	rills, crusts	Severe

Appendix B. Modelling and suspended sediment measurements



Fig. B.1 Sites of turbidity and discharge measurements: (a) Donga-Pont, (b) Lower Aguima, (c) Donga-Kolonkonde, (d) Terou-Igbomakoro (Date: September 2004, 2006).

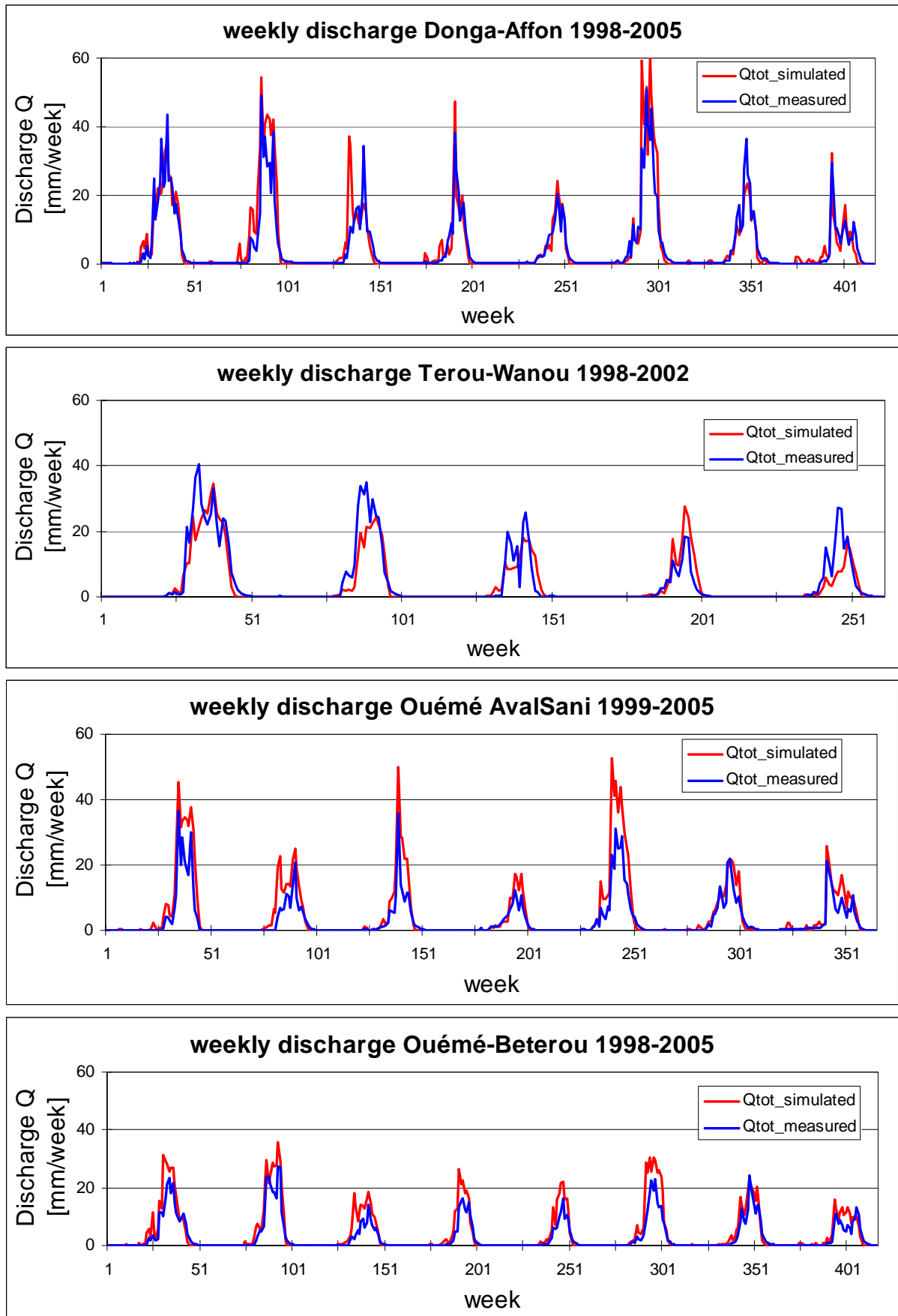


Fig. B.2 Spatial validation: Comparison of measured and simulated weekly discharge at the validation outlets.

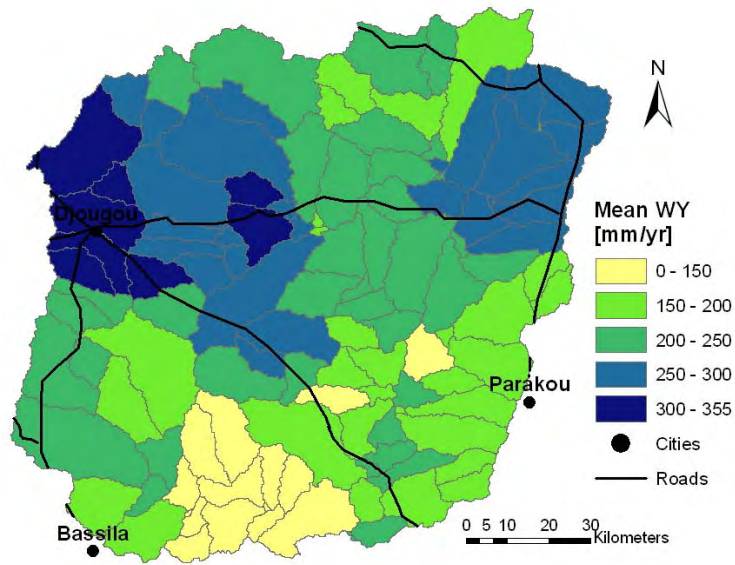


Fig. B.3 Spatial distribution of the mean total discharge in the Upper Ouémé catchment for the original model (1998-2005).

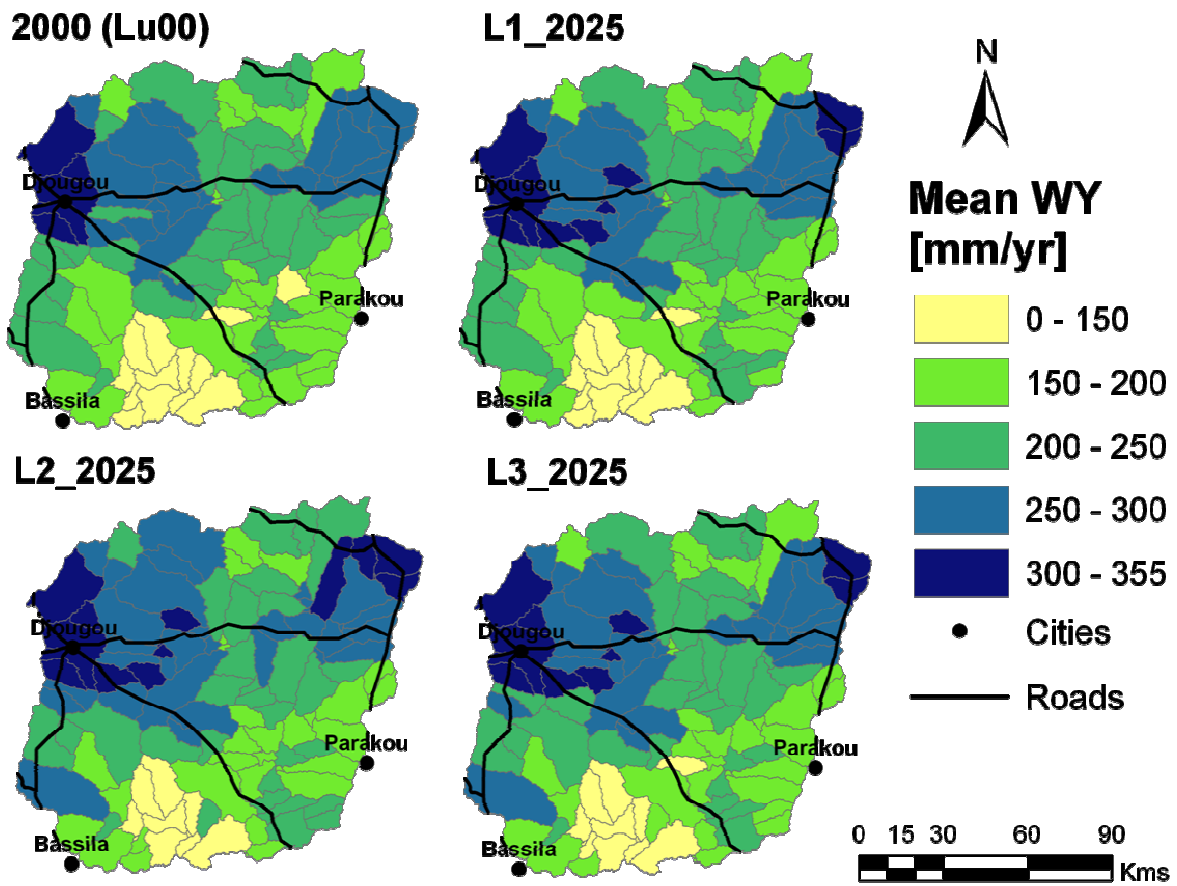


Fig. B.4 Spatial distribution of the mean total discharge in the Upper Ouémé catchment for the land use scenarios L1 to L3 and the Lu00 model.

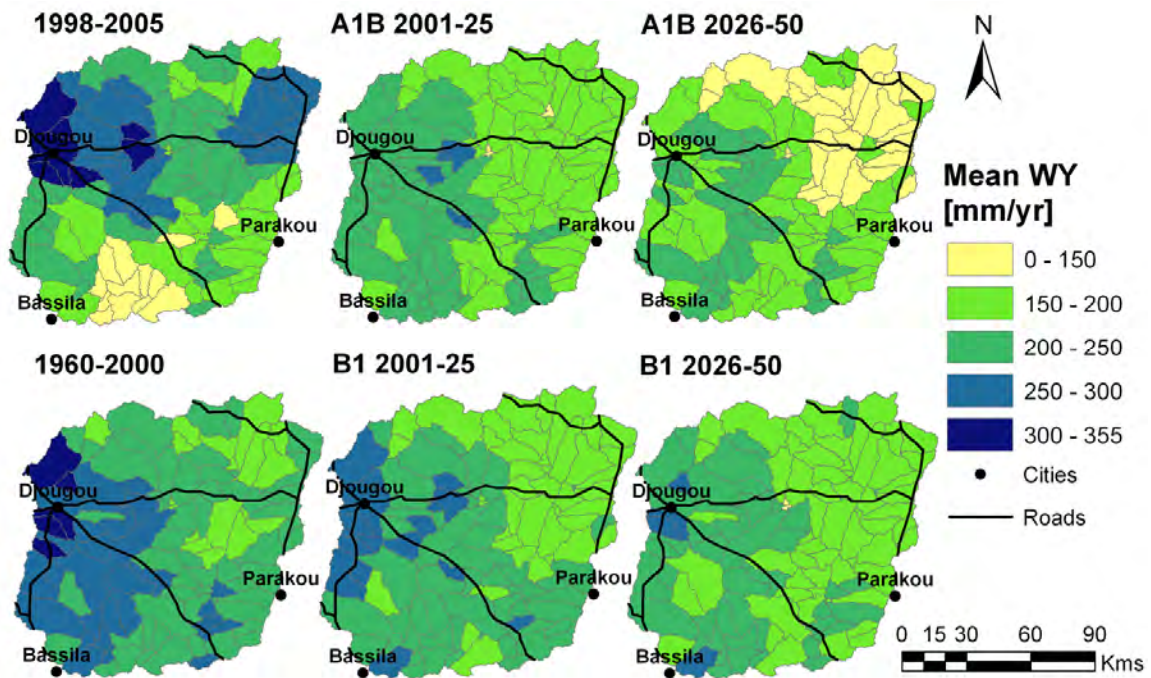


Fig. B.5 Mean spatial distribution of water yield for the climate scenarios A1B and B1 for the periods 2001-2025 and 2026-2050 compared to the original model (1998-2005) and the model with REMO data for 1960-2000.

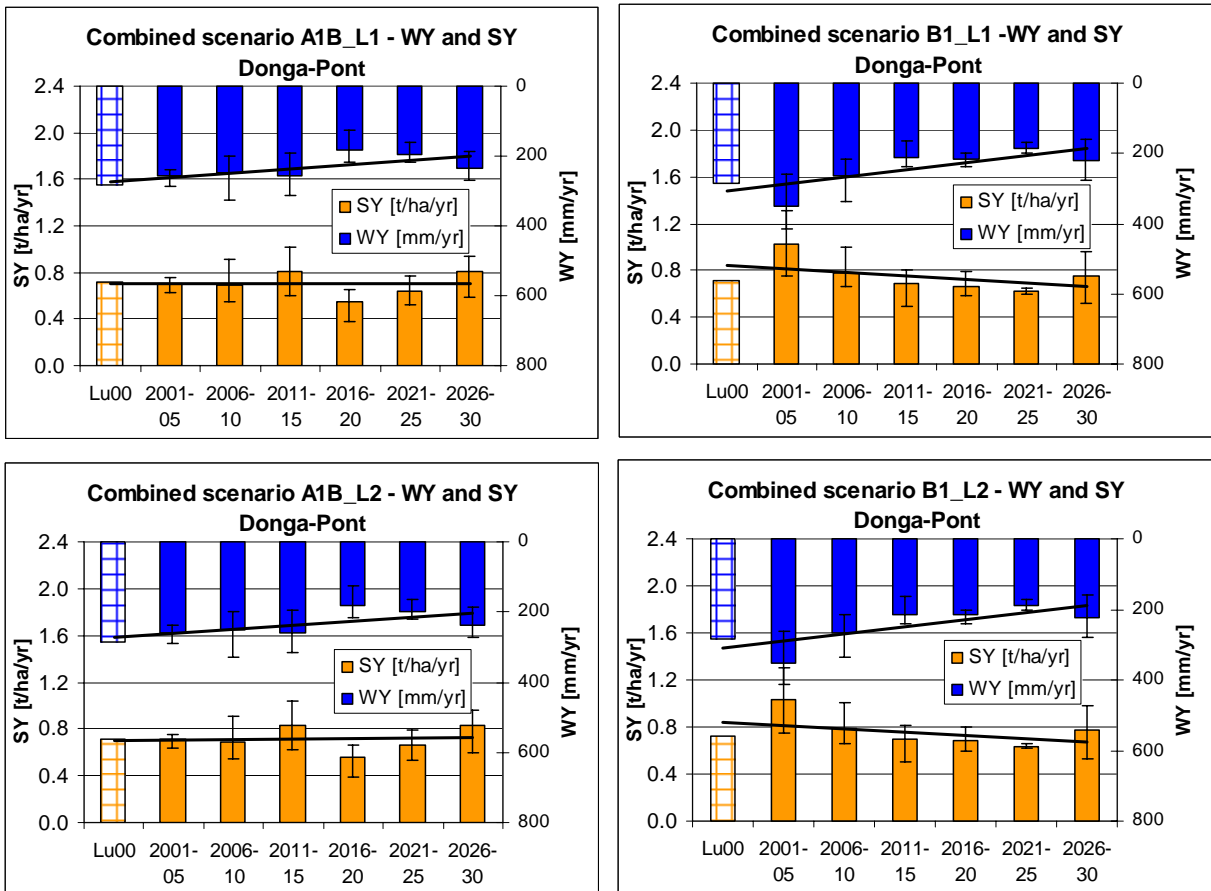


Fig. B.6 Mean simulated annual values of rainfall, sediment yield (SY) and water yield (WY) in the Donga-Pont subcatchment for the combination of the land use scenarios L1 and L2 with the climate change scenarios for the period 2000 to 2030. The presented results are averages of three ensemble runs for each climate scenario.

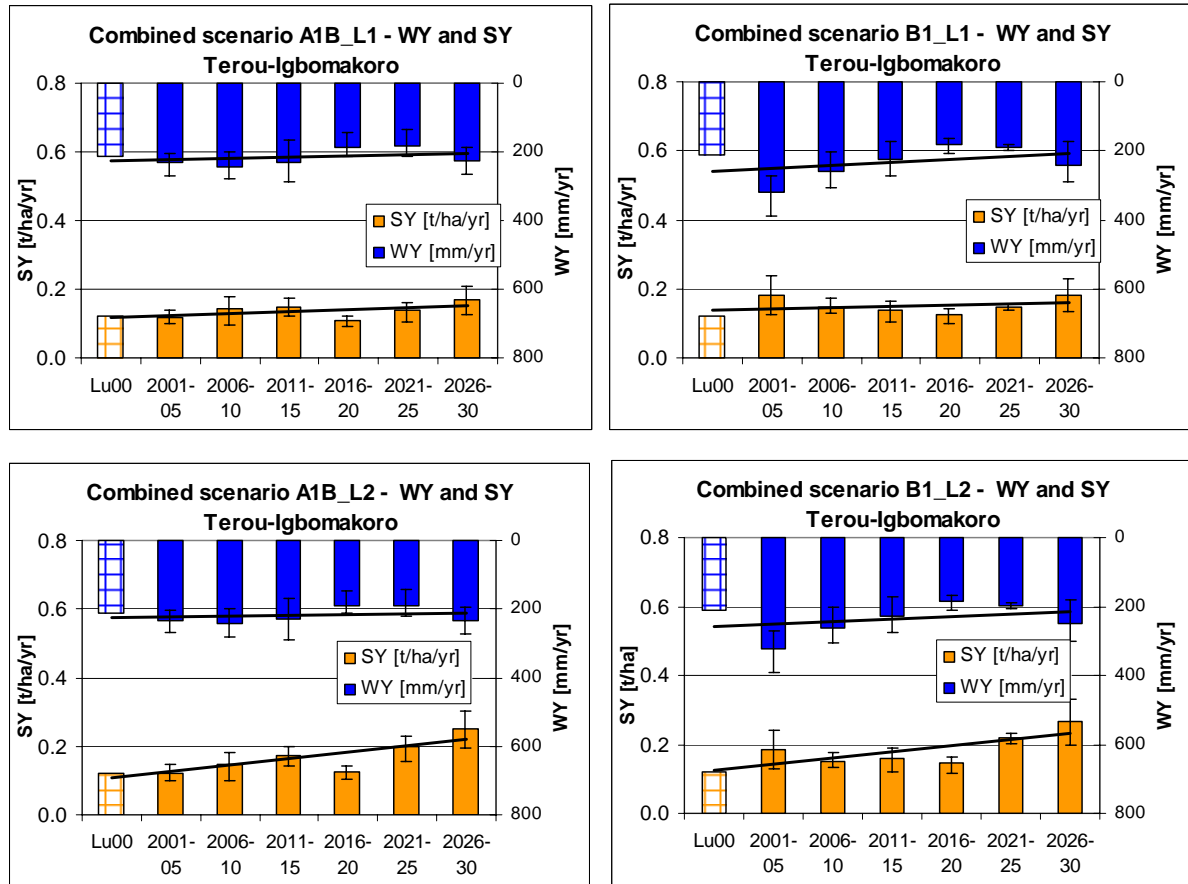


Fig. B.7 Mean simulated annual values of rainfall, sediment yield (SY) and water yield (WY) in the Terou-Igbomakoro subcatchment for the combination of the land use scenarios L1 and L2 with the climate change scenarios for the period 2000 to 2030. The presented results are averages of three ensemble runs for each climate scenario.

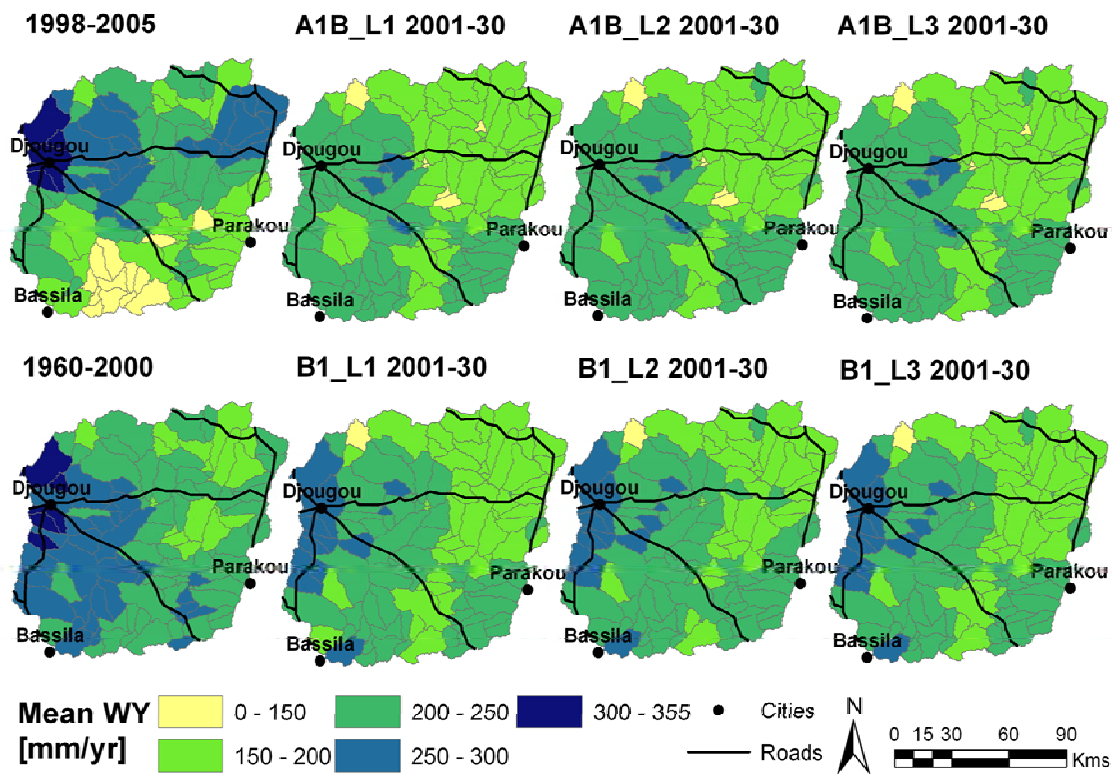


Fig. B.8 Mean spatial distribution of water yield for the combinations of the climate scenarios A1B and B1 with the land use scenarios L1-L3 for the period 2001-2030 compared to the Lu00 model (1998-2005) and the model with REMO data for 1960-2000.

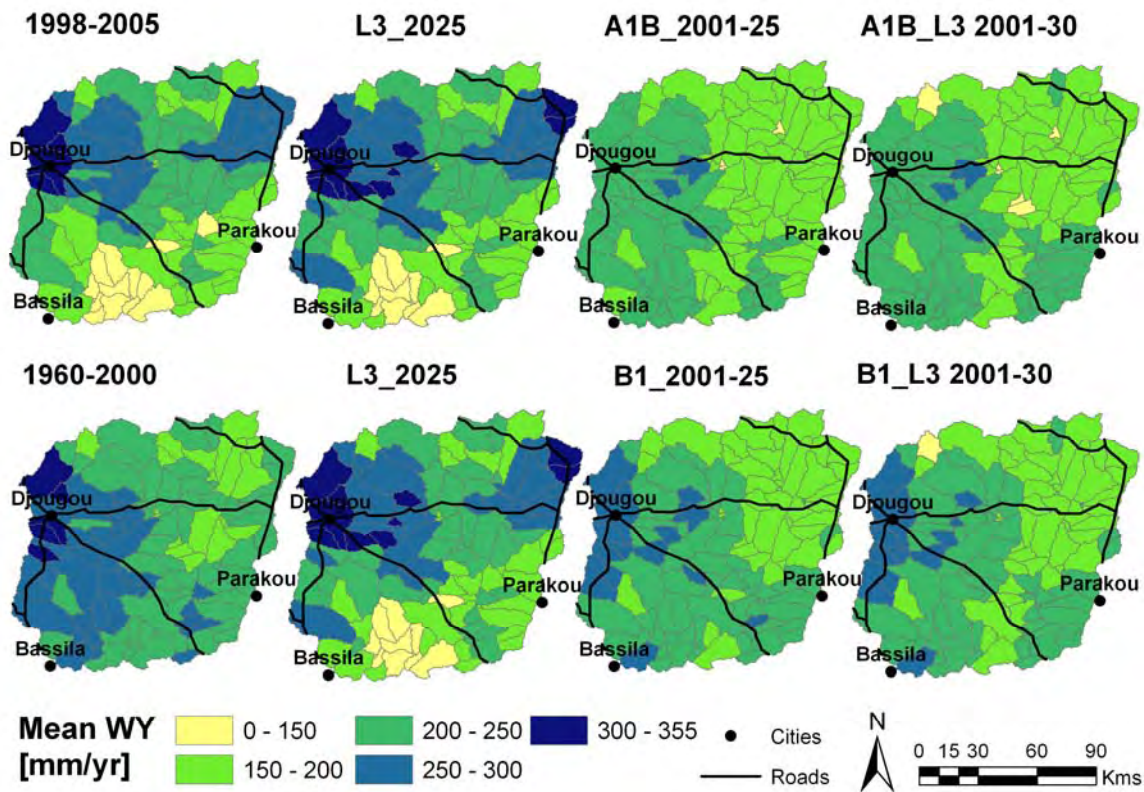


Fig. B.9 Mean spatial distribution of water yield for the land use, climate and combined scenarios compared to the Lu00 model (1998-2005) and the model with REMO climate data for 1960-2000.

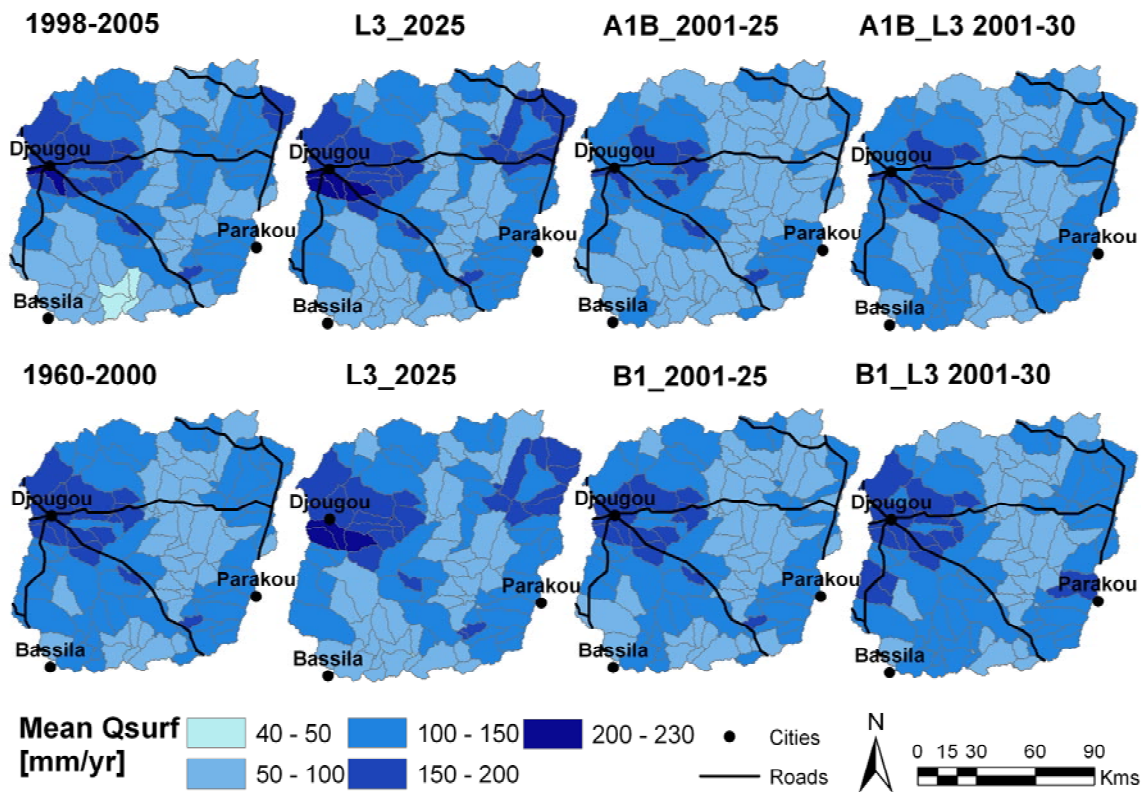


Fig. B.10 Mean spatial distribution of surface runoff for the land use, climate and combined scenarios compared to the Lu00 model (1998-2005) and the model with REMO climate data for 1960-2000.

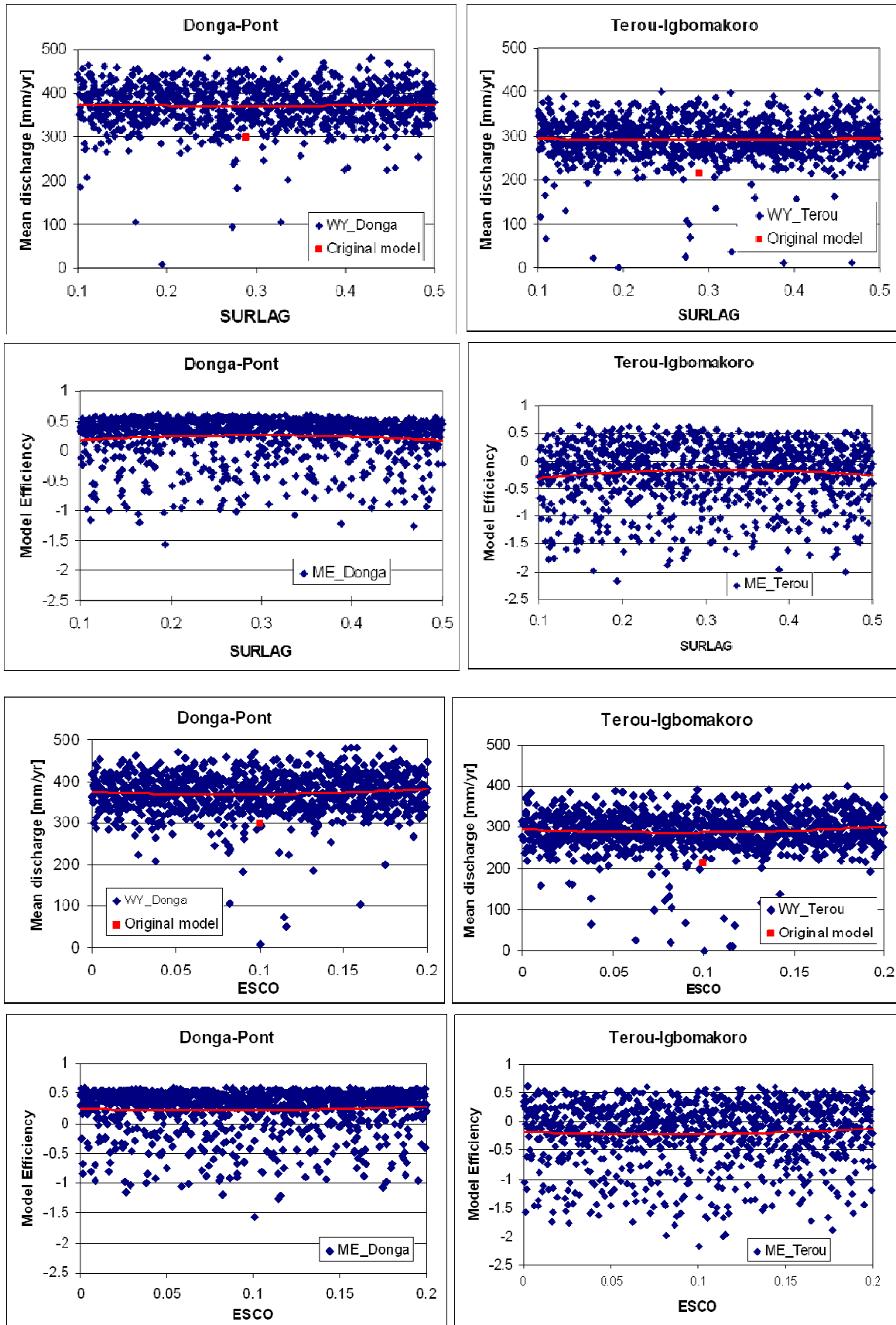


Fig. B.11 Sensitivity of mean annual discharge and model efficiency to changes of the parameters ESCO and SURLAG (red dot: parameter value and simulated mean discharge for the period 1998-2001, red line: polynomial regression).

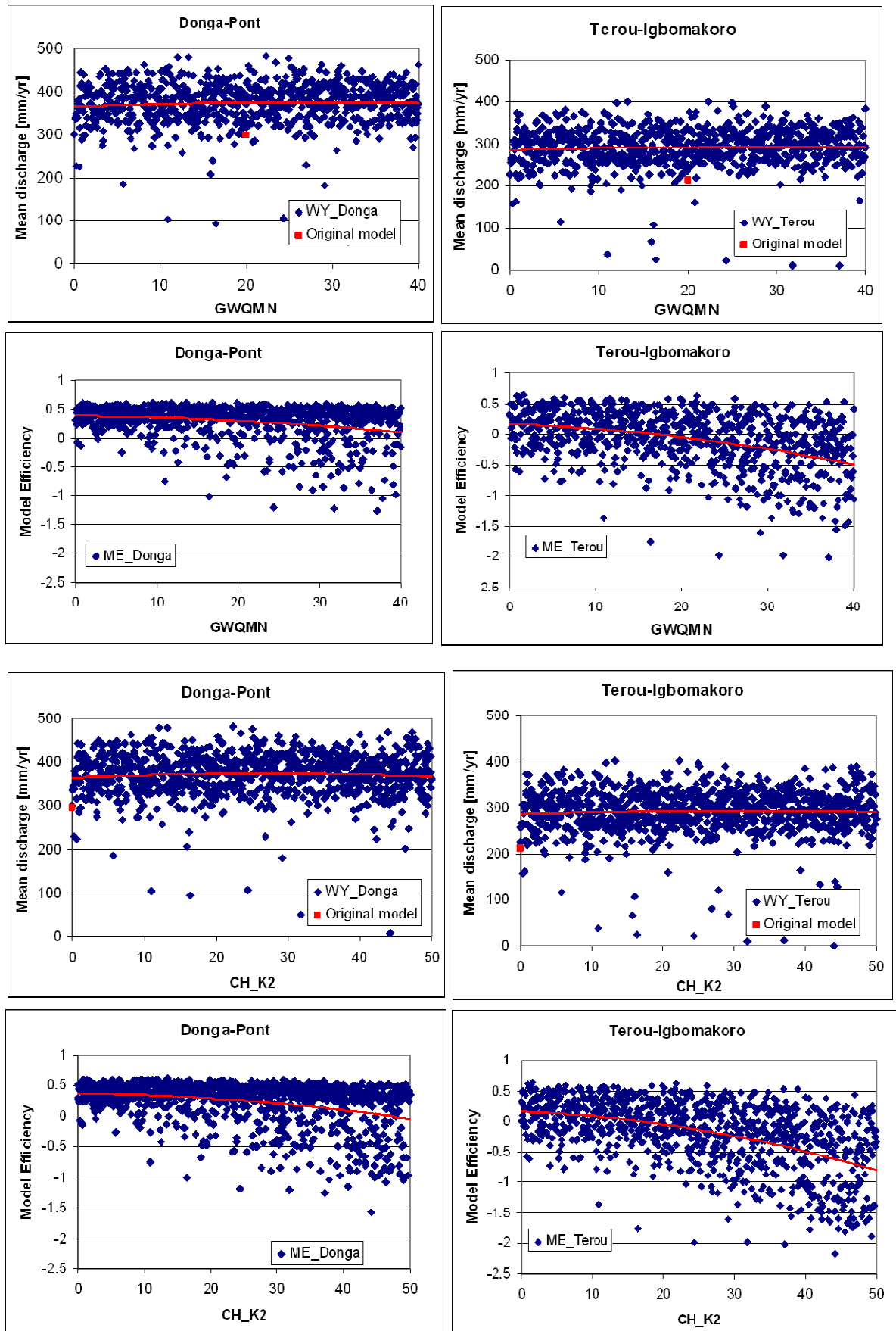


Fig. B.12 Sensitivity of mean annual discharge and model efficiency to changes of the parameters GWQMN and CH_K2 (red dot: parameter value and simulated mean discharge for the period 1998-2001, red line: polynomial regression).

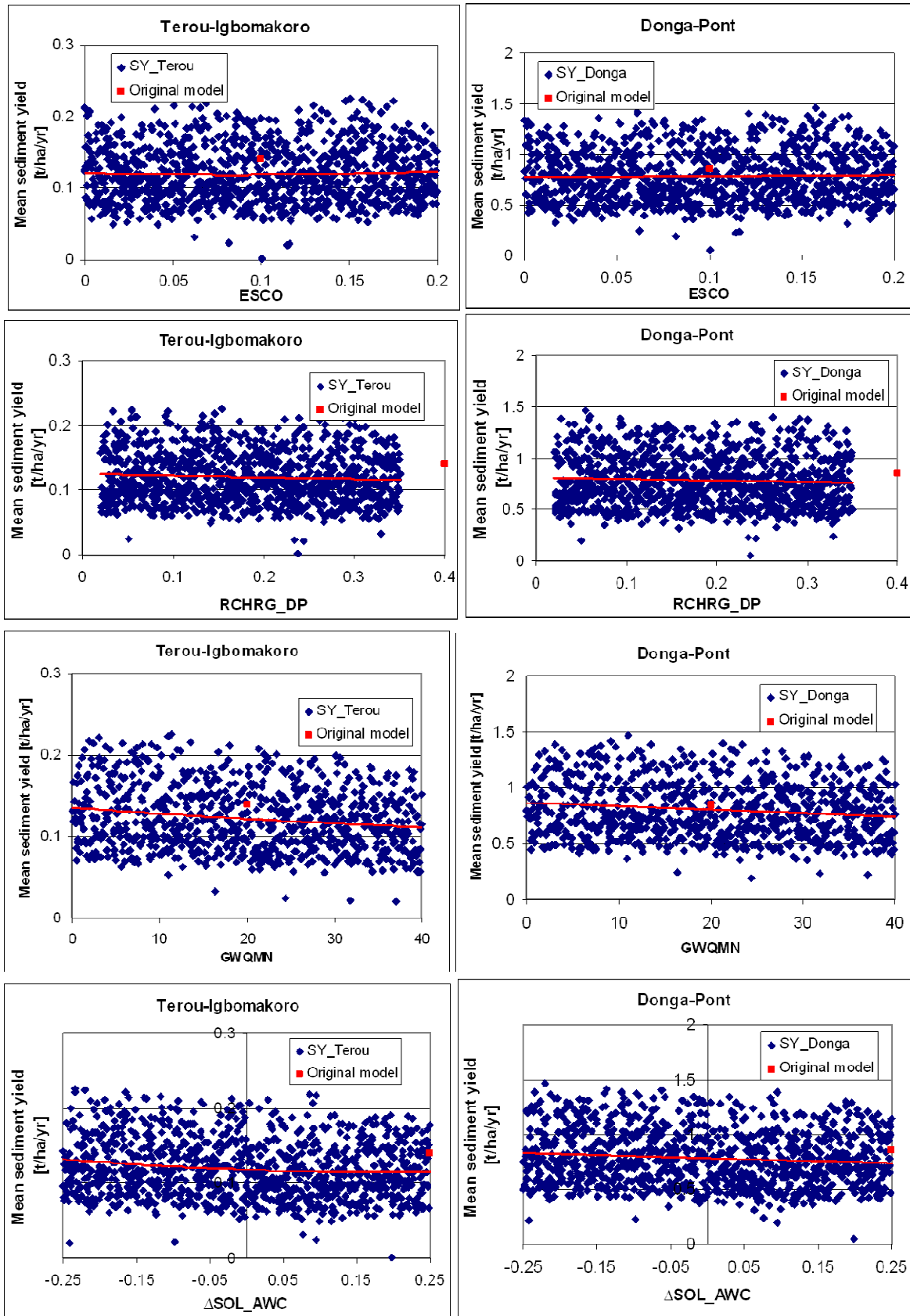


Fig. B.13 Sensitivity of mean annual sediment yield to changes of the parameters ESCO, SURLAG, GWQMN and SOL_AWC (red dot: parameter value and simulated mean discharge for the period 1998-2001, red line: polynomial regression).

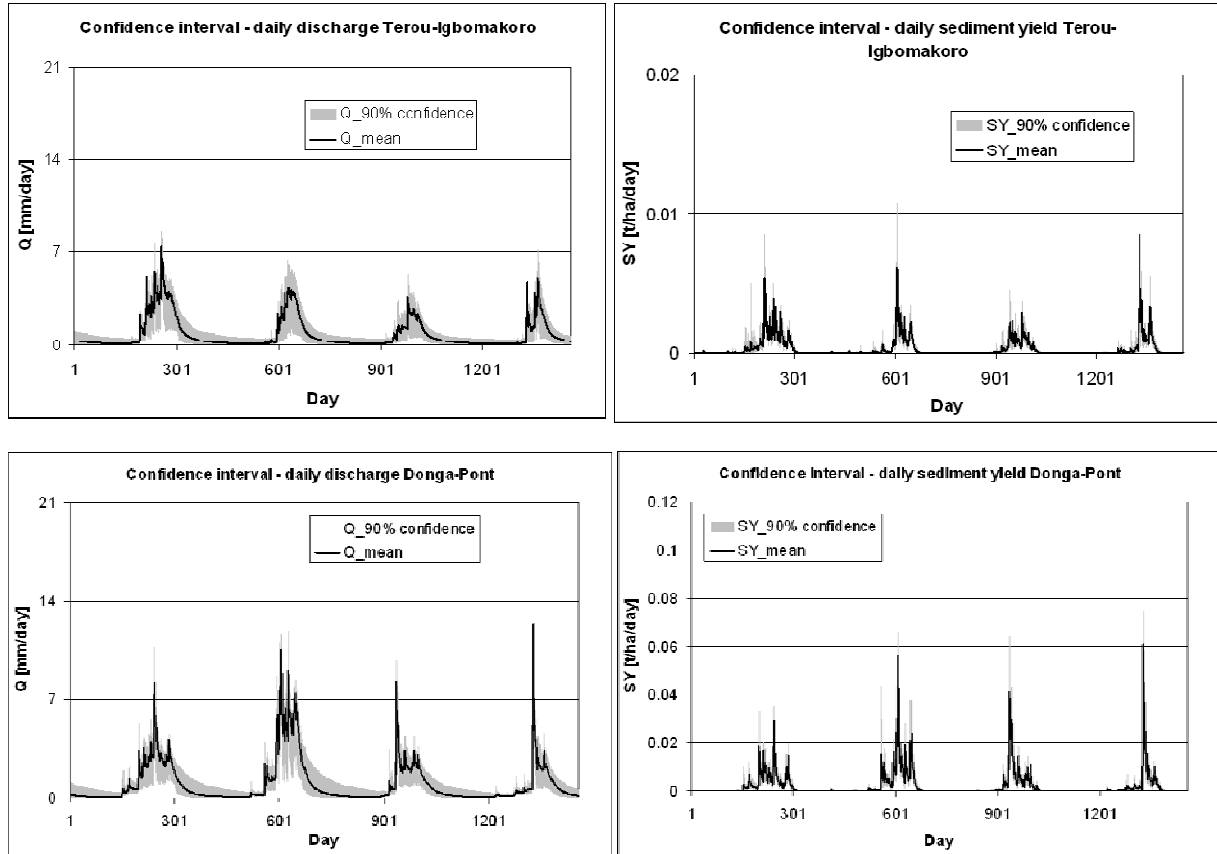


Fig. B.14 Confidence interval (90%) for mean daily discharge and sediment yield at the Terou-Igbomakoro and Donga-Pont outlets.

Appendix C. Soil conservation

Table C.1 Main finished and ongoing development projects in Benin concerning soil degradation (Sources: Singer, 2005; MEHU, 2005; own investigations).

Project title	Budget 10 ⁶ FCFA	Funding institutions	Period	Intervention zone	Objectives
Projet pour la lutte contre le feux de brousse	-	UNDP, FAO	1986-1990	Boukoubé	Combat of bush fire
PADSA (Phase I)	13	DANIDA, Benin	1997-2003	22 communes (e.g. Ouenou in Ndali)	Development of the agricultural sector
PAGER	6.7	FIDA, DANIDA, Benin	1997-2004	Whole country	Financing of income generating activities
PDE	6	BAD, Benin	1998-2002	Northern Benin	Reinforcement of food security by the promotion of sustainable animal husbandry
PAZH	1.45	Netherlands, Benin	1998-2001	Southern Benin	Elaboration of a strategy for the management of the humid zones of Benin
AGRE	-	DANIDA, Benin	Since 1998	Whole country	Management of water ressources
UNSO	3.5	FEM, UNDP, Worldbank, Benin	1989-1999	Forests of Sota, Goungoun, Goroubi	Carbon sequestration through reforestation
PGRN	16	AFD, Worldbank, UNDP, GTZ, GEF, Benin	1992-1999	Whole country	Forest and watershed management
PADEL	3.053,862	UNDP, FENU, Benin	1995-2001	East Borgou, West Atacora	Local development and promotion of local collectives
PADSE	5.5	AFD, Benin, OPA	1998-2004	Alibori, Borgou (e.g. Ouenou), Zou/Collines	Soil fertility, agro-forestry, integration of agriculture and animal husbandry, diversification
PPRF	-	GTZ, Benin	1999-2004	Bassila	Forest management and land tenure
PGTRN	11	GTZ, AFD, Benin	1999-2005	Mono/Couffo, Zou/Colline, Atacora/Donga	Land tenure and land-use planning, upscaling of management activities from PGRN
PSSA	1.846,130	FAO, Vietnam, Benin	1999-2007	Atacora, Zou, Atlantique, Ouémé, Borgou	Improve alimentation of population
PCNCC	290	FEM, Benin	2000-2003	Whole country	Vulnerability and adaptation of the socio-economic sectors to climate change
Projet Axe Vert et plantation d'arbres	305	Benin	2000-2003	Urban centres	Reforestation of urban centres
PGFTR	41.536	Worldbank, FEM, Benin	2000-2006	22 forêts classée	Forest management

... continued

Project title	Budget 10 ⁶ FCFA	Funding institutions	Period	Intervention zone	Objectives
PDRT		Worldbank, IFAD, BOAD, Benin	2001-2008	Whole country	Filiere de cassava, sustainable agriculture
PAMF	13.701	BAD, BADEA, Benin	2002-2007	Agoua, Wari- Maro, Monts Kouffè	Integrated forest management
PNGE	49.812,6	Benin, local partner collectives	2002-2008 (Phase I)	Whole country	Efficient and sustainable use of environmental ressources
Projet d'établissement d'un corps de jeunes pour l'environnement	431,6	Vénézuela, UNDP, PAM, Benin	2004-2007	Djidja, Ouaké	Generation of employment for young people, restauration and protection of natural ressources
ProCGRN	7.97	GTZ, KFW, Worldbank, AFD, BAD, Benin	2004-2014	Atacora, Donga, Cotonou, Atlantique	Sustainable management of natural resources in rural area, integrates earlier projects: PGTRN, PPEFB, PRRF
ANCR	200	FEM, Benin	2005-2007	Whole country	Capacity building concerning environmental issues
GERBES	7.105,5	Worldbank, Benin	2005-2014	Region Atchérigb- Tchaourou	Effective domestic energy use, reducing the pressure on natural ressources
PAC/MEHU	1.017	Benin, partners	2005-2010	Whole country	Capacity building in the communes concerning environmental management
PAEB Nord		DWHH, DED, EU	2007-2009	Bassila, Ndali	Sustainable agriculture, natural ressources management
Millenium villages		DWHH	2007-2010	Selected villages	E.g. agro-forestry, micro credits, water sector
FALMP		GEF, Worldbank	2007-2011	e.g. Parakou, Abomey, Djougou and Natitingou	Upscale community-based forest management component of PGRN to the remaining gazetted forests, forest adjacent lands, and four urban forest plantations

Table C.2 Main soil conservation measures in Benin: Effects, advantages and constraints from the Beninese farmer's point of view. Sources: ¹Lal (1990), ²oral comm. Azontonde, ³oral comm. Loconon, ⁴UNDP (2002), ⁵Gandonou (2000), ⁶FAO (2001a), ⁷Mulindabigwi (2006), ⁸Fadohan (2004), ⁹Donovan and Casey (1998), ¹⁰Godjo et al. (2003), ¹¹Floquet et al. (2002), ¹²Maliki et al. (2001), ¹³Gantoli (1997), ¹⁴Floquet et al. (2006).

Type of measure	Effect	Advantages	Constraints	Adoption in Benin
1. Cultural technology & soil tillage				
Field limits (parcelling, earth wall, stones, bush); discharge barriers on pathways	Reduction of slope length, decrease of Q_{surf} and erosion	Demarcation of field borders	High labour demand installation/maintenance, no short-term benefit, no significant increase of crop yield	Only widespread in Atacora region with steep slopes and stony soils
Tillage against the slope	Reduction of slope length, decrease of Q_{surf} and erosion	Simple and cheap measure	Worse drainage, no protection against severe storms	Often on the mid-slope
Ox-Ploughing	Higher infiltration rate ²	Reduced labour demand	Most farmers have no cattle, animal diseases	Only common in northern Benin
2. Plant management				
Early seeding, dense seeding, early combat of weeds and pest	Increase in vegetation cover and crop biomass reduce Q_{surf} and erosion	Higher crop yield	Labour demand	
Adapted varieties, diversification		Higher crop yield, improved food security	Lack of access to efficient seeds, high labour demand	Diversification widespread
No bush fire	Increase of topsoil C_{org} and vegetation cover result in less erosion and better soil nutrient status	Higher crop yield on degraded soils	Traditional burning for multiple purposes (e.g. hunting, land preparation, pest and weed control, quick nutrient release)	Only in areas with high land pressure or with additional benefit (e.g. honey production) ³ ; therefore often propagation of early fires
Mulching top of yam mounds	Lower raindrop impact due to increased shear strength ¹ , more earthworms due to regulated soil temperature ⁷ , less evaporation losses, better infiltration ⁷	Reduced topsoil loss, higher crop yield; simple and cheap measure		Widespread; if not enough biomass cover with soil mottles until yam plants long enough to enrol the plant around the mound top (northern HVO) ⁷
Improved crop rotation (groundnut, niebe, cowpea)	Legumes improve soil fertility due to N-fixation	Increased soil fertility, partially compensates shorter fallow period	Food preferences	Groundnut widespread part of the crop cycle in northern Benin, cowpea and niebe more widespread in southern Benin

... continued

Type of measure	Effect	Advantages	Constraints	Adoption in Benin
Vetiver hedges	Strips along contour-lines as runoff absorber and to encourage sedimentation	Reduced topsoil loss	High labour demand for installation, access to Vetiver grass	Only sporadic on steep slopes and next to big erosion rills
Agro-Forestry: <i>Gliricidia sepium</i>	Increase soil fertility due to N-fixation, reduced erosion due to increase of vegetation cover	Increase of soil fertility, option for settled yam cropping → reduces deforestation, increase of crop yield ⁸ , drought-resistant ¹² , suitable as fodder ¹²	High labour demand installation/maintenance; sophisticated handling of seeds ^{2,8} , restricts crop cycle in growing phase ² , difficult access to seeds/plants ¹² , space demand ¹²	Limited adoption in project intervention areas
Agro-Forestry: <i>Leucaena leucocephala</i>	Increase soil fertility due to N-fixation, reduced erosion due to increase of vegetation cover	fire-resistant ² , additional benefit (fodder, wood), increase maize yields ²	High labour demand installation/maintenance, sometimes reduced crop yield due to competition ⁶ , excessive spreading ² , needs sufficient P in soil, sensible to termite attacks and severe disease defoliation, poor biomass production on low fertility and acidic soils ⁹	Farmers in southern Benin prefer <i>Mucuna</i> or <i>Cajanus</i> ² ; <i>Leucaena</i> preferred by herders in region Bassila because of additional benefit as fodder and wood ³
Agro-Forestry: <i>Acacia auriculiformis</i>	As fallow on degraded soils, tree harvest after 4-5 years, since 3 rd year cultivation of maize in the litter possible ¹²	Improves soil properties and crop yields after fallow, low labour demand, valuable as fire wood and timber ¹¹	Space demand, farmers prefer second crop in the south, land tenure, shadowing, costs, difficult access and transport ¹¹	High adoption rates in southern Benin ¹⁴
Agro-Forestry: <i>Cajanus cajan</i>	Increase soil fertility due to N-fixation, reduced erosion due to increase of vegetation cover;	fire- and drought-resistant ² , leaves as fodder ¹³ , auto-consumption and commerce with <i>Cajanus</i> ⁸ , suppression of weeds like <i>Imperata</i> ¹³	not as efficient as <i>Gliricidia</i> ² , high labour demand for installation and maintenance, competition with annual crops due to shadowing, difficult weeding of young plants ⁸ , dislikes pH<5 and inundations ¹³	Preferred by farmers in region Bassila due to additional benefit as food product ³

... continued

Type of measure	Effect	Advantages	Constraints	Adoption in Benin
Cover crops: <i>Mucuna pruriens</i>	Minimised erosion due to fast dense vegetation cover; increase soil fertility due to N-fixation, through shadowing protection against weeds	Very efficient in combat of Imperata and Striga ^{2,14} , farmers can produce their own seeds ² , lower labour-demand than for Agro-Forestry, reduces labour needed for tilling and weeding ⁹	Not fire-resistant ^{2,11} , long lifecycle 150-200 days ² , often yield decline except for new fertilized maize species ⁶ , treatment of biomass with traditional tools difficult and labour intensive ¹⁰ , poor growth on waterlogged or heavily degraded, acid soils ^{11,4}	Above all in South Benin; rarely in North Benin due to bush fire, shorter rainy period and destruction by livestock ² , in South Benin competition with permanent food crop cultivation ¹¹ ; promotion in region Bassila failed ³
Cover crops: Niebe	Reduced erosion due to increase of vegetation cover; increase soil fertility due to N-fixation	Variety Vohounvo very effective; additional benefit (food), lower labour-demand than for agro-forestry	Food preferences: Niebe only common in some regions	Widespread in Couffo (North Mono) and other parts of South Benin; as second crop after maize or groundnut ²
Improved fallow	Kept trees on fields improve physical and chemical soil properties	Fire-wood, easy to handle, no competition between trees and crops ⁹ , higher crop yield	In land-scarce regions too space demanding ⁹	
3. Fertiliser				
Organic fertiliser from animal husbandry	Compensates nutrient loss	Increased yields, in particular maize	High labour demand, many farmers have no cattle, lack of equipment for transport/ incorporation ⁹ , poor quality ⁹	Farmers often allow herders grazing after harvest, trade with manure uncommon
Organic fertiliser from composting	Compensates nutrient loss	Increased yields, in particular maize, cheap	Labour demand for transport too high, little big amounts, often poor quality ⁹	Partially in home gardens and house maize fields (e.g. in Northern Borgou and Bokoumbé region ⁵)
Mineral fertiliser	Compensates nutrient loss, increases soil fertility	Increase of crop yield	Difficult access, on the long run acidification	